



NATO Science for Peace and
Chemistry and

Advances in R
Medicine:
Nanotechno
Engineering

Advances in Regenerative Medicine: Role of Nanotechnology, and Engineering Principles

NATO Science for Peace and Security Series

This Series presents the results of scientific meetings supported under the NATO Programme: Science for Peace and Security (SPS).

The NATO SPS Programme supports meetings in the following Key Priority areas: (1) Defence Against Terrorism; (2) Countering other Threats to Security and (3) NATO, Partner and Mediterranean Dialogue Country Priorities. The types of meeting supported are generally "Advanced Study Institutes" and "Advanced Research Workshops". The NATO SPS Series collects together the results of these meetings. The meetings are coorganized by scientists from NATO countries and scientists from NATO's "Partner" or "Mediterranean Dialogue" countries. The observations and recommendations made at the meetings, as well as the contents of the volumes in the Series, reflect those of participants and contributors only; they should not necessarily be regarded as reflecting NATO views or policy.

Advanced Study Institutes (ASI) are high-level tutorial courses intended to convey the latest developments in a subject to an advanced-level audience

Advanced Research Workshops (ARW) are expert meetings where an intense but informal exchange of views at the frontiers of a subject aims at identifying directions for future action

Following a transformation of the programme in 2006 the Series has been re-named and re-organised. Recent volumes on topics not related to security, which result from meetings supported under the programme earlier, may be found in the NATO Science Series.

The Series is published by IOS Press, Amsterdam, and Springer, Dordrecht, in conjunction with the NATO Public Diplomacy Division.

Sub-Series

A.	Chemistry and Biology	Springer
B.	Physics and Biophysics	Springer
C.	Environmental Security	Springer
D.	Information and Communication Security	IOS Press
E.	Human and Societal Dynamics	IOS Press

<http://www.nato.int/science>

<http://www.springer.com>

<http://www.iospress.nl>



Series A: Chemistry and Biology

Advances in Regenerative Medicine: Role of Nanotechnology, and Engineering Principles

Edited by

Venkatram Prasad Shastri

Universität Freiburg
Institute of Makromolekulare Chemie
Germany

George Altankov

ICREA & Institute of Bioengineering Catalunya
Barcelona
Spain

Andreas Lendlein

Institute of Polymer Research and Berlin-Brandenburg Center for
Regenerative Therapies
GKSS Research Center Geesthacht GmbH
Teltow
Germany

 Springer

Published in Cooperation with NATO Public Diplomacy Division

Proceedings of the NATO Advanced Research Workshop on Nanoengineered
Systems for Regenerative Medicine Varna, Bulgaria
21–24 September 2007

Library of Congress Control Number: 2010929479

ISBN 978-90-481-8789-8 (PB)
ISBN 978-90-481-8788-1 (HB)
ISBN 978-90-481-8790-4 (e-book)

Published by Springer,
P.O. Box 17, 3300 AA Dordrecht, The Netherlands.

www.springer.com

Printed on acid-free paper

All Rights Reserved

© 2010 Springer Science+Business Media B.V.

No part of this work may be reproduced, stored in a retrieval system, or transmitted in any form-or by any means, electronic, mechanical, photocopying, microfilming, recording or otherwise, without written permission from the Publisher, with the exception of any material supplied specifically for the purpose of being entered and executed on a computer system, for exclusive use by the purchaser of the work.

Preface

This book summarizes the NATO Advanced Research Workshop (ARW) on “Nanoengineered Systems for Regenerative Medicine” that was organized under the auspices of the NATO *Security through Science Program*. I would like to thank NATO for supporting this workshop via a grant to the co-directors.

The objective of ARW was to explore the various facets of regenerative medicine and to highlight role of the “the nano-length scale” and “nano-scale systems” in defining and controlling cell and tissue environments. The development of novel tissue regenerative strategies require the integration of new insights emerging from studies of cell-matrix interactions, cellular signalling processes, developmental and systems biology, into biomaterials design, via a systems approach. The chapters in the book, written by the leading experts in their respective disciplines, cover a wide spectrum of topics ranging from stem cell biology, developmental biology, cell-matrix interactions, and matrix biology to surface science, materials processing and drug delivery. We hope the contents of the book will provoke the readership into developing regenerative medicine paradigms that combine these facets into clinically translatable solutions.

This NATO meeting would not have been successful without the timely help of Dr. Ulrike Shastri, Sanjeet Rangarajan and Ms. Sabine Benner, who assisted in the organization and implementation of various elements of this meeting. Thanks are also due Dr. Fausto Pedrazzini and Ms. Alison Trapp at NATO HQ (Brussels, Belgium). The commitment and persistence of Ms. Wil Bruins at Springer in getting this book published is very much appreciated. Last but not least, I would like to thank Prof. George Altankov my co-Director and Prof. Andreas Lendlein for their supportive role.

Co-Director, Freiburg

V. Prasad Shastri

Contents

1 Cell Adhesions and Signaling: A Tool for Biocompatibility	
Assessment	1
1.1 Introduction.....	2
1.2 Cell-Matrix Adhesions.....	3
1.2.1 Integrin Receptors and Integrin Cytoplasmic Complexes	3
1.2.2 Focal Adhesions.....	5
1.2.3 Fibrillar Adhesions.....	9
1.2.4 Three-Dimensional Matrix Adhesions.....	10
1.2.5 Dynamics of Cell Adhesions	12
1.3 Concluding Remarks.....	14
References.....	15
2 Development of Provisional Extracellular Matrix on Biomaterials Interface: Lessons from In Vitro Cell Culture	19
2.1 Introduction.....	20
2.2 Initial Cell–Materials Interaction.....	20
2.2.1 Development of Focal Adhesion Complex	21
2.2.2 Substratum Properties Affect Focal Adhesions Formation	22
2.3 Development of Provisional Extracellular Matrix at the Biomaterials Interface	23
2.3.1 Development of Early Matrix	23
2.3.2 Development of Late Fibronectin Matrix	25
2.4 Integrin Receptors Dynamics and Provisional Extracellular Matrix Formation	26
2.4.1 Studies on Integrin Dynamics.....	26
2.4.2 Integrin Dynamics Depend on Substratum Properties.....	29
2.5 Development of Extracellular Matrix at “Real” Biomaterials Interface.....	30
2.5.1 Effects of Substratum Chemistry on Matrix Formation: A View of Biosensors Application.....	30

- 2.5.2 Development of Extracellular Matrix on Biomimetic Hydroxyapatite Cements Surfaces..... 33
- 2.5.3 Development of Extracellular Matrix on Different Rough Titanium Surfaces 36
- References..... 41
- 3 Endothelial Progenitor Cells for Tissue Engineering and Tissue Regeneration 45**
 - 3.1 Introduction..... 46
 - 3.2 Vascular Networks for TE Constructs..... 46
 - 3.3 Sources of Human Endothelial Cells for TE
 - Vascular Networks 47
 - 3.3.1 Mature Vessel-Derived Endothelial Cells 47
 - 3.3.2 Human Embryonic Stem Cells..... 47
 - 3.3.3 Blood-Derived EPCs..... 48
 - 3.3.4 Bone Marrow-Derived Cells for Tissue Vascularization 49
 - 3.4 Blood-Derived EPCs for Creating Vascular Networks 50
 - 3.4.1 Isolation and Culture of Human EPCs and HSVSMCs..... 50
 - 3.4.2 In Vivo Assay for Vascularization..... 51
 - 3.4.3 Summary: Vasculogenic Potential of Human EPCs 51
 - References..... 52
- 4 Dermal Precursors and the Origins of the Wound Fibroblast..... 55**
 - 4.1 Introduction..... 55
 - 4.2 Mesenchymal Stem Cells..... 56
 - 4.2.1 Marrow Derived Fibroblast Populations 57
 - 4.2.2 Fibrocytes..... 58
 - 4.2.3 Factors for Mobilization and Recruitment of Marrow Populations..... 61
 - 4.3 Defining the Dermal Fibroblast 62
 - 4.3.1 Dermal Progenitors 62
 - 4.3.2 Evidence for Progenitor Populations 63
 - 4.4 Clinical Applications 65
 - 4.5 Novel Healing Properties of MSC 66
 - 4.6 Summary 66
 - References..... 67
- 5 Cell Based Therapies: What Do We Learn from Periosteal Osteochondrogenesis? 71**
 - 5.1 General Introduction 72
 - 5.1.1 Cell Based Therapies 72
 - 5.2 Periosteum..... 73

- 5.2.1 Embryological Development of Bone, Cartilage, and Periosteum..... 74
- 5.2.2 Periosteum in Bone and Cartilage Repair..... 75
- 5.3 Differential Survival of Periosteal Progenitor Cells Versus Chondrocytes..... 77
 - 5.3.1 Introduction..... 77
 - 5.3.2 Cell Labeling and Scaffolds..... 77
 - 5.3.3 Chondrocytes Survive Transplantation Better than Periosteal Progenitor 78
 - 5.3.4 Hyaluronan Increases the Number of Viable Periosteal Progenitors 78
 - 5.3.5 Discussion..... 79
- 5.4 A Model to Study Periosteal Osteochondrogenesis In Vivo..... 79
 - 5.4.1 Introduction..... 79
 - 5.4.2 Periosteal Callus Recapitulates the Sequential Steps of Endochondral Bone Formation 80
 - 5.4.3 HIF-1 α Activation and BMP Expression..... 81
 - 5.4.4 Periostin Activation During Periosteal Callus Formation..... 83
- 5.5 Repair of Osteochondral Defects with Cartilage from Periosteum..... 84
 - 5.5.1 Introduction..... 84
 - 5.5.2 Improved Repair of Osteochondral Defects..... 84
 - 5.5.3 Discussion..... 86
- 5.6 Evidence That Endochondral Bone Formation Can Be Manipulated in the IVB..... 87
 - 5.6.1 Introduction..... 87
 - 5.6.2 Growth Factors..... 87
 - 5.6.3 Hypoxia..... 87
 - 5.6.4 Calcium..... 88
- 5.7 Discussion..... 88
- References..... 89

- 6 Bioreactor Systems in Regenerative Medicine 95**
 - 6.1 Introduction..... 95
 - 6.2 Bioreactors in Regenerative Medicine: Key Features..... 96
 - 6.2.1 Cell Seeding on Three-Dimensional Matrices..... 96
 - 6.2.2 Maintenance of a Controlled Culture Environment..... 97
 - 6.2.3 Physical Conditioning of Developing Tissues 99
 - 6.2.4 Predicting Mechanical Functionality of Engineered Tissues 100
 - 6.3 Bioreactor-Based Manufacturing of Tissue Engineering Products..... 101
 - 6.3.1 Automating Conventional Cell Culture Techniques 103

6.3.2	Automating Tissue Culture Processes.....	104
6.3.3	Streamlining Tissue Engineering Processes.....	106
6.3.4	Different ‘Manufacturing’ Concepts.....	109
6.4	Conclusions and Future Perspectives.....	110
	References.....	111
7	Biomimetic Approaches to Design of Tissue	
	Engineering Bioreactors	115
7.1	Introduction.....	116
7.2	Cardiac Tissue Engineering	116
7.2.1	Myocardium (Cardiac Muscle)	116
7.2.2	Tissue Engineering.....	117
7.3	Cartilage Tissue Engineering	120
7.3.1	Articular Cartilage	120
7.3.2	Tissue Engineering.....	121
7.4	Conclusions.....	125
	References.....	126
8	The Nature of the Thermal Transition Influences	
	the Shape-Memory Behavior of Polymer Networks	131
8.1	Introduction.....	131
8.2	Architectures of Different Polymer Networks	136
8.2.1	Synthesis	136
8.2.2	Thermomechanical Properties	139
8.3	Shape-Memory Capability	143
8.4	Degradation.....	151
8.5	Summary	153
8.6	Outlook	154
	References.....	155
9	Nanoengineered Systems for Regenerative Medicine	
	Surface Engineered Polymeric Biomaterials	
	with Improved Bio-Contact Properties	157
9.1	Introduction.....	157
9.2	Polymeric Materials with Improved	
	Bio-Contact Properties.....	158
9.2.1	Strong Hydrophilic “Water-Like” Protein	
	Repellent Surfaces.....	158
9.2.2	Protein Repellent Plasma Films	164
9.2.3	Polydimethylsiloxane (PDMS) with Improved	
	Interactions with Living Cells.....	164
9.3	Conclusions.....	172
	References.....	172

10	Nanocomposites for Regenerative Medicine.....	175
10.1	Perspective	175
10.2	A Nanophase for the Mechanical Reinforcement of Tissue Engineering Scaffolds	177
10.2.1	Introduction.....	177
10.2.2	Nanocomposite Scaffolds for Hard Tissue Engineering.....	178
10.2.3	Nanocomposite Scaffolds for Soft Tissue Engineering.....	185
10.2.4	Conclusion and Future Direction	189
10.3	A Nanophase for Drug Delivery Applications.....	191
10.3.1	Introduction.....	191
10.3.2	Nanofibrous and Nanoporous Biomaterials.....	191
10.4	Conclusions.....	201
	References.....	201
11	Role of Spatial Distribution of Matricellular Cues in Controlling Cell Functions.....	207
11.1	Introduction.....	207
11.2	Cell-Matrix Interaction	210
11.2.1	Effect of Matrix on Cell Migration.....	212
11.2.2	Matrix Effect on Embryonic Development.....	218
11.2.3	Matrix Effect on Angiogenic Processes.....	222
11.3	Development of Novel Biofunctional Materials	223
11.4	Conclusions.....	228
	References.....	228
12	Materials Surface Effects on Biological Interactions	233
12.1	Introduction.....	233
12.1.1	First Generation	235
12.1.2	Second Generation	236
12.1.3	Third Generation.....	237
12.1.4	Biomaterials for Substitution, Repair and Regeneration	238
12.1.5	Stem Cells Sources	239
12.2	Surface Modification to Improve Cell–Material Interactions	240
12.2.1	Surface Topography	242
12.2.2	Surface Chemistry.....	243
12.3	Oxidation Treatment of NiTi Shape Memory Alloys to Obtain Ni-Free Surfaces and to Enhance Biocompatibility.....	244
12.4	Surface Characterisation of Fully Biodegradable Composite Scaffolds for Bone Regeneration.....	246
12.5	Micro and Nanopatterned Surfaces for Biomedical Applications	247
	References.....	248

13	Chemical and Physical Modifications of Biomaterial	
	Surfaces to Control Adhesion of Cells.....	253
13.1	General Introduction	254
13.1.1	Basics of Cell Adhesion on Material Surfaces	254
13.1.2	Short Overview on Techniques to Modify Surfaces of Biomaterials	257
13.1.3	Methods to Generate Nanostructured Surface	258
13.2	Self Assembled Monolayers Based on Organosiloxanes.....	259
13.2.1	Background	259
13.2.2	Effect of SAM on Fibroblast Adhesion, Spreading and Growth	260
13.3	Photochemical Immobilization of Polyethyleneglycol on Hydrophobic Biomaterials	264
13.3.1	Background	264
13.4	Effect of Photochemical Immobilization of Poly (Ethylene Glycol) on Adhesion of Cells	265
13.5	Application of Layer-by-Layer Technique on Charged Surfaces	270
13.5.1	Background of Layer-by-Layer Technique.....	270
13.5.2	Application of LbL Technique to Inorganic Surfaces	271
13.5.3	Application of LbL Technique to Poly (L-Lactide) (PLLA) for Tissue Engineering Applications.....	275
13.6	Summary and Conclusions	279
	References.....	279
14	Results of Biocompatibility Testing of Novel, Multifunctional Polymeric Implant Materials In-Vitro and In-Vivo.....	285
14.1	Introduction.....	286
14.1.1	Regenerative Medicine.....	286
14.1.2	Functionalized Implant Materials	287
14.1.3	Clinical Application of Polymer-Based Implant Materials	287
14.2	Materials and Methods.....	290
14.2.1	Polymer-Based, Biodegradable Implant Materials	290
14.2.2	Sterilization Methods	290
14.2.3	Investigation of In-Vitro Toxicity	290
14.2.4	In-Vivo Assessment of Tissue Compatibility of Biomaterials.....	291
14.2.5	Animal Model	291
14.2.6	Statistical Evaluation.....	292
14.3	Results.....	292
14.3.1	Detailed Evaluation of In-Vitro Biocompatibility Testing.....	292

14.3.2	In-Vivo Assessment of Tissue Compatibility of Biomaterials.....	294
14.4	Discussion.....	296
	References.....	298
15	UFOs, Worms, and Surfboards: What Shapes Teach Us About Cell–Material Interactions	301
15.1	Introduction.....	302
15.2	Particulate Drug Delivery Systems.....	302
15.2.1	Role of Physical Properties in Particle Function.....	304
15.3	Phagocytosis.....	306
15.3.1	Attachment.....	306
15.3.2	Internalization.....	307
15.4	Fabrication of Non-spherical Polymer Particles.....	307
15.4.1	General Method.....	308
15.4.2	Specific Shapes.....	309
15.5	Effect of Particle Shape on Phagocytosis.....	312
15.5.1	Shape Internalization.....	312
15.5.2	Quantification of Shape.....	314
15.5.3	Correlation Between Internalization, Shape and Size.....	315
15.6	Design of Non-spherical Particles for Drug Delivery.....	318
15.6.1	Optimal Shapes for Avoiding Phagocytosis.....	318
15.6.2	Fabrication of Non-spherical Biodegradable Drug Carriers.....	319
15.7	Conclusions and Future Directions.....	320
15.7.1	Drug Delivery.....	320
15.7.2	Cell–Material Interactions.....	320
	References.....	321
16	Nano-engineered Thin Films for Cell and Tissue-Contacting Applications	325
16.1	Introduction.....	325
16.2	Resonant Infrared Pulsed Laser Deposition of Thin Films.....	326
16.3	Resonant Infrared Laser Ablation of Thermally Labile Polymers.....	328
16.3.1	Poly(Ethylene Glycol) – PEG.....	328
16.3.2	Poly(DL-Lactide-Co-Glycolide) – PLGA.....	331
16.3.3	Proteins and Nucleic Acids.....	332
16.3.4	Poly(Tetrafluoroethylene).....	334
16.4	Deposition of Functional Nanoparticles.....	336
16.5	Discussion and Conclusions.....	338
16.5.1	Evidence for Low-Temperature Character of RIR-PLD.....	339
16.5.2	The RIR-PLD Mechanism and Its Consequences.....	340

16.5.3	Prospects for Table-Top RIR-PLD Laser Technology.....	341
16.6	Conclusions.....	343
	References.....	344
17	Injectable Hydrogels: From Basics to Nanotechnological Features and Potential Advances.....	347
17.1	Introduction.....	347
17.1.1	The Concept of Scaffold.....	348
17.2	Hydrogels.....	350
17.2.1	Methods of Preparation.....	351
17.3	Properties Exploitable in Tissue Engineering.....	358
17.4	Major Issues of Injectable Materials in Tissue Engineering.....	364
17.5	Conclusions.....	365
	References.....	365
18	Polyelectrolyte Complexes as Smart Nanoengineered Systems for Biotechnology and Gene Delivery.....	383
18.1	Introduction.....	379
18.2	Complex Formation and Competitive Reactions in Solutions of Oppositely Charged Polyelectrolytes.....	383
18.2.1	Polyelectrolyte Complexes and Their Properties.....	383
18.3	DNA-Containing PECs and Their Properties.....	389
18.3.1	Stability of DNA-Containing Complexes.....	389
18.3.2	Selectivity of Competitive Reactions in DNA Solutions.....	390
18.3.3	Complexing of DNA with Polycations for Cell Transfection.....	391
18.4	Complexes of Proteins with Oppositely Charged Polyions.....	393
18.4.1	Soluble Complexes and Competitive Reactions in Their Solutions.....	393
18.4.2	Artificial Chaperones.....	396
18.5	Polyelectrolyte Multilayer Films and Capsules.....	397
	References.....	399

Chapter 1

Cell Adhesions and Signaling: A Tool for Biocompatibility Assessment

Roumen Pankov and Albena Momchilova

Abstract Interactions between cells and extracellular environment are mediated through specific cell adhesion sites. These structures are responsible for transmitting environmental signals, which affect essentially all aspects of a cell's life, including proliferation, differentiation and death. The morphology, organization and type of signaling transmitted through these adhesions depend on the chemical identity, geometry and the physical properties of the substrate. Here we outline the cell adhesions organized by fibroblasts on natural two- and within three-dimensional substrates, the signaling associated with these structures and discuss the possible use of this knowledge in assessment of surface biocompatibility of new materials, prepared for regenerative medicine.

Keywords Cell adhesions • Focal contacts • Fibrillar adhesions • Three-dimensional matrix adhesions • Integrins • Extracellular matrix • Cell signaling • Biocompatibility • Nanomaterials

R. Pankov (✉)

Sofia University "St. Kliment Ohridski", Sofia 1164, Bulgaria
and

Laboratory of Cell and Developmental Biology, National Institute of Dental
and Craniofacial Research, National Institutes of Health,
Bethesda, MD 20892, USA

and

Department of Cytology, Histology and Embryology, Faculty of Biology,
Sofia University, 8 Dragan Tzankov str, 1164 Sofia, Bulgaria
e-mail: rpankov@biofac.uni-sofia.bg

A. Momchilova

Institute of Biophysics, Bulgarian Academy of Sciences,
1113 Sofia, Bulgaria

1.1 Introduction

The current view for development of successful implants for regenerative medicine is evolving towards the perception that the opportunities of biomimetic or bioartificial materials significantly exceed those of the existing prosthetic implants. It was a widely held belief that prostheses must be biologically inert (biologically “invisible”), i.e. they must not interact by no means with the surrounding cells and tissues. Currently, an advanced concept emerges and it is based on the principle of construction of artificial materials that imitate to a maximum extent the tissue they are implanted in and are actively interacting with its cells (Brown and Phillips 2007). Presumably, the materials for construction of biomimetic implants must possess proper physical (strength, elasticity, specific three-dimensional structure, etc.) and chemical (to cause no inflammation and to be non-toxic) characteristics. These materials must secure the cells with a friendly environment which provides all major signals directing cell physiology and metabolism.

The available data indicate that these signals cannot be completely substituted through supra-physiological doses of soluble cytokines, growth factors or other pharmaceutical agents. What is absolutely necessary is the “integration” of signals in the surface structures of the biomimetic materials that are capable of interaction and activation of the integrin cell receptors (see below). The simulation of normal extracellular matrix (ECM) characteristics in the structure of novel materials is a highly developed trend in the field of modern nanomaterials and tissue engineering (Badylak 2005). Innovative and more complex physical and chemical methods for production of artificial porous and fibrous matrices are in a continuous process of invention and application. These materials are modeled with surfaces and organization that are imitating to an utmost extent the structure of extracellular matrices typical for all human tissues and organs (Katti 2004; Hemmrich and von Heimburg 2006; Nair and Laurencin 2006).

Without neglecting the advance in the field, the usefulness and possible application of these novel materials can be determined only after an assessment of their biocompatibility. The first step in this usually long-termed process is an *in vitro* culturing of appropriate cells on the surface of artificial materials, followed by assessment of their behavior. The capability of artificial materials to provide the cells with the correct adhesivity, and to assure proliferation and formation of own extracellular matrix (features that are obligatory for a successful implantation in a living organism) is evaluated through diverse cell and molecular biology methods.

In this chapter we explore the possibility that the type, morphological characteristics and the specific signaling of cell contacts with ECM can serve as reliable markers for estimation of functional state of the cells and as a consequence – for biological assessment of the surface features of nanoengineered materials, prepared for regenerative medicine.

1.2 Cell-Matrix Adhesions

Cell adhesion occurs through the binding of specific adhesion receptors – integrins (Hynes 1987), to matrix proteins. These are essential interactions contributing to normal processes such as differentiation, embryonic development, and wound healing as well as the progression of diseases and pathological conditions. Denial of appropriate matrix or detachment of anchorage-dependent cells from the substrate induces a special form of apoptosis termed “anoikis” (Frisch and Francis 1994) illustrating the importance of cell adhesion.

Adhesions with the ECM are formed by essentially all types of adherent cell, but their morphology, size and subcellular distribution can be quite heterogeneous. Nevertheless, most of these adhesions share two common features – they are mediated by integrins, and they interact with the actin cytoskeleton at the cell interior. Integrin receptors bind extracellular matrix proteins (e.g. fibronectin, vitronectin, laminin and various collagens) through their large ectodomain and engage the cytoskeleton via their short cytoplasmic tails. These interactions provide cells with physical link to the extracellular environment, necessary for cell anchorage and mechanical support for movements. But cell adhesions are not simply static architectural entities. As suggested by Rosales et al. (1995) and confirmed by numerous later studies, they are dynamic units that are capable of capturing, integrating and propagating signals from the extracellular environment. These features of the adhesion contacts are determined both by the integrin receptors and by the specific set of cytoplasmic adhesion plaque proteins (integrin complexes).

1.2.1 *Integrin Receptors and Integrin Cytoplasmic Complexes*

The integrins are a family of cell-surface glycoproteins that act as receptors for extracellular matrix. Each integrin is a heterodimer that contains an α and a β subunit with each subunit having a large extracellular domain, a single membrane-spanning region, and in most cases (other than $\beta 4$), a short cytoplasmic domain. The integrin receptor family of vertebrates includes at least 18 distinct α subunits and eight β subunits which can associate to form more than 24 distinct integrins. The α/β pairings specify the ligand-binding abilities of the integrin heterodimers (Arnaout et al. 2007).

The $\alpha 5\beta 1$ integrin plays a major part in fibroblasts adhesion as it secures the binding to fibronectin (Humphries et al. 2006). After plating on surfaces coated with this ECM molecule, part of the $\alpha 5\beta 1$ integrin receptors on the cell surface generates contacts with this ligand (ligation) and aggregates are formed as a result (clusterization). The last two events mark the activation of integrins and lead to subsequent conformational changes in the extracellular domain as well as in the cytoplasmic domains (Arnaout et al. 2007; Shimaoka et al. 2002). Current studies

confirm that in an inactive state the cytoplasmic tail of $\alpha 5$ blocks the ability of $\beta 1$ tail to interact with other proteins and by that means it keeps the integrin heterodimer in an inactive state (Giancotti 2003). As a result of the ligation and clusterization, the interaction between the two cytoplasmic tails weakens, providing the $\beta 1$ cytoplasmic domain with an opportunity to form complexes with other cytoplasmic proteins. The consequence of these processes is the formation of two populations of $\alpha 5 \beta 1$ integrins on the cell membrane – active and inactive. They can be distinguished with specific antibodies which identify conformational epitopes expressed only by activated $\beta 1$ integrins (Humphries 2004). The investigations with such antibodies allow visualization of cell adhesions and reveal the fact that the activated $\beta 1$ integrins are located mainly in these structures while the inactive ones diffusively occupy the entire cell surface (Pankov et al. 2000).

The activated cytoplasmic domain of $\beta 1$ integrin attracts and forms complexes with a variety of cytoskeletal, adaptor and signaling cytoplasmic molecules (Zaidel-Bar et al. 2007a, b). The cytoskeleton and adaptor proteins execute the physical contact between transmembrane integrins and actin cytoskeleton, whereas the signaling molecules activate different kinases and phosphatases as well as their substrates. Here, we will present a brief description of some of the best studied integrin-complex proteins that are widely used for labeling of cell adhesions. Their specific localization into the adhesion contacts and the availability of good commercial antibodies makes them a matter of choice when substrate-induced changes in cell adhesions are studied:

- Talin is a large (~270 kDa) intracellular protein of the cytoskeletal protein group which forms antiparallel dimers (Critchley 2000). Two domain structures form its molecule – a head (amino end) and a tail (carboxy end). A trilobed FERM domain (4.1, ezrin, radixin, and moeisin) is located in the head through which talin binds to the β integrin subunits, the focal adhesion kinase (FAK), phosphatidylinositol phosphate kinase type $I\gamma$ and phosphatidylinositol-(4,5)-bisphosphate (PIP2) (Brakebusch and Fassler 2003). Three binding sites for vinculin and a binding site for actin are located in the tail (Hemmings et al. 1996). A major function of talin *in vivo* is to form the connection between the integrin clusters and the actin cytoskeleton. The adapter protein paxillin, which is incorporated together with talin in early focal complexes, may link talin to the integrin α -cytoplasmic tail, enhancing resistance of matrix–integrin–talin complexes to mechanical stress (Alon et al. 2005). The binding of talin also directs the destruction of α - and β -tails interaction and induces activation of integrin and/or strengthening of the interaction between integrins and their extracellular ligands (Calderwood 2004).
- Vinculin also belongs to the cytoskeletal protein group. It is a common cytoplasmic protein with a molecular weight of 116 kDa. Electron microscopy studies demonstrate the existence of two main domains within vinculin molecule – a globular head and rod-like tail (Molony and Burridge 1985). The head contains binding sites for talin and α -actinin whereas the tail contains sites for actin and paxillin. The binding between vinculin and talin is under regulation by PIP2

which after an interaction with vinculin induces unfolding of the otherwise inactive molecule and exposure of the talin-binding sites (Gilmore and Burridge 1996; Bois et al. 2006).

- Tensin is a dimer comprised of two 200 kDa polypeptide chains. Each of them contains multiple regions that can bind to actin. The diversity of interactions with actin (Lo et al. 1994) suggests a significant role of tensin in the regulation of interactions between the integrin complexes and the actin cytoskeleton. This possibility is also supported by the fact that tensin undergoes post-synthetic modifications after the integrin activation. The focal adhesion kinase phosphorylates tensin after the activation of integrins by fibronectin (Bockholt and Burridge 1993) which can cause an alteration of its ability for interaction with actin. The PTB domain of tensin binds the β -tail in a talin-like manner, but with lower affinity (McCleverty et al. 2007).
- Paxillin is originally identified as a 68–70 kDa phosphoprotein in cells transformed with Src (Glenney and Zokas 1989). Further studies reveal its adaptor function and association with integrins. Its molecule contains a proline-rich region that provides the interactions with SH3-containing molecules and five LD and four LIM motifs with the ability to execute protein – protein recognition (Turner 2000). These motifs provide the binding of paxillin to cytoskeleton proteins, tyrosine and serine/threonine kinases as well as other adaptor proteins. The presumption that the main function of paxillin is coordination of integrin-dependent signals which regulate the substrate adhesion of cells and their migration in the focal adhesion contacts results from its phosphorylation as a consequence of integrin activation (Schaller 2001).

The best-characterized adhesions, formed on the surface of fibroblasts are the ‘classical’ focal adhesions (FA) (also termed focal contacts), fibrillar adhesions (FbA), and 3D-matrix adhesions (3D-MA). These contacts reflect different stages of interaction of cells with the ECM, and each is formed and disrupted in a dynamic, cyclical manner through sequential recruitment and loss of different integrin receptors, cytoskeletal and signaling molecules from the cytoplasm (Geiger et al. 2001; Webb et al. 2004).

1.2.2 Focal Adhesions

Focal adhesions are first described by Abercrombie et al. (1971) as locations of the closest contact between cell and substrate. From dozens to hundreds FA that differ in size (from half to several square micrometers) can be determined in a typical cell in a monolayer culture (Fig. 1.1). The size and distribution of FA vary depending on the type of substrate, nutrition medium and density of cell culture. Usually, they are characterized with oval shape, more or less elongated morphology and location near the cell periphery.

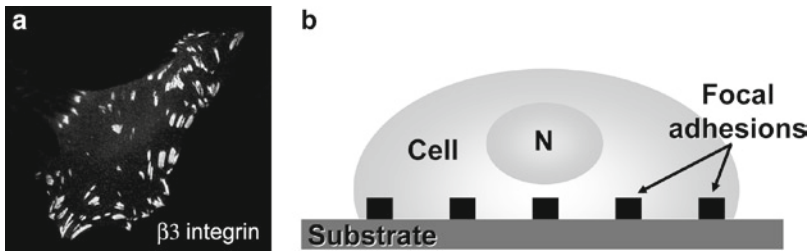


Fig. 1.1 Focal adhesions. (a) FA on the dorsal surface of primary human fibroblast visualized after immunofluorescent labeling with antibody against $\beta 3$ integrin. (b) Scheme depicting the position of focal adhesions, relative to the substrate, N – cell nucleus

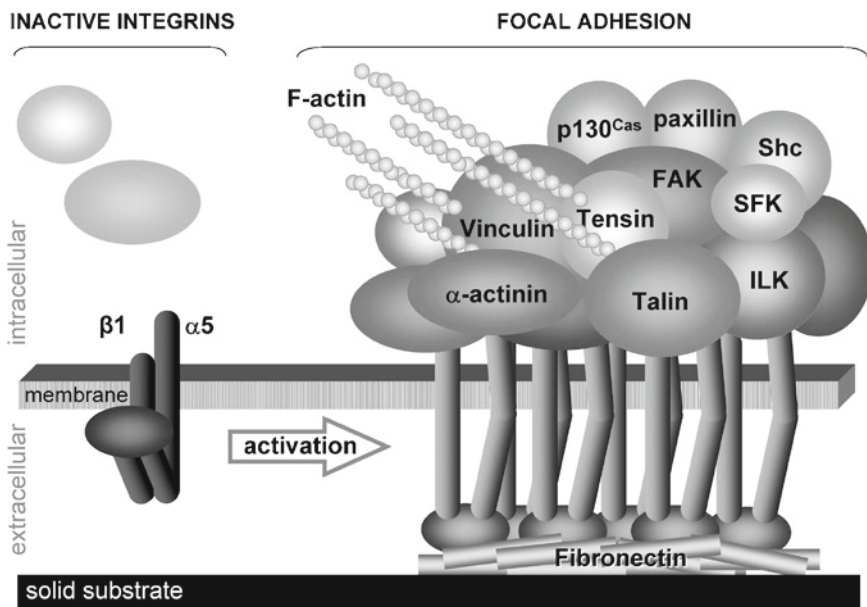


Fig. 1.2 Schematic representation of the complexity of focal adhesions. Inactive integrins are diffusely distributed on the cell surface. Ligated and clustered integrins go through conformational changes that allow recruitment of specific cytoplasmic proteins and building up of focal contact. Note that bundles of actin filaments anchor into this adhesion site

Immunofluorescent and immunoelectron microscopic studies reveal that FA comprise of surprisingly great number (>90) of diverse protein molecules (Zaidel-Bar et al. 2007a) organized in large assemblies of molecules (Fig. 1.2). The most common integrins found in focal adhesions are $\alpha 5\beta 1$ and $\alpha V\beta 3$ (vitronectin receptor), although depending on the substrate other integrins may be present. In the cytoplasm, several groups of focal adhesion proteins can be

identified (Geiger et al. 2001). A small group of proteins (talin, α -actinin, tensin and filamin) can function as direct integrin–actin linkers. Additional integrin-associated molecules do not interact directly with actin, but bind to the cytoskeleton indirectly through other components of the integrin complexes. Some of them, such as focal adhesion kinase (FAK), integrin-linked kinase (ILK) and 14-3-3 β , are signalling molecules. An additional group of focal-adhesion-associated proteins includes actin-binding proteins, not interacting directly with integrins (vinculin, vasodilator-stimulated phosphoprotein/Ena and ezrin–radixin–moesin proteins). In this group vinculin plays a major role as it interacts with many plaque proteins (including talin, α -actinin, ponsin, vinexin and protein kinase C), as well as with membranes and actin. A very large group of proteins consists of adaptor proteins, which interact with actin-bound and integrin-bound components and link them to each other (e.g. p130 Cas, merlin, Crk). Beyond their protein–protein binding specificities, many of the focal adhesion proteins are enzymes falling into two general categories – kinases and phosphatases.

The functions of FA characterized up to date can be divided into two groups – mechanical and signaling. The mechanical functions illustrate the role of FA as cell surface sites where the actin cytoskeleton binds to the extracellular matrix. Thus, FA secure a support for cell movements and allow the cell to model the matrix through alteration of the stress in certain locations (Halliday and Tomasek 1995). The stress applied is marked as tension or contractility and is generated by the actomyosin cell system. In this process of force transmission major role is played by the talin/vinculin connection (Evans and Calderwood 2007). The cell tension in its turn is essential for maintenance of the focal adhesive contacts. The activity of one of the major contractility regulators – Rho is necessary for the formation and stabilization of FA. Its suppression by the Rho-kinase inhibitor Y-27632 or agents that block the acto-myosin activity provokes their rapid destruction (Rottner et al. 1999).

The close relation of FA with mechanical tension exchanged between the cells and environment, offers the opportunity to consider these structures as mechanosensors which transmit information about physical characteristics of the substrate and allow the cell to respond with adequate contractility (Bershadsky et al. 2003). These properties of the focal adhesion contacts define them as suitable sensors for assessment of the physical specificity of various cell substrates including the surface properties of nanoengineered materials.

A well established fact is that focal adhesion contacts are not merely mechanical formations. They also possess the ability to register and transmit chemical signals. The activation of integrins induces a cascade of specific biochemical events known generally as integrin signaling. The short integrin cytoplasmic tails lack enzymatic activity, and so depend on recruitment of adaptor and signaling molecules (Geiger et al. 2001). These include activation of tyrosine kinases such as focal adhesion kinase (FAK) and Src; serine/threonine kinases such as integrin linked kinase (ILK), MAP kinases, jun kinase (JNK), and protein kinase C (PKC); intracellular

ions such as protons and calcium; the small GTPase Rho; and lipid mediators such as phosphoinositides, diacylglycerol, and arachidonic acid metabolites (Giancotti and Tarone 2003; Thiery 2003).

Most of the integrin signaling is initiated through formation of particular complexes that include specific set of focal adhesion molecules. A well studied example of this type of integrin signaling is FAK-mediated signal transduction pathway. FAK activation occurs after integrin clustering and starts with autophosphorylation at tyrosine 397 either in an inter- or intramolecular manner. The phosphorylation on Tyr397 creates a high-affinity binding site for the SH2 domain of Src family kinases and leads to the recruitment and activation of Src through the formation of a bipartite kinase complex. Tyr397-dependent activation of FAK and the recruitment of Src have been implicated in the efficient tyrosine phosphorylation of additional sites on FAK. Binding of the SH2 domain-containing adaptor protein GRB2/SOS (growth factor receptor bound 2/homologue of *Drosophila melanogaster* “son of sevenless” protein) to the FAK tyrosine 925 site seems to play a major role in activating the pro-survival Ras/Raf/MEK/MAPK pathway. Phosphorylation of ERK2 in response to binding of GRB2/SOS to FAK activates the myosin light chain kinase, which promotes cell survival and proliferation (Hanks et al. 2003).

Integrin signaling may also depend on the specific interactions with particular sequences along the $\beta 1$ integrin cytoplasmic domain. Recently we have identified the tryptophan residue at position 775 of human $\beta 1$ integrin as specific and necessary for integrin-mediated protein kinase B/Akt survival signaling (Pankov et al. 2003). Stable expression of a $\beta 1$ integrin mutated at this amino acid in GD25 $\beta 1$ -null cells results in reduction of Akt phosphorylation and as a consequence, the cells become substantially more sensitive to serum starvation-induced apoptosis. This inactivation of Akt results from increased dephosphorylation by an activated population of protein phosphatase 2A localized in $\beta 1$ integrin cytoplasmic complexes. Interestingly, the mutation of Trp775 specifically affects Akt signaling, without effects on focal adhesion morphology and other integrin-activated pathways including phosphoinositide 3-kinase, MAPK, JNK, and p38 nor does it influence activation of the integrin-responsive kinases FAK and Src. These results identify a novel mechanism employed by integrins that controls the level of Akt phosphorylation via local activity of the phosphatase PP2A. Thus, mutations or inappropriate matrix conditions, inducing conformational changes in integrin molecule that “mask” Trp775, may lead directly to altered cell survival decisions without any other obvious effects (Fig. 1.3).

The signaling events, routed through focal contacts offer an additional tool for fine assessment of surface biocompatibility. Simple tests (e.g. Western blotting with phosphospecific antibodies against FAK, Src, Akt or MAPK) of the activity of major signal transduction pathways would allow fine evaluation of the ability of new materials to ensure normal cell survival and growth. It should be noted that several signaling pathways must be evaluated, considering their relative independence as demonstrated by the Trp775 mutation.

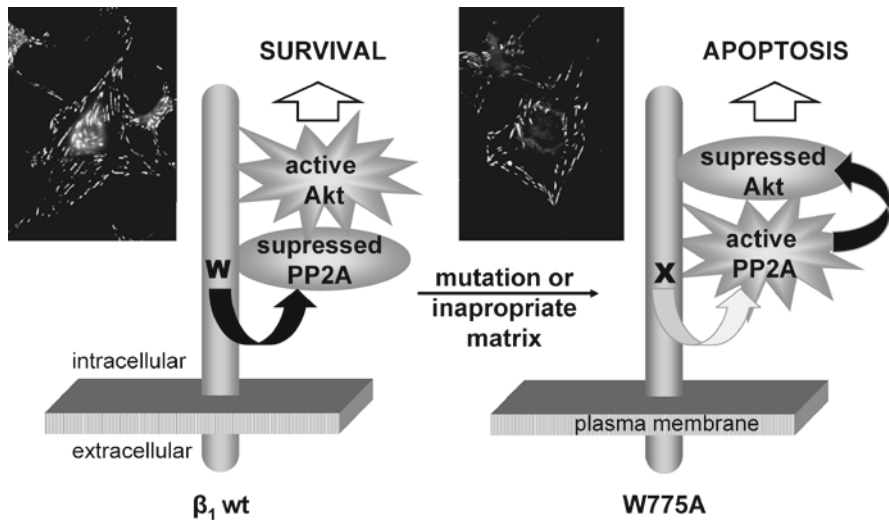


Fig. 1.3 Integrin signaling mediated by tryptophan residue at position 775 of human β_1 cytoplasmic tail. In wild type integrin (β_1 wt) Trp775 (W) interacts and blocks protein phosphatase 2A (PP2A) which in turn leaves Akt active and promotes survival. When this residue is mutated (X in W775A mutant integrin), PP2A is active. This leads to inactivation of Akt and initiation of apoptosis. Note that focal contacts organized by wild type (*left image*) and mutant (*right image*) integrins and revealed by staining with anti-integrin antibody, have normal appearance

1.2.3 Fibrillar Adhesions

A second, major type of cell adhesions are the ECM adhesions (Chen and Singer 1982) which were later renamed to fibrillar adhesions (Zamir et al. 1999). These structures appear when cells start to deposit fibronectin fibrils in the extracellular space and mark the contacts between these fibrils and the cell surface (Fig. 1.4). Contrary to the integrin diversity in FA, in the structure of FbA just one integrin heterodimer is determined – $\alpha_5\beta_1$. The cytoplasmic complex, organized around integrin tails in FbA contains a single major cytoskeletal protein – tensin. Recently non-phosphorylated paxillin is also found to be present in FbA although its quantity is less than 30% of the amount, associated with focal adhesions. Tensin and non-phosphorylated paxillin are important for formation and maintenance of fibrillar adhesions. It has been demonstrated that disruption of tensin function with dominant-negative inhibitor causes FbA to disappear while overexpression of nonphosphorylatable paxillin mutant displays formation of prominent FbA (Pankov et al. 2000; Zaidel-Bar et al. 2007b). Molecules with phosphorylated tyrosine are abundant in the FA but in contrast FbA are found to be negative after staining with phosphotyrosine antibodies (Katz et al. 2000). $\alpha_5\beta_1$ integrins, tensin and paxillin are structured in fibrils (axis ratio >7) which are positioned along the actin filaments located under the cytoplasmic membrane. As mentioned above, a representative

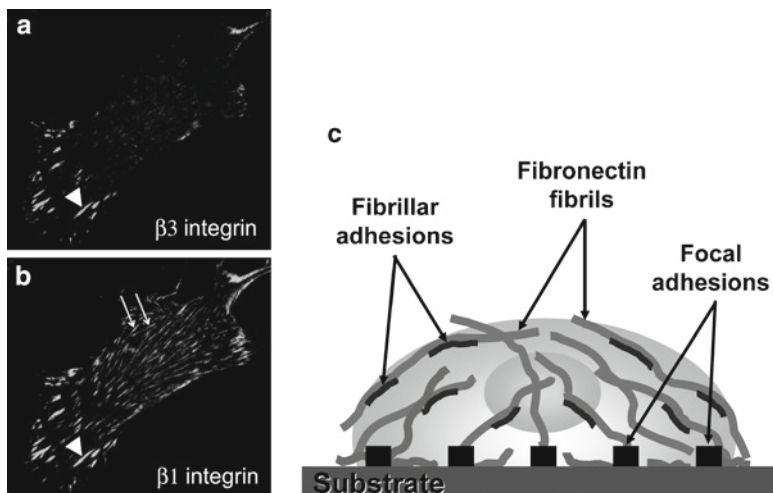


Fig. 1.4 Fibrillar adhesions. While anti- $\beta 3$ integrin antibody labels only focal contacts (**a**, *arrowhead*) in primary human fibroblasts, staining with anti- $\beta 1$ integrin antibody reveals both focal (**b**, *arrowhead*) and fibrillar (**b**, *arrows*) adhesions. (**c**) Schematic representation of cell surface distribution of FA and FbA. Note that while FAs are associated with the solid substrate, FbAs are connected to the fibronectin fibrils

component of the FbA are also the fibronectin fibrils located on the outer side of the cell and bound to $\alpha 5\beta 1$ integrins.

The formation of fibrillar adhesion contacts is executed by a population of highly activated $\alpha 5\beta 1$ which together with tensin rapidly depart from the regions of focal contacts and through actin filaments transfer towards the centre of the cell body (Pankov et al. 2000; Clark et al. 2005). A possible molecular mechanism underlying this integrin movement may involve phosphorylation of the NPxY motif within $\beta 1$ integrin tail by Src. Phosphorylated and ligand-occupied integrins dissociate from talin (Ling et al. 2003; McCleverty et al. 2007), making them available for binding to tensin and translocation along actin filaments. This movement provides a potential mechanism for integrins to apply tensile forces to stretch fibronectin molecules and induce fibronectin fibrillogenesis. The deposition and maturation of these fibrils leads to the formation of extracellular matrix. Since this specific integrin dynamics and the ability of cells to organize fibronectin fibrils depends strongly on the properties of the substrate (Halliday and Tomasek 1995; Katz et al. 2000; Faucheux et al. 2006; Tzoneva et al. 2007) it can be utilized as an additional sensor element to assess surface biocompatibility of nanoengineered materials.

1.2.4 Three-Dimensional Matrix Adhesions

Most of our current knowledge about cell adhesive contacts is based on studies carried out with conventional, monolayer (two dimensional, 2D) cell cultures. Under these conditions cells are forced to adjust to unnaturally flat and rigid plastic

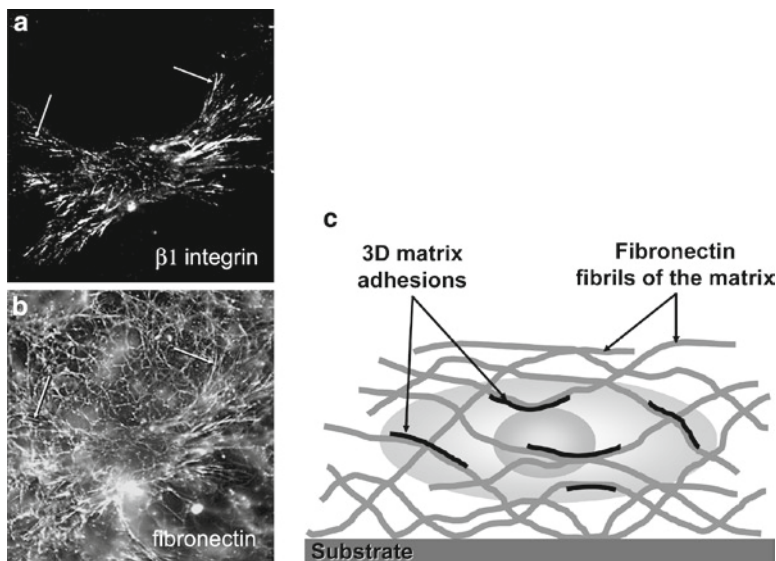


Fig. 1.5 Three-dimensional matrix adhesions. 3D-MAs on the surface of primary human fibroblasts are revealed by staining with anti- $\beta 1$ integrin antibody (a). These adhesion contacts align with fibronectin fibrils of the three dimensional matrix (b, arrows) visualized by staining with anti-fibronectin antibody. (c) Schematic representation 3D-MA. Note that within 3D environment, cells interact only with matrix fibrils and do not contact solid substrate

or glass surfaces that greatly differ from natural extracellular matrix, surrounding most cells in living organisms. Increasingly, researchers are recognizing the limitations of these 2D cell cultures and an alternative three-dimensional (3D) cell culture approach, offering a means to study cells under conditions that reproduce an *in vivo* environment, has been established (Cukierman et al. 2001; Edelman and Keefe 2005).

In natural environment or in laboratory-produced cell-derived 3D matrices (Cukierman et al. 2001), the fibroblasts contact with extracellular matrix which is three-dimensional, elastic and has complex chemical nature. An important feature of this environment is the absence of the artificial dorso-ventral polarization, typical for fibroblasts in 2D conditions. In such *in vivo*-like settings, fibroblasts form a new type of integrin adhesive structures – three-dimensional matrix adhesions, which has been denominated as the third basic type of adhesions (Cukierman et al. 2001, 2002) (Fig. 1.5). It is important to note that same adhesions are also identified in tissue sections, supporting the concept that these are the natural structures, formed by fibroblasts in living organisms.

3D-matrix adhesions are distinct from both the focal adhesions and the fibrillar adhesions. They exhibit specific morphology which is characterized by extraordinary elongation – four to nine orders of magnitude than the length of FbA. Another distinctive feature of 3D-MA contacts is their composition. They are formed by combination of molecules which in 2D conditions are separated between FA or FbA (Table 1.1).

Table 1.1 Basic characteristics of adhesion contacts

Characteristics	Focal adhesion contacts (FA)	Fibrillar adhesion contacts (FBA)	Three-dimensional matrix adhesion contacts (3D-MA)
Location	Cell periphery	Cell body	Cell body
Morphology	Oval	Fibrillar	Fibrillar
Dimensions	2–5 μm	1–10 μm	10–30 μm
Marker proteins	$\alpha\text{v}\beta\text{3}$	(–)	(–)
	$\alpha\text{5}\beta\text{1}$	$\alpha\text{5}\beta\text{1}$	$\alpha\text{5}\beta\text{1}$
	Tensin	Tensin	Tensin
	Vinculin	(–)	Vinculin
	Talin	(–)	Talin
	Paxillin	Paxillin (<30%)	Paxillin
	α -Actinin	(–)	α -Actinin
	FAK	(–)	FAK
	FAK(Tyr ³⁹⁷)	(–)	(–)

The formation of 3D-MA is accompanied by important alterations in cell behavior. The cells cultured within 3D matrices demonstrate increased proliferation, faster migration and altered morphology in comparison with cells cultured on solid tissue culture plates. These changes reflect a different type of signaling initiated by activated $\alpha\text{5}\beta\text{1}$ integrins. For example, in 3D cultures, the steady-state level of activity of MAPK is enhanced when compared with MAPK activation level, sustained by 2D environment. This is due to increase in the steady state level of activation of the tyrosine kinase Src, suggesting that at least some of the 3D matrix stimulatory signals are routed through Src, bypassing FAK (Cukierman et al. 2001; Damianova et al. 2008).

Whether cells sense the artificial materials prepared for implantation as a “true” 3D environment is a difficult question to answer. However, the existence of different balances between signal transduction pathways in 3D versus 2D environment, together with the specific morphological characteristics of 3D-MA may provide a very sensitive tool for assessment of three-dimensionality and allow precise characterization of diverse artificial scaffolds prepared for use in regenerative medicine.

1.2.5 Dynamics of Cell Adhesions

The accumulated data demonstrate that all types of matrix adhesions are related and appear in a specific consequence. These results allow identifying a model for in vitro evolution or maturation of cell-matrix adhesions (Cukierman et al. 2002; Geiger et al. 2001). The model is best illustrated by following the events that occur after plating of fibroblast cells on a solid, two-dimensional substrate (Fig. 1.6).

The first small integrin complexes that are formed at cell contacts with the substrate are commonly termed focal complexes. These structures contain talin and can be transient or evolve to focal adhesions. Their stabilization and growth into focal

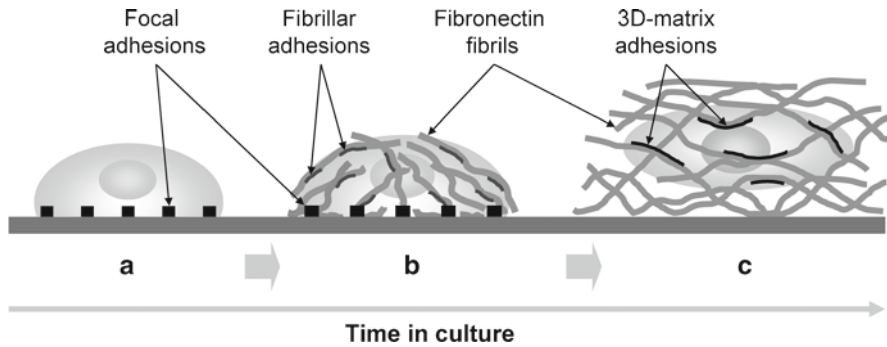


Fig. 1.6 Schematic presentation of the sequence of formation of different matrix-adhesion contacts on the surface of fibroblasts. (a) Within half an hour after plating, cells attach firmly to the solid substrate via focal adhesions. (b) Fibrillar adhesions, in addition to focal adhesions appear when fibroblasts start to organize and deposit fibrils of polymerized fibronectin. This process starts about an hour after plating and can proceed for several days. (c) When enough matrix is deposited, cells detach from the solid substrate and focal adhesions are substituted with 3D matrix adhesions

adhesions depends on mechanical forces generated internally by the intracellular contractile machinery. In this process the activation of a member of the of small GTPase family – Rho A plays an important role (Geiger and Bershadsky 2001). Maturation of these initial adhesion sites into focal adhesions is marked by recruitment of other plaque proteins like paxillin, vinculin, FAK, α -actinin and building up of a strong connection to the actin cytoskeleton (Arnaout et al. 2007) (Fig. 1.6a). Thus, the transformation of initial integrin adhesion complexes into cytoskeleton-restrained focal adhesions depends on the firmness of the connection with the substrate and indicates a mechanism for rapid local mechanosensing.

Although focal adhesions mediate attachment, migration and signalling on extracellular substrates, they have equally important roles in the creation and organization of cell's own ECM. Several studies (Ohashi et al. 2002; Pankov et al. 2000) have shown that focal adhesions serve as sites of support from which activated $\alpha 5 \beta 1$ integrins, bound to fibronectin, depart and move centripetally. This translocation drives the formation of a different type of cell–matrix adhesion, the fibrillar adhesions. These structures are believed to apply tension to fibronectin, exposing cryptic sites for polymerization and thereby facilitating fibronectin fibrillogenesis (Fig. 1.6b).

Ongoing fibrillogenesis leads to accumulation of a thick matrix, which presents a new three-dimensional environment for the cells. Under these conditions fibroblasts lose their focal contacts, detach from the solid substrate and become completely embedded in the three-dimensional fibronectin matrix. The adaptation to the altered environment stimulates the formation of new adhesion contacts analogous to those in a multicellular organism – 3D-MA (Fig. 1.6c).

Thus, the adhesion contacts emerge consecutively and in relation to the changing environment. For example, inhibition of Rho or cell contractility prevents the

transition of focal complexes into focal adhesions (Geiger and Bershadsky 2001) and inhibition of $\alpha 5\beta 1$ integrin translocation out of focal adhesions abolishes the formation of fibrillar adhesions (Pankov et al. 2000). The entire process may be considered as a way of adaptation of cells to the unnatural flat and rigid laboratory plates. This *in vitro* progression of cell adhesions most probably represents a means for cultured cells to improve their microenvironment by bringing it closer to *in vivo* conditions. Such process most probably would appear on the surface of artificial materials after implantation, therefore it should be considered when assessing new materials for biocompatibility.

1.3 Concluding Remarks

Our current understanding for the molecular organization and function of cell adhesions demonstrates that cells have elaborated an extremely responsive sensor system for examination and evaluation of different parameters of the extracellular environment. The reoccurring theme throughout this article is the possibility of using this natural sensor as a precise tool for assessment of surface biocompatibility of artificial materials designed to work in tissue environment.

As discussed above, integrin receptors will respond with conformational changes, clusterization and attachment to the actin cytoskeleton only if their ligands are properly presented and firmly attached to the substrate. This response can be easily followed with conformation-specific anti-integrin antibodies and can be utilized to tailor material surfaces with improved protein adsorption. The assembly of focal adhesions guarantees not only mechanical support but also influences integrin signaling. This adds another level of complexity for biocompatibility assessment of the new materials allowing to go beyond simple attachment. Examination of the activity of different integrin-mediated signal transduction pathways makes possible to predict and follow the ability of cells to migrate, proliferate, differentiate or die when plated on the tested material.

The natural ability of the cells to organize and deposit their own extracellular matrix is an important feature needed for successful integration of artificial implants into the host tissue. Thus, the capacity of the new material to support formation of fibrillar adhesions, 3D matrix adhesions and deposition of fibronectin matrix is also an essential factor for biocompatibility that can be easily tested. The differences observed in two-dimensional versus 3D adhesions and signaling emphasize the importance and provide a way of evaluating three-dimensionality when drawing conclusions about artificial 3D support scaffolds.

Although much more remains to be learned about the mechano-chemical interactions taking place at matrix-integrin-cytoskeleton interface, it is clear that the available data already allow *in vitro* testing of biocompatibility at several levels. Furthermore, the knowledge on the molecular mechanisms, operating at different cell adhesion sites permits identification and avoidance of potential flaws in the design of the new materials.

Acknowledgements This work was supported in part through grants BY-B-1/05 and 1404/04 by the Bulgarian National Fund for Scientific Research.

References

- Abercrombie M, Heaysman JE, Pegrum SM (1971) The locomotion of fibroblasts in culture. IV. Electron microscopy of the leading lamella. *Exp Cell Res* 67:359–367
- Alon R, Feigelson SW, Manevich E, Rose DM, Schmitz J, Overby DR, Winter E, Grabovsky V, Shinder V, Matthews BD, Sokolovsky-Eisenberg M, Ingber DE, Benoit M, Ginsberg MH (2005) Alpha4beta1-dependent adhesion strengthening under mechanical strain is regulated by paxillin association with the alpha4-cytoplasmic domain. *J Cell Biol* 171:1073–1084
- Arnaout MA, Goodman SL, Xiong JP (2007) Structure and mechanics of integrin-based cell adhesion. *Curr Opin Cell Biol* 19:1–13
- Badylak SF (2005) Regenerative medicine and developmental biology: the role of the extracellular matrix. *Anat Rec B New Anat* 287:36–41
- Bershadsky AD, Balaban NQ, Geiger B (2003) Adhesion-dependent cell mechanosensitivity. *Annu Rev Cell Dev Biol* 19:677–695
- Bockholt SM, Burridge K (1993) Cell spreading on extracellular matrix proteins induces tyrosine phosphorylation of tensin. *J Biol Chem* 268:14565–14567
- Bois PR, O'Hara BP, Nietlispach D, Kirkpatrick J, Izard T (2006) The vinculin binding sites of talin and alpha-actinin are sufficient to activate vinculin. *J Biol Chem* 281:7228–7236
- Brakebusch C, Fassler R (2003) The integrin-actin connection, an eternal love affair. *EMBO J* 22:2324–2333
- Brown RA, Phillips JB (2007) Cell responses to biomimetic protein scaffolds used in tissue repair and engineering. *Int Rev Cytol* 262:75–150
- Calderwood DA (2004) Integrin activation. *J Cell Sci* 117:657–666
- Chen WT, Singer SJ (1982) Immunoelectron microscopic studies of the sites of cell-substratum and cell-cell contacts in cultured fibroblasts. *J Cell Biol* 95:205–222
- Clark K, Pankov R, Travis MA, Askari JA, Mould AP, Craig SE, Newham P, Yamada KM, Humphries MJ (2005) A specific $\alpha 5 \beta 1$ -integrin conformation promotes directional integrin translocation and fibronectin matrix formation. *J Cell Sci* 118:291–300
- Critchley DR (2000) Focal adhesions – the cytoskeletal connection. *Curr Opin Cell Biol* 12:133–139
- Cukierman E, Pankov R, Stevens DR, Yamada KM (2001) Taking cell matrix adhesions to the third dimension. *Science* 294:1708–1712
- Cukierman E, Pankov R, Yamada KM (2002) Cell interactions with three-dimensional matrices. *Curr Opin Cell Biol* 14:633–639
- Damianova R, Stefanova N, Cukierman E, Momchilova A, Pankov R (2008) Three-dimensional matrix induces sustained activation of ERK1/2 via Src/Ras/Raf signaling pathway. *Cell Biol Int* 32:229–234
- Edelman D, Keefer E (2005) A cultural renaissance: in vitro cell biology embraces three-dimensional context. *Exp Neurol* 192:1–6
- Evans EA, Calderwood DA (2007) Forces and bond dynamics in cell adhesion. *Science* 316:1148–1153
- Faucheux N, Tzoneva R, Nagel MD, Groth T (2006) The dependence of fibrillar adhesions in human fibroblasts on substratum chemistry. *Biomaterials* 27:234–245
- Frisch SM, Francis H (1994) Disruption of epithelial cell-matrix interactions induces apoptosis. *J Cell Biol* 124:619–626
- Geiger B, Bershadsky A (2001) Assembly and mechanosensory function of focal contacts. *Curr Opin Cell Biol* 13:584–592

- Geiger B, Bershadsky A, Pankov R, Yamada KM (2001) Transmembrane crosstalk between the extracellular matrix-cytoskeleton crosstalk. *Nat Rev Mol Cell Biol* 2:793–805
- Giancotti FG (2003) A structural view of integrin activation and signaling. *Dev Cell* 4:149–151
- Giancotti FG, Tarone G (2003) Positional control of cell fate through joint integrin/receptor protein kinase signaling. *Annu Rev Cell Dev Biol* 19:173–206
- Gilmore AP, Burridge K (1996) Regulation of vinculin binding to talin and actin by phosphatidylinositol-4-5-bisphosphate. *Nature* 381:531–535
- Glenny JR Jr, Zokas L (1989) Novel tyrosine kinase substrates from Rous sarcoma virus-transformed cells are present in the membrane skeleton. *J Cell Biol* 108:2401–2408
- Halliday NL, Tomasek JJ (1995) Mechanical properties of the extracellular matrix influence fibronectin fibril assembly in vitro. *Exp Cell Res* 217:109–117
- Hanks SK, Ryzhova L, Shin NY, Brabek J (2003) Focal adhesion kinase signaling activities and their implications in the control of cell survival and motility. *Front Biosci* 8:d982–d996
- Hemmings L, Rees DJ, Ohanian V, Bolton SJ, Gilmore AP, Patel B, Priddle H, Trevithick JE, Hynes RO, Crichtley DR (1996) Talin contains three actin-binding sites each of which is adjacent to a vinculin-binding site. *J Cell Sci* 109:2715–2726
- Hemmerich K, von Heimburg D (2006) Biomaterials for adipose tissue engineering. *Expert Rev Med Devices* 3:635–6345
- Humphries MJ (2004) Monoclonal antibodies as probes of integrin priming and activation. *Biochem Soc Trans* 32:407–411
- Humphries JD, Byron A, Humphries MJ (2006) Integrin ligands at a glance. *J Cell Sci* 119:3901–3903
- Hynes RO (1987) Integrins: a family of cell surface receptors. *Cell* 48:549–554
- Katti KS (2004) Biomaterials in total joint replacement. *Colloids Surf B Biointerfaces* 39:133–142
- Katz BZ, Zamir E, Bershadsky A, Kam Z, Yamada KM, Geiger B (2000) Physical state of the extracellular matrix regulates the structure and molecular composition of cell-matrix adhesions. *Mol Biol Cell* 11:1047–1060
- Ling K, Doughman RL, Iyer VV, Firestone AJ, Bairstow SF, Mosher DF, Schaller MD, Anderson RA (2003) Tyrosine phosphorylation of type I γ phosphatidylinositol phosphate kinase by Src regulates an integrin–talin switch. *J Cell Biol* 163:1339–1349
- Lo SH, Janmey PA, Hartwig JH, Chen LB (1994) Interactions of tensin with actin and identification of its three distinct actin-binding domains. *J Cell Biol* 125:1067–1075
- McCleverty CJ, Lin DC, Liddington RC (2007) Structure of the PTB domain of tensin1 and a model for its recruitment to fibrillar adhesions. *Protein Sci* 16:1223–1229
- Molony L, Burridge K (1985) Molecular shape and self-association of vinculin and metavinculin. *J Cell Biochem* 29:31–36
- Nair LS, Laurencin CT (2006) Polymers as biomaterials for tissue engineering and controlled drug delivery. *Adv Biochem Eng Biotechnol* 102:47–90
- Ohashi T, Kiehart DP, Erickson HP (2002) Dual labeling of the fibronectin matrix and actin cytoskeleton with green fluorescent protein variants. *J Cell Sci* 115:1221–1229
- Pankov R, Cukierman E, Katz B-Z, Matsumoto K, Lin DC, Lin S, Hahn C, Yamada KM (2000) Integrin dynamics and matrix assembly: tensin-dependent translocation of $\alpha(5)\beta(1)$ integrins promotes early fibronectin fibrillogenesis. *J Cell Biol* 148:1075–1090
- Pankov R, Cukierman E, Clark K, Matsumoto K, Hahn C, LaFlamme SE, Poulin B, Yamada KM (2003) Specific $\beta(1)$ integrin site selectively regulates Akt/PKB signaling via local activation of PP2A. *J Biol Chem* 278:18671–18681
- Rosales C, O'Brien V, Kornberg L, Juliano RL (1995) Signal transduction by cell adhesion receptors. *Biochim Biophys Acta* 1242:77–98
- Rottner K, Hall A, Small JV (1999) Interplay between Rac and Rho in the control of substrate contact dynamics. *Curr Biol* 9:640–648
- Schaller MD (2001) Paxillin: a focal adhesion-associated adaptor protein. *Oncogene* 20:6459–6472
- Shimaoka M, Takagi J, Springer TA (2002) Conformational regulation of integrin structure and function. *Annu Rev Biophys Biomol Struct* 31:485–516

- Thiery JP (2003) Cell adhesion in development: a complex signaling network. *Curr Opin Gen Dev* 13:365–371
- Turner CE (2000) Paxillin interactions. *J Cell Sci* 113:4139–4140
- Tzoneva R, Faucheux N, Groth T (2007) Wettability of substrata controls cell-substrate and cell-cell adhesions. *Biochim Biophys Acta* 1770:1538–1547
- Webb DJ, Donais K, Whitmore LA, Thomas SM, Turner CE, Parsons TF, Horwitz AF (2004) FAK-Src signalling through paxillin, ERK and MLCK regulates adhesion disassembly. *Nat Cell Biol* 6:154–161
- Zaidel-Bar R, Itzkovitz S, Ma'ayan A, Iyengar R, Geiger B (2007a) Functional atlas of the integrin adhesome. *Nat Cell Biol* 9:858–867
- Zaidel-Bar R, Milo R, Kam Z, Geiger B (2007b) A paxillin tyrosine phosphorylation switch regulates the assembly and form of cell-matrix adhesions. *J Cell Sci* 120:137–148
- Zamir E, Katz BZ, Aota S, Yamada KM, Geiger B, Kam Z (1999) Molecular diversity of cell-matrix adhesions. *J Cell Sci* 112:1655–1669

Chapter 2

Development of Provisional Extracellular Matrix on Biomaterials Interface: Lessons from In Vitro Cell Culture

George Altankov, Thomas Groth, Elisabeth Engel, Jonas Gustavsson, Marta Pegueroles, Conrado Aparicio, Francesc J. Gil, Maria-Pau Ginebra, and Josep A. Planell

Abstract The initial cellular events that take place at the biomaterials interface mimic to a certain extent the natural interaction of cells with the extracellular matrix (ECM). The cells adhering to the adsorbed soluble matrix proteins, such as fibronectin (FN) and fibrinogen (FNG) tend to re-arrange them in fibril-like pattern. Using model surfaces we have demonstrated that this cellular activity is abundantly dependent on the surface properties of materials, such as wettability, surface chemistry, charge and topography. This raises the possibility that tissue compatibility of materials is connected with the allowance of cells to remodel substratum associated proteins presumably to form provisional ECM. We have further shown that antibodies which bind β_1 and α_v integrins (subunits of the FN and FNG receptors respectively) may induce their linear rearrangement on the dorsal surface of living cells – a phenomenon presumably related to the same early molecular events of fibrillar matrix assembly. Because the quantitative measurements revealed that this receptor dynamics is strongly altered on the low compatible (hydrophobic) substrata we hypothesized that in order to be biocompatible, materials need to adsorb matrix proteins loosely, i.e. in such a way that the cells can easily remove and organize them in matrix-like fibrils via coordinated functioning of integrins. More recent studies on the fate of

G. Altankov (✉)

Institute of Biophysics Bulgarian Academy of Sciences, Sofia, Bulgaria

and

ICREA (Institucio Catala para Recercia i Estudis Avancats), Barcelona, Spain

and

Institute for Bioengineering of Catalonia, Feixa Llarga Pavello Govern 1º, 1121

08907 L'Hospitalet de Llobregat Barcelona, Spain

e-mail: george.altankov@icrea.es

T. Groth

Department of Pharmacy, Martin-Luther University Halle-Wittenberg, Kurt-Mothes-Strasse

106120, Halle (Saale), Germany

E. Engel, J. Gustavsson, M. Pegueroles, C. Aparicio, F.J. Gil, M.-P. Ginebra, and J.A. Planell

Department of Material Science, Universitat Politècnica de Catalunya, Av. Diagonal 64708028,

Barcelona, Spain

FN on some real biomaterial surfaces, including different rough titanium (Ti) and hydroxyapatite (HA) cements and the surface of biosensors confirmed this point of view. They also show that quantitative measurements of adsorbed matrix proteins and their dynamic rearrangement at cell-material interface might provide insight to the biocompatibility of given material and even predict its tissue integration.

Keywords Biomaterials interface • Fibronectin matrix • Reorganization • Provisional ECM • Cellular interaction

2.1 Introduction

The interaction of living cells with foreign materials is fundamental for biology and medicine and is a key for understanding the phenomena of biocompatibility (Thiery 2003). After searching during long time for the “ideal” bioinert surface, it became clear that proper cellular interaction with manmade biomaterials is rather desirable property (Thiery 2003; Spie 2002; Griffin and Naughton 2002; Henche and Polak 2002). Cell adhesion and the generation of adequate cellular responses are prerequisite for the successful incorporation of implants, the colonization of scaffolds and for many other tissue engineering applications (Spie 2002; Griffin and Naughton 2002). In fact, successful cell adhesion triggers complicated molecular cascades where both early and late events may be distinguished. Within early events are the recognition of adsorbed proteins at the material surface and the physical interaction of cells, followed by the generation of proper biological signals that could be transmitted to the cell interior. All this usually ends with the colonization of biomaterials or scaffolds with living cells. The later events are connected with the proliferation of cells and with their proper differentiation which also needs an exchange of biological signals with the material surface that support cell functionality (Thiery 2003; Spie 2002; Griffin and Naughton 2002; Henche and Polak 2002). In vivo the cellular interaction is further complicated by the local inflammatory response and the biodegradation of material (Spie 2002) – events which are out of the scope of this paper.

2.2 Initial Cell–Materials Interaction

The initial cellular events that take place at the biomaterials interface mimic to a certain extent the natural adhesive interaction of cells with the ECM (Grinnell 1986; Hynes 2002). The cells cannot interact directly with the foreign material surfaces as they do not recognize them, but they readily attach to the adsorbed protein layer (see Fig. 2.1), containing adhesive sequences that are specifically recognized by the cells (e.g., RGD). Among these proteins it seems FN, vitronectin (VN) and FNG play a crucial role. In fact, these are natural matrix proteins but in soluble form, thus uniformly available in most biological fluids (Grinnell 1986).

Thus, according to the classical ligand-receptor theory the initial cell–materials interaction has to be considered as a complex multi-step paradigm, well described in the

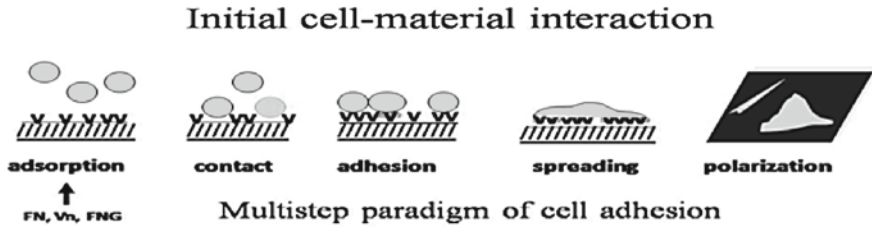


Fig. 2.1 Initial cell-materials interaction is approximated with the process of cell adhesion

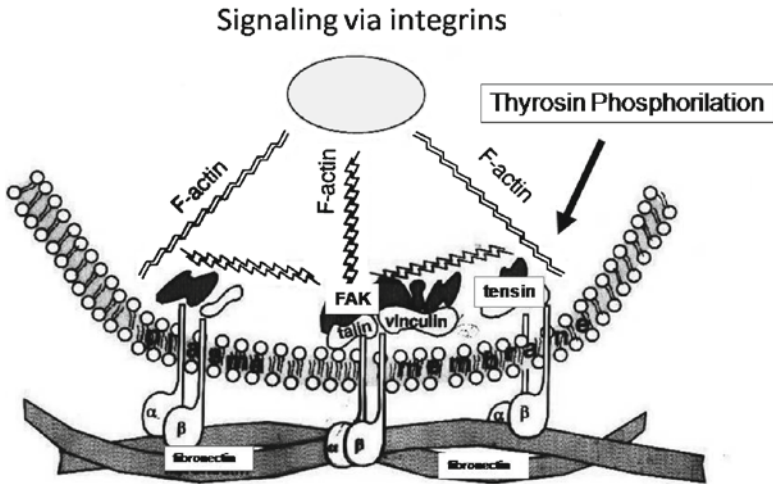


Fig. 2.2 Development of focal adhesion complex

literature (Grinnell 1986), which starts with the adsorption of proteins from the surrounding medium, followed by cell adhesion, spreading and polarization (Fig. 2.1).

2.2.1 Development of Focal Adhesion Complex

The cells recognize adsorbed adhesive proteins via integrins – a family of cell surface receptors that provide trans-membrane links between the ECM and cytoskeleton (Hynes 2002). When integrins are occupied they clusterize and become activated which result in the development of focal adhesion complex (see Fig. 2.2). The focal adhesions are the places where the actual anchorage of the cells take place and where subsequent cellular response is triggered (Hynes 2002). By these structures the cells receive points on the substratum for traction that support the development of their normal shape. The focal adhesion complexes also act as signaling units by their capacity to accumulate various signaling intermediates (Denen et al. 2002) such as Rho-GTP-ases and their effector proteins (Pankov et al. 2000). Studies have revealed presence of tyrosine kinases (Src, FAK, PUK2, Csk and Abl), serine/threonine

kinases (ILK, PKC and PAK) and other enzymes (Pi3-kinase, protease calpan II, tyrosine phosphatases, etc.), as well as the cytoskeletal components α -actinin, tensin, paxillin, talin and vinculin (Zamir and Geiger 2001). Upon clustering of integrins most of them undergo a common mechanism of activation (tyrosine phosphorylation) resulting in the direct binding to actin filaments (via vinculin, tensin, α -actinin, FAK, etc.) (Denen et al. 2002; Pankov et al. 2000; Zamir and Geiger 2001). Thus, the focal adhesion complexes act as trans-membrane mechanical links between adsorbed matrix proteins and the cytoskeleton.

2.2.2 *Substratum Properties Affect Focal Adhesions Formation*

The assessment of materials biocompatibility relies heavily on analysis of macroscopic cellular responses to material interaction (Yamad et al. 2003). A line of investigation has shown that the formation of focal adhesion complexes is strongly dependent on the surface properties and is altered on low biocompatible materials. In contact with such low compatible materials cells are usually less spread and cannot develop their normal shape. Morphologically, they remain shrunken or rounded and often present irregular protrusions. In Fig. 2.3, reprinted from our previous work (Groth and Altankov 1996), altered focal adhesion formation is shown when fibroblasts adhere on hydrophobic octadecylsilane (ODS) surface. These focal adhesion complexes are viewed by alpha-v integrins and compared to cells adhering

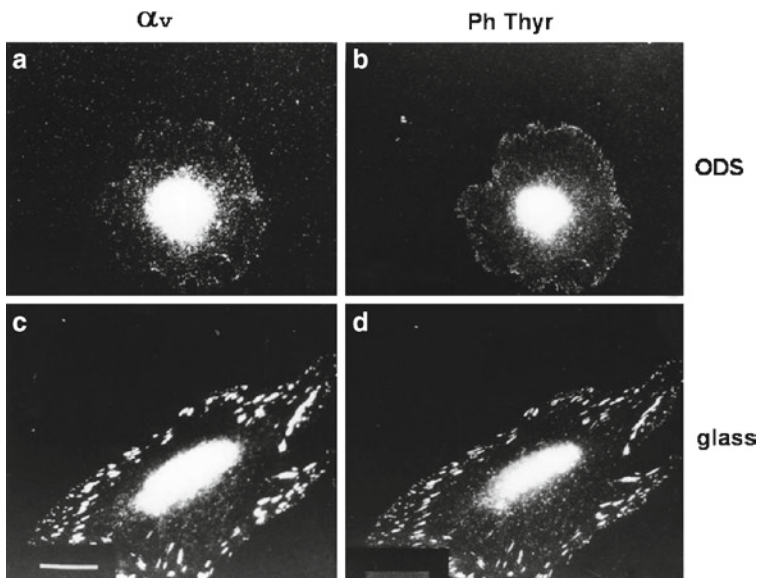


Fig. 2.3 Development of focal adhesion complexes of αv integrins (a, c) and colocalization with the phosphotyrosine activity (b, d) of human fibroblasts adhering on hydrophilic (c, d) and hydrophobic (a, b) substrata

on hydrophilic glass. The co-localization of phosphotyrosine activity (viewed by anti-phosphotyrosine antibodies) in focal adhesions on hydrophilic substrata show that the cells not only attach successfully but also transmit proper signals to the cell interior. Conversely, cells on hydrophobic ODS neither develop focal adhesion complexes nor transmit signals to the cell (Fig. 2.3, upper panel). We anticipate that such substrates are low biocompatible, as cells do not receive adequate signals from the materials interface (Groth and Altankov 1996).

Thus, the initial formation of focal adhesion complexes reflects the successful cellular interaction. However, in vivo this interaction is more complicated and bi-directional: cells surrounded by tissue are continuously receiving information from their environment, and they recognize specific structural cues within this matrix (Yamad et al. 2003). At the same time they are frequently remodeling this matrix (Hynes 2002; Denen et al. 2002; Pankov et al. 2000; Tzoneva et al. 2002). Many cells are able to imprint specific biological information within the ECM, which other cells later can read. Such information however is rarely found on foreign materials interface. Therefore, it is not surprising that many primary cells cannot adapt in vitro and grow poorly in contact with foreign materials. Others however, adapt more easily. What is the reason for this difference? One possible explanation is that some cells easily can develop their own matrix at the materials interface, and thus enable their own survival.

2.3 Development of Provisional Extracellular Matrix at the Biomaterials Interface

The next level of complexity comes from the fact that cells not only interact with the adsorbed matrix proteins in vitro, but also tend to reorganize them on the substratum in a specific fibril-like pattern, presumably as an attempt to arrange their own matrix (Grinnell 1986; Pankov et al. 2000; Altankov and Groth 1994; Altankov et al. 1997; Altankov and Groth 1996; Tzoneva et al. 2002). This is particularly pronounced for stromal cells like fibroblasts, presumably because their main function is to produce ECM. But also other cell types like endothelial cells (Tzoneva et al. 2002), keratinocytes (Altankov et al. 2001), osteoblasts (Gustavsson et al. 2007), and even cancer cells (Maneva-Radicheva et al. 2008) may possess ability to organize provisional ECM in vitro. This matrix forming activity might be distinguished in two types: *early* and *late* matrix formation.

2.3.1 Development of Early Matrix

As previously shown, when fibroblasts or endothelial cells are seeded on FN, within few hours they start to rearrange this protein in a specific fibrillar pattern (Altankov and Groth 1994) (see Fig. 2.4):

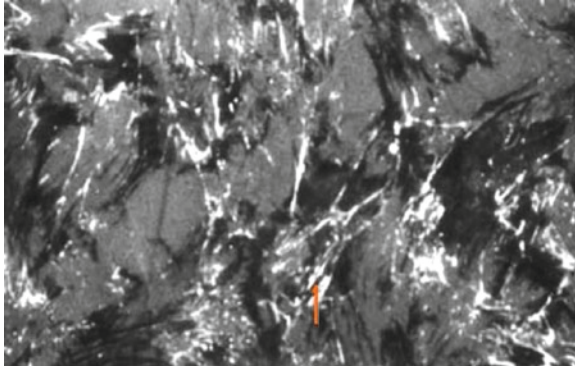
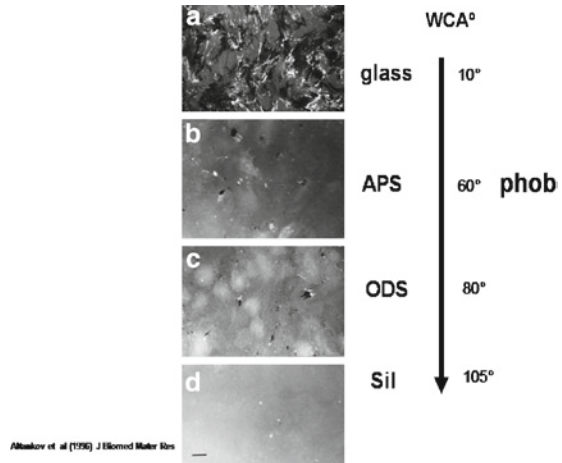


Fig. 2.4 Reorganization of adsorbed fibronectin by fibroblasts within 4 h of incubation (Altankov and Groth 1994)

Fig. 2.5 Altered reorganization of adsorbed FITC-fibronectin with increasing the wettability of substratum



It has to be noted however, that this cellular activity is abundantly dependent on the surface properties of materials, such as wettability (Altankov and Groth 1994; Tzoneva et al. 2002), surface chemistry and charge (Gustavsson et al. 2007).

The data presented in Fig. 2.5 demonstrate that with increased surface hydrophobicity, fibroblast reorganization of substratum associated FN is altered. Even on moderately wettable substrata (with water contact angle, WCA, around 60°) the FN reorganization is blocked (Altankov and Groth 1994). Moreover, this cellular activity is not specific only to FN, but similar altered cellular reorganization was recently reported for adsorbed FNG in contact with endothelial cells (Tzoneva et al. 2002).

2.3.2 Development of Late Fibronectin Matrix

When fibroblasts are cultured in vitro they synthesize and tend to arrange secreted FN in a specific fibrillar pattern on the materials interface and such FN matrix is formed only in the presence of cells (Lutolf and Hubbell 2005). Figure 2.2 represents the typical “late” FN matrix deposited by fibroblasts after 4 days of culture on glass substrata visualized by immunofluorescence. Morphologically these FN fibrils look similar to the FN matrix fibrils that might be obtained in vivo (Hynes 1990) (Fig. 2.6).

It has to be noted however, that the development of this late provisional FN matrix is once again strongly altered on low biocompatible (hydrophobic) substrata, as has been demonstrated previously (Altankov and Groth 1996) and which is shown in Fig. 2.7. These substrates (identical as in Fig. 2.5) possess a step-wise increase of surface hydrophobicity and it correlates with altered FN deposition (Altankov and Groth 1994).

Based on above observations, in fact confirmed for various cell models including endothelial cells (Tzoneva et al. 2002), osteoblasts (Gustavsson et al. 2007), keratinocytes (Altankov et al. 2001), and even carcinoma cells (Maneva-Radicheva et al. 2008), one can support the existence of a common cellular mechanism for the provisional ECM formation on biomaterials interface. Moreover, the cells show ability to arrange different matrix proteins such as FN (Grinnell 1986; Groth and Altankov 1996; Altankov and Groth 1994; Altankov et al. 1997; Altankov and Groth 1996), FNG (Tzoneva et al. 2002) and even adsorbed collagen IV, which (note!) is not fibrillar protein. It seems FN play a leading role as it co-localize with both rearranged FNG and collagen IV in a specific linear pattern, similar but not identical with FN fibrils (Tzoneva et al. 2002; Maneva-Radicheva et al. 2008). On the other hand, these spatially arranged proteins co-aligns with some actin fibers and transiently co-localize with FN fibrils, as well as with $\beta 1$ and $\alpha 2$ integrin,

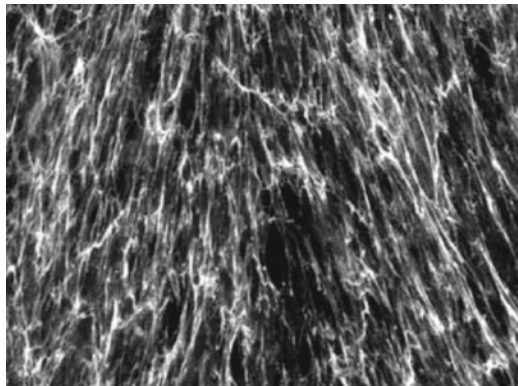


Fig. 2.6 Fibronectin matrix deposited by fibroblasts on glass slide after 4 days in culture

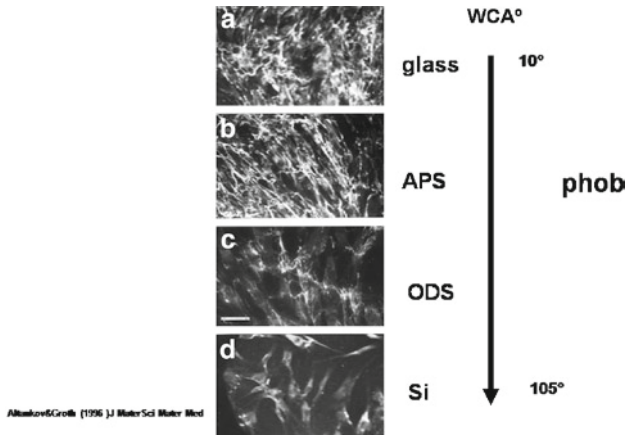


Fig. 2.7 Altered fibronectin matrix formation with increasing the substratum hydrophobicity

respectively, suggesting a cell-driven process (Tzoneva et al. 2002; Maneva-Radicheva et al. 2008). Finally, our current investigations show that adsorbed collagen IV remodeling is once again altered (similarly to FN and FNG) on low biocompatible hydrophobic substrata (Coelho et al. 2009).

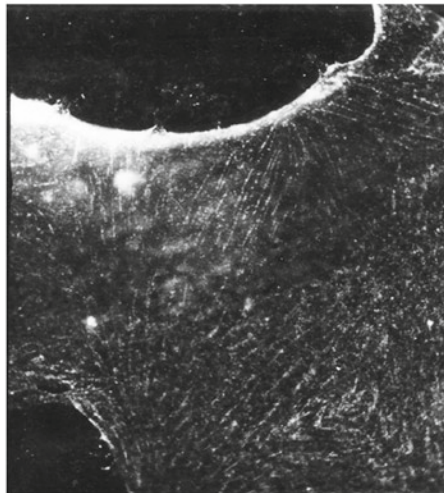
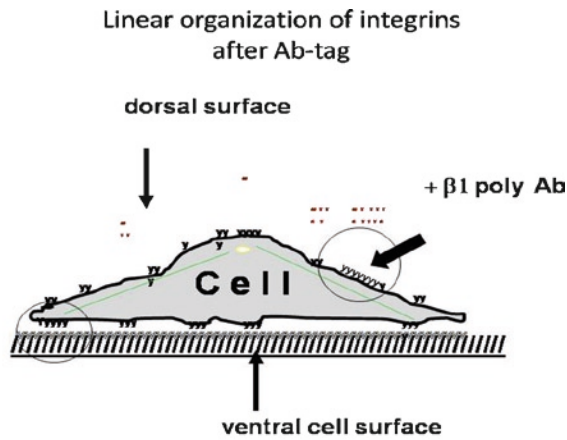
Collectively, all these studies provide evidences that *tissue compatibility of materials is strongly dependent on the allowance of cells to remodel surface associated proteins* and to form provisional extracellular matrix. Presumably this matrix is very similar to the matrix obtained during wound healing (Altankov et al. 2005; Clark et al. 1982), as it is well documented that FN and FNG readily accumulate in the extravascular space during injury where they serve as substrate for cells migration towards the wound surface (Clark et al. 1982). In this respect, the existence of mechanisms for collagen remodeling during regeneration is a great deal in our understanding of wound healing (Altankov et al. 2005; Clark et al. 1982; Donaldson et al. 1989). Apart from this, however, our current studies show that reorganization of substrate associated collagen IV together with FN and FNG might be a useful morphological tool for studies on biocompatibility (Clark et al. 1982).

2.4 Integrin Receptors Dynamics and Provisional Extracellular Matrix Formation

2.4.1 Studies on Integrin Dynamics

Another line of our research highlights the dynamic behavior of integrins, i.e. the cellular adhesive machinery that controls the adhesion strength and matrix assembly. In these studies we are interested in learning more on how cells “imprint” specific

biological information at the biomaterials interface. We anticipate that it should relate to the functionality of integrins and their ability to organize surrounding ECM. Previously, we have shown that antibodies which bind $\beta 1$ and αV integrins (subunits of the main FN and FNG receptors) can induce their linear rearrangement on the dorsal surface of living cells (Altankov and Grinnell 1995) – a phenomenon presumably related to the same early molecular events that are responsible for the matrix assembly *in vitro* (Altankov and Groth 1994; Altankov et al. 1997). Figure 2.8 represents the experimental design of these studies (e.g. antibody tag of living fibroblasts adhering to FN) and the main results obtained with this approach, namely the *linear organization of $\beta 1$ integrins on the dorsal cell surface of living cells* when they are treated with antibody (30–60 min).



Altankov & Grinnell, 1995, *Exp Cell Res*

Fig. 2.8 Linear rearrangement of $\beta 1$ integrins upon antibody tag

Two important issues were considered (Pereira et al. 2002) when we designed these experiments. First, the antibodies as polyvalent ligands are expected to clusterize and activate the integrins, thus, their behavior would mimic, to a certain extent the physiological ligand binding. Second, when we follow the functional distribution of integrins on the dorsal cell surface, we will actually follow the behavior of these integrins which are “invisible” for the classical immunomorphological studies. Thus, completely different information can be obtained depending on the experimental protocol:

As demonstrated in Fig. 2.9 (upper panel), if antibody is added to the fixed and permeabilized samples it will stain the integrins mainly on the ventral cell surface, i.e. we will see the *classical focal adhesion complexes* (c). The dorsal integrins will not be seen due to their diffuse pattern. Conversely, on non-permeabilized samples antibody will visualize mostly integrins located on the dorsal cell surface, seen because no staining of the ventral integrins. The dorsal integrins typically represent a diffuse pattern (b, e). Finally, when the antibody is added to living cells it will induce *linear rearrangement of the integrins* (a, c) presumably caused by the reversible association of these antibody-receptor clusters with the actin cytoskeleton. The later is demonstrated on the lower panel, where fibroblasts are double stained

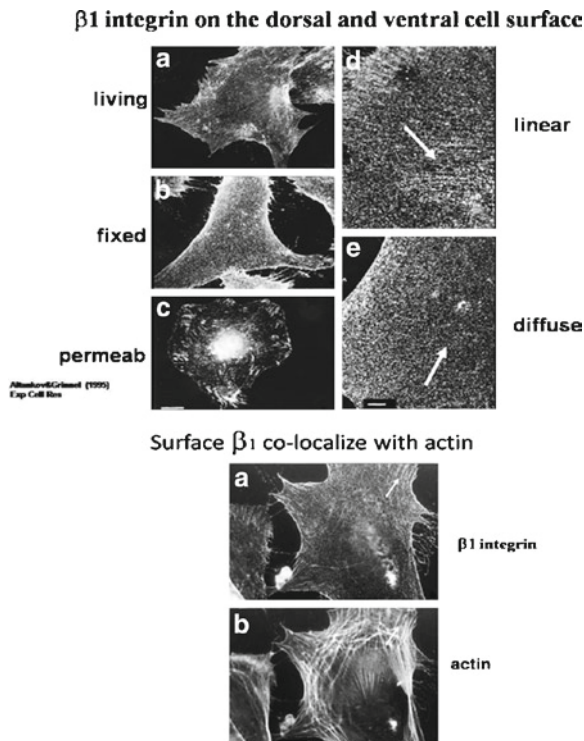


Fig. 2.9 Distribution of β_1 integrins depending on the way of staining

for $\beta 1$ integrin (a) and actin (b) and where linearly arranged $\beta 1$ integrins (arrow) co-align with longitudinal actin stress fibres (b).

2.4.2 Integrin Dynamics Depend on Substratum Properties

How do the underlying surface properties affect integrin dynamics? To address this question we designed experiments aiming to follow the behavior of $\beta 1$ integrins on both the dorsal and the ventral cell surface when cells adhere to model hydrophilic (glass) and hydrophobic ODS substrata respectively. The main results of this study are presented on Fig. 2.10.

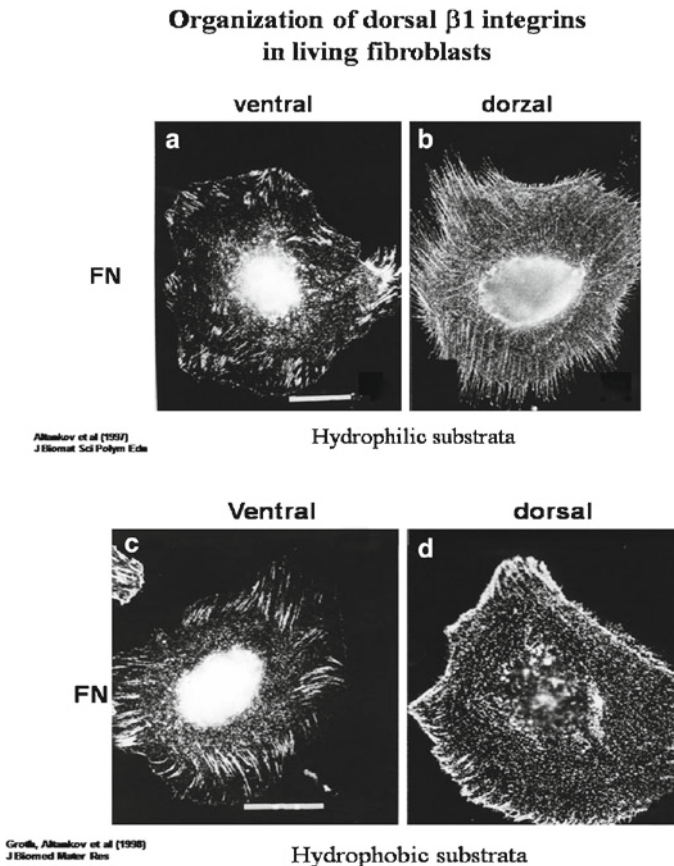


Fig. 2.10 Linear organization of antibody tagged integrins on hydrophilic substrata coated with fibronectin (**b**, top panel). Note its absence on hydrophobic ODS substrata (**d**, bottom panel) while focal adhesions on the ventral cell surface (**a**, **c**) remains unaffected in both cases

When looking on the ventral cell surface no big difference between hydrophilic (a) and hydrophobic (c) substrata is found, i.e. the development of focal adhesion contacts is similar on both FN coated substrates (a, c). However, when looking on the behavior of integrins on the dorsal cell surface, a clear difference between hydrophilic (b) and hydrophobic (d) substrata can be observed: a well pronounced linear arrangement of antibody tagged $\beta 1$ clusters can be seen on hydrophilic glass (b), but is almost absent on hydrophobic ODS surface (d).

From these studies, published in details elsewhere (Altankov et al. 1997), we concluded that the antibody-induced functional rearrangement of $\beta 1$ integrins on the dorsal cell surface is strongly altered on low biocompatible substrata. It is interesting to note, that the molecular events that take place on the dorsal cell surface were more sensitive to the substratum hydrophobicity than those on the ventral cell surface (focal adhesion complexes), although the later face directly the material surface. We hypothesized that stronger interaction of adhesive proteins with the hydrophobic substrata immobilize part of integrins at the ventral cell surface, and because these integrins (already activated) are important for the further linear arrangement of dorsal integrins (Ab tagged) this will block their linear reorganization. Conversely, on hydrophilic substrata that loosely bind adhesive proteins, activated integrins can easily translocate to the dorsal cell surface where joining the Ab tagged integrins will support their linear rearrangement. Indeed, a line of subsequent investigations confirmed this view (Pankov et al. 2000; Altankov et al. 1997; Tzoneva et al. 2002; Zlatanov et al. 2005).

2.5 Development of Extracellular Matrix at “Real” Biomaterials Interface

Most of the above presented research is based on the experiments using model surfaces, which provide many advantages, such as simple experimental design and easier analysis of the results, but suffers from a main disadvantage: they are far from the real biomaterials application. In fact, most of the clinically used biomaterials are polymers, metals or ceramics that provide broad range of surface chemistries and topography. Moreover, the majority of real biomaterials represent highly rough surfaces. How ECM is formed on such biomaterials and how it is organized on their interface is of particular bioengineering interest.

2.5.1 Effects of Substratum Chemistry on Matrix Formation: A View of Biosensors Application

The main event in tissue repair is the ability of cells to produce matrix and to restore the integrity of damaged tissue. The abnormal deposition of matrix, however, could lead to negative consequences, such as scar formation and fibrosis. Another example

of such negative impact is the one of biosensors – here viewed as bioengineered devices put in close contact with cells or tissues, to monitor distinct environmental changes, such as pH, ion balance, gases, and even cell growth and differentiation – where ECM deposition may alter significantly their sensitivity and/or stability. In this respect their interaction with matrix proteins, such as FN, VN and FNG could be of critical importance. Moreover as shown above these proteins can undergo remodelling by adhering cells (Altankov and Groth 1994; Altankov et al. 1997; Altankov and Groth 1996; Tzoneva et al. 2002) and thus cells themselves may affect the properties of the sensor. Therefore we asked whether we can control and even tailor the cellular interaction and the provisional matrix formation on such sensing materials to improve their properties. A suitable alternative was using self assembled monolayers (SAMs) that have been successfully applied with other materials to obtain control over the protein adsorption and cellular responses.

As a low pressure chemically vapour deposited thin film silicon nitride (Si_3N_4) is used as the sensitive material in miniaturized chemical biosensors such as the *ion-selective field effect transistor* (ISFET) (Neumann et al. 2004) or the *electrolyte/insulator/semiconductor* microtransducer (Schöning et al. 1998). Using human osteoblast-like MG-63 cells as an in vitro model for bone we found that Si_3N_4 surface does not provide optimal conditions for osseointegration (Kue et al. 1999; Sohrabi et al. 2000) as the cells tend to detach from its surface when cultured over confluence. In an attempt to improve its biological properties Si_3N_4 was modified with SAMs bearing functional end groups of primary amine (NH_2), carboxyl (COOH) and methyl (CH_3), representing distinct surface chemistries and wettability.

The adsorption of FITC-labeled FN to each of these surfaces was fluorimetrically quantified after extraction with 0.2 M NaOH, showing low adsorption to Si_3N_4 while significantly higher on NH_2 followed by CH_3 and COOH (Fig. 2.11).

Furthermore we observed that the NH_2 functionality promoted cell proliferation, but delayed cell differentiation (Gustavsson et al. 2007). This raised the possibility that stronger FN interaction could disturb the cell functionality, particularly in respect to the organization of ECM. To address this, we studied the fate of both adsorbed and secreted FN by MG-63 cells to learn more about the impact of above functionalities on matrix formation. Indeed, as shown in Fig. 2.12 the ability of MG-63 cells to remove and reorganise adsorbed FITC-labelled FN after 4 h (i.e. early matrix) was present only on the COOH chemistry and on the positive control glass, while on both Si_3N_4 and NH_2 the pre-adsorbed FN was completely intact (Fig. 2.12, left column).

When reaching confluency, MG63 cells grew in a film-like structure that served as a rather three dimensional environment. It obviously made cells less dependent of the substrate chemistry as the spatial organization of FN produced by the cells after 5 days in culture did not show much difference between the surfaces (Fig. 2.12, right column). The osteoblasts-like cells generally deposited FN fibrils in a facet-like pattern following the specific organisation of cell layer. However, while this film-like structure was observed to be very well attached on NH_2 , and somewhat less strongly to COOH , it was loosely associated with the Si_3N_4 and CH_3 surfaces where it was easily removed by washing or changing the medium.

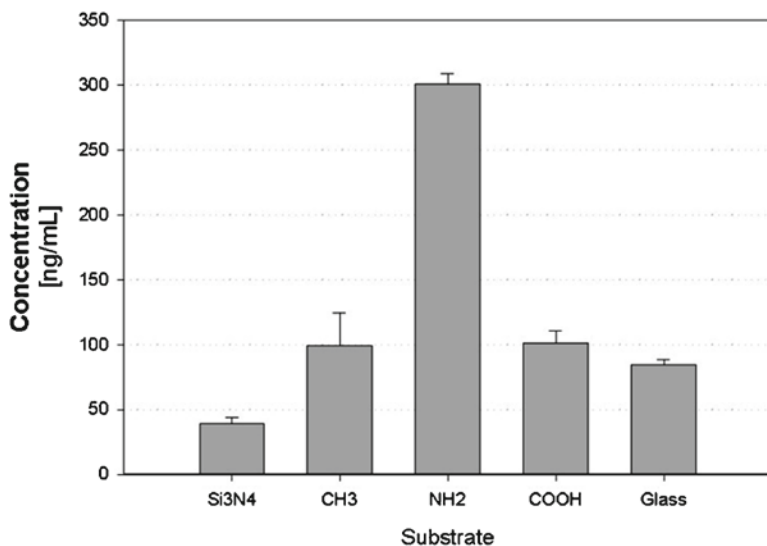


Fig. 2.11 Adsorption of FITC-labeled fibronectin measured on different surface chemistries

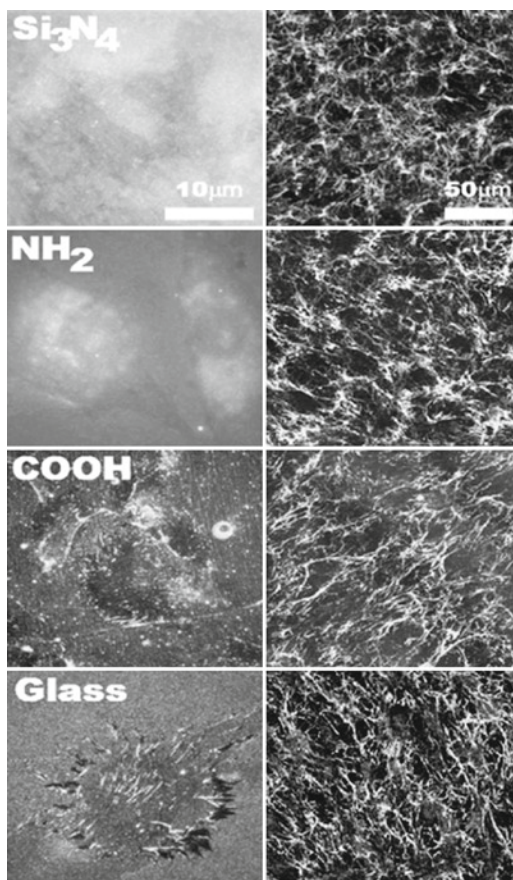


Fig. 2.12 Adsorption of FITC-labelled fibronectin measured on different surface chemistry

On the other hand, the observation that NH_2 delays the differentiation of MG-63 cells while Si_3N_4 promote it (Gustavsson et al. 2007) provokes a conclusion that although a strong surface interaction with matrix proteins is an important event for osseointegration, it may at the same time disturb the proper osteoblasts functionality. Further studies are now on the way to confirm or to exclude the above puzzling conclusion.

2.5.2 Development of Extracellular Matrix on Biomimetic Hydroxyapatite Cements Surfaces

Bone is among the most complex examples of biomineralized material where the hydroxyapatite (HA) nanocrystals grow within bone in intimate contact with collagen fibres, building up a nanostructured composite with characteristic mechanical behaviour (Baumann et al. 1999). In the past few decades bone mineralization was visualized as being a physicochemical phenomena in which the ECM (mostly collagen) acts as template upon which the mineral crystals are formed. The observation that the production and composition of ECM are carefully modulated during osteoblastic differentiation (Lowenstain and Weiner 1989) suggests an important regulatory role of cell-matrix interaction. Apart from collagen, the distribution of FN in the areas of skeletogenesis suggests that it is also involved in early stages of bone formation (Maurisi et al. 1996). Its role in matrix organization is further suggested by ultrastructural colocalization of FN with individual type I collagen fibrils (Gronowicz et al. 1991). Indeed, addition of anti FN antibodies in osteoblasts culture reduces subsequent formation of nodules showing that FN is required for the normal osteogenesis (Lowenstain and Weiner 1989).

On the other hand, a large number of investigations have been conducted to develop filling-in-materials for bone tissue repair. In this respect, calcium phosphates represents a good alternative as they are known to be biocompatible and in most cases osteoinductive. An interesting alternative is the application of calcium phosphates as cements made of mixtures between one or several calcium phosphate powders. Upon mixture with water, the calcium phosphate powders dissolve and precipitate into another calcium phosphate. Through this precipitation, the paste hardens forming a fine homogenous nano or micro porous matrix.

Previous research (Nordahi et al. 1995) revealed that depending on the size of the initial powder the HA cement may produce surfaces with unique topography. Specifically, it has been shown that by controlling the particle size (through milling process) it is possible to develop calcium phosphate materials with tailored surface structure at the micro and nano-scale levels (Nordahi et al. 1995). Figure 2.13 represents an example of such structures: the SEM pictures of two types of cements. Fine (particle size of about 1 μm) and coarse (10 μm size), which were obtained by low-temperature setting of a calcium phosphate cements (CPC), where calcium deficient HA is formed through the hydrolysis of α -tricalcium phosphate (α -TCP) (Nordahi et al. 1995).

In respect to the biological properties, in the direct contact studies, no differences in the initial cell adhesion between the two substrates were observed, but cell spreading

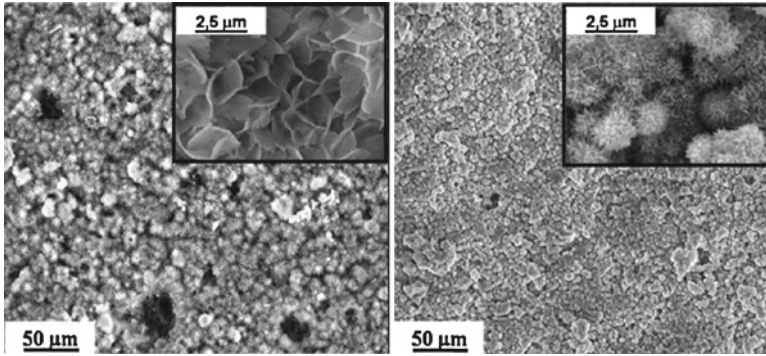


Fig. 2.13 SEM micrographs of coarse (*left*) and fine cement (*right*) surface microstructures, showing the differences in size and morphology of crystals

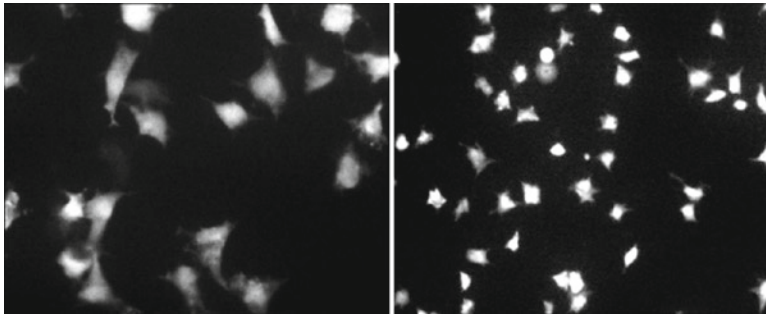
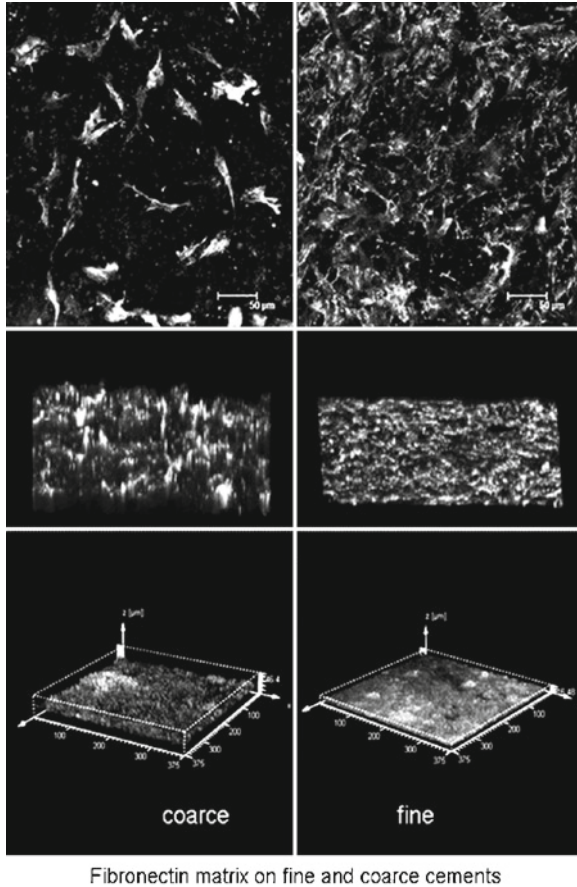


Fig. 2.14 Overall morphology MG 63 cells adhering on fibronectin coated coarse (*left*) and fine (*right*) cement surface

was more pronounced on Coarse cement, when it was coated with FN (Fig. 2.14). This result is in agreement with the work of Deligianni et al. who reported an increased cellular interaction with increased surface roughness of sintered HA (Ginebra et al. 2004). Similarly to these and also other studies we observed a generally lower cell adhesion and proliferation on these apatite substrates than in the control TC polystyrene (Ginebra et al. 2004; Deligianni et al. 2001).

The same trend was found also for cell proliferation. MG 63 cells grew much better on the surface of Coarse cement and significant differences between the two CPC substrates appeared from day 7, suggesting that osteoblasts on fine cements tended to stop earlier their proliferation.

Increased surface roughness that is characteristic for Coarse cements however depressed FN matrix formation (Fig. 2.15, top and middle panels – left). Although the cells still organize FN, it is arranged in a different way. FN fibrils are very rich and well organized on the surface of Fine cement (top and middle panels – right)



Fibronectin matrix on fine and coarse cements

Fig. 2.15 3D LSM images of the late FN matrix organized by osteoblast-like MG63 cells on the surface of Coarse and Fine cements. At the (*top panel*) images are shown as maximum projection while they are reconstructed (*middle panel*) and quantified (*lower panel*) in 3D

apart from the Coarse where FN represents rather sheet-like structure (top and middle panels –left). Nevertheless, more precise measurements show that MG 63 cells respond to the topography by increasing the thickness of their produced matrix (Fig. 2.15, lower panel), presumably together with collagen, which may be already extrapolated to the subsequent osseointegration.

Finally, it is interesting to mention that the less matrix organization on Coarse cements correlates with the significantly depressed differentiation of MG 63 cells on this surface (not shown here), judged by both osteocalcin and alkaline phosphatase measurements (Yuasa et al. 2004). This suggest that the allowance of HA cement surface to promote organization of late FN matrix would be a beneficial property in respect to osteoinductivity.

2.5.3 Development of Extracellular Matrix on Different Rough Titanium Surfaces

The development of bone-implant interfaces depend on the direct interactions of osteoblasts and the subsequent deposition of bone matrix. Therefore, the proper cell adhesion and the formation of ECM are essential steps for the successful osseointegration of any material (Engel et al. 2008; Jayaraman et al. 2004). Although controversial results exist (Lange et al. 2002), the fact that surface topography strongly influences the behavior of adhering cells is widely accepted in the literature (Richards 1996; Boyan et al. 2001; Schwartz et al. 1996), and particularly for the Titanium (Ti) surface (Engel et al. 2008; Jayaraman et al. 2004; Lange et al. 2002; Richards 1996; Boyan et al. 2001; Schwartz et al. 1996; Chesmel et al. 1995; Aparicio et al. 2002) which at present is probably the most widely used biomaterial. For example fibroblasts adhering on grooved Ti surface extend their body in the direction of surface grooves and these aligned cells attach better than the spherical ones (Anselme et al. 2000). Similar orientations on grooved surfaces undergo osteoblasts (Eisenbarth et al. 2002; Ponsonnet et al. 2003); on smooth substrate they were found randomly oriented, while they line up in parallel to the grooves of 5 μm deep. Conversely, the osteoblasts did not assess topography of 0.5 μm (Eisenbarth et al. 2002) (Fig. 2.16).

To learn more about the effect of surface topography MG-63 osteoblasts-like cell were cultured on substrate disks of cp-Titanium (Ti) blasted with different sized SiC or Al_2O_3 particles to produce surfaces with defined and gradually increasing roughness (Ponsonnet et al. 2003). The roughness parameters R_a and R_l characterized via light interferometry showed a significant and stepwise increase with augmenting the blasting particles size (not shown here) (Ponsonnet et al. 2003).

FITC-labeled FN was adsorbed on these surfaces (marked A3, A6 and A9 for aluminum and S3, S6 and S9, respectively, for Si blasting particles) and studied for its 3D organization by LSM (Fig. 2.17). The amount of adsorbed FN was quantified

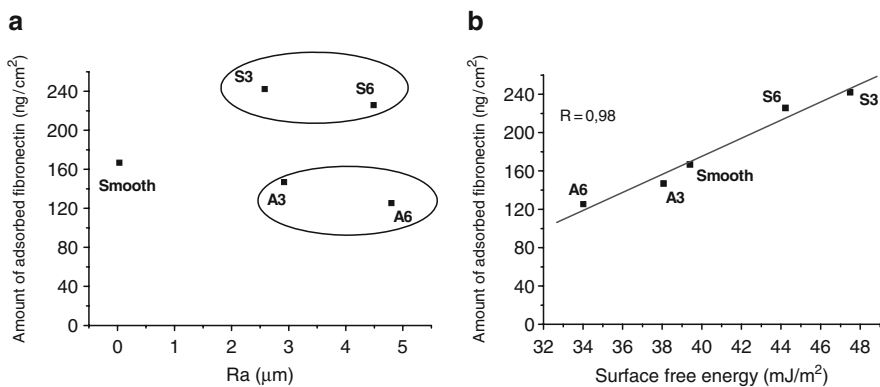


Fig. 2.16 Fibronectin adsorption profile in correlation with: (a) roughness parameter R_a and (b) surface free energy of different Ti surfaces

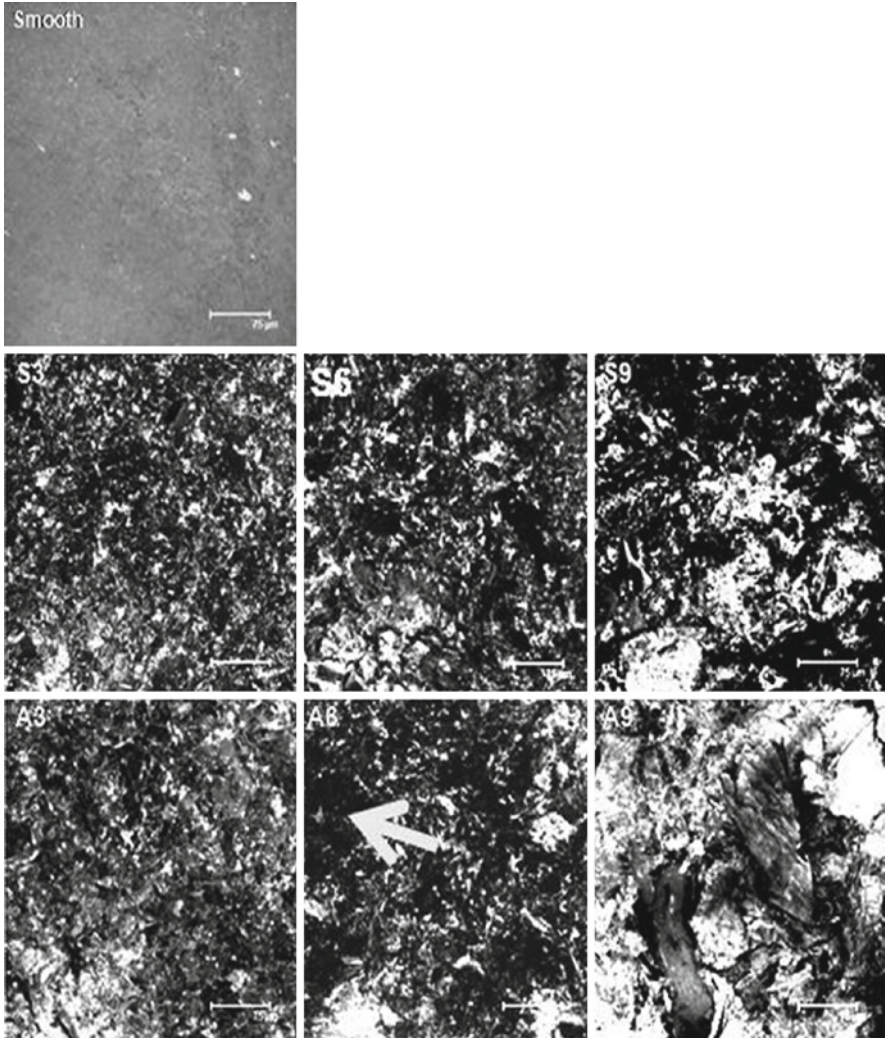


Fig. 2.17 3D reconstructed images of FITC-labeled fibronectin adsorbed on the different Ti samples. “Smooth” represents plane non-blasted Ti surface. The roughness of silica (S_{3-9}) or aluminum (A_{3-9}) particle blasted surfaces increase step-wise from *left* to *right* (Ponsonnet et al. 2003)

after NaOH extraction and was found to correlate positively with the values of SFE ($r = 0.986$) (Fig. 2.16, right), but not with the roughness parameter Ra (left panel). An irregular pattern of FN adsorption (Fig. 2.17), more at peaks than at valleys of the underlining topography, was observed apart from its homogenous distribution on smooth Ti surface.

Adhesion of MG 63 cells tended to increase with augmenting the roughness (Fig. 2.18). It is interesting to note that although the cells spread less with increasing

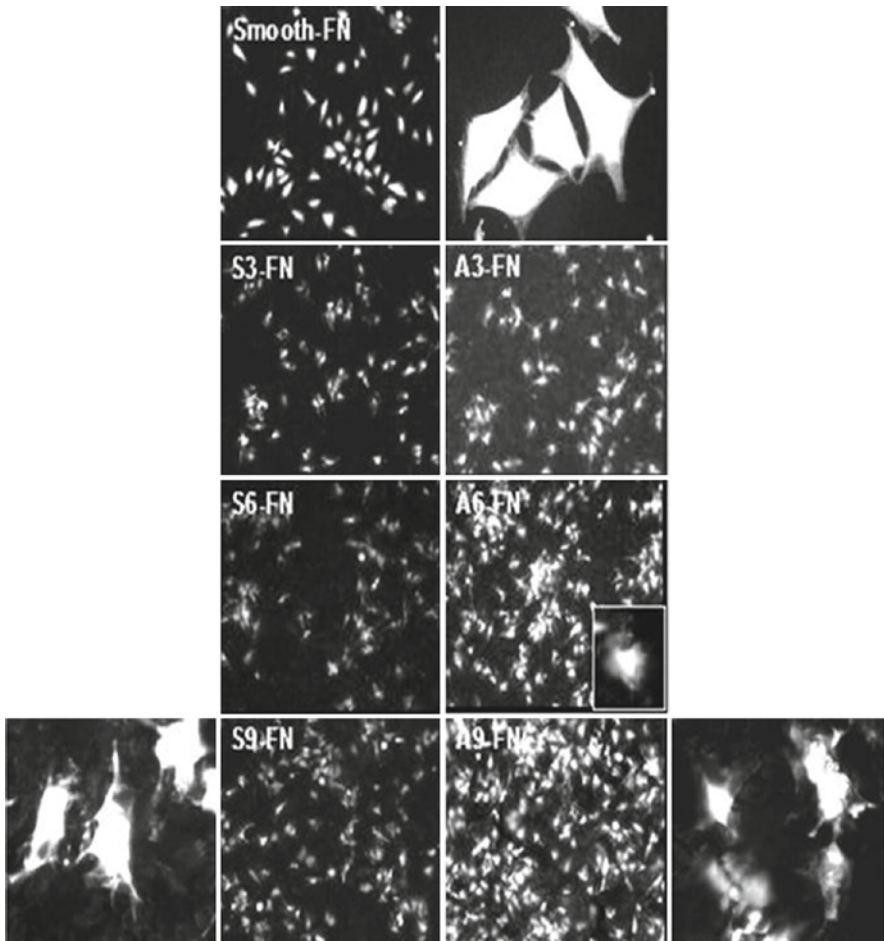


Fig. 2.18 Overall morphology of adhering MG63 cells viewed with fluorescein diacetate. All Ti samples were pre-coated with fibronectin. Stellate morphology is viewed at higher magnification (1000 \times) (Ponsonnet et al. 2003)

roughness they developed a rather stellate morphology – a typical shape for cells cultured in 3D environment. One can support that MG 63 cells respond on topography because they sense the adsorbed FN in its third dimension.

The overall organization of secreted FN matrix at fourth day of incubation (Fig. 2.19) shows, that on rough Ti surfaces it appears thicker and did not follow the unevenness of the underlining topography. Instead, FN matrix grows as film like structure that overly the top of the samples. To learn more about the overall 3D organization of FN matrix, the fluorescent images were reconstituted simultaneously with the topography viewed at the LSM reflection mode (not shown). Precise measurements at the seventh day of culture revealed that increasing the dimensions

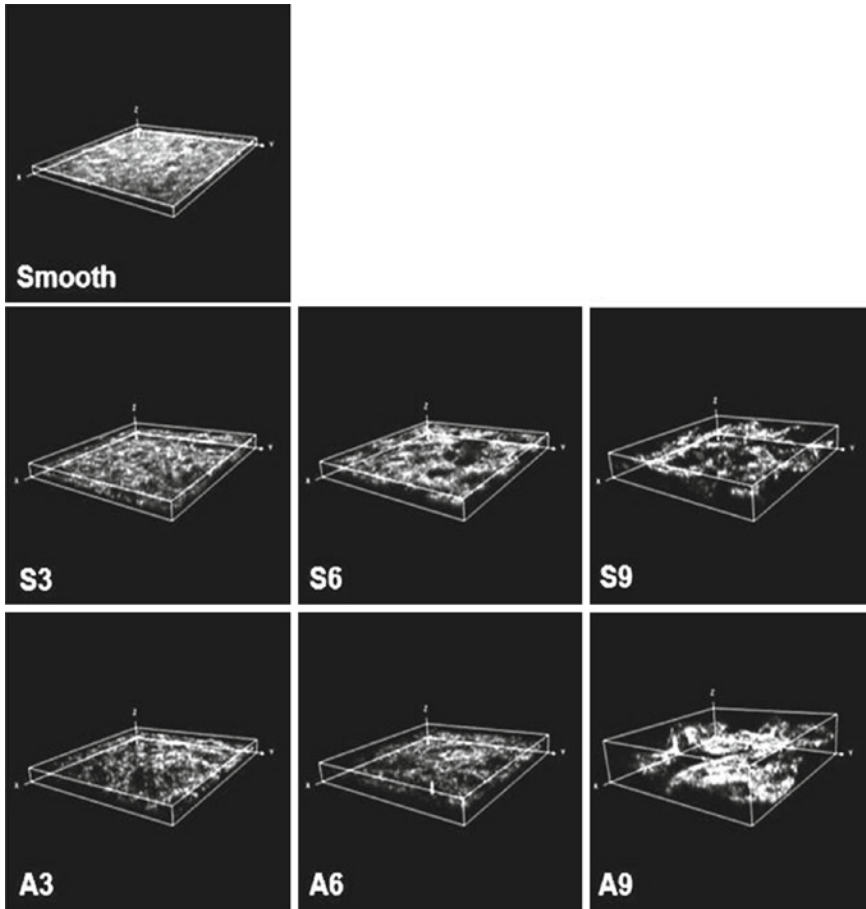


Fig. 2.19 3D reconstruction of the extracellular fibronectin matrix formed by MG63 cells on different Ti samples. Images were obtained by LSM (Z stack mode) at magnification $\times 60$ and viewed by the corresponding software (Ponsonnet et al. 2003)

of underlying topography result in a proportional augmenting the thickness of FN matrix, however, without penetrating more than $1/2$ in depth (i.e. the cross point, see the graph inserted in the Table 2.1).

The main observation from this study (Ponsonnet et al. 2003) that the newly developed FN matrix overly only the upper part of the rough Ti surface and did not penetrate more than a half from the peak to valley distance rises the possibility that on very rough surfaces the cells may tend to ignore topography.

Systematic studies of Boyan's group (Richards 1996; Boyan et al. 2001) shows that cells cultured on microrough Ti exhibited reduced proliferation and enhanced differentiation when compared to smooth Ti substrates, a fact that was also confirmed in our previous studies (Pegueroles et al. 2009). Collectively all this suggests that

Table 2.1 Some dimensions of the secreted fibronectin matrix corroborated with the topography parameters (Ponsonnet et al. 2003)

Samples	Ry (um)	ECM (um)	Cross point (um)	Above ECM (um)	Graph parameters
Control	\emptyset	11.295 ± 0.666	\emptyset	\emptyset	
Smooth	15.267 ± 2.678	11.255 ± 1.367	5.682 ± 1.592	1.670 ± 1.707	
S3	25.691 ± 2.336	16.379 ± 2.109	12.194 ± 1.405	2.882 ± 1.417	
S6	29.339 ± 3.529	18.397 ± 2.311	16.265 ± 2.684	5.323 ± 1.449	
S9	48.768 ± 6.864	27.503 ± 3.233	24.630 ± 3.769	3.365 ± 2.575	
A3	35.436 ± 2.011	18.215 ± 1.353	20.396 ± 2.253	3.175 ± 1.885	
A6	41.518 ± 5.433	23.052 ± 4.413	19.150 ± 1.948	0.684 ± 0.920	
A9	50.955 ± 7.028	26.206 ± 3.529	24.953 ± 4.421	0.204 ± 0.645	

the cells reside rather well on rough Ti interface. Therefore, further experiments are now under way to evaluate the strength of matrix-to-substratum interaction, which will be a direct link to the osseointegration.

References

- Altankov G, Grinnell F (1995) Fibronectin receptor internalization and AP-2 complex reorganization in potassium depleted fibroblasts. *Exp Cell Res* 216:299–309
- Altankov G, Groth Th (1994) Reorganization of substratum-bound fibronectin on hydrophilic and hydrophobic materials is related to biocompatibility. *J Mater Sci: Mater Med* 5:732–737
- Altankov G, Groth Th (1996) Fibronectin matrix formation and the biocompatibility of materials. *J Mater Sci: Mater Med* 7:425–429
- Altankov G, Groth Th, Krasteva N, Albrecht W, Paul D (1997) Morphological evidence for different fibronectin receptor organization and function during fibroblast adhesion on hydrophilic and hydrophobic glass substrata. *J Biomater Sci Polym Ed* 8:721–740
- Altankov G, Hecht J, Dimoudis N (2001) Serum-free cultured keratinocytes fail to organize fibronectin matrix and possess different distribution of beta-1 integrins. *Exp Dermatol* 10:80–89
- Altankov G, Albrecht W, Richau K, Groth Th, Lendlein A (2005) On the tissue compatibility of poly(ether imide) membranes: an in vitro study on their interaction with human dermal fibroblast and keratinocytes. *J Biomater Sci Polym Ed* 16(1):23–42
- Anselme K, Bigerelle M, Noel B, Dufresne E, Judas D, Iost A, Hardouin P (2000) Qualitative and quantitative study of human osteoblast adhesion on materials with various surface roughnesses. *J Biomed Mater Res* 49:155–166
- Aparicio C, Gil FJ, Planell JA, Engel E (2002) Human osteoblast proliferation and differentiation on grit-blasted and bioactive titanium for dental applications. *J Mater Sci: Mater Med* 13:1105–1111
- Baumann WH, Lehmann M, Schwinde A, Ehret R, Brischwein M, Wolf B (1999) Microelectric sensor system for microphysiological application on living cells. *Sens Actuat B* 55:77–89
- Boyan BD, Lohmann CH, Dean DD, Sylvia VL, Cochran DL, Schwartz Z (2001) Mechanisms involved in osteoblast response to implant surface morphology. *Annu Rev Mater Res* 31:357–371
- Chesmel KD, Clark CC, Brighton CT, Black J (1995) Cellular-responses to chemical and morphologic aspects of biomaterial surfaces. Biosynthetic and migratory response of bone cell-populations. *J Biomed Mater Res* 29:1101–1110
- Clark RA, Lanigan JM, DellaPelle P, Manseau E, Dvorak HF, Colvin RB (1982) Fibronectin and fibrin provide a provisional matrix for epidermal cell migration during wound reepithelialization. *J Invest Dermatol* 79:264–269
- Coelho NM, Sánchez MS, Plannell J, Altankov G (2009) Assembly of adsorbed type IV collagen on hydrophilic and hydrophobic substrata determine its biological activity (under preparation)
- Deligianni DD, Katsala ND, Koutsoukos PG, Missirlis YF (2001) Effect of surface roughness of hydroxyapatite on human bone marrow cell adhesion, proliferation, differentiation and detachment strength. *Biomaterials* 22(1):87–89
- Denen EHJ, Sonneveld P, Brakebusch C, Fassler R, Sonneberg A (2002) The fibronectin binding integrins $\alpha 5\beta 1$ and $\alpha v\beta 3$ differentially modulate RhoA-GTP loading, organization of cell matrix adhesionism and fibronectin fibrillogenesis. *J Cell Biol* 159:1071–1086
- Donaldson DJ, Mahan JT, Amrani D, Hawiger J (1989) Fibrinogen-mediated epidermal cell migration: structural correlates for fibrinogen function. *J Cell Sci* 94:101–108
- Eisenbarth E, Linez P, Biehl V, Velten D, Breme J, Hildebrand HF (2002) Cell orientation and cytoskeleton organisation on ground titanium surfaces. *Biomol Eng* 19:233–237

- Engel E, Del Valle S, Aparicio C, Altankov G, Asin L, Planell JA, Ginebra MP (2008). Discerning the role of topography and ion exchange in cell response to bioactive tissue engineering scaffolds. *Tissue Engineering Part A* 14(8):1341–1351
- Ginebra MP, Driessens FC, Planell JA (2004) Effect of the particle size on the micro and nano-structural features of a calcium phosphate cement: a kinetic analysis. *Biomaterials* 25(17): 3453–3462
- Griffin L, Naughton G (2002) Tissue engineering – current challenges and expanding opportunities. *Science* 259:1009–1014
- Grinnell F (1986) Focal adhesion sites and the removal of substratum-bound fibronectin. *J Cell Biol* 103:2697–2706
- Gronowicz G, DeRome ME, McCarthy MB (1991) Glucocorticoids inhibit fibronectin synthesis and messenger RNA levels in cultured rat parietal bones. *Endocrinology* 128:1007–1114
- Groth Th, Altankov G (1996) Studies on the cell-biomaterial interaction: role of tyrosine phosphorylation during fibroblasts spreading on surfaces varying in wettability. *Biomaterials* 17:1227–1234
- Gustavsson J, Altankov G, Errachid A, Samitier J, Planell J, Engel E (2007) Surface modifications of silicon nitride for biosensors application. *J Mater Sci: Mater Med* 19(4):1839–1850
- Henche LL, Polak JM (2002) Third generation biomedical materials. *Science* 259:1014–1017
- Hynes RO (1990) *Fibronectins*. Springer, New York
- Hynes RO (2002) Integrins: bidirectional, allosteric signaling machines. *Cell* 110:673–678
- Jayaraman M, Meyer U, Buhner M, Joos U, Wiesmann HP (2004) Influence of titanium surfaces on attachment of osteoblast-like cells in vitro. *Biomaterials* 25:625–631
- Kue R, Sohrabi A, Nagle D, Frondoza C, Hungerford D (1999) Enhanced proliferation and osteocalcin production by human osteoblast like MG-63 cells on silicon nitride ceramic discs. *Biomaterials* 20:1195–1201
- Lange R, Luthen F, Beck U, Rychly J, Baumann A, Nebe B (2002) Cell-extracellular matrix interaction and physico-chemical characteristics of titanium surfaces depend on the roughness of the material. *Biomol Eng* 19:255–261
- Lowenstain HA, Weiner S (1989) *On biomineralisation*. Oxford University Press, Oxford
- Lutolf MP, Hubbell JA (2005) Synthetic biomaterials as instructive extracellular microenvironments for morphogenesis in tissue engineering. *Nat Biotechnol* 23(1):47–55
- Maneva-Radicheva L, Ebert U, Dimoudis N, Altankov G (2008) Fibroblast remodeling of collagen type IV is altered in contact with cancer cells. *Histol Histopathol* 23:833–841
- Mauri AM, Damsky CH, Lull J, Zimmerman D, Doty S, Aota S-I, Globus RK (1996) Fibronectin regulates calvarial osteoblasts differentiation. *J Cell Sci* 109:1369–1380
- Neumann A, Reske T, Held M, Jahnke K, Ragov C, Maier HR (2004) Comparative investigation of the biocompatibility of various silicon nitride ceramic qualities in vitro. *J Mater Sci: Mater Med* 15(10):1135–1140
- Nordahi J, Mangarelli-Widholm S, Hulthen K, Reinhold FP (1995) Ultrastructural immunolocalization of fibronectin in epiphyseal and metaphyseal bone of young rats. *Calcif Tissue Int* 57:442–449
- Pankov R, Cukierman E, Katz B-Z, Matsumoto K, Lin DC, Lin Sh, Hahn C, Yamada K (2000) Integrin dynamics and Matrix Assembly: tensin-dependent translocation of $\alpha 5 \beta 1$ Integrins promotes Early Fibronectin Fibrillogenesis. *J Cell Biol* 148:1075–1090
- Pegueroles M, Bosio M, Gil FJ, Planell JA, Engel E, Aparicio C, Altankov G (2009) Development of early fibronectin matrix by osteoblasts on different rough titanium interface. *Acta Biomater* (in press). Available in Internet. doi:10.1016/j.actbio.2009.07
- Pereira M, Rybarczyk BJ, Odrlijn TM, Hocking DC, Sottile J, Simpson-Haidaris J (2002) The incorporation of fibrinogen into extracellular matrix is dependent on active assembly of a fibronectin. *J Cell Sci* 115:609–617
- Ponsonnet L, Reybier K, Jaffrezic N, Comte V, Lagneau C, Lissac M, Martelet C (2003) Relationship between surface properties (roughness, wettability) of titanium and titanium alloys and cell behaviour. *Mater Sci Eng C-Biomim Supramol Syst* 23:551–560

- Richards RG (1996) The effect of surface roughness on fibroblast adhesion in vitro. *Inj-Int J Care Inj* 27:38–43
- Schöning MJ, Thust M, Müller-Veggian M, Kordoš P, Lüth H (1998) A novel silicon-based sensor array with capacitive EIS structures. *Sens Actuat B* 47:225–230
- Schwartz Z, Martin JY, Dean DD, Simpson J, Cochran DL, Boyan BD (1996) Effect of titanium surface roughness on chondrocyte proliferation, matrix production, and differentiation depends on the state of cell maturation. *J Biomed Mater Res* 30:145–155
- Sohrabi A, Holland C, Kue R, Nagle D, Hungerford DS, Frondoza CG (2000) Proinflammatory cytokine expression of IL-1 and TNF- by human osteoblast-like MG-63 cells upon exposure to silicon nitride in vitro. *J Biomed Mater Res* 50(1):43–49
- Spie J (2002) Tissue engineering and reparative medicine. *Ann NY Acad Sci* 961:1–9
- Thiery JP (2003) Cell adhesion in development: a complex signaling network. *Curr Opin Genet Dev* 13:365–371
- Tzoneva R, Groth Th, Altankov G, Paul D (2002) Remodeling of fibrinogen by endothelial cells in dependence of fibronectin matrix assembly. Effect of substratum wettability. *J Mater Sci Mater Med* 13:1235–1244
- Yamad KM, Pankov R, Cuyerman E (2003) Dimensions and dynamics of integrin function. *J Med Biol Res* 36:959–966
- Yuasa T, Miyamoto Y, Ishikawa K, Takechi M, Momota Y, Tatehara S, Nagayama M (2004) Effects of apatite cements on proliferation and differentiation of human osteoblasts in vitro. *Biomaterials* 25:1159–1166
- Zamir E, Geiger B (2001) Molecular complexity and dynamics of cell-matrix adhesions. *J Cell Sci* 114:3583–3590
- Zlatanov A, Groth Th, Lendlein A, Altankov G (2005) Dynamics of β 1- integrin in living fibroblast-effect of substratum wettability. *Biophys J* 89:3555–3562

Chapter 3

Endothelial Progenitor Cells for Tissue Engineering and Tissue Regeneration

Endothelial Progenitor Cells

Joyce Bischoff

Abstract Vascularization of tissues is a major challenge of tissue-engineering and tissue regeneration. We hypothesize that blood-derived endothelial progenitor cells (EPCs) have the required proliferative and vasculogenic activity to create vascular networks in vivo. To test this, EPCs from human umbilical cord blood or from adult peripheral blood, and human smooth muscle cells as a source of perivascular cells, were combined in Matrigel and implanted subcutaneously into immunodeficient mice. An extensive network of human endothelial cell-lined vessels filled with red blood cells was seen after 1 week, indicating formation of functional anastomoses with the host vasculature. Quantitative analyses showed the microvessel density was significantly superior to that generated by human dermal microvascular endothelial cells but similar to that generated by human umbilical vein endothelial cells. Our findings strongly support the use of human EPCs to form vascular networks in engineered organs and tissues and for regeneration of vascular networks in vivo. In this Chapter, previous studies on strategies for creating microvascular networks, sources of endothelial cells and EPCs for cardiovascular tissue-engineering and studies using bone marrow-derived progenitors for tissue regeneration will be discussed.

Keywords Endothelial progenitor cells (EPCs) • Vasculogenesis • Angiogenesis • Microvascular networks • Human endothelial cells

J. Bischoff (✉)
Vascular Biology Program and Department of Surgery,
Children's Hospital Boston and Harvard Medical School,
Boston, MA 02115, USA
e-mail: joyce.bischoff@childrens.harvard.edu

3.1 Introduction

Nearly all of the organs and tissues in the human body require a healthy vascular network to deliver oxygen and nutrients. Hence, it is widely accepted in the field of tissue-engineering (TE) that a vascular network must be incorporated into a TE construct, or its formation rapidly induced after *in vivo* implantation, in order for the nascent organ or tissue to survive (Nomi et al. 2002). For tissue regeneration, it is well-established that formation of new blood vessels is required. For example, liver regeneration that occurs after hepatectomy requires angiogenesis (Drixler et al. 2002) and the extent of angiogenesis in the regenerating liver may even dictate the eventual organ mass (Folkman 2007). Bone formation requires a vascular network, with recent studies showing hypoxia-inducible factor- α (HIF- α) as a critical link between osteogenesis and angiogenesis (Wang et al. 2007). In TE experiments, co-implantation of endothelial cells with bone marrow stromal cells (MSCs) has been reported to stimulate bone formation by the MSCs (Kaigler et al. 2005), suggesting that the endothelium provides signals for tissue regeneration that go beyond the delivery of oxygen and nutrients. Further evidence that the vasculature provides inductive cues comes from studies on organ development during embryogenesis: two landmark papers showed that signals derived from endothelial cells are required for proper development of the pancreas and liver (Lammert et al. 2001; Matsumoto et al. 2001). In summary, the vasculature provides not only critically needed delivery of oxygen and nutrients but may also drive tissue development and tissue regeneration. Thus, the importance of vascular networks for TE may be twofold.

3.2 Vascular Networks for TE Constructs

A variety of approaches have been proposed to vascularize TE constructs. These strategies include embedding an angiogenic factor, e.g., basic FGF (Lee et al. 2002), or receptors needed for vascular development, e.g., ephrin-A1 (Moon et al. 2007) into the scaffold to promote ingrowth and assembly of host microvessels. An exciting new area is self-assembling nanostructures coated with heparin which in turn can bind bFGF or VEGF; the authors showed that these structures stimulate new blood vessel formation *in vivo* and propose that these nanostructures could be used to promote neovascularization for TE (Rajangam et al. 2006). Technologies to create microfluidic networks seeded with endothelial cells suggest the possibility of creating pre-fabricated vascular channels (Chrobak et al. 2006; Golden and Tien 2007). Recently, endothelial cells cultured on patterned substrates generated by optical lithography were shown to form tubular networks when transferred to tissue and implanted into mice (Kobayashi et al. 2007). Several microfabrication technologies are being used to create endothelial-lined channels directly within a biocompatible scaffold, as reviewed by Langer, Vacanti and colleagues (Khademhosseini et al. 2006). The strategy described herein will rely on the inherent vasculogenic capability of EPCs to form physiologic vascular networks.

3.3 Sources of Human Endothelial Cells for TE Vascular Networks

3.3.1 Mature Vessel-Derived Endothelial Cells

For any of the above mentioned strategies, it will be important to identify the most suitable sources of endothelial cells. The feasibility of using human endothelial cells to pre-construct a microvascular network *in vitro* was shown by Schechner and colleagues (Schechner et al. 2000; Enis et al. 2005). In these studies, human umbilical vein endothelial cells (HUVECs) genetically modified to express caspase-resistant Bcl-2 were embedded in collagen/fibronectin gels for 24 h to allow assembly into tubular structures. The constructs were then implanted into immunodeficient mice; a microvascular network formed after 31 days with multi-layered vessel structures seen after 60 days. In a similar study, human dermal microvascular endothelial cells (HDMECs) seeded on biopolymer constructs were also shown to form human microvessels after 21 days (Nor et al. 2001). These studies clearly demonstrated the feasibility of using mature human endothelial cells to construct microvessels *in vivo*. However, the requirement for Bcl-2 expression to minimize apoptosis and the time frame needed for vessel formation may preclude therapeutic use. Furthermore, the clinical use of mature ECs derived from healthy autologous vascular tissue would pose certain limitations: the isolation relies on an invasive procedure and sacrifice of healthy tissue, mature ECs show relatively low proliferative potential and it is difficult to obtain a sufficient number of cells from a small biopsy of autologous tissue. These limitations have prompted the search for other sources of ECs with more proliferative and vasculogenic activities.

3.3.2 Human Embryonic Stem Cells

Embryonic stem cells (ESCs) have been studied in many laboratories for potential to differentiate into vascular structures. For example, murine ESCs are well known for ability to form CD31+ or PECAM-1+ structures within embryoid bodies *in vitro*. Furthermore, vascular progenitors with both endothelial and smooth muscle cell differentiation potential have been identified in murine embryos (Yamashita et al. 2000). More recently, the endothelial differentiation potential of human ESCs has been explored in many laboratories (Levenberg et al. 2002; Gerecht-Nir et al. 2003). Similar to murine embryoid bodies, endothelial differentiation becomes evident in three-dimensional human embryoid bodies after 10–15 days of culture. However, in two-dimensional cultures, the endothelial character of the cells was less apparent. Furthermore, the studies on endothelial functional capabilities of hESC-derived endothelium are somewhat limited at this time – for review see (Levenberg et al. 2007). One recent study showed that seeding of endothelial cells derived from embryonic stem cells along with myoblasts and

embryonic fibroblasts resulted in the formation of skeletal muscle tissue (Levenberg et al. 2005). At present, ethical considerations along with a nascent understanding of the mechanisms controlling the differentiation of embryonic stem cells are hurdles that need to be overcome before these cells can be used in a clinical setting.

3.3.3 *Blood-Derived EPCs*

Peripheral blood represents a third source of human endothelial cells that can be used to create vascular networks for tissue engineering or regeneration applications. The presence of endothelial progenitor cells (EPCs) circulating in blood has been studied intensively for nearly a decade since the seminal reports from the Isner and colleagues (Asahara et al. 1997) and Hebbel and colleagues (Lin et al. 2000). The EPCs that will be discussed here are defined by (a) high proliferative capacity in vitro (over 70 population doublings); (b) expression of endothelial markers and lack of expression of hematopoietic markers (CD45 and CD14) or mesenchymal markers (CD90); and (c) ability to form blood vessels in vivo. Importantly, the EPCs are well-delineated from the hematopoietic cells sometimes referred to as EPCs or “early EPCs” (Yoder et al. 2007).

The feasibility of using blood-derived EPCs for cardiovascular TE has been established in large animal models. For example, we reported in 2001 that autologous ovine EPCs expanded ex vivo could be used to make TE neovessels that showed patency and arterial function in vivo (Kaushal et al. 2001). Subsequent in vitro studies by others showed that such an approach could be attempted with human blood-derived EPCs (Shirota et al. 2003). TE of blood vessels from human umbilical cord blood-derived EPCs and vessel wall-derived myofibroblasts has also been demonstrated in vitro (Schmidt et al. 2005; Schmidt et al. 2006a). (TE of small-diameter blood vessels with human cells is limited to in vitro studies because of a lack of immunodeficient large animals, such as sheep, in which many TE approaches have been pioneered. Furthermore, TE small-diameter vessels appropriate for mouse or rat, for which immunodeficient strains are available, are technically challenging from a surgical standpoint. A recent study expanded upon the sheep and human studies by creating TE jugular veins using sheep blood-derived EPCs and bone marrow-derived SMPC; the TE venular segments showed excellent histology, including organized elastin fibrils (Liu et al. 2007).

EPCs have also been used to construct TE heart valves for replacement of the pulmonary valve in children born with congenital heart defects. In one study, EPCs from cord blood and fetal mesenchymal progenitor cells isolated from chorionic villus sampling were used to construct TE heart valve; the in vitro results showed the TE valves were highly comparable to native neonatal heart valves (Schmidt et al. 2006b). TE heart valves created by seeding autologous peripheral blood-derived EPCs onto de-cellularized human PV allografts have been implanted in two pediatric patients, ages 11 and 13, with follow-up at 3.5 years indicating good function and growth (Cebotari et al. 2006). These studies further indicate the promise and progress of EPCs for cardiovascular TE and TE in general.

3.3.4 Bone Marrow-Derived Cells for Tissue Vascularization

Bone marrow is an accessible source of stem/progenitor cells that has been studied extensively over the past several years in order to elucidate cellular/molecular mechanisms and to develop cell-based therapies, including TE approaches. The types of stem/progenitor cells in bone marrow include hematopoietic stem cells, mesenchymal stromal or stem cells (MSCs)(Pittenger et al. 1999), endothelial progenitor cells (EPCs)(Asahara et al. 1999), smooth muscle-like progenitors(SMPCs)(Shimizu et al. 2001) and cardiac progenitor cells (CPCs)(Orlic et al. 2001; Ballard and Edelberg 2007). Some therapeutic approaches have involved mobilization of stem/progenitor cells to leave the bone marrow with the hope that the cells will home to sites where needed. Attempts to specify the homing process have been pursued, for example using anti-CD34-coated stents to attract EPCs to provide an endothelial lining at sites of vascular stenosis (Rotmans et al. 2005). However, the adherence of CD34-positive cells resulted in increased neointimal hyperplasia despite the efficient endothelialization (Rotmans et al. 2005). Some successes have been reported with unfractionated nucleated bone marrow-derived cells. Shin'oka and colleagues have used autologous bone marrow cells harvested at the time of surgery to seed vascular conduits and patches constructed from a biodegradable scaffold. Studies are ongoing, but results up to 32 months after surgery indicate vascular patency and function (Shin'oka et al. 2005).

The delivery of bone marrow- derived cells to sites of limb and myocardial ischemia has been studied in mice and evaluated in clinical trials in humans. Itescu and colleagues have suggested that improving homing of bone marrow endothelial precursors to the myocardium will increase vasculogenesis and angiogenesis and thereby help to maintain cardiomyocyte viability, reduce collagen deposition and improve cardiac function – for review see (Itescu et al. 2003). One of the first papers to attract attention to this concept tested the effect of locally-injected eGFP-labeled bone marrow cells, purified by negative selection for blood cell lineage markers and positive selection for c-kit, into viable myocardium surrounding an infarcted region in mice (Orlic et al. 2001). Another early study showed that bone marrow endothelial precursors or angioblasts could directly contribute to new blood vessel formation at the site of myocardial infarction and indirectly stimulate the proliferation of pre-existing vessels; the long term net effect was an attenuation of nearly all of the events leading to cardiac remodeling (Kocher et al. 2001). Follow-up studies from the same group showed that increasing the number of endothelial precursors in ischemic myocardium resulted in improved cardiac function, decreased apoptosis and proliferation of cardiomyocytes (Schuster et al. 2004). These studies, and work from many other laboratories, have led to clinical trials in humans. One clinical trial used blood-derived cells expanded *ex vivo* for a period of time as well as bone marrow-derived mononuclear cells. The cells were delivered within 7 days to >3 months after myocardial infarction into coronary vessels supplying the affected region of the heart (For review and most recent update on the trial see Ballard and Edelberg 2007; Assmus et al. 2007). A second study isolated CD34+ progenitor cells from the blood of patients with intractable angina

and, after thorough ex vivo analyses, injected the cells intramyocardially (Losordo et al. 2007). These studies highlight the use of patient-derived cells for in situ tissue regeneration. Although a promising area of research, the concerns regarding the use of bone marrow-derived cells are (a) the heterogeneity of the cell populations, including the CD34-positive cells, (b) the insufficient understanding of the cellular differentiation pathways that might occur in different pathological settings and how this might impact long-term outcomes, and (c) an incomplete understanding of the cellular mechanisms involved.

3.4 Blood-Derived EPCs for Creating Vascular Networks

As presented at the NATO Advanced Research Workshop entitled “Nanoengineered Systems for Regenerative Medicine” in September 2007, we reported in 2007 that cord blood EPCs, as well as adult peripheral blood EPC, are able to form vascular networks with anastomoses to the murine circulation after 7 days in vivo when combined with human SMCs (Melero-Martin et al. 2007).

3.4.1 Isolation and Culture of Human EPCs and HSVSMCs

Both cord blood-derived EPCs (cbEPCs) and adult peripheral blood-derived EPCs were obtained from the mononuclear cell (MNC) fraction isolated from 25 ml of cord blood or 50 ml of adult peripheral blood using Ficoll-histopaque and Accuspin columns from Sigma-Aldrich Inc. MNCs were seeded on 1% gelatin-coated tissue culture plates in Endothelial Basal Medium (EBM-2), 20% FBS (Hyclone, Logan, UT), 1× glutamine-penicillin-streptomycin (GPS; Invitrogen, Carlsbad, CA), 15% autologous plasma, and SingleQuots. EBM-2 and SingleQuots are commercially available from Lonza Biologics, Inc. The hydrocortisone aliquot was omitted from the SingleQuots. Forty-eight hours after plating cord blood MNCs, or 4 days after plating adult peripheral blood MNCs, unbound cells were removed and the adherent cell fraction was then maintained in culture using EBM-2 supplemented with 20% FBS, SingleQuots (except for hydrocortisone) and 1× GPS (this medium is referred to as EBM-2/20%). Colonies of endothelial-like cells were allowed to grow until confluence, trypsinized and purified using CD31-coated magnetic beads (DynaL Biotech, Brown Deer, WI). CD31-selected EPCs were serially passaged and cultured on fibronectin-coated (FN; 1 µg/cm²; Chemicon International, Temecula, CA) plates at a density of 5×10^3 cell/cm² in EBM-2/20%. Human saphenous vein smooth muscle cells (HSVSMCs) were grown in DMEM (Invitrogen), 10% FBS, 1× GPS and 1× non-essential amino acids (Sigma-Aldrich, Inc). Sufficiently large numbers of EPCs from cord blood and adult peripheral blood were obtained in 4–6 weeks from several different cord blood and adult peripheral blood donors (Melero-Martin et al. 2007). Both EPCs and HSVSMCs were characterized extensively

by flow cytometry, western blotting and RT-PCR for expression of phenotypic markers to firmly establish the homogeneity and expected characteristics of these cell populations (Melero-Martin et al. 2007).

3.4.2 In Vivo Assay for Vascularization

The in vivo assay used will be described briefly here. Adult peripheral blood or cord blood EPCs were combined with human saphenous vein SMCs (HSVSMCs) (total 1.9×10^6 cells) in 200 μ l of ice-cold Matrigel. The HSVSMCs served as a source of perivascular cells, as our previous studies had shown would be required (Wu et al. 2004). The cell/Matrigel suspension was injected subcutaneously into immunodeficient male mice at 6 weeks of age. Matrigel forms a gel at 37°C effectively localizing the cells in vivo.

At specified time points, but typically at 7 days, the Matrigel implants were harvested from the mice, processed for paraffin-sectioning, and stained with hematoxylin and eosin (H&E). Functional blood vessels were counted as luminal structures containing murine red blood cells (RBCs), which were readily apparent in the H&E sections. The average vessel density seen after 7 days in vivo was 47.5 ± 8 microvessels/ mm^2 indicating robust vasculogenesis. Matrigel containing either cbEPCs or HSVSMCs alone failed to form microvessels after 1 week, indicating a requirement for a two-cell system to construct vascular networks in a reasonable time frame in a relatively short time frame. Previous studies using mature human ECs alone detected microvessels in implants in immunodeficient mice at 21–30 days. As an additional control, injections of Matrigel alone resulted in the appearance of few host cells infiltrated into the borders of the implants but no vascular structures. To verify that vessel lumens were composed of human endothelial cells, sections were stained with a human-specific CD31 antibody (Melero-Martin et al. 2007). The location of the smooth muscle cells was detected using anti- α -SMA. Importantly, this two-cell system contained no added growth factors or supplements. Prior to injection, the cell monolayers were washed, harvested by trypsinization, resuspended in Matrigel and kept ice-cold until injection.

3.4.3 Summary: Vasculogenic Potential of Human EPCs

We reported that blood-derived EPCs have an inherent vasculogenic ability to create functional microvascular networks in vivo (Melero-Martin et al. 2007). Implantation of EPCs with HSVSMCs resulted in the formation of an extensive blood vessel network after 1 week in vivo. The presence of HSVSMCs was found to be critical, as EPCs alone did not form vessels at the 7 day time point. The presence of human EC-lined lumens containing murine erythrocytes throughout the implants indicated not only a process of vasculogenesis by the implanted cells, but also the

formation of functional anastomoses with the host circulatory system. Our results are the first to demonstrate the robust *in vivo* vasculogenic potential of blood-derived EPCs. A future goal will be to identify a source of smooth muscle cells or smooth muscle progenitors that can be obtained non-invasively, expanded into large numbers *in vitro* as a homogeneous population with defined characteristics, and used in place of vein-derived SMCS.

For tissue engineering and tissue regeneration applications, it is of interest to determine the time course and the sequence of events that leads to the formation of functional microvessels and how this might be accelerated and optimized. Our *in vivo* model of tissue vascularization is well-suited for the investigation of such strategies and for the study of the physiology of microvessel development. In summary, our results strongly support the therapeutic potential of using human EPCs to form vascular networks that will allow sufficient vascularization of engineered organs and tissues. For infants, other sources such as HUVECs may also be isolated and used for this purpose. Further efforts are required to implement strategies for controlled vasculogenesis in tissue engineered constructs using autologous vascular endothelial and smooth muscle cells obtained from perinatal and adult blood.

References

- Asahara T, Murohara T, Sullivan A, Silver M, van der Zee R, Li T, Witzenbichler B, Schatteman G, Isner JM (1997) Isolation of putative progenitor endothelial cells for angiogenesis. *Science* 275:964–967
- Asahara T, Masuda H, Takahashi T, Kalka C, Pastore C, Silver M, Kearne M, Magner M, Isner JM (1999) Bone marrow origin of endothelial progenitor cells responsible for postnatal vasculogenesis in physiological and pathological neovascularization. *Circ Res* 85:221–228
- Assmus B, Fischer-Rasokat U, Honold J, Seeger FH, Fichtlscherer S, Tonn T, Seifried E, Schachinger V, Dimmeler S, Zeiher AM (2007) Transcoronary transplantation of functionally competent BMCs is associated with a decrease in natriuretic peptide serum levels and improved survival of patients with chronic postinfarction heart failure: results of the TOPCARE-CHD Registry. *Circ Res* 100:1234–1241
- Ballard VL, Edelberg JM (2007) Stem cells and the regeneration of the aging cardiovascular system. *Circ Res* 100:1116–1127
- Cebotari S, Lichtenberg A, Tudorache I, Hilfiker A, Mertsching H, Leyh R, Breymann T, Kallenbach K, Maniuc L, Batrinac A et al (2006) Clinical application of tissue engineered human heart valves using autologous progenitor cells. *Circulation* 114:1132–1137
- Chrobak KM, Potter DR, Tien J (2006) Formation of perfused, functional microvascular tubes *in vitro*. *Microvasc Res* 71:185–196
- Drixler TA, Vogten MJ, Ritchie ED, van Vroonhoven TJ, Gebbink MF, Voest EE, Borel Rinke IH (2002) Liver regeneration is an angiogenesis-associated phenomenon. *Ann Surg* 236:703–711; discussion 711–702
- Enis DR, Shepherd BR, Wang Y, Qasim A, Shanahan CM, Weissberg PL, Kashgarian M, Pober JS, Schechner JS (2005) Induction, differentiation, and remodeling of blood vessels after transplantation of Bcl-2-transduced endothelial cells. *Proc Natl Acad Sci USA* 102:425–430
- Folkman J (2007) Angiogenesis: an organizing principle for drug discovery? *Nat Rev Drug Discov* 6:273–286

- Gerecht-Nir S, Ziskind A, Cohen S, Itskovitz-Eldor J (2003) Human embryonic stem cells as an in vitro model for human vascular development and the induction of vascular differentiation. *Lab Invest* 83:1811–1820
- Golden AP, Tien J (2007) Fabrication of microfluidic hydrogels using molded gelatin as a sacrificial element. *Lab Chip* 7:720–725
- Itescu S, Kocher AA, Schuster MD (2003) Myocardial neovascularization by adult bone marrow-derived angioblasts: strategies for improvement of cardiomyocyte function. *Heart Fail Rev* 8:253–258
- Kaigler D, Krebsbach PH, West ER, Horger K, Huang YC, Mooney DJ (2005) Endothelial cell modulation of bone marrow stromal cell osteogenic potential. *FASEB J* 19:665–667
- Kaushal S, Amiel GE, Guleserian KJ, Shapira OM, Perry T, Sutherland FW, Rabkin E, Moran AM, Schoen FJ, Atala A et al (2001) Functional small-diameter neovessels created using endothelial progenitor cells expanded ex vivo. *Nat Med* 7:1035–1040
- Khademhosseini A, Langer R, Borenstein J, Vacanti JP (2006) Microscale technologies for tissue engineering and biology. *Proc Natl Acad Sci USA* 103:2480–2487
- Kobayashi A, Miyake H, Hattori H, Kuwana R, Hiruma Y, Nakahama K, Ichinose S, Ota M, Nakamura M, Takeda S et al (2007) In vitro formation of capillary networks using optical lithographic techniques. *Biochem Biophys Res Commun* 358:692–697
- Kocher AA, Schuster MD, Szabolcs MJ, Takuma S, Burkhoff D, Wang J, Homma S, Edwards NM, Itescu S (2001) Neovascularization of ischemic myocardium by human bone-marrow-derived angioblasts prevents cardiomyocyte apoptosis, reduces remodeling and improves cardiac function. *Nat Med* 7:430–436
- Lammert E, Cleaver O, Melton D (2001) Induction of pancreatic differentiation by signals from blood vessels. *Science* 294:564–567
- Lee H, Cusick RA, Browne F, Ho Kim T, Ma PX, Utsunomiya H, Langer R, Vacanti JP (2002) Local delivery of basic fibroblast growth factor increases both angiogenesis and engraftment of hepatocytes in tissue-engineered polymer devices. *Transplantation* 73:1589–1593
- Levenberg S, Golub JS, Amit M, Itskovitz-Eldor J, Langer R (2002) Endothelial cells derived from human embryonic stem cells. *Proc Natl Acad Sci USA* 99:4391–4396
- Levenberg S, Rouwkema J, Macdonald M, Garfein ES, Kohane DS, Darland DC, Marini R, van Blitterswijk CA, Mulligan RC, D'Amore PA et al (2005) Engineering vascularized skeletal muscle tissue. *Nat Biotechnol* 23:879–884
- Levenberg S, Zoldan J, Basevitch Y, Langer R (2007) Endothelial potential of human embryonic stem cells. *Blood* 110:806–814
- Lin Y, Weisdorf DJ, Solovey A, Hebbel RP (2000) Origins of circulating endothelial cells and endothelial outgrowth from blood. *J Clin Invest* 105:71–77
- Liu JY, Swartz DD, Peng HF, Gugino SF, Russell JA, Andreadis ST (2007) Functional tissue-engineered blood vessels from bone marrow progenitor cells. *Cardiovasc Res* 75(3):618–628
- Losordo DW, Schatz RA, White CJ, Udelson JE, Veereshwarayya V, Durgin M, Poh KK, Weinstein R, Kearney M, Chaudhry M et al (2007) Intramyocardial transplantation of autologous CD34+ stem cells for intractable angina: a phase I/IIa double-blind, randomized controlled trial. *Circulation* 115:3165–3172
- Matsumoto K, Yoshitomi H, Rossant J, Zaret KS (2001) Liver organogenesis promoted by endothelial cells prior to vascular function. *Science* 294:559–563
- Melero-Martin JM, Khan ZA, Picard A, Wu X, Paruchuri S, Bischoff J (2007) In vivo vasculogenic potential of human blood-derived endothelial progenitor cells. *Blood* 109:4761–4768
- Moon JJ, Lee SH, West JL (2007) Synthetic biomimetic hydrogels incorporated with ephrin-A1 for therapeutic angiogenesis. *Biomacromolecules* 8:42–49
- Nomi M, Atala A, Coppi PD, Soker S (2002) Principles of neovascularization for tissue engineering. *Mol Aspects Med* 23:463–483
- Nor JE, Peters MC, Christensen JB, Sutorik MM, Linn S, Khan MK, Addison CL, Mooney DJ, Polverini PJ (2001) Engineering and characterization of functional human microvessels in immunodeficient mice. *Lab Invest* 81:453–463

- Orlic D, Kajstura J, Chimenti S, Jakoniuk I, Anderson SM, Li B, Pickel J, McKay R, Nadal-Ginard B, Bodine DM et al (2001) Bone marrow cells regenerate infarcted myocardium. *Nature* 410:701–705
- Pittenger MF, Mackay AM, Beck SC, Jaiswal RK, Douglas R, Mosca JD, Moorman MA, Simonetti DW, Craig S, Marshak DR (1999) Multilineage potential of adult human mesenchymal stem cells. *Science* 284:143–147
- Rajangam K, Behanna HA, Hui MJ, Han X, Hulvat JF, Lomasney JW, Stupp SI (2006) Heparin binding nanostructures to promote growth of blood vessels. *Nano Lett* 6:2086–2090
- Rotmans JJ, Heyligers JM, Verhagen HJ, Velema E, Nagtegaal MM, de Kleijn DP, de Groot FG, Stroes ES, Pasterkamp G (2005) In vivo cell seeding with anti-CD34 antibodies successfully accelerates endothelialization but stimulates intimal hyperplasia in porcine arteriovenous expanded polytetrafluoroethylene grafts. *Circulation* 112:12–18
- Schechner JS, Nath AK, Zheng L, Kluger MS, Hughes CC, Sierra-Honigmann MR, Lorber MI, Tellides G, Kashgarian M, Bothwell AL et al (2000) In vivo formation of complex microvessels lined by human endothelial cells in an immunodeficient mouse. *Proc Natl Acad Sci USA* 97:9191–9196
- Schmidt D, Mol A, Neuenschwander S, Breyman C, Gossi M, Zund G, Turina M, Hoerstrup SP (2005) Living patches engineered from human umbilical cord derived fibroblasts and endothelial progenitor cells. *Eur J Cardiothorac Surg* 27:795–800
- Schmidt D, Asmis LM, Odermatt B, Kelm J, Breyman C, Gossi M, Genoni M, Zund G, Hoerstrup SP (2006) Engineered living blood vessels: functional endothelia generated from human umbilical cord-derived progenitors. *Ann Thorac Surg* 82:1465–1471; discussion 1471
- Schmidt D, Mol A, Breyman C, Achermann J, Odermatt B, Gossi M, Neuenschwander S, Pretre R, Genoni M, Zund G et al (2006b) Living autologous heart valves engineered from human prenatally harvested progenitors. *Circulation* 114:I125–I131
- Schuster MD, Kocher AA, Seki T, Martens TP, Xiang G, Homma S, Iescu S (2004) Myocardial neovascularization by bone marrow angioblasts results in cardiomyocyte regeneration. *Am J Physiol Heart Circ Physiol* 287:H525–H532
- Shimizu K, Sugiyama S, Aikawa M, Fukumoto Y, Rabkin E, Libby P, Mitchell RN (2001) Host bone-marrow cells are a source of donor intimal smooth-muscle-like cells in murine aortic transplant arteriopathy. *Nat Med* 7:738–741
- Shin'oka T, Matsumura G, Hibino N, Naito Y, Watanabe M, Konuma T, Sakamoto T, Nagatsu M, Kurosawa H (2005) Midterm clinical result of tissue-engineered vascular autografts seeded with autologous bone marrow cells. *J Thorac Cardiovasc Surg* 129:1330–1338
- Shirota T, He H, Yasui H, Matsuda T (2003) Human endothelial progenitor cell-seeded hybrid graft: proliferative and antithrombotic potentials in vitro and fabrication processing. *Tissue Eng* 9:127–136
- Wang Y, Wan C, Deng L, Liu X, Cao X, Gilbert SR, Boussein ML, Faugere MC, Guldberg RE, Gerstenfeld LC et al (2007) The hypoxia-inducible factor alpha pathway couples angiogenesis to osteogenesis during skeletal development. *J Clin Invest* 117:1616–1626
- Wu X, Rabkin-Aikawa E, Guleserian KJ, Perry TE, Masuda Y, Sutherland FW, Schoen FJ, Mayer JE Jr, Bischoff J (2004) Tissue-engineered microvessels on three-dimensional biodegradable scaffolds using human endothelial progenitor cells. *Am J Physiol Heart Circ Physiol* 287:H480–H487
- Yamashita J, Itoh H, Hirashima M, Ogawa M, Nishikawa S, Yurugi T, Naito M, Nakao K, Nishikawa S (2000) Flk1-positive cells derived from embryonic stem cells serve as vascular progenitors. *Nature* 408:92–96
- Yoder MC, Mead LE, Prater D, Krier TR, Mroueh KN, Li F, Krasich R, Temm CJ, Prchal JT, Ingram DA (2007) Redefining endothelial progenitor cells via clonal analysis and hematopoietic stem/progenitor cell principals. *Blood* 109:1801–1809

Chapter 4

Dermal Precursors and the Origins of the Wound Fibroblast

Jeffrey M. Davidson

Abstract Tissue repair demands the efficient restoration of connective tissue integrity and architecture. The brunt of the task falls on the fibroblast, a cell type strongly committed to the production of extracellular matrix. Recent investigation has refined the historical concept that the bone marrow and circulating precursors can make a significant, transient contribution to wound healing during the formation of granulation tissue. In parallel, there is mounting evidence that a subset of dermal mesenchymal cells have pluripotent properties that could contribute to the restoration and even regeneration of wound sites. The interrelationships between mesenchymal stem cells, circulating fibrocytes, and dermal progenitors are still an evolving area of investigation. Nevertheless, the manipulation of these cell types for wound healing and tissue engineering applications is a promising strategy.

Keywords Wound healing • mesenchymal stem cell • fibrocyte • progenitor

4.1 Introduction

The process of wound healing is initiated by hemostasis, which creates a fibrin clot that forms the first provisional matrix at the injury site. Blood platelets, as well as local cells immediately begin to release signals that lead to the recruitment of inflammatory cells from the circulation to control infection and to stimulate restoration of tissue integrity by the deposition of new vasculature and connective tissue. Local cells at the wound periphery are also activated. Until recently, the traditional

J.M. Davidson (✉)

Department of Pathology, Vanderbilt University School of Medicine,
Nashville, TN 37232, USA

and

Research Service, VA Tennessee Valley Healthcare System,
1310 24th Ave. South, Nashville, TN 37212, USA

e-mail: jeff.davidson@vanderbilt.edu

view had held that the infiltration of the provisional matrix by fibroblasts and microvascular endothelial cells was largely due to migration from the wound margins, while extravasation from the blood gave entry to successive cohorts of inflammatory leukocytes, first neutrophils and then monocytes and lymphocytes. Nevertheless, several observations in the past had suggested that blood-borne leukocytes might actually assume a connective tissue phenotype once having entered the wound environment. Indeed, Conheim and others had put forward this hypothesis on morphological grounds in the middle of the nineteenth century (Cohnheim 1867; Paget 1863), and Lindblad and others provided biochemical evidence of the capacity of macrophages to produce collagen, a hallmark of a fibroblastic phenotype, in the latter part of last century (Lindblad 1998; Lindblad et al. 1987; Stirling and Kakkar 1969; Allgower and Hulliger 1960). The concept of circulating precursors was placed on firmer ground by the description of the fibrocyte, a leukocyte that infiltrates early wounds and expressed collagen, by Bucala et al. (Abe et al. 2001; Quan et al. 2004; Chesney et al. 1997; Bucala et al. 1994), and the circulating endothelial progenitor cell (EPC), initially characterized by Ashahara and co-workers (Eguchi et al. 2007; Asahara et al. 1997, 1999). These findings and subsequent follow-up have provided clear evidence of the existence of several leukocyte, and hence marrow-derived, populations that can participate in the wound healing process. The quantitative contribution of these leukocytes to the process of tissue repair, their specific role, and their necessity for successful healing is less well understood.

There are many recent reviews on the participation of stem cells in wound repair (Asahara et al. 1999; Abraham et al. 2007; Bellini and Mattoli 2007; Cha and Falanga 2007; Cotsarelis 2006; Falanga 2004; Gurtner et al. 2007; Hennessy et al. 2004; Li et al. 2005; Roh and Lyle 2006). This discussion focuses on the more restricted issue of the relationships between putative fibroblast precursors in three tissue compartments: the bone marrow, the circulation, and the skin (dermis). Several key issues are considered: the criteria used to identify fibroblast precursors, the evidence for their participation in tissue repair, the quantitative contribution of these cells to connective tissue restoration, and the therapeutic applications of this segment of stem cell biology.

4.2 Mesenchymal Stem Cells

Mesenchymal stem cells (also known as marrow stromal cells, MSC) were the first progenitors to be characterized as multipotential, self-renewing source of many connective tissue cell types. The concept was initially put forward by Friedenstein (Friedenstein 1995; Friedenstein et al. 1974; Friedenstein and Kuralesova 1971) based on studies of marrow-derived precursors of osteogenic cells and then extended to many other lineages by the work of Caplan (Caplan 2007; Caplan 1991), Pittenger (Le Blanc and Pittenger 2005; Pittenger et al. 1999), and their colleagues. Originally conceptualized as a part of the “mesengenic process” (Caplan 1994), *in vitro* experimentation ultimately established two key elements: culture conditions

under which MSC could be isolated from whole marrow aspirates and maintained as long-lived, stably undifferentiated progenitors; culture conditions under which these stable MSC could be induced down the osteogenic, adipogenic, myogenic, chondrogenic, and fibrogenic pathways. Isolation methods for these cells are remarkably simple, since most of the other marrow-derived cell populations are not strongly adherent to a tissue culture surface. Although MSC are reported to express potentially distinctive cell surface markers such as Stro-1 (Stewart et al. 2003; Dennis et al. 2002; Gronthos et al. 1994; Simmons and Torok-Storb 1991), this antigen has not routinely gained use as a means of MSC fractionation. The predominant surface characteristics used in are presence of CD49a ($\alpha 1$ integrin) and low or absent CD45 and CD11b. Thus, the MSC is principally defined by its adhesive properties in vitro rather than its anatomic localization or its cell surface properties.

MSC have been widely popularized as a potential source for tissue engineering constructs because of their wide range of potential differentiation pathways. Osteogenic and chondrogenic applications predominate, but these cells have potential applications in muscle, skin, and other connective tissues. In addition, many other connective tissues harbor mesenchymal progenitors with nearly equivalent developmental potential, including skeletal muscle, adipose tissue, amniotic cells, placenta, and – as will be amplified below – the dermis. While commercial development of MSC as sources for cartilage repair is advancing (Ahmed et al. 2007; De Bari and Dell’accio 2007; Richter 2007), these other sources of MSC-like cells may be easier to obtain, potentially of autologous origin, and more flexible in terms of tissue engineering and cell-based therapies. As with marrow derived MSC, isolation and purification of these cell strains depends on appropriate culture conditions as much as cell surface marker selection.

4.2.1 Marrow Derived Fibroblast Populations

Although there is ample evidence that marrow-derived cells enter the wound site during and after the inflammatory phase, only recently have techniques and evidence for the contribution of the marrow-derived cells to the fibroblast lineage been established. Most of these studies have relied on adoptive transfer of genetically or biochemically-distinct bone marrow to marrow-ablated hosts (Fathke et al. 2004; Ishii et al. 2005; Opalenik and Davidson 2005). Early studies with adoptive transfer for potential correction of the bone disorder osteogenesis imperfecta had strengthened the concept that bone marrow cells could be mobilized to remote connective tissue compartments (Pereira et al. 1998). General support for the concept in wound healing came from a study using eGFP-marked donor marrow in mice followed by excisional wounding after engraftment was ascertained (Badiavas et al. 2003). Although this experimental design could not discriminate fibroblasts from other marrow sources, many eGFP-positive cells took up the appropriate position and assumed the appropriate morphology to suggest that a significant fraction of the wound fibroblast population was marrow derived. This laboratory adopted an

approach that could more precisely identify the wound fibroblast population by using a mouse marrow donor that contained transgenes expressing β -galactosidase and luciferase under the control of the COL1A2 promoter and enhancer that is relatively selective for fibroblasts (Opalenik and Davidson 2005). While collagen 1 is expressed at low levels in several cell types, high-level collagen expression is restricted to mesenchymal cells such as fibroblasts and vascular smooth muscle cells. Experimental sponge implants were placed in engrafted mice and harvested at time points from 5 to 28 days, thus covering the phases of inflammation, granulation tissue expansion, and remodeling. Histochemistry identified a β -galactosidase rich population of spindle-shaped cells in collagen-rich regions of granulation tissue that also expressed the fibroblast marker, fibroblast specific protein-1 (Iwano et al. 2002; Okada et al. 1997). Enumeration of donor-derived fibroblasts indicated that the relative content of marrow-derived fibroblasts peaked at approximately 38%, suggesting that – at least in this wound model and species – the marrow is a significant source of matrix-producing cells in traumatic wounds. Quantitation of donor-derived collagen production as a function of time after wounding showed that these cells contributed maximally at 28 days, during the remodeling phase of tissue repair (Table 4.1).

Similar studies have been independently reported by two laboratories using morphological and biochemical methods to show values of 30–40% marrow contribution to skin wound fibroblast population (Fathke et al. 2004; Ishii et al. 2005). These studies also showed that marrow-derived fibroblasts contributed minimally to normal skin (turnover), and fully resolved wounds showed a return of marrow-derived mesenchymal cells to a basal level. This decline is not unexpected, since wound fibroblasts gradually undergo apoptosis as a dense collagen matrix replaces the highly cellular granulation tissue. Since the relative abundance of these cells returned towards baseline, these findings suggest a selective loss of the marrow-derived population. One might hypothesize that marrow/blood-derived mesenchymal cells are designed to serve a temporary role in tissue reorganization, at least in non-pathological states. Tracing the marrow precursor to the wound has been challenging, since the fibroblast phenotype (high collagen expression) is not present in circulating cells, and the fibroblast lacks distinctive surface markers. In addition, it is reasonable to assume that these precursors, as they are mobilized from bone marrow and recruited to the wound site, are behaving more like circulating leukocytes. The factors that mobilize MSC and attract them to sites of injury are undefined. SDF-1 and PDGF are the most likely candidates at this juncture.

4.2.2 *Fibrocytes*

During and somewhat before the notion that MSC or marrow-derived fibroblasts were significant in wound healing, the innovative work of Bucala and colleagues revived the nineteenth-century notion of the circulating fibrocyte (Abe et al. 2001; Quan et al. 2004; Bucala et al. 1994). Their studies showed that early wound fluid (the plasma exudates within the wound site) contained a distinctive population of

Table 4.1 Characteristics of dermal progenitor cells

Designation	Origin	Cultivation Method	Markers	Phenotype	Differentiation	Reference
Skin-derived precursors (SKP)	Dissociated skin	Spheres in FGF-2/EGF	Nestin, FN, slug, snail, twist, versican, Wnt5a	Neural crest	Neuron, glia, smooth muscle, adipocyte, dermal papillae	Fernandes et al. (2008)
Neonatal dermis	Dissociated mouse skin	Fractionation, 3-D cultures	CD34 ⁺ , CD49f ^{lo} , MRP8	Dermal papilla	Bone, cartilage, fat, muscle	Crigler et al. (2007)
Follicular dermal cells	Whisker follicles	MEM, FBS	CD44 ⁺ , CD73 ⁺ , CD90 ⁺ , CD34 ⁻	Dermal sheath and papilla	Bone, fat, adipocyte, cartilage (muscle), nestin, NG2	Hoogdujin et al. (2006)
Fibroblast	Human foreskin	Collagenase-DMEM	CD29, CD13, CD49d, CD105, CD34 ⁻	Fibroblast	Bone, adipose, cartilage, nestin+	Chen et al. (2007)
Dermal MSC	Human foreskin	Clonal subcultivation in DMEM + mercaptoethanol	CD90, CD105, CD34 ⁻ , c-kit ⁻ , CD133 ⁻	Fibroblast	Fat, bone, muscle	Bartsch et al. (2005)
Dermal stem cell	Avian dermis	Clonal analysis		Stellate morphology	Muscle, fat, cartilage, bone, connective tissue	Young et al. (1993, 1995)
Dermal sheath and papilla	Rat hair follicles	Clonal analysis in conditioned medium	Rhodamine 123 dye exclusion	Fibroblast	Fat, bone	Jahoda et al. (2003)

leukocytes that expressed a mixture of cell surface markers that included mononuclear cells (CD11b, CD45), dendritic cells, and fibroblasts (collagen I). This cell population, which appears to take on multiple roles with wound tissue, is abundant in advance of the major appearance of classical fibroblasts and myofibroblasts in granulation tissue, and at least some lineage studies suggest that these cells ultimately persist in the resolved wound/scar as dendritic/antigen-presenting cells (Chesney et al. 1997). Unlike the elusive circulating MSC, fibrocytes can be fractionated from blood and wound fluid by combinations of antibodies recognizing CD11b, CD45, CD16, and collagen I. The relationship between the fibrocyte and the MSC is somewhat difficult to establish, since primary, circulating fibrocytes are principally defined by a collection of mononuclear leukocyte cell surface markers, while MSC are defined by *lack* of CD11b and a multipotential differentiation capability after prolonged cultivation and expansion *in vitro*. Fibrocytes are not reported to be capable of differentiation into multiple mesenchymal lineages, although they do seem to be capable of differentiation into fibroblasts and myofibroblasts under the influence of fibrogenic factors such as TGF- β (Wang et al. 2007). A current review of fibrocyte biology illustrates the complex pathways that can lead to fibrocyte recruitment, activation, and differentiation (Bellini and Mattoli 2007). Several publications have emphasized the fibrocyte population as having multiple, diverse roles in inflammation and repair. It is not clear that the fibrocyte is a homogeneous population. The effector and fibrogenic roles may derive from the nature of the microenvironment, or they may depend on different fibrocyte subpopulations.

In contrast to the MSC, which retains a multipotential phenotype under appropriate growth conditions, fibrocytes only appear to have one mesenchymal pathway: towards fibroblasts and thence to myofibroblasts. There is considerable difference in the fibrocyte repertoire as a mononuclear cell, where many effector functions can be expressed. Given the early appearance of fibrocytes at sites of injury, it would seem likely that the immune effector functions of mononuclear cells predominate in early wounds, with a progressive transition to either fibrogenic or dendritic cell functions. Although fibrocytes participate in the normal healing process, there is not much quantitative information on their relative contribution, perhaps due to the variable phenotype. Much more attention has been given to the participation and role of the fibrocyte in pathological fibrosis in the kidney, lung, and other tissues (Okada and Kalluri 2005; Bucala 2008; Quan et al. 2006). Experimental data has begun to accumulate to suggest that the recruitment and the cytokine environment of the fibrocyte can be driven towards an exaggerated accumulation of collagen and the development of the contractile myofibroblast phenotype (Bellini and Mattoli 2007). Pharmacological interventions are under study, among which the effect of serum amyloid protein appears promising, since this protein appears to retard the differentiation of fibrocytes to a fibroblastic phenotype (Pilling et al. 2003). Aggregated IgG also appears to retard fibrocyte differentiation. It should be stressed that under many conditions the fibrocyte may continue to express relatively low levels of collagen until provoked by high levels of signals such as TGF- β and CTGF or low levels of IL-12 and IFN- γ .

4.2.3 Factors for Mobilization and Recruitment of Marrow Populations

The foregoing material presents compelling information that fibrocyte and fibroblast precursors can mobilize from the bone marrow, enter the circulation, and extravasate into sites of tissue damage to execute a program that includes the elaboration of new connective tissue. There are still many challenges in understanding what signals lead to mobilization and exit of these precursors from their point of origin. The principal circulating factors that are implicated in mesenchymal precursor mobilization are SDF-1 (Lama and Phan 2006), which is also known to be a key factor for EPC mobilization, PDGF (Ponte et al. 2007), and TGF- β , whose serum levels have been shown to be elevated in correlation with circulating fibrocyte levels (Yang et al. 2002). All of these factors are rapidly released at sites of tissue injury. They interact with distinct receptors: CXCR4 for SDF-1, PDGF receptors A and B for PDGF, and the TGF β -R1/R2 heterodimers for TGF- β family members. Thus, rate-limiting steps for mobilization could be the concentration of these signal molecules or their receptors. The extravasation and recruitment of fibrocytes may involve MCP-1, CXCL12 and the ligands of CCR7, CCL19 and CCL21, depending on the pathological condition and the nature of the inflammatory infiltrate (Bellini and Mattoli 2007). In this sense, fibrocytes behave much like other mononuclear cells in terms of chemoattraction and adhesion to the vascular wall prior to extravasation. Once within the tissue/wound compartment, fibrocytes appear to transform from a precursor state (CD45⁺CD34⁺MMP9⁺⁺Collagen I⁺Fibronectin⁺ α -SMA⁻) to a more typical fibroblast state (CD45^{+/low}CD34^{low/-}MMP9⁺⁺Collagen I-III⁺⁺Fibronectin⁺⁺) state. Endothelin-1 and TGF- β 1 are implicated in this process. Expression of α -SMA signifies the further transition to myofibroblasts under the influence of the TGF- β /CTGF axis.

Despite the great interest in understanding and utilizing potential fibroblast precursors from the marrow and the circulation, there is still no strong evidence that this resource is rate limiting for wound repair. Indeed, the greatest interest to date has concentrated on the contribution of fibrocytes to pathological wound healing/fibrosis (Bellini and Mattoli 2007; Quan et al. 2006). Much more investigation is needed to determine whether healing-impaired states such as (diabetic) ulcers are due, at least in part, to lower mobilization, recruitment, extravasation, proliferation, or differentiation of these cell populations. There is some early evidence that elevation of mobilization/recruitment factors such as SDF-1 may enhance the healing of ischemic wounds in mice, but the focus of these studies has been on the EPC rather than the MSC/fibrocyte lineage (Ceradini and Gurtner 2005). The weight of the evidence certainly points to local sources for the bulk of connective tissue replacement in any healing organ. Thus, the question to be addressed is which cells and in which location are responsible for connective tissue replacement.

4.3 Defining the Dermal Fibroblast

The term “*fibroblast*” implies, by analogy with cell nomenclature in other lineages, that the cell has the qualities of a progenitor, yet there has been little evidence to date that fibroblasts – defined by classical histological appearance and by characteristics when grown in culture – normally give rise to differentiated progeny. The main business of this cell type in tissue is to elaborate and maintain the extracellular matrix by the secretion of fibrillar collagens (types I, III, and V) and proteoglycans that provide tissue mechanical properties. Many other lesser constituents of the matrix are produced as well. The origin of the wound fibroblast has been attributed to several sources, including adjacent intact fibroblasts, microvascular pericytes, adjacent fascial planes, and even adjacent adipose tissue. Unlike extravasation of mononuclear cells (among which may occur fibrocytes) and granulocytes, the mass infiltration of connective tissue cells into the wound site often involves a delay of several days, suggesting that certain modifications must occur within the provisional matrix and that signaling to the wound margin leads to the activation of a relatively latent population. The work of McLain et al in pig excisional wounds suggested that the limiting step was mesenchymal activation (McClain et al. 1996). We now appreciate that the activation signal largely comprises expression of a cascade of growth factors and cytokines that bring about cell migration, proliferation and differentiation. However, it is less certain what fraction of the mesenchymal cells in the wound periphery respond. This is due, in no small part, to our limited ability to define precisely the fibroblast phenotype, which many view as a default pathway in the mesenchymal lineage. The cells are predominantly distinguished from other mesenchymal cell types by high collagen synthetic capacity, which is accompanied by high-level expression of the associated enzymes, prolyl and lysyl hydroxylase, lysyl oxidase, and Hsp47. Fibroblast-specific protein 1 (S100A4) is also a potential marker of the fibroblast lineage (Iwano et al. 2002), and it has been used to study epithelial-mesenchymal transformation (Okada et al. 1997). Fibroblasts regrettably lack useful, distinctive, surface markers.

4.3.1 *Dermal Progenitors*

The search for the fibroblast progenitor evolved, in part, from studies in other connective tissues that had shown evidence of pluripotent, MSC-like cells. These tissues include adipose (Dicker et al. 2005; Kim et al. 2007; Prichard et al. 2007), skeletal muscle (Peng and Huard 2004), and placenta (Delo et al. 2006), among others. In addition, studies on hair development had suggested that there were specialized fibroblast populations in both the dermal papilla (Jahoda et al. 2003; Hunt et al. 2008; Fernandes et al. 2004; Lako et al. 2002) and the hair shaft (Jahoda et al. 2003; Gharzi et al. 2003). Investigation of Label Retaining Cells in the region of the follicle identified two populations of slow-cycling cells: epidermal cells in the

follicle and fibroblasts in the adjacent area. The dermal papilla cells in particular were targeted for investigation since their interaction with overlying epidermis is the initiating event in de novo hair follicle formation and hence epidermal regeneration. Microdissection of both dermal papilla and follicular hair shaft cells has led to the propagation of MSC-like cells from the dermis. However, there may be other sites within the skin that harbor progenitors. Dermal dissociation followed by a variety of specialized cultivation techniques has also given rise to cultures of multipotential cells. Together, these findings in dermis suggest that the skin, as true of many other organs, contains cells with an unusually broad developmental potential. Some of the MSC-like cultures are reported to transdifferentiate into nerve as well.

The study of precursor cells within dermis has not yet yielded specific markers for histological localization. The results do suggest that certain dermal cells, in the proper microenvironment, could express more regenerative features than previously appreciated. The regenerative capacity of skin is lost in mammals during the latter part of gestation, as the adaptive immune system develops. Fetal regeneration transforms into healing and scar formation as the need to rapidly close a wound and restore both mechanical and epithelial integrity overrides the precise construction methods used during development. Excess matrix formation and coarse rearrangement of tissue architecture further impedes complete regeneration. It is conceivable that appropriate chemical and mechanical cues could take advantage of the developmental potential presumed to be harbored in resident dermal MSC to create a superior form of repair. Given the very recent revelation that even routinely grown fibroblasts can be transformed into pluripotential cells by overexpression of as few as three transcription factors (Lowry et al. 2008; Maherali et al. 2007; Yamanaka 2008), it may be that the lowly fibroblast will provide a remarkably rich reserve for tissue regeneration. These findings also imply that appropriate signals and genes could dramatically alter the plasticity of cells in damaged tissue and convert healing into regeneration.

4.3.2 Evidence for Progenitor Populations

Young et al. (1993, 2001) provided the earliest definitive evidence of multipotential progenitors in a variety of mesodermal tissues including the dermis. Cells were cultured under standard conditions with varying amounts of dexamethasone. According to their data, 30% of isolated cells were lineage-committed, while the balance was multipotential. These populations were positive for CD34 and CD90 and negative for a wide range of other markers including CD36, CD45, and CD117 (Young et al. 2001).

Several recent reports have provided considerable support for the existence of resident dermal stem cells. Fernandes et al. (2004) and Toma et al. (2001) have described a skin progenitor designated SKP by special cultivation methods that can be differentiated into mesenchymal, neural, and mesothelial phenotypes. SKP appear to be derived from a stem cell niche in the dermal papilla (Sieber-Blum et al. 2004). There are suggestions, particularly based on the neural differentiation

capability, that these cells are related to embryonic neural crest, since they can be isolated from embryonic, juvenile, and adult rodent tissue. Toma et al. have reported that similar cell types can be isolated from neonatal human foreskin (Toma et al. 2005), although this source obviously lacks follicular structures. The multipotential activity of human SKP also extended to neuronal and glial phenotypes as well as the usual mesenchymal pathways. Young et al. (2001) have reported mesenchymal progenitors in dermis from fetal through aged donors, and Chunmeng (Chunmeng and Tianmin 2004) has also successfully isolated a mesenchymal progenitor population from the dermis. Several reports have suggested the reservoir for resident stem cells is in the follicular sheath (Jahoda et al. 2003; Gharzi et al. 2003; Richardson et al. 2005) (Jahoda/Ghrazi/Richardson), and Hoogduijn (Hoogduijn et al. 2006) have recently shown that follicular dermal stem cells present a typical dermal stem cell repertoire. Many of these findings point to cells in or near the follicle having the greatest developmental plasticity.

Bartsch et al. (2005) reported the clonal expansion of MSC from human foreskin specimens by initial attachment of trypsinized cells to untreated plastic dishes. Cells were diluted to clonality, although this aspect was not formally proven. These cells expressed CD90 (Thy-1), CD105 (endoglin, a TGF- β receptor), and the embryonic stem cell marker SSEA4. Little or no expression of other common stem cell markers CD34, c-kit, CD133, SSEA3, Oct-4, TRA 1-60 or TRA 1-81 was detected by FACS analysis. The authors assert that long term (6d) storage of the tissue after harvest may have selected for the most robust cell population. The site of origin of these cells was undetermined, although foreskin lacks follicular structures.

Gharzi et al. (2003) emphasize the developmental potential of the lower follicle dermal sheath cells from the rat. Using dye-labeled cells to trace their lineage, they showed that this population was important, together with fibroblasts derived from the dermal papilla, for regeneration of both dermal and epidermal structures. These lower sheath cells can also repopulate the dermis and damaged adjacent hair follicles during wound repair. In addition, the dermal sheath cells were able to reconstitute an engineered dermis. The multipotentiality of the dermal sheath fibroblast population was not addressed in this study.

Crigler et al. (2007) recently reported the characterization of a multilineage cell population from neonatal mouse skin using a complex fractionation scheme of differential adhesion and centrifugation after collagenase/DNase digestion to separate a hair follicle dermal component from several other dermal cell fractions. FACS analysis showed enrichment of CD34+ and CD49^{hi/low} clusters in the side population of the principal dermal fraction. These cells also had detectable CD117 and CD90. Interestingly, these cells distinctly expressed S100A8/MRP8, which we have recently shown to mark regenerative healing in MRL/MpJ mouse ear wound (Caldwell et al. 2008). The nonadherent dermal fraction showed typical multipotential mesenchymal properties.

Toma et al. (2001) have isolated a somewhat different population of progenitors from juvenile and adult mice that are described as skin-derived precursors (SKP). In addition to the usual range of mesenchymal phenotypes, SKP could be differentiated into fibronectin-positive nestin-positive neurons and glia. Skin was dissociated

by relatively standard techniques, and dissociated cells were cultured with B-27 (Gibco; a serum-free supplement for neuronal differentiation) in relatively high concentrations of EGF (20 ng/ml) and bFGF (40 ng/ml), conditions that appeared to promote growth of floating clusters or spheroids. These structures were mechanically dissociated for further propagation, and eventually individual cells were propagated on poly-D-lysine/laminin coated surfaces. In low serum, α -smooth muscle actin could be detected in cultures, while high serum encouraged differentiation of an adipogenic phenotype. The nonadherent SKP population sharply contrasted with the flattened, adherent phenotype of conventional, marrow-derived MSC. The SKP population lacked convincing evidence of a *bona fide* mesenchymal precursor. Fernandes et al. (2006) reviewed additional data, which lead them to the conclusion that SKP represent a neural crest lineage residing in the dermal papilla.

The follicular reserve of MSC was investigated by Hoogdujin et al.(2006), resulting in the isolation of a CD44⁺, CD73⁺, CD90⁺ and CD34⁻ multipotential progenitors that could be driven into both the characteristic mesenchymal lineages exhibited by bone marrow MSC as well as expressing neuroprogenitor markers. Under the culture conditions used by these investigators, interfollicular cells did not differentiate. Intact hair follicles showed osteogenic induction within cells associated with the hair shaft and the lower part of the dermal papillae, not the bulge region that is associated with epidermal regeneration. Nevertheless, all regions of the follicle were capable of propagating adherent cells with MSC properties.

4.4 Clinical Applications

Given the remarkable developmental plasticity of these various sources of progenitor populations, one might assume that all the resources for complete restoration of many types of connective tissue lie within the capability of both recruited and resident mesenchymal precursors. Yet the reality of wound healing is that its resolution in humans in most tissues and in postnatal life is far from perfect. Scar tissue replaces normal matrix organization, and overlying epithelial structures are not regenerated after injuries that destroy the follicle and other adnexal structures. Thus, there may be properties inherent to the wound healing environment or the species/strain that limit the otherwise exciting potential of these cells. There is a strong belief that such cells can become a (universal) source of engineered connective tissues, although there are limitations of production costs and tissue compatibility inherent in any cell-based device. On the other hand, it may be safer and more cost-effective to use the individual's own progenitors as a resource for not only restoration of the hematopoietic bone marrow as currently practiced, but for generation of MSC pools for tissue repair applications. This latter type of intervention is now being tested in various forms of tissue injury, including myocardial, neurologic, musculoskeletal, and cutaneous applications. The MSC sources include bone marrow, skeletal muscle, and adipose tissue. Recently a preliminary report describes the application of marrow-derived cells to wounds in a fibrin spray (Falanga et al. 2007). While some favorable results

have been obtained in a growing number of similar studies, there is still little if any evidence of engraftment of the host cells into the injury site. They may simply have an effector function, similar to that observed with current engineered skin substitutes.

Besides the direct introduction of progenitors into injured tissue, there is also the aspect of MSC mobilization and recruitment. This is a poorly understood area, largely because few markers are available to identify specifically the circulating MSC. If one postulates that the fibrocyte represents such a population, then there are some suggestions that severe (burn) injury increases their mobilization into plasma (Yang et al. 2002). The potential mediator of recruitment is currently SDF-1, which is a ligand for the CXCR4 receptor. Other cytokines such as CXCL12 and the ligands of CCR7 and CCR2 may well be involved (Bellini and Mattoli 2007). SDF-1 has previously been implicated strongly in the recruitment of endothelial progenitor cells to sites of injury and hypoxia. Given that these circulating progenitors are recruited, at least in part, concurrently with other leukocytes, many of the same attraction and adhesion mechanisms may be operative. Recruitment factors for endogenous progenitors could be a more practical and efficient strategy to enhance stem cell participation in tissue repair.

4.5 Novel Healing Properties of MSC

The key to regenerative capacity may be related to the biology of the MSC. Recent work from our group has suggested that a strain of mice that has the highest regenerative capacity, the MRL/MpJ mouse (Davis and Lennon 2005; Heber-Katz et al. 2004) may have MSC with an unusually high capacity to restore tissue integrity. This trait is polygenic (Li et al. 2001; Yu et al. 2007), and many aspects of signaling may be altered in this strain. We have recently examined a portion of the proteomic profile of wounds in this strain, and there is evidence that several calcium-binding proteins are more highly expressed (Caldwell et al. 2008). In addition, morphological examination of the cutaneous wounds in the MRL strain suggest an unusually large influx of mononuclear cells into the healing lesions. In light of these observations, we have begun testing the hypothesis that MSC from this strain may confer improved healing properties. Preliminary data confirm that MRL MSC can accelerate connective tissue repair (Alfaro et al. 2009). Proteomic profiling of these cells has suggested that altered Wnt signaling may be responsible, in part, for the enhanced healing properties of these cells. Recent findings also indicate p21 as an important factor in the MRL/MpJ regenerative phenotype (Bedelbaeva et al. 2010).

4.6 Summary

The interrelationship between dermal precursors in marrow, blood and tissue compartments certainly needs further clarification. It has taken many decades of concerted effort to develop a clearly defined lineage hierarchy in the hematopoietic system.

The tissue fibroblast lacks a distinct set of selectable markers to signify its differentiation. This generic phenotype might even suggest the plasticity of the phenotype. The recent, revolutionary discovery that a simple set of transcription factors can revert skin fibroblasts to totipotent (IPS) cells that can fully reconstitute an organism suggests that the definition of precursor/progenitor/stem cells (Lowry et al. 2008; Maherali et al. 2007; Yamanaka 2008). While the fibrocyte could represent an intermediate between marrow and tissue, it appears to retain many leukocyte characteristics while expressing modest levels of connective tissue protein. We can look forward to many significant advances in the coming years.

Acknowledgements The author is grateful to Pampee P. Young, Susan R. Opalenik, and Mariagabriella Giro for their contributions to this work. Supported by the Department of Veterans Affairs and NIH grants AG06528 and AR041943.

References

- Abe R et al (2001) Peripheral blood fibrocytes: differentiation pathway and migration to wound sites. *J Immunol* 166(12):7556–7562
- Abraham DJ et al (2007) New developments in fibroblast and myofibroblast biology: implications for fibrosis and scleroderma. *Curr Rheumatol Rep* 9(2):136–143
- Ahmed N, Stanford WL, Kandel RA (2007) Mesenchymal stem and progenitor cells for cartilage repair. *Skeletal Radiol* 36(10):909–912
- Alfaro MP et al (2009) The Wnt modulator sFRP2 enhances mesenchymal stem cell engraftment, granulation tissue formation and myocardial repair. *Proc Natl Acad Sci USA* 105:18366–18371
- Allgower M, Hulliger L (1960) Origin of fibroblasts from mononuclear blood cells: a study on the in vitro formation of the collagen precursor, hydroxyproline, in buffy coat cultures. *Surgery* 47:603–609
- Asahara T et al (1997) Isolation of putative progenitor endothelial cells for angiogenesis. *Science* 275(5302):964–967
- Asahara T et al (1999) Bone marrow origin of endothelial progenitor cells responsible for postnatal vasculogenesis in physiological and pathological neovascularization. *Circ Res* 85(3):221–228
- Badiavas EV et al (2003) Participation of bone marrow derived cells in cutaneous wound healing. *J Cell Physiol* 196(2):245–250
- Bartsch G et al (2005) Propagation, expansion, and multilineage differentiation of human somatic stem cells from dermal progenitors. *Stem Cells Dev* 14(3):337–348
- Bedelbaeva K et al (2010) Lack of p21 expression links cell cycle control and appendage regeneration in mice. *Proc Natl Acad Sci USA* 107:5845–5850
- Bellini A, Mattoli S (2007) The role of the fibrocyte, a bone marrow-derived mesenchymal progenitor, in reactive and reparative fibroses. *Lab Invest* 87(9):858–870
- Bucala R (2008) Circulating fibrocytes: cellular basis for NSF. *J Am Coll Radiol* 5(1):36–39
- Bucala R et al (1994) Circulating fibrocytes define a new leukocyte subpopulation that mediates tissue repair. *Mol Med* 1(1):71–81
- Caldwell RL et al (2008) Tissue profiling MALDI mass spectrometry reveals prominent calcium-binding proteins in the proteome of regenerative MRL mouse wounds. *Wound Repair Regen* 16:442–449
- Caplan AI (1991) Mesenchymal stem cells. *J Orthop Res* 9(5):641–650
- Caplan AI (1994) The mesengenic process. *Clin Plast Surg* 21(3):429–435
- Caplan AI (2007) Adult mesenchymal stem cells for tissue engineering versus regenerative medicine. *J Cell Physiol* 213(2):341–347

- Ceradini DJ, Gurtner GC (2005) Homing to hypoxia: HIF-1 as a mediator of progenitor cell recruitment to injured tissue. *Trends Cardiovasc Med* 15(2):57–63
- Cha J, Falanga V (2007) Stem cells in cutaneous wound healing. *Clin Dermatol* 25(1):73–78
- Chen FG et al (2007) Clonal analysis of nestin vimentin + multipotent fibroblasts isolated from human dermis. *J Cell Sci* 120(Pt 16):2875–2883
- Chesney J et al (1997) The peripheral blood fibrocyte is a potent antigen-presenting cell capable of priming naive T cells in situ. *Proc Natl Acad Sci USA* 94(12):6307–6312
- Chunmeng S, Tianmin C (2004) Skin: a promising reservoir for adult stem cell populations. *Med Hypotheses* 62(5):683–688
- Cohnheim J (1867) Ueber Entzündung und Eiterung. *Path Anat Physiol Klin Med* 40:1–79
- Cotsarelis G (2006) Epithelial stem cells: a folliculocentric view. *J Invest Dermatol* 126(7):1459–1468
- Crigler L et al (2007) Isolation of a mesenchymal cell population from murine dermis that contains progenitors of multiple cell lineages. *FASEB J* 21(9):2050–2063
- Davis TA, Lennon G (2005) Mice with a regenerative wound healing capacity and an SLE autoimmune phenotype contain elevated numbers of circulating and marrow-derived macrophage progenitor cells. *Blood Cells Mol Dis* 34(1):17–25
- De Bari C, Dell'Accio F (2007) Mesenchymal stem cells in rheumatology: a regenerative approach to joint repair. *Clin Sci (Lond)* 113(8):339–348
- Delo DM et al (2006) Amniotic fluid and placental stem cells. *Methods Enzymol* 419:426–438
- Dennis JE et al (2002) The STRO-1+ marrow cell population is multipotential. *Cells Tissues Organs* 170(2–3):73–82
- Dicker A et al (2005) Functional studies of mesenchymal stem cells derived from adult human adipose tissue. *Exp Cell Res* 308(2):283–290
- Eguchi M, Masuda H, Asahara T (2007) Endothelial progenitor cells for postnatal vasculogenesis. *Clin Exp Nephrol* 11(1):18–25
- Falanga V (2004) The chronic wound: impaired healing and solutions in the context of wound bed preparation. *Blood Cells Mol Dis* 32(1):88–94
- Falanga V et al (2007) Autologous bone marrow-derived cultured mesenchymal stem cells delivered in a fibrin spray accelerate healing in murine and human cutaneous wounds. *Tissue Eng* 13(6):1299–1312
- Fathke C et al (2004) Contribution of bone marrow-derived cells to skin: collagen deposition and wound repair. *Stem Cells* 22(5):812–822
- Fernandes KJ et al (2004) A dermal niche for multipotent adult skin-derived precursor cells. *Nat Cell Biol* 6(11):1082–1093
- Fernandes KJ et al (2006) Analysis of the neurogenic potential of multipotent skin-derived precursors. *Exp Neurol* 201(1):32–48
- Fernandes KJ, Toma JG, Miller FD (2008) Multipotent skin-derived precursors: adult neural crest-related precursors with therapeutic potential. *Philos Trans R Soc Lond B Biol Sci* 363:185–198
- Friedenstein AJ (1995) Marrow stromal fibroblasts. *Calcif Tissue Int* 56(Suppl 1):S17
- Friedenstein A, Kuralesova AI (1971) Osteogenic precursor cells of bone marrow in radiation chimeras. *Transplantation* 12(2):99–108
- Friedenstein AJ et al (1974) Precursors for fibroblasts in different populations of hematopoietic cells as detected by the in vitro colony assay method. *Exp Hematol* 2(2):83–92
- Gharzi A, Reynolds AJ, Jahoda CA (2003) Plasticity of hair follicle dermal cells in wound healing and induction. *Exp Dermatol* 12(2):126–136
- Gronthos S et al (1994) The STRO-1+ fraction of adult human bone marrow contains the osteogenic precursors. *Blood* 84(12):4164–4173
- Gurtner GC, Callaghan MJ, Longaker MT (2007) Progress and potential for regenerative medicine. *Annu Rev Med* 58:299–312
- Heber-Katz E et al (2004) Spallanzani's mouse: a model of restoration and regeneration. *Curr Top Microbiol Immunol* 280:165–189

- Hennessy B, Korbling M, Estrov Z (2004) Circulating stem cells and tissue repair. *Panminerva Med* 46(1):1–11
- Hoogduijn MJ, Gorjup E, Genever PG (2006) Comparative characterization of hair follicle dermal stem cells and bone marrow mesenchymal stem cells. *Stem Cells Dev* 15(1):49–60
- Hunt DP et al (2008) A highly enriched niche of precursor cells with neuronal and glial potential within the hair follicle dermal papilla of adult skin. *Stem Cells* 26(1):163–172
- Ishii G et al (2005) In vivo characterization of bone marrow-derived fibroblasts recruited into fibrotic lesions. *Stem Cells* 23(5):699–706
- Iwano M et al (2002) Evidence that fibroblasts derive from epithelium during tissue fibrosis. *J Clin Invest* 110(3):341–350
- Jahoda CA et al (2003) Hair follicle dermal cells differentiate into adipogenic and osteogenic lineages. *Exp Dermatol* 12(6):849–859
- Kim WS et al (2007) Wound healing effect of adipose-derived stem cells: a critical role of secretory factors on human dermal fibroblasts. *J Dermatol Sci* 48(1):15–24
- Lako M et al (2002) Hair follicle dermal cells repopulate the mouse haematopoietic system. *J Cell Sci* 115(Pt 20):3967–3974
- Lama VN, Phan SH (2006) The extrapulmonary origin of fibroblasts: stem/progenitor cells and beyond. *Proc Am Thorac Soc* 3(4):373–376
- Le Blanc K, Pittenger M (2005) Mesenchymal stem cells: progress toward promise. *Cytotherapy* 7(1):36–45
- Li X et al (2001) Genetic control of the rate of wound healing in mice. *Heredity* 86(Pt 6):668–674
- Li WW et al. (2005) The role of therapeutic angiogenesis in tissue repair and regeneration. *Adv Skin Wound Care* 18(9):491–500; quiz 501–502
- Lindblad WJ (1998) Perspective article: collagen expression by novel cell populations in the dermal wound environment. *Wound Repair Regen* 6(3):186–193
- Lindblad WJ et al (1987) Induction of prolyl hydroxylase activity in a nonadherent population of human leukocytes. *Biochem Biophys Res Commun* 147(1):486–493
- Lowry WE et al (2008) Generation of human induced pluripotent stem cells from dermal fibroblasts. *Proc Natl Acad Sci USA* 105(8):2883–2888
- Maherali N et al (2007) Directly reprogrammed fibroblasts show global epigenetic remodeling and widespread tissue contribution. *Cell Stem Cell* 1(1):55–70
- McClain SA et al (1996) Mesenchymal cell activation is the rate-limiting step of granulation tissue induction. *Am J Pathol* 149(4):1257–1270
- Okada H, Kalluri R (2005) Cellular and molecular pathways that lead to progression and regression of renal fibrogenesis. *Curr Mol Med* 5(5):467–474
- Okada H et al (1997) Early role of Fsp1 in epithelial-mesenchymal transformation. *Am J Physiol* 273(4 Pt 2):F563–F574
- Opalenik SR, Davidson JM (2005) Fibroblast differentiation of bone marrow-derived cells during wound repair. *FASEB J* 19(11):1561–1563
- Paget J (1863) Lectures on surgical pathology. Longmans, London, p 848
- Peng H, Huard J (2004) Muscle-derived stem cells for musculoskeletal tissue regeneration and repair. *Transpl Immunol* 12(3–4):311–319
- Pereira RF et al (1998) Marrow stromal cells as a source of progenitor cells for nonhematopoietic tissues in transgenic mice with a phenotype of osteogenesis imperfecta. *Proc Natl Acad Sci USA* 95(3):1142–1147
- Pilling D et al (2003) Inhibition of fibrocyte differentiation by serum amyloid P. *J Immunol* 171(10):5537–5546
- Pittenger MF et al (1999) Multilineage potential of adult human mesenchymal stem cells. *Science* 284(5411):143–147
- Ponte AL et al (2007) The in vitro migration capacity of human bone marrow mesenchymal stem cells: comparison of chemokine and growth factor chemotactic activities. *Stem Cells* 25(7):1737–1745
- Prichard HL, Reichert WM, Klitzman B (2007) Adult adipose-derived stem cell attachment to biomaterials. *Biomaterials* 28(6):936–946

- Quan TE et al (2004) Circulating fibrocytes: collagen-secreting cells of the peripheral blood. *Int J Biochem Cell Biol* 36(4):598–606
- Quan TE, Cowper SE, Bucala R (2006) The role of circulating fibrocytes in fibrosis. *Curr Rheumatol Rep* 8(2):145–150
- Richardson GD et al (2005) Plasticity of rodent and human hair follicle dermal cells: implications for cell therapy and tissue engineering. *J Investig Dermatol Symp Proc* 10(3):180–183
- Richter W (2007) Cell-based cartilage repair: illusion or solution for osteoarthritis. *Curr Opin Rheumatol* 19(5):451–456
- Roh C, Lyle S (2006) Cutaneous stem cells and wound healing. *Pediatr Res* 59(4 Pt 2):100R–103R
- Sieber-Blum M et al (2004) Pluripotent neural crest stem cells in the adult hair follicle. *Dev Dyn* 231(2):258–269
- Simmons PJ, Torok-Storb B (1991) Identification of stromal cell precursors in human bone marrow by a novel monoclonal antibody, STRO-1. *Blood* 78(1):55–62
- Stewart K et al (2003) STRO-1, HOP-26 (CD63), CD49a and SB-10 (CD166) as markers of primitive human marrow stromal cells and their more differentiated progeny: a comparative investigation in vitro. *Cell Tissue Res* 313(3):281–290
- Stirling G, Kakkar V (1969) Cells in the circulating blood capable of producing connective tissue. *Br J Exp Pathol* 50:51–55
- Toma JG et al (2001) Isolation of multipotent adult stem cells from the dermis of mammalian skin. *Nat Cell Biol* 3(9):778–784
- Toma JG et al (2005) Isolation and characterization of multipotent skin-derived precursors from human skin. *Stem Cells* 23(6):727–737
- Wang JF et al (2007) Fibrocytes from burn patients regulate the activities of fibroblasts. *Wound Repair Regen* 15(1):113–121
- Yamanaka S (2008) Induction of pluripotent stem cells from mouse fibroblasts by four transcription factors. *Cell Prolif* 41(Suppl 1):51–56
- Yang L et al (2002) Peripheral blood fibrocytes from burn patients: identification and quantification of fibrocytes in adherent cells cultured from peripheral blood mononuclear cells. *Lab Invest* 82(9):1183–1192
- Young HE et al (1993) Pluripotent mesenchymal stem cells reside within avian connective tissue matrices. *In Vitro Cell Dev Biol Anim* 29A(9):723–736
- Young HE et al (1995) Mesenchymal stem cells reside within the connective tissues of many organs. *Dev Dyn* 202(2):137–144
- Young HE et al (2001) Human reserve pluripotent mesenchymal stem cells are present in the connective tissues of skeletal muscle and dermis derived from fetal, adult, and geriatric donors. *Anat Rec* 264(1):51–62
- Yu H et al (2007) Mouse chromosome 9 quantitative trait loci for soft tissue regeneration: congenic analysis and fine mapping. *Wound Repair Regen* 15(6):922–927

Chapter 5

Cell Based Therapies: What Do We Learn from Periosteal Osteochondrogenesis?

Peter J. Emans, Tim J.M. Welting, and Venkatram Prasad Shastri

Abstract Unraveling isolation, cultivation and transplantation protocols is often difficult and time consuming but essential to exploit the full potential of cell based therapies. Studying periosteal callus formation, may give novel insights how this tissue can be used to repair cartilage and bone defects and thus bypass optimization of the protocols mentioned above.

Periosteal callus can be induced in vivo without breaking the bone. During periosteal callus formation, osteochondrogenic progenitor cells which reside in the cambium cambium layer, differentiate via the sequential steps of endochondral bone formation; chondrogenesis is initiated then chondrocytes differentiate into hypertrophic cells. These hypertrophic chondrocytes release pro-angiogenic factors, mineralize and bone is deposited.

Grafts can be harvested during the chondrogenic phase. Compared to isolated undifferentiated periosteal cells, cells in these grafts survive the transplantation into an osteochondral defect much better. By injecting a gel between bone and periosteum, the micro-environment can be manipulated. Per example inhibition of vascularization and induction of hypoxia enhances periosteal chondrogenesis both in vitro and in vivo.

Taken together, studying repair processes of the body in detail may not only give essential information for different cell based therapies, but can even lead to a complete other approach in which the body its own regenerative capacity is used.

Keywords Chondrogenesis • Osteogenesis • Osteochondral defects • Periosteum

P.J. Emans (✉) and T.J.M. Welting
Department Orthopaedic Surgery, University Hospital Maastricht,
P.O. Box 5800, 6202 AZ Maastricht, The Netherlands
e-mail: pj.emans@orthop.unimaas.nl

V.P. Shastri
Faculty of Chemistry, Pharmacy and Earth Sciences, Institute for Macromolecular Chemistry
and Bioss-Center for Cell Signalling Studies, University of Freiburg,
Freiburg, Germany

5.1 General Introduction

5.1.1 Cell Based Therapies

Up to date several cell based therapies have reached the clinic. Examples are bone marrow transplantation for leukemia, adult stem cell transplantation after myocardial infarction, and Autologous Chondrocyte Transplantation (ACT) for cartilage defects.

Cells for “orthopaedic” tissues such as bone, cartilage and ligaments originate from the mesenchymal cell line. For cell based therapies, cells can be released from their matrix, selected and expanded in vitro. This way a relatively small amount of tissue a can be used as appropriate cell source.

Generally bone marrow, blood, periosteum, fat tissue, synovium, dental mould and perichondrium can serve as a source for pluripotent cells (Park et al. 2005; Nathan et al. 2003; Bouwmeester et al. 1997; Chu et al. 1997; Emans et al. 2005; Engkvist et al. 1975a; Homminga et al. 1991; Hunziker and Rosenberg 1996; Ito et al. 2001; O’Driscoll et al. 1986, 2001; Skoog and Johansson 1976; Wakitani et al. 1994; Bruder et al. 1994). If perichondrial cells are truly pluripotent remains unclear (Chu et al. 1995).

Human embryonic stem cells (hES) are another attractive population because they can be maintained by well established protocols, and greatly expanded. However hES face immune rejection after transplantation and there are ethical issues regarding the usage of human embryos. These concerns may be overcome if stem cells can be induced from fibroblasts by retroviral introduction of three transcription factors (Okita et al. 2007). Okita et al. showed that retroviral introduction of Oct3/4, Sox2, and Klf4 of mouse fibroblasts results in induced pluripotent cells stem cells (iPS)(Okita et al. 2007). These iPS are similar to ES cells in morphology and teratoma formation. Subsequent selection for Nanog expression leads to increased ES-cell-like gene expression and DNA methylation patterns (Okita et al. 2007).

For bone and cartilage repair, some authors prefer the use of differentiated cells (e.g. chondrocytes or bone from the iliac crest) for transplantation while others prefer the use of undifferentiated pluripotent cells (Park et al. 2005; Nathan et al. 2003; Bouwmeester et al. 1997; Chu et al. 1997; Emans et al. 2005; Engkvist et al. 1975a; Homminga et al. 1991; Hunziker and Rosenberg 1996; Ito et al. 2001; O’Driscoll et al. 1986, 2001; Skoog and Johansson 1976; Wakitani et al. 1994; Bruder et al. 1994; Brittberg et al. 1994; Hauselmann et al. 1994; Lindahl et al. 2003). Using ES for cell based therapies, there is a tendency to differentiate these cells prior to transplantation (Nussbaum et al. 2007; Laflamme et al. 2007; Harper et al. 2004). It has been reported that this approach enhances cell survival and avoids teratoma formation when ES cells are used (Nussbaum et al. 2007; Laflamme et al. 2007; Harper et al. 2004).

Another approach is to stimulate progenitor cells in vivo to differentiate in the desired tissue. This approach bypasses in vitro engineering of tissues using human culture-expanded autologous cells which pose several challenges primarily variability in tissue quality, cost and complex logistics. In addition, studying in vivo differentiation of progenitor cells may provide useful insights for cell based

therapies. In this chapter we examine periosteum for the repair of osteochondral defects using a “classic” *in vitro* step and *in vivo* differentiation of periosteum.

5.2 Periosteum

The outer surface of bone is covered by a condensed, fibrocollagenous layer called periosteum. This periosteal layer is attached to the underlying bone by extrinsic collagen fibers. These Sharpey’s fibers penetrate deep into the outer cortical tissue. Two layers can be found in periosteum (a) the outer, thicker fibrous layer, and (b) the layer adjacent to the bone called the cambium layer (Fig. 5.1). The name “cambium” derives from the cambium layer of a trunk of a tree (Ito et al. 2001; Duhamel 1739). This cambium layer contains mesenchymal stem cells with osteochondrogenic potential.

Periosteum is highly active during fetal development when it generates osteoblasts for the appositional growth of bone. Parathyroidhormone related protein (PTHrP) is expressed by periosteum (Kartsogiannis et al. 1997). Indian Hedgehog and PTHrP are two signaling molecules that interact in a negative feedback loop regulating the pace of hypertrophic differentiation of the chondrocytes in the growth plate, thus growth of long bones is also influenced by periosteum (Vortkamp 2001). The thickness and chondrogenic potential of periosteum decreases with age (O’Driscoll et al. 2001). Periostin is another molecule expressed by periosteum, this adhesion molecule is believed to play a role in the recruitment of osteoblast precursors (Horiuchi et al. 1999). Periosteum remains important in fracture healing. Periostin is highly up-regulated during fracture repair at mechanical stress

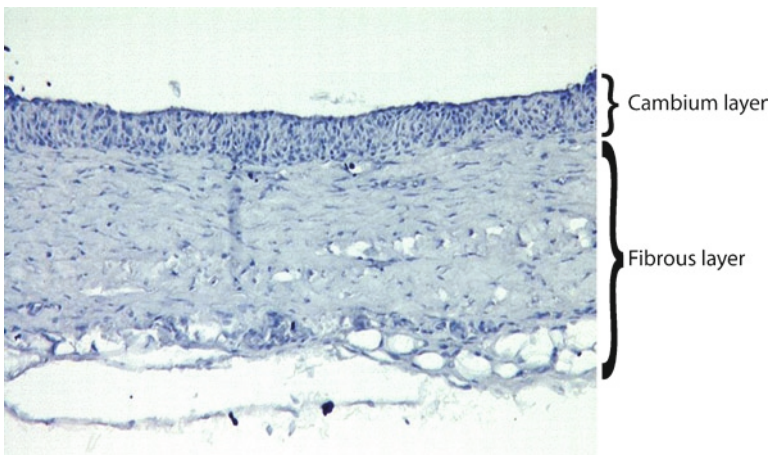


Fig. 5.1 Periosteum, the cambium layer with its osteochondral progenitor cells is attached to the bone

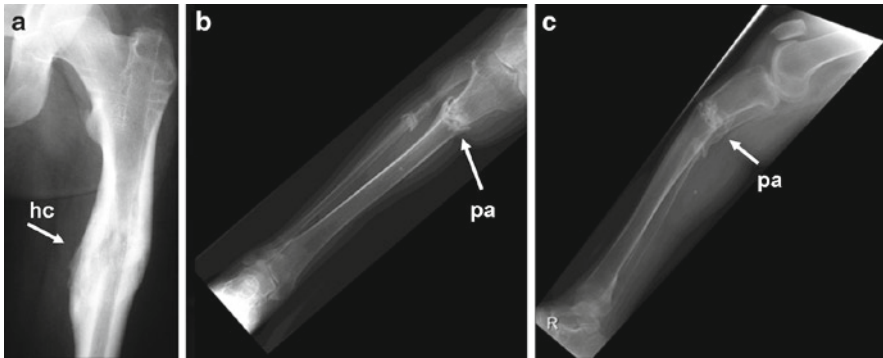


Fig. 5.2 (a) A femoral fracture treated with intramedullary nailing (the nail is already removed), the fracture is nicely healed and a large quantity of hard callus (hc) is deposited. (b and c) shown a tibial fracture which was not treated, this failed to heal and resulted in an pseudoarthrosis (pa), periosteal callus has resulted in a novel joint formation which is not painful in this case. These pictures nicely illustrate how, depending the mechanical forces (microenvironment), (a) bone is generated via the endochondral pathway or (b) the callus remains cartilage

(Wilde et al. 2003; Nakazawa et al. 2004). If it is absent, e.g. within the joint capsule of the femoral neck, fractures heal slowly. Removing periosteum surrounding a fracture leads to absence of cartilage in the fracture callus (Hall and Jacobson 1975).

Thus periosteum plays an important role in bone healing which has, up to a certain level, a high regenerative capacity. Bone often heals without “scar tissue” and has even the capacity to remodel as described in “Wolfs law”. In case of fracture instability and persistent motion, bone fails to heal and “neo joint” called pseudo-arthrosis is formed (Fig. 5.2). In case of a so called hypertrophic pseudoarthrosis, periosteum may be the most important source of cartilage in hypertrophic pseudo arthrosis.

Taken together, periosteum has unique features. Exploring the regenerative capacity of periosteum may give novel insights that are essential to understand and use periosteum for regeneration of cartilage and bone defects.

5.2.1 Embryological Development of Bone, Cartilage, and Periosteum

Bone and cartilage develop from the same mesenchyme, but they have completely different structures, compositions and functions. The diaphyseal cartilage is replaced by bone before birth (primary ossification), most of the cartilaginous epiphysis turns into bone after birth (secondary ossification) leaving cartilage, not covered by a perichondral layer, only at the articulating surfaces of joints. In the adult, bone and overlying articular cartilage are attached by an interface of calcified cartilage (Schenk et al. 1986). This interface distributes forces and stresses applied during load bearing and acts as a barrier to nutrients.

Chondrogenesis is a key event in developing limb buds beginning in the center of condensed mesenchyme. The earliest form of cartilage development is suggested to be 300 million years ago (Urist 1976). In humans the first rudiments develop during the fifth week of gestation. In the 8 week of the embryological life a relatively cell-poor intermediate zone begins to develop. This will form the joint cavity (Aydelotte and Kuettner 1992; Anderson 1962; Gray and Gardner 1950). The epiphysis is covered by a vascularized perichondrium and characterized by appositional growth. Interestingly, epiphyseal cartilage lacks a perichondrial layer and interstitial growth is the only form of expansion. Nutrients for the growing epiphyseal cartilage are supplied by two sources: (1) the synovial cavity and (2) the vascularized cartilage canals (Kuettner and Pauli 1983; McKibbin and Maroudas 1979). Cartilage and synovium merge at a transitional zone which persists in the adult and is the site of osteophyte formation. These osteophytes are derived from periosteum under the influence of TGF- β , which is highly present in degenerative joints (van der Kraan and van den Berg 2007).

5.2.2 *Periosteum in Bone and Cartilage Repair*

5.2.2.1 **Natural Bone Healing and Periosteum**

As described above, endochondral bone formation drives skeletal growth. The same sequential steps of endochondral bone formation are largely responsible for fracture healing of long bones (O'Driscoll et al. 2001; Skoog and Johansson 1976). It is known that periosteum is the main source of progenitor cells capable of creating large volumes of non-vascularized cartilage surrounding a fracture (Wakitani et al. 1994). This first phase of endochondral bone formation is called soft callus. During the second phase chondrocytes become hypertrophic, mineralize (hard callus) (Fig. 5.2), secrete pro-angiogenic factors such as VEGF and are replaced by bone. In the final phase bone is vascularized and will remodel under influence of mechanical forces. While interaction of Indian Hedgehog (Ihh) and Parathyroid hormone related Protein (PTHrP) is the best known regulatory mechanism in the growthplate, such an interplay is unknown for fracture healing (Okita et al. 2007; Brittberg et al. 1994a; Hauselmann et al. 1994). Chondrocytes at different stages of maturation release cytokines and growth factors such as Fibroblast Growth Factor (FGF), Transforming Growth Factor (TGF)- β , BMP's and VEGF (Lindahl et al. 2003; Nussbaum et al. 2007; Laflamme et al. 2007). For instance FGF-2 and TGF- β control endochondral ossification by inhibition of proliferation, hypertrophy and apoptosis (Nussbaum et al. 2007). From our own findings we know that TGF- β is important for (osteo)chondrogenesis both in *ex vivo* and *in vivo* models (Harper et al. 2004). Neo-vascularization under influence of VEGF ensures vessel formation which supply oxygen and nutrients to osteoblast and osteoclasts. The latter produce MMP-9 and -13 which degrade the matrix surrounding terminally hypertrophic chondrocytes (Lindahl et al. 2003). It has been shown that by blocking

VEGF the hypertrophic zone in the growth plate does not degrade and therefore enlarges (Lindahl et al. 2003).

Also Ca^{2+} levels are of interest in the mineralization process and promotes cell death dose-dependent (Kartsoginnis et al. 1997). Chondrocytes are more sensitive to Ca^{2+} than osteoblasts (Vortkamp 2001). Ca^{2+} concentrations are high in late hypertrophy chondrocytes (Okita et al. 2007), while mitochondrial Ca^{2+} levels drop upon matrix mineralization.

5.2.2.2 Periosteal Arthroplasty

Periosteal arthroplasty is an interesting way of treating cartilage defects since many have reported the chondrogenic potential of periosteum (Emans et al. 2005; O'Driscoll et al. 1986, 1988, 2001; Gally et al. 1994; Zarnett and Salter 1989; Iwasaki et al. 1993, 1994, 1995; Nakata et al. 1992; Nakahara et al. 1990, 1991a, b). More than 90% of collagen type II has been reported in the hyaline cartilage formed in the cartilage defects treated with periosteal grafts in rabbits (O'Driscoll et al. 1986, 1988). The cambium layer should be placed so that it faces towards the joint surface (fibrin layer towards the subchondral bone). Anchoring the graft with sutures through the subchondral bone ensures a good fixation. This way the graft can be placed deep into the defect avoiding shear forces. If these measures are taken, and the meticulous procedures of harvesting and handling the grafts are followed (ensuring the presence of a vital cambium layer), the use of this technique seems quite promising. However results in human studies are, compared to rabbits studies, disappointing.

5.2.2.3 Periosteum in Autologous Chondrocyte Transplantation

Chondrocytes are capable of producing cartilage under the appropriate conditions. After selection and expansion, the main challenge is to keep these cells in the damaged area of the joint and this challenge becomes even greater in larger defects (Bentley and Greer 1971). Grande et al. reported that only 8% of the total number of cells in the healing tissue originated from transplanted chondrocytes (Grande et al. 1989). Chondrocytes can be maintained in the defect by suturing a periosteal flap or a collagen mesh over the defect (Brittberg et al. 1994; Grande et al. 1989; Bartlett et al. 2005). In general, human defects appeared to have healed and histological evidence of repair with hyaline cartilage was seen in 13 biopsy specimens (Brittberg et al. 1994). However disparity between clinical results raises questions regarding the contribution of the transplanted cells.

5.2.2.4 Periosteal Differentiation In Vivo for Bone and Cartilage Repair

An interesting variation to periosteal arthroplasty and ACT is a report by Takahashi et al. who used the early fracture callus, induced at the iliac crest (Takahashi et al. 1995). The early fracture callus was implanted into osteochondral defects of rabbit knees with excellent results. Recently Stevens et al. published an interesting paper of inducing

chondrogenesis by subperiosteal injection of a hyaluronan based gel containing the antiangiogenic factor Suramin. The resulting tissue also resembled cartilage of early fracture callus (Stevens et al. 2005). The main advantage of this approach is that the body is used as its own “*in situ* incubator”; cells provide their own matrix and complex and costly isolation, selection and culturing procedures are bypassed.

5.3 Differential Survival of Periosteal Progenitor Cells Versus Chondrocytes

5.3.1 Introduction

As mentioned before chondrocytes are used to repair cartilage defects using the ACT technique as first described by Brittberg et al. (1994a). While this technique is suitable for articular cartilage defects, in a situation where bone formation is required, such as osteochondral defects (involvement of the subchondral bone), pluripotent cells might be a better cell source.

Using these cell based therapies, cultured cells are transferred into chondral or osteochondral defects. Immediately at implantation, cells will be exposed to a dramatically changed environment. Cell culture conditions have been optimized for either proliferation or (re)differentiation of cells. Once transplanted in an osteochondral woundbed, cells are exposed to the hostile conditions of the primary wound healing reaction, including polymorphonuclear cells, catabolic enzymes and deleterious cytokines (TNF α , IL-1). Other potential harmful factors are mechanical forces and changes in the supply of nutrients and oxygen. Factors which may affect cell viability upon transplantation are amongst others: (1) immunological, due to traces of foreign body proteins from culture media (i.e. fetal bovine serum [FBS]), (2) the presence of extracellular matrix, which may protect the cells and keep them well differentiated, and (3) interconnectivity of pores within the scaffold, which will determine the nutrient and oxygen supply. The effectiveness of any cellular repair approach will depend on the retention of cell viability early after implantation (Kruyt et al. 2003a; Chen et al. 1997). Surprisingly, little is known of the survival of transplanted cells (Kruyt et al. 2003b). The aim of this study was to determine the viability of two cell types currently considered for cellular therapies of cartilage defects: chondrocytes and progenitor cells, shortly after exposure to an osteochondral defect in rabbit knees.

5.3.2 Cell Labeling and Scaffolds

Autogenic chondrocytes and periosteal cells were labeled with Cmdil fluorochrome, seeded in PEGT/PBT scaffolds, transferred into osteochondral defects, harvested 5 days post-implantation, and analyzed for cell viability. Three-dimensional micro-computed tomography (μ CT) was used to characterize scaffold architecture

(Malda et al. 2004). The scaffolds had a comparable porosity of approximately 80%. The average pore sizes for the Compression Moulded (CM)- and Rapid Prototyped (RP)-scaffolds were 182 and 525 μm , respectively. The accessible pore volume (measure for interconnectivity) at a pore size of 200 μm was 20% for the CM scaffold. By contrast, the RP-scaffolds had an accessible pore volume of 98%. In order to further elucidate factors effecting cell viability within our model system, we investigated the effect of (1) serum (2) scaffold interconnectivity, and (3) hyaluronan as a known cell protectant. Controls included scaffolds with devitalized cells and scaffolds analyzed at implantation.

5.3.3 Chondrocytes Survive Transplantation Better than Periosteal Progenitor

We found that viability of periosteum cells (14%) but not of chondrocytes (65–95%) was significantly decreased after implantation (Fig. 5.3a). Surprisingly, cell viability in less interconnected compression-moulded scaffolds was higher compared to fully interconnected scaffolds produced by rapid prototyping. All other factors tested did not affect viability significantly.

5.3.4 Hyaluronan Increases the Number of Viable Periosteal Progenitors

Addition of hyaluronan increased periosteum cell viability to 44% ($p < 0.05$) (Fig. 5.3b). Periosteal cells are known to display MSC characteristics (Ghilzon et al. 1999; Zohar et al. 1997) and to express the receptor CD44 for hyaluronan (Noonan et al. 1996). Hyaluronan may protect periosteal cell from cell death through its CD44 receptor (Pohl et al. 2000; Lisignoli et al. 2001). Therefore, addition of hyaluronan, in combination with the induction of chondrogenic differentiation

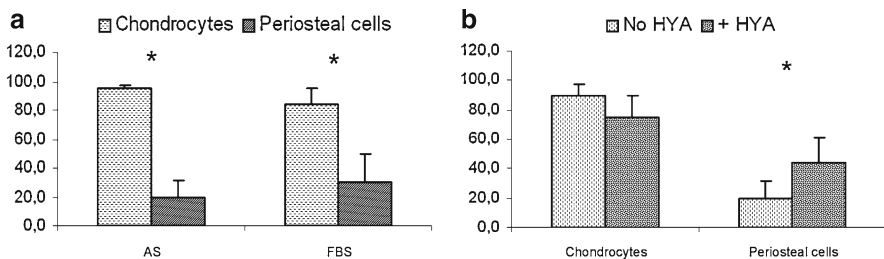


Fig. 5.3 (a) Viability of chondrocytes and periosteal cells after implantation into osteochondral defects when expanded in Autologous Serum (AS) or fetal bovine serum. (b) The effect of hyaluronan on viability of chondrocytes and periosteal cells when cultured in autologous serum (* indicates a significant difference at $p < 0.05$)

of progenitor cells prior to implantation, may increase cell viability for bone and cartilage tissue engineering purposes and requires further research.

5.3.5 Discussion

There are few data in the literature about the fate of implanted cells in tissue engineered constructs. To our knowledge, we report here for the first time a detailed analysis on cell viability in the initial osteochondral repair phase. Quintavalla et al. studied fluorescently labeled mesenchymal stem cells after implantation in osteochondral defects in goats. Although some of the labeled cells were present 2 weeks post-implantation, cell viability was not assessed (Quintavalla et al. 2002). Mierisch et al. and Dell'Accio et al. studied the contribution of transplanted chondrocytes in a rabbit and a goat model of autologous chondrocyte transplantation, respectively (Dell'Accio et al. 2003; Mierisch et al. 2003). Mierisch et al. found the labeled cells not incorporated in the repair tissue and therefore the authors doubt whether the implanted cells contribute to the repair process. Dell'Accio et al. showed fluorescently labeled, transplanted chondrocytes to be present up to 14 weeks in defects in which the periosteal flap covering the defect was not delaminated. It was also shown that labeled cells contributed to tissue repair suggesting that these cells are still vital after 14 weeks. Surprisingly, we did not find differences in chondrocyte viability after seeding in CM- or PR-scaffolds, except in the presence of extracellular matrix. Apparently, nutrient supply and diffusion towards cells within scaffolds does not depend on scaffold interconnectivity, but on the effect of extracellular matrix in fully interconnected scaffolds.

Hyaluronan contributed to the survival of progenitor cells. Laflamme et al. described a survival cocktail which spectacularly increased the percentage of ES cells surviving the transplantation after myocardial infarction (Laflamme et al. 2007). Next to unraveling these factors for different cell based therapies, differentiating progenitor cells may enhance cell survival as has been described for ES cells used for repair of motoneurons in the spinal cord and cardiomyocytes (Laflamme et al. 2007; Harper et al. 2004). Studying periosteum derived callus formation may unravel novel insights (e.g. survival factors) and lead to in vivo differentiated tissue which can be used for bone and cartilage repair.

5.4 A Model to Study Periosteal Osteochondrogenesis In Vivo

5.4.1 Introduction

Damaging periosteum may be a way to generate ectopic cartilage or bone, which may be useful for the repair of articular cartilage and bone defects. If ectopic cartilage develops, studying this periosteal callus formation, may provide useful information for the field of regenerative medicine.

To this end, periosteum was bilaterally dissected from the proximal medial tibia of New Zealand white rabbits. Reactive periosteal tissue was harvested at 10, 20 and 40 days post-surgery and analyzed for expression of Collagen Types I, II and X, aggrecan by RT-PCR and Collagen Types I and II by immunohistochemistry.

5.4.2 Periosteal Callus Recapitulates the Sequential Steps of Endochondral Bone Formation

Reactive tissue was present in 93% of the cases. Histologically this tissue consisted of hyaline cartilage at 10 and 20 days follow-up. Expression of Collagen Type II and aggrecan was present at 10 and 20 days post-surgery. Highest expression was at 10 days. Expression of Collagen Type X increased up to 20 days. Immunohistochemistry confirmed the presence of cartilage, which was positive for Collagen Types I and II at 10 days and only for Collagen Type II at 20 days. At 20 days post-surgery also the onset of bone formation was observed. At 40 days post-surgery, the reactive tissue had almost completely turned into bone (Fig. 5.4).

Thus a novel in vivo model for osteochondrogenesis, in which periosteum is damaged without breaking the bone and accessing the bone marrow is established and recapitulates the sequential steps of endochondral bone formation (Emans et al. 2005). Studies on endochondral bone formation in vivo often use whole embryos or growth plates as paradigms (Lefebvre et al. 1997, 1998, 2001). In addition, fracture healing models in adult rodents are used in which the bone marrow is penetrated (Einhorn 2005; Bostrom et al. 1995). To date, experimental models for endochondral bone formation in adult organisms have, to our knowledge, not been described, whereas such models are likely relevant in respect to clinical situations.

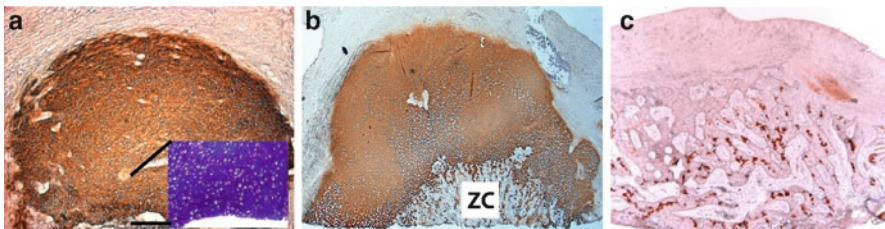


Fig. 5.4 The sequential steps of endochondral bone formation during periosteal callus formation are illustrated by immunohistochemical detection of collagen type II in periosteal reactive tissue (callus); (a) 10 days post-surgery this collagen is present in the newly formed cartilage (a thionine stained section is enlarged). (b) At 20 days post-surgery the presence of Collagen Type II decreases at the zone of calcification (ZC) and bone formation. (c) 40 days post-surgery remnants of Collagen Type II are still visible (*brown*). Original magnification (a) $\times 16$; (b) $\times 16$; (c) $\times 16$; insert in (a) $\times 100$

5.4.3 HIF-1 α Activation and BMP Expression

Numerous growth and transcription factors have been implicated in endochondral bone formation of the growth plate. Many of these factors are up-regulated during hypoxia and down stream of Hypoxia-Inducible Factor (HIF)-1 α activation. However, the specific function of these factors, in the context of oxygenation and metabolic adaptation during adult periosteal endochondral bone formation are largely unknown. Here, we studied HIF-1 α and the possible roles of (HIF-1 α related) growth and transcription factors.

During the chondrogenic phase of periosteal callus formation, we find that cells of the cambium layer first commit to a chondrogenic cell fate; mRNA of the transcription factors Sox9, Ihh, is up-regulated. In addition, during periosteal chondrogenesis, an increase in mRNA expression levels of GAPDH and HIF-1 α and the presence of HIF-1 α protein are indicative of a response to a change in oxygenation, and a metabolic shift indicative of adaptation to hypoxia (Fig. 5.5).

Under normoxia, the HIF-1 α subunit is rapidly degraded via a concerted action of prolyl hydroxylases, which hydroxylate HIF-1 α , and the von Hippel-Lindau tumour suppressor gene product VHL, which ubiquitylates HIF-1 α and thereby targets it for proteasomal degradation. Oxygen deprivation blocks hydroxylation and thereby stabilizes HIF-1 α . These processes play an important role in chondrocyte growth arrest and survival under hypoxia (Schipani et al. 2001; Lee et al. 2004). During the chondrogenic phase many essential factors are activated by HIF-1 α dependent mechanisms (Horiuchi et al. 1999; Robins et al. 2005; Minchenko et al. 1994; Levy et al. 1998; Lu et al. 2002). HIF-1 α plays an important role in the “Pasteur effect” which includes decreased oxidative phosphorylation and an increase in glycolysis (Seagroves et al. 2001). Since glycolytic ATP-production is significantly less efficient per molecule of glucose compared to that by oxidative phosphorylation, glycolytic metabolism is upregulated to sustain free ATP levels in the hypoxic cell. In good agreement with published data in other model systems,

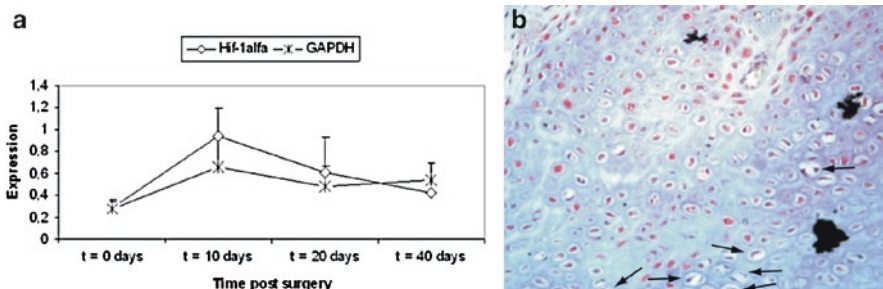


Fig. 5.5 (a) mRNA levels of HIF-1 α and GAPDH are upregulated during periosteal chondrogenesis. (b) Immunohistochemical staining of HIF-1 α confirms presence and stabilization of this protein. No HIF-1 α staining is found in hypertrophic chondrocytes (arrows). Original magnification (b) $\times 200$

our periosteal callus formation model shows a concomitant increase of HIF-1 α and GAPDH mRNA levels, one of the key-enzymes in glycolysis and a known HIF-1 α target (Lu et al. 2002).

Interestingly, while the mRNA expression levels of BMP-2, -4 and -7 were significantly decreased during chondrogenesis, these growth factors were readily detectable by immunohistochemical staining at 10 and 40 days post operative (Fig. 5.6).

Reports on BMP expression levels during chondrogenesis are inconsistent: Yaoita et al. report an unaffected expression of BMPs after inducing a fracture, while Kloen et al. report a positive staining of BMPs in human callus (Yaoita et al. 2000; Kloen et al. 2003). The results of the study presented herein, indicate that throughout periosteal callus formation and osteochondrogenic differentiation, BMP expression is regulated both by transcriptional and post-transcriptional mechanisms. Increased association with polysomes during conditions of cell stress (e.g. hypoxia) has recently been shown to result in preferential translation of select mRNAs (Koritzinsky et al. 2006). It is tempting to speculate such mechanisms act on BMP and other mRNAs. The exact mechanism of translational regulation of cartilage matrix molecules, BMP's, Sox9, Ihh, PTHrP and periostin during chondrogenesis under conditions of lowered oxygen availability, remains unknown and are subject of further study in our labs.

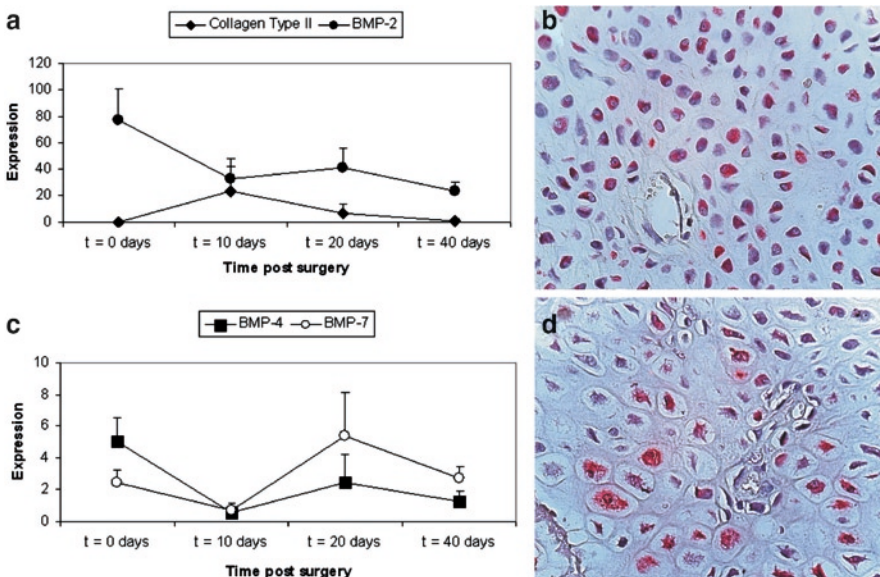


Fig. 5.6 (a) mRNA levels for BMP2 decrease during periosteal chondrogenesis. (b) Note that immunohistochemical staining confirms BMP2 during the chondrogenic phase of periosteal callus formation, 10 days post-surgery. The same pattern was observed for BMP4, (c) mRNA levels decrease while (d) the protein of BMP4 is detected immunohistochemically. Original magnification (b) $\times 200$; (d) $\times 400$

5.4.4 Periostin Activation During Periosteal Callus Formation

In contrast to other reports (Horiuchi et al. 1999; Nakazawa et al. 2004), in which periostin mRNA was not detected in chondrocytes, the present study shows that periostin protein was detectable in mature chondrocytes (Fig. 5.7).

Periostin is an extra cellular matrix/adhesion molecule (Takeshita et al. 1993), however its exact function during osteo- and chondrogenesis is unclear. Our immuno-localization studies confirmed this notion, in that periostin is also detected in the cartilaginous matrix around periostin-positive chondrocytes. Periostin expression, both at the mRNA and protein level, is increased during fracture healing possibly to enhance the recruitment and adhesion of chondro- and osteoprogenitors from essential sources such as bone marrow and blood (Nakazawa et al. 2004). The higher number of peripherally located periostin-positive cells in the newly formed cartilage is consistent with this idea. In line with our observation that both TGF- β and periostin have similar mRNA expression profile, several studies report a TGF- β dependency of periostin regulation (Chen et al. 2006). Periostin expression is regulated down-stream of cellular stress responses, including hypoxia, i.e. during vascular remodeling in different systems (Chen et al. 2006; Li et al. 2004, 2005). Ectopic periostin expression in several models increases adhesion, migration and invasiveness (Yan and Shao 2006; Kii et al. 2006).

We have provided evidence that HIF-1 α is activated during the chondrogenic phase of periosteal callus formation, which suggests that conditions during callus formation and differentiation are, at least transiently, hypoxic. Interestingly, expression of BMP's appears to be regulated at a post-transcriptional level during these processes.

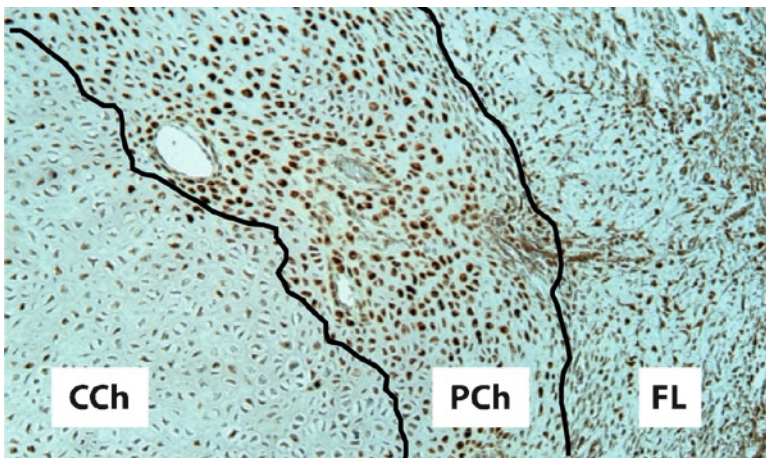


Fig. 5.7 Immuno-histochemical detection of periostin in chondrocytes of periosteal callus. Ten days post-surgery the number of periostin-positive cells is higher in the peripheral chondrocytes (PCh) compared to the chondrocytes localized centrally (CCh). FL indicates the overlying fibrous layer. Original magnification $\times 200$

5.5 Repair of Osteochondral Defects with Cartilage from Periosteum

5.5.1 Introduction

Cartilage has a poor regenerative capacity. Different treatment modalities are currently available, such as autologous perichondrium transplantation (Engkvist et al. 1975b; Engkvist and Wilander 1979; Homminga et al. 1989, 1990), debridement combined with microfracture or subchondral drilling (Pridie 1959; Steadman et al. 2001; Blevins et al. 1998), Mosaic Plasty (Hangody et al. 1997, 1998) and Autologous Chondrocyte Transplantation (ACT) (Brittberg et al. 1994).

In most of these techniques, undifferentiated cells (e.g. periosteum and perichondrium transplantation) and differentiated cells (e.g. ACT and Mosaic Plasty) are transplanted in the cartilage defect. Using techniques such as microfracture and subchondral drilling cells are not transplanted and it is unknown whether cells from the bone marrow have differentiated upon invasion into the cartilage defect. Interestingly, approaches using undifferentiated cells have failed to repair cartilage defects in a clinical setting in the long-term. In contrast, Mosaic Plasty and ACT are currently used for the repair of osteochondral defects. Mosaic Plasty and ACT both require harvesting of osteochondral plugs from less-weight-bearing sites of the affected joint, and the fate of the donor sites is unclear. There are experimental indications, that damaged cartilage, also in less-weight-bearing sites will result in OA (McDevitt and Muir 1976). Other drawbacks of ACT are the costs and safety requirements of the cell-culture procedure which come with this method. In a randomized trial comparing ACT with the microfracture technique, no clinical differences were found at 2 years of follow-up (Knutsen et al. 2004).

The use of ectopically produced cartilage, derived from periosteum might be a novel method to heal osteochondral defects.

5.5.2 Improved Repair of Osteochondral Defects

Ectopic cartilage was produced by dissecting a piece of periosteum from the tibia of rabbits. After 14 days the reactive tissue at the dissection site was harvested and a graft was cored out and press-fit implanted in an osteochondral defect in the medial condyle of the femur with or without addition of hyaluronan. The progress of the repair was evaluated using histology at 3 weeks and 3 months. Thionine and collagen type II stained sections were evaluated for graft viability, ingrowth of the graft and joint surface repair.

Empty defects remained empty at 3 weeks follow-up, ectopic cartilage filled the defect to the level of the surrounding cartilage. Histologically, the grafts were viable, consisted mainly out of cartilage and showed a variable pattern of ingrowth.

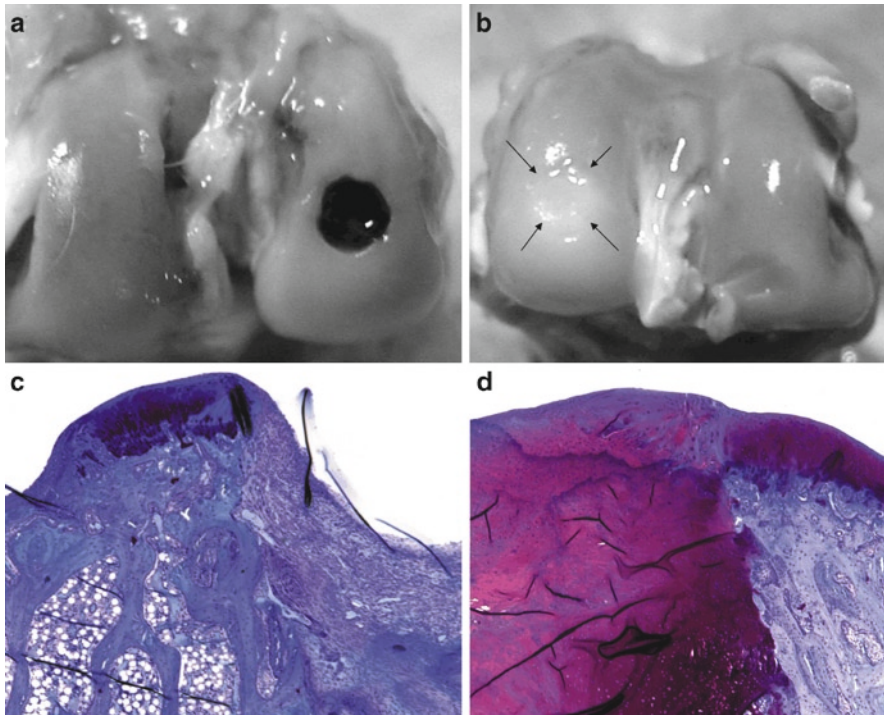


Fig. 5.8 (a) Macroscopic view after 3 weeks of follow up of an empty osteochondral defect. (b) Macroscopic view after 3 weeks of an osteochondral defect treated with an ectopic cartilage graft (*arrows*). The defect is filled up to the level of the surrounding tissue. (c) Thionine staining of an empty osteochondral defect treated with hyaluronan after 3 weeks (magnification $\times 50$). (d) Thionine staining of an osteochondral defect in which ectopic cartilage (no HYA) has been implanted. The joint surface level was restored, the graft appeared viable and a good tissue in growth was observed (magnification $\times 50$)

Three months after implantation empty defects with or without hyaluronan were primarily filled with fibrocartilaginous tissue. With ectopic cartilage treated defects contained mixtures of fibro-cartilaginous and hyaline cartilage (Fig. 5.8).

In some cases a tidemark was observed in the new articular cartilage and the orientation of the cells was similar as in healthy articular cartilage (Schenk et al. 1986; Urist 1976; Aydelotte and Kuettner 1992). Subchondral bone repair was excellent. The modified O'Driscoll scores for empty defects without and with hyaluronan were 12.7 ± 6.4 and 15.3 ± 3.2 ; for treated defects scores were better 15.4 ± 3.9 and 18.2 ± 2.9 (Fig. 5.9).

The thickness of the ectopic cartilage at 14 days post-induction was 2.05 mm, which is quite sufficient to repair articular cartilage in a rabbit, which is 120–200 μm thick. The thickness of human articular cartilage is 2–6 mm, so in order to repair human articular cartilage defects thicker ectopic cartilage needs to be induced.

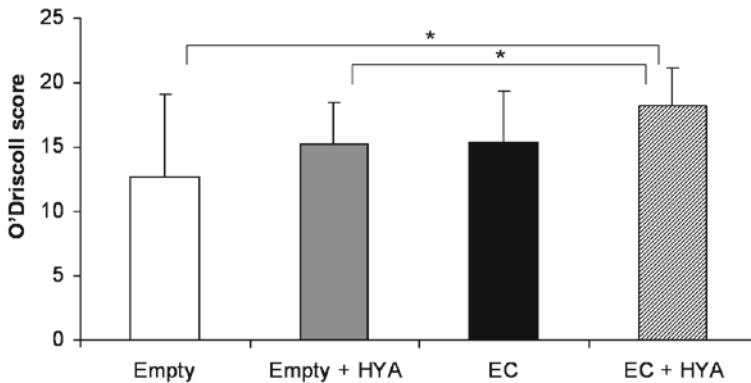


Fig. 5.9 Modified O'Driscoll scores after 3 months follow-up for the groups of empty defects without and with Hyaluronan (HYA) were 12.7 ± 6.4 and 15.3 ± 3.2 , respectively. The scores were 15.4 ± 3.9 and 18.2 ± 2.9 for the groups treated with ectopic cartilage (ec) grafts without and with HYA were. The differences between the two groups with empty defects, $-/+$ HYA, and the group with treated defects + HYA were significant ($*p < 0.02$)

5.5.3 Discussion

The described procedure of repair of an osteochondral defect with ectopically produced cartilage has several advantages over the tissue engineering methods currently used in the clinic. First of all, there is no need to harvest cartilage from the affected joint, so in this joint there will be no donor site morbidity. Then, the time span between induction and transplantation of ectopic cartilage was 14 days (in rabbits).

This is relatively short compared to the time needed to isolate, expand and seed chondrocytes from harvested cartilage. These procedures are prone to mistakes and infections and require a number of safety requirements, which make them very expensive. Using the own body as a cartilage generating reactor eliminates all these issues and may evolve in a cheap and versatile way to produce cartilage for articular surface repair.

In contrast to isolated periosteal cells, differentiated cell in the grafts were viable after transplantation in a osteochondral defect (Emans et al. 2006). This finding supports other reports describing that differentiating cells prior to transplantation improves post-transplantation outcome (Nussbaum et al. 2007; Laflamme et al. 2007; Harper et al. 2004).

In order to use this procedure in the clinic a success rate close to 100% may be necessary. This may be achieved by optimizing the induction method of ectopic cartilage from periosteum. Other ways to stimulate periosteal cells to proliferate and differentiate have been explored (Simon et al. 2001; Stevens et al. 2004) and may result in higher success rates and more reproducible, high quality tissue. A more recent advancement in the de novo engineering of tissue is the In Vivo Bioreactor (IVB) (Stevens et al. 2005). The advantage of the IVB lies in the possibility to manipulate the microenvironment of periosteum and thus enhancing the properties of the periosteum derived tissue prior to transplantation (Stevens et al. 2005).

5.6 Evidence That Tissue Formation Can Be Manipulated in the IVB

5.6.1 Introduction

Studies in the rabbit model using this IVB approach show very promising results: large quantities of mature bone can be engineered, which excellent integration at the transplanted site (Stevens et al. 2005). More importantly the formation of bone occurs via the mere introduction of a calcium-rich bipolymer-derived hydrogel (Biogel). Osteosynthesis is invoked by triggering a wound healing response within the confined space of the IVB, interestingly this process commences without damaging or fracturing the bone. This novel technology bypasses complex and costly isolation and culturing procedures. By injecting a gel containing a drug that can promote hypoxia in combination with growth factors that can stimulate chondrogenesis in the periosteal cells between bone and periosteum progenitor cells can be induced towards chondrogenesis in situ (Stevens et al. 2005).

The use of a biologically active gel (Biogel), which releases important factors to control the fate of tissue development with the IVB shows that the microenvironment can be modified which gives us a powerful tool to control the process of endochondral bone formation and thus the quantity and quality of the generated bone. Examples hereof are illustrated below:

5.6.2 Growth Factors

From our own findings and from literature we know that TGF- β is essential for (osteo)chondrogenesis of periosteum in in vitro and ex-vivo models (Stevens et al. 2004; O'Driscoll 1986; O'Driscoll 1988). In the ex vivo model a piece of periosteum is harvested and cultured in a sandwich of agarose under the influence of growth factors. Such periosteum agarose cultures enable us to rapidly assess the effects of microenvironmental changes on (osteo)chondrogenesis.

Modification of the gel environment by incorporation of TGF- β has also been shown to invoke a chondrogenic response, with hypertrophic chondrocytes that resemble the first step in endochondral bone formation (Stevens et al. 2005). One can envision that such cartilaginous tissue can be transplanted to promote new bone formation at ectopic or osseous site.

5.6.3 Hypoxia

Previous research in our lab suggest that during first phase of formation of periosteum derived endochondral bone, a Hypoxia Inducible Factor (HIF)-1 α dependent hypoxic response is activated (Grande et al. 1989). In addition,

preliminary analysis on cell cultures point to a beneficial effect of hypoxic conditions. Similarly, HIF-1 α has been described as an essential factor for chondrocyte survival and differentiation (O'Driscoll et al. 2001). Our findings suggest that inhibition of vascularity (by incorporation of Suramin, an angiogenesis inhibitor) promotes cartilage formation in the IVB, which may further remodel into bone via the endochondral ossification process (Stevens et al. 2005).

5.6.4 Calcium

Ca²⁺ promotes cell death, with chondrocytes being more sensitive than osteoblasts (Vortkamp 2001). Since Ca²⁺ concentrations are high in hypertrophic chondrocytes (Okita et al. 2007), it is evident that this mineral plays an important role in endochondral bone formation. In close agreement with this, Shastri and co-workers described that after injection of the IVB with a calcium rich alginate gel resulted process of *neo*-bone formation via an intramembranous pathway that yields woven bone incorporating large (40–180 μ m) vascular canals (Stevens et al. 2005). The presence of a good blood supply and local deposition of calcium salts will induce osteogenic cells to differentiate into bone. Interestingly, if the IVB was filled with an alginate solution that was not crosslinked with calcium ions, the volume of *neo*-bone regenerated was tenfold less compared to a calcium rich gel after 6 weeks (Stevens et al. 2005). Based on these observations one can envisage altering the fate of cells within the IVB by varying the physico-chemical characteristics of the biogel.

5.7 Discussion

More and more cell based therapies are reaching the clinic. Many potential cell sources, isolation, cultivation and differentiation protocols are described and are being unraveled. In order to make cell based therapies successful, a thorough understanding of post-transplantation requirements (e.g. cell survival, mechanical loading, [electrical] integration, etc.) is needed. Cells may be manipulated (e.g. differentiate cells prior to transplantation) and their environment may be manipulated (e.g. transplant cells in a survival cocktail as described by Laflamme et al. (2007). The latter is also illustrated by isolated periosteal progenitor cells which survive the hostile environment of an osteochondral defect much better when hyaluronan is added (Emans et al. 2006).

In addition, harvesting, isolating and culturing cells is prone to infections, expensive and time consuming. Generating cartilage from periosteum *in vivo* is possible; this provides homologous ectopically produced cartilage grafts which are large enough to fill large osteochondral defects (in rabbits).

This novel method can also be used as a model to study periosteal endochondral bone formation. Studying this process shows that during mineralization and ossification, many of the chondrocytes which derived from the periosteal progenitor cells become hypertrophic and subsequently die. This observation leads to the

question if a cell based therapy is required for regenerative medicine of bone. In other words would it be easier and better to use a “smart” scaffold that resembles the matrix with its growth-factors (e.g. BMP’s and HIF-1 α) that is deposited by hypertrophic chondrocytes during callus formation?

Finally, implantation of periosteum derived cartilage improved the repair of osteochondral defects. The repair was further enhanced by the addition of hyaluronan. This novel way of tissue regeneration bypasses expensive and time consuming laboratory techniques without further damage to the joint, thus holds promise as a procedure for articular cartilage repair.

By injecting a biologically active gel between the bone and the periosteum the microenvironment can be manipulated without damage or loss to the cells which reside in the periosteum (Stevens et al. 2005). Using this approach we expect to control the quantity and quality of ectopically periosteum derived cartilage, which not only may be very suitable to repair osteochondral defect but also gives essential data which may unravel the secrets of the regenerative capacity of periosteum.

Acknowledgements The authors like to acknowledge Roel Kuijer, Sjoerd Bulstra, Lodewijk van Rhijn, and Willem Voncken for their input and support.

References

- Anderson H (1962) Histochemical studies of the human hip joint. *Acta Anat* 48:258–292
- Aydelotte M, Kuettner K (1992) Heterogeneity of articular chondrocytes and cartilage matrix. Marcel Dekker, New York
- Bartlett W, Skinner JA, Gooding CR, Carrington RW, Flanagan AM, Briggs TW et al (2005 May) Autologous chondrocyte implantation versus matrix-induced autologous chondrocyte implantation for osteochondral defects of the knee: a prospective, randomised study. *J Bone Joint Surg Br* 87(5):640–645
- Bentley G, Greer RB 3rd (1971 Apr 9) Homotransplantation of isolated epiphyseal and articular cartilage chondrocytes into joint surfaces of rabbits. *Nature* 230(5293):385–388
- Blevins FT, Steadman JR, Rodrigo JJ, Silliman J (1998) Treatment of articular cartilage defects in athletes: an analysis of functional outcome and lesion appearance. *Orthopedics* 21(7):761–768
- Bostrom MP, Lane JM, Berberian WS, Missri AA, Tomin E, Weiland A et al (1995 May) Immunolocalization and expression of bone morphogenetic proteins 2 and 4 in fracture healing. *J Orthop Res* 13(3):357–367
- Bouwmeester SJ, Beckers JM, Kuijer R, van der Linden AJ, Bulstra SK (1997) Long-term results of rib perichondrial grafts for repair of cartilage defects in the human knee. *Int Orthop* 21(5):313–317
- Brittberg M, Lindahl A, Nilsson A, Ohlsson C, Isaksson O, Peterson L (1994a) Treatment of deep cartilage defects in the knee with autologous chondrocyte transplantation. *N Engl J Med* 331(14):889–895
- Bruder SP, Fink DJ, Caplan AI (1994 Nov) Mesenchymal stem cells in bone development, bone repair, and skeletal regeneration therapy. *J Cell Biochem* 56(3):283–294
- Chen AC, Nagrampa JP, Schinagl RM, Lottman LM, Sah RL (1997 Nov) Chondrocyte transplantation to articular cartilage explants in vitro. *J Orthop Res* 15(6):791–802
- Chen YF, Feng JA, Li P, Xing D, Ambalavanan N, Oparil S (2006 Apr 27) Atrial natriuretic peptide-dependent modulation of hypoxia-induced pulmonary vascular remodeling. *Life Sci* 79(14):1357–1365

- Chu CR, Coutts RD, Yoshioka M, Harwood FL, Monosov AZ, Amiel D (1995 Sept) Articular cartilage repair using allogeneic perichondrocyte-seeded biodegradable porous polylactic acid (PLA): a tissue-engineering study. *J Biomed Mater Res* 29(9):1147–1154
- Chu CR, Douchis JS, Yoshioka M, Sah RL, Coutts RD, Amiel D (1997 July) Osteochondral repair using perichondrial cells. A 1-year study in rabbits. *Clin Orthop Relat Res* 340:220–229
- Dell'Accio F, Vanlauwe J, Bellemans J, Neys J, De Bari C, Luyten FP (2003 Jan) Expanded phenotypically stable chondrocytes persist in the repair tissue and contribute to cartilage matrix formation and structural integration in a goat model of autologous chondrocyte implantation. *J Orthop Res* 21(1):123–131
- Duhamel H (1739) Cited by Basset CAL in current concepts of bone formation. *J Bone Joint Surg Am* 44-A:1217–1244
- Einhorn TA (2005 (Nov–Dec)) The science of fracture healing. *J Orthop Trauma* 19(10 Suppl): S4–S6
- Emans PJ, Surtel DA, Frings EJ, Bulstra SK, Kuijer R (2005 (March–Apr)) In vivo generation of cartilage from periosteum. *Tissue Eng* 11(3–4):369–377
- Emans PJ, Pieper J, Hulsbosch MM, Koenders M, Kreijveld E, Surtel DA et al (2006 June) Differential cell viability of chondrocytes and progenitor cells in tissue-engineered constructs following implantation into osteochondral defects. *Tissue Eng* 12(6):1699–1709
- Engkvist O, Wilander E (1979) Formation of cartilage from rib perichondrium grafted to an articular cartilage defect in the femoral condyle of the rabbit. *Scand J Plast Reconstr Surg* 13:371–376
- Engkvist O, Johansson SH, Ohlsen L, Skoog T (1975a) Reconstruction of articular cartilage using autologous perichondrial grafts. A preliminary report. *Scand J Plast Reconstr Surg* 9(3):203–206
- Engkvist O, Ohlsen L, Johansson S, Skoog T (1975b) Reconstruction of articular cartilage using autologous perichondrial grafts. A preliminary report. *Scand J Plast Reconstr Surg* 9:203
- Gallay SH, Miura Y, Commisso CN, Fitzsimmons JS, O'Driscoll SW (1994 July) Relationship of donor site to chondrogenic potential of periosteum in vitro. *J Orthop Res* 12(4):515–525
- Ghilzon R, McCulloch CA, Zohar R (1999 Jan) Stromal mesenchymal progenitor cells. *Leuk Lymphoma* 32(3–4):211–221
- Grande DA, Pitman MI, Peterson L, Menche D, Klein M (1989) The repair of experimentally produced defects in rabbit articular cartilage by autologous chondrocyte transplantation. *J Orthop Res* 7(2):208–218
- Gray DJ, Gardner E (1950 March) Prenatal development of the human knee and superior tibiofibular joints. *Am J Anat* 86(2):235–287
- Hall BK, Jacobson HN (1975 Jan) The repair of fractured membrane bones in the newly hatched chick. *Anat Rec* 181(1):55–69
- Hangody L, Kish G, Kárpáti Z, Szerb I, Udvarhelyi I (1997) Arthroscopic autogenous osteochondral mosaicplasty for the treatment of femoral condylar articular defects. *Knee Surg Sports Traumatol Arthrosc* 5:262–267
- Hangody L, Kish G, Kárpáti Z, Udvarhelyi I, Szigeti I, Bély M (1998) Mosaicplasty for the treatment of articular cartilage defects: application in clinical practice. *Orthopedics* 21(7):751–756
- Harper JM, Krishnan C, Darman JS, Deshpande DM, Peck S, Shats I et al (2004 May 4) Axonal growth of embryonic stem cell-derived motoneurons in vitro and in motoneuron-injured adult rats. *Proc Natl Acad Sci USA* 101(18):7123–7128
- Hauselmann HJ, Fernandes RJ, Mok SS, Schmid TM, Block JA, Aydelotte MB et al (1994 Jan) Phenotypic stability of bovine articular chondrocytes after long-term culture in alginate beads. *J Cell Sci* 107(Pt 1):17–27
- Homminga GN, van der Linden AJ, Terwindt-Rouwenhorst EAW, Drukker J (1989) Repair of articular defects by perichondrial grafts. Experiments in the rabbit. *Acta Orthop Scand* 60(3):326–329
- Homminga GN, Bulstra SK, Bouwmeester PSM, van der Linden AJ (1990) Perichondral grafting for cartilage lesions of the knee. *J Bone Joint Surg [Br]* 72-B(6):1003–1007

- Homminga GN, Bulstra SK, Kuijjer R, van der Linden AJ (1991 Oct) Repair of sheep articular cartilage defects with a rabbit costal perichondrial graft. *Acta Orthop Scand* 62(5):415–418
- Horiuchi K, Amizuka N, Takeshita S, Takamatsu H, Katsuura M, Ozawa H et al (1999 July) Identification and characterization of a novel protein, periostin, with restricted expression to periosteum and periodontal ligament and increased expression by transforming growth factor beta. *J Bone Miner Res* 14(7):1239–1249
- Hunziker EB, Rosenberg LC (1996 May) Repair of partial-thickness defects in articular cartilage: cell recruitment from the synovial membrane. *J Bone Joint Surg Am* 78(5):721–733
- Ito Y, Fitzsimmons JS, Sanyal A, Mello MA, Mukherjee N, O'Driscoll SW (2001 Apr) Localization of chondrocyte precursors in periosteum. *Osteoarthritis Cartilage* 9(3):215–223
- Iwasaki M, Nakata K, Nakahara H, Nakase T, Kimura T, Kimata K et al (1993 Apr) Transforming growth factor-beta 1 stimulates chondrogenesis and inhibits osteogenesis in high density culture of periosteum-derived cells. *Endocrinology* 132(4):1603–1608
- Iwasaki M, Nakahara H, Nakase T, Kimura T, Takaoka K, Caplan AI et al (1994 Aug) Bone morphogenetic protein 2 stimulates osteogenesis but does not affect chondrogenesis in osteochondrogenic differentiation of periosteum-derived cells. *J Bone Miner Res* 9(8):1195–1204
- Iwasaki M, Nakahara H, Nakata K, Nakase T, Kimura T, Ono K (1995 Apr) Regulation of proliferation and osteochondrogenic differentiation of periosteum-derived cells by transforming growth factor-beta and basic fibroblast growth factor. *J Bone Joint Surg Am* 77(4):543–554
- Kartsogiannis V, Moseley J, McKelvie B, Chou ST, Hards DK, Ng KW et al (1997 Nov) Temporal expression of PTHrP during endochondral bone formation in mouse and intramembranous bone formation in an in vivo rabbit model. *Bone* 21(5):385–392
- Kii I, Amizuka N, Minqi L, Kitajima S, Saga Y, Kudo A (2006 Apr 14) Periostin is an extracellular matrix protein required for eruption of incisors in mice. *Biochem Biophys Res Commun* 342(3):766–772
- Kloen P, Di Paola M, Borens O, Richmond J, Perino G, Helfet DL et al (2003 Sept) BMP signaling components are expressed in human fracture callus. *Bone* 33(3):362–371
- Knutsen G, Engebretsen L, Ludvigsen TC, Drogset JO, Grontvedt T, Solheim E et al (2004 March) Autologous chondrocyte implantation compared with microfracture in the knee. A randomized trial. *J Bone Joint Surg Am* 86-A(3):455–464
- Koritzinsky M, Magagnin MG, van den Beucken T, Seigneuric R, Savelkoul K, Dostie J et al (2006 March 8) Gene expression during acute and prolonged hypoxia is regulated by distinct mechanisms of translational control. *EMBO J* 25(5):1114–1125
- Kruyt MC, de Bruijn JD, Wilson CE, Oner FC, van Blitterswijk CA, Verbout AJ et al (2003a) Viable osteogenic cells are obligatory for tissue-engineered ectopic bone formation in goats. *Tissue Eng* 9(2):327–336
- Kruyt MC, De Bruijn J, Veenhof M, Oner FC, Van Blitterswijk CA, Verbout AJ et al (2003b) Application and limitations of chloromethyl-benzamidodialkylcarbocyanine for tracing cells used in bone Tissue engineering. *Tissue Eng* 9(1):105–115
- Kuettner K, Pauli B (1983) *Vascularity of cartilage*. Academic, New York
- Laflamme MA, Chen KY, Naumova AV, Muskheli V, Fugate JA, Dupras SK et al (2007 Sept) Cardiomyocytes derived from human embryonic stem cells in pro-survival factors enhance function of infarcted rat hearts. *Nat Biotechnol* 25(9):1015–1024
- Lee JW, Bae SH, Jeong JW, Kim SH, Kim KW (2004 Feb 29) Hypoxia-inducible factor (HIF-1) alpha: its protein stability and biological functions. *Exp Mol Med* 36(1):1–12
- Lefebvre V, Huang W, Harley VR, Goodfellow PN, de Crombrughe B (1997 Apr) SOX9 is a potent activator of the chondrocyte-specific enhancer of the pro alpha1(II) collagen gene. *Mol Cell Biol* 17(4):2336–2346
- Lefebvre V, Li P, de Crombrughe B (1998 Oct 1) A new long form of Sox5 (L-Sox5), Sox6 and Sox9 are coexpressed in chondrogenesis and cooperatively activate the type II collagen gene. *EMBO J* 17(19):5718–5733
- Lefebvre V, Behringer RR, de Crombrughe B (2001) L-Sox5, Sox6 and Sox9 control essential steps of the chondrocyte differentiation pathway. *Osteoarthritis Cartilage* 9(Suppl A):S69–S75

- Levy NS, Chung S, Furneaux H, Levy AP (1998 March 13) Hypoxic stabilization of vascular endothelial growth factor mRNA by the RNA-binding protein HuR. *J Biol Chem* 273(11): 6417–6423
- Li P, Oparil S, Feng W, Chen YF (2004 Oct) Hypoxia-responsive growth factors upregulate periostin and osteopontin expression via distinct signaling pathways in rat pulmonary arterial smooth muscle cells. *J Appl Physiol* 97(4):1550–1558; discussion 1549
- Li G, Oparil S, Sanders JM, Zhang L, Dai M, Chen LB et al (2006 Oct) Phosphatidylinositol-3-kinase signaling mediates vascular smooth muscle cell expression of periostin in vivo and in vitro. *Atherosclerosis* 188(2):292–300
- Lindahl A, Brittberg M, Peterson L (2003) Cartilage repair with chondrocytes: clinical and cellular aspects. *Novartis Found Symp* 249:175–186; discussion 186–179, 234–178, 239–141
- Lisignoli G, Grassi F, Zini N, Toneguzzi S, Piacentini A, Guidolin D et al (2001 Aug) Anti-Fas-induced apoptosis in chondrocytes reduced by hyaluronan: evidence for CD44 and CD54 (intercellular adhesion molecule 1) involvement. *Arthritis Rheum* 44(8):1800–1807
- Lu S, Gu X, Hoestje S, Epner DE (2002 March 19) Identification of an additional hypoxia responsive element in the glyceraldehyde-3-phosphate dehydrogenase gene promoter. *Biochim Biophys Acta* 1574(2):152–156
- Malda J, Woodfield TBF, van der Vloodt F, Kooy FK, Martens DE, Tramper J et al (2004 Nov) The effect of PEGT/PBT scaffold architecture on oxygen gradients in tissue engineered cartilaginous constructs. *Biomaterials* 25(26):5773–5780
- McDevitt CA, Muir H (1976 Feb) Biochemical changes in the cartilage of the knee in experimental and natural osteoarthritis in the dog. *J Bone Joint Surg Br* 58(1):94–101
- McKibbin B, Maroudas A (1979) Adult articular cartilage. *Piman Med* 2E:461–486
- Mierisch CM, Wilson HA, Turner MA, Milbrandt TA, Berthoux L, Hammarskjold ML et al (2003 Sept) Chondrocyte transplantation into articular cartilage defects with use of calcium alginate: the fate of the cells. *J Bone Joint Surg Am* 85-A(9):1757–1767
- Minchenko A, Bauer T, Salceda S, Caro J (1994 Sept) Hypoxic stimulation of vascular endothelial growth factor expression in vitro and in vivo. *Lab Invest* 71(3):374–379
- Nakahara H, Bruder SP, Goldberg VM, Caplan AI (1990 Oct) In vivo osteochondrogenic potential of cultured cells derived from the periosteum. *Clin Orthop Relat Res* 259:223–232
- Nakahara H, Dennis JE, Bruder SP, Haynesworth SE, Lennon DP, Caplan AI (1991a) In vitro differentiation of bone and hypertrophic cartilage from periosteal-derived cells. *Exp Cell Res* 195(2):492–503
- Nakahara H, Goldberg VM, Caplan AI (1991b) Culture-expanded human periosteal-derived cells exhibit osteochondral potential in vivo. *J Orthop Res* 9(4):465–476
- Nakata K, Nakahara H, Kimura T, Kojima A, Iwasaki M, Caplan AI et al (1992 March 16) Collagen gene expression during chondrogenesis from chick periosteum-derived cells. *FEBS Lett* 299(3):278–282
- Nakazawa T, Nakajima A, Seki N, Okawa A, Kato M, Moriya H et al (2004 May) Gene expression of periostin in the early stage of fracture healing detected by cDNA microarray analysis. *J Orthop Res* 22(3):520–525
- Nathan S, De Das S, Thambyah A, Fen C, Goh J, Lee EH (2003 Aug) Cell-based therapy in the repair of osteochondral defects: a novel use for adipose tissue. *Tissue Eng* 9(4):733–744
- Noonan KJ, Stevens JW, Tammi R, Tammi M, Hernandez JA, Midura RJ (1996 July) Spatial distribution of CD44 and hyaluronan in the proximal tibia of the growing rat. *J Orthop Res* 14(4):573–581
- Nussbaum J, Minami E, Laflamme MA, Virag JA, Ware CB, Masino A et al (2007 May) Transplantation of undifferentiated murine embryonic stem cells in the heart: teratoma formation and immune response. *FASEB J* 21(7):1345–1357
- O'Driscoll SW, Keeley FW, Salter RB (1986 Sept) The chondrogenic potential of free autogenous peri art grafts for biological resurfacing of major full-thickness defects in joint surfaces under the influence of continuous passive motion. An experimental investigation in the rabbit. *J Bone Joint Surg Am* 68(7):1017–1035
- O'Driscoll SW, Keeley FW, Salter RB (1988 Apr) Durability of regenerated articular cartilage produced by free autogenous periosteal grafts in major full-thickness defects in joint surfaces

- under the influence of continuous passive motion. A follow-up report at one year. *J Bone Joint Surg Am* 70(4):595–606
- O'Driscoll SW, Recklies AD, Poole AR (1994 Jul) Chondrogenesis in periosteal explants. An organ culture model for in vitro study. *J Bone Joint Surg Am* 76(7):1042–1051
- O'Driscoll SW, Saris DB, Ito Y, Fitzimmons JS (2001 Jan) The chondrogenic potential of periosteum decreases with age. *J Orthop Res* 19(1):95–103
- Okita K, Ichisaka T, Yamanaka S (2007 July 19) Generation of germline-competent induced pluripotent stem cells. *Nature* 448(7151):313–317
- Park Y, Sugimoto M, Watrin A, Chiquet M, Hunziker EB (2005 Jun) BMP-2 induces the expression of chondrocyte-specific genes in bovine synovium-derived progenitor cells cultured in three-dimensional alginate hydrogel. *Osteoarthritis Cartilage* 13(6):527–536
- Pohl M, Sakurai H, Stuart RO, Nigam SK (2000 Aug 15) Role of hyaluronan and CD44 in in vitro branching morphogenesis of ureteric bud cells. *Dev Biol* 224(2):312–325
- Pridie KH (1959) A method of resurfacing osteoarthritic knee joints. *J Bone Joint Surg [Br]* 41-B:618–619
- Quintavalla J, Uziel-Fusi S, Yin J, Boehnlein E, Pastor G, Blancuzzi V et al (2002) Fluorescently labeled mesenchymal stem cells (MSCs) maintain multilineage potential and can be detected following implantation into articular cartilage defects. *Biomaterials* 23(1):109–119
- Robins JC, Akeno N, Mukherjee A, Dalal RR, Aronow BJ, Koopman P et al (2005 Sept) Hypoxia induces chondrocyte-specific gene expression in mesenchymal cells in association with transcriptional activation of Sox9. *Bone* 37(3):313–322
- Schen R, Egli P, Hunziker E (1986) *Articular cartilage morphology*. Raven, New York
- Schipani E, Ryan HE, Didrickson S, Kobayashi T, Knight M, Johnson RS (2001 Nov 1) Hypoxia in cartilage: HIF-1 α is essential for chondrocyte growth arrest and survival. *Genes Dev* 15(21):2865–2876
- Seagroves TN, Ryan HE, Lu H, Wouters BG, Knapp M, Thibault P et al (2001 May) Transcription factor HIF-1 is a necessary mediator of the Pasteur effect in mammalian cells. *Mol Cell Biol* 21(10):3436–3444
- Simon T, Van Sickle D, Kunishima D, Jackson D (2001) Cambium cell stimulation response to surgical release of overlying periosteal tissue. 47th Annual Meeting, ORS; Poster 0503
- Skooog T, Johansson SH (1976 Jan) The formation of articular cartilage from free perichondrial grafts. *Plast Reconstr Surg* 57(1):1–6
- Steadman JR, Rodkey WG, Rodrigo JJ (2001 Oct) Microfracture: surgical technique and rehabilitation to treat chondral defects. *Clin Orthop* 391S:S362–S369
- Stevens MM, Qanadilo HF, Langer R, Prasad Shastri V (2004 Feb) A rapid-curing alginate gel system: utility in periosteum-derived cartilage tissue engineering. *Biomaterials* 25(5):887–894
- Stevens MM, Marini RP, Schaefer D, Aronson J, Langer R, Shastri VP (2005 Aug 9) In vivo engineering of organs: the bone bioreactor. *Proc Natl Acad Sci USA* 102(32):11450–11455
- Takahashi S, Oka M, Kotoura Y, Yamamuro T (1995 March) Autogenous callo-osseous grafts for the repair of osteochondral defects. *J Bone Joint Surg Br* 77(2):194–204
- Takeshita S, Kikuno R, Tezuka K, Amann E (1993 Aug 15) Osteoblast-specific factor 2: cloning of a putative bone adhesion protein with homology with the insect protein fasciclin I. *Biochem J* 294(Pt 1):271–278
- Urist M (1976) *Biogenesis of bone: calcium and phosphorus in the skeleton and blood in vertebrate evolution*. American Physiological Society, Washington, DC
- van der Kraan PM, van den Berg WB (2007 March) Osteophytes: relevance and biology. *Osteoarthritis Cartilage* 15(3):237–244
- Vortkamp A (2001) Interaction of growth factors regulating chondrocyte differentiation in the developing embryo. *Osteoarthritis Cartilage* 9(Suppl A):S109–S117
- Wakitani S, Goto T, Pineda SJ, Young RG, Mansour JM, Caplan AI et al (1994 Apr) Mesenchymal cell-based repair of large, full-thickness defects of articular cartilage. *J Bone Joint Surg Am* 76(4):579–592
- Wilde J, Yokozeki M, Terai K, Kudo A, Moriyama K (2003 Jun) The divergent expression of periostin mRNA in the periodontal ligament during experimental tooth movement. *Cell Tissue Res* 312(3):345–351

- Yan W, Shao R (2006 May 15) Transduction of a mesenchyme-specific gene periostin into 293T cells induces cell invasive activity through epithelial-mesenchymal transformation. *J Biol Chem* 281:19700–19708
- Yaoita H, Orimo H, Shirai Y, Shimada T (2000) Expression of bone morphogenetic proteins and rat distal-less homolog genes following rat femoral fracture. *J Bone Miner Metab* 18(2):63–70
- Zarnett R, Salter RB (1989 May) Periosteal neochondrogenesis for biologically resurfacing joints: its cellular origin. *Can J Surg* 32(3):171–174
- Zohar R, Sodek J, McCulloch CA (1997 Nov 1) Characterization of stromal progenitor cells enriched by flow cytometry. *Blood* 90(9):3471–3481

Chapter 6

Bioreactor Systems in Regenerative Medicine

Ivan Martin, Stefania A. Riboldi, and David Wendt

Abstract In this chapter, the functions and potential applicability of bioreactors from a technical, scientific and clinical perspective will be reviewed in the context of tissue engineering and regenerative medicine. In particular, examples will be given to illustrate the role of bioreactors in (a) establishing and maintaining 3D cell cultures, (b) standardizing physicochemical culture parameters, (c) physically conditioning engineered grafts, (d) predicting mechanical functionality of constructs to be implanted, (e) automating conventional tissue culture processes, (f) streamlining tissue manufacturing strategies. The critical role of bioreactors to make tissue engineered products clinically accessible, safe and commercially competitive will finally be discussed.

Keywords Tissue engineering • Cell-based therapy • Graft manufacturing • Physical conditioning • Perfusion flow

6.1 Introduction

“Bioreactors”, a term generally associated with classical industrial bioprocesses such as fermentation, was initially used in Tissue Engineering (TE) applications to describe little more than simple mixing of a Petri dish. Over the last 2 decades, bioreactors used in TE research evolved, not only for the function of engineering in vitro various types of biological tissues (e.g., skin, tendons, blood vessels, cartilage and bone), but also to serve as defined model systems supporting investigations on cell function and tissue development. In recent years, as bioreactors continued to progress in sophistication, the term has gradually become synonymous

I. Martin (✉), S.A. Riboldi, and D. Wendt
Institute for Surgical Research and Hospital Management, Departments of Surgery
and of Biomedicine, University Hospital Basel, Hebelstrasse 20, 4031 Basel, Switzerland
e-mail: imartin@uhbs.ch

with sophisticated devices enabling semi-automated, closely monitored and tightly controlled cell and tissue culture. In particular, by controlling specific physico-chemical culture parameters at defined levels, bioreactors provide the technological means to perform controlled studies aimed at understanding the effects of specific biological, chemical or physical cues on basic cell functions in a three-dimensional (3D) spatial arrangement. Moreover, bioreactors successfully make up for limitations of conventional manual methods when driving the development of structurally uniform and functionally effective 3D engineered constructs.

Despite the impressive progress achieved by researchers in the field of bioreactor-based TE, it is evident that the need for safe and clinically effective autologous tissue substitutes still remains unsatisfied. In order to successfully translate TE technologies from bench to bedside numerous challenges remain to be addressed. To this end, of prime consideration is the fact that the clinical efficacy of a tissue engineered product will need to be accompanied by a *cost-effective manufacturing process* and *compliance to the evolving regulatory framework* in terms of Quality Control (QC) and Good Manufacturing Practice (GMP) requirements. TE products manufactured by labor-intensive manual benchtop cell and tissue culture protocols may find difficulty in competing with alternative therapeutic options, concerning safety and cost-benefit ratio. On the contrary, *bioreactors* as a means to generate and maintain a controlled culture environment and enabling directed tissue growth could represent the key element for the development of automated, standardized, traceable, cost-effective and safe manufacturing of engineered tissues for clinical applications.

In this chapter we discuss the role of bioreactors in the translational paradigm of TE approaches from basic research to streamlined tissue manufacturing. In particular, examples will be given to illustrate the role of bioreactors in (a) establishing and maintaining 3D cell cultures (Section 6.2.1), (b) standardizing physicochemical culture parameters (Section 6.2.2), (c) physically conditioning engineered grafts (Section 6.2.3), (d) predicting mechanical functionality of constructs to be implanted (Section 6.2.4), (e) automating conventional cell and tissue culture processes (Sections 6.3.1 and 6.3.2), (f) streamlining tissue manufacturing strategies (Section 6.3.3). The critical role of bioreactors to make tissue engineered products clinically accessible, safe and commercially competitive will also be discussed (Section 6.3.4).

6.2 Bioreactors in Regenerative Medicine: Key Features

6.2.1 Cell Seeding on Three-Dimensional Matrices

Traditionally, the delivery of a cell suspension within a three-dimensional scaffold is manually performed by means of pipettes and relying on gravity as a leading principle for cell settlement and subsequent adhesion to the scaffold pores. Such a seeding method, besides being scarcely reproducible due to marked intra- and

inter-operator variability, is inevitably characterized by poor efficiency and non-uniformity of the resulting cell distribution within the scaffold (Wendt et al. 2003). The usual “static” seeding method may yield particularly inhomogeneous results when *thick and/or low-porosity scaffolds* are used, since gravity may not suffice for the cells to penetrate throughout the scaffold pores. When dealing with *human cell sources*, optimizing the efficiency of seeding will be crucial in order to maximize the utilization of cells that can be obtained from the rather limited tissue biopsies.

Hence a variety of “dynamic” cell seeding techniques, relying on the use of bioreactors, have been recently developed with the aim to increase quality, reproducibility, efficiency and uniformity of the seeding process as compared to conventional static methods. Spinner flasks (Vunjak-Novakovic et al. 1999), wavy-walled reactors (Bueno et al. 2007) and rotating wall vessels (Freed and Vunjak-Novakovic 1997) are only examples of the numerous devices found in the literature. However, the most promising approach, enabling efficient and uniform seeding of different cell types in scaffolds of various morphologies and porosities, proved to be “perfusion seeding”, consisting in direct perfusion of a cell suspension through the pores of a 3D scaffold (Braccini et al. 2005; Janssen et al. 2006a, b; Kitagawa et al. 2006; Sun et al. 2005; Timmins et al. 2007; Wendt et al. 2003, 2006; Zhao and Ma 2005; Chen and Lin 2006). Such an efficient method, relying on active driving forces rather than on gravity for the fluid to penetrate the scaffold pores, revealed to be particularly suitable when seeding cells into thick scaffolds of low porosity (Wendt et al. 2003). Interestingly, the principle of perfusion has been recently used in the field of heart valve tissue engineering also for in vitro transformation of porcine valves into human valves, enabling decellularization of valve grafts of xenogenic origin and subsequent re-cellularization with human cells (Karim et al. 2006).

When defining and optimizing seeding protocols (i.e., the selection of parameters such as cell concentration in the seeding suspension, medium flow rate, flow directions and timing of the perfusion pattern), most of the studies found in the literature have relied upon experimental, application-specific, trial and error investigations, without the support of theoretical models. However, the inherent complexity of a dynamic seeding system represents a major challenge for modeling, due to high dependence on the specific cell type and scaffold implemented (i.e., complex pore architecture and related fluid-dynamics, kinetics of cell adhesion, molecular mechanics, biomaterial properties, etc.). A notable effort in this direction was described by Li and co-authors, who developed and validated a mathematical model allowing predictive evaluation of the maximum seeding density achievable within matrices of different porosities, in a system enabling filtration seeding at controlled flow rates (Li et al. 2001).

6.2.2 Maintenance of a Controlled Culture Environment

Early bioreactors, developed for research purposes in the 1980s and 1990s of the last century, were generally meant to be positioned inside cell culture incubators

while in use. In such configurations, monitoring and control of key environmental parameters for homeostatic maintenance of cell cultures (such as temperature, atmosphere composition and relative humidity) were supplied by the incubators themselves. More recently, a spreading demand for automated, user-friendly and operationally simple bioreactor systems for cell and tissue culture catalyzed research towards the development of stand-alone devices integrating the key function of traditional cell culture incubators, namely environmental control.

Bioreactors are known to play a key role also in the maintenance of *local* homeostasis, at a level of the engineered construct, specifically via oxygen and metabolite supply and waste product removal. The high degree of structure heterogeneity of 3D engineered constructs cultured in static conditions (i.e., presence of a necrotic central region, surrounded by a dense layer of viable cells) suggests that diffusional transport does not properly assure uniform and efficient mass transfer within the constructs (Fassnacht and Portner 1999). On the contrary, convective media flow around the construct and, even at a greater extent, direct medium perfusion through its pores, can aid overcoming diffusional transport limitations. Bioreactors that perfuse culture medium directly through the pores of a scaffold have therefore been employed in the engineering of various tissues, demonstrating that perfusion enhances calcified matrix deposition by marrow-derived osteoblasts (Bancroft et al. 2002; Janssen et al. 2006a, b; Sikavitsas et al. 2005), viability, proliferative capacities and expression of cardiac-specific markers of cardiomyocytes (Dvir et al. 2006; Radisic et al. 2004b), cell proliferation in engineered blood vessels (Kitagawa et al. 2006) and extra-cellular matrix deposition, accumulation and uniform distribution by chondrocytes (Davisson et al. 2002b; Wendt et al. 2006). In this context, a deep understanding of the basic mechanisms underlying perfusion-associated cell proliferation/differentiation and matrix production will be challenging to achieve, since the relative effects of perfusion-induced mechanical stresses acting on cells and enhanced mass transfer of chemical species, or a combination of the factors, cannot be easily discerned. As a result, similar to perfusion seeding parameters, optimization of perfusion culture conditions is commonly achieved from an experimental, trial-and-error approach. In future applications, both the design of new perfusion bioreactors and the optimization of their operating conditions will derive significant benefits from computational fluid dynamics modeling aimed at estimating fluid velocity and shear profiles (Cioffi et al. 2006; Galbusera et al. 2007; Porter et al. 2005), as well as biochemical species concentrations within the pores of 3D scaffolds. A more comprehensive strategy that could help to elucidate and decouple the effects of mechanical stimuli and specific species should (a) combine theoretical and experimental approaches, i.e., validate simplified models with experimental data (Raimondi et al. 2006) and (b) make use of sensing and control technologies to monitor the culture progression and adapt the culture conditions in a feedback-controlled loop, aimed at re-establishing homeostatic parameters.

Another noteworthy factor heavily hindering homeostatic control in cell culture systems is the abrupt change in the concentration of metabolites/catabolites, signal molecules, as well as pH, when culture medium is exchanged in periodic batches.

In traditional static culture procedures, the smoothening of these step-shaped variations can be achieved by performing partial medium changes, however requiring additional repeated manpower involvement. Bioreactor technology offers a better solution by enabling either semi-continuous automatic replenishment of exhausted media at defined time-points or feedback-controlled addition of fresh media, aimed at re-establishing a homeostatic parameter to a pre-defined set point (e.g., pH) (Kino-Oka et al. 2005; Prenosil and Kino-Oka 1999; Sun et al. 2005).

6.2.3 *Physical Conditioning of Developing Tissues*

A number of in vivo and ex vivo studies over centuries contributed to demonstrate that physical forces (i.e., hydrodynamic/hydrostatic, mechanical and electrical) play a key role in the development of tissues and organs during embryogenesis, as well as their remodeling and growth in postnatal life. Based on these findings, and in an attempt to induce the development of biological constructs that resemble the structure and function of native tissues, tissue engineers have aimed to recreate in vitro a physical environment similar to the one experienced by tissues in vivo. For this purpose, numerous bioreactors have been developed, enabling controlled and reproducible dynamic conditioning of three-dimensional constructs for the generation of functional tissues.

Bioreactors applying *fluid-driven mechanical stimulation*, for example, were employed for the investigation of developmental mechanisms via establishment of shear stress acting directly on cells (e.g., in the case of cartilage (Raimondi et al. 2006), bone (Bancroft et al. 2002), cardiac tissue (Radisic et al. 2003)), via creation of a differential pressure (e.g., for blood vessels [Thompson et al. 2002] and heart valves [Mol et al. 2005]) or combining these two mechanisms (again with vessels [Hahn et al. 2007; Hoerstrup et al. 2001; Niklason et al. 1999; Sodian et al. 2002] and heart valves [Flanagan et al. 2007]). Furthermore, coherently with what was expected on the basis of in vivo findings, the development of tissues natively experiencing relevant mechanical cues was enhanced by means of bioreactors enabling *mechanical conditioning*, namely direct tension (e.g., tendons, ligaments, skeletal muscle tissue [Altman et al. 2002; Mantero et al. 2007; Powell et al. 2002], cardiac tissue [Fink et al. 2000]), compression (e.g., cartilage [Davisson et al. 2002a; Demartean et al. 2003]) and bending (e.g., bone [Mauney et al. 2004]). Similarly, interesting findings on the effect of *electrical stimulation* on the development of excitable tissues were derived by conditioning skeletal muscle (Pedrotty et al. 2005; Powell et al. 2002) and cardiac constructs (Radisic et al. 2004a). Moreover, a promotion of neural gene expression by activation of calcium channels was observed as a result of the application of physiological electrical patterns to primary sensory neurons (Brosenitsch and Katz 2001).

Consistent with the tight correlation existing in nature between the *structure* and *function* of biological tissues (the spatial arrangement of load-bearing structures in long bones and the presence of tightly parallel arrays of fibers in

skeletal muscles being just two examples of this principle), appropriate tissue structural arrangements have been induced *in vitro* via the dynamic conditioning of engineered tissues. Physical conditioning was shown to be an effective means to improve cell/tissue structural organization, mainly entering the mechanism of mutual influence that cells and extracellular proteins reciprocally exert via integrin binding (Chen and Lin 2006; Grad et al. 2005; Shangkai et al. 2007; Wernike et al. 2007).

As previously discussed with respect to flow-associated effects in perfusion bioreactors, it is imperative to underline that current scientific knowledge is far from allowing a deep understanding of the mechano-responsive dynamics of cell function. As a consequence, the idea of precisely directing tissue development *in vitro* by means of specific physical cues still remains an immense challenge. In evidence of this fact, one only needs to examine the vast array of model systems that can be found in the literature, and moreover, the various magnitudes, frequencies and durations of the applied physical stimuli, even with reference to one single tissue type. Deriving conclusions from different model systems becomes more challenging when considering that the same physical cue (e.g., compression) may result in the alteration of many secondary variables (e.g., tension, hydrostatic pressure, flow-shear, streaming potentials and mass transfer) according to the distinguishing features of the model system and, in particular, to the specific scaffold employed.

6.2.4 Predicting Mechanical Functionality of Engineered Tissues

One of the most compelling questions in the engineering of grafts for clinical use is related to the minimal stage of development required for safe and successful implantation. Especially in the context of the musculoskeletal system, this issue is often addressed by the effort to improve the mechanical properties of the tissue to be implanted. However, an alternative way to answer the question ‘how good is good enough?’ is related to the use of bioreactor-based *in vitro* model systems to test and predict the behavior of engineered grafts upon implantation and associated exposure to physiological loading regimes.

One example in this direction, in the context of articular cartilage repair, is provided by Demarteau et al. (2003). With the ultimate goal to define the effective functionality of engineered human cartilage, the authors exposed engineered constructs at different stages of development to a loading regime resembling a mild post-operative rehabilitation. Results clearly indicated that the response of engineered tissues to dynamic compression was correlated with the amount of glycosaminoglycans in the constructs prior to loading. Despite the limitation to a specific scaffold type and loading regime, the study indicates a possible role of bioreactors as functional quality control for engineered tissues, towards the definition of minimal requirements for implantation and immediate loading. Conversely, the same experimental setup could be exploited to identify potential

regimes of physical rehabilitation which are most appropriate for a specific graft. In this regard, quantitative analysis and computational modeling of stresses and strains which are experienced by tissues *in vivo* for a variety of activities, and by engineered tissues in bioreactors would be necessary to establish more precise comparisons of *in vivo* and *in vitro* mechanical conditioning.

The same concept and paradigm described above can be used to address fundamental questions relevant to the selection of appropriate cell sources. For example, the use of nasal chondrocytes for the repair of articular cartilage defects has long been proposed, mostly due to the higher and more reproducible chondrogenic capacity as compared to articular chondrocytes (Kafienah et al. 2002). However, the possible use of nasal chondrocytes in a joint critically depends on their capacity to respond to physical forces similarly to articular chondrocytes. Before more complex and costly animal models are introduced, bioreactors can provide a technical solution for addressing the raised question. In fact, Candrian et al. used different types of bioreactor systems to demonstrate that nasal chondrocytes not only can increase the synthesis and accumulation of extracellular matrix molecules in response to dynamic compression, but also can upregulate the expression of lubricating molecules, typically expressed by cells in the surface zone of articular cartilage, in response to surface motion (Fig. 6.1) (Candrian et al. 2007).

6.3 Bioreactor-Based Manufacturing of Tissue Engineering Products

During the initial phase of the emerging TE field, we have been mainly consumed by the new biological and engineering challenges posed in establishing and maintaining three-dimensional cell and tissue cultures. After nearly 2 decades, with exciting and promising research advancements, tissue engineering is now at the stage where it must begin to translate this research-based technology into large-scale and commercially successful products. However, just as other biotech and pharmaceutical industries came to realize in the past, we are ultimately faced with the fact that even the most clinically successful products will need to demonstrate: (a) cost-effectiveness and cost-benefits over existing therapies, (b) absolute safety for patients, manufacturers and the environment, and (c) compliance to the current regulations.

But what has been hindering cell-based engineered products from reaching the market and what can be done to increase their potential for clinical and commercial success? In this section, we describe and discuss several commercial manufacturing strategies that allowed the first cell-based products to enter the clinical practice. Moreover, we comment on the potential of bioreactor-based manufacturing approaches to improve the clinical and commercial success of engineered products by controlling, standardizing, and automating cell and tissue culture procedures in a cost-effective and regulatory-compliant manner. In particular, brief insight will be given with regards to techniques aimed at automating conventional

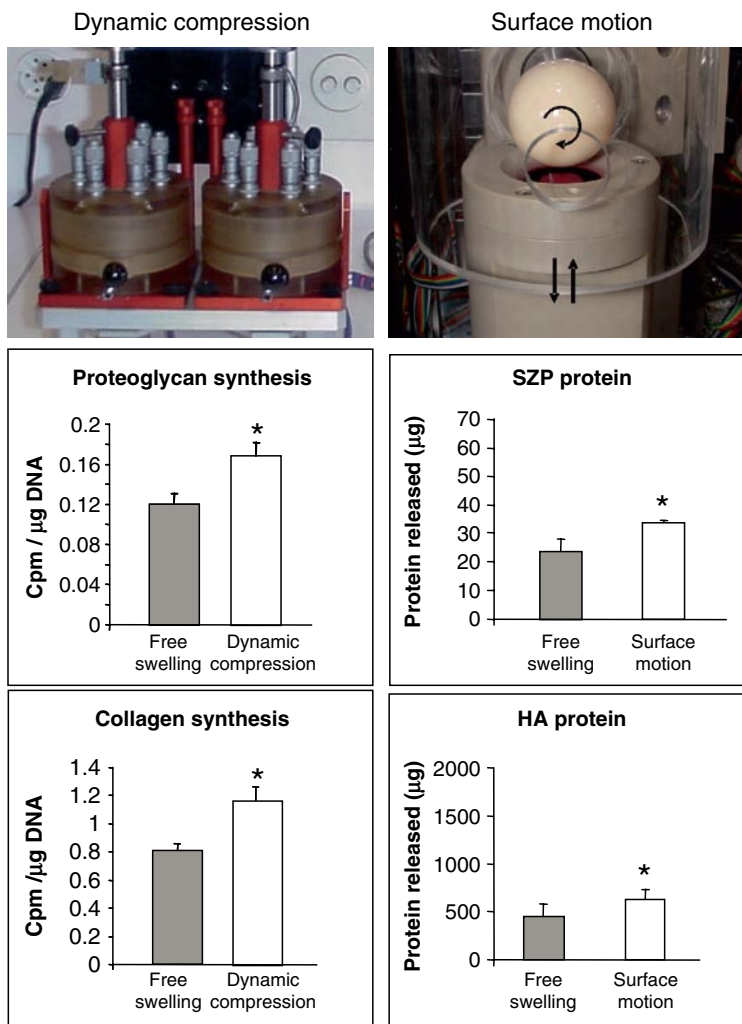


Fig. 6.1 Response of nasal chondrocytes to physical stimuli that simulate joint loading. Amounts of newly synthesized proteoglycans and collagen, measured by the incorporation of $[^{35}\text{S}]\text{SO}_4$ and $[^3\text{H}]\text{proline}$, respectively, were significantly higher in constructs subjected to a single application of *dynamic compression* as compared to those maintained under free swelling. Proteins involved in joint-lubrication (superficial zone protein “SZP” and hyaluronan “HA”) were released into the culture medium in significantly higher amounts when constructs were subjected to intermittent applications of *surface motion* as compared to those maintained under free swelling conditions (Candrian et al. 2007)

cell culture techniques (i.e., bi-dimensional monolayer cell expansion), strategies to automate and streamline tissue culture processes (i.e., comprising automation of the three-dimensional culture phase), as well as a critical analysis of different manufacturing concepts.

6.3.1 Automating Conventional Cell Culture Techniques

As described above, the basic procedures for generating engineered tissues have traditionally been based around conventional manual benchtop cell and tissue culture techniques. It is therefore quite natural that these manual techniques, due to their simplicity and wide-spread use, were included in the initial phases of product development, and ultimately in the final manufacturing processes of early cell-based products. Manual techniques still remain particularly appealing for start-up companies since the simple level of technology minimizes initial development time and investment costs, allowing for more rapid entry to clinical trials and into the market. An example of the straightforward benchtop-based manufacturing process is that employed by Genzyme Tissue Repair (Cambridge, MA, USA) for the production of Carticel[®], an *autologous* cell transplantation product for the repair of articular cartilage defects currently used in the clinic. To manufacture the Carticel product, a cartilage biopsy is harvested upon surgical intervention and sent to a central facility where the chondrocytes are isolated and expanded in monolayer culture to generate a sufficient number of cells (Mayhew et al. 1998) using routine culture systems (i.e., manually by a lab technician, inside a biological safety cabinet, housed in a Class 10,000 clean room). Hyalograft C[™], marketed by Fidia Advanced Biopolymers (Abano Terme, Italy), is an alternative *autologous* cell-based product for the treatment of articular cartilage defects, also manufactured through conventional benchtop techniques. Similar to the production of Carticel, chondrocytes are first isolated from a biopsy and expanded in tissue culture flasks by highly trained technicians at a central manufacturing facility. To generate the Hyalograft C cartilage graft, the expanded chondrocytes are then manually seeded onto a 3D scaffold and cultured for 14 days by specialized technicians using routine tissue culture techniques (Scapinelli et al. 2002). For both of these products, the simple production systems kept initial product development costs down as the products were established within the marketplace. However, these manufacturing processes require a large number of manual and labor-intensive manipulations, and moreover, due to the autologous nature of the products, each cell preparation must be treated individually. For instance, whereas in general lab practices a large quantity of flasks are routinely processed simultaneously in a sterile hood in parallel, for manufacturing autologous products, cells/flasks derived from a single donor would be removed from the incubator, introduced into the sterile hood, and processed individually (e.g., media exchanged, cells trypsinized and passaged, etc.), and only following a detailed and validated cleaning/decontamination procedure would the entire procedure be repeated with cells/flasks derived from a different donor. As a result, the production costs of these products are rather high, they possess inherent risks for contamination and intra- and inter-operator variability, and would be difficult to scale as product demands increase. It is therefore becoming more and more evident that tissue engineering firms will inevitably have to follow in the footsteps of other biotechnology fields and begin to introduce process engineering into their manufacturing strategies.

Robotic systems have proven highly effective in automating and controlling sophisticated manufacturing process for a wide variety of industries such as the

computer and automotive fields. Recently, robotics have also been developed for use in biotechnology applications (e.g., Cell^{host} system, from Hamilton AG, Bonaduz, Switzerland; and SelecTTM, from The Automation Partnership, Royston, UK), capable of performing a number of routine but laborious cell culture processes such as the maintenance and expansion of multiple simultaneous cell lines and the automated culture of embryonic stem cells. Robotics could also be an attractive option in the tissue engineering field (Knoll et al. 2004; Mason and Hoare 2007). For instance, in an attempt at automating the labor-intensive phase of expanding epithelial cells for dermal tissue engineering purposes, a closed bioreactor system with integrated robotics technology was designed to perform both automated medium exchange and cell passaging (Kino-Oka et al. 2005). Online measurements of medium components and simulations of cell growth kinetics could be used to determine the timing for medium exchanges and to predict cell confluence and scheduling cell passages. Moreover, the automatic and closed environment of the system minimized the number of potential aseptic handling steps, reducing the number of contaminations as compared to manual performance of the same process. This study demonstrates the significance of monitoring and control for bioreactors discussed earlier in this chapter, as well as the value of implementing innovative technological concepts more conducive to automation. However, it still remains questionable whether complex and rather costly robotic systems could actually demonstrate a real cost-benefit by replacing manual cell culture techniques in a manufacturing process.

As an alternative to essentially mimicking established manual procedures, bioreactor systems that implement novel concepts and techniques that streamline the conventional engineering processes will likely have the greatest impact on manufacturing. As opposed to the standard process for cell expansion, in which cells are cultured in a flask until reaching confluence, trypsinized, and re-plated in multiple flasks, culturing cells on an expandable membrane could minimize or bypass the need of cell passages. Using a bioreactor developed by Cytomec GmbH (Spiez, Switzerland), cells can be seeded onto a small circular membrane that can be gradually stretched radially by the bioreactor (similar to the iris of the eye) to continually provide cells with space to grow, without the need for serial passaging (Vonwil et al. 2007). Technology used to engineer cell-sheets (Yang et al. 2007) could also be implemented within a bioreactor design to facilitate the streamlining and automation of the cell expansion process. Culture surfaces in the bioreactor could be coated with the temperature-responsive polymer poly(N-isopropylacrylamide), which allows for the detachment of cells by simply lowering the temperature, thereby eliminating the need for trypsin and the associated time-consuming processing steps.

6.3.2 Automating Tissue Culture Processes

While the systems described in Section 6.3.1 illustrate various approaches to automate and streamline traditional *cell culture* processes, these “2D phases” are typically only the starting point for most tissue engineering strategies, and represent

only one component of the numerous key bioprocesses required to generate three-dimensional tissue grafts. As discussed in [Section 6.2](#), the structure, function, and reproducibility of engineered constructs can be dramatically enhanced by employing bioreactor-based strategies to establish, maintain, and possibly physically condition cells within the 3D environment (the “3D phases”). Therefore, ideally, bioreactor systems would be employed to automate and control the entire manufacturing process (both 2D and 3D phases), from cell isolation through generation of a suitable graft. The advantages of this comprehensive approach would be manifold. A closed, standardized, and operator-independent system would possess great benefits in terms of safety and regulatory compliance, and despite incurring high product development costs initially, these systems would have great potential to improve the cost-effectiveness of a manufacturing process, maximizing the potential for large-scale production in the long-term.

Advanced Tissue Sciences was the first tissue engineering firm to address the issues of automation and scale-up for their production of Dermagraft®, an *allogenic* product manufactured with dermal fibroblasts grown on a scaffold for the treatment of chronic wounds such as diabetic foot ulcers (Marston et al. 2003) (currently manufactured by Smith and Nephew, London, UK). Skin grafts were generated in a closed manufacturing system within bioreactor bags inside which cells were seeded onto a scaffold, cell-scaffold constructs were cultivated, cryopreservation was performed, and finally that also served as the transport container in which the generated grafts were shipped to the clinic (Naughton 2002). Eight grafts could be manufactured within compartments of a single bioreactor bag, and up to 12 bags could be cultured together with automated medium perfusion using a manifold, allowing the scaling of a single production run to 96 tissue grafts. Nevertheless, despite this early effort to automate the tissue engineering process, the production system was not highly controlled and resulted in many batches that were defective, ultimately contributing to the overall high production costs (Martin et al. 2004). Considering that significant problems were encountered in the manufacturing of this *allogenic* product, tremendous challenges clearly lie ahead in order to automate and scale the production of *autologous* grafts (technically, biologically, and in terms of regulatory issues), particularly since cells from each patient will be highly variable and cells must be processed as completely independent batches.

A particularly appealing approach to automate the production of autologous cell based products would be based on a modular design, where the bioprocesses for each single cell source are performed in individual, dedicated, closed system sub-units. In this strategy, a manufacturing process can be scaled-up, or perhaps more appropriately considered “scaled-out” (Mason and Hoare 2006), simply by adding more units to the production as product demand increases. This strategy is exemplified by the concept of ACTES™ (Autologous Clinical Tissue Engineering System), pioneered by Millenium Biologix and currently being developed by Octane Medical Group (Kingston, Ontario). As a compact, modular, fully automated and closed bioreactor system, ACTES would digest a patient’s cartilage biopsy, expand the chondrocytes, and provide either (1) an autologous cell suspension, or (2) an osteochondral graft generated by seeding and culturing the cells onto

the surface of an osteoconductive porous scaffold. Clearly, full automation of an entire tissue engineering process possesses the greatest risks upfront, requiring considerable investment costs and significant time to develop a highly technical and complex bioreactor system such as ACTES.

For the enthusiastic engineer, developing a fully automated and controlled system would probably necessitate state-of-the-art systems to monitor and control a full range of culture parameters, and when possible, to monitor cell behavior and tissue development throughout the production process (Martin et al. 2004). Significant benefits would derive from implementing sensing and monitoring devices within the manufacturing system in terms of *traceability* and *safety* of the process itself, features that are crucial to compliantly face current GMP guidelines. However, sensors and control systems will add significant costs to the bioreactor system. Keeping in mind low-cost bioreactor systems will be required for a cost-effective manufacturing process, it will be imperative to identify the essential process and construct parameters to monitor and control to standardize production and which can provide meaningful quality control and traceability data. In this context, the monitoring and control of bioreactor systems will be crucial at the research stage of product development in order to identify these key parameters and to establish standardized production methods.

6.3.3 *Streamlining Tissue Engineering Processes*

Bioreactor designs could be dramatically simplified, and related development costs significantly reduced, if we re-evaluate the conventional tissue engineering paradigms and could streamline the numerous individual processing steps. A bioreactor-based concept was recently described by Braccini et al. for the engineering of osteoinductive bone grafts (Braccini et al. 2005), which would be particularly appealing to implement in a simple and streamlined manufacturing process. In this approach, cells from a bone marrow aspirate were introduced directly into a perfusion bioreactor, without the conventional phase of selection and cell expansion on plastic dishes; bone marrow stem cells could be seeded and expanded directly within the 3D ceramic scaffold, ultimately producing a highly osteoinductive graft, in a single perfusion bioreactor system. Remarkably, expansion of human bone marrow stromal cells directly within the ceramic scaffold pores under perfusion flow supported the generation of constructs more reproducibly osteogenic than traditional cell expansion in monolayer (Fig. 6.2). This example thus highlights that modification of typical manufacturing processes as opposed to their automation can not only lead to more streamlined procedures, but also to improved standardization, which is often still an unresolved issue in regenerative medicine products.

The paradigm to generate a cell-based graft by direct expansion of cells within the scaffold pores in a 3D environment was recently shown to be valid even for other cell sources. For example, Scherberich et al. demonstrated that 3D perfusion culture of human adipose tissue-derived cells results in the generation of both vasculogenic

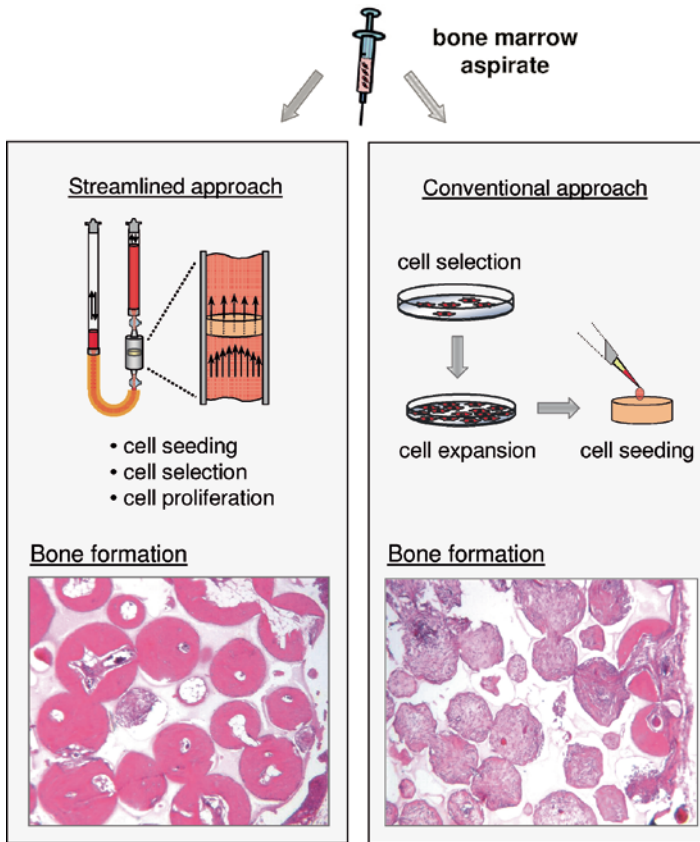


Fig. 6.2 Bone tissue formation by bone marrow stromal cells (BMSC) expanded by conventional monolayer culture or under the streamlined 3D perfusion bioreactor approach. Images show representative hematoxylin/eosin stained cross-sections of BMSC-ceramic constructs implanted ectopically in nude mice and harvested after 8 weeks. BMSC expanded directly in the ceramic scaffolds for 19 days in the bioreactor system reproducibly yielded high amounts of uniformly distributed bone tissue. In contrast, the same number of BMSC loaded in the ceramic following the conventional expansion in Petri dishes typically generated fibrous tissue, or in the most osteogenic specimens, limited amounts of bone localized at the periphery of the constructs (Braccini et al. 2005)

and osteogenic constructs, unlike typical monolayer expansion of cells derived from the same donors (Scherberich et al. 2007) (Fig. 6.3). Interestingly, the use of adipose tissue as a cell source, due to the relatively higher frequency of osteoprogenitor cells as compared to the bone marrow, allowed to reduce the culture times from 3 weeks down to 5 days, opening the challenging prospective to further shorten the processing time and develop a procedure which is compatible with intraoperative schedules (see Section 6.3.4.2).

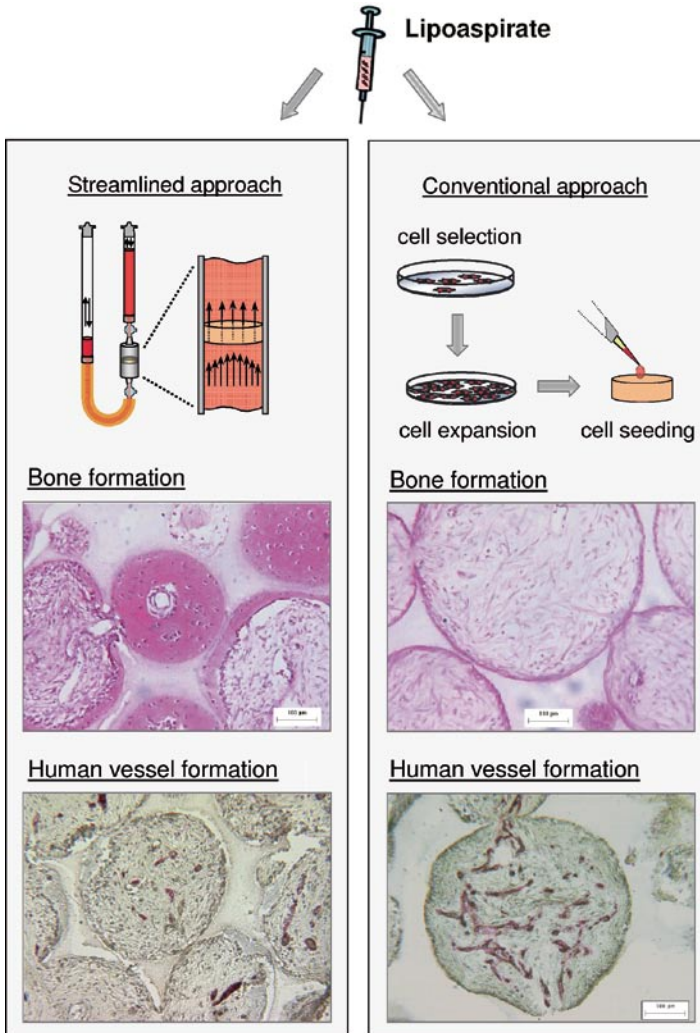


Fig. 6.3 Bone tissue and human blood vessel formation by adipose tissue-derived cells. Images show representative hematoxylin/eosin (bone formation) or anti-human CD34 (human endothelial cells) stained cross-sections of constructs implanted ectopically in nude mice and harvested after 8 weeks. When stromal vascular fraction (SVF) cells derived from human adipose tissue were cultured in ceramic-based scaffolds under perfusion for only 5 days and then implanted, significant amounts of bone tissue were observed. In contrast, SVF cells loaded in the ceramic following the conventional expansion in Petri dishes typically generated only fibrous tissue *in vivo*. Interestingly, during implantation, SVF cell-ceramic constructs generated by both approaches formed blood vessels, comprised of *human* endothelial cells, which had connected to the vasculature of the host mouse (Scherberich et al. 2007)

Simplified tissue engineering processes could be key to future manufacturing strategies by requiring a minimal number of bioprocesses and unit operations, facilitating simplified bioreactor designs with reduced automation requirements, permitting compact designs, with the likely result of reduced product development and operating costs.

6.3.4 Different ‘Manufacturing’ Concepts

6.3.4.1 Centralized Versus De-centralized Production Facilities

To date, all TE products currently on the market have been and continue to be manufactured within *centralized* production facilities. While manufacturing a product at central locations has the clear advantage of enabling close supervision over the entire production process, this requires establishing and maintaining large and expensive GMP facilities. But unlike in the production of other biotech products such as pharmaceuticals, critical processes and complicated logistical issues (e.g., packaging, shipping and tracking of living biopsies and engineered grafts), and the considerable associated expenses, must be considered for the centralized production of engineered tissue grafts.

As an alternative to manufacturing engineered products within main centralized production facilities, a *de-centralized* production system, such as a fully automated closed-bioreactor system (e.g., ACTES), could be located on-site within the confines of a hospital. This would eliminate complex logistical issues of transferring biopsies and engineered products between locations, eliminate the need for large and expensive GMP tissue engineering facilities, facilitate scale-up, and minimize labor-intensive operator handling. On the other hand, as previously mentioned in the context of fully automated closed bioreactors systems, a de-centralized manufacturing strategy will clearly involve the greatest upfront risks in terms of development time and costs.

6.3.4.2 Intraoperative Approaches

During the first 2 decades of the tissue engineering field, most research was aimed at the *in vitro* generation of tissue grafts that resemble the composition and function of native tissues. Trends may be changing. Perhaps due in part to the realization of the current high costs to engineer mature tissue grafts, there is now great emphasis on determining the *minimal* maturation stage of the graft (i.e., only cells seeded onto a scaffold, cells primed for (re-)differentiation within a scaffold, or a functional graft) that will promote defect repair *in vivo* (capitalizing on the *in vivo* “bioreactor”), with the ultimate goal of developing intraoperative therapies. In spite of a potential future paradigm shift, bioprocess engineering will continue to serve numerous vital roles in the tissue engineering/regenerative medicine field. Bioreactors could be used to

automate the isolation of cells from a biopsy for inter-operative cell therapies (e.g., Biosafe from Sepax, Eysins, Switzerland), or to rapidly seed the isolated cells into a 3D scaffold for immediate implantation. Moreover, bioreactors will continue to be critical for in vitro research applications to identify the requirements for the “in vivo bioreactors” (Stevens et al. 2005), and supporting the shift from tissue engineering approaches to the more challenging field of regenerative medicine.

6.4 Conclusions and Future Perspectives

The ex vivo generation of living tissue grafts has presented new biological and engineering challenges for establishing and maintaining cells in three-dimensional cultures, therefore necessitating the development of new biological models as compared to those long established for traditional cell culture. In this context, bioreactors represent a key tool in the tissue engineering field, from the initial phases of basic research through the final manufacturing of a product for clinical applications.

As we have seen from past and present tissue engineering manufacturing strategies, manual benchtop-based production systems allowed engineered products to reach the clinic, despite their rather high cost and limitations for potential scale-up. Higher-level technology involves longer development time, increased costs, and the risk of technical difficulties, but on the other hand, maximizes the potential for a safe, standardized, scaleable and cost-effective manufacturing process. Therefore, fundamental knowledge gained through the use of well-defined and controlled bioreactor systems at the research level will be essential to define, optimize, and moreover, streamline the key processes required for efficient manufacturing models.

The translation of bioreactors initially developed for research applications into controlled and cost-effective commercial manufacturing systems would benefit from collaborations between tissue engineering firms, academic institutions, and industrial partners with expertise in commercial bioreactor and automation systems. Academic partners would be key to provide the fundamental aspects of the system, while industrial partners could provide essential elements of automation, as well as making the system user-friendly and compliant with regulatory criteria. Working towards this ambitious goal, a number of multi-disciplinary consortiums have already been established within Europe (e.g., REMEDI, AUTOBONE, STEPS) to develop automated and scaleable systems and processes to streamline and control the engineering of autologous cell-based grafts, such that the resulting products meet specific regulations and criteria regarding efficacy, safety and quality, in addition to being cost-effective. Efforts in this direction will help to make tissue engineered products more clinically accessible and will help the translational paradigm of TE approaches from research-based technology to a competitive commercial field.

References

- Altman GH, Lu HH, Horan RL et al (2002) Advanced bioreactor with controlled application of multi-dimensional strain for tissue engineering. *J Biomech Eng* 124:742–749
- Bancroft GN, Sikavitsas VI, van den DJ et al (2002) Fluid flow increases mineralized matrix deposition in 3D perfusion culture of marrow stromal osteoblasts in a dose-dependent manner. *Proc Natl Acad Sci USA* 99:12600–12605
- Braccini A, Wendt D, Jaquierey C et al (2005) Three-dimensional perfusion culture of human bone marrow cells and generation of osteoinductive grafts. *Stem Cells* 23:1066–1072
- Brosenitsch TA, Katz DM (2001) Physiological patterns of electrical stimulation can induce neuronal gene expression by activating N-type calcium channels. *J Neurosci* 21:2571–2579
- Bueno EM, Laevsky G, Barabino GA (2007) Enhancing cell seeding of scaffolds in tissue engineering through manipulation of hydrodynamic parameters. *J Biotechnol* 129:516–531
- Candrian C, Vonwil D, Barbero A et al (2007) Engineered cartilage generated by nasal chondrocytes is responsive to physical forces resembling joint loading. *Arthritis Rheum* 58:197–208
- Chen JP, Lin CT (2006) Dynamic seeding and perfusion culture of hepatocytes with galactosylated vegetable sponge in packed-bed bioreactor. *J Biosci Bioeng* 102:41–45
- Cioffi M, Boschetti F, Raimondi MT et al (2006) Modeling evaluation of the fluid-dynamic microenvironment in tissue-engineered constructs: a micro-CT based model. *Biotechnol Bioeng* 93:500–510
- Davissou T, Kunig S, Chen A et al (2002a) Static and dynamic compression modulate matrix metabolism in tissue engineered cartilage. *J Orthop Res* 20:842–848
- Davissou T, Sah RL, Ratcliffe A (2002b) Perfusion increases cell content and matrix synthesis in chondrocyte three-dimensional cultures. *Tissue Eng* 8:807–816
- Demartean O, Wendt D, Braccini A et al (2003) Dynamic compression of cartilage constructs engineered from expanded human articular chondrocytes. *Biochem Biophys Res Commun* 310:580–588
- Dvir T, Benishti N, Shachar M et al (2006) A novel perfusion bioreactor providing a homogenous milieu for tissue regeneration. *Tissue Eng* 12:2843–2852
- Fassnacht D, Portner R (1999) Experimental and theoretical considerations on oxygen supply for animal cell growth in fixed-bed reactors. *J Biotechnol* 72:169–184
- Fink C, Ergun S, Kralisch D et al (2000) Chronic stretch of engineered heart tissue induces hypertrophy and functional improvement. *FASEB J* 14:669–679
- Flanagan TC, Cornelissen C, Koch S et al (2007) The in vitro development of autologous fibrin-based tissue-engineered heart valves through optimised dynamic conditioning. *Biomaterials* 28:3388–3397
- Freed LE, Vunjak-Novakovic G (1997) Microgravity tissue engineering. *In Vitro Cell Dev Biol Anim* 33:381–385
- Galbusera F, Cioffi M, Raimondi MT et al (2007) Computational modeling of combined cell population dynamics and oxygen transport in engineered tissue subject to interstitial perfusion. *Comput Methods Biomech Biomed Eng* 10:279–287
- Grad S, Lee CR, Gorna K et al (2005) Surface motion upregulates superficial zone protein and hyaluronan production in chondrocyte-seeded three-dimensional scaffolds. *Tissue Eng* 11:249–256
- Hahn MS, McHale MK, Wang E et al (2007) Physiologic pulsatile flow bioreactor conditioning of poly(ethylene glycol)-based tissue engineered vascular grafts. *Ann Biomed Eng* 35:190–200
- Hoerstrup SP, Zund G, Sodian R et al (2001) Tissue engineering of small caliber vascular grafts. *Eur J Cardiothorac Surg* 20:164–169
- Janssen FW, Hofland I, van OA et al (2006a) Online measurement of oxygen consumption by goat bone marrow stromal cells in a combined cell-seeding and proliferation perfusion bioreactor. *J Biomed Mater Res A* 79:338–348

- Janssen FW, Oostru J, Oorschot A et al (2006b) A perfusion bioreactor system capable of producing clinically relevant volumes of tissue-engineered bone: in vivo bone formation showing proof of concept. *Biomaterials* 27:315–323
- Kafienah W, Jakob M, Demartean O et al (2002) Three-dimensional tissue engineering of hyaline cartilage: comparison of adult nasal and articular chondrocytes. *Tissue Eng* 8:817–826
- Karim N, Golz K, Bader A (2006) The cardiovascular tissue-reactor: a novel device for the engineering of heart valves. *Artif Organs* 30:809–814
- Kino-Oka M, Ogawa N, Umegaki R et al (2005) Bioreactor design for successive culture of anchorage-dependent cells operated in an automated manner. *Tissue Eng* 11:535–545
- Kitagawa T, Yamaoka T, Iwase R et al (2006) Three-dimensional cell seeding and growth in radial-flow perfusion bioreactor for in vitro tissue reconstruction. *Biotechnol Bioeng* 93:947–954
- Knoll A, Scherer T, Poggendorf I et al (2004) Flexible automation of cell culture and tissue engineering tasks. *Biotechnol Prog* 20:1825–1835
- Li Y, Ma T, Kniss DA et al (2001) Effects of filtration seeding on cell density, spatial distribution, and proliferation in nonwoven fibrous matrices. *Biotechnol Prog* 17:935–944
- Mantero S, Sadr N, Riboldi SA et al (2007) A new electro-mechanical bioreactor for soft tissue engineering. *JABB* 5:107–116
- Marston WA, Hanft J, Norwood P et al (2003) The efficacy and safety of Dermagraft in improving the healing of chronic diabetic foot ulcers: results of a prospective randomized trial. *Diabetes Care* 26:1701–1705
- Martin I, Wendt D, Heberer M (2004) The role of bioreactors in tissue engineering. *Trends Biotechnol* 22:80–86
- Mason C, Hoare M (2006) Regenerative medicine bioprocessing: the need to learn from the experience of other fields. *Regen Med* 1:615–623
- Mason C, Hoare M (2007) Regenerative medicine bioprocessing: building a conceptual framework based on early studies. *Tissue Eng* 13:301–311
- Mauney JR, Sjostrom S, Blumberg J et al (2004) Mechanical stimulation promotes osteogenic differentiation of human bone marrow stromal cells on 3-D partially demineralized bone scaffolds in vitro. *Calcif Tissue Int* 74:458–468
- Mayhew TA, Williams GR, Senica MA et al (1998) Validation of a quality assurance program for autologous cultured chondrocyte implantation. *Tissue Eng* 4:325–334
- Mol A, Driessen NJ, Rutten MC et al (2005) Tissue engineering of human heart valve leaflets: a novel bioreactor for a strain-based conditioning approach. *Ann Biomed Eng* 33:1778–1788
- Naughton GK (2002) From lab bench to market: critical issues in tissue engineering. *Ann N Y Acad Sci* 961:372–385
- Niklason LE, Gao J, Abbott WM et al (1999) Functional arteries grown in vitro. *Science* 284:489–493
- Pedrotty DM, Koh J, Davis BH et al (2005) Engineering skeletal myoblasts: roles of three-dimensional culture and electrical stimulation. *Am J Physiol Heart Circ Physiol* 288:H1620–H1626
- Porter B, Zauel R, Stockman H et al (2005) 3-D computational modeling of media flow through scaffolds in a perfusion bioreactor. *J Biomech* 38:543–549
- Powell CA, Smiley BL, Mills J et al (2002) Mechanical stimulation improves tissue-engineered human skeletal muscle. *Am J Physiol Cell Physiol* 283:C1557–C1565
- Prenosil JE, Kino-Oka M (1999) Computer controlled bioreactor for large-scale production of cultured skin grafts. *Ann N Y Acad Sci* 875:386–397
- Radisic M, Euloth M, Yang L et al (2003) High-density seeding of myocyte cells for cardiac tissue engineering. *Biotechnol Bioeng* 82:403–414
- Radisic M, Park H, Shing H et al (2004a) Functional assembly of engineered myocardium by electrical stimulation of cardiac myocytes cultured on scaffolds. *Proc Natl Acad Sci USA* 101:18129–18134
- Radisic M, Yang L, Boublik J et al (2004b) Medium perfusion enables engineering of compact and contractile cardiac tissue. *Am J Physiol Heart Circ Physiol* 286:H507–H516

- Raimondi MT, Moretti M, Cioffi M et al (2006) The effect of hydrodynamic shear on 3D engineered chondrocyte systems subject to direct perfusion. *Biorheology* 43:215–222
- Scapinelli R, Aglietti P, Baldovin M et al (2002) Biologic resurfacing of the patella: current status. *Clin Sports Med* 21:547–573
- Scherberich A, Galli R, Jaquiere C et al (2007) Three-dimensional perfusion culture of human adipose tissue-derived endothelial and osteoblastic progenitors generates osteogenic constructs with intrinsic vascularization capacity. *Stem Cells* 25:1823–1829
- Shangkai C, Naohide T, Koji Y et al (2007) Transplantation of allogeneic chondrocytes cultured in fibroin sponge and stirring chamber to promote cartilage regeneration. *Tissue Eng* 13:483–492
- Sikavitsas VI, Bancroft GN, Lemoine JJ et al (2005) Flow perfusion enhances the calcified matrix deposition of marrow stromal cells in biodegradable nonwoven fiber mesh scaffolds. *Ann Biomed Eng* 33:63–70
- Sodian R, Lemke T, Fritsche C et al (2002) Tissue-engineering bioreactors: a new combined cell-seeding and perfusion system for vascular tissue engineering. *Tissue Eng* 8:863–870
- Stevens MM, Marini RP, Schaefer D et al (2005) In vivo engineering of organs: the bone bioreactor. *Proc Natl Acad Sci U S A* 102:11450–11455
- Sun T, Norton D, Haycock JW et al (2005) Development of a closed bioreactor system for culture of tissue-engineered skin at an air-liquid interface. *Tissue Eng* 11:1824–1831
- Thompson CA, Colon-Hernandez P, Pomerantseva I et al (2002) A novel pulsatile, laminar flow bioreactor for the development of tissue-engineered vascular structures. *Tissue Eng* 8:1083–1088
- Timmins NE, Scherberich A, Fruh JA et al (2007) Three-dimensional cell culture and tissue engineering in a T-CUP (tissue culture under perfusion). *Tissue Eng* 13:2021–2028
- Vonwil D, Barbero A, Quinn T et al (2007) Expansion of adult human chondrocytes on an extendable surface: a strategy to reduce passage-related dedifferentiation. *Eur Cell Mater* 13:17
- Vunjak-Novakovic G, Martin I, Obradovic B et al (1999) Bioreactor cultivation conditions modulate the composition and mechanical properties of tissue-engineered cartilage. *J Orthop Res* 17:130–138
- Wendt D, Marsano A, Jakob M et al (2003) Oscillating perfusion of cell suspensions through three-dimensional scaffolds enhances cell seeding efficiency and uniformity. *Biotechnol Bioeng* 84:205–214
- Wendt D, Stroebel S, Jakob M et al (2006) Uniform tissues engineered by seeding and culturing cells in 3D scaffolds under perfusion at defined oxygen tensions. *Biorheology* 43:481–488
- Wernike E, Li Z, Alini M et al (2007) Effect of reduced oxygen tension and long-term mechanical stimulation on chondrocyte-polymer constructs. *Cell Tissue Res*
- Yang J, Yamato M, Shimizu T et al (2007) Reconstruction of functional tissues with cell sheet engineering. *Biomaterials* 28:5033–5043
- Zhao F, Ma T (2005) Perfusion bioreactor system for human mesenchymal stem cell tissue engineering: dynamic cell seeding and construct development. *Biotechnol Bioeng* 91:482–493

Chapter 7

Biomimetic Approaches to Design of Tissue Engineering Bioreactors

Bojana Obradovic, Milica Radisic, and Gordana Vunjak-Novakovic

Abstract Tissue engineering is an attractive strategy to address the increasing clinical need for tissue replacement. Engineered tissues can also serve as high-fidelity models for studies of development, disease and therapeutic modalities. Cultivation of three-dimensional tissue equivalents is necessarily based on the use of bioreactors, which are designed to provide controlled steady state cultivation conditions as well as required biochemical and physical regulatory signals. In this chapter, we review the design and operation of tissue engineering bioreactors, with the focus on biomimetic approaches to provide in vivo-like environments for rapid and orderly tissue development by cells cultured on a scaffold. Specifically, we focus on bioreactors for tissue engineering of two distinctly different tissues – articular cartilage and myocardium.

Keywords Tissue engineering • Cartilage • Myocardium • Bioreactor • Oxygen transport • Mechanical stimulation

B. Obradovic (✉)
Department of Chemical Engineering, Faculty of Technology
and Metallurgy, University of Belgrade, Karnegijeva 4, 11120 Belgrade, Serbia
e-mail: bojana@tmf.bg.ac.rs

M. Radisic
Institute of Biomaterials and Biomedical Engineering, University of Toronto,
164 College St, Toronto, Ontario, M5S3G9, Canada

G. Vunjak-Novakovic
Department of Biomedical Engineering,
Columbia University, 363G Engineering Terrace,
Mail Code 8904, 1210 Amsterdam Avenue New York, NY 10027, USA

7.1 Introduction

Tissue engineering aims to provide functional biological substitutes of native tissues for potential clinical application in the repair of damaged or diseased tissues and organs. Ideally, a lost or damaged tissue could be replaced by an engineered graft that can re-establish appropriate structure, composition, cell signaling, and function of the native tissue. Thus, an engineered graft should provide regeneration, rather than repair, and undergo remodeling in response to environmental factors (Buckwalter and Mankin 1998; Einhorn 1998; O'Driscoll 2001). In addition, functional constructs can also serve as physiologically relevant models for in vitro studies of tissue development and help distinguishing the effects of specific environmental signals from the complex milieu of factors present in vivo.

One approach to tissue engineering is in vitro cultivation of functional tissue equivalents by mimicking the native cell environment and recapitulating processes during normal in vivo tissue development. This approach is biomimetic in nature, and based on reparative cells, a cell support that provides structural template for cell attachment and tissue regeneration, and bioreactor cultivation that provides facilitated transport of nutrients and metabolites, and provision of molecular and biophysical regulatory factors. The cell support should be biocompatible and biodegradable at the same rate as the rate of tissue assembly. Structure of the cell support determines the transport of nutrients, metabolites and regulatory molecules to and from the cells, whereas the biomaterial chemistry may have an important role in cell attachment and differentiation. The bioreactor should maintain controlled conditions in culture medium (e.g. temperature, pH, osmolality, levels of oxygen, nutrients, metabolites, regulatory molecules), facilitate mass transfer to and from the engineered tissue surfaces, and provide physiologically relevant physical signals (e.g., interstitial fluid flow, shear, pressure, compression) (Freshney et al. 2007). By the integrated design of the cell support and the bioreactor configuration and cultivation conditions, it is aimed to precisely regulate the local cellular microenvironment in order to induce appropriate cellular responses.

Biomimetic approaches to design of tissue engineering systems rely on the knowledge and understanding of cell and tissue biology and physiology. These studies can also serve to reveal underlying mechanisms of structural tissue development. In this chapter we provide description of biomimetic approaches to design of bioreactor systems for engineering of myocardium and cartilage, two distinctly different tissues regarding the metabolic activity, structure, and function.

7.2 Cardiac Tissue Engineering

7.2.1 Myocardium (*Cardiac Muscle*)

The myocardium (cardiac muscle) is a highly differentiated tissue that couples electrical and mechanical outputs to provide blood flow throughout the organism. It is composed of cardiac myocytes and fibroblasts with a dense supporting vasculature

and collagen-based extracellular matrix. The myocytes form a three-dimensional syncytium that enables propagation of electrical signals across specialized intracellular junctions to produce coordinated mechanical contractions that pump blood forward. Contractile apparatus of cardiac myocytes consists of sarcomeres arranged in parallel myofibrils. Cardiomyocytes comprise only 20–40% of the cells in the heart but they occupy 80–90% of the heart volume. Their high metabolic activity is supported by the high density of mitochondria in the cells (MacKenna et al. 1994; Brilla et al. 1995), and vast amounts of oxygen supplied by convection of blood through capillary networks and by diffusion into the tissue space surrounding each capillary. Under physiological conditions, oxygen dissolved in blood plasma accounts for only ~1.5% of total oxygen content of the blood (Fournier 1998) while the majority of oxygen carrying capacity of the blood comes from hemoglobin, a natural oxygen carrier.

7.2.2 Tissue Engineering

Cardiac muscle has a limited ability to regenerate after myocardial infarction or congenital injury. Currently, the only definitive treatment for end stage heart failure is cardiac transplantation, which is limited by the availability of donor organs. Numerous studies have been focused on possibilities for myocardial tissue replacement. Repair of myocardial injuries has been attempted by injection of myogenic cells into scarred myocardium (Soonpaa et al. 1994; Scorsin et al. 1996; Connold et al. 1997) and the replacement of scarred tissue with engineered grafts (Li et al. 1999; Leor et al. 2000; Zimmermann et al. 2002). To serve as grafts for myocardial repair, engineered constructs must be thick and compact, contain physiologic density of metabolically active, differentiated, electromechanically coupled cells, and contract synchronously in response to electrical stimulation.

Three-dimensional tissue constructs that express structural and physiological features characteristic of native cardiac muscle have been engineered using fetal or neonatal rat cardiac myocytes (CM) cultured in collagen gels with mechanical stimulation (Eschenhagen et al. 1997; Fink et al. 2000; Zimmermann et al. 2000, 2002), on collagen fibers (Akins et al. 1999), polyglycolic acid meshes (Bursac et al. 1999; Carrier et al. 1999, 2002a, b; Papadaki et al. 2001), and collagen sponges (Li et al. 1999, 2000; Radisic et al. 2003, 2004). Cells were seeded onto scaffolds and cultivated in dishes (Carrier et al. 1999; Li et al. 1999; Leor et al. 2000; Papadaki et al. 2001), spinner flasks (Bursac et al. 1999; Carrier et al. 1999; Papadaki et al. 2001) or in rotating vessels (Akins et al. 1999; Carrier et al. 1999; Papadaki et al. 2001). Oxygen dissolved in the culture medium was transported to the cells by molecular diffusion, which alone could support only ~100 μm thick outer layer of functional tissue but not the construct interior, which remained relatively acellular (Bursac et al. 1999; Carrier et al. 1999; Papadaki et al. 2001; Zimmermann et al. 2000). Perfusion of constructs by culture medium markedly improved the uniformity of cell distribution, but the overall cell density remained low due to diffusional limitations of oxygen supply during scaffold seeding (Carrier et al. 2002a, b). Generally, oxygen transport during cell seeding and cultivation

of engineered constructs was shown to be one of the key factors for cell survival. Furthermore, measurements of oxygen concentrations and cell viability within engineered cardiac constructs clearly indicated the need to maintain the oxygen concentration above $\sim 100 \mu\text{M}$ at all points within the engineered tissue (Radisic et al. 2006a).

7.2.2.1 Biomimetic Bioreactor Culture System

In order to enhance oxygen supply to the cells within engineered constructs, a biomimetic approach was adopted, where oxygen is supplied to the cells by mechanisms similar to those in the native heart. Highly porous, channeled scaffolds, culture medium supplemented with oxygen carriers, and perfusion bioreactors were utilized to provide convective transport of oxygen through the tissue constructs mimicking *in vivo* mechanisms of oxygen delivery to the cells (Fig. 7.1) (Radisic et al. 2006b, c, 2007).

To mimic the capillary network, rat cardiomyocytes alone or in a co-culture with fibroblasts isolated from 1 to 2 day old neonatal rats were seeded on a highly porous elastomer (Wang et al. 2002) with a parallel array of channels (Radisic et al. 2006b).

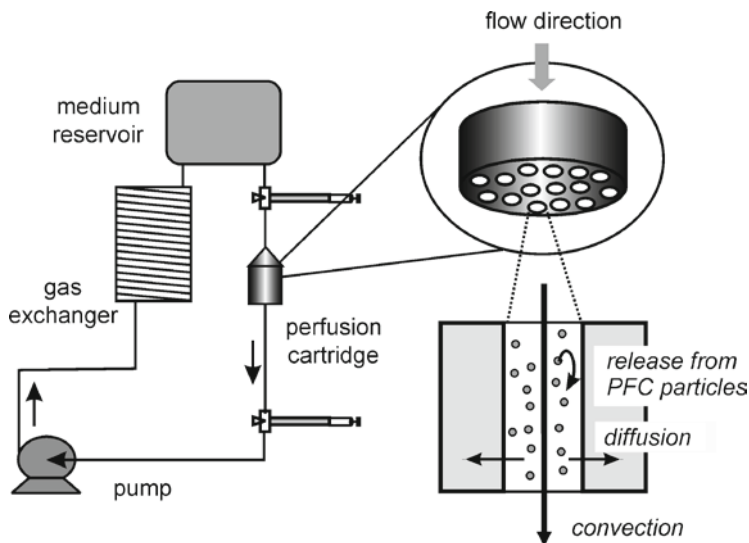


Fig. 7.1 Biomimetic cardiac culture system. Cardiac cells were seeded onto channeled scaffolds and each cell-polymer construct was fitted into a perfusion cartridge connected to a perfusion loop, which incorporated a medium reservoir and a gas exchanger. Two syringes served for medium exchange and extraction of gas bubbles. Unidirectional medium flow at a physiologic velocity was provided by a multichannel peristaltic pump. Supply of oxygen to the tissue was provided by medium flow through the channels (convection) and diffusion through the tissue. Spent oxygen in medium was replenished by release from PFC particles

The sequential coculture of cardiac fibroblasts and myocytes was shown to support cardiomyocyte attachment, differentiation, and contractile function, presumably due to scaffold conditioning by cultured fibroblasts (Radisic et al. 2008). Gel-cell inoculated constructs (5–6 mm diameter \times 2 mm thick discs) were fitted in 1.5-ml polycarbonate perfusion cartridges (one construct per cartridge) between two O rings (5 mm ID, 10 mm OD) and stainless steel screens, in order to provide culture medium flow directly through the tissue. Each cartridge was connected to a perfusion loop with the total volume of 30 ml, which incorporated a reservoir bag and a gas exchanger (a coil of silicone tubing, 3 m long). Constructs were subjected to unidirectional medium flow by a multichannel peristaltic pump at a flow rate of 0.1 ml/min for 3 days of cultivation. This flow rate corresponded to the velocity of 560 $\mu\text{m/s}$, comparable to blood velocity through capillaries in native heart ($\sim 500 \mu\text{m/s}$).

Furthermore, to mimic the role of hemoglobin, the culture medium was supplemented with a synthetic oxygen carrier (OxygentTM). OxygentTM is a 60%w/v (32%v/v) phospholipid stabilized emulsion of perfluorooctyl bromide as a principal component and a small percentage of perfluorodecyl bromide (Kraft et al. 1998). Since perfluorocarbon (PFC) droplets are immiscible with the aqueous phase, they served as rechargeable oxygen reservoirs, replenishing oxygen in the aqueous phase of culture medium by diffusion. Overall, the oxygen partial pressures measured in the aqueous phase of PFC-supplemented and unsupplemented (control) medium were the same, and the PFC particles replenished oxygen consumed by the cells without increasing oxygen concentration in the aqueous phase of culture medium.

Comparison of conditions in the *in vivo* heart tissue and in the biomimetic bioreactor system is summarized in the Table 7.1.

7.2.2.2 Cardiac Tissue Engineering in the Biomimetic Culture System

Medium supplementation with PFC emulsion at a concentration of $\sim 5.4\%v/v$ increased availability of oxygen for the cultivated cells such that the total oxygen concentration consumed by the control constructs was smaller (62 μM) as compared

Table 7.1 Comparison of the *in vivo* (native heart) and *in vitro* (bioreactor) conditions

	In vivo (native heart)	In vitro (bioreactor)
Cells	$\sim 10^8$ cell/cm ³ 33% myocytes and mostly fibroblasts	$\sim 0.3 \times 10^8$ cell/cm ³ Myocytes, fibroblasts, and endothelial cells; or stem cells
Geometry	Capillary network: $\sim 7 \mu\text{m}$ diameter, $\sim 30 \mu\text{m}$ spacing	Parallel channel array: 335 μm diameter, 364 μm spacing
Mass transport	Blood velocity $\sim 500 \mu\text{m/s}$	Medium velocity: 560 $\mu\text{m/s}$
Oxygen carrier	Hemoglobin (arterial blood) O ₂ dissolved in plasma: 130 μM O ₂ as oxyhemoglobin: 8,500 μM	5.4% PFC emulsion O ₂ dissolved in aq. phase: 220 μM O ₂ in PFC particles: 230 μM

to the PFC supplemented constructs (82 μM). In addition, PFC supplementation induced significantly lower oxygen decrease in medium passing through the tissue constructs (28 mmHg) as compared to the constructs perfused with control culture medium (45 mmHg) (Radisic et al. 2006b).

Higher availability of oxygen resulted in markedly and significantly higher contents of DNA and cardiac proteins (troponin I and connexin-43) in tissue constructs cultured with the PFC supplemented medium as compared to those cultured in control medium (Radisic et al. 2006b). Final cell densities were 0.27 and 0.43×10^8 cell/cm³ in the control and PFC supplemented group, respectively. Supplementation of medium with PFC emulsion resulted in less cell damage and death as seen also from the lower release of LDH as compared to the control group. The expressions of troponin I and connexin-43 were 53% and 135% in the control group and 77% and 163% in the PFC group, respectively, calculated on the basis of values measured for isolated cardiomyocytes.

Constructs cultivated in PFC supplemented medium expressed also enhanced contractile properties as compared to those cultured in control medium (Radisic et al. 2006b). Excitation thresholds were 3.8 ± 0.2 and 2.7 ± 0.1 V in the control and PFC group, respectively, while maximum capture rates were 162 ± 6 and 127 ± 15 bpm in the control and PFC group, respectively.

The enhanced structural and contractile properties of constructs cultured in PFC supplemented medium are indicative of improved development toward an adult cardiac phenotype, which could be correlated to the efficient oxygen supply to the cells, by a combined use of channeled scaffolds and PFC emulsion.

7.3 Cartilage Tissue Engineering

7.3.1 Articular Cartilage

Skeletally mature articular cartilage is an avascular tissue composed of relatively low number of cells (chondrocytes) embedded in abundant extracellular matrix (ECM), consisting of a fibrous network of collagen type II and glycosaminoglycan (GAG)-rich proteoglycans (Buckwalter and Mankin 1997). Chondrocytes are well adapted to hypoxic conditions since the adult articular cartilage is supplied by oxygen and nutrients from the synovial fluid by diffusion and by fluid flow during joint loading (O'Hara et al. 1990). In contrast, immature cartilage is vascularized and efficiently supplied with oxygen and exhibits high metabolic activity.

The main function of articular cartilage is to allow joint mobility while transferring compressive and shear forces. During joint movements, articular cartilage is dynamically exposed to compressive stresses, which can be as high as 6–18 MPa (Ateshian and Hung 2003). Mechanical loading was shown to strongly affect metabolic activity of articular chondrocytes consequently altering composition, structure and biomechanical properties of articular cartilage in vivo and in vitro.

In general, static compression of cartilage leads to loss of proteoglycans (Palmski et al. 1979; Vanwanseele et al. 2002), while moderate exercise (Saamanen et al. 1987; Kiviranta et al. 1988) and cyclic dynamic loading may stimulate synthesis of proteoglycans and proteins, in a way that depends on the frequency, intensity, and duration of the stimulus (Gray et al. 1989; Sah et al. 1989; Parkkinen et al. 1993; Steinmeyer and Knue 1997; Wong et al. 1999; Grodzinsky et al. 2000).

7.3.2 Tissue Engineering

Adult cartilage under physiologic conditions has practically no capacity for self-repair after an injury (Buckwalter and Mankin 1997). Cartilage tissue engineering based on the integrated use of chondrogenic cells, biodegradable scaffolds, and bioreactors was proposed for in vitro regeneration of tissue equivalents that would ideally have site- and scale-specific structural and biomechanical properties of native articular cartilage, and integrate firmly and completely to the adjacent host tissues (Freed and Vunjak-Novakovic 2000a, b; Chao et al. 2007).

Cells mostly used in this approach, are chondrocytes (fully differentiated cells) or osteochondral progenitor cells isolated from bone marrow (herein referred to as bone marrow stromal cells – BMSC). BMSC have the advantage in higher proliferative and regenerative capacity as compared to cultures of differentiated chondrocytes, but these cells require additional biochemical regulatory signals to induce chondrogenic differentiation. Efficient mass transfer of regulatory molecules is thus one of the main requirements in cultures of BMSC.

Biomaterials used for cartilage tissue engineering have varied regarding chemistry (e.g. collagen, alginate, agarose, synthetic polymers), geometry and structure (e.g. gels, fibrous meshes, sponges). One of the extensively used scaffolds is the highly porous mesh made of biodegradable fibrous polyglycolic acid (PGA), which was shown to biodegrade at a rate comparable to that of ECM synthesis in cell-polymer constructs cultivated under appropriate in vitro conditions (Freed et al. 1994a, b). Alginate is also one of the most important scaffold materials since it was shown to support cultures of chondrogenic cells and synthesis of cartilaginous components (Weber et al. 2002; Masuda et al. 2003; Grunder et al. 2004; Sharma and Elisseff 2004). The beneficial effects of scaffolds were amplified in hydrodynamically active environments (Pei et al. 2002).

Variety of bioreactors were investigated for cartilage tissue engineering including static and mixed flasks, rotating vessels, perfusion cartridges, packed bed bioreactors, and bioreactors with mechanical stimulation (Radisic et al. 2005). Among these, rotating bioreactors were shown to promote in vitro chondrogenesis by dynamic laminar flow and efficient supply of oxygen to the cultivated tissue (Vunjak-Novakovic et al. 1999, 2002; Obradovic et al. 1999, 2000, 2001). The resulting engineered cartilage after 6 weeks of cultivation had physiological cellularities and spatially uniform distributions of cartilaginous components. However, the fraction of collagen remained at 39% of physiologic level even after 7 months

of cultivation in rotating bioreactors (Martin et al. 2000). Consistently, dynamic stiffness and streaming potential of engineered cartilage were 46% and 28% of those of native cartilage, respectively (Martin et al. 2000).

Taken together, these studies indicated that optimal conditions for functional tissue engineering of cartilage will be likely determined by the integrated design of scaffolds, physical stimuli in the bioreactor, and provision of growth factors necessary to induce chondrogenic differentiation of progenitor cells (Obradovic et al. 2005).

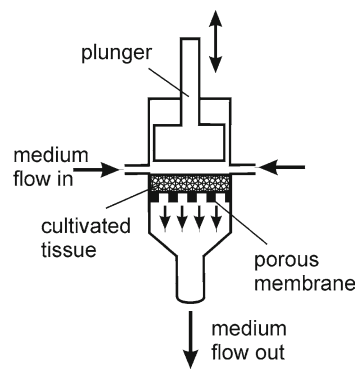
7.3.2.1 Biomimetic Approaches to Design of Bioreactor Systems

In this chapter we focus on attempts to design bioreactors for functional cartilage tissue engineering providing efficient mass transfer and adequate physical stimuli. A possible design of such a bioreactor is presented in Fig. 7.2 and provides dynamic tissue compression by a plunger and tissue perfusion by the cultivating medium (Petrovic et al. 2009). In order to determine optimal operating conditions in this bioreactor, we review here cartilage tissue engineering in bioreactors with mechanical stimulation and bioreactors with interstitial fluid flow.

Bioreactors with Mechanical Stimulation

Bioreactors with controlled dynamic loading were proposed to mimic biomechanical stimuli that native articular cartilage is normally exposed to in vivo (Mauck et al. 2000, 2002, 2003a, b; Demarteau et al. 2003a, b). In this bioreactor design (Fig. 7.3), tissue constructs are placed in wells and dynamically compressed by plungers to reproduce physiological joint loading (5–10% strain, 0.1–1 Hz frequency). In alginate and agarose gels seeded with bovine chondrocytes, intermittent deformational loading (10% strain, 1 Hz frequency, 1 h on/1 h off, 3 h/day, 5 days/week) stimulated deposition of cartilaginous ECM components and enhanced of biomechanical

Fig. 7.2 Novel bioreactor with mechanical stimulation and tissue perfusion. Culture medium is supplied from the sides and forced through the cultivated tissue. Dynamic compression of the tissue can be performed independently or simultaneously with perfusion (Petrovic et al. 2009)



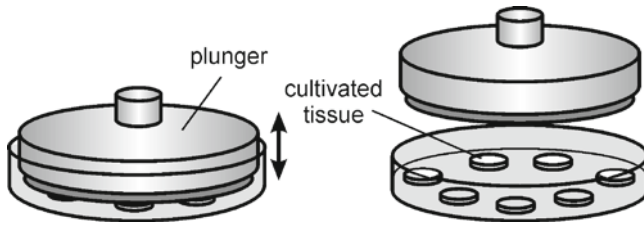


Fig. 7.3 Basic design of a bioreactor with dynamic compression. Cultivated tissue samples are placed in one or more wells filled with medium and unconfinely, dynamically compressed by a plunger

properties of engineered cartilage over time (Mauck et al. 2000). Over 28 days of cultivation, equilibrium aggregate modulus in dynamically loaded discs increased approximately 21-fold as compared to the initial discs (Mauck et al. 2000). In addition, dynamically loaded constructs exhibited significantly higher values of dynamic and equilibrium Young's moduli as compared to static free swelling cultures after 1–2 months of culture (Mauck et al. 2002, 2003b). Notably, the enhancement of biomechanical properties by dynamic compression as compared to free swelling cultures was observed even though no significant differences in GAG and collagen contents were measured, which implied different structural organizations of the produced ECM (Mauck et al. 2003b).

Furthermore, growth factors provided in conjunction with dynamic loading during culture had a synergistic effect on compositions and mechanical properties of cultured constructs (Mauck et al. 2003a). Dynamic loading of cell-polymer constructs based on dually-transfected bovine MSCs with an aggrecan-luciferase reporter construct and a constitutive CMV-Renilla plasmid, modulated aggrecan promoter activity, such that it increased over time resulting in increased proteoglycan content (Mauck et al. 2006).

However, still is little known about specific regimes of application of mechanical loading (i.e. magnitude, frequency, continuous or intermittent, duty cycle) that are stimulatory for *in vitro* development of all structural and functional properties of native cartilage tissue. Dynamic compression of expanded adult human chondrocytes seeded in Polyactive foams stimulated GAG formation only in already developed cartilaginous tissues (Demartean et al. 2003b), which implies that engineered tissues at different stages of development might require different regimes of mechanical conditioning.

Bioreactors with Interstitial Fluid Flow

A limitation of the above bioreactors with dynamic loading is that the surface for mass transfer is reduced to only through the outer cylindrical surface of the engineered tissue. Efficient mass transfer can be achieved by the use of perfusion cartridges and porous scaffolds (Fig. 7.4a) similar to the biomimetic bioreactor system applied for cardiac tissue engineering. Expanded human adult BMSC and bovine

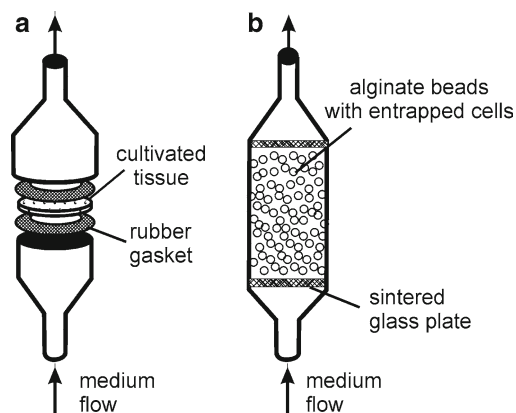


Fig. 7.4 Bioreactors with interstitial medium flow. **(a)** Perfusion cartridge: cells are seeded onto a porous scaffold, clamped between gaskets, and directly perfused by the cultivation medium. **(b)** Packed bed bioreactor: cells are entrapped in alginate beads, which are then packed and perfused by the cultivation medium

calf chondrocytes were seeded onto collagen sponges and fibrous PGA scaffolds, respectively, and cultivated under continuous interstitial medium flow at physiological velocities (20–40 $\mu\text{m/s}$).

In order to achieve efficient mass transfer and protection of cells from the shear stresses induced by medium flow, we have designed and utilized packed bed bioreactors with small diameter alginate beads as cell supports (Osmokrovic et al. 2006; Obradovic et al. 2007). Bovine calf chondrocytes were immobilized in 2.5 mm alginate beads at a concentration of 120×10^6 cell/ml and cultivated under continuous medium flow of 2.5 ml/min in packed bed bioreactors (Fig. 7.4b). Each bioreactor was connected to a separate perfusion loop, which included a medium reservoir and a tubing coil serving as a gas exchanger. After 2 weeks of perfusion, tissue formation induced clumping of alginate beads and blockage of the bioreactors (Fig. 7.5a). Large tissue buds protruded from surfaces of the bioreactor cultivated beads (Fig. 7.5b), feature that was not observed in statically cultivated beads.

Integration of the beads in large tissue lumps even though not uniform, implied that parameters of this cultivation system could be optimized to obtain cartilaginous equivalents for potential clinical treatments of fairly large defects (over 10 mm in diameter). However, histological appearances of the bead cross-sections revealed synthesis of GAG preferentially in superficial regions, indicating mass transfer limitations in the bead interiors (Obradovic et al. 2007). These results suggested that the cell density and the bead size should be decreased in order to achieve shorter distances for diffusion within alginate matrices and more uniform ECM regeneration.

Electrostatic droplet generation was shown to be a suitable technique for controlled production of alginate microbeads down to 50 μm in diameter based on

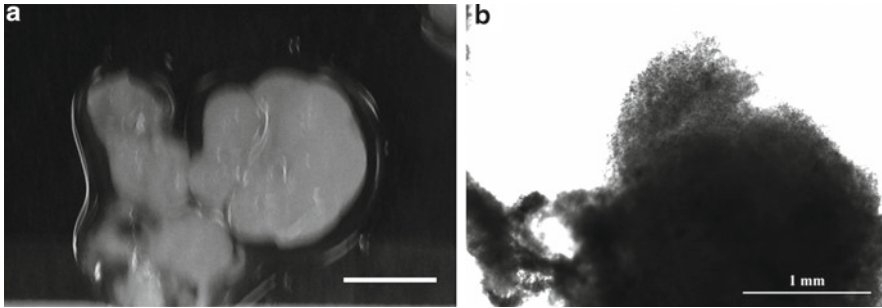


Fig. 7.5 Appearance of alginate beads with immobilized chondrocytes cultivated in packed bed bioreactors for 20 days in total, including 2 weeks of continuous bioreactor perfusion. (a) Clump of beads (scale bar = 5 mm). (b) Surface of a bead (scale bar = 1 mm)

the use of electrostatic forces (Bugarski et al. 1994; Poncelet et al. 1999; Manojlovic et al. 2006). We have also demonstrated that this technique could be successfully used for immobilization of murine BMSC (Obradovic et al. 2004; Bugarski et al. 2005). Alginate microbeads 500 μm in diameter with immobilized murine BMSC at a concentration of 5×10^6 cell/ml were cultivated for 5 weeks in the packed bioreactor under continuous medium flow of 0.18 ml/min. In this study, microbeads preserved the shape and consistency and only in rare cases merged together (Osmokrovic et al. 2006; Obradovic et al. 2007). These results implied that the cell concentration used (5×10^6 cell/ml) was too low to result in tissue formation.

In sum, optimization of initial cell density, alginate microbead size and perfusion flowrate in this system could provide efficient delivery of regulatory molecules to the immobilized cells and precise control of the cellular microenvironment in cartilage tissue engineering.

7.4 Conclusions

Biomimetic approaches to design of tissue engineering systems are aimed at recapitulating conditions during normal *in vivo* tissue development. By this strategy it is intended to precisely regulate the cellular microenvironment by adequate and timely provision of biochemical and biophysical regulatory signals and thus induce regeneration of structurally and functionally competent tissue equivalents. In addition, design and operation of biomimetic systems could be powerful tools to study the effects of specific signals on cells and tissues and reveal fundamental mechanisms of functional tissue assembly.

We described here examples of biomimetic systems for cardiac and cartilage tissue engineering. Highly porous, channeled scaffolds mimicking a capillary network, medium supplemented with oxygen carriers fulfilling the role of hemoglobin in

blood, and tissue perfusion at physiologic velocities were used to enhance oxygen delivery, resulting in improved structural and contractile properties of engineered cardiac constructs. In addition, dynamic deformational loading, with optimized parameters mimicking compressive stresses found in vivo, and appropriate biochemical signals could facilitate the growth of a structurally organized cartilage tissue substitute.

Acknowledgements The authors would like to acknowledge funding of their research was funded by the Ministry of Science of the Republic of Serbia, grant 142075, Swiss National Science Foundation, grant IB73B0-111016/1 (BO), NIH grants P41 EB002520-01, R01 DE016525 and R01 HL076485-01 (GV), and ARTEC and NSERC Discovery Grant (MR).

References

- Akins RE, Boyce RA, Madonna ML, Schroedl NA, Gonda SR, McLaughlin TA, Hartzell CR (1999) Cardiac organogenesis in vitro: reestablishment of three-dimensional tissue architecture by dissociated neonatal rat ventricular cells. *Tissue Eng* 5:103–118
- Ateshian GA, Hung CT (2003) Functional properties of native articular cartilage. In: Guilak F, Butler DL, Goldstein SA, Mooney DJ (eds) *Functional tissue engineering*. Springer, New York, pp 46–68
- Brilla CG, Maisch B, Rupp H, Sunck R, Zhou G, Weber KT (1995) Pharmacological modulation of cardiac fibroblast function. *Herz* 20:127–135
- Buckwalter JA, Mankin HJ (1997) Articular cartilage, part II: degeneration and osteoarthritis, repair, regeneration, and transplantation. *J Bone Joint Surg Am* 79A:612–632
- Buckwalter JA, Mankin HJ (1998) Articular cartilage: degeneration and osteoarthritis, repair, regeneration, and transplantation. *Instr Course Lect* 47:487–504
- Bugarski B, Li Q, Goosen MFA (1994) Electrostatic droplet generation: mechanism of polymer droplet formation. *AIChE J* 40:1026–1031
- Bugarski D, Obradovic B, Petakov M, Jovicic G, Stojanovic N, Bugarski B (2005) Alginate microbeads as potential support for cultivation of bone marrow stromal cells. In: Uskokovic DP, Milonjic SK, Rakovic DI (eds) *Materials science forum*, vol. 494. Progress in advanced materials processes. Trans Tech Publications Ltd, Zurich, pp 525–530
- Bursac N, Papadaki M, Cohen RJ, Schoen FJ, Eisenberg SR, Carrier R, Vunjak-Novakovic G, Freed LE (1999) Cardiac muscle tissue engineering: toward an in vitro model for electrophysiological studies. *Am J Physiol Heart Circ Physiol* 277:H433–H444
- Carrier RL, Papadaki M, Rupnick M, Schoen FJ, Bursac N, Langer R, Freed LE, Vunjak-Novakovic G (1999) Cardiac tissue engineering: cell seeding, cultivation parameters and tissue construct characterization. *Biotechnol Bioeng* 64:580–589
- Carrier RL, Rupnick M, Langer R, Schoen FJ, Freed LE, Vunjak-Novakovic G (2002a) Effects of oxygen on engineered cardiac muscle. *Biotechnol Bioeng* 78:617–625
- Carrier RL, Rupnick M, Langer R, Schoen FJ, Freed LE, Vunjak-Novakovic G (2002b) Perfusion improves tissue architecture of engineered cardiac muscle. *Tissue Eng* 8:175–188
- Chao PhG, Grayson W, Vunjak-Novakovic G (2007) Engineering cartilage and bone using human mesenchymal stem cells. *J Orthop Sci* 12:398–404
- Connold AL, Frischknecht R, Dimitrakos M, Vrbova G (1997) The survival of embryonic cardiomyocytes transplanted into damaged host myocardium. *J Muscle Res Cell Motil* 18:63–70
- Demarteau O, Jakob M, Schafer D, Heberer M, Martin I (2003a) Development and validation of a bioreactor for physical stimulation of engineered cartilage. *Biorheology* 40:331–336
- Demarteau O, Wendt D, Braccini A, Jakob M, Schafer D, Heberer M, Martin I (2003b) Dynamic compression of cartilage constructs engineered from expanded human articular chondrocytes. *Biochem Biophys Res Commun* 310:580–588

- Einhorn TA (1998) The cell and molecular biology of fracture healing. *Clin Orthop* 355S:S7–S21
- Eschenhagen T, Fink C, Remmers U, Scholz H, Wattchow J, Woil J, Zimmermann WD, Schafer H, Bishopric N, Wakatsuki T, Elson E (1997) Three-dimensional reconstitution of embryonic cardiomyocytes in a collagen matrix: a new heart model system. *FASEB J* 11:683–694
- Fink C, Ergun S, Kralisch D, Remmers U, Weil J, Eschenhagen T (2000) Chronic stretch of engineered heart tissue induces hypertrophy and functional improvement. *FASEB J* 14:669–679
- Fournier RL (1998) Basic transport phenomena in biomedical engineering. Taylor & Francis, Philadelphia, PA
- Freed LE, Vunjak-Novakovic G (2000a) Tissue engineering bioreactors. In: Lanza RP, Langer R, Vacanti J (eds) *Principles of tissue engineering*. Academic, Boston, MA, pp 143–156
- Freed LE, Vunjak-Novakovic G (2000b) Tissue engineering of cartilage. In: Bronzino JD (ed) *The biomedical engineering handbook*. CRC Press, Boca Raton, FL, pp 124-1–124-26
- Freed LE, Marquis JC, Vunjak-Novakovic G, Emmanuel J, Langer R (1994a) Composition of cell-polymer cartilage implants. *Biotechnol Bioeng* 43:605–614
- Freed LE, Vunjak-Novakovic G, Biron R, Eagles D, Lesnoy D, Barlow S, Langer R (1994b) Biodegradable polymer scaffolds for tissue engineering. *Biotechnology* 12:689–693
- Freshney RI, Obradovic B, Grayson W, Cannizzaro C, Vunjak-Novakovic G (2007) Principles of tissue culture and bioreactor design. In: Lanza RP, Langer R, Vacanti J (eds) *Principles of tissue engineering*. Elsevier, San Deigo, CA, pp 155–183
- Gray ML, Pizzanelli AM, Lee RC, Grodzinsky AJ, Swann DA (1989) Kinetics of the chondrocyte biosynthetic response to compressive load and release. *Biochim Biophys Acta* 991:415–425
- Grodzinsky AJ, Levenston ME, Jin M, Frank EH (2000) Cartilage tissue remodeling in response to mechanical forces. *Annu Rev Biomed Eng* 2:691–713
- Grunder T, Gaissmaier C, Fritz S, Stoop R, Hortschansky P, Mollenhauer J, Aicher WK (2004) Bone morphogenetic protein (BMP)-2 enhances the expression of type II collagen and aggrecan in chondrocytes embedded in alginate beads. *Osteoarthritis Cartilage* 12:559–567
- Kiviranta I, Tammi M, Jurvelin J, Saamanen AM, Helminen HJ (1988) Moderate running exercise augments glycosaminoglycans and thickness of articular cartilage in the knee joint of young beagle dogs. *J Orthop Res* 6:188–195
- Kraft MP, Riess JG, Weers JG (1998) The design and engineering of oxygen-delivering fluorocarbon emulsions. In: Benita S (ed) *Submicron emulsions in drug targeting and delivery*. Harwood Academic Publishers, Amsterdam, pp 235–333
- Leor J, Aboulafia-Etzion S, Dar A, Shapiro L, Barbash IM, Battler A, Granot Y, Cohen S (2000) Bioengineered cardiac grafts: a new approach to repair the infarcted myocardium? *Circulation* 102:III56–III61
- Li R-K, Jia ZQ, Weisel RD, Mickle DAG, Choi A, Yau TM (1999) Survival and function of bioengineered cardiac grafts. *Circulation* 100:II63–II69
- Li R-K, Yau TM, Weisel RD, Mickle DAG, Sakai T, Choi A, Jia ZQ (2000) Construction of a bioengineered cardiac graft. *J Thorac Cardiovasc Surg* 119:368–375
- MacKenna DA, Omens JH, McCulloch AD, Covell JW (1994) Contribution of collagen matrix to passive left ventricular mechanics in isolated rat heart. *Am J Physiol* 266:H1007–H1018
- Manojlovic V, Djonlagic J, Obradovic B, Nedovic V, Bugarski B (2006) Investigation of cell immobilization in alginate: rheological and electrostatic extrusion studies. *J Chem Technol Biotechnol* 81:505–510
- Martin I, Obradovic B, Treppo S, Grodzinsky AJ, Langer R, Freed LE, Vunjak-Novakovic G (2000) Modulation of the mechanical properties of tissue engineered cartilage. *Biorheology* 37:141–147
- Masuda K, Sah R, Hejna M, Thonar EJ-MA (2003) A novel two-step method for the formation of tissue-engineered cartilage by mature bovine chondrocytes: the alginate-recovered-chondrocyte (ARC) method. *J Orthop Res* 21:139–148
- Mauck RL, Soltz MA, Wang CCB, Wong DD, Chao PG, Valhmu WB, Hung CT, Ateshian GA (2000) Functional tissue engineering of articular cartilage through dynamic loading of chondrocyte-seeded agarose gels. *J Biomech Eng* 122:252–260

- Mauck RL, Seyhan SL, Ateshian GA, Hung CT (2002) Influence of seeding density and dynamic deformational loading on the developing structure/function relationships of chondrocyte-seeded agarose hydrogels. *Ann Biomed Eng* 30:1046–1056
- Mauck RL, Nicoll SB, Seyhan SL, Ateshian GA, Hung CT (2003a) Synergistic action of growth factors and dynamic loading for articular cartilage tissue engineering. *Tissue Eng* 9:597–611
- Mauck RL, Wang CC-B, Oswald ES, Ateshian GA, Hung CT (2003b) The role of cell seeding density and nutrient supply for articular cartilage tissue engineering with deformational loading. *Osteoarthritis Cartilage* 11:879–890
- Mauck RL, Byers BA, Yuan X, Rackwitz L, Tuan RS (2006) Cartilage tissue engineering with MSC-laden hydrogels: effect of seeding density, exposure to chondrogenic medium and loading. 52nd Annual Meeting of the Orthopaedic Research Society, Chicago, Illinois, 19–22 March 2006, Paper No: 0336
- O'Driscoll SW (2001) Preclinical cartilage repair: current status and future perspectives. *Clin Orthop* 391(Suppl):S397–S401
- O'Hara BP, Urban JPG, Maroudas A (1990) Influence of cyclic loading on the nutrition of articular cartilage. *Ann Rheum Dis* 49:536–539
- Obradovic B, Carrier RL, Vunjak-Novakovic G, Freed LE (1999) Gas exchange is essential for bioreactor cultivation of tissue engineered cartilage. *Biotechnol Bioeng* 63:197–205
- Obradovic B, Meldon JH, Freed LE, Vunjak-Novakovic G (2000) Glycosaminoglycan deposition in engineered cartilage: experiments and mathematical model. *AIChE J* 46:1860–1871
- Obradovic B, Martin I, Freed LE, Vunjak-Novakovic G (2001) Bioreactor studies of natural and tissue engineered cartilage. *Ortop Traumatol Rehabil* 3:181–189
- Obradovic B, Bugarski D, Petakov M, Jovic G, Stojanovic N, Bugarski B, Vunjak-Novakovic G (2004) Cell support studies aimed for cartilage tissue engineering in perfused bioreactors. In: Uskokovic DP, Milonjic SK, Rakovic DI (eds) *Materials science forum*, vol. 453–454. Progress in advanced materials processes. Trans Tech Publications Ltd, Zurich, pp 549–555
- Obradovic B, Radisic M, Vunjak-Novakovic G (2005) Tissue engineering of cartilage and myocardium. In: Nedovic V, Willaert RG (eds) *Focus on biotechnology*, vol. 8b. Applications of cell immobilisation biotechnology. Springer, Dordrecht/Berlin/Heidelberg/New York, pp 99–133
- Obradovic B, Osmokrovic A, Bugarski B, Bugarski D, Vunjak-Novakovic G (2007) Alginate microbeads as cell support for cartilage tissue engineering: bioreactor studies. In: Uskokovic DP, Milonjic SK, Rakovic DI (eds) *Materials science forum*, vol. 555. Progress in advanced materials processes. Trans Tech Publications Ltd, Zurich, pp 417–422
- Osmokrovic A, Obradovic B, Bugarski D, Bugarski B, Vunjak-Novakovic G (2006) Development of a packed bed bioreactor for cartilage tissue engineering. *FME Trans* 34:65–70
- Palmoski M, Perricone E, Brandt KD (1979) Development and reversal of a proteoglycan aggregation defect in normal canine knee cartilage after immobilization. *Arthritis Rheum* 22:508–517
- Papadaki M, Bursac N, Langer R, Merok J, Vunjak-Novakovic G, Freed LE (2001) Tissue engineering of functional cardiac muscle: molecular, structural and electrophysiological studies. *Am J Physiol Heart Circ Physiol* 280:H168–H178
- Parkkinen JJ, Ikonen J, Lammi MJ, Laakkonen J, Tammi M, Helminen HJ (1993) Effects of cyclic hydrostatic pressure on proteoglycan synthesis in cultured chondrocytes and articular cartilage explants. *Arch Biochem Biophys* 300:458–465
- Pei M, Solchaga LA, Seidel J, Zeng L, Vunjak-Novakovic G, Caplan AI, Freed LE (2002) Bioreactors mediate the effectiveness of tissue engineering scaffolds. *FASEB J* 16:1691–1694
- Petrovic M, Mitrakovic D, Bugarski B, Vonwil D, Martin I, Obradovic B (2009) A novel bioreactor with mechanical stimulation for skeletal tissue engineering. *CI&CEQ* 15:41–44
- Poncelet D, Babak VG, Neufeld RJ, Goosen M, Bugarski B (1999) Theory of electrostatic dispersion of polymer solutions in the production of microgel beads containing biocatalyst. *Adv Colloid Interface Sci* 79:213–228
- Radisic M, Euloth M, Yang L, Langer R, Freed LE, Vunjak-Novakovic G (2003) High density seeding of myocyte cells for tissue engineering. *Biotechnol Bioeng* 82:403–414

- Radisic M, Yang L, Boublik J, Cohen RJ, Langer R, Freed LE, Vunjak-Novakovic G (2004) Medium perfusion enables engineering of compact and contractile cardiac tissue. *Am J Physiol Heart Circ Physiol* 286:H507–H516
- Radisic M, Obradovic B, Vunjak-Novakovic G (2005) Functional tissue engineering of cartilage and myocardium: bioreactor aspects. In: Ma PX, Elisseeff J (eds) *Scaffolding in tissue engineering*. Marcel Dekker, New York, pp 491–520
- Radisic M, Malda J, Epping E, Geng W, Langer R, Vunjak-Novakovic G (2006a) Oxygen gradients correlate with cell density and cell viability in engineered cardiac tissue. *Biotechnol Bioeng* 93:332–343
- Radisic M, Park H, Chen F, Salazar-Lazzaro JE, Wang Y, Dennis RG, Langer R, Freed LE, Vunjak-Novakovic G (2006b) Biomimetic approach to cardiac tissue engineering: oxygen carriers and channeled scaffolds. *Tissue Eng* 12:1–15
- Radisic M, Cannizzaro C, Vunjak-Novakovic G (2006c) Scaffolds and fluid flow in cardiac tissue engineering. *FDMP: Fluid Dynamics Mater Process* 2:1–15
- Radisic M, Park H, Gerecht-Nir S, Cannizzaro C, Langer R, Vunjak-Novakovic G (2007) Biomimetic approach to cardiac tissue engineering. *Phil Trans R Soc B* 362:1357–1368
- Radisic M, Park H, Salazar-Lazaro JE, Wang Y, Langer R, Freed LE, Vunjak-Novakovic G (2008) Pretreatment of synthetic elastomeric scaffolds by cardiac fibroblasts improves engineered heart tissue. *J Biomed Mater Res A* 86:713–724
- Saamanen AM, Tammi M, Kiviranta I, Jurvelin J, Helminen HJ (1987) Maturation of proteoglycan matrix in articular cartilage under increased and decreased joint loading. A study in young rabbits. *Connect Tissue Res* 16:163–175
- Sah RLY, Kim YJ, Doong JYH, Grodzinsky AJ, Plaas AHK, Sandy JD (1989) Biosynthetic response of cartilage explants to dynamic compression. *J Orthop Res* 7:619–636
- Scorsin M, Marotte F, Sabri A, Le Dref O, Demirag M, Samuel J-L, Rappaport L, Measche P (1996) Can grafted cardiomyocytes colonize peri-infarct myocardial areas? *Circulation* 94:II337–II340
- Sharma B, Elisseeff J (2004) Engineering structurally organized cartilage and bone tissues. *Annals Biomed Eng* 32:148–159
- Soonpaa MH, Koh GY, Klug MG, Field LJ (1994) Formation of nascent intercalated disks between grafted fetal cardiomyocytes and host myocardium. *Science* 264:98–101
- Steinmeyer J, Knue S (1997) The proteoglycan metabolism of mature bovine articular cartilage explants superimposed to continuously applied cyclic mechanical loading. *Biochem Biophys Res Co* 240:216–221
- Vanwanseele B, Lucchinetti E, Stussi E (2002) The effects of immobilization on the characteristics of articular cartilage: current concepts and future directions. *Osteoarthritis Cartilage* 10:408–419
- Vunjak-Novakovic G, Martin I, Obradovic B, Treppo S, Grodzinsky AJ, Langer R, Freed LE (1999) Bioreactor cultivation conditions modulate the composition and mechanical properties of tissue engineered cartilage. *J Orthop Res* 17:130–138
- Vunjak-Novakovic G, Obradovic B, Martin I, Freed LE (2002) Bioreactor studies of native and tissue engineered cartilage. *Biorheology* 39:259–268
- Wang Y, Ameer GA, Sheppard BJ, Langer R (2002) A tough biodegradable elastomer. *Nat Biotechnol* 20:602–606
- Weber M, Steinert A, Jork A, Dimmler A, Thurmer F, Schutze N, Hendrich C, Zimmermann U (2002) Formation of cartilage matrix proteins by BMP-transfected murine mesenchymal stem cells encapsulated in a novel class of alginates. *Biomaterials* 23:2003–2013
- Wong M, Siegrist M, Cao X (1999) Cyclic compression of articular cartilage explants is associated with progressive consolidation and altered expression pattern of extracellular matrix proteins. *Matrix Biol* 18:391–399
- Zimmermann WH, Fink C, Kralish D, Remmers U, Weil J, Eschenhagen T (2000) Three-dimensional engineered heart tissue from neonatal rat cardiac myocytes. *Biotechnol Bioeng* 68:106–114
- Zimmermann WH, Schneiderbanger K, Schubert P, Didie M, Munzel F, Heubach JF, Kostin S, Nehuber WL, Eschenhagen T (2002) Tissue engineering of a differentiated cardiac muscle construct. *Circ Res* 90:223–230

Chapter 8

The Nature of the Thermal Transition Influences the Shape-Memory Behavior of Polymer Networks

Andreas Lendlein, Marc Behl, and Stefan Kamlage

Abstract Degradable shape-memory polymer networks intended for biomedical applications are highlighted. These polymer networks were synthesized from oligo(ϵ -caprolactone)dimethacrylate (PCL), or oligo[(L-lactide)-*ran*-glycolide] dimethacrylate (PLG), or from starlike hydroxytelechelic oligo[(*rac*-lactide)-*co*-glycolide] and a low molecular weight linker. While the thermal transition related to the switching phase is a melting point in case of the PCL-based materials, the switching transition of oligo[(L-lactide)-*ran*-glycolide]dimethacrylate networks and copolyesterurethane networks is a glass transition. In this chapter, the influence of the nature of thermal transition on the shape-memory behavior of polymer networks is described. Furthermore, different polymer network architectures are introduced, which enable the tailoring of polymer network properties as well as the shape-memory capability.

Keywords Shape-memory polymer • Polymer networks • Biomaterials • Biodegradability • Poly(ϵ -caprolactone) • Poly[(L-lactide)-*ran*-glycolide] • Copolyesterurethane

8.1 Introduction

Shape-memory materials are known for about 60 years (Bühler et al. 1963; Chang and Read 1951; He et al. 1996; Hu et al. 1995; Lendlein and Kelch 2002; Lendlein 1999; Li et al. 1997; Osada and Matsuda 1995). These materials have the capability

A. Lendlein (✉), M. Behl, and S. Kamlage
Institute of Polymer Research and Berlin-Brandenburg Center for
Regenerative Therapies, GKSS Research Center, Geesthacht GmbH,
Teltow, Germany
e-mail: andreas.lendlein@gkss.de

A. Lendlein
Berlin-Brandenburg Center for Regenerative Therapies, Campus Virchow Klinikum Charité,
Berlin, Germany

of changing their shape upon exposure to an external stimulus. Consequently shape-memory polymers belong to the group of “actively moving” polymers. The vast majority of shape-memory polymers are dual-shape polymers (Behl and Lendlein 2007a). They can actively change from a temporarily fixed shape A to a permanent shape B. The temporary shape A is obtained by mechanical deformation of the material’s permanent shape B at a temperature $T > T_{\text{switch}}$ and subsequent fixation of the deformation at $T < T_{\text{switch}}$. This process also determines the movement of the polymer which ideally is directly opposed to the programming. In most shape-memory polymers heat or light has been used as the stimulus (Behl and Lendlein 2007b).

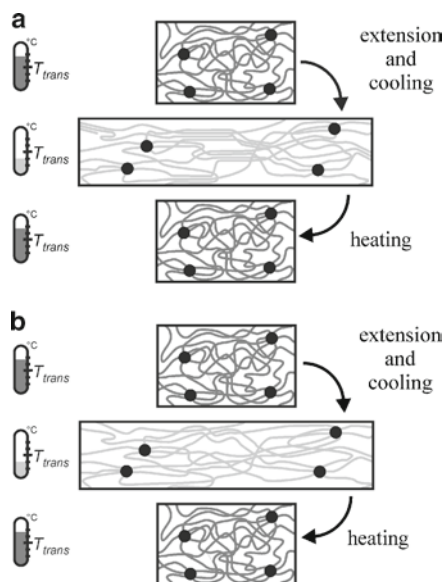
An active change in shape caused by an increase in temperature is called a thermally-induced shape-memory effect. Such an effect is not related to a specific material property of single molecules. The effect rather results from a combination of a polymer structure and a programming process (Lendlein and Kelch 2002; Otsuka et al. 1998; Lendlein and Langer 2002).

The driving force of the shape recovery is the entropy elasticity of (amorphous) network chains (Lendlein and Kelch 2002). The random coil-like state is favored by the entropy. On this account the chains are aimed to return to the random coil-like state after being fixed in an oriented conformation. The capability of switching results from the thermal transition T_{trans} , which is related to domains formed by these network chains (Choi and Lendlein 2007). It is important for shape-memory polymers to differentiate between the properties and the functionality of the polymer. The intrinsic material properties are given by nature. The functionality of the polymer is a result of the combination of a polymer architecture and a specific process and does not require specific repeating units. The unexpected combination of material functionalizations like the combination of biofunctionality, hydrolytic degradability, and shape-memory functionality is referred to as multifunctionality (Lendlein and Kelch 2005; Behl et al. 2010). The development of such multifunctional materials is often application-driven (Behl and Lendlein 2007b; Lendlein and Kelch 2005).

Shape-memory polymers are elastic polymer networks that are equipped with suitable stimuli-sensitive switches. A scheme for such polymer networks consisting of molecular switches (lines in Fig. 8.1) and netpoints (dots in Fig. 8.1) is given in Fig. 8.1. Netpoints determine the permanent shape of the polymer network and can be formed by chemical reactions (covalent bonds) or physical (intermolecular) interactions. Physically crosslinked shape-memory polymers require a morphology which consists of at least two segregated domains. An example for a polymer type being able to form such a morphology are block copolymers. The netpoints are formed by domains with the highest thermal transition (hard segment), while the molecular switches are consisting of domains formed by chain segments related to the second highest thermal transition (T_{trans}) (switching segment) (Behl and Lendlein 2007b).

The switching segment of a shape-memory polymer can be either crystallizable associated to a melting point (T_m) or amorphous related to a glass transition (T_g). T_g resembles a second order thermodynamic transition. For a melting transition the first derivatives of G with respect to temperature T and pressure p is a continuous transition, therefore this transition resembles a first order thermodynamic transition. T_{trans} of amorphous materials however, depends on the cooling rate of the melt and the heat capacity (C_p) at $T < T_g$ is lower than C_p at $T > T_g$. Thus, the glass transition

Fig. 8.1 Molecular mechanism of the thermally-induced shape-memory effect. Fixation of the temporary shape in polymer networks with switching segments triggered by T_m (a) and T_g (b) (Lendlein and Kelch 2002). Copyright Wiley-VCH Verlag GmbH & Co. KGaA. Reproduced with permission



is not a thermodynamic transition but a kinetic phenomenon. Shape-memory polymers with $T_{trans} = T_m$ exhibits a different behavior at the phase transition compared to polymers with $T_{trans} = T_g$.

The crystallinity of a shape-memory polymer has a strong influence on its mechanical properties and its biodegradability. The experimentally determinable melting enthalpy correlates in most cases with the crystalline proportion of the polymer and is therefore a highly important property

Figure 8.1 shows the schematic representation of the molecular mechanism of the thermally-induced shape-memory effect of covalently crosslinked polymer networks with $T_{trans} = T_m$ (Fig. 8.1a) and $T_{trans} = T_g$ (Fig. 8.1b). If the temperature is increased to a temperature above T_{trans} of the switching segments, these segments are flexible (shown in dark gray) and the polymer can be deformed elastically. The temporary shape is created in a process called programming, in which the sample is mechanically deformed and subsequently fixed by cooling. The deformation leading to the temporary shape defines the change of shape (shown in light gray). When exposed to a temperature $T > T_{trans}$, shape-memory polymers recover their permanent shape. This shape recovery is determined by gain of entropy elasticity. The process of programming and recovery can be repeated several times with different temporary shapes in subsequent cycles (Lendlein and Kelch 2002).

The shape-memory effect can be quantified in cyclic, thermomechanical tests, which are performed in a tensile tester under strain- or stress-control. In the strain-controlled tests the stress on the specimen while in stress-controlled tests the strain of the specimen is recorded at defined thermal conditions. A single cycle includes programming of the test piece and recovering of its permanent shape.

The strain-controlled test consists of four steps: (1) heating of the sample to the upper working temperature T_{high} ; stretching to a certain extension (ϵ_m) at a defined strain rate (expressed as $\text{mm}\cdot\text{min}^{-1}$) for a fixed period of time; (2) cooling to the lower working temperature T_{low} with a certain rate (β_c) while ϵ_m is kept constant; (3) unloading of the specimen to zero stress at T_{low} ; (4) clamp distance is driven back to original starting distance, heating up to T_{high} while keeping $\sigma = 0$ MPa, afterwards start of next cycle (1). In these tests the strain applied to the sample with respect to the relative distance of the clamps of the tensile tester is controlled while developing stress is recorded. T_{high} and T_{low} are held constant at least for 10 min before loading or unloading of the specimen. In stress-controlled cyclic thermomechanical tests steps (1) and (2) are modified, by keeping the stress constant at σ_m instead of ϵ_m . In stress-controlled tests the deformation of the sample with respect to the distance of the clamps is monitored while a defined stress is kept. T_{high} and T_{low} are adjusted to $T_{\text{trans}} \pm (20\text{--}30)$ K of the investigated polymer network. The cyclic thermomechanical tests are typically performed five times. The first cycle erases irregularities arising from the polymers thermal history. Generally, the cycles two to five are used for the quantification. Besides stress- or strain-controlled protocols different procedures of sample programming are possible (cold drawing at $T < T_{\text{trans}}$ or temporarily heating up of the test piece to $T > T_{\text{trans}}$) (Lendlein and Kelch 2002; Choi and Lendlein 2007; Bellin et al. 2006; Choi et al. 2006; Kelch et al. 2007; Lendlein et al. 2001). In case of thermoplasts it is important not to exceed the highest thermal transition T_{perm} , which would cause the polymer sample to melt (Lendlein and Kelch 2002). The result of such cyclic thermomechanical measurement is usually presented in a $\epsilon - \sigma$ curve (Fig. 8.2a; $\sigma =$ tensile stress; $\epsilon =$ strain).

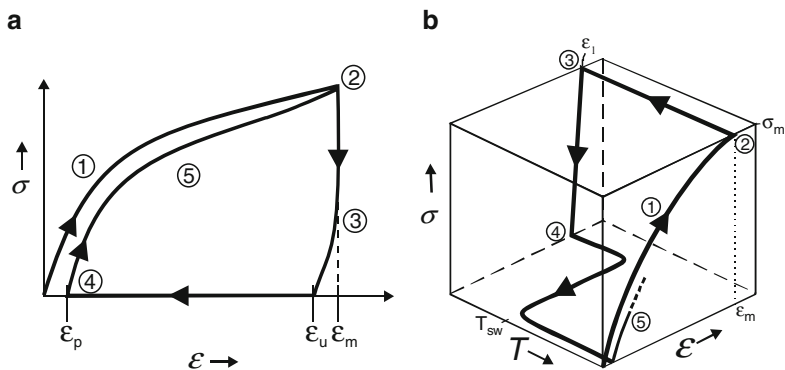


Fig. 8.2 Schematic representation of the results of the cyclic thermomechanical explorations for two different tests: **(a)** ϵ - σ diagram ① – stretching to ϵ_m at T_{high} ; ② – cooling to T_{low} while ϵ_m is kept constant; ③ – clamp distance is driven back to original distance; ④ – at $\epsilon = 0\%$ heating up to T_{high} ; ⑤ – start of the second cycle. **(b)** ϵ - T - σ diagram: ① – stretching to ϵ_m at T_{high} ; ② – cooling down to T_{low} with cooling rate $k_{\text{cool}} = dT/dt$ while σ_m is kept constant; ③ – clamp distance is reduced until the stress-free state $\sigma = 0$ MPa is reached; ④ – heating up to T_{high} with a heating rate $k_{\text{heat}} = dT/dt$ at $\sigma = 0$ MPa; ⑤ – start of the second cycle (Lendlein and Kelch 2002) Copyright Wiley-VCH Verlag GmbH & Co. KGaA. Reproduced with permission

Such an experiment is called a “two-dimensional measurement” as the temperature is changed throughout the test protocol. Figure 8.2b represents the three-dimensional diagram of a stress-controlled test procedure. In this measurement the sample is cooled in a controlled way at a strain of ε_m (maximum strain) and a constant tensile stress σ_m (maximum stress). When the stretched specimen is cooled (position ② in Fig. 8.2a) different effects of the sample behavior have to be considered. Examples are the change of the expansion coefficient of the stretched specimen at temperatures above and below T_{trans} as a result of entropy elasticity, as well as volume changes arising from crystallization in case of $T_{\text{trans}} = T_m$ (Lendlein and Kelch 2002).

The elastic modulus $E(T_{\text{high}})$ at T_{high} can be determined from the initial slope in the measurement range ① (Fig. 8.2a). Additionally E of the stretched sample at T_{low} can also be determined from the slope of the curve at ③ (Fig. 8.2a) (Lendlein and Kelch 2002). The proper description of the shape-memory properties requires the determination of the strain recovery ratio R_r and the strain fixity ratio R_f at a strain ε_m . Both can be determined from cyclic, thermo-mechanical measurements according to Eqs. (8.1) or (8.3) and (8.2) or (8.4), depending on the used test protocol.

	Strain-controlled	Stress-controlled
Shape fixity ratio	$R_f(N) = \frac{\varepsilon_u(N)}{\varepsilon_m} \quad (8.1)$	$R_f(N) = \frac{\varepsilon_u(N)}{\varepsilon_l(N)} \quad (8.3)$
Shape recovery ratio	$R_r(N) = \frac{\varepsilon_m - \varepsilon_p(N)}{\varepsilon_m - \varepsilon_p(N-1)} \quad (8.2)$	$R_r(N) = \frac{\varepsilon_l(N) - \varepsilon_p(N)}{\varepsilon_l(N) - \varepsilon_p(N-1)} \quad (8.4)$

In a strain-controlled protocol R_f is given by the ratio of the strain in the stress-free state after the retraction of the tensile stress in the N th cycle $\varepsilon_u(N)$ and the maximum strain ε_m (Eq. 8.1) In such a protocol R_r quantifies the ability of the material to memorize its permanent shape and is a measure of how far a strain that was applied in the course of the programming $\varepsilon_m - \varepsilon_p(N-1)$ is recovered in the following shape-memory transition. For this purpose the strain that occurs during the programming step in the N th cycle $\varepsilon_m - \varepsilon_p(N-1)$ is compared to the change in strain that occurs during the shape-memory effect $\varepsilon_m - \varepsilon_p(N)$ (Eq. 8.2). The strain of the samples in two successively passed cycles in the stress-free state before application of yield stress is represented by $\varepsilon_p(N-1)$ and $\varepsilon_p(N)$. In case of a stress-controlled protocol R_f is given by the ratio of the retraction of the tensile strain ε_u and the strain in the strain-free state after cooling of the N th cycle $\varepsilon_l(N)$ (Eq. 8.3). In such a protocol R_r quantifies the ability of the material to memorize its permanent shape and is a measure of how far a strain that was applied in the course of the programming $\varepsilon_l(N) - \varepsilon_p(N-1)$ is recovered in the following shape-memory transition. For this purpose the strain that occurs during the programming step in the N th

cycle $\varepsilon_1(N) - \varepsilon_p(N-1)$ is compared to the change in strain that occurs with the shape-memory effect $\varepsilon_1(N) - \varepsilon_p(N)$ (Eq. 8.4).

Besides the shape-memory functionality the investigated networks exhibit another important functionality: biodegradability. Amorphous and crystalline switching segments display a different degradation characteristic. The degradation of the amorphous segments is much faster than of the crystalline ones, because the water penetrates more easily into the amorphous parts, if the rate of hydrolysis of the ester-bonds is similar in both cases. The permeation into the crystalline parts is inhibited by the high density packing in these areas.

8.2 Architectures of Different Polymer Networks

8.2.1 Synthesis

Four different polymer network architectures are described in this chapter. The first polymer network consists of one kind of chain segments (shown in gray in Fig. 8.3a) and netpoints (shown in black). The second polymer network consists of two different kind of chain segments (shown in light and dark gray in Fig. 8.3b) and netpoints.

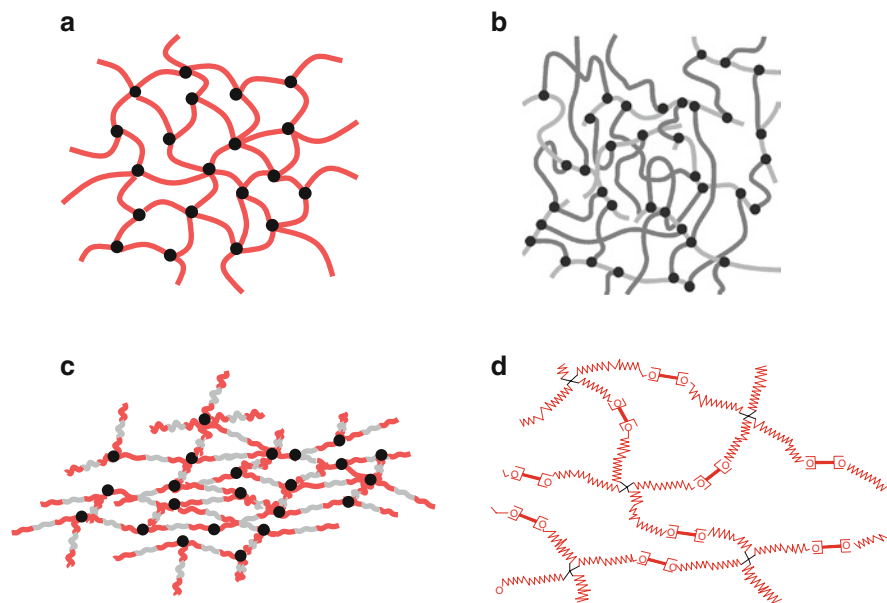


Fig. 8.3 $\color{red}{\curvearrowright}$ chain segment, \bullet netpoint, \square linker, \times initiator forming a netpoint (a) covalent polymer network; (b) covalent AB polymer network; (c) covalent ABA polymer network; (d) copolyesterurethane network

Both types of polymer chain segments form links between two netpoints and contribute to the elasticity of the whole polymer network. The third polymer network consists of triblock copolymers, which form ABA chain segments. Each chain segment is built of two different blocktypes (shown in dark and light gray in Fig. 8.3c). The chains are connected by netpoints. The fourth network architecture consists of crosslinked starlike hydroxytelecheles, which are acting as netpoints (shown in black in Fig. 8.3d). The chain segments (shown in dark gray) of the starlike hydroxytelechelic oligomers were built by two arms from two different telechels linked by a junction unit (shown in dark gray). The chain segments of the four presented polymer network architectures can be amorphous or crystallizable. In shape-memory polymer networks these segments are acting as switching segments (Fig. 8.4), Table 8.1.

Covalent crosslinking of the polymer networks can be realized by polymerization of macrodimethacrylates or by linking of hydroxytelechelic star-shaped oligomers by low molecular weight junction units. The synthesis of methacrylate polymer networks requires the conversion of macrodiols into macrodimethacrylates. Usage of different *co*-monomers enables the synthesis of semicrystalline (ϵ -caprolactone plus diglycolide) or amorphous (L,L-dilactide plus diglycolide) macrodiols (Lendlein et al. 2000). The different sets of comonomers used in the synthesis of macrodiols are shown in Fig. 8.4. The macrodiols were transferred into macrodimethacrylates in an esterification reaction with methacryloyl chloride. Depending on the macrodiols these macrodimethacrylates can be used for polymer network formation with amorphous or crystalline switching segments. The polymer networks with $T_{\text{trans}} = T_m$ or $T_{\text{trans}} = T_g$ according to type 1 (Fig. 8.3a) are formed from acrylate or methacrylate functionalized oligomers by irradiation with UV-light (Choi et al. 2006).

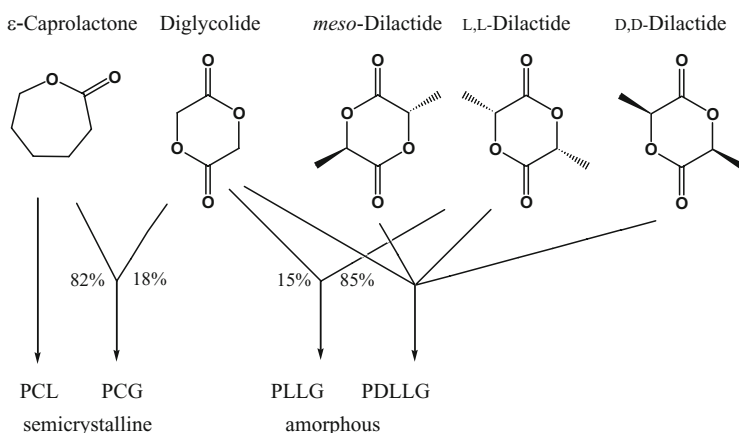
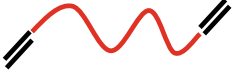


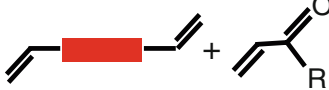
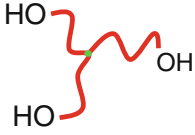


Fig. 8.4 Synthesis of macrodiols by ring opening polymerization of lactones or cyclic diesters with a low molecular weight hydroxy telechelic initiator, e.g. ethylene glycol. PCL: poly(ϵ -caprolactone); PCG: poly[(ϵ -caprolactone)-*co*-glycolide]; PLLG: poly[(L-lactide)-*co*-glycolide]; PDLLG: poly[(*rac*-lactide)-*co*-glycolide] (Kelch et al. 2009). Copyright 2009, with permission from the Material Research Society

Table 8.1 Starting materials in the synthesis of different polymer network architectures, switching segments are shown in *gray*

amorphous switching segment	crystallizable switching segment
 <p>Macrodimerethacrylates (Fig. 8.3a)</p>	 <p>Macrodimerethacrylates (Fig. 8.3a)</p>
 <p>ABA Triblockdimerethacrylates (Fig. 8.3c)</p>	 <p>Macrodimerethacrylate and acrylic comonomers (Fig. 8.3b)</p>
 <p>Hydroxy telechelic star-shaped oligomers as starting materials for copolyesterurethanes (Fig. 8.3d)</p>	

AB copolymer networks according to type 2 (Fig. 8.3b) with $T_{\text{trans}} = T_m$ were prepared from oligo[ϵ -caprolactone]-*co*-glycolide]dimerethacrylate and *n*-butyl acrylate. The networks with *n*-butyl acrylate as *co*-monomer contain amorphous and non crystallizable soft segments of poly(*n*-butyl acrylate). *n*-Butyl acrylate is used because of the low glass transition temperature of poly(*n*-butyl acrylate) [$T_g = -55^\circ\text{C}$] (Lendlein et al. 2001).

ABA networks with $T_{\text{trans}} = T_g$ (Fig. 8.3c) can be formed by suitable oligomers of different molar masses. The macrodiols were prepared by a ring opening polymerization (ROP) of *rac*-dilactide with poly(propylene oxide) as macroinitiator in presence of dibutyltin oxide as catalyst. These ABA triblock copolymer diols with a middle block of poly(propylene oxide) were endgroup functionalized with methacrylate groups. Polymer networks based on such macrodimerethacrylates were obtained by photocrosslinking using UV-light (Choi et al. 2006).

Copolyesterurethane networks with $T_{\text{trans}} = T_g$ (Fig. 8.3d) were prepared by crosslinking of star-shaped hydroxytelechelic *co*-oligoesters. The crosslink points were introduced by ROP of α -hydroxy acids with hydroxytelechelic initiators. The *co*-oligoester segments were synthesized by copolymerization of diglycolide and *rac*-dilactide forming the oligo[*rac*-lactide]-*co*-glycolide]. 1,1,1-tris(hydroxymethyl)ethane or pentaerythrite were used as initiators. The use of 1,1,1-tris(hydroxymethyl)ethane results in trifunctional netpoints (N-T-LG: networks from poly[*rac*-lactide]-*co*-glycolide] and the use of pentaerythrite results in tetrafunctional netpoints (N-P-LG: networks from poly[*rac*-lactide]-*co*-glycolide]. These telechelic oligomers are called three-armed *co*-oligoesters and four-armed

co-oligoesters. The crosslinking reaction was performed by adding an isomeric mixture of 1,6-diisocyanato-2,2,4-trimethylhexane and 1,6-diisocyanato-2,4,4-trimethylhexane to the *co*-oligoesters and subsequent heating resulted in the formation of the final polymer networks (Alteheld et al. 2005; Lendlein et al. 2009).

8.2.2 Thermomechanical Properties

Macrodiols and macrodimethacrylates of PLGA, PCL and PCG exhibit a similar correlation of transition temperature with molecular weight of the oligomers. With

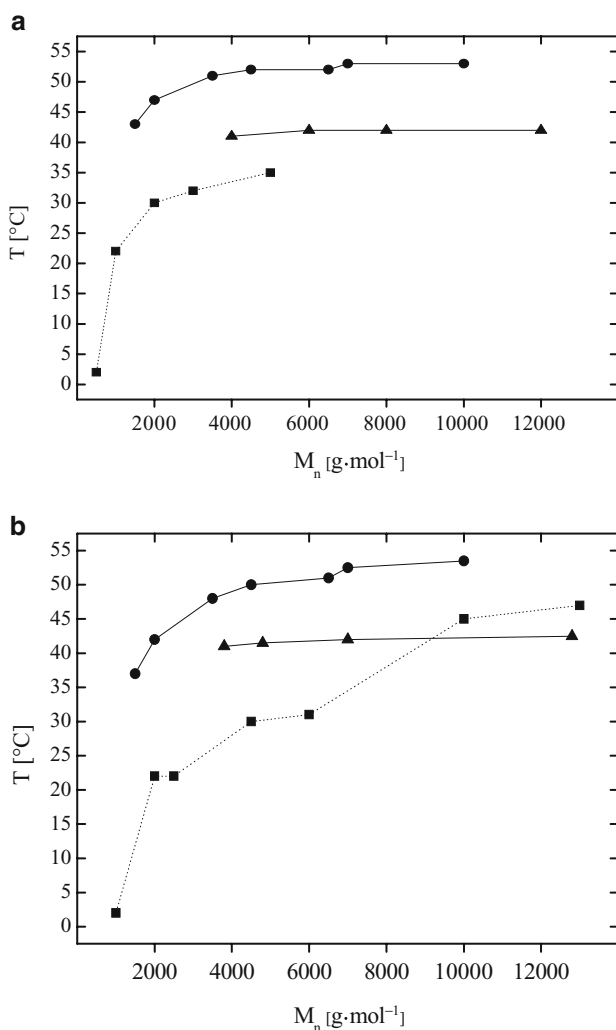


Fig. 8.5 Thermal transition of telechelics with $T_{\text{trans}} = T_m$; —, telechelics with $T_{\text{trans}} = T_g$; ..., (a) macrodiols of ■ PLGA, ● PCL, ▲ PCG; (b) macrodimethacrylates of ■ PLGA, ● PCL, ▲ PCG; M_n was determined by ¹H-NMR (.... and — are guidelines to the eye)

increasing molecular weight (M_n) the telechelics reach individual maximum T_{trans} (Fig. 8.5, the data are obtained from Choi et al. 2006, Kelch et al. 2007, and Middleton and Tipton 2000). The melting enthalpy (ΔH_m) of macrodiols of PCL without *co*-monomer is independent of M_n of the macrodiols. ΔH_m of PCL polymer systems containing *co*-monomers increases slightly with M_n of the used macrodimethacrylates and ΔH_m decreases strongly with increasing glycolide content (Kelch et al. 2007).

If the molecular weights of the macrodimethacrylate precursors are above 2 kD, the glass transition temperatures of PLGA networks are independent of the molecular weight of the precursor. In contrast, the melting temperatures of PCG networks are increasing with increasing molecular weight of the used oligomers (Fig. 8.6, the data are obtained from Choi et al. 2006, Kelch et al. 2007, and Middleton and Tipton 2000). In case of PCL the dependence of T_m for macrodimethacrylates and polymer networks thereof is similar.

Two different kinds of polymer networks with oligo[(ϵ -caprolactone)-*co*-glycolide] segments were synthesized: on one hand the homo networks according to Fig. 8.3a derived from the dimethacrylate functionalized oligomers dimethacrylate only and on the other hand AB networks according to Fig. 8.3b containing poly[(ϵ -caprolactone)-*co*-glycolide]dimethacrylate and *n*-butyl acrylate. The thermal properties of the shape-memory polymer networks can be adjusted by the M_n of the used oligomers having the same glycolide content. The mechanical properties are influenced by M_n of the oligomers and its glycolide content. In AB polymer networks the mechanical properties can be tuned by the content of comonomer forming an amorphous phase related to a low T_g .

The mechanical properties of amorphous PLGA networks are independent from glycolide content for glycolide contents ranging between 15–50 wt% (Middleton

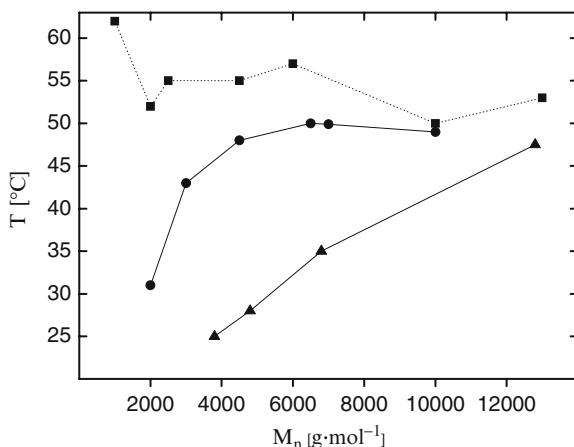


Fig. 8.6 Thermal transition of polymer networks from macrodimethacrylates with $T_{\text{trans}} = T_m$: —, polymer networks with $T_{\text{trans}} = T_g$; ···, depending on M_n of the macrodiol used as starting material in the synthesis (■ PLGA, ● PCL, ▲ PCG; M_n was determined by ¹H-NMR (.... and — are guidelines to the eye)

and Tipton 2000). E is in the range of 2 GPa and ε in the range of 3–10% for all polymer networks at room temperature.

E of semicrystalline polymer networks with a randomized sequence structure (N-CG: poly[(ε -caprolactone)-*co*-glycolide]dimethacrylate networks) decreases with increasing glycolide amount from about 90 to 2 MPa. In case of semicrystalline copolymer network (AB-CG: copolymer networks based on poly[(ε -caprolactone)-*co*-glycolide]dimethacrylate and *n*-butyl acrylate) the value of E is decreasing, too, but only from about 10 to 2 MPa (Fig. 8.7a). The same tendencies can be observed for σ (Fig. 8.7b). In case of ε (Fig. 8.7c) no obvious tendency can be noticed either at room temperature or at 70 °C. At 70 °C E and σ are in the same range for all polymer networks mentioned in Fig. 8.7 (the data are obtained from Kelch et al. 2007).

T_m of the formed AB-type shape-memory polymer is decreasing with increasing *n*-butyl acrylate content. In such networks an increasing *n*-butyl acrylate content causes a decrease in crystallinity and in ΔH_m (Kelch et al. 2007). The content of acrylate also influences the mechanical properties of the polymer networks. These polymer networks become elastic with a high amount of acrylate. A similar behavior was shown for AB networks from *n*-butyl acrylate and poly(ε -caprolactone)dimethacrylate. The influence is stronger for oligomers with a smaller molar mass than for larger oligomers (Lendlein et al. 2001).

Generally, the switching segment is formed by a pure phase. In ABA polymer networks built from *rac*-dilactide with poly(propylene oxide)-dimethacrylate precursors (PRxtytN) a T_g of the phase built by the poly(propylene oxide) of -50°C and a T_g of 50°C by the phase provided by the poly(*rac*-lactide) is expected. A clear phase separation of the resulting polymer networks can be observed for macrodiol-dimethacrylate precursors with $M_n > 10$ kD. In case of ABA polymer networks built from macrodiol dimethacrylate precursors with $M_n < 10$ kD besides the T_g of the poly(propylene oxide) an additional mixed phase between the poly(propylene oxide) and the poly(*rac*-lactide) can be spotted. The thermomechanical properties of three polymer networks from ABA triblockdimethacrylates are shown in Fig. 8.8 (Choi et al. 2006). The influence of the mixed phase can be observed in the dynamic mechanical experiments at varied temperature (DMTA) curves of ABA-networks.

Figure 8.9a presents the dependence of T_g of hydroxytelechelic oligomers as a function of M_n of the oligomers. The influence of M_n of the *co*-oligoester on T_g of the copolyesterurethane networks is shown in Fig. 8.9b. It can be noticed that T_g of hydroxytelechelic oligomers depends on M_n of the precursor but not on the number of hydroxyl groups of the initiator (Fig. 8.9a). In contrast, T_g of the polymer networks is independent from M_n of the precursors (Fig. 8.9b). At 70 °C, approximately 20 °C above T_g , the copolyesterurethane networks are in a rubber-elastic state. E and ε_b depend on the segment length and the functionality of the netpoints determined by the type of initiator. E of copolyesterurethane networks based on three or four armed telechelics is decreasing with increasing chain length while ε_b is increasing with increasing chain length. Generally, E of the four armed copolyesterurethane networks are higher than E of the three armed networks in case of the same M_n of

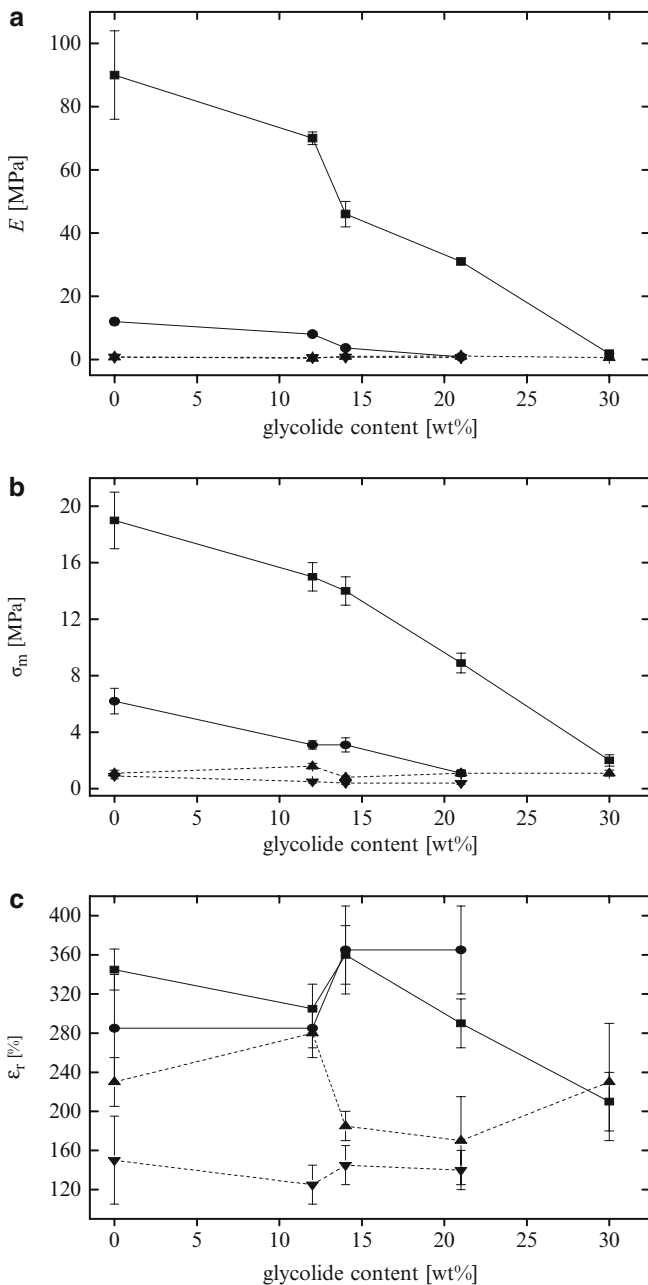


Fig. 8.7 Mechanical properties of shape-memory polymer networks from oligo[(ϵ -caprolactone)-*co*-glycolide]dimethacrylate (N-type) or AB-type polymer networks from oligo[(ϵ -caprolactone)-*co*-glycolide]dimethacrylate with *n*-butyl acrylate (AB-type) depending on glycolide content, — at rt, --- at 70°C (a) E of N-type (■ N-CG at rt, ▲ N-CG at 70°C) and AB-type (● AB-CG at rt, ▼ AB-CG at 70°C). (b) σ of N-type (■ N-CG at rt, ▲ N-CG at 70°C) and AB-type (● AB-CG at rt, ▼ AB-CG at 70°C). (c) ϵ of N-Type (■ N-CG at rt, ▲ N-CG at 70°C) and AB-type (● AB-CG at rt, ▼ AB-CG at 70°C) (.... and — are guidelines to the eye)

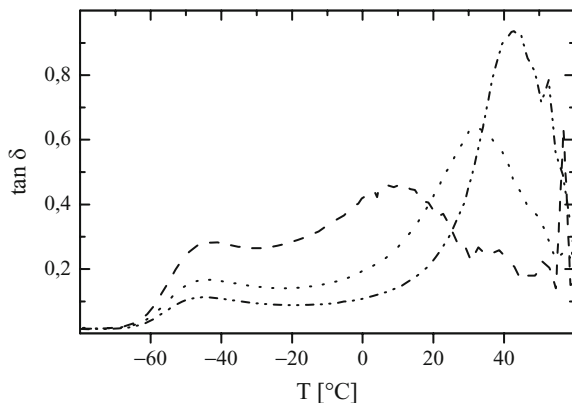


Fig. 8.8 Thermomechanical properties of networks from ABA triblockdimethacrylates determined by DMTA (M_n [NMR] of macrodiols: --- 6 kD, 8 kD, - · - · - · 10 kD) (Choi et al. 2006). Copyright Wiley-VCH Verlag GmbH & Co. KGaA. Reproduced with permission

the oligomer starting material. The values of ϵ_b of the three armed networks are higher than the values of the four armed networks in case of the same M_n of the oligomer starting material (Alteheld et al. 2005).

The mechanical properties of the described polymer networks are summarized in Table 8.2 (the data are obtained from Choi and Lendlein 2007, Choi et al. 2006, Kelch et al. 2007, Lendlein et al. 2001, Middleton and Tipton 2000). The transition temperatures of these polymer networks are in the range from 25 °C to 65 °C. At room temperature E and ϵ_b are strongly depending on the kind of switching segment. E of polymer networks with amorphous switching segments is a magnitude higher compared to networks with crystallizable switching segments. According to these results ϵ_b of networks with crystallizable switching segments is higher than ϵ_b of polymer networks with amorphous switching segments. At 70 °C, when all switching segments are in the molten state, E of all polymer networks decrease while the values of ϵ_b remain constant or increase compared to the values at room temperature.

8.3 Shape-Memory Capability

Cyclic, thermomechanical tensile tests are performed using two different experimental setups (Lendlein and Kelch 2002; Kelch et al. 2007; Mohr et al. 2006). On the one hand, programming and strain recovery are performed in presence of air. On the other hand, to simulate conditions relevant for medical applications in the body, the strain recovery of conventionally programmed samples is performed in water (Lendlein and Kelch 2002; Mohr et al. 2006). The result of a strain-controlled

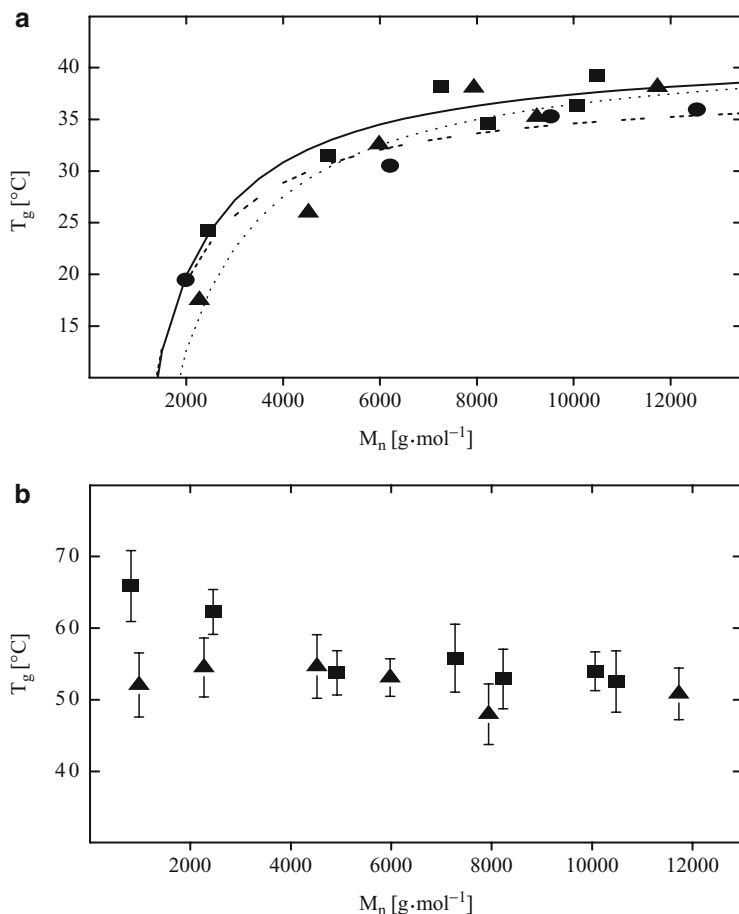
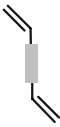

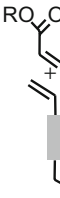
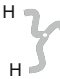


Fig. 8.9 (a) T_g of oligomers as a function of the molecular weight of the precursor (initiated with ● or --- ethylene glycol, ▲ or - - - tris(hydroxymethyl)ethane, ■ or — pentaerythrite) (b) T_g of copolyesterurethane networks from the second heating cycle as a function of the molecular weight of the telechelic cooligoester precursors (▲ macrotriol (tris(hydroxy-methyl)-ethane), ■ macrotetrol(pentaerythrite). Number average molecular weight of all precursors determined by ¹H NMR spectroscopy (Alteheld et al. 2005). Copyright Wiley-VCH Verlag GmbH & Co. KGaA. Reproduced with permission

cyclic thermomechanical tests of a network from PCL-dimethacrylate is shown in Fig. 8.10. The sample is loaded (a) and afterwards cooled to T_{low} , resulting in crystallization of the switching segments. Lowering of T leads to a decrease in stress, caused by entropy elasticity of the amorphous chain segments (b). The crystallization following this process results in a dramatic increase of stress to a maximum stress at T_{low} (after thermal contraction; σ_l) during the ongoing cooling process (c). The formed crystallites act as physical crosslinks, fixing the tensile-loaded shape of the

Table 8.2 Mechanical properties of different covalently crosslinked polymer networks below and above T_{trans}

Polymer networks system	Mechanical properties	Room temperature	70 °C
 Fig. 8.3a	E ϵ_b	2.4–71 MPa 16–296%	1.8–6.0 MPa 18–210%
 Fig. 8.3a	E ϵ_b	900–3,000 MPa 50%	3.7–11.3 MPa 50–195%
 Fig. 8.3b	E ϵ_b	0.8–12 MPa 71–210%	0.4–1.0 MPa 187–382%
 Fig. 8.3d	E ϵ_b	330–600 MPa 90–305%	0.9–2.8 MPa 115–875%

sample. With unloading, the stress-strain curve intersects the σ axis at a temporary strain (ϵ_u), which represents the actual fixed shape of the specimen (d). After reheating and the recovery of the permanent shape a residual strain (ϵ_p) remains, and the second cycle ($N = 2$) is slightly different. In general, the permanent shape is recovered by more than 90%, but this value might be increased in subsequent cycles because the preorientation of the sample resulting from processing of the shaped body is deleted. A typical protocol consists of five cycles (Lendlein et al. 2005).

Strain-controlled thermomechanical cycles of AB polymer networks from PCG-dimethacrylate and *n*-butylacrylate are shown in Fig. 8.11. The introduction of the amorphous *n*-butyl acrylate phase influences the ratio of crystalline domains acting as switching domains and thus the mechanical properties of the polymer network below T_{trans} . The curves of the polymer networks N-CG(14)-7 and N-CG(14)-10 are similar to the curve described in Fig. 8.10. The curves of the polymer networks N-CG(14)-3 and N-CG(14)-5 differ from the curves described in Fig. 8.10 because the ϵ -hydroxycaproate-sequences dominated segments are relatively short forming less stable crystallites, stabilizing the temporary shape (Kelch et al. 2007).

AB copolymer networks of N-CG with varying content of glycolide exhibit complete strain recovery in stress-controlled, cyclic thermo-mechanical tests (Fig. 8.12). Heating of the specimen at $T < T_{\text{trans}}$ causes a slight increase of strain due to the positive thermal expansion coefficient. The temperature at the inflection point of the strain-recovery curve is correlated with T_{switch} and increases with

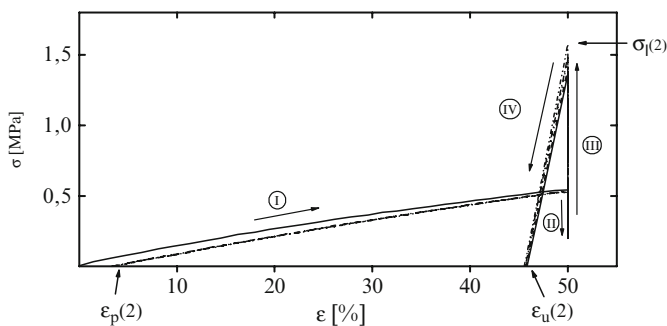


Fig. 8.10 Cyclic, thermomechanical strain-controlled test of a network from PCL-dimethacrylate with $T_h = 70^\circ\text{C}$, $T_l = 0^\circ\text{C}$, and $\varepsilon_m = 50\%$ ($\sigma = \text{stress}$) in air. The data of the graph are obtained from five cycles (Lendlein et al. 2005). Copyright John Wiley and Sons. Reproduced with permission

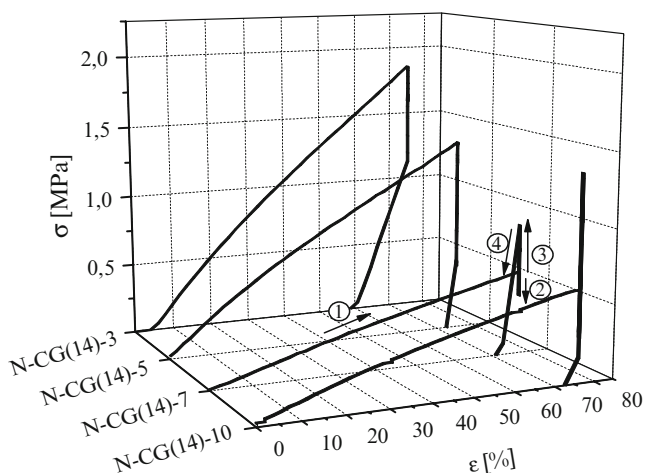


Fig. 8.11 Fifth cycle of a strain-controlled cyclic, thermomechanical tensile test of copolymer networks N-CG(14)-X from macrodimethacrylates with X = 3, 5, 7 or 10 kD of the oligomer in air. $T_h = 70^\circ\text{C}$, $T_l = 0^\circ\text{C}$, $\varepsilon_m = 75\%$. Reprinted from (Kelch et al. 2007) with permission. Copyright 2007 American Chemical Society

increasing glycolide content during measurements in air and water in a very similar way (Kelch et al. 2007).

AB-networks from PCL-dimethacrylate (C10) and *n*-butyl acrylate reach uniform deformation properties with R_f of more than 99% after three cycles (Lendlein et al. 2001). Total strain recovery rates ($R_{r,\text{tot}}$) show values between 93% and 98% and are increasing with increasing rates of *n*-butyl acrylate. R_f displays average values of around 95% at a *n*-butyl acrylate content of less than 50% but is decreasing to a value of 82% in case of a *n*-butyl acrylate content of 70 wt% (Fig. 8.13). This fact could be explained by the low overall crystallinity of this polymer network (Lendlein et al. 2001).

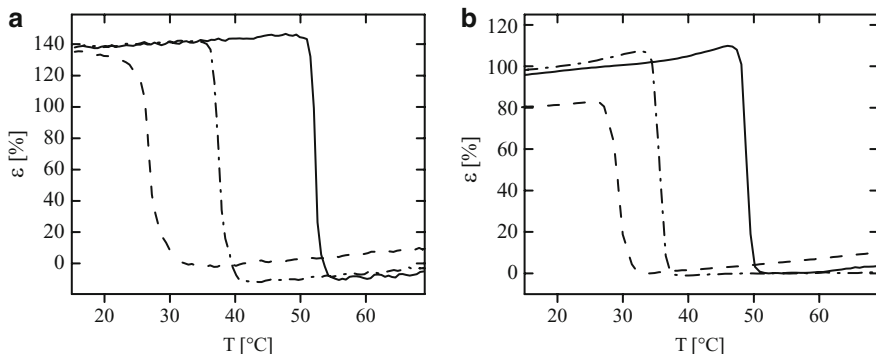


Fig. 8.12 Strain ϵ as a function of the temperature T of copolymer networks N-CG-10 with varying glycolide content in wt% in the recovery process of a stress-controlled thermomechanical tensile test in air (a) and in water (b). (··: N-CG(21)-10; - - -: N-CG(14)-10; —: N-CG(0)-10). The programming of the samples was performed strain-controlled in air. The variation in strain at the beginning of the strain recovery results from different programming processes. $T_{\text{high}} = 70^\circ\text{C}$, $\epsilon_m = 100\%$, $T_{\text{low}} = 15^\circ\text{C}$, and $N = 1$. Reprinted from (Kelch et al. 2007) with permission. Copyright 2007 American Chemical Society

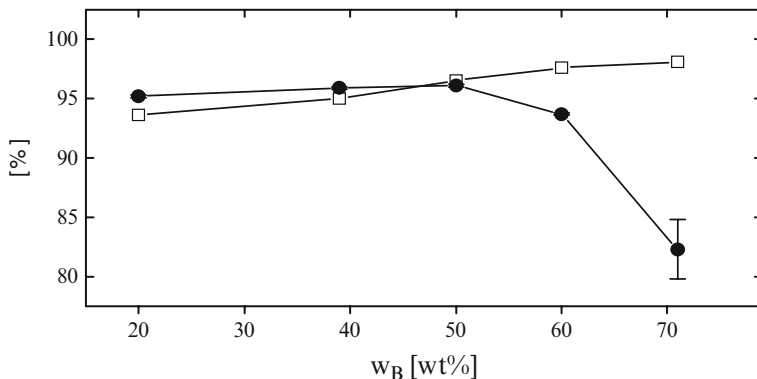


Fig. 8.13 Shape-memory properties of AB polymer networks from C10 and *n*-butyl acrylate as a function of comonomer content w_B at $T_h = 70^\circ\text{C}$, $T_l = 0^\circ\text{C}$, $\epsilon_m = 200\%$. \square : total strain recovery rate $R_{r,\text{tot}}$; \bullet : average strain fixity rate R_f (Lendlein et al. 2001). Copyright 2007 National Academy of Sciences, U.S.A. (— guideline to the eye)

In polymer networks with $T_{\text{trans}} = T_m$ fixation of the temporary shape needs to be adjusted to the crystallization process. Detailed information about the crystallization process are necessary to optimize the programming process. The programming process can be controlled by the cooling rate β_c (from the melt) and variation of T_{low} , at which the sample is kept for crystallization. Cooling of the samples from the melt at various β_c values enables investigation of non-isothermal crystallization. It was shown for polymer networks from oligo(ϵ -caprolactone)dimethacrylates that the heat of crystallization is independent of β_c for all investigated materials

(Lendlein et al. 2005). The data obtained from the non-isothermal crystallization can be analyzed according to the Ozawa equation (Eq. 8.5). According to this equation the mass fraction transformed from the melt to the crystal phase in the processes of crystallization depends on β_c :

$$-(n \cdot \log \beta_c) - \log k_{ni}(T) = \log[-\ln(1 - \alpha(T))] \quad (8.5)$$

in which $k_{ni}(T)$ is a temperature function and n the Avrami constant, depending on the crystallization mode of nucleation and crystallization geometry. Application of this equation to the non-isothermal crystallization processes of polymer networks from oligo(ϵ -caprolactone)dimethacrylates indicated a strong relationship between the crystallization temperatures and different β_c constants and between crystallization and crystal growth (Lendlein et al. 2005; Ozawa 1971; Pena et al. 1994).

Isothermal crystallization data of polymer networks from oligo(ϵ -caprolactone)dimethacrylates C10, were analyzed according to the Avrami equation (Eq. 8.6) in which n can be determined: (Lendlein et al. 2005; Avrami 1941; de Carvalho and Bretas 1998; Mandelkern 1964; Wunderlich 1976)

$$-\ln[1 - \alpha(t)] = k_i(T) \cdot t^n \quad (8.6)$$

with $k_i(T)$ is a kinetic constant of the crystallization process and $\alpha(t)$ is given by the ratio of the crystallization enthalpy evolved at time t to the crystallization enthalpy of the overall process.

The plot of $\log\{-\ln[1 - \alpha(t)]\}$ against $\log t$ for different crystallization temperatures allowed determination of n and $k_i(T)$ by linear least-square fitting for each crystallization temperature. The double logarithmic plots are shown in Fig. 8.14.

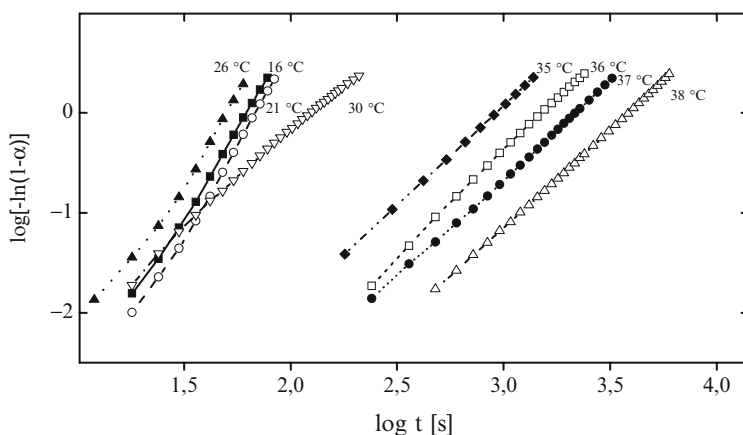


Fig. 8.14 Master plot of an Avrami analysis of the isothermal crystallization process of photoset networks from oligo(ϵ -caprolactone)dimethacrylate C10 (Lendlein et al. 2005). Copyright John Wiley and Sons. Reproduced with permission

n was shown to be different at crystallization temperatures below and above 26 °C. It varies between 3.1 and 3.6 for the lower crystallization temperatures and about 1.9 and 2.1 for crystallization temperatures above 26 °C. This indicates a change in the mechanism of crystallization between 26 °C and 30 °C. For C10 the plot of $\log\{-\ln[1-\alpha(t)]\}$ against $\log t$ at 30 °C is similar to the plots for crystallization temperatures between 16 °C and 26 °C in the beginning and in the upper part it displays behavior like plots for crystallization temperatures between 35 °C and 38 °C (Lendlein et al. 2005).

The dependence of T_m of selected AB-polymer networks based on oligo (ϵ -caprolactone) segments regarding to the process of crystallization has been investigated in isothermal crystallization experiments at different crystallization temperatures T_{cr} . No dependence of T_m on T_{cr} can be observed up to temperatures of 25 °C for crosslinked C10 (Fig. 8.15) (Lendlein et al. 2005). On base of these data, a Hoffman-Weeks analysis has been performed for determination of the equilibrium melting temperature T_m^∞ . T_m^∞ is given by the intersection of the solid line formed by plotting $T_m = T_{cr,iso}$ to the extrapolated lines of T_m (Hoffman and Weeks 1962). For C10, this method led to a T_m^∞ of 64 °C. The same method applied for networks from PCLDMA with M_n of the oligomer = 3 kD (C3) and C10 (with 39 wt% of n -butyl acrylate as comonomer) in both cases resulted in a T_m^∞ of 55 °C. It can be concluded that a lower molecular weight of oligo(ϵ -caprolactone) segments or the presence of an amorphous phase as poly(n -butyl acrylate) led to an obvious change in the crystallization behavior of the oligo(ϵ -caprolactone) phase.

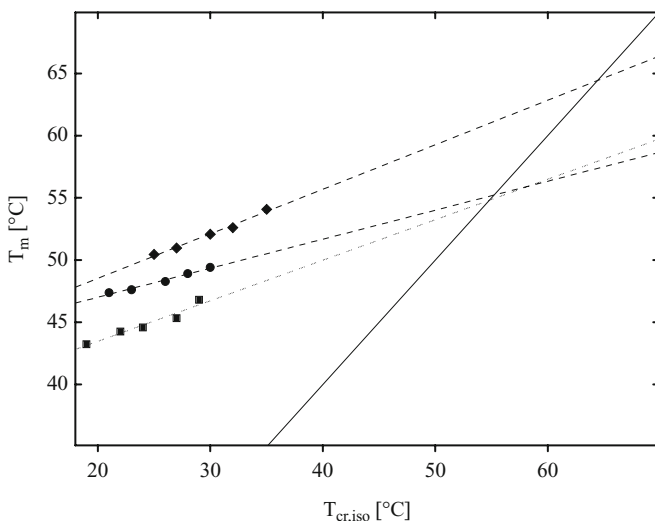


Fig. 8.15 Hoffmann-Weeks plot of isothermal crystallization processes. \blacktriangle : C3, M_n of macromonomer: 3,500 g·mol⁻¹; \blacksquare : C10, M_n of macromonomer = 10 kD; \bullet : C10B(39), $w_B = 39\%$, M_n of macromonomer = 10 kD; —, $T_m = T_{cr,iso}$ (Lendlein et al. 2001). Copyright 2007 National Academy of Sciences, U.S.A.

These results emphasize the importance of the crystallization behavior on the programming process of the temporary shape of a shape-memory polymer network (Lendlein et al. 2001).

Besides programming, temperature plays a prominent role in the recovery process of polymer networks. An example are polymer networks with $T_{\text{switch}} = T_g$. In such polymer networks the temperature range of the strain recovery can be influenced by the heating rate. With lower heating rates the strain recovery starts and ends at lower temperatures, and the temperature intervals during recovery get smaller with decreasing heating rates (Choi and Lendlein 2007).

Figure 8.16 shows the characteristic strain ε during shape recovery of polymer networks with $T_{\text{trans}} = T_m$ (Fig. 8.16a) and $T_{\text{trans}} = T_g$ (Fig. 8.16b). Although the graphs of both systems are looking similar, the differences of both systems become obvious with respect to the first derivation of strain. In polymer networks with $T_{\text{trans}} = T_m$ the first derivation shows a sharp peak (Fig. 8.16a) whereas the first derivation for polymer networks with $T_{\text{trans}} = T_g$ exhibits a broader peak (Fig. 8.16b). In the latter case the broadness of the peak can be influenced by the heating rate: the faster the heating rate is the broader the peak becomes. The clearly visible differences in the thermomechanical properties of the polymer systems reflect in the shape-memory capabilities of such systems.

The recovery rate v_r is given as the ratio of R_r over the temperature interval of recovery ΔT_r (Eq. 8.7). ΔT_r is given by the end temperature of the transition (T_e) minus the temperature at the beginning of the transition (T_s) (Eq. 8.8) (Kelch et al. 2008).

$$v_r = \frac{R_r}{\Delta T_r} \quad (8.7)$$

$$\Delta T_r = T_e - T_s \quad (8.8)$$

The results obtained from cyclic thermomechanical tensile tests of different triblock polymer networks are shown in Fig. 8.17.

T_{sw} is defined as inflection point of the recovery sector in thermocycles displayed in Fig. 8.17. As expected, T_{sw} occurred at a higher temperature with increasing T_g found for the ABA polymer network. The temperature interval of the strain recovery ΔT_r also increased between 29 and 37 K with increasing molecular weight of the chain segments. R_r is increasing with increasing molecular weight of the poly(*rac*-lactide) blocks. The chain segments reshape into the random coil conformation at T_{switch} in the order PR4t6tN < PR4t8tN < PR4t10tN. An explanation for these results is the increase in the molecular weight of the chain segment per unit volume. In these polymer systems the highest measured entropy gain, which is also the driving force of the strain recovery, is detected for the block copolymer network PR4t10tN. Consequently, the highest R_r value of 99.5% was measured in case of PR4t10tN. The highest value for v_r was measured for PR4t10tN, too (Choi et al. 2006).

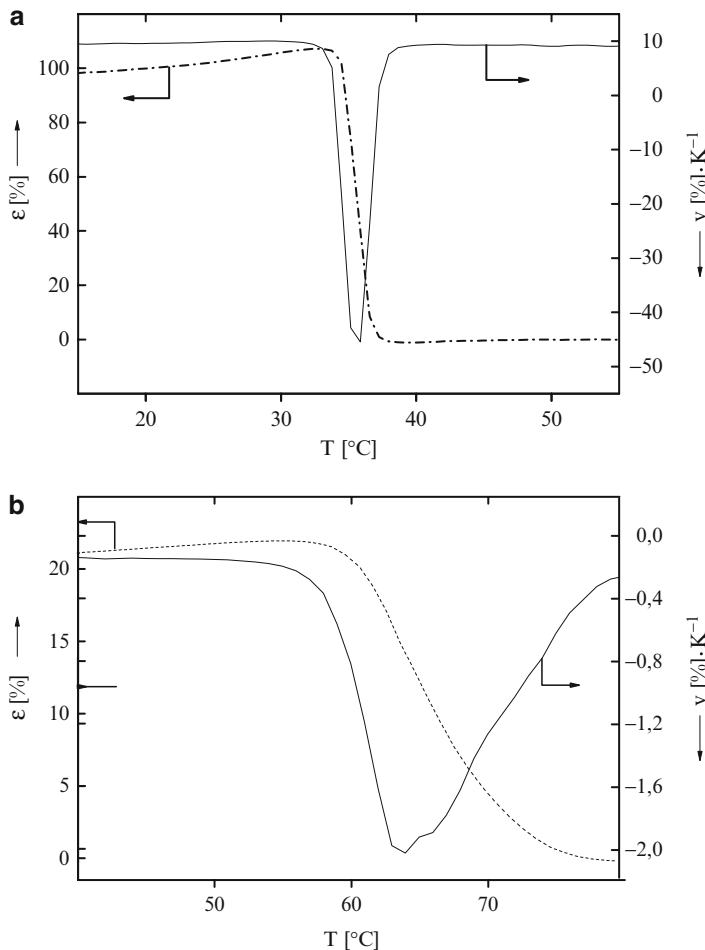


Fig. 8.16 (a) - - - Recovery of strain ϵ of polymer network N-CG(14)-10 at a heating rate of 2 K·min⁻¹; — First derivation of ϵ of polymer network N-CG(14)-10 (Kelch et al. 2007). (b) ---- Recovery of strain ϵ of polymer network from oligo[(L-lactide)-ran-glycolide] at a heating rate of 3 K·min⁻¹; — First derivation of ϵ of polymer network from oligo[(L-lactide)-ran-glycolide] (Choi and Lendlein 2007). Figures from (Behl et al. 2010) Copyright Wiley-VCH Verlag GmbH & Co. KGaA. Reproduced with permission

8.4 Degradation

Generally, two different hydrolytic degradation mechanisms are described: surface or bulk degradation. In surface degradation the cleavage of the hydrolyzable bonds is faster than the diffusion of water into the polymer matrix. In contrast polymers showing bulk degradation are initially swelling in water followed by hydrolytic chain cleavage. The process of bulk degradation of polymer networks can be

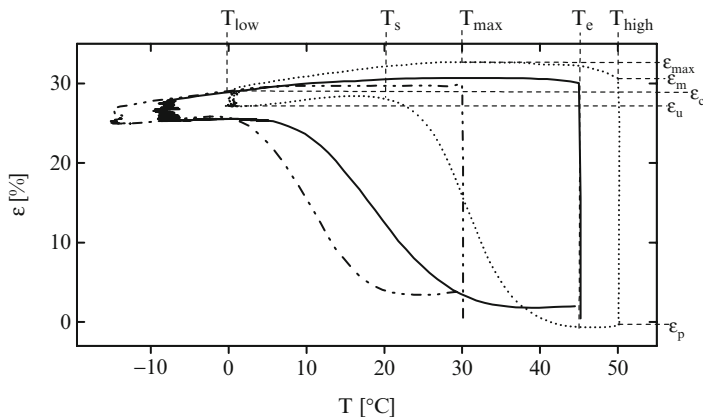


Fig. 8.17 Cyclic, thermomechanical tensile experiment at constant stress σ_m during cooling and $\sigma = 0$ during reheating for polymer networks from poly(*rac*-lactide)-*b*-poly(propylene oxide)-*b*-poly(*rac*-lactide)dimethacrylates. (--- PR4t6tN; — PR4t8tN; PR4t10tN) (Choi et al. 2006) Copyright Wiley-VCH Verlag GmbH & Co. KGaA. Reproduced with permission

subdivided into three steps: swelling and induction period (1), reduction of molecular weight and reduction of mechanical strength (2), and mass loss (3) (Alteheld et al. 2005; Pitt et al. 1981).

The degradation behavior of different shape-memory polymer networks has been investigated in phosphate buffer solution at pH 7.0 and 37 °C. Mass loss over time (72 weeks) of polymer networks from oligo-(ϵ -caprolactone)dimethacrylate, from poly(ϵ -caprolactone)dimethacrylate and *n*-butyl acrylate, and oligo-[(ϵ -caprolactone)-*co*-glycolide]dimethacrylate with different glycolide content is depicted in Fig. 8.18a (Kelch et al. 2007). The hydrolytic degradation of this polymer system results from a hydrolysis of the ester bonds in the main chain. For polymer networks from oligo(ϵ -caprolactone)dimethacrylate, from poly(ϵ -caprolactone)dimethacrylate and *n*-butyl acrylate mass losses of only 10% were observed during 72 weeks. Introduction of glycolide units in the copolyester segment increases the number of easily hydrolyzable bonds and therefore accelerated mass loss. In case of polymer networks derived from oligo-[(ϵ -caprolactone)-*co*-glycolide]dimethacrylate with a glycolide content of 9 wt% a period of induction of 20 weeks can be observed. After 53 weeks a total mass loss of 15% was detected. A glycolide content of 13 wt% resulted in a period of induction of 20 weeks as well. However, after 58 weeks a total mass loss of 60% was detected. In polymer networks with a glycolide content of 14 wt% and more a decrease in crystallinity of the polymer network can be observed. As water penetrates faster into the amorphous parts than in crystalline parts, this should lead to additional acceleration of degradation (Kelch et al. 2007).

Copolyesterurethane networks were degraded up to > 90% within 100–150 days (Fig. 8.18b) (Alteheld et al. 2005). An induction period of 120 days can be observed in the degradation experiments of copolyesterurethane networks from oligomeric telechelics having M_n around 10 kD. For copolyesterurethane networks from oligomers with $M_n = 1$ kD an induction period of 100 days can be observed. Copolyesterurethane

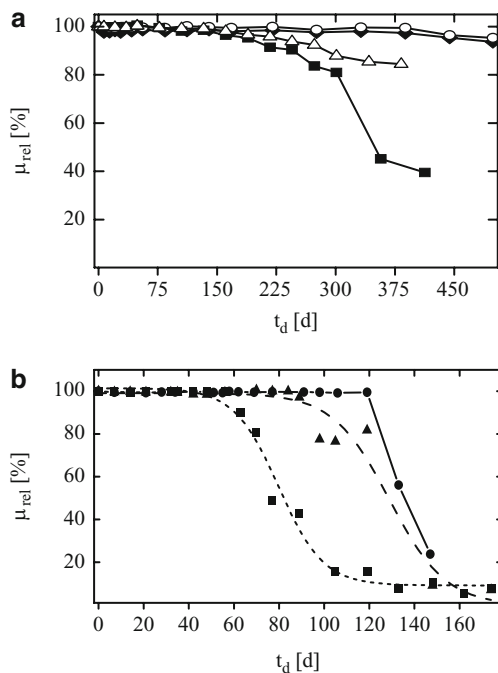


Fig. 8.18 (a) Hydrolytic degradation of polymer networks from ϵ -caprolactone based on different acrylate networks (\circ : poly(ϵ -caprolactone)dimethacrylate, \diamond : poly(ϵ -caprolactone)dimethacrylate and *n*-butyl acrylate, \triangle : poly[(ϵ -caprolactone)-*co*-glycolide]dimethacrylate (9 wt%), \blacksquare : poly[(ϵ -caprolactone)-*co*-glycolide]dimethacrylate (13 wt%). Reprinted from (Kelch et al. 2007) with permission. Copyright 2007 American Chemical Society; (b) hydrolytic degradation of copolyesterurethane networks (M_n of macrotetraoles: \blacktriangle : 1 kD, \blacksquare : 5 kD, \bullet : 10 kD) (Alteheld et al. 2005). Copyright Wiley-VCH Verlag GmbH & Co. KGaA. Reproduced with permission. (....., ---, and — are guidelines to the eye)

networks with M_n of the oligomers = 1 kD are densely crosslinked polymer networks, which prevent a fast diffusion of water into the core of the network. The copolyesterurethane network with M_n of the oligomers = 5 kD exhibits an induction period of 50 days. This result demonstrates, that the diffusion of water is not only influenced by the crosslink density but also by the hydrophilicity of polymer networks, which increases with increasing content of diurethane units as well as the number of easily hydrolyzable bonds, which increases with growing M_n of the starting materials.

8.5 Summary

Shape-memory polymer networks with crystallizable or non-crystallizable amorphous switching segments have been described. The polymer networks with crystallizable switching segments were synthesized from macrodimethacrylates derived from PCL or PCG, which in case of AB polymer networks are copolymerized with

n-butylacrylate. The described amorphous polymer networks contain of PLGA- or PLLG- or poly[(*rac*-lactide)-*b*-poly(propylene-oxide)-*b*-poly(*rac*-lactide)]-segments. Alternatively three or four arm star-shaped telechelic oligomers were linked with diisocyanates to copolyesterurethane networks.

In polymer networks with amorphous switching segments the glass transition temperature (T_g) is independent from the molecular weight of the oligomers used as starting materials. However, the melting temperature (T_m) of polymer networks from PCL- or PCG-dimethacrylates with crystallizable switching segments depends on the molecular weight of the oligomers.

In shape-memory polymer networks with $T_{trans} = T_m$ only the crystalline parts of the switching segments are contributing to the fixation of the temporary shape. In contrast in shape-memory polymer networks with $T_{trans} = T_g$ the whole polymer network is acting as switching segment, as shown for networks from PLGA-dimethacrylates.

AB polymer networks were prepared to achieve shape-memory polymer networks with suitable elastic properties in their permanent and temporary shape. The disadvantage of AB polymer networks with an *n*-butyl acrylate content of more than 50 wt% is the decrease in the strain fixity rate. To obtain elastic polymer networks at $T < T_{switch}$ and to avoid the low strain fixity ratio of AB polymer networks ABA polymer networks of poly(*rac*-lactide)-*b*-poly(propylene oxide)-*b*-poly(*rac*-lactide) dimethacrylate were synthesized.

The hydrolytic degradation rate of polymer networks can be influenced by the number of easily hydrolyzable ester bonds and by increasing the amorphous fraction of the polymeric material. All described polymer networks display bulk degradation.

The systematic variation of molecular parameters results in a comprehensive database enabling the analysis of structure-property relationship. These insights are the basis for a knowledgebased approach to tailored properties and functions of shape-memory polymer networks to the requirement of specific applications. In copolyester based polymer networks with $T_{trans} = T_m$, T_{sw} can be adjusted by the comonomer ratio. Another example for the tailoring of material properties is the adjustment of elastic properties for $T > T_{trans}$ by variation of molecular weights of oligomers as starting materials in polymer network synthesis.

8.6 Outlook

In addition to the thermally-induced stimulation of shape-memory polymers other kinds of stimuli can be applied, i.e. a magnetic field or light (Mohr et al. 2006; Narendra Kumar et al. 2010). The development of systems with types of stimulation other than temperature will be further investigated during the next years. Another interesting field of shape-memory polymers are triple shape polymers, having two different switching temperatures related to three different shapes (Bellin et al. 2006, 2007; Behl et al. 2008; Zotzmann et al. 2010). Also shape-memory systems with segment chains which are specially tailored for certain applications, e.g. polydepsipeptides, are currently under investigation (Feng et al. 2008).

References

- Alteheld A, Feng Y, Kelch S, Lendlein A (2005) Biodegradable, amorphous copolyesterurethane networks having shape-memory properties. *Angew Chem Int Ed* 44:1188–1192
- Avrami M (1941) Granulation, phase change and microstructure. Kinetics of phase change. III. *J Chem Phys* 9:177–193
- Behl M, Lendlein A (2007a) Actively moving polymers. *Soft Matter* 3(1):58–67
- Behl M, Lendlein A (2007b) Shape-memory polymers. *Mater Today* 10(4):20–28
- Behl M, Razaq MY, Lendlein A (2010) Multifunctional shape-memory polymers. *Adv Mater*, in press, doi:10.1002/adma.200904447
- Behl M, Bellin I, Kelch S, Wagermaier W, Lendlein A (2008) One-Step Process for Creating Triple-Shape Capability of AB Polymer Networks 19:102–108
- Bellin I, Kelch S, Langer R, Lendlein A (2006) Polymeric triple-shape materials. *Proc Natl Acad Sci* 103(48):18043–18047
- Bellin I, Kelch S, Lendlein A (2007) Dual-shape properties of triple-shape polymer networks with crystallizable network segments and grafted side chains. *J Mater Chem* 17(29):2885–2891
- Bühler WJ, Gilfrich JW, Wiley RC (1963) Effect of low-temperature phase changes on the mechanical properties of alloys near composition TiNi. *J Appl Phys* 34:1475
- Chang LC, Read TA (1951) Plastic deformation and diffusionless phase changes in metals. The gold-cadmium beta phase. *Trans AIME* 189:47
- Choi N-Y, Lendlein A (2007) Degradable shape-memory polymer networks from oligo [(L-lactide)-ran-glycolide] dimethacrylates. *Soft Matter* 3:901–909
- Choi N-Y, Kelch S, Lendlein A (2006) Synthesis, shape-memory functionality and hydrolytical degradation studies on polymer networks from poly(*rac*-lactide)-*b*-poly(propylene oxide)-*b*-poly(*rac*-lactide) dimethacrylates. *Adv Eng Mater* 8(5):439–445
- de Carvalho B, Bretas RES (1998) Quiescent crystallization kinetics and morphology of isotactic polypropylene resins for injection molding. I. Isothermal crystallization. *J Appl Polym Sci* 68(7):1159–1176
- Feng YK, Behl M, Kelch S, Lendlein A (2008) Biodegradable multiblock copolymers based on oligodepsipeptides with shape-memory properties. *Macromol Biosci* 9:45–54
- He X, Oishi Y, Takahara A, Kajiyama T (1996) Higher order structure and thermo-responsive properties of polymeric gel with crystalline side chains. *Polym J* 28:452–457
- Hoffman JD, Weeks JJ (1962) Melting process and equilibrium melting temperature of poly(chlorotrifluoroethylene). *J Res Natl Bur Stand Section A* 66:13
- Hu Z, Zhang X, Li Y (1995) Synthesis and application of modulated polymer gels. *Science* 269:525–527
- Kelch S, Behl M, Kamlage S, Lendlein A (2009) Multiphase Polymer Networks with Shape-Memory. *Mater Res Soc Symp Proc* 1190:3–11
- Kelch S, Choi NY, Wang ZG, Lendlein A (2008) Amorphous, elastic AB copolymer networks from acrylates and poly[(L-lactide)-ran-glycolide]dimethacrylates. *Adv Eng Mat* 10:494–502
- Kelch S, Steuer S, Schmidt AM, Lendlein A (2007) Shape-memory polymer networks from oligo[ϵ -hydroxycaproate-co-glycolate] dimethacrylates and butyl acrylate with adjustable hydrolytic degradation rate. *Biomacromolecules* 8:1018–1027
- Lendlein A (1999) Polymere als Implantatwerkstoffe. *Chem in unserer Zeit* 33:279–295
- Lendlein A, Kelch S (2002) Shape-memory polymers. *Angew Chem Int Ed Engl* 41:2034–2057
- Lendlein A, Kelch S (2005) Degradable, multifunctional polymeric biomaterials with shape-memory. *Material Science Forum*, 492-493:219–223
- Lendlein A, Langer R (2002) Biodegradable elastic shape-memory polymers for potential biomedical applications. *Science* 296:1673–1676
- Lendlein A, Schmidt AM, Langer R (2001) AB-polymer networks based on oligo(ϵ -caprolactone) segments showing shape-memory properties. *Proc Natl Acad Sci* 98(3):842–847
- Lendlein A, Neuenschwander P, Suter UW (2000) Hydroxy-telechelic copolyesters with well defined sequence structure through ring-opening polymerization. *Macromol Chem Phys* 201:1067–1076

- Lendlein A, Schmidt AM, Schroeter M, Langer R (2005) Shape-memory polymer networks from oligo(ϵ -caprolactone)dimethacrylates. *J Polym Sci Part A: Polym Chem* 43:1369–1381
- Lendlein A, Zotzmann J, Feng YK, Alteheld A, Kelch S (2009) Controlling the switching temperature of biodegradable, amorphous shape-memory poly(rac-lactide)urethane networks by incorporation of different comonomers. *Biomacromolecules* 10:975–982
- Li Y, Hu Z, Chen Y (1997) Shape memory gels made by the modulated gel technology. *J Appl Polym Sci* 63(9):1173–1178
- Mandelkern L (1964) *Crystallization of polymers*. McGraw-Hill, New York
- Middleton JC, Tipton AJ (2000) Synthetic biodegradable polymers as orthopedic devices. *Biomaterials* 21(23):2335–2346
- Mohr R, Kratz K, Weigel T, Lucka-Gabor M, Moneke M, Lendlein A (2006) Initiation of shape-memory effect by inductive heating of magnetic nanoparticles in thermoplastic polymers. *Proc Natl Acad Sci* 103(10):3540–3545
- Narendra Kumar U, Kratz K, Wagermaier W, Behl M, Lendlein A (2010) Non-contact actuation of triple-shape effect in multiphase polymer network nanocomposites in alternating magnetic field. *J Mater Chem* 20:3404–3415
- Osada Y, Matsuda A (1995) Shape memory in hydrogels. *Nature* 376:219
- Otsuka K, Wayman CM, Saburi T, Tadaki T, Maki T, Suzuki Y, Humbeeck JV, Stalmans R, Uchino K, Miyazaki S (1998) *Shape memory materials*. Cambridge University Press, Cambridge
- Ozawa T (1971) Kinetics of non-isothermal crystallization. *Polymer* 12(3):150–158
- Pena B, Delgado JA, Bello A, Perez E (1994) Crystallization kinetics of isotactic poly(1-hexadecene). *Polymer* 35(14):3039–3045
- Pitt CG, Gratzl MM, Kimmel GL, Surlis J, Schindler A (1981) Aliphatic polyesters II. The degradation of poly (DL-lactide), poly (ϵ -caprolactone), and their copolymers in vivo. *Biomaterials* 2:215–220
- Wunderlich B (1976) *Macromolecular physics*. Academic, New York, p 132
- Zotzmann J, Behl M, Hofmann D, Lendlein A (2010) Reversible Triple-Shape Effect of Polymer Networks Containing Poly(pentadecalactone)- and Poly(ϵ caprolactone)-Segments. *Adv Mater* in press, DOI: 10.1002/adma.200904202

Chapter 9

Nanoengineered Systems for Regenerative Medicine Surface Engineered Polymeric Biomaterials with Improved Bio-Contact Properties

Todorka Vladkova and Natalia Krasteva

Abstract Some examples of surface engineered polymeric biomaterials with nano-size modified layers that have controlled protein adsorption and initial cell adhesion potentially applicable at blood and/or tissue contacting devices, scaffolds for cell culture, tissue engineering, etc. as well as the approaches to their preparation are presented here.

Keywords Polymeric biomaterials • surface engineered • controlled protein adsorption and initial cell adhesion • nano-layers with controlled parameters: chemical composition • hydrophilic/hydrophobic balance • topography and roughness, etc.

9.1 Introduction

On a lot of parameters polymeric materials satisfy most fully the requirements of regenerative medicine applications. But the last ones are limited in the major cases by the non-sufficient bio-contact properties of the polymers. Surface engineering leading to creation of nano-size layers with controlled parameters, such as chemical composition, topography and roughness, hydrophilic/hydrophobic balance, etc. emerged as a simple, useful and versatile approach to solution the problem.

T. Vladkova (✉)

Department of Polymer Engineering, University of Chemical Technology and Metallurgy,
8 Kl. Ohridski Blvd, 1756 Sofia, Bulgaria
e-mail: TGV@uctm.edu; DoraVladkova@abv.bg

N. Krasteva

Institute of Biophysics, BAS, 1113 Sofia, Bulgaria

For a long time we and other authors are developing polymer surfaces with controlled protein adsorption and initial cell adhesion potentially applicable at blood and/or tissue contacting devices, scaffolds for cell culture, patterning of proteins, etc. We present here some examples of such materials as well as the approaches to their preparation.

9.2 Polymeric Materials with Improved Bio-Contact Properties

9.2.1 Strong Hydrophilic “Water-Like” Protein Repellent Surfaces

Such type surfaces are potentially applicable at bio-inert biomaterials for blood and/or tissue contacting devices, intraocular lenses, patterned supports for tissue engineering, scaffolds for cell culture, etc.

The biological cascade of all non-desirable response reactions against biomaterials begins with deposition of proteins. Therefore the low protein adsorption is accepted now as the most important pre-requisite to bio-inertness and bio-fouling resistance. In addition, the initial interaction between cells and material surfaces is mediated by adsorption of adhesive proteins.

Because of their versatile nature many proteins can be adsorbed on many mechanisms when they are in front of complementary surfaces (Hlady et al. 1985). This makes very difficult the protein adsorption prevention. Many current investigations are devoted to study the single well defined proteins adsorption or the concurrent adsorption from double or multi-component systems (Gölander 1986; Malmsten 1998). It is known nowadays (Gölander 1986; Altankov 2003; Drotleff 2006; Jager et al. 2007) that the protein adsorption and bio-contact properties of the polymers depend on the: surface chemical composition and topography, surface hydrophilic/hydrophobic balance and charge, the mobility of the surface functional groups, the thickness and density of the modifying layer, etc. Hence, changing some of them we can control the protein adsorption.

Ikada, Suzuki and Tamada (Ykada et al. 1984) theoretically predict that the work of adhesion in aqueous media approaches zero when the water contact angle approaches 0° or 90° . This theoretical prediction has been experimentally proven by bovine serum albumin (BSA) adsorption on various polymer surfaces in phosphate buffer. It means that there are two possibilities for material surface to have work of adhesion approaching 0, in other words to be non-adhesive: one is to create super hydrophilic, that is water-like surface and the other is to create super hydrophobic surface. This is the start point in the development of strong hydrophilic or strong hydrophobic non-adhesive protein repellent biomaterials and bio-fouling release surfaces as well as of moderate hydrophilic materials supporting the cell adhesion and proliferation.

Table 9.1 Cross-section corrected intensities of characteristic functional groups for various hydrophilic photo-polymeric films: N-vinylpyrrolidone (NVP), acrylic acid (AA) or polyethylene glycol mono-acrylates (PEG) on PE-OSO₃H and PVC after adsorption of bovine serum albumin (BSA)

	C-O/-CH ₂ -	-COO-/-CH ₂ -	O(1s)/-CH ₂ -	N/-CH ₂ -	N ⁺ /-CH ₂ -	Cl(2p)/-CH ₂ -	I- _{CH₂} - (cs ⁻¹ eV ⁻¹)
PE-OSO ₃ H	0.57	0.27	0.45	0.15	0.04		2,706
NVP	0.84	0.29	1.13	0.17	0.11		1,040
AA	1.29	0.38	1.18	0.15	0.15		1,062
PEG550	1.08	0.28	1.39	0.04	0.02		1,402
PEG1900	2.06	0.46	1.47	0.03	0.01		1,145
PEG5000	1.81	0.30	1.23	0.03	>0.01		1,226
TMP(EO) ₂₀	2.32	0.25	1.55	0.06	>0.01		1,086
PVC	0.72	0.21	0.41	0.13	0.04	0.23	1,693
PEG550	0.80	0.20	0.64	0.09	0.02	0.18	1,600
PEG1900	1.32	0.24	0.80	0.04	0.02	0.18	1,332
PEG5000	2.20	0.30	1.35	0.11	0.03	0.11	1,051
TMP(EO) ₂₀	0.76	0.19	0.55		0.04	0.11	1,694

A lot of strong hydrophilic and strong hydrophobic surfaces have been developed by us and other authors to decrease protein adsorption at biomaterials (Elbert and Hubbell 1996; Chu et al. 2002). A comparative protein adsorption ESCA study on different strong hydrophilic surfaces: positively charged (N-vinyl-pyrrolidone), negatively charged (Acrylic Acid) and non-charged (PEG) clearly demonstrate the advantages of non-charged strong hydrophilic surfaces (Gölander et al. 1986). As it is seen from Table 9.1, the nitrogen content, originating from adsorbed BSA, is one order and even more lowly on all PEG coated surfaces as compared to NVP or AA coated hydrophilic surfaces or to non-coated PE-SO₃H and PVC surfaces. Similar are the results of ellipsometry measurements (Gölander et al. 1987; Malmsten and Van Alstin 1996).

Polyethylene glycols (PEGs) – called now “gold” of the biomaterials are the most often used in the creation of protein repellent bio-inert materials. Many researches are oriented to the study the mechanisms of protein resistance of different PEG coated surfaces, for example surfaces with adsorbed or PEG-graft copolymers (Pasche 2004). The outstanding protein repellent properties of PEG are most often explained with the structural similarity of -CH₂CH₂O- unit to the water and the strong hydrogen bonding to the O-atom that rationalizes its miscibility with water and engage of the -CH₂-groups by a water network (Bailey and Koleske 1976; Harris 1992). Hence, when a foreign moiety approaches PEG coated surface in fact it contacts with water.

A number of experimental techniques were used to introduce PEG groups on different polymer surfaces, such as PE, PVC, PMMA, NR, PDMS, PS, etc. by wet chemistry or by plasma treatment (Gölander et al. 1986; Harris 1992; Vladkova 2001; Vladkova et al. 1997; Chan 1993; Chan et al. 1996). Wet chemistry methods include deposition of photopolymer hydrogel PEG coatings including a two step

Fig. 9.1 Schematic drawing that shows the structural features of PEG layers obtained by different coating: photo-polymerization, grafting and adsorption

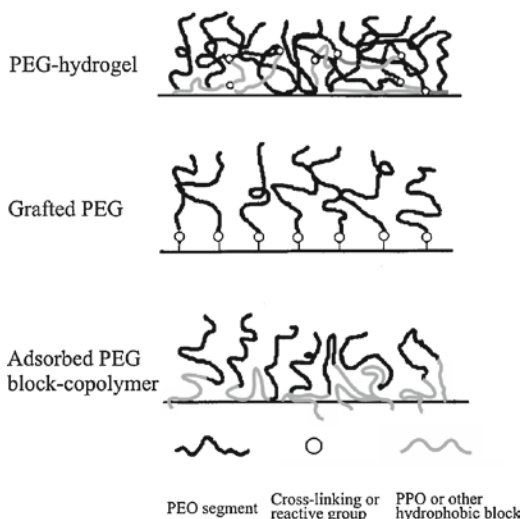
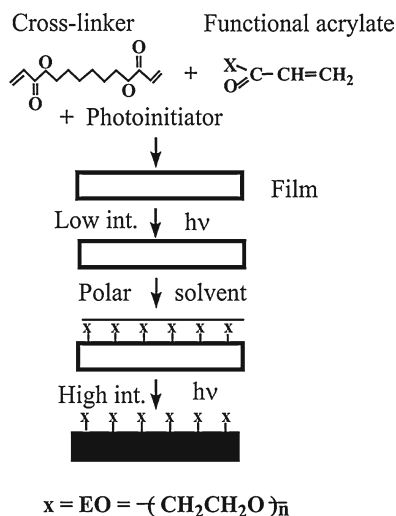


photo polymerization procedure to increase the surface density of PEG chains (Gölander et al. 1984), grafting or adsorption of PEG chains on the substrate surface (Gölander 1986). Structural features of PEG layers obtained by different coating: photo-polymerization, grafting and adsorption are presented in Fig. 9.1. The examples of PEG coated surfaces, described here, are only a small part of all described in the special literature.

9.2.1.1 PEG Hydrogel Coatings

PEG hydro-gel coatings could be created by polymerization in situ of deposited on a substrate PEG containing polymerizable resin. PEG acrylates or methacrylates are suitable for free radical polymerization, initiated thermally by azobisisobutyronitrile (AIBN) or peroxides or photo-chemically using photo-initiators like benzophenones, thioxanth, etc. (Gölander et al. 1986). Concentrating PEG chains through a creation of brush type surface coatings using mono-functional PEG-acrylates and two-step UV polymerization are prepared super-hydrophilic (water contact angle $< 10^\circ$) surfaces with exclusively low (below 0.05 mg/m^2) protein adsorption (Gölander et al. 1984). A structural model of PEG hydro-gel is displayed in Fig. 9.1 and the principle sketch of the two-step procedure for the photo-curing of a PEG-acrylate layer for enhancement of the surface density of EO groups, in Fig. 9.2.

Fig. 9.2 Two-step procedure for the photo-curing of a PEG-acrylate layer for enhancement of the surface density of EO groups



9.2.1.2 Chemically Immobilized and PEG Grafted Surfaces

PEG-aldehyde (Vladkova 2001; Gölander et al. 1987; Kiss et al. 1987) and PEG-epoxide grafting or PEG-epoxide/PEI copolymer quasi-irreversible adsorption (Vladkova 2001) at optimal reaction conditions leads also to the formation of surfaces with very low protein adsorption – below 0.05 mg/m² (by ellipsometry).

A number of methods for covalent attachment of PEG to different polymer surfaces are known requiring employment of PEG with derivative terminal OH groups, the last ones able to interact with a functionalized substrate surface. In case of strong hydrophobic chemically inert polymers, surface pre-activation is necessary by plasma treatment or wet chemistry prior to the grafting of the functionalized PEG.

The next Fig. 9.3 shows schematically the coupling procedure of PEG-aldehyde by Schiff base reaction with surface –NH₂ groups and Fig. 9.1 the structural model of the PEG surface. This reaction is convenient to use in aqueous media where it could be driven to completion by addition of NaCNBH₃, acting as a selective reducing agent for the imine product –CH=N– in presence of aldehyde. In order to increase the surface density of PEG chains the immobilization reaction is performed under solution conditions close to the cloud point when the repulsion between PEG chains is small. To induce clouding at lower reaction temperatures, “salting out” with potassium sulfate is performed.

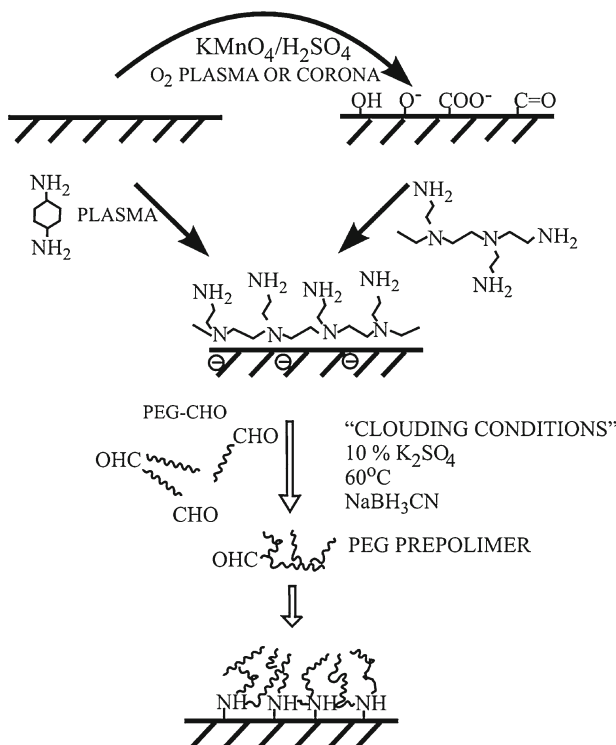


Fig. 9.3 Grafting of PEG by the Schiff base reaction between PEG-CHO and polymer surfaces aminated in various ways, for example by treatment in di-amino-cyclohexane (DACH) plasma or by deposition of polyethyleimine (PEI) on pre-oxidated polymer surface

9.2.1.3 PEG-Coated Surfaces Prepared by Quasi-Irreversible Adsorption with Very Low Protein Adsorption and Unexpected Good Initial Cellular Interactions

High molecular weight copolymers of PEG can be adsorbed irreversibly attaching at multiple adsorption sites. Although the free energy of adsorption for each side may be relatively small, the attachment of a molecule to several sides leads to a multiplication effect, so that the total free energy of adsorption of a polymer becomes quite large. For this reason polymers tend to be adsorbed very strongly in a lot of cases.

One approach to achieving a firmly attached PEG coating at negatively charged surfaces is to physically adsorb a graft copolymer of PEG and a polycation such as polyethylene imine (PEI). A one-step preparation procedure could be used to achieve enough high density of PEG chains on the surface (Vladkova et al. 1999; Malmsten and Van Alstin 1996). PEI/PEG-epoxyde adducts are employed for the above described quasi-irreversible adsorption. All prepared in this way PEG coatings are strong hydrophilic (equilibrium water contact angle $<10^\circ$) and characterize with very low adsorption of HSA, IgG, Fng, Fn, C3 and Cq1 ($< 0.05 \text{ mg/m}^2$ by ellipsometry) – Table 9.2.

Table 9.2 Protein adsorption (mg/m^2) as measured by ellipsometry

Surface	A_{HSA}	A_{IgG}	A_{Fgn}	A_{Fn}	A_{C3}	A_{C1q}
Silica	0.35	1.10	2.9	1.90	3.10	1.90
PEI/PEG1500	–	<0.05	<0.05	–	–	–
PEI/PEG6000	<0.05	<0.05	<0.05	<0.05	<0.05	<0.05
PEI/PEG12500	–	<0.05	<0.05	–	–	–

HAS – human serum albumin; IgG – immunoglobulin; Fgn – fibrinogen; Fn – fibronectin; C3 – complement component; C1q – complement component

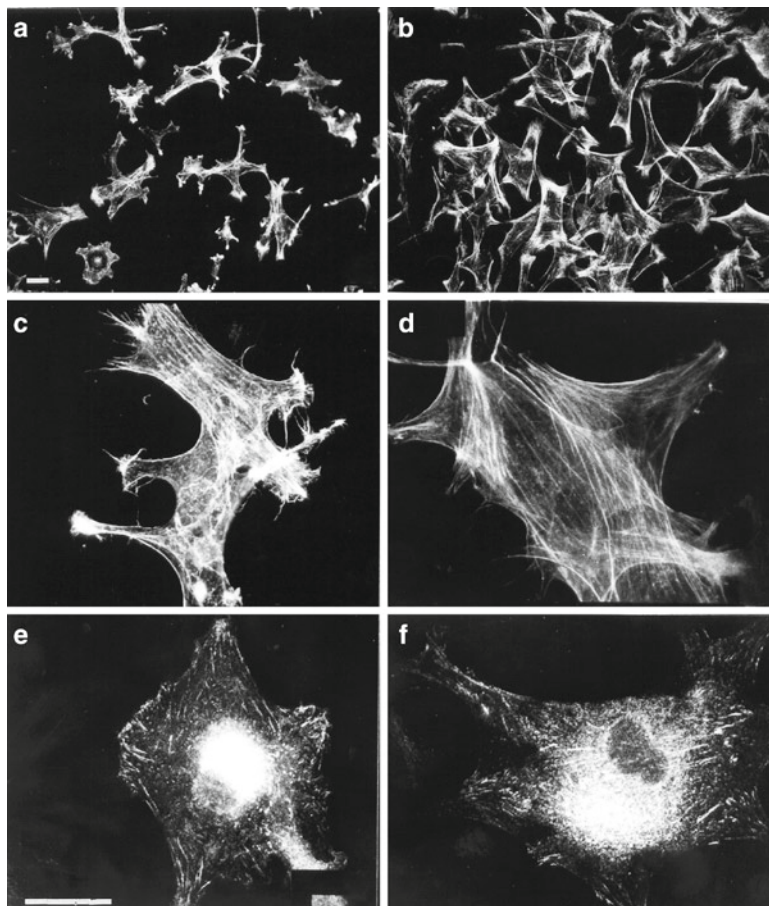


Fig. 9.4 Morphology of human fibroblasts adhered to PEI/PEG6000-epoxyde in absence (**a, b, e**) and in presence (**b, d, f**) of pre-adsorbed fibronectin. Fibroblasts were incubated on the surface for 2 h, then fixed and processed for fluorescence microscopy to visualize actin (**a–d**) and $\beta 1$ integrin (**e, f**)

In general, for such surfaces is expected good biocompatibility, in sense of bio-inertness but low cellular interactions. Surprisingly, these surfaces demonstrate very good initial cellular interaction: spreading, proliferation and adhesion (Fig. 9.4).

No direct correlation was found in this case between the protein adsorption and cellular interaction suggesting that cell-surface interaction depends on many other factors including the conformation of the adsorbed proteins and the polymer chains organization that, in turn, is influenced by their length and structure.

The described up to now three types, namely PEG hydrogel, PEG-grafted and PEI/PEG irreversibly adsorbed coatings, characterizes with exclusively low adsorption of different type proteins ($<0.05 \text{ mg/m}^2$); weak complement system activation, low platelet adhesion, excellent bio-inertness and thrombi-resistance proven not only in vitro but also in vivo (Kicheva et al. 2002a, b). In addition, the quasi irreversible deposited PEI/PEG coatings, in spite of their very low adsorption of plasma proteins unexpectedly characterize with very good interactions with living cells (Fig. 9.4) thought due to their specific structuring (Vladkova et al. 1999).

9.2.2 Protein Repellent Plasma Films

“Dray” chemistry methods, including plasma treatment, ion-beam, etc. offer a possibility to regulate all surface parameters influencing the bio-contact properties of the polymeric materials, including chemical composition, hydrophilic/hydrophobic balance, topography and roughness of the surface. They could be used also to activate chemically inert polymer surfaces for further chemical modification or bio-fictionalization.

Plasma treatment in vacuum or at normal pressure, in atmosphere of different gases, as well as ion- or electron beam are accepted now as convenient approaches to polymer surface engineering aimed at creation of modified nano-layers with desired properties to control the bio-contact properties of the polymeric material.

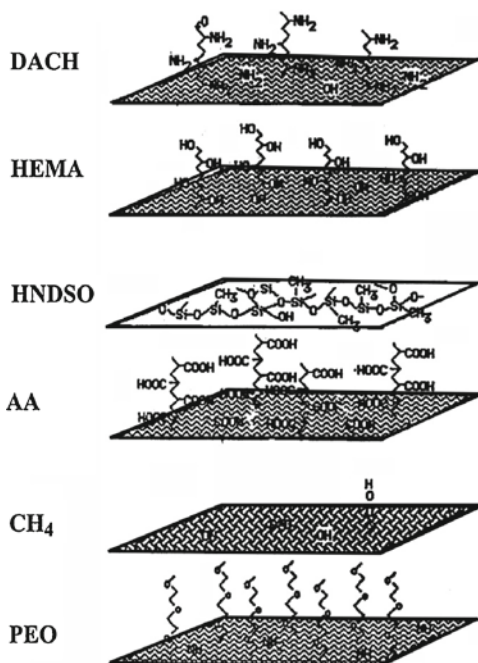
Figure 9.5 shows a simple sketch of the chemical composition of different radio frequency (RF) plasma discharge deposited films, based on the results from X-ray photoelectron spectroscopy (XPS).

Comparative study of similar plasma deposited films (Vladkova 1995; Kicheva et al. 2002a, b) indicates that both, strong hydrophobic silicon and strong hydrophilic PEG surfaces characterizes with very low protein adsorption, weak complement system activation and low cell and platelet adhesion that is in a compliance with the prediction of Ikada, Susuki and Tamada (Ykada et al. 1984).

9.2.3 Polydimethylsiloxane (PDMS) with Improved Interactions with Living Cells

Despite that the mechanism of the cell/surface interaction remains still not clear enough, a lot of physical–chemical factors influencing this interaction are known

Fig. 9.5 Chemical composition of plasma deposited polymer films: diaminocyclohexane (DACH), hydroxyethylmetacrylate (HEMA), hexamethyldisiloxane (HMDS), acrylic acid (AA), methane (CH_4) and polyethylene oxide (PEO)



nowadays that could be used for its control. Leading theories attempt to correlate both kind and intensity of the biological responses to

- Surface thermodynamic characteristics, such as hydrophilic/hydrophobic balance – an optimum interaction with cells is observed at moderate hydrophilicity (water contact angle of $\sim 40\text{--}60^\circ$)
- Surface chemical composition – the chemical functional groups oppress it in the following raw: $-\text{NH}_2 > -\text{OH} > \text{epoxy} > -\text{SO}_3 > -\text{COOH} > -\text{CF}_3$
- Total negative charge on the surface – not only the grafted functional groups but also the adsorbed ions influence the interaction
- Bonding of fibronectin and other matrix proteins – the synthesis and organization of fibronectin matrix by cells is better on surfaces bonding weakly fibronectin and other matrix proteins
- Conformation of the adsorbed adhesive proteins
- Surface roughness and topography, etc. (Altankov 2003; Jager et al. 2007; Vladkova et al. 1999)

Here are presented three examples of surface modification of strong hydrophobic chemically inert PDMS by creation of hydrophilic modified surface nano-layers that improves its interaction with living cells.

9.2.3.1 Plasma Based Ar⁺ Beam Treated PDMS

Cold plasma obtained in low pressure glow discharge has been often used to activate polymer surface, including siloxane membranes (Chu et al. 2002; Chan et al. 1996; Abbasi et al. 2001; Lee et al. 1996) for further grafting of suitable monomers like acrylic acid (AA), hydroxyl-ethyl-metacrylate (HEMA), etc. aimed at improvement of its interaction with living cells. On the other hand, ion-beam without following grafting (Satriano et al. 2001, 2002) is known as other possible way to improve bio-contact properties of polysiloxanes (Vladkova et al. 2004a, b). Plasma based Ar⁺ beam performed in RF (13,56 MHz) low-pressure with a serial capacitance can be employed for surface modification of PDMS to combine some advantages of both: ion-beam and plasma treatment, namely the durability of the modifying effect of the ion-beam with the simplicity of the plasma as compared to ion-beam equipment (Hippler et al. 2000). The presence of a serial capacitance ensures arise of an ion-flow inside the plasma volume directed toward the treated sample (Fig. 9.6) and the discharge power varying ensures varied ion-flow density.

A partially mineralized surface layer, similar to that obtained after a conventional ion-beam is the result of plasma based Ar⁺ beam treatment of PDMS surface as proven by XPS analysis and contact angle measurements (Vladkova et al. 2005). Plasma based Ar⁺ beam treatment transforms the initially strong hydrophobic PDMS surface into a durably hydrophilic one (Fig. 9.7), mainly due to raising of the polar component of the surface tension, this effect being most probably due to an enrichment of the modified surface layer with permanent dipoles of a [SiOx]-based network and elimination of the original methyl groups (Vladkova et al. 2005).

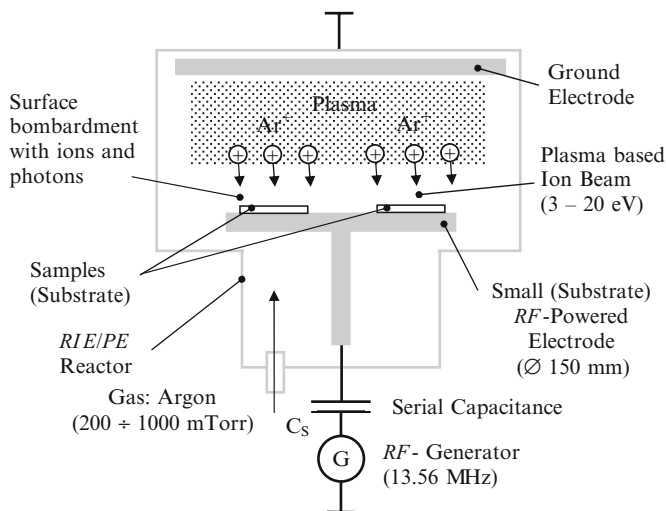


Fig. 9.6 Parallel plate single-wafer reactor in variant of plasma based Ar⁺ beam (AIB) mode of surface treatment

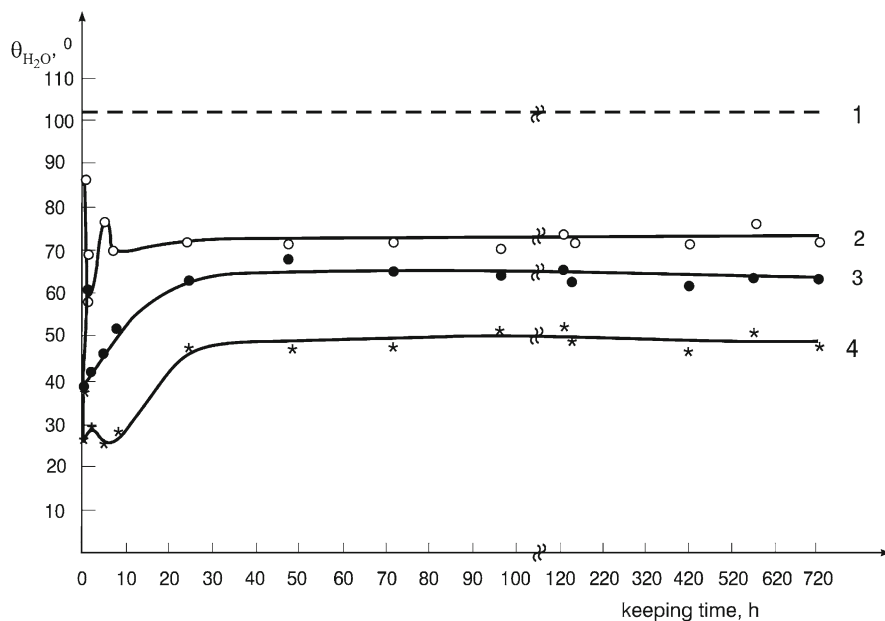


Fig. 9.7 Dependence of the water contact angle, $\theta_{\text{H}_2\text{O}}$ on the keeping time at room conditions for different PDMS surfaces: non-modified – (curve 1); plasma based Ar^+ beam treated for 1 min at a varied discharge power of 100 (curve 2), 1,200 (curve 3) and 2,500 W (curve 4)

Such modification is accompanied also with altering of the surface topography and roughness (Shanggun 2003) (Fig. 9.8, Table 9.3) and leads to significant improvement of the initial cell adhesion not only in presence but also in absence of pre-coated fibronectin (Vladkova et al. 2005; Keranov et al. 2007a) (Fig. 9.9).

9.2.3.2 Acrylic Acid (AA) Grafted Plasma Based Ar^+ Beam Pre-Activated PDMS

Ar^+ beam treatment opens also a way to further grafting of suitable monomers, arising radicals and hence activating PDMS surface. AA grafting to in this way activated surfaces, proven by XPS analysis and Toluidin Blue O adsorbance (Sano et al. 1993), leads to creation of moderate hydrophilic surfaces with water contact angle of 62–73° depending on the AA grafting density (Hippler et al. 2000). These values are close to the water contact angle value (~70°) of AA coated surfaces prepared earlier by photopolymerization (Gölander et al. 1986). The initial cell adhesion, studied by using of human fibroblast model, appears to be significantly better to AA grafted surfaces than to non-modified PDMS surface but only in presence of pre-coated fibronectin – compare Fig. 9.9a, b to Fig. 9.10a, b.

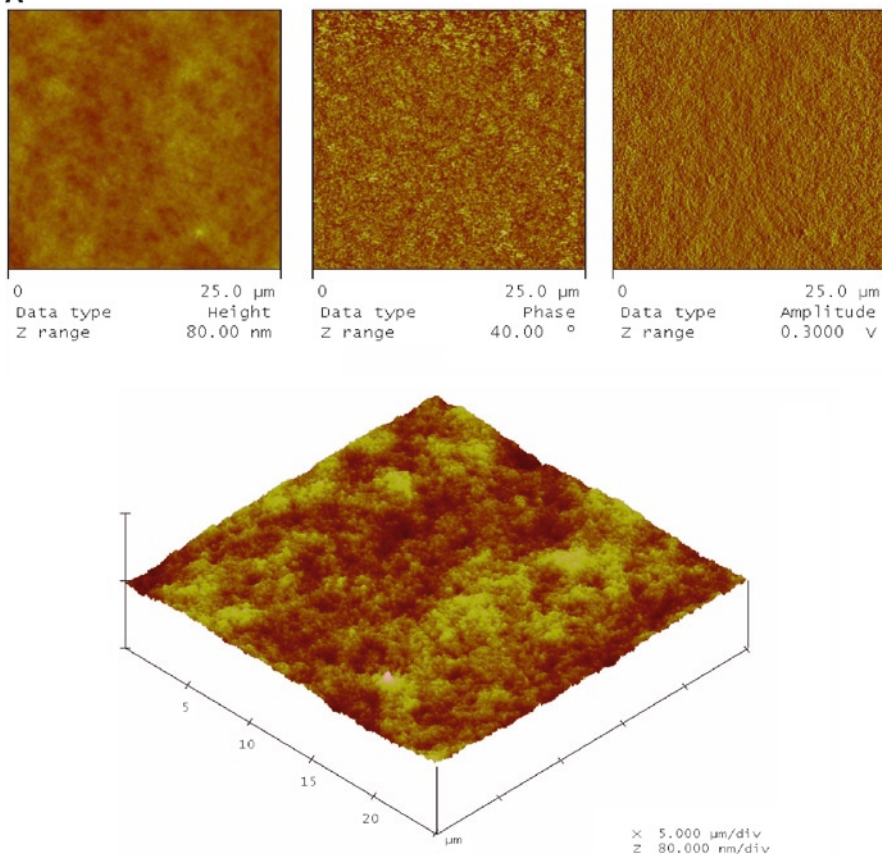
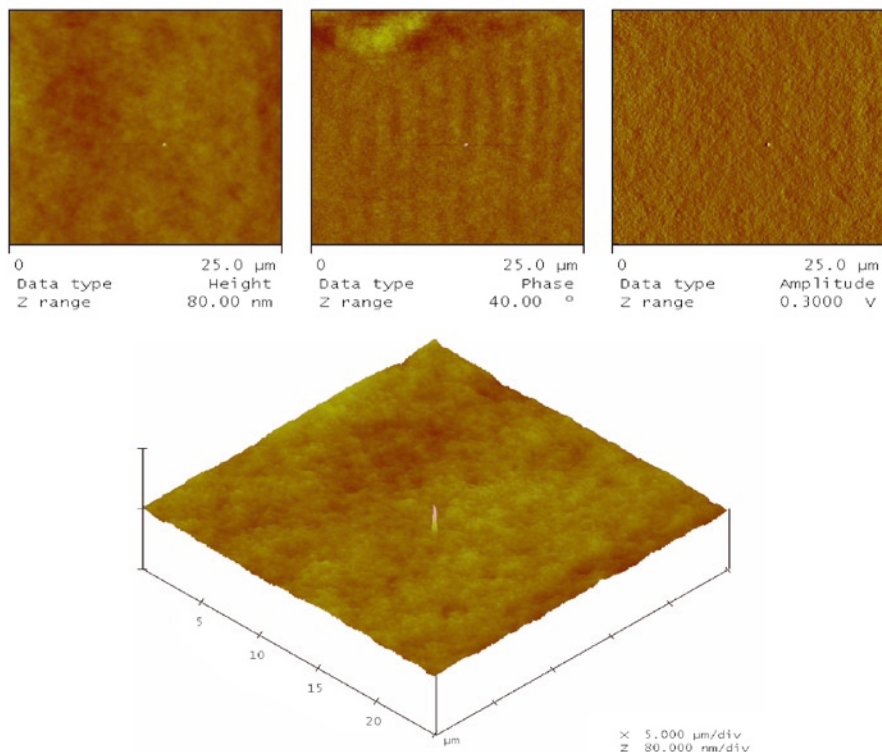
A

Fig. 9.8A AFM images: 2D height (a), phase (b) and amplitude (c); 3D height (d). Of non-modified PDMS (A) and treated by plasma based Ar^+ beam performed at discharge power of 1,200 W for 1 min (B)

9.2.3.3 Collagen Immobilized PDMS Surfaces

Bio-molecules (peptides, proteins, etc.) immobilization onto the polymer surface is another way to improvement of its interaction with cells, the last one of great importance in cell culture, tissue engineering and bio-integrating biomaterials. Bio-molecules immobilization could be achieved by different techniques based on either physical adsorption or covalent bonding. Unfortunately the direct covalent bonding of bio-molecules to chemically inert polymer surfaces such as polyethylene, polytetrafluorethylene (PTFE), PDMS, etc. is difficult and surface pre-activation, followed by a multi-step bonding procedure is necessary. For example, pre-activation of PTFE by plasma treatment opens a way to a multi-step procedure for peptide immobilization on its surface (Baquey et al. 1999).

B**Fig. 9.8B** (continued)**Table 9.3** Mean roughness, R_a and Root-mean-square roughness, R_q of non-modified (control) and plasma based Ar^+ beam treated PDMS for 1 min at different discharge power: 100, 1,200 and 2,500 W

Sample	Scan size μm	R_a nm	R_q nm
PDMS non-modified	25	1.593	2.013
PDMS treated for 1 min at 100 W	25	1.284	1.656
PDMS treated for 1 min at 1,200 W	25	1.201	1.064
PDMS treated for 1 min at 2,500 W	25	3.868	5.808

Plasma based Ar^+ beam treatment of PDMS also opens a way to its biofunctionalization by a multi-step procedure that includes AA grafting and flexible PEG-spacer coupling prior to a collagen immobilization by peptide synthesis reaction (Keranov et al. 2007b). AA grafted PDMS surfaces are reacted with PEG bearing two terminals NH_2 -groups (Baquay et al. 1999). A known peptide synthesis reaction (Keranov et al. 2007b; Shanggun 2003; Ho and Yasuda 1990) is used for the immobilization of collagen, type I on the AA grafted and PEG spacer coupled samples. Surface chemical composition, wet ability, topography and roughness are controlled on every stage

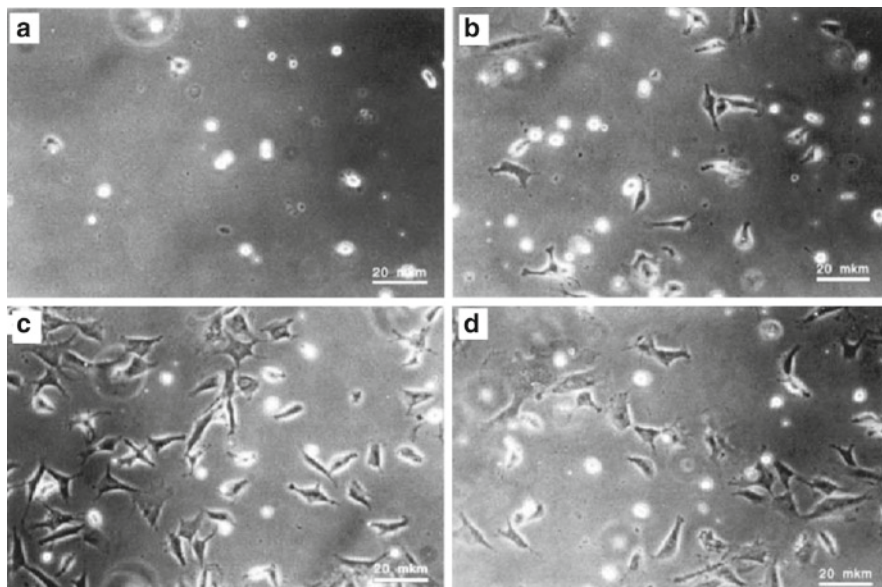


Fig. 9.9 Initial cell adhesion of human fibroblasts to non-modified PDMS (a, b) or treated by plasma based Ar^+ beam performed at 1,200 W/1 min (c, d) in absence (a, c) and in presence (b, d) of pre-coated fibronectin

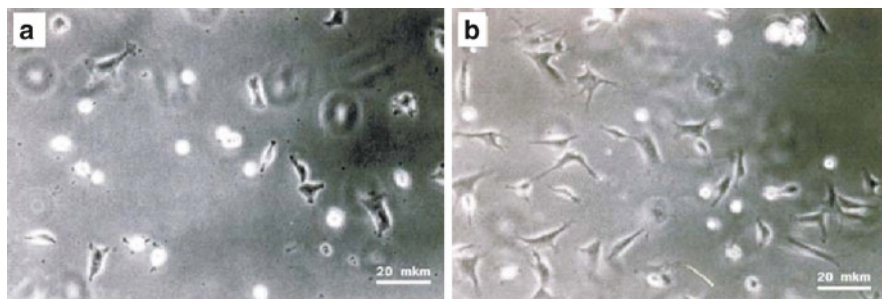


Fig. 9.10 Initial cell adhesion of human fibroblasts to AA grafted plasma based Ar^+ beam pre-treated PDMS in absence (a) and in presence (b) of pre-coated fibronectin

of the multi-step procedure by XPS analysis, contact angle measurements and AFM observations. Collagen immobilization via flexible spacer improves significantly the cellular interaction (Figs. 9.11 and 9.12) on the scarcely adhesive PDMS surface this effect depending on the length of the PEG chain.

This multi-step procedure to bio-functionalization of strong hydrophobic chemically inert polymer surfaces has a potential to be used whenever need arises to control cellular interaction with the siloxane rubber, for example cell culture, tissue engineering, bio-integrating biomaterials.

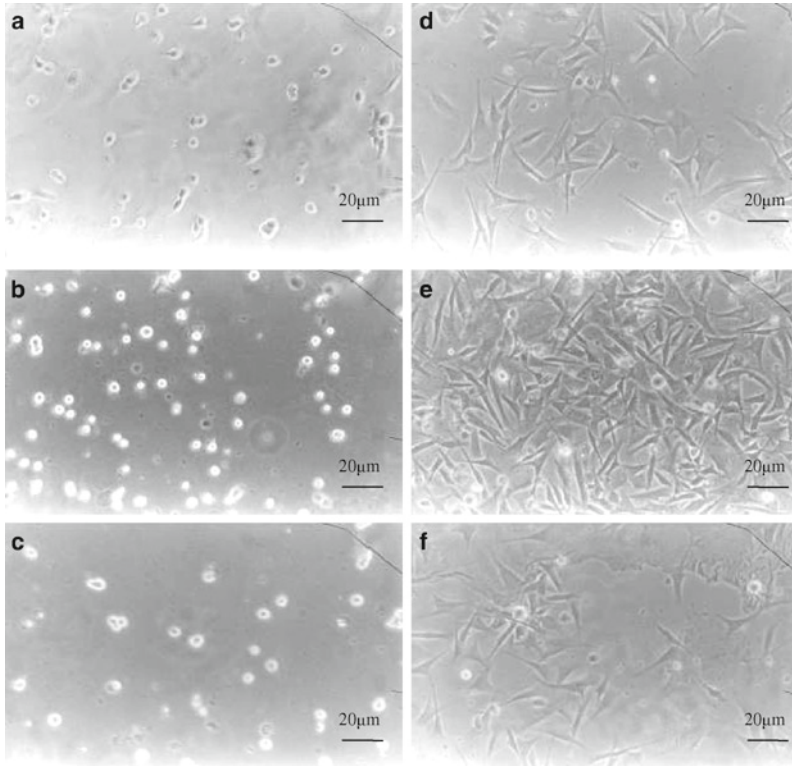


Fig. 9.11 Overall cell morphology of human fibroblast cells on plasma based Ar⁺ beam treated and AA grafted PDMS surfaces, coupled with PEG-spacer: (a) di-NH₂PEG2000, (b) di-NH₂PEG6000, (c) di-NH₂PEG20000 and collagen, type I immobilized: (d) di-NH₂PEG2000/collagen, (e) di-NH₂PEG6000/collagen and (f) di-NH₂PEG20000/collagen

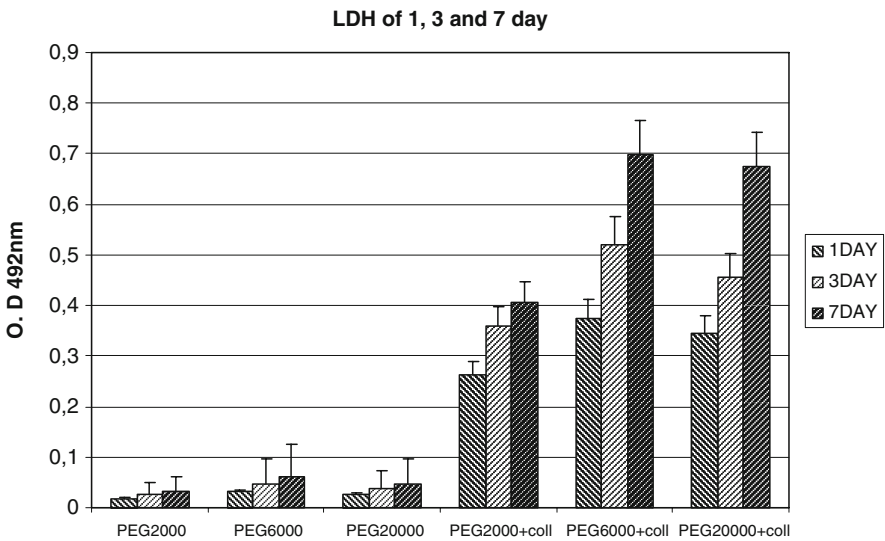


Fig. 9.12 LDH cell assay on PEG coupled and collagen immobilized PDMS surfaces

Evidently, plasma based Ar⁺ beam treatment successfully activates PDMS surface for subsequent functionalization and bio-functionalization. Such treatment in itself and following AA grafting as well as collagen immobilization turn PDMS from strong hydrophobic in moderate hydrophilic material due to altering its surface chemical composition, polarity, topography and roughness, these depending on the operation conditions. No direct correlation is observed between the surface hydrophilicity and the initial cellular interaction presumably due to the simultaneous influence of other factors like surface chemical composition and roughness. The cellular interaction on a scarcely adhesive PDMS surface is significantly improved by all the three surface modification techniques due to creation of modified nano-size layers with suitable physical–chemical properties. The above described three approaches to PDMS surface engineering offers new possibilities to the control of cellular interactions with siloxane rubber surfaces.

9.3 Conclusions

Biomaterials with controlled protein adsorption and initial cell adhesion potentially applicable in the regenerative medicine could be developed on the base of conventional polymers such as PE, PP, PVC, PS, PTFE, NR, PDMS, etc. by creation of modified nano-size layers with controlled parameters employing different surface engineering chemical and plasma-chemical techniques. Suitable surface engineering could alter the surface chemical composition, hydrophilic/hydrophobic balance, topography and roughness in a desirable direction to control the protein adsorption, platelet and cell adhesion, complement system activation, etc. The choice of a surface treatment technique depends on the polymer substrate properties as well as on the desirable physical–chemical and bio-contact properties of the surface modified layer.

References

- Abbasi F, Mirzadeh A, Katbab A-A (2001) Modification of polysiloxane polymers for biomedical applications: a review. *Polym Int* 50:1279–1287
- Altankov B (2003) взаимодействие на клетки с биоматериални повърхности, Дисертация за доктор на биологическите науки, БАН, Институт по биофизика, 2003 г
- Bailey FE, Koleske JV (1976) Poly(ethylene Oxide). Academic, New York/San Francisco/London
- Baquey Ch, Palumbo F, Porte-Durrieu MC, Legeay G, Tressaud A, d'Agostino R (1999) Plasma treatment of expanded PTFE offers a way to a biofunctionalization of its surface. *Nucl Instrum Methods Phys Res B* 151:255–262
- Chan CM (1993) Polymer surface modification and characterization, Chapters 5–7. Hanser, Brookfield, WI
- Chan CM, Ko T-M, Hiraoka H (1996) Polymer surface modification by plasmas and photons. *Surf Sci Rep* 24(1–2):1–54
- Chu PK, Chen JY, Wang LP, Huang N (2002) Plasma-surface modification of biomaterials. *Mater Sci Eng R36*:143–206

- Drotleff S (2006) Polymers and protein-conjugates for tissue engineering. PhD Thesis, University of Regensburg, Germany
- Elbert DL, Hubbell JA (1996) Thin polymer layers formed using multiarm poly(ethylene glycol) vinylsulfone by a covalent layer-by-layer method. *Annu Rev Mater Sci* 26:365–394;
- Sakiyama-Elbert SE, Hubbell JA (2001) Functional biomaterials: design of novel biomaterials. *Annu Rev Mater Res* 31:183–201
- Gölander C-G (1986) Preparation and properties of functionalized polymer surfaces. PhD Thesis, The Royal Institute of Technology, Stockholm, Sweden
- Gölander C-G, Jönsson E-S, Vladkova TG (1984) A surface coated article, process and means for the preparation of thereof and use of thereof, Swed. Pat. No 8404866-9/1984; Bulg. Pat. No 67997/1984; Europ. Pat. No 022966/1984; PCT SE85/00376/1984
- Gölander C-G, Jönsson E-G, Vladkova TG, Stenius P, Eriksson J-C (1986) Preparation and protein adsorption properties of photo-polymerized hydrophilic films coating N-Vinyl pyrrolidone (NVP), Acrylic Acid (AA) or Ethylene oxide (EO) units as studied by ESCA. *Colloids Surf* 21:149–166
- Gölander C-G, Jönsson E-S, Vladkova T, Stenius P, Eriksson J-C, Kisch E (1987) Protein adsorption on some photo-polymerized hydrophilic films. *Proc IUPAC'87*, July 13–18, Sofia, 8.27
- Harris JM (ed) (1992) Poly(ethylene Glycol) chemistry. biotechnical and biomedical applications. Plenum, New York/London, pp 1–7
- Hippler R, Pfau S, Schmidt M, Schönbach K (eds) (2000) Low temperature plasma physics. Fundamental aspects and applications. Willey-VCH, Berlin/New York/Chichester/Brisbane/Toronto
- Hlady V, VanWagenen RA, Andrade JD (1985). In: Andrade JD (ed) Surface and interfacial aspects of biomedical polymers, vol 2. Plenum, New York, p 81
- Ho C-P, Yasuda H (1990) A hydrophilic plasma polymerized film composite for application in sensors. *J Appl Polym Sci* 39:154–160
- Jager M, Zilkens C, Zanger K, Krauspe R (2007) Significance of nano- and microtopography for cell-surface interactions in orthopedic implants. *J Biomed Biotechnol* 2007. Article ID 69036, doi:10.1155/2007/69036
- Keranov I, Vladkova T, Minchev M, Kostadinova A, Altankov G, Dineff P (2009) Topography characterization and initial cellular interaction of plasma based Ar+ beam treated PDMS surfaces. *J Appl Polym Sci* 111:2637–2646
- Keranov I, Vladkova T, Minchev M, Kostadinova A, Altankov G (2008) Preparation, characterization and cellular interactions of collagen immobilized PDMS surfaces. *J Appl Polym Sci* 110:321–330
- Kicheva Y, Vladkova T, Kostov V, Gölander C-G (2002a) Preparation of PVC drain tubing and in vivo study for their biocompatibility. *JUCTM* 37:77–84
- Kicheva Y, Kostov V, Mateev M, Vladkova T (2002) In vitro and in vivo evaluation of biocompatibility of PVC materials with modified surfaces. Proceedings of VIth Colloquium on Biomaterials, Aachen, Germany, 24–25 Sept 2002
- Kiss E, Gölander C-G, Eriksson J-C (1987) Surface grafting of polyethyleneoxide optimized by means of ESCA. *Progress Colloid Polym Sci* 74:113–118
- Lee Sh-D, Hsiue G-H, Kao Ch-Y (1996) Preparation and characterization of a homo-bi-functional silicone rubber membrane grafted with acrylic acid via plasma-induced graft copolymerization. *J Polym Sci A: Polym Chem* 34:141–148
- Malmsten M (ed) (1998) Biopolymers at interfaces. Marcel Dekker, New York
- Malmsten M, Van Alstin JM (1996) Reduction of protein adsorption by polyethylene glycol coatings. *Colloids Surf B80*:159–165
- Pasche S (2004) Mechanisms of protein resistance of adsorbed PEG-graft copolymers. DSC Thesis, Swiss Federal Institute of Technology, Zurich
- Sano S, Kato K, Ikada Y (1993) Introduction of functional groups onto the surface of polyethylene for protein immobilization. *Biomaterials* 14(11):817–822
- Satriano C, Conte E, Marletta G (2001) Surface chemical structure and cell adhesion onto ion beam modified polysiloxane. *Langmuir* 17:2243–2250

- Satriano C, Carpazza S, Guglielmino S, Marletta G (2002) *Langmuir* 18:9469–9476
- Shanggun N (2003) Methods for amide formation. *J Am Chem Soc* 125:7754–7755
- Vladkova T (1995) Modification of polymer surfaces for medical application. Proceedings of XIIIth Science Conference. “Modification of Polymers”, Kudowa Zdroj, Poland, 11–15 Sept 1995
- Vladkova T (2001) Some possibilities to polymer surface modification. UCTM Ed. Centre, Sofia
- Vladkova TG, Gölander C-G, Christoskova St Ch, Jönsson E-S (1997) Mechanically stable hydrophilic films based on oxialkylated macromers polymerizable by UV irradiation. *Polym Adv Technol* 8:347–353
- Vladkova T, Krasteva N, Kostadinova A, Altankov G (1999) Preparation of PEG-coated biomedical surfaces and study for their interaction with living cells. *J Biomater Sci Polym Ed* 10(6): 609–620
- Vladkova T, Keranov I, Altankov G (2004) Preparation and properties of PDMS surfaces grafted with acrylic acid via plasma pretment or ion-beam induced graft co-polymerization. Proceedings of 4th International Conference of the Chemical Societies of the South-Eastern European Countries (ICOSECS), Belgrad, Serbia, A-P 26, 18–21 July 2004
- Vladkova T, Keranov I, Dineff P, Altankov G (2004) Ion-beam assisted surface modification of PDMS. Proceedings of XVIIIth Congres of Chemists and Technologist of Macedonia, Ohrid, PPM-16, 21–25 Sept 2004
- Vladkova T, Keranov I, Dineff P, Youroukov S, Avramova I, Krasteva N, Altankov G (2005) Plasma based Ar⁺ beam assisted poly(dimethylsiloxane) surface modification. *Nucl Instrum Methods Phys Res B* 236:552–562
- Ykada Y, Suzuki M, Tamada Y (1984) Polymer surfaces possessing minimal interaction with blood components. In: Shalaby SW, Hoffman AS, Ratner BD (eds) *Polymers as biomaterials*. Plenum, New York

Chapter 10

Nanocomposites for Regenerative Medicine

Ryan Hoshi, Antonio R. Webb, Hongjin Qiu, and Guillermo A. Ameer

Abstract This chapter describes properties and applications of nanocomposites in tissue engineering and regenerative medicine with an emphasis on the impact of the nanophase on nanocomposite function. The nanophase can be used as a means to engineer new physical properties that improve the utility of tissue engineering scaffolds. Several examples of the use of the nanophase for mechanical reinforcement or drug delivery are discussed with an emphasis on understanding how nanoparticles are used to achieve the controlled release of macromolecules. Advances in nanotechnology, knowledge of mechanical reinforcement at the nanoscale level, and new strategies for controlled drug release will contribute to the next generation of nanocomposite-based scaffolds designed for regenerative medicine.

Keywords Nanocomposites • Tissue engineering • Nanotechnology • Drug delivery • Nanofibers • Electrospinning • Nanopores

10.1 Perspective

The field of biomaterials has experienced an exponential growth in the development or modification of materials for biomedical applications ranging from drug delivery to tissue engineering-based therapies. The establishment of new biomaterials

G.A. Ameer (✉)

Biomedical Engineering Department, Northwestern University, 2145 Sheridan Rd E310, Evanston, IL 60208, USA

and

Department of Surgery, Feinberg School of Medicine, Northwestern University, 303 E Chicago, Chicago, IL 60611, USA

and

Institute for BioNanotechnology in Medicine (IBNAM), Northwestern University, 303 East Superior Street, Suite 11-131, Chicago, Illinois 60611-2875

e-mail: g-ameer@northwestern.edu

R. Hoshi, A.R. Webb, and H. Qiu

Biomedical Engineering Department, Northwestern University, 2145 Sheridan Rd E310, Evanston, IL 60208, USA

programs at research institutions world-wide has resulted in the rapid growth of new biomaterials literature. The irony is that despite the large number of biomaterials that have been described at a preclinical level, there is little diversity of materials used in the clinical or hospital setting. Furthermore, with such a large variety of biomaterials described in the literature it becomes increasingly difficult to justify the generation or development of new materials for medical applications. The biomaterials scientist or engineer will have to carefully re-evaluate the rationale for designing and implementing a novel biomaterial in a medical application. This fact points to the importance of defining a very important target application and problem with an unmet need. Nevertheless, developments that combine knowledge in nanotechnology with composite materials may provide new and radical solutions to very old problems. With the emergence of nanotechnology, researchers are emphasizing the impact that nanoscale engineering can have on the functions of biomaterials. Some of these nanotechnology byproducts are being implemented in composite biomaterials used in scaffolds for tissue engineering. However, without defining specific applications or problems that would significantly benefit from a novel device, biomaterials science and engineering will run the risk of becoming irrelevant to the growing field of regenerative medicine.

This chapter will discuss new developments in the medical applications of nanocomposites. Nanocomposites are defined as materials that contain a distinct nanophase that typically consists of a different material from that in the bulk or macrophase. At least one dimension of the nanophase should be less than 100 nm. Caution should be used when using definitions. Rather than categorizing a nanocomposite based only on size scale arguments, one should take into consideration whether there is a step change in a particular function or property. The mechanism of the step change should involve phenomena that can be attributed to nano-scale structures. To address the issue of incongruity when it comes to nanophase research, herein we describe the role of the nanophase in modulating the properties or function of a composite. The first section, discusses the nanophase as a means to tailor the mechanical properties of scaffolds used in tissue engineering applications, placing particular emphasis on orthopaedic tissue engineering. The second section discusses drug delivery applications using nanostructures. In some cases the nanostructures may consist of nanofibers or nanopores while in other cases the nanostructures may be nanoparticles that can be incorporated within a macrophase.

In the end, the goal for the biomaterials scientist is to provide biomaterials that can be used in devices that mimic the function and/or properties of natural tissues. With continued scientific progress in nanotechnology research, we have the capabilities to engineer and design biomaterials at sub 100 nm scale. As we will describe later, the impact of nanotechnology is not only limited to bulk properties of a composite but also to surface interactions where nanoscale surface features can have a significant impact on protein adsorption, conformation, and subsequent cellular interactions. The challenge in this field is to develop novel and innovative approaches to enhance the efficacy of devices used for regenerative medicine, which can lead to clinical application and improved healthcare. Ultimately, this challenge will only be met if there is collaborative engagement across academia, industry and regulatory agencies.

10.2 A Nanophase for the Mechanical Reinforcement of Tissue Engineering Scaffolds

10.2.1 Introduction

Tissue engineering is a rapidly developing interdisciplinary field that combines engineering and life sciences to repair or regenerate diseased or damaged biological tissues (Langer and Vacanti 1993; Vacanti and Langer 1999). This field often requires the use of three-dimensional porous scaffolds on which cells and growth factors can be seeded on to promote cell attachment, proliferation, migration and extracellular matrix (ECM) synthesis. When engineering tissues that have specific biomechanical requirements such as bone and a variety of soft tissues, the mechanical properties of the scaffold can be particularly important (Webb et al. 2004; Yang et al. 2001). For example, elastomeric scaffolds that can withstand cyclic loading are beneficial for cartilaginous, ligamentous, and smooth muscle containing tissues as mechanical stimulation during *in vitro* tissue development has been shown to modulate cell differentiation, increase extracellular matrix synthesis, and enhance the mechanical properties of the resulting tissue (Kim and Mooney 2000; Nerem 2003; Niklason et al. 1999; Waldman et al. 2003; Kim et al. 1999). Likewise, for *in vivo* tissue engineering, the scaffold should withstand normal physiological loads during tissue development and provide gradual stress transfer to the developing tissue as the scaffold degrades (Yang et al. 2005). Since many tissues have specific biomechanical properties that are critical for normal *in vivo* performance, successful tissue engineering will require the development of scaffolds that can mimic these biomechanical properties (Bulter et al. 2000).

Poly(hydroxyortho esters) such as poly(glycolic acid) (PGA), poly(lactic acid) (PLA), and copolymers thereof are often used for the fabrication of scaffolds for tissue engineering due to their long history in the clinical setting (Atala and Lanza 2001). However, for soft tissues where mechanical stimulation during development may be beneficial, these materials are of limited use due to their inability to undergo large reversible elastic deformations when stressed (Yang et al. 2001). Poly(ϵ -caprolactone) (PCL) may undergo reversible elastic deformations, but is not used as often due to its slow degradation and limited compatibility with cells due to its hydrophobicity (Pachence and Kohn 2000; Kweon et al. 2003). Similarly, for hard tissues, poly(hydroxyortho esters) are also of limited use due to their lack of osseointegration with existing bone and inadequate mechanical properties in high load bearing applications (Singh and Sinha Ray 2007; Bleach et al. 2002).

In an attempt to improve the mechanical properties and biocompatibility of polymeric scaffolds, researchers have investigated the inclusion of a second component or phase, often made of fibers, whiskers, or particles, to create a composite material (Jordan et al. 2005). The resulting composite often has a new range of properties that cannot be achieved with either phase alone. Although composites were traditionally reinforced with micron scale inclusions, recent advances in processing technology have allowed the size of inclusions to decrease to the nanoscale (Jordan et al. 2005).

This transition from micro- to nano-sized inclusions often brings dramatic increases in mechanical properties. Herein, a review of recent literature on nanocomposite tissue engineering scaffolds with enhanced mechanical properties will be presented. The discussion will be divided into scaffolds for hard and soft tissue engineering.

10.2.2 Nanocomposite Scaffolds for Hard Tissue Engineering

With the aging population, there is a huge need for bone and dental tissue engineering products. Traditionally, bio-inert materials such as metals, ceramics, and alloys have been used as bone replacements with the goal of providing minimal toxicity and mechanical properties that match those of the replaced tissue (Hench and Polak 2002). However, these materials usually elicit a host response which results in a fibrous capsule forming around the tissue and prevents proper integration with the native tissue environment (Ratner and Bryant 2004). Therefore, many researchers have investigated the tissue engineering approach for bone and hard tissue substitutes with improved biocompatibility. Although biodegradable polymers such as poly(L-lactic acid) (PLLA), poly(glycolic acid) (PGA), and their copolymers (PLGA) have traditionally been used as tissue engineering scaffolds due to their biocompatibility and biodegradability, their poor mechanical properties compared to bone and lack of osteoconductivity have limited their usefulness for bone tissue engineering (Singh and Sinha Ray 2007). Bioceramics such as hydroxyapatite are another class of materials used for bone repair. Although these materials are similar to the mineral component of bone and show good osteoconductivity, they are inherently brittle and difficult to process into tissue engineering scaffolds (LeGeros 2002; Cooke 1992). The development of composite materials is one strategy that researchers have used to combine the osteoconductivity of bioceramics with the biocompatibility and processability of biodegradable polymers.

Since nanometer scale apatite in natural bone is considered to be important for mechanical properties and osteoconductivity, synthetic nano-hydroxyapatite (nano-HA) can be used to resemble natural bone in both size and morphology at the nanometer scale (Rho et al. 1998; Du et al. 1999; Du et al. 1998). A number of studies have utilized nano-hydroxyapatite for composite bone tissue engineering scaffolds for improved osteoconductivity and biocompatibility; however, there are few reports of scaffolds with enhanced mechanical properties (Du et al. 1999; Cool et al. 2007; Nie and Wang 2007; Sachols et al. 2006). The following section will discuss recent literature on novel nano-HA scaffolds for hard tissue engineering that show enhanced mechanical properties.

10.2.2.1 Synthetic/Nano-hydroxyapatite Scaffolds for Hard Tissue Engineering

Synthetic materials such as poly(ortho esters) and poly(amides) have been used as polymer matrices for bone tissue engineering nanocomposite scaffolds.

For instance Kim et al. created PLGA/nano-HA scaffolds for bone tissue engineering using gas foaming and particulate leaching methods (Kim et al. 2006). Gas foaming is beneficial since it eliminates harmful residual solvents that may be left behind using traditional solvent casting and particulate leaching techniques. Gas foamed scaffolds exhibited increased compressive (4.5 ± 0.3 versus 2.3 ± 0.4 MPa) and tensile (26.9 ± 0.2 versus 2.0 ± 0.1 MPa) moduli compared to solvent cast scaffolds. The decrease in mechanical properties was attributed to residual solvent in the cast scaffolds acting as a plasticizer. However, there was no mechanical testing of unreinforced scaffolds or scaffolds with micron sized HA, so it is impossible to determine if the nano-HA provided any reinforcement. Nevertheless, the compressive modulus was well within the range reported for cancellous bone (2–10 MPa) (Gibson 1985).

In addition to PLGA, poly(lactic acid) has been used extensively as a polymer matrix for composite bone tissue engineering scaffolds. Wei and Ma at the University of Michigan created nano-HA/PLLA composites using a thermally induced phase separation technique (Wei and Ma 2004). Briefly, nano-HA powder was first dispersed in dioxane and this solvent/HA mixture used to dissolve PLLA. The mixture was then poured into a Teflon mold, transferred to a freezer to induce phase separation, and finally the solvent removed via freeze drying. The compressive modulus of nano-HA/PLLA scaffolds increased with nano-HA content (Fig. 10.1). In addition, compressive modulus of nano-HA reinforced scaffolds increased compared to that of micro-HA reinforced scaffolds (Fig. 10.1). Once again, the compressive modulus for the 30% and 50% nano-HA scaffolds compare favorably to the upper range reported for cancellous bone.

Since previous studies have shown that scaffolds with nanofibrous pore walls have increased osteoblast cell attachment (Woo et al. 2003), Wei and Ma further refined their nanocomposite scaffolds by introducing a nanofibrous PLLA network combined with nano-HA (Wei and Ma 2006). In addition, large macropores were introduced

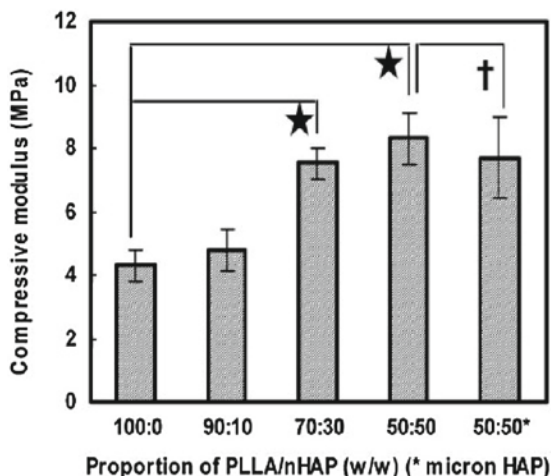


Fig. 10.1 Effect of nano-HA content on the compressive modulus of nano-HA/PLLA composites (Reprinted with permission from Wei and Ma 2004)

using sugar spheres as a porogen during the gelation step. However, the compressive moduli of these scaffolds were all less than 1 MPa. The low compressive modulus of these scaffolds may be due to high porosity (98% in this study versus 92% in previous work), as well as the different morphology of the pore walls (nanofibrous versus solid). Nonetheless, the authors speculate that the nanofibrous structure of the pore wall, which mimics the nanostructure of collagen, should improve cell attachment and provide a better environment for bone growth and cell differentiation.

Researchers have shown that under certain conditions, addition of HA particles can improve the mechanical properties of elastomeric poly(1,8-octanediol citrate) (POC) when used in a composite blend (Qiu et al. 2006). The composite of POC with HA had the desired characteristics of a bioceramic suitable for hard tissue engineering but with improved processability, mechanical properties, and degradation characteristics. Its mechanical properties can be tailored by simply changing reaction conditions such as reaction temperature and time, and the ratio of 1,8-octanediol to citric acid as well as HA particle size (Yang et al. 2004a; Yang et al. 2006a). Varying the percent of nanocrystals in the POC-HA nanocomposites resulted in a material with mechanical properties ranging from flexible to hard. The latter characteristic allows for interference screw fabrication by machine processing. Compared with HA microparticles, the incorporation of HA nanocrystals into the POC polymer matrix significantly improves the mechanical properties (strength and modulus of bending and compression). These findings may be attributed to the small size and higher contact surface area of HA nanocrystals relative to microparticles at a fixed particle weight fraction (Crosby and Lee 2007a). Interfacial adhesion between the polymer and the ceramic is increased resulting in a significant change in mechanical properties (Deng et al. 2001). The bioceramic-elastomer composite has a wide range of mechanical properties and a hydroxyapatite content that is similar to that of bone. The mechanical property measurements of the POC-HA composites evaluated in this study were within the range of values reported for biodegradable polymers and composites intended for bone fixation devices (Daniels et al. 1990). Therefore the fabrication of composites of polymers with bioceramics can be considered a suitable compromise to meet mechanical property requirements and achieve osteointegration of the implant. Moreover, these materials are inexpensive and easy to synthesize, which is advantageous for clinical application.

Although the above composites are similar to natural bone in bioceramic composition and hierarchical microstructure, they are missing collagen which is the main non-mineral component of natural bone. A nano-HA/collagen/PLA composite was created by biomimetic synthesis with faster degradation rates (Liao et al. 2004). Briefly, nano-HA was mineralized onto collagen I, harvested, and then added to PLA solutions to create the composite. The mechanical properties increased with increasing PLA concentration and approached the lower limits of cancellous bone (Fig. 10.2). In addition, the compressive modulus is similar to that of trabecular bone (50 MPa) (Shea et al. 2000). However, these materials could not support implantation due to their low compressive strength.

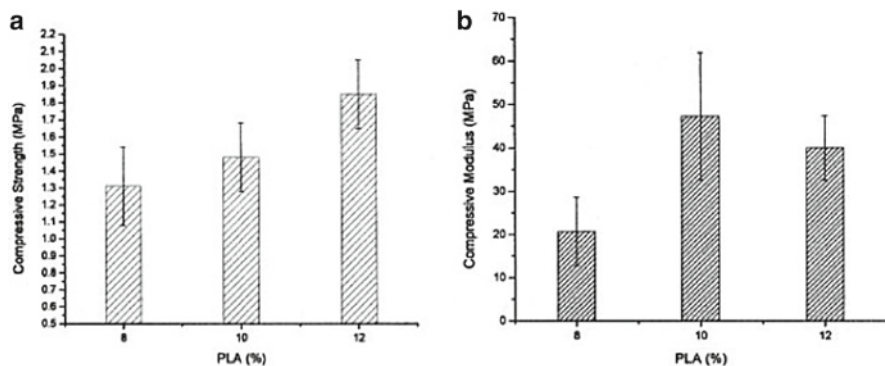


Fig. 10.2 (a) Compressive strength and (b) compressive modulus of nano-HA/collagen/PLA composite vs PLA concentration (Reprinted with permission from Liao et al. 2004)

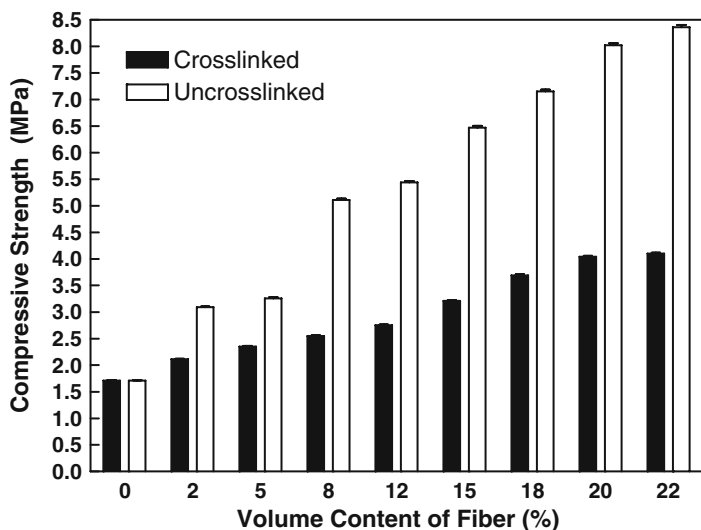
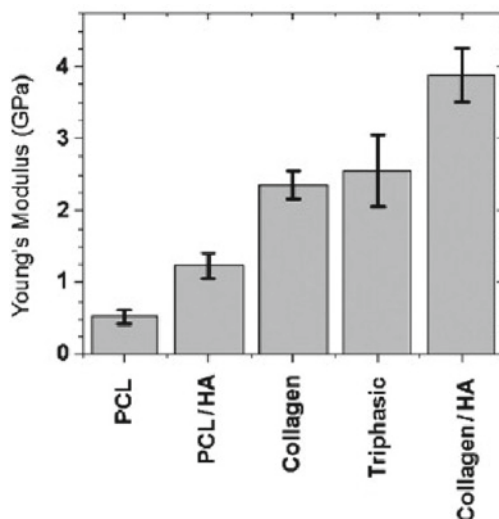


Fig. 10.3 Compressive strength of nano-HA/collagen/chitin fiber nanocomposites as a function of fiber content (Recreated from data published in Li et al. 2006)

In a similar study, Li et al. developed nano-HA/collagen/PLLA composites but the mechanical properties were much lower than that of cancellous bone (Wang et al. 1995; Du et al. 2000). To overcome these limitations, chitin fibers were added to the nano-HA/collagen scaffold to provide reinforcement (Li et al. 2006). When the volume content of the scaffolds increased, the mechanical properties increased (Fig. 10.3). By crosslinking the chitin fibers to the PLLA polymer, the mechanical properties could be increased further and approach the upper range reported for cancellous bone (Fig. 10.3).

Fig. 10.4 Young's modulus of PCL/collagen/nano-HA composites (Reprinted with permission from Catledge et al. 2007)



Catledge et al. created electrospun poly(caprolactone)/collagen/nano-HA triphasic scaffolds for bone tissue engineering (Catledge et al. 2007). The nano-HA deposits itself between tangled collagen/PCL fibers and provides reinforcement (Fig. 10.4). The increase in Young's modulus may be due to mechanical interlocking or calcium ion bridges between the tangled fibers increasing resistance to deformation and hindering plastic deformation (Catledge et al. 2007). However, it should be noted that the mechanical properties were tested on pressure consolidated pellets and thus may not be representative of a porous three dimensional scaffold under in vivo conditions.

Poly(amides) (PA) are another class of polymers that have proven beneficial for bone tissue engineering nanocomposites. In particular, poly(amides) are known to possess good biocompatibility with various human cells and tissues due to its similarity to collagen in chemical structure and active groups (Springer et al. 2001; Koji et al. 2001; Upadhyay et al. 2004). In addition, PA's exhibit excellent mechanical properties due to strong hydrogen bonding between amide groups and poly(amide) macromolecules. In one study, nanocomposites of PA66 (nylon 6,6) and nano-HA were created by precipitating nano-HA particles in the presence of a poly(amide) solution (Jie and Yubao 2004). Mechanical properties of the composites are shown in Table 10.1. For the 64.25% nano-HA composites, the bending, tensile, and compressive strength compare favorably to that of natural bone (bending = 80–100 MPa, tensile = 60–120 MPa, compressive = 50–140 MPa). In addition, although the elastic modulus was much lower than that of bioceramics and metals, the values are closer to that of natural bone (3–25 GPa). This fact should eliminate the stress shielding effect seen with bioceramics and metals that leads to loosening of the implant and eventual failure and resorption of bone. However, it should be noted that mechanical properties were not tested on porous samples and thus will decrease dramatically when a 3D-porous structure is fabricated.

Table 10.1 Mechanical properties of dense nano-HA/PA66 composites (Reprinted with permission from Jie and Yubao 2004)

Nano-HA content (%)	Tensile strength (MPa)	Bending strength (MPa)	Compressive strength (MPa)	Elastic modulus (GPa)
38.71 ± 0.208	65 ± 4	77 ± 5.0	93 ± 7.1	3.6 ± 0.3
45.06 ± 0.012	71 ± 1	85 ± 2.3	106 ± 2.6	4 ± 0.5
51.78 ± 0.252	74 ± 3	87 ± 3.6	112 ± 6.0	4.9 ± 0.2
64.25 ± 0.270	87 ± 2	95 ± 5.2	117 ± 4.1	5.6 ± 0.3

Table 10.2 Compressive mechanical properties of 40% nano-HA/PA66 composites with different porosities (Reprinted with permission from Li et al. 2005a)

Porogen/composite (w/w)	Porosity (%)	Compressive strength (MPa)
1:1	37.0	31.0
3:1	65.5	15.2
4:1	85.0	8.7

A later study by Li et al. using a 40% nano-HA/60% PA66 nanocomposites showed a significant decrease in mechanical properties with the addition of pores (Table 10.2) (Li et al. 2005a). Likewise, a 2007 study by Wang et al. also demonstrated compressive strength values (13.2 ± 0.34 MPa for a 70% porous 60% nano-HA/40% PA) similar to that reported by Li et al. and also showed a similar decrease with increasing porosity (Wang et al. 2007). Since porosities greater than 90% are often required for tissue engineering scaffolds, it is unlikely that these materials can be used for in vivo tissue engineering without further reinforcement.

10.2.2.2 Natural Material/Nano-hydroxyapatite Scaffolds for Hard Tissue Engineering

Natural materials have also been used as bone tissue engineering scaffolds due to their excellent biocompatibility and in some cases structural similarity to native bone. Chitosan is a natural biodegradable polymer that has shown significant promise in a number of biomedical applications (Madhally and Matthew 1999; Mi et al. 2002; VandeVord et al. 2002). However, similar to synthetic poly(hydroxyortho esters), chitosan lacks bone bonding bioactivity. Therefore, composites with nano-hydroxyapatite and chitosan have been created to increase biocompatibility and osseointegration. Although a number of chitosan/nano-HA composites have been created for bone tissue engineering, few have been concerned with the increase in mechanical properties provided by the chitosan (Kong et al. 2006; Kong et al. 2005). In a study by Li et al., chitosan/nano-HA composites demonstrated compressive strengths of up to 120 MPa with a 30:70 chitosan to nano-HA ratio (Li et al. 2005b). As noted by the authors, the strength of these materials should be great enough to be used in load bearing sites of bone tissue. However, since the polymers created by Li et al. lacked porosity for three-dimensional cell seeding the material is limited for use as a bone filler material. The degradation rate of the chitosan may also be a concern.

Calcium phosphates have generated great interest for bone tissue engineering since they are a principal inorganic component of natural bone. It has been shown that the combination of HA/ β -tricalcium phosphate (β -TCP) ceramics are more effective in bone repair and regeneration than either phase alone (Kwon et al. 2003; Ryu et al. 2002; Kohri et al. 1993). Although researchers have demonstrated porous HA scaffolds with compressive moduli of up to 5 MPa, which is on the order of cancellous bone, there is still further need to increase mechanical properties for other types of bone (Gibson 1985; Ramay and Zhang 2003). Accordingly, Ramay et al. incorporated HA-nanofibers into a β -TCP scaffold and demonstrated that both the compressive strength and compressive modulus increased dramatically with small percentages of nanofibers added (Fig. 10.5) (Ramay and Zhang 2004). For scaffolds containing 5 wt% HA nanofibers and a porosity of 73%, the compressive strength (9.8 ± 0.3 MPa) compares favorably to the high end reported for cancellous bone (2–10 MPa) (Gibson 1985). These improvements in mechanical properties are promising; however, there is still a need to further increase the porosity of the composites to greater than 90% for uniform cell seeding and efficient transport of nutrients throughout the scaffold (Yang et al. 2001).

Since natural bone also contains polysaccharides, other strategies have included the addition of structural polysaccharides to improve the mechanical properties of nano-HA/collagen scaffold composites. In one study, nano-HA/collagen/alginate composites were created by mixing nano-HA/collagen with sodium alginate and crosslinking with calcium (Zhang et al. 2003a). While unreinforced nano-HA/collagen scaffolds had a compressive yield strength of only 62 kPa, with increases in alginate content both the yield strength and modulus of the nanocomposite increased dramatically and approached that of natural bone (Fig. 10.6).

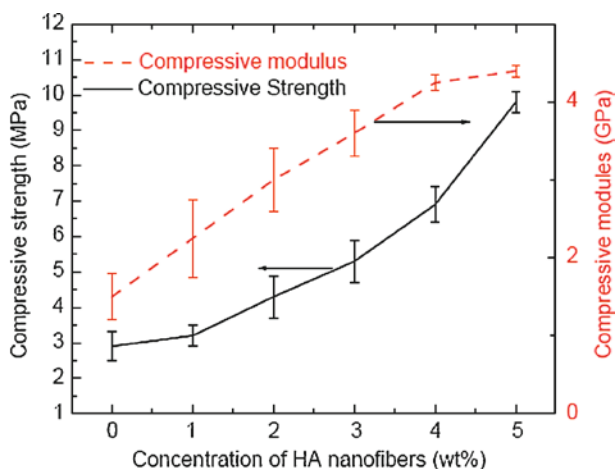


Fig. 10.5 Compressive strength and modulus of β -TCP composite scaffold reinforced with nano-HA fibers (Reprinted with permission from Ramay and Zhang 2004)

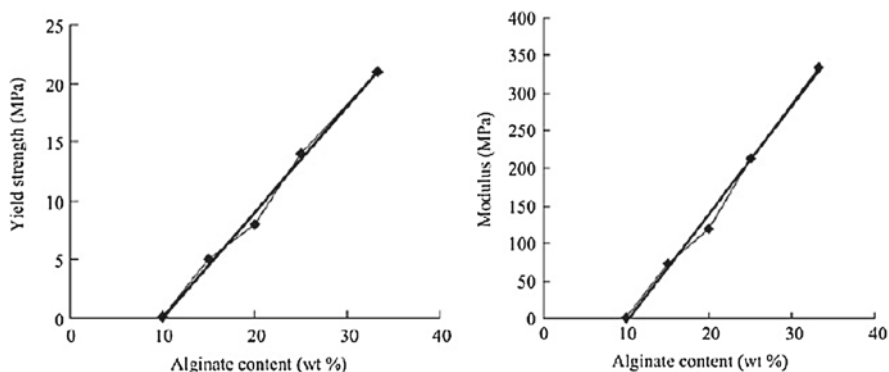


Fig. 10.6 Compressive yield strength and modulus of nano-HA/collagen/alginate composites (Reprinted with permission from Zhang et al. 2003b)

10.2.3 Nanocomposite Scaffolds for Soft Tissue Engineering

Although there are many reports of nanocomposite scaffolds utilizing hydroxyapatite for hard tissue engineering, to date, only one study has been published on biodegradable nanocomposite scaffolds for soft tissue engineering (Webb et al. 2007). Due to the stiffness and lack of elasticity of commonly used poly(hydroxyortho esters) and their composites, biodegradable materials with elastomeric properties have recently received attention for their potential use in the engineering of soft tissues (Webb et al. 2004; Wang et al. 2002, 2003; Yang et al. 2004b; Lee et al. 2003; Pego et al. 2003). In particular, we have developed a novel family of biodegradable elastomeric polyesters referred to as poly(diols citrates) (Yang et al. 2004b, 2006b, c). The mechanical properties of poly(diols citrates) can be adjusted depending on the selection of diols and the post-polymerization conditions (Yang et al. 2006b). However, the mechanical properties that can be obtained may not meet the demanding requirements of musculoskeletal tissues such as ligament or cartilage, which are often exposed to relatively large tensile or compressive loading forces. To further address this problem, we developed a novel elastomeric nanocomposite material in which the macrophase consists of a poly(diols citrate) elastomer and the nanophase consists of a poly(L-lactic acid) (PLLA) nanofibrous network or poly(lactic-co-glycolic acid) (PLGA) nanoparticles (Webb et al. 2007).

10.2.3.1 Poly(diols Citrate)-PLLA Nanofibrous Composites

Poly(diols citrate)-PLLA nanofibrous composites were fabricated via thermally induced gelation followed by solvent exchange and freeze drying (Ma and Zhang 1999; Zhang and Ma 2000). After drying, the PLLA nanofibrous network was impregnated with the poly(1,10-decanediol-co-citrate) (PDC) pre-polymer solution to create the resulting composite (Fig. 10.7).

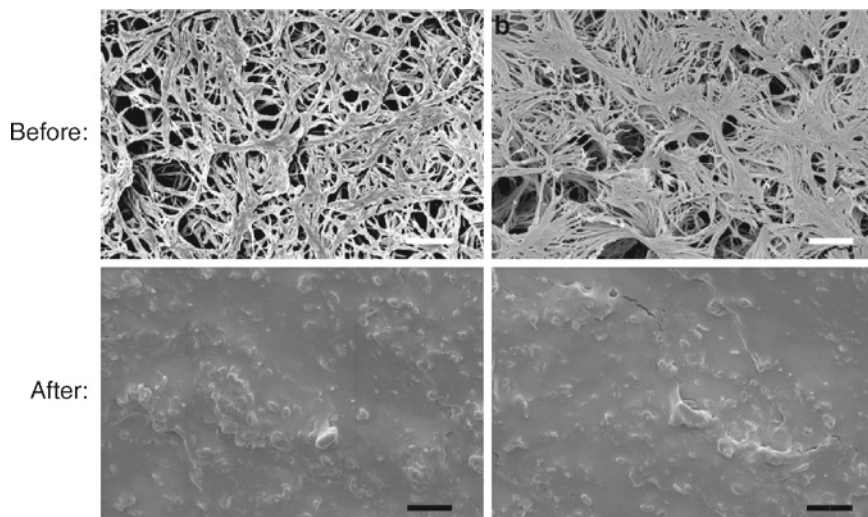


Fig. 10.7 SEM micrographs of (a) 5% and (b) 10% PLLA nanofibrous networks before and after filling the pores with PDC (scale bars = 2 μm)

Poly(diols citrate)-PLLA nanofibrous composites showed greatly enhanced mechanical properties compared to either component alone (Fig. 10.8). The PLLA nanofibrous network provided reinforcement to the poly(diols citrate) matrix as demonstrated by the increased tensile strength, modulus, and elongation at break. The tensile strength of a 10% PLLA-PDC nanocomposite increased over 150% compared to PDC alone and over 400% compared to the PLLA nanofiber network alone. Similarly, the modulus increased by 1,000% compared to PDC without PLLA reinforcement. Although the modulus of the composite decreased relative to that of the PLLA network, the addition of the non-elastic PLLA nano-phase increased the elongation at break from 200% for the PDC control to 300% for the 10% nanocomposite. In contrast, the elongation at break for PLLA controls was less than 5%. PDC nanocomposites could also be elongated with little permanent plastic deformation. The ability of the nanocomposites to be elongated to many times their original length without significant permanent plastic deformation should be beneficial for soft tissue engineering scaffolds since mechanical stimulation during *in vitro* tissue development has proven beneficial for the development of many tissues (Kim and Mooney 2000; Nerem 2003; Niklason et al. 1999; Waldman et al. 2003; Kim et al. 1999).

Since tissue engineering often requires a three dimensional porous scaffold on which cells can be seeded, porous nanocomposites were also created through the incorporation of salt particles during the gelation step (Zhang and Ma 2000). Both the 5% and 10% nanocomposites exhibited an open and interconnected pore structure with high porosity (Fig. 10.9). In addition to a highly porous structure,

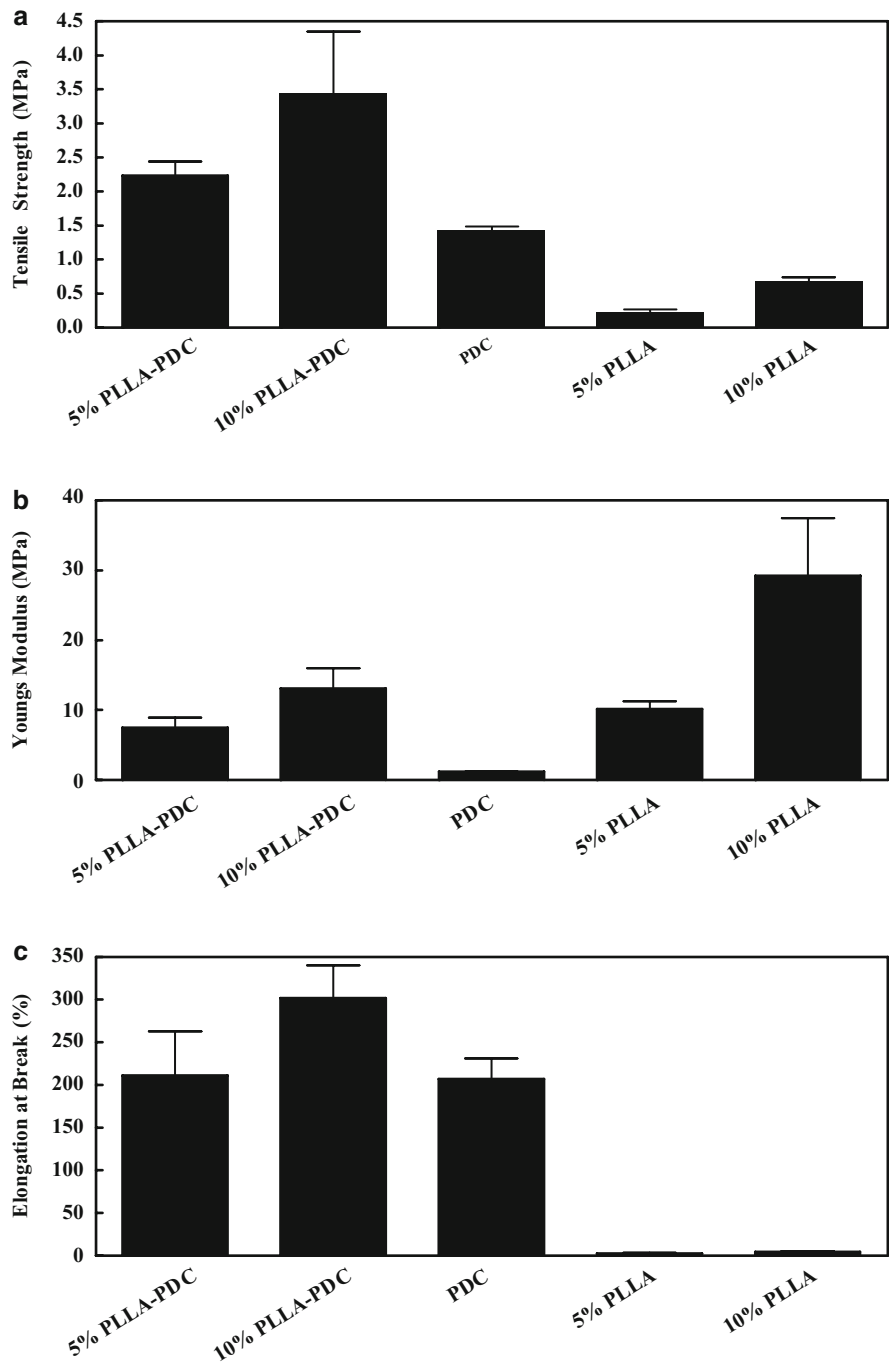


Fig. 10.8 (a) Tensile strength (b) young's Modulus, and (c) elongation at break of poly(diols citrate) nanofibrous composites and controls

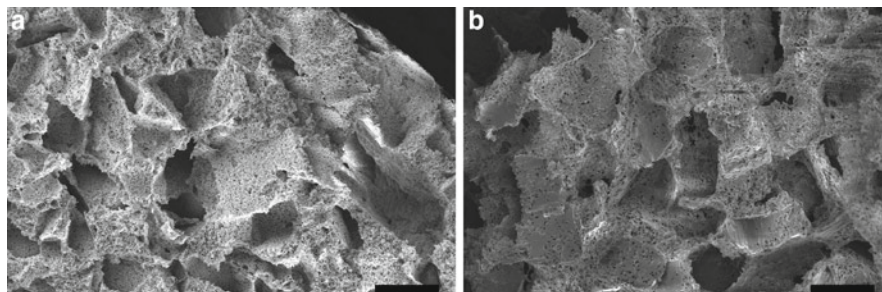


Fig. 10.9 (a) 10% PLLA nanofibrous scaffold with large micropores (~90–120 μm). (b) 10% PLLA-PDC nanocomposites (magnification = 500 \times , scale bar = 100 μm)

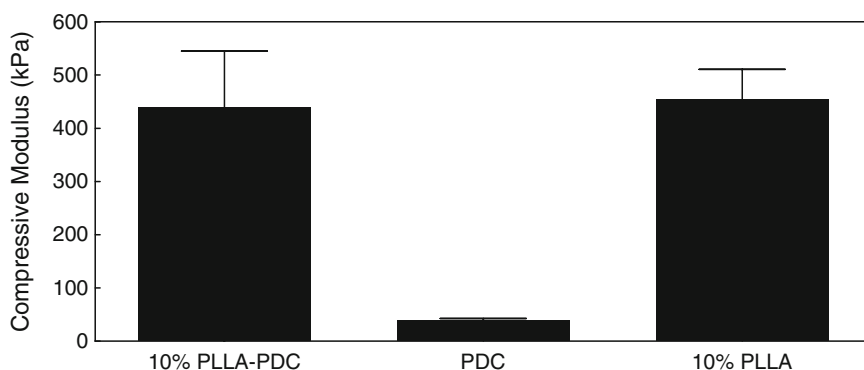


Fig. 10.10 Compressive modulus of PDC-PLLA nanocomposites and controls

the mechanical properties of the scaffold should match the host tissue at the site of implantation (Webb et al. 2007). For porous nanocomposite scaffolds, the compressive modulus increased with increasing PLLA concentration (Fig. 10.10). For the 10% PLLA-PDC composition, the compressive modulus was 439 ± 106 kPa, similar to that of human (581 ± 168 kPa) and bovine (310 ± 180 kPa) articular cartilage (Jurvelin et al. 2003; Korhonen et al. 2002).

10.2.3.2 Poly(diols citrate)-PLGA Nanoparticle Composites

Our lab has also created poly(diols citrate) nanocomposites using nanoparticles for reinforcement. PLGA nanoparticles with various ratios of lactic to glycolic acid as well as poly(D,L-lactic acid) and poly(L-lactic acid) nanoparticles were produced using a modified spontaneous emulsion and solvent diffusion method (Table 10.3) (Murakami et al. 2000; Murakami et al. 1999). By creating nanoparticles from PLGA with various ratios of lactic to glycolic acid and PLLA, the degradation rate of the particles can be tailored to match that of the surrounding nanocomposite matrix or to the regeneration rate of the developing tissue. This is important as the

Table 10.3 Size and polydispersity of various nanoparticles

Sample	Size (nm)	Polydispersity	Recovery (%)
PLGA (85:15)	178.1	0.005	103.84
PLGA (50:50)	190.1	0.005	99.23
PLA	177.4	0.005	98.00
PLLA	183.7	0.045	87.95

PLGA = poly(lactic-co-glycolic acid) with the ratio of lactic to glycolic acid designated by (Lactic:Glycolic); PLA = poly(D,L-lactic acid); PLLA = poly(L-lactic acid)

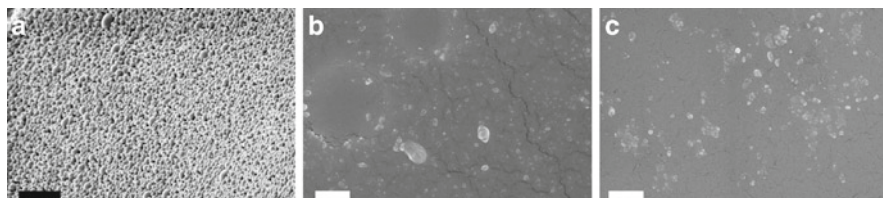


Fig. 10.11 SEM micrographs of (a) PLGA nanoparticles (scale bar = 1 μm), (b) 5% PLGA-PDC nanocomposite (scale bar = 2 μm), (c) 10% PLGA-PDC nanocomposite (scale bar = 2 μm)

degradation rate of a tissue engineering scaffolds should match the regeneration rate of the developing tissue (Yang et al. 2005). The modified spontaneous emulsion method also yields a uniform size of nanoparticles as demonstrated by the low polydispersity as well as minimal aggregation and high recovery.

Nanocomposites were fabricated with either 5% (w/w) or 10% (w/w) PLGA nanoparticles. SEM micrographs of the PLGA nanoparticles and resulting composites are shown in Fig. 10.11. The mechanical properties of the composites are shown in Fig. 10.12. Although the mechanical property increases were not as great as with nanofibrous scaffolds for reinforcement, nanoparticles added to the PDC matrix act as additional crosslink points and increase the strength and stiffness (Young's modulus) while decreasing the elongation at break. However, it should be noted that while the elongation at break decreases, the nanocomposites still maintain the ability to be elongated to many times their original length before rupture. The increase in mechanical properties is most likely due to good matrix/nanoparticle interactions. Since the modified spontaneous emulsion method uses poly(vinyl alcohol) as a surfactant to coat the nanoparticles and prevent aggregation, the large number of alcohol groups provided by the PVA coating on nanoparticles likely forms covalent bonds with the poly(diols citrate) matrix.

10.2.4 Conclusion and Future Direction

As the field of tissue engineering continues to grow, there is a need for scaffolds that are capable of matching the biomechanical properties of native tissues.

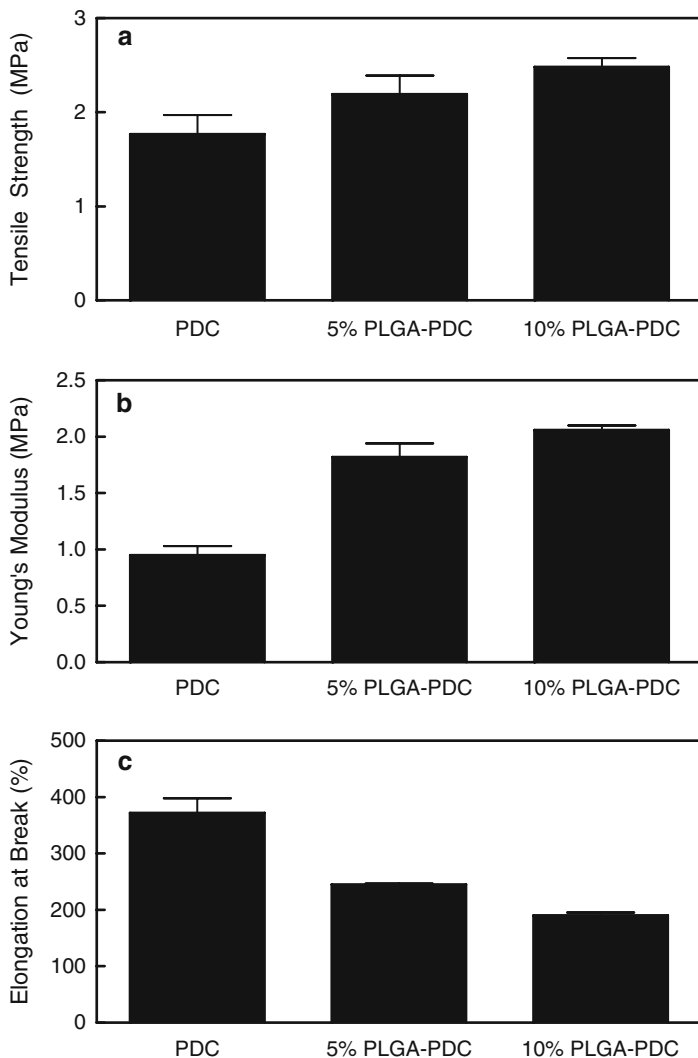


Fig. 10.12 (a) Tensile strength, (b) Young's modulus, (c) elongation at break of PLLA-PDC nanoscaffold composites and PDC control that were polymerized at 80°C for 3 days without vacuum ($n = 4$) (* $p < 0.01$ from control)

Although there are promising nanocomposites with enhanced mechanical properties for both hard and soft tissue engineering, proper engineering design and safety needs to effectively evaluate their performance. The mechanical properties of a polymer nanocomposite are dictated by a complex mix of microstructural parameters such as the properties of the polymer matrix, the properties and distribution of the filler, interfacial bonding between the filler and polymer matrix, and the processing

methods used to make the composite (Crosby and Lee 2007b). Although a detailed explanation of these parameters and the theory behind mechanical reinforcement is beyond the scope of this chapter, it is important to note that a careful selection of polymer matrix and nanofiller is critical if one is to design a nanocomposite with enhanced mechanical properties. Further complicating matters is the requirement for a tissue engineering scaffold to be biodegradable and biocompatible. As seen in scaffolds for bone tissue engineering, the incorporation of a nanofiller that closely resembles natural bone greatly benefits osseointegration and biocompatibility. However, more research must be done to find nanophase materials that can both increase biocompatibility with other tissues as well as increase mechanical properties. Furthermore, since many tissues have specific nanoarchitecture, nanoscale fillers that can mimic these structural parameters while also providing mechanical reinforcement will also be beneficial in improving biocompatibility. Further advances in nanotechnology and knowledge of mechanical reinforcement at the nanoscale level will help researchers design and develop the next generation of tissue engineering scaffolds.

10.3 A Nanophase for Drug Delivery Applications

10.3.1 Introduction

Nanotechnology can potentially improve the efficacy, controllability and versatility of current drug therapies as well as the possibility of creating new drugs and drug delivery technologies for the more effective treatment of disease. Since this is a broad field of rapidly emerging research, it can be a daunting task to attempt to name and define all the nanotechnology applications for drug delivery therapies and systems. Indeed, the interdisciplinary nature of nanotechnology-related research can also make the development process difficult to define, regulate and evaluate for efficacy. A recent commentary in *Nature Materials* highlighted the need to better understand the development processes involved in emerging technologies utilizing nanoscale systems where there needs to be a more concerted effort between academia, industry and regulatory agencies (Eaton 2007). Ultimately, an understanding of applied nanotechnology for drug delivery therapies depends upon the final medical application. This section will highlight emerging types of nanotechnology platforms for drug delivery that can be combined with scaffolds for regenerative medicine.

10.3.2 Nanofibrous and Nanoporous Biomaterials

Polymer nanofibers have received increased interest in recent years for their potential uses in a number of biomedical applications. Due to their high surface

area to volume ratio, they may be good candidates for drug delivery applications (Pham et al. 2006; Zhang et al. 2005). Within the extracellular matrix (ECM), protein components such as collagen and elastin fibers have nano-scale dimensions and play important functions in regulating complex cellular signals and providing mechanical properties to tissue (Ma et al. 2005). It should be noted that the exact definition of a “nanofiber” can be somewhat arbitrary since some publications define it as being 100 nm or less in diameter while others refer to a “nanofiber” as being anything on the order of hundreds of nanometers in diameter (Zhang et al. 2005).

While there is significant interest and research activity on the development of better processing techniques to produce polymer nanofibers, electrospinning remains one of the more popular fabrication methods (Zhang et al. 2005). The electrospinning process uses an applied electric field to create a charge on a loaded polymer solution and upon reaching a critical charge to overcome surface tension forces, the polymer solution is ejected in a uniform stream towards a ground plate (Pham et al. 2006). Varying the electric field strength, polymer mixture and chamber conditions can modulate the nanofiber properties, such as fiber width and density of the woven mesh (Zhang et al. 2005). Despite the general ease of fabrication, there are a number of issues which stem from using this fabrication technique for drug incorporation. For example, proteins with charge sensitivity and other macromolecular drugs which are immiscible in the polymer solutions may have difficulty during incorporation. In addition, the use of organic solvents to dissolve polymer blends may also denature some protein-based drugs.

Electrospun poly(ϵ -caprolactone) (PCL) nanofibers have been used for the delivery of heparin for cardiovascular tissue engineering strategies (Luong-Van et al. 2006). A PCL nanofiber network that incorporated heparin was able to show sustained release for up to 14 days and was capable of inhibiting vascular smooth muscle cell proliferation *in vitro*. Poly(vinyl alcohol) (PVA) based electrospun nanofibers have also been investigated for the incorporation of model non-steroidal anti-inflammatory drugs to determine the effect of drug solubility on release and incorporation (Taepaiboon et al. 2006) (Fig. 10.13). Although the morphological appearance of electrospun nanofibers varied depending on the water solubility of the model drug, the overall chemical integrity of the incorporated drugs was maintained. The drug release from the electrospun PVA also showed a faster release compared to cast films of PVA with incorporated drug; an important property to take into consideration if there is an unintended burst release profile.

Another issue in using electrospinning techniques is modulating and controlling the final mechanical properties of the nanofiber material. For example, electrospinning for co-drug encapsulation may affect the mechanical properties. Chew et al., observed a considerable discrepancy in the mechanical performance for electrospun nanofibers composed of poly(ϵ caprolactone) (PCL), and its copolymer, poly(caprolactone-co-ethyl ethylene phosphate) (PCLEEP) after encapsulating retinoic acid and bovine serum albumin as model drugs (Chew et al. 2006). The nanofibers which were 200–300 nm in average diameter had an improvement in mechanical properties with 1–20 wt% loading with retinoic acid, however showed an opposite effect when loaded with 10–20 wt% bovine serum albumin (Chew et al. 2006).

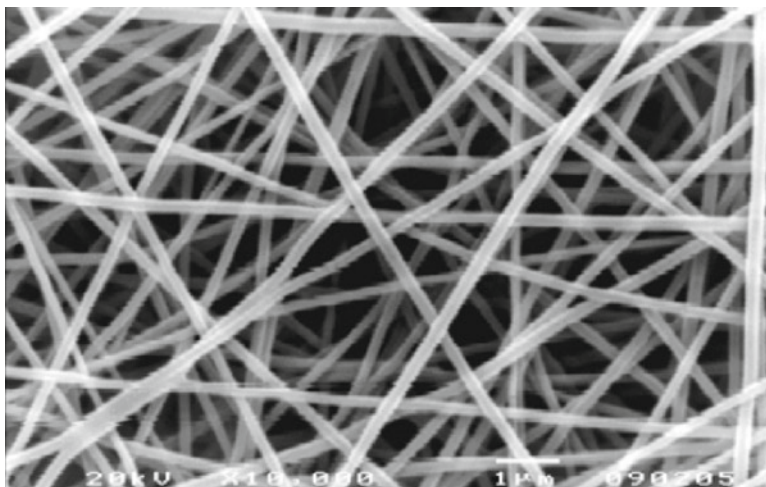


Fig. 10.13 Scanning electron micrograph (SEM) of electrospun PVA nanofibers. Scale bar: 1 μm (Image reprinted with permission from Taepaiboon et al. 2006.)

The research highlights the need to better understand not just drug encapsulation efficiency, stability and controlled release, but also mechanical performance when designing scaffolds for tissue engineering strategies.

Coaxial electrospinning is a modified electrospinning technique for use in the incorporation of bioactive molecules for drug delivery applications. Unlike electrospinning methods with polymer/drug blends and mixtures which directly incorporate the drug and/or bioactive molecules into the solution, coaxial electrospinning feeds two different solutions through capillary channels to generate composite nanofibers (Zhang et al. 2006). Since the polymer and drug solutions can be kept separate through the capillary channels, this method can minimize the interaction of bioactive proteins with harsh organic solvents. Zhang et al. used the coaxial electrospinning technique for the incorporation of bovine serum albumin (BSA) to serve as the model protein therapeutic in nanofiber composites made up of PCL and PEG (Zhang et al. 2006). Although Zhang et al. were able to demonstrate incorporation of the protein through the coaxial technique, an evaluation of the BSA stability was not performed and a majority of the encapsulated protein was released within the first 48–72 h. Jiang et al. also evaluated the capabilities of PCL and PEG based nanofibers for coaxial electrospinning using BSA (Jiang et al. 2006). The release rate showed modulation with faster release of protein with higher concentrations of PEG incorporated within the PCL fibers. Jian et al. also evaluated the stability of lysozyme using this technique and showed no significant loss of activity over the course of the 4 week period of release. Future work is promising to demonstrate the application of coaxial electrospinning methods for incorporation of protein based therapeutics. However, as mentioned previously, protein incorporation with blended electrospun polymer scaffolds can have a negative effect on the mechanical properties of the system and these initial studies concerning coaxial nanofibers have not been evaluated for changes in mechanical performance.

Our laboratory has been investigating the use of nanoporous biodegradable elastomers to address issues associated with growth factor drug delivery which may include complicated fabrication steps, rapid burst release kinetics and limited bioactivity of growth factors upon release (Sheridan et al. 2000; Elcin and Elcin 2006; Gu et al. 2007). In particular, this approach takes advantage of interfacial instabilities that lead to pore collapse thereby entrapping and controlling the release of macromolecules. We recently fabricated a novel nanoporous biodegradable elastomer based on poly(1,8 octanediol-co-citric acid) (POC) copolymer using polyethylene glycol dimethyl ether (PEGDM) as the porogen template. Using this technique we can obtain elastomeric films that are 80% porous prior to pore collapse. Drug or macromolecule entrapment is achieved by incubating the nanoporous POC in a solution of the macromolecule, followed by solvent removal. Unlike other nano-scale porous polymer networks (Raman and Palmese 2005; Zhou et al. 2006), POC copolymer is ideal for drug delivery and tissue engineering strategies since it is biodegradable and biocompatible (Motlagh et al. 2007; Asuri et al. 2006; Yang et al. 2006d). These nanoporous elastomers are currently being explored for the release of platelet-derived growth factor-BB (PDGF-BB) for wound healing applications.

Another area of research has been the use of self-assembled hydrogels comprised of peptide amphiphile (PA) for tissue engineering and drug delivery strategies (Hosseinkhani et al. 2007). PA is formed through a self-assembly, covalent capture and mineralization process which is capable of recreating the nanostructured organization of natural bone (Hartgerink et al. 2001). A more in depth explanation of these self-assembly systems is described in the landmark paper published by the Stupp research group at Northwestern University in the journal, *Science* (Hartgerink et al. 2001). To demonstrate application of this novel nanostructured material, Hosseinkhani et al. incorporated bone morphogenetic protein-2 (BMP-2) into self-assembled hydrogels composed of PA to facilitate ectopic bone formation (Hosseinkhani et al. 2007). An in vivo rat model was able to demonstrate that injectable PA/BMP-2 hydrogel was able to improve tissue regenerative responses towards bone formation as a result of the hydrogel scaffold and sustained release of BMP-2. Although it was demonstrated that BMP-2 could be released over 20 days in vitro, the interactions between the protein and the hydrogel as the nano-scaffold degrades is still not well characterized.

Self assembly of peptide amphiphiles to form nanofibers has also been used to entrap biologically relevant molecules within a gel (Guler et al. 2005; Bull et al. 2005). For example, in the development of enhanced magnetic resonance imaging (MRI) contrast agents for better understanding the fate of tissue engineered scaffolds and biomolecules in vivo, peptide amphiphile (PA) self-assembled nanofibers have been created with active MRI peptides (Bull et al. 2005). These self-assembled nanofiber materials have individual fiber lengths greater than 100 nm and widths of approximately 20 nm. Similar PAs have also been developed for encapsulation of drug molecules for drug delivery applications (Guler et al. 2005). These modified PAs were capable of encapsulating model hydrophobic drugs such as pyrene within the cylindrical self-assembled nanostructures. Furthermore these same PAs

were also modified to contain the cell adhesion recognition peptide RGDS to allow for potential cellular targeting of drug molecules to cell membrane through ligand–integrin interactions.

In a drastically different approach and mechanism of release, Hu et al., developed a unique magnetic responsive porous hydrogel biomaterial which was fabricated in the presence of magnetic nanoparticles (Hu et al. 2007). The “nano-ferrosponge” consisted of gelatin with in situ co-precipitation synthesis of iron oxide nanoparticles within the gel matrix. The introduction of the magnetic nanoparticles in the porous hydrogel system was able to increase the sensitivity of the material to changes in magnetic field strength due to the relatively large density of nanoparticles within the polymer pore walls. The “nano-ferrosponge” had tailored average pore size distributions from 4.6 to 9.1 nm in diameter depending on treatment with an externally applied magnetic field. This magnetic responsive hydrogel has potential to be used in site specific targeted drug delivery whereby the mechanism of release can be mediated by a non-invasive externally applied electric field. The biocompatibility of such a system remains unknown.

10.3.2.1 Elastin-Like Polypeptides

Research concerning elastin-like polypeptides (ELP) has led to novel drug delivery platforms with nano-scale dimensions. ELPs are an example of an artificial extracellular matrix (aECM) component that can be engineered to be biosynthetically produced with tailored biological and mechanical properties that mimic naturally occurring mammalian elastin (Simnick et al. 2007). The structural repeating unit for ELPs consists of Val-Pro-Gly-Xaa-Gly and is ideal as a material for biomedical applications because of a well defined molecular weight, structural sequence and a lower critical solution temperature (LCST) transition behavior (Simnick et al. 2007).

Due to these unique properties, ELPs have been researched as potential constructs in controlled drug delivery applications (Megeed et al. 2006). Megeed et al. engineered an elastin-like polypeptide linkage to single-chain antibodies to have a temperature dependent binding affinity based on the structural transition of the elastin-like peptide motif $(VPGXG)_n$ (Megeed et al. 2006). Since the elastin-like polypeptide linkage has unique thermally induced phase transitions (Urry and Pattanaik 1997), which has been traditionally used for protein purification strategies, it was hypothesized that the same unique structural transitions could be used to modulate the binding affinity of attached single-chain antibodies. In related drug delivery research, genetically engineered ELPs were used to selectively accumulate in solid tumors when subjected to localized hyperthermia as a novel mechanism for targeted and controlled cancer treatment (Hu et al. 2007). Liu et al. developed ELPs such that they remained soluble when introduced to physiologic temperatures, but would undergo phase transition and aggregation when exposed to induced hyperthermic conditions at specific tumor sites (Hu et al. 2007). Other research has also focused on tailoring ELP surface topography on the nanoscale (Reguera et al. 2004).

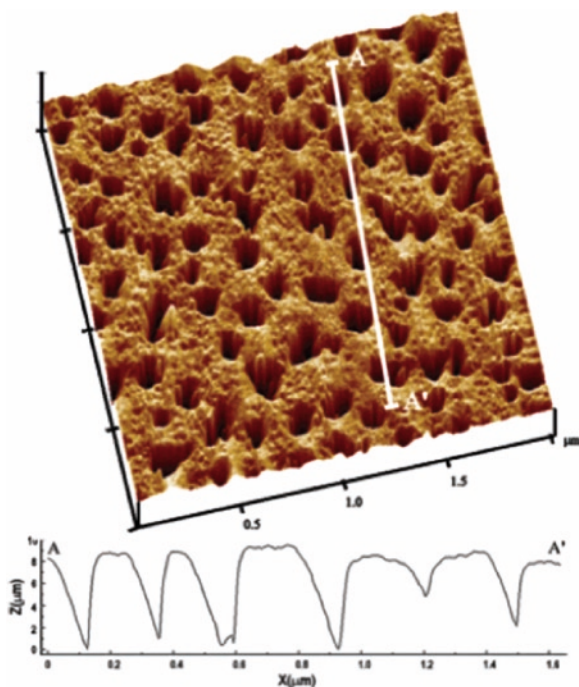


Fig. 10.14 Tapping mode atomic force microscopy (TMAFM) image of self-assembled ELPs from basic medium (Image reprinted with permission from Reguera et al. 2004)

Reguera et al. developed a process for creating nanopores (~ 70 nm in diameter) by modulating the pH of the solution during ELP self-assembly (Fig. 10.14). Different biofunctionalities can be added to these ELP nanoporous substrates thereby enabling specific biological interactions.

10.3.2.2 Polymeric Micelles

Polymeric micelles can be fabricated on the scale of 10–100 nm in size and are ideal candidates for drug delivery due to their ability to incorporate water-insoluble drugs with limited denaturation (Kabanov and Gendelman 2007). In drug targeting, since the size scale of the polymeric micelles prevents them from being phagocytosed by mononuclear cells, they can serve as passive targets for cancerous tissues (Gaucher et al. 2005). Micelles consisting of block copolymers for example, are formed through the self-assembly of amphiphilic copolymers or electrostatic interactions between oppositely charged copolymer chains (Gaucher et al. 2005). The hydrophobic portion of the copolymer comprises the inner core of the micelle whereas the hydrophilic moiety makes up the outer shell membrane. These copolymer micelle systems can be easily tailored for their size, drug

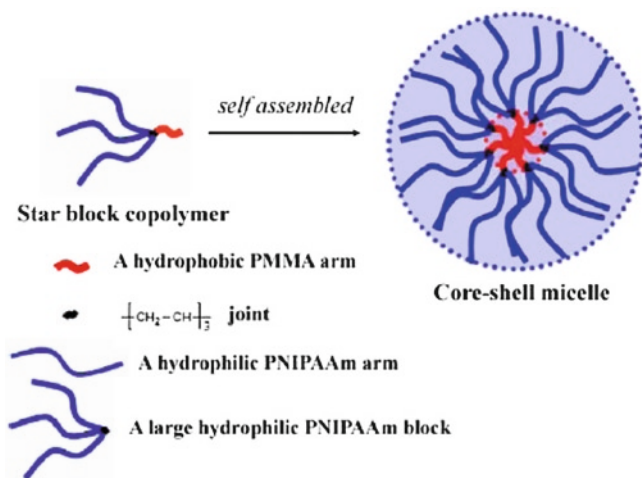


Fig. 10.15 Graphic representation for self-assembled thermosensitive core-shell micelle consisting of PMMA and PNIPAAm (Image reprinted with permission from Wei et al. 2007)

encapsulation and release rates depending on the polymer composition (Nishiyama and Kataoka 2006). An amphiphilic star block copolymer micelle drug delivery system based on poly methyl methacrylate (PMMA) and poly(N-isopropylacrylamide) (PNIPAAm) was shown to have reversible aggregation and dispersion characteristics in a temperature sensitive manner (Wei et al. 2007) (Fig. 10.15). The polymeric micelles, having an average particle diameter of 50 nm were shown to have differential drug release profiles using the model hydrophobic drug, prednisone acetate, in a temperature dependent response (Wei et al. 2007). However, there are still drawbacks in using this thermoresponsive polymeric micelle strategy, where there is a considerable burst release profile within the first 48 h. Inorganic polymer “nanocapsules” or polymeric micelles have also been developed as potential carriers for drug delivery (Perkin et al. 2005). Perkin et al., were able to fabricate hybrid nanostructures which were 50–70 nm in diameter made from cross-linked poly(acrylic acid) enclosed within an amorphous calcium phosphate shell (Perkin et al. 2005).

Worm micelles which can be <100 nm in diameter and on the order of several microns in length have also been investigated for controlled drug release (Kim et al. 2005). Unlike other polymeric spherical micelles, worm micelles offer advantages such as increased time in the circulation, flexibility and better penetration through nanoporous media and capacity to serve as carriers of multiple drugs (Kim et al. 2005; Ahmed et al. 2006). Worm micelles made of PLA were shown to have sustained release of hydrophobic drugs such as Triamterene and were degradable through PLA hydrolysis. In an in vivo animal model, these nano-carriers were also capable of delivering paclitaxel and doxorubicin within 24 h of systemic circulation, which caused a significant decrease in tumor size compared to drugs delivered directly into circulation (Ahmed et al. 2006).

10.3.2.3 Nanoparticles

Nanoparticle research for drug delivery applications often consist of insoluble polymers whereby the drug or protein based therapeutic is encapsulated within the polymer nanoparticle using conventional water-in-oil-emulsion techniques (Kabanov and Gendelman 2007). A common method for encapsulation uses organic solvents, which may adversely affect the activity of biomacromolecular drugs and several research aims have focused on dealing with the issue of denaturation and stability during release (Kabanov and Gendelman 2007).

Nanoparticle technology has improved drug targeting for neurodegenerative disorders. For example, in drug targeting to the central nervous system, a major obstacle towards effective therapy is the poor transportation of macromolecular drugs across the blood-brain barrier (BBB) and the rapid removal and degradation of those drugs once introduced into the bloodstream (Vinogradov et al. 2004). The use of nanoparticles (100 nm or less in dimension) can enable better transport across the BBB and if modified with different surface functional groups, can increase the residence time in the bloodstream (Vinogradov et al. 2004; Kreuter 2001). Vinogradov et al. developed a nanoscale network of poly(ethylene glycol) and polyethylenimine which is capable of binding to negatively charged oligonucleotides forming a polyelectrolyte nanoparticle complex (Vinogradov et al. 2004). Preliminary findings were able to show that the nanoparticle complexes were capable of crossing the BBB and decreased the degradation rates of the model oligonucleotide drugs. Recently, it was hypothesized that surface modification of poly(butyl cyanoacrylate) (PBCA) nanoparticles using apolipoprotein A-I could enhance the receptor mediated endocytosis of nanoparticles across the BBB (Petri et al. 2007). Promising preliminary results were able to show a correlation between the surface modified PBCA nanoparticles and their corresponding translocation across the BBB. This work by Petri et al. shows the ability to develop better chemotherapy delivery strategies for targeting tumors across the BBB.

Gao et al. synthesized novel nanoparticle protein drug delivery systems based on conjugated (PLA) to ethylenediamino or diethylenetriamino bridged to bis(β -cyclodextrin)s (bis-CDs) (Gao et al. 2007). It is argued that the cyclodextrin components could create a more favorable environment for protein activity due to the CD interaction with the hydrophobic PLA domains (Gao et al. 2007). Although the system was able to extend release on the order of weeks using model bovine serum albumin (BSA) protein, there was still a characteristic burst release and the issue of protein degradation and inactivation still has to be addressed with the PLA conjugate nanoparticle system. Other research by Lee et al. has also tried to address the issue of hydrophobic residues on the surface of PLA nanoparticle drug delivery systems and the problems associated with protein denaturation during encapsulation (Lee et al. 2007). Nanoparticles based upon poly(lactide)-tocopheryl polyethylene glycol succinate (PLA-TPGS) copolymers were proposed as a novel biodegradable polymer drug delivery system due to the more water-soluble nature and hydrophilicity of the TPGS moiety (Lee et al. 2007). Using BSA as a model protein, it was shown that modulating the ratio weight content of PLA:TPGS could affect the burst release characteristics from the nanoparticles.

Other research concerning polymer based drug delivery system includes the use of microgels and nanogels. Micro and nano-gels are a type of hydrogel which consist of stable colloidal particles of cross-linked polymer networks (Oh et al. 2007). Recently, a nanogel system comprising stable disulfide linkages using inverse miniemulsion atom transfer radical polymerization (ATRP) was devised for use in drug delivery applications (Oh et al. 2007). Similar to research with nanoparticles, nanogels are also ideal in biomedical applications due to the large surface area for functionalization and control in their mechanical and biodegradation properties. Oh et al., demonstrated the functionalization of the nanogels (~150–250 nm in average size) with biotin-streptavidin conjugation as well as the release of an anti-cancer therapeutic, Doxorubicin (Oh et al. 2007). However, the extended release characteristics of the drug delivery system is still not well characterized.

Nanoparticle based drug delivery systems may also be useful in cancer treatment since these therapies are often limited due to the adverse side effects associated with intravenous and systemic delivery of drugs (Devalapally et al. 2007). A pH sensitive poly(ethylene oxide) (PEO)-modified poly(beta-amino ester) (PbAE) nanoparticle based system (100–200 nm) encapsulating the anti-tumor drug, paclitaxel, was shown to enhance drug efficacy by inhibiting tumor growth in vivo and decreasing drug toxicity when administered intravenously (Devalapally et al. 2007). Furthermore, since the system was pH sensitive, it exploited the nature of cancerous tissues which tend to have pH slightly lower than the systemic circulation (Devalapally et al. 2007).

Nanoparticulate based drug delivery systems have also been proposed as therapeutics for neural tissue engineering (Das et al. 2007). Cerium oxide nanoparticles (2–5 nm) were shown to have a neuroprotective effect on adult rat spinal cord neurons in vitro (Das et al. 2007). Since spinal cord neurons are prone to oxidative damage, Das et al. proposed that the neuroprotective effect of the cerium oxide nanoparticle delivery arises from the anti-oxidant behavior of cerium to scavenge for free radicals (Das et al. 2007). Furthermore, the unique large specific surface area of nanoparticle cerium oxide allowed for more effective anti-oxidative properties.

Nanoparticles have also been investigated as possible gene delivery vehicles (Chorny et al. 2007). A novel approach utilizing nanoparticle gene delivery strategies was combined with a magnetically driven gene delivery system using superparamagnetic nanoparticles using poly(lactide) with the incorporation of oleate-coated iron oxide and polyethylenimine (PEI) for DNA binding. Using an in vitro cell culture model with green fluorescent protein reporter gene transfection, an externally applied magnetic field (500 G) was able to enhance gene transfer using the superparamagnetic nanoparticle delivery system (Chorny et al. 2007). It was also shown that transfection followed a nanoparticle size dependence, where nanoparticles with mean diameter 375 nm had great transfection efficiency compared with nanoparticles 185–240 nm in diameter.

New particles for drug delivery based on “nanodiamonds” have been studied by Dean Ho’s group at Northwestern University. These nanodiamonds consist of nanostructured diamond particulates between 2–8 nm. It was shown with the model drug doxorubicin (DOX), that a significant amount of DOX could be adsorbed within aggregates of nanodiamonds with simple variations in salt concentration during

drug loading (Huang et al. 2007). Furthermore, DOX adsorbed nanodiamonds were able to serve as intracellular carriers to induce apoptosis *in vitro*, which gives promising support for their use in targeted cancer drug therapies.

10.3.2.4 Carbon Nanotubes

Carbon nanotubes have also been investigated for their potential use in drug delivery systems (Singh et al. 2005; Feazell et al. 2007; Liu et al. 2007). The relatively large specific surface area of carbon nanotubes creates an ideal substrate to have tailored surface chemistry to influence interaction with biological systems. More interestingly, it has been shown that single-walled carbon nanotubes (SWNTs) have the ability to stabilize proteins in the presence of organic solvents and increased temperatures compared to conventional flat surfaces (Asuri et al. 2006).

Ammonium-functionalized single-walled and multiwalled carbon nanotubes have been explored as potential gene delivery systems for plasmid DNA (Singh et al. 2005). These modified cationic carbon nanotubes were able to condense DNA to form nanotube-DNA complexes through electrostatic interactions. *In vitro* cell culture studies were able to demonstrate that the nanotube-DNA complexes were able to upregulate gene expression, however, the exact mechanisms by which the complexes enter the cell and how the condensed DNA is removed from the nanotube wall intracellularly is still not well characterized.

In the area of cancer research, one of the major obstacles towards effective drug dosage and delivery is the relatively poor circulation of systemically administered platinum drugs and their loss of biological activity before targeting to sites of tumor growth (Feazell et al. 2007). Functionalized carbon nanotubes have the potential to serve as carriers for platinum based prodrugs to tumor cells by allowing for cellular internalization and reduction when internalized by endosomes (Feazell et al. 2007).

Other surface functionalization strategies have included that addition of multiple chemical species such as poly(ethylene glycol) (PEG) to increase the surface hydrophilicity and solubility as well as drugs for chemotherapies and fluorescent molecules for signaling and recognition (Liu et al. 2007). Using a model cancer drug, doxorubicin, Liu et al. were able to load a significant amount of drug stacked onto functionalize carbon nanotubes and show the drug release in a pH dependent manner (Liu et al. 2007). These modified carbon nanotubes were also functionalized with the cell binding motif, RGD, for specific cellular targeting coupled with the doxorubicin drug delivery.

As with every emerging technology, the issues of safety and efficacy must be addressed before widespread clinical application. In the case of carbon nanotubes it is still unclear which parameters may pose potentially harmful cytotoxicity, *i.e.* nanotube size and surface chemistry. For instance, multi-walled carbon nanotubes were shown to significantly alter the protein expression profiles for epithelial cells, which may lead to serious health complications with repeated exposure (Witzmann and Monteiro-Riviere 2006). Another report evaluating the cardiovascular effects of pulmonary exposure to carbon nanotubes was able to demonstrate cellular oxidative

stress and accelerated plaque formation in transgenic mouse models *in vivo*. However, in recent reports concerning carbon nanotube cytotoxicity, it has been stressed that the type of viability assay used in experimentation needs to be standardized because carbon nanotube interactions with assay reagents can give misleading results (Worle-Knirsch et al. 2006; Casey et al. 2007).

10.4 Conclusions

We have attempted to describe the importance of nanocomposites in regenerative medicine and specifically the impact of the nanophase on potential applications of these novel materials. The nanophase can be used as a means to engineer new physical properties that would otherwise not be possible with the bulk or macrophase only. Several examples of the use of the nanophase for mechanical reinforcement have been discussed. Use of the nanophase for drug delivery has also been discussed with an emphasis on understanding how nanoparticles can be used to achieve controlled drug delivery. Although we have presented the work of several research groups, it is important to realize that the context for the use of these materials is what will determine whether nanocomposite biomaterials will have a meaningful impact on regenerative medicine.

References

- Ahmed F et al (2006) Biodegradable polymersomes loaded with both paclitaxel and doxorubicin permeate and shrink tumors, inducing apoptosis in proportion to accumulated drug. *J Control Release* 116(2):150–158
- Asuri P et al (2006) Increasing protein stability through control of the nanoscale environment. *Langmuir* 22(13):5833–5836
- Atala A, Lanza RP (2001) *Methods of tissue engineering*. Academic, San Diego, CA
- Bleach NC et al (2002) Effect of filler content on mechanical and dynamic mechanical properties of particulate biphasic calcium phosphate-poly lactide composites. *Biomaterials* 23: 1579–1585
- Bull SR et al (2005) Self-assembled peptide amphiphile nanofibers conjugated to MRI contrast agents. *Nano Lett* 5(1):1–4
- Bulter DL, Goldstein SA, Guilak F (2000) Functional tissue engineering: the role of biomechanics. *J Biomech Eng* 122:570–575
- Casey A et al (2007) Spectroscopic analysis confirms the interactions between single walled carbon nanotubes and various dyes commonly used to assess cytotoxicity. *Carbon* 45(7):1432
- Catledge SA et al (2007) An electrospun triphasic nanofibrous scaffold for bone tissue engineering. *Biomed Mater* 2:142–150
- Chew S et al (2006) Mechanical properties of single electrospun drug-encapsulated nanofibres. *Nanotechnology* 17:3880–3891
- Chorny M et al (2007) Magnetically driven plasmid DNA delivery with biodegradable polymeric nanoparticles. *FASEB J* 21(10):2510–2519
- Cooke FW (1992) Ceramics in orthopedic surgery. *Clin Orthop Relat Res* 6:135–146

- Cool SM et al (2007) Poly(3-hydroxybutyrate-co-3-hydroxyvalerate) composite materials for bone tissue regeneration: in vitro performance assessed by osteoblast proliferation, osteoclast adhesion and resorption, and macrophage proinflammatory response. *J Biomed Mater Res* 82:599–610
- Crosby AJ, Lee JY (2007a) Polymer nanocomposites: the “nano” effect on mechanical properties. *Polym Rev* 47(2):217–229
- Crosby AJ, Lee J-Y (2007b) Polymer nanocomposites: the “nano” effect on mechanical properties. *Polym Rev* 47:217–229
- Daniels AU, Chang MK, Andriano KP (1990) Mechanical properties of biodegradable polymers and composites proposed for internal fixation of bone. *J Appl Biomater* 1(1):57–78
- Das M et al (2007) Auto-catalytic ceria nanoparticles offer neuroprotection to adult rat spinal cord neurons. *Biomaterials* 28(10):1918–1925
- Deng X, Hao J, Wang C (2001) Preparation and mechanical properties of nanocomposites of poly(D, L-lactide) with Ca-deficient hydroxyapatite nanocrystals. *Biomaterials* 22(21):2867–2873
- Devalapally H et al (2007) Poly(ethylene oxide)-modified poly(beta-amino ester) nanoparticles as a pH-sensitive system for tumor-targeted delivery of hydrophobic drugs: part 3. Therapeutic efficacy and safety studies in ovarian cancer xenograft model. *Cancer Chemother Pharmacol* 59(4):477–484
- Du C et al (1998) Tissue response to nano-hydroxyapatite/collagen composite implants in marrow cavity. *J Biomed Mater Res* 42:540–548
- Du C et al (1999) Three-dimensional nano-HAp/collagen matrix loading with osteogenic cells in organ culture. *J Biomed Mater Res* 44:407–415
- Du C et al (2000) Formation of calcium phosphate/collagen composites through mineralization of collagen matrix. *J Biomed Mater Res* 50:518–527
- Eaton M (2007) Nanomedicine: industry-wise research. *Nat Mater* 6(4):251–253
- Elcin AE, Elcin YM (2006) Localized angiogenesis induced by human vascular endothelial growth factor-activated PLGA sponge. *Tissue Eng* 12(4):959–968
- Feazell RP et al (2007) Soluble single-walled carbon nanotubes as longboat delivery systems for platinum(IV) anticancer drug design. *J Am Chem Soc* 129(27):8438–8439
- Gao H et al (2007) Conjugates of poly(DL-lactide-co-glycolide) on amino cyclodextrins and their nanoparticles as protein delivery system. *J Biomed Mater Res A* 80(1):111–122
- Gaucher G et al (2005) Block copolymer micelles: preparation, characterization and application in drug delivery. *J Control Release* 109(1–3):169–188
- Gibson LJ (1985) The mechanical behavior of cancellous bone. *Biomechanics* 18:317–328
- Gu F, Neufeld R, Amsden B (2007) Sustained release of bioactive therapeutic proteins from a biodegradable elastomeric device. *J Control Release* 117(1):80–89
- Guler M, Claussena R, Stupp SI (2005) Encapsulation of pyrene within self-assembled peptide amphiphile nanofibers. *J Mater Chem* 15:4507–4512
- Hartgerink JD, Beniash E, Stupp SI (2001) Self-assembly and mineralization of peptide-amphiphile nanofibers. *Science* 294(5547):1684–1688
- Hench LL, Polak JM (2002) Third-generation biomedical materials. *Science* 295:1014–1017
- Hosseinkhani H et al (2007) Bone regeneration through controlled release of bone morphogenetic protein-2 from 3-D tissue engineered nano-scaffold. *J Control Release* 117(3):380–386
- Hu SH et al (2007) Nano-ferrosponges for controlled drug release. *J Control Release* 121(3):181–189
- Huang H et al (2007) Active nanodiamond hydrogels for chemotherapeutic delivery. *Nano Lett* 7(11):3305–3314
- Jiang H et al (2006) Modulation of protein release from biodegradable core-shell structured fibers prepared by coaxial electrospinning. *J Biomed Mater Res B Appl Biomater* 79(1):50–57
- Jie W, Yubao L (2004) Tissue engineering scaffold material of nano-apatite crystals and polyamide composite. *Eur Polym J* 40:509–515
- Jordan J et al (2005) Experimental trends in polymer nanocomposites – a review. *Mater Sci Eng A* 393:1–11

- Jurvelin JS, Buschmann MD, Hunziker EB (2003) Mechanical anisotropy of the human knee articular cartilage in compression. *Proc Inst Mech Eng [H]* 217(3):215–219
- Kabanov AV, Gendelman HE (2007) Nanomedicine in the diagnosis and therapy of neurodegenerative disorders. *Progress Polym Sci* 32(8–9):1054–1082
- Kim BS, Mooney DJ (2000) Scaffolds for engineering smooth muscle under cyclic mechanical strain conditions. *J Biomech Eng* 122(3):210–215
- Kim BS et al (1999) Cyclic mechanical strain regulates the development of engineered smooth muscle tissue. *Nat Biotechnol* 17(10):979–983
- Kim Y et al (2005) Polymeric worm micelles as nano-carriers for drug delivery. *Nanotechnology* 16:S484–S491
- Kim S et al (2006) Poly(lactide-co-glycolide)/hydroxyapatite composite scaffolds for bone tissue engineering. *Biomaterials* 27:1399–1409
- Kohri M et al (1993) In vivo stability of biphasic calcium phosphate ceramics. *Biomaterials* 14:299–304
- Koji H et al (2001) Prospects for bone fixation development of new cerclage fixation techniques. *Mater Sci Eng C* 17(1–2):19–26
- Kong L et al (2005) Preparation and characterization of nano-hydroxyapatite/chitosan composite. *J Biomed Mater Res* 75:275–282
- Kong L et al (2006) A study on the bioactivity of chitosan/nano-hydroxyapatite composite scaffolds for bone tissue engineering. *Eur Polym J* 42:3171–3179
- Korhonen RK et al (2002) Comparison of the equilibrium response of articular cartilage in unconfined compression, confined compression and indentation. *J Biomech* 35(7):903–909
- Kreuter J (2001) Nanoparticulate systems for brain delivery of drugs. *Adv Drug Deliv Rev* 47(1):65–81
- Kweon H et al (2003) A novel degradable polycaprolactone networks for tissue engineering. *Biomaterials* 24(5):801–808
- Kwon SH et al (2003) Synthesis and dissolution behavior of B-TCP and HA/B-TCP composite powders. *J Eur Ceramic Soc* 23:1039–1045
- Langer R, Vacanti JP (1993) Tissue engineering. *Science* 260(5110):920–926
- Lee SH et al (2003) Elastic biodegradable poly(glycolide-co-caprolactone) scaffold for tissue engineering. *J Biomed Mater Res* 66A(1):29–37
- Lee SH, Zhang Z, Feng SS (2007) Nanoparticles of poly(lactide)-tocopheryl polyethylene glycol succinate (PLA-TPGS) copolymers for protein drug delivery. *Biomaterials* 28(11):2041–2050
- LeGeros RZ (2002) Properties of osteoconductive biomaterials: calcium phosphates. *Clin Orthop Relat Res* 395:81–98
- Li Z et al (2005a) Studies on the porous scaffold made of the nano-HA/PA66 composite. *J Mater Sci* 40:107–110
- Li Z et al (2005b) Preparation and in vitro investigation of chitosan/nano-hydroxyapatite composite as bone substitute materials. *J Mater Sci: Mater Med* 16:213–219
- Li X et al (2006) Chemical characteristics and cytocompatibility of collagen-based scaffold reinforced by chitin fibers for bone tissue engineering. *J Biomed Mater Res* 77:219–226
- Liao SS et al (2004) Hierarchically biomimetic bone scaffold material: nano-HA/collagen/PLA composite. *J Biomed Mater Res* 69(2):158–165
- Liu Z et al (2007) Supramolecular chemistry on water soluble carbon nanotubes for drug loading and delivery. *ACS NANO* 1(1):50–56
- Luong-Van E et al (2006) Controlled release of heparin from poly(epsilon-caprolactone) electrospun fibers. *Biomaterials* 27(9):2042–2050
- Ma P, Zhang R (1999) Synthetic nano-scale fibrous extracellular matrix. *J Biomed Mater Res* 46:60–72
- Ma Z et al (2005) Potential of nanofiber matrix as tissue-engineering scaffolds. *Tissue Eng* 11(1–2):101–109
- Madhally SV, Matthew HW (1999) Porous chitosan scaffolds for tissue engineering. *Biomaterials* 20(12):1133–1142

- Megeed Z, Winters RM, Yarmush ML (2006) Modulation of single-chain antibody affinity with temperature-responsive elastin-like polypeptide linkers. *Biomacromolecules* 7(4):999–1004
- Mi F-L et al (2002) In vivo biocompatibility and degradability of a novel injectable chitosan based implant. *Biomaterials* 23(1):181–191
- Motlagh D et al (2007) Hemocompatibility evaluation of poly(diols citrate) in vitro for vascular tissue engineering. *J Biomed Mater Res A* 80(3):661–668
- Murakami H et al (1999) Preparation of poly(DL-lactide-co-glycolide) nanoparticles by modified spontaneous emulsification solvent diffusion method. *Int J Pharm* 187:143–152
- Murakami H et al (2000) Further application of a modified spontaneous emulsification solvent diffusion method to various types of PLGA and PLA polymers for preparation of nanoparticles. *Powder Technol* 107:137–143
- Nerem RM (2003) Role of mechanics in vascular tissue engineering. *Biorheology* 40:281–287
- Nie H, Wang C-H (2007) Fabrication and characterization of PLGA/HAp composite scaffolds for delivery of BMP-2 plasmid DNA. *J Control Release* 120:111–121
- Niklason LE et al (1999) Functional arteries grown in vitro. *Science* 284(5413):489–493
- Nishiyama N, Kataoka K (2006) Current state, achievements, and future prospects of polymeric micelles as nanocarriers for drug and gene delivery. *Pharmacol Ther* 112(3):630–648
- Oh JK et al (2007) Biodegradable nanogels prepared by atom transfer radical polymerization as potential drug delivery carriers: synthesis, biodegradation, in vitro release, and bioconjugation. *J Am Chem Soc* 129(18):5939–5945
- Pachence JM, Kohn J (2000) Biodegradable polymers. In: Lanza RP, Langer R, Vacanti J (eds) *Principles of tissue engineering*. Academic, San Diego, CA, pp 263–277
- Pego AP et al (2003) Biodegradable elastomeric scaffolds for soft tissue engineering. *J Control Release* 87:69–79
- Perkin KK et al (2005) Fabrication of hybrid nanocapsules by calcium phosphate mineralization of shell cross-linked polymer micelles and nanocages. *Nano Lett* 5(7):1457–1461
- Petri B et al (2007) Chemotherapy of brain tumour using doxorubicin bound to surfactant-coated poly(butyl cyanoacrylate) nanoparticles: revisiting the role of surfactants. *J Control Release* 117(1):51–58
- Pham QP, Sharma U, Mikos AG (2006) Electrospinning of polymeric nanofibers for tissue engineering applications: a review. *Tissue Eng* 12(5):1197–1211
- Qiu H et al (2006) A citric acid-based hydroxyapatite composite for orthopedic implants. *Biomaterials* 27(34):5845–5854
- Raman VI, Palmese GR (2005) Nanoporous thermosetting polymers. *Langmuir* 21(4):1539–1546
- Ramay HR, Zhang M (2003) Preparation of porous hydroxyapatite scaffolds by combination of the gel-casting and polymer sponge methods. *Biomaterials* 24:3293–3302
- Ramay HR, Zhang M (2004) Biphasic calcium phosphate nanocomposite porous scaffolds for load-bearing bone tissue engineering. *Biomaterials* 25:5171–5180
- Ratner BD, Bryant SJ (2004) Biomaterials: where we have been and where we are going. *Annu Rev Biomed Eng* 6:41–75
- Reguera J et al (2004) Nanopore formation by self-assembly of the model genetically engineered elastin-like polymer [(VPGVG)₂(VPGEG)(VPGVG)₂]₁₅. *J Am Chem Soc* 126(41):13212–13213
- Rho JY, Kuhn-Spearing L, Zioupos P (1998) Mechanical properties and the hierarchical structure of bone. *Med Eng Phys* 20:92–102
- Ryu HS et al (2002) An improvement in sintering property of B-tricalcium phosphate by addition of calcium pyrophosphate. *Biomaterials* 23:909–914
- Sachols E, Gotoro D, Czernuszka J (2006) Collagen scaffolds reinforced with biomimetic composite nano-sized carbonate-substituted hydroxyapatite crystals and shaped by rapid prototyping to contain internal microchannels. *Tissue Eng* 12(9):2479–2487
- Shea LD et al (2000) Engineering bone development from a pre-osteoblast cell line on three-dimensional scaffolds. *Tissue Eng* 6:605–617
- Sheridan MH et al (2000) Bioabsorbable polymer scaffolds for tissue engineering capable of sustained growth factor delivery. *J Control Release* 64(1–3):91–102

- Simnick A, Lim DW, Chilkoti A (2007) Biomedical and biotechnological applications of elastin-like polypeptides. *J Macromol Sci* 47:121–154
- Singh S, Sinha Ray S (2007) Polylactide based nanostructured biomaterials and their applications. *J Nanosci Nanotechnol* 7:2596–2615
- Singh R et al (2005) Binding and condensation of plasmid DNA onto functionalized carbon nanotubes: toward the construction of nanotube-based gene delivery vectors. *J Am Chem Soc* 127(12):4388–4396
- Springer I et al (2001) Culture of cells gained from temporomandibular joint cartilage on non-absorbable scaffolds. *Biomaterials* 22:2569–2577
- Taepaiboon P, Rungsardthong U, Supaphol P (2006) Drug-loaded electrospun mats of poly(vinyl alcohol) fibres and their release characteristics of four model drugs. *Nanotechnology* 17:2317–2329
- Upadhyay DJ et al (2004) A comparative study of the surface activation of polyamides using an air dielectric barrier discharge. *Colloids Surf A: Physicochem Eng Aspects* 248(1–3):47–56
- Urry DW, Pattanaik A (1997) Elastic protein-based materials in tissue reconstruction. *Ann N Y Acad Sci* 831:32–46
- Vacanti JP, Langer R (1999) Tissue engineering: the design and fabrication of living replacement devices for surgical reconstruction and transplantation. *Lancet* 354:SI32–SI34
- VandeVord PJ et al (2002) Evaluation of the biocompatibility of a chitosan scaffold in mice. *J Biomed Mater Res* 59:585–590
- Vinogradov SV, Batrakova EV, Kabanov AV (2004) Nanogels for oligonucleotide delivery to the brain. *Bioconjug Chem* 15(1):50–60
- Waldman SD et al (2003) Effect of biomechanical conditioning on cartilaginous tissue formation in vitro. *J Bone Joint Surg Am* 85A(Suppl 2):101–105
- Wang RZ et al (1995) Synthesis of nanophase hydroxyapatite collagen composite. *J Mater Sci Lett* 14:490–492
- Wang Y et al (2002) A tough biodegradable elastomer. *Nat Biotechnol* 20(6):587–591
- Wang Y, Kim YM, Langer R (2003) In vivo degradation characteristics of poly(glycerol sebacate). *J Biomed Mater Res* 66A:192–197
- Wang H et al (2007) Biocompatibility and osteogenesis of biomimetic nano-hydroxyapatite/polyamide composite scaffolds for bone tissue engineering. *Biomaterials* 28:3338–3348
- Webb A, Yang J, Ameer GA (2004) Biodegradable polyester elastomers in tissue engineering. *Expert Opin Biol Ther* 4(6):801–812
- Webb AR, Kumar V, Ameer GA (2007) Biodegradable poly(diols citrate) nanocomposite elastomers for soft tissue engineering. *J Mater Chem* 17:900–906
- Wei G, Ma PX (2004) Structure and properties of nano-hydroxyapatite/polymer composite scaffolds for bone tissue engineering. *Biomaterials* 25:4749–4757
- Wei G, Ma PX (2006) Macroporous and nanofibrous polymer scaffolds and polymer/bone-like apatite composite scaffolds generated by sugar spheres. *J Biomed Mater Res* 78:306–315
- Wei H et al (2007) Self-assembled, thermosensitive micelles of a star block copolymer based on PMMA and PNIPAAm for controlled drug delivery. *Biomaterials* 28(1):99–107
- Witzmann FA, Monteiro-Riviere NA (2006) Multi-walled carbon nanotube exposure alters protein expression in human keratinocytes. *Nanomedicine* 2(3):158–168
- Woo KM, Chen VJ, Ma PX (2003) Nano-fibrous scaffolding architecture selectively enhances protein adsorption contributing to cell attachment. *J Biomed Mater Res* 67:531–537
- Worle-Knirsch JM, Pulskamp K, Krug HF (2006) Oops they did it again! Carbon nanotubes hoax scientists in viability assays. *Nano Lett* 6(6):1261–1268
- Yang S et al (2001) The design of scaffolds for use in tissue engineering. Part I. Traditional factors. *Tissue Eng* 7(6):679–689
- Yang J, Webb AR, Ameer GA (2004a) Novel citric acid-based biodegradable elastomers for tissue engineering. *Adv Mater* 16(6):511–516
- Yang J, Webb A, Ameer G (2004b) Novel citric acid-based biodegradable elastomers for tissue engineering. *Adv Mater* 16(6):511–516

- Yang J, Webb AR, Ameer GA (2005) Biodegradable elastomeric polymers for tissue engineering. In: Mallapragda S, Narasimhan B (eds) Handbook of biodegradable polymeric materials and their applications. American Scientific Publishers, Valencia
- Yang J et al (2006a) Synthesis and evaluation of poly(diols citrate) biodegradable elastomers. *Biomaterials* 27(9):1889–1898
- Yang J et al (2006b) Synthesis and evaluation of novel biodegradable elastomeric polyesters. *Biomaterials* 27:1889–1898
- Yang J et al (2006c) Modulating expanded polytetrafluoroethylene vascular graft host response via citric acid-based biodegradable elastomers. *Adv Mater* 18(12):1493–1498
- Yang M, Yunhui Y, Yanli L, Guoli S, Ruqin Yu (2006d) Platinum nanoparticles-doped sol-gel/carbon nanotubes composite electrochemical sensors and biosensors. *Biosens Bioelectron* 21(7):1125–1131
- Zhang R, Ma PX (2000) Synthetic nano-fibrillar extracellular matrices with predesigned macroporous architecture. *J Biomed Mater Res* 52(2):430–438
- Zhang SM et al (2003a) Synthesis and biocompatibility of porous nano-hydroxyapatite/collagen/alginate composite. *J Mater Sci: Mater Med* 14(7):641–645
- Zhang SM et al (2003b) Synthesis and biocompatibility of porous nano-hydroxyapatite/collagen/alginate composite. *J Mater Sci: Mater Med* 14:641–645
- Zhang Y et al (2005) Recent development of polymer nanofibers for biomedical and biotechnological applications. *J Mater Sci Mater Med* 16(10):933–946
- Zhang YZ et al (2006) Coaxial electrospinning of (fluorescein isothiocyanate-conjugated bovine serum albumin)-encapsulated poly(epsilon-caprolactone) nanofibers for sustained release. *Biomacromolecules* 7(4):1049–1057
- Zhou N, Bates FS, Lodge TP (2006) Mesoporous membrane templated by a polymeric bicontinuous microemulsion. *Nano Lett* 6(10):2354–2357

Chapter 11

Role of Spatial Distribution of Matricellular Cues in Controlling Cell Functions

Daniela Guarnieri and Paolo A. Netti

Abstract The extracellular matrix (ECM) represents the quintessential material for tissue engineering (TE) applications, because it provides a structural support and regulates tissue development. Therefore, the main challenge in TE is to recreate ECM analogues that recapitulate the structural and molecular microenvironment to promote and guide tissue growth. Apart from composition, the distribution and presentation of molecular cues within the matrix are pivotal in controlling morphogenetic process. However, the role of matricellular signal presentation in terms of spatial and temporal orchestration is still poorly understood. This article overviews the development of systems able to control the spatial and temporal exposure of matricellular cues to the aim of guide cell response for tissue engineering applications.

Keywords Bioactive scaffold • Signals presentation • Cell guidance

11.1 Introduction

The main challenges of regenerative medicine and tissue engineering include the development of integrated medical devices specifically designed to replace existing tissues and organs and the development of new generation materials with appropriate mechanical, physical and biological properties able to guide and control cell response (Lavik and Langer 2004; Mikos et al. 2006).

D. Guarnieri and P.A. Netti (✉)

Department of Materials and Production Engineering, University of Naples “Federico II”,
P.le Tecchio 80, 80125, Naples, Italy

and

Interdisciplinary Research Centre on Biomaterials (CRIB), University of Naples “Federico II”,
P.le Tecchio 80, 80125, Naples, Italy

e-mail: nettipa@unina.it; nettipa@cds.unina.it

The tissue engineering paradigm implies the possibility to restore or engineer virtually any kind of tissue through a controlled interplay of a defined combination of factors, either soluble and/or insoluble (Niklason and Langer 2001; Goldberg et al. 2007). Hence, the key step of all tissue engineering strategies is the preliminary identification of the relevant factors and the design of suitable material scaffolds able to chrono-program their release (Mikos et al. 2006; Matsumoto and Mooney 2006; Hutmacher 2001).

The first approach of TE for a guided tissue regeneration is based on the use of a synthetic matrix that conducts the host cells to populate the tissue defect site and repair the damaged tissue (Lavik and Langer 2004). In this approach, the role of scaffold is limited to a structural inert support rather than actively guide and control cell attachment, migration, proliferation and differentiation. On the other hand, a second TE strategy concerns the stimulation of tissue formation by delivering and releasing specific growth factors in the tissue defect site to induce the cells to regenerate the tissue (Biondi et al. 2008). This strategy typically uses drug delivery systems, to target drugs to specific cell populations. Even if the direct delivery of growth factor has shown to be effective in the induction of physiological response, the main drawback of this approach still remains the difficulty to achieve long-term release of functional proteins because of their short biological half life at physiological conditions. Therefore, in order to improve the sustained delivery of biological factors, novel controlled delivery systems have been introduced. The basic concept of these delivery systems is to mimic the ECM in the sequestration and temporal release of growth factors (GFs) after controlled proteolysis of ECM. An alternative and more sophisticated approach to elicit the desired biological responses relies on the use of transfected cells able to synthesize and secrete the desired protein in situ according to a paracrine mechanism. In this way, cells genetically induced to secrete proteins may act as point-source delivery systems, allowing a prolonged and more specific effect (Lu et al. 2001; Savarino et al. 2007; Shen et al. 2004). Cells can be transfected in vitro and then transplanted in the damaged tissue or, in alternative, the plasmid DNA, encoding for the inductive factor, can be delivered in place of the protein (Panyam et al. 2002). However, the direct injection of the plasmid may lead to an inadequate response because of the scarce transfection efficiency. In this case, the deliver of the plasmid needs to be optimized to induce transfection of the host cells and, hence, the production of sufficient doses of the desired protein to produce physiologically observable effects. Finally, the last approach of TE involves the transplantation of a specific cell population, directly delivered to the damaged tissue site to permit neo-tissue formation (Atala 2007). The main drawbacks of this strategy are due to the scarce integration of transplanted cells with host tissue and/or death or dedifferentiation of most transplanted cells after delivery.

In all of these approaches, the main “tools” of TE, namely cells, scaffolds and signals, are used separately. However, in order to obtain a successfully engineered tissue, it is fundamental to acquire a deep knowledge, from developmental and cell-material interaction studies, of all biological mechanisms occurring in naturally extracellular microenvironment. The integration of the cues controlling

this interaction is essential for designing appropriate biomaterials for specific-tissue or organ engineering. In addition, another important aspect that governs cellular responses is scaffold three-dimensional structure and its deformability or stiffness. Indeed, a variety of studies of cells cultured in three-dimensional gels and reconstituted basement membrane matrix have highlighted the importance of mechanical and stereomorphological configuration of cells seeded in a 3D context (Discher et al. 2005; Ingber 2006; Lo et al. 2000; Zaari et al. 2004; Curtis et al. 2001; Cukierman et al. 2001; Yamada et al. 2003). Therefore, an ideal scaffold should possess a three-dimensional and well defined microstructure with an interconnected pore network, mechanical properties similar to those of natural tissues, be biocompatible and bio-resorbable at a controllable degradation and resorption rate as well as provide the control over the sequestration and delivery of specific bioactive factors to enhance and guide the regeneration process (Hutmacher 2001; Tabata 2005).

Biomaterials used as TE scaffolds may be from natural or synthetic origin or hybrids. Natural materials have the advantage to interact with cellular receptors and promote cellular recognition, nevertheless they show limited source, batch-to-batch variability and, in general, their mechanical properties are not modulable. Conversely, synthetic materials present the advantage that their mechanical, structural and chemical properties can be modulated during their synthesis, but for a specific cellular recognition they need to be functionalised with active biomolecules (e.g. proteins and peptides) (Karp and Langer 2007). Peptides or proteins activated polymers are currently being studied as valuable hybrid platforms able to combine the advantage of natural and synthetic materials (Maheshwari et al. 2000).

In this context, a novel vision of material scaffold for TE is developing that considers the scaffold as a “drug” able to repair tissue defects by actively direct cell response and guide tissue development by supplying not only a structural support for cells, but also specific biological signals, such as GFs, in a controlled spatio-temporal pattern to induce tissue formation. Therefore, the major scientific and technological challenge in TE today is represented by the possibility to enhance further the functionality of material scaffolds by encoding in them the capability to expose an array of biological signals with an adequate dose and for a desired time frame.

Nevertheless, several aspects of the cell-material interaction mechanism remain to be explored. In particular, a better understanding of the role of the material properties and density of distribution of biological sites within the material on cell behaviour needs to be gained in order to establish and optimize design guidelines for these bioactive materials.

By summarizing results from recent studies, this chapter outlines the role played by soluble and insoluble extracellular signals in controlling cell functions. In particular, it focuses on the effect of density and spatial distribution of biological signals on cell response in terms of adhesion, migration, growth and differentiation. This chapter will attempt to address some issues that represent emerging challenges in the design of biofunctional scaffolds for TE.

11.2 Cell-Matrix Interaction

Processes of tissue remodelling occurring during development, after damage or in pathological condition are the results of a complex orchestrated interplay spatio-temporal controlled of numerous signals both biochemical and biophysical, soluble (growth factors, cytokines, chemokines) and insoluble (the ECM macromolecules) (Beningo et al. 2004; Hynes 1992). The response and behaviour of all cellular populations forming a tissue are regulated by bidirectional and dynamic molecular interactions between cells and their micro-environmental surroundings (Giancotti and Ruoslahti 1999; Schoenwaelder and Burridge 1999; Humphries and Newham 1998). The extracellular microenvironment is a complex highly hydrated network composed of various insoluble macromolecules (Hay 1991). ECM includes structural fibrillar proteins such as collagen and elastin, adhesion glycoproteins such as fibronectin and laminin, that form, together with glycosaminoglycans and proteoglycans, an interwoven network incorporating soluble macromolecules such as growth factors, cytokines and chemokines (Hay 1991; Hynes 1990). The composition of the ECM (in particular its contents of insoluble macromolecules) determines the physical properties of tissues; for instance, the presence of collagen fibrils or of the glycosaminoglycans and proteoglycans provides resistance to tensile and compressive stresses respectively (Hsu et al. 1994).

Although the ECM has long been viewed as an inert structural support, it is becoming clear that extracellular matrix not only provides a structural scaffold for cells, supplying both a spatial barrier and a physical resistance to the tissues, but also it actively interplays with the surrounding cells by storing and presenting biological signals able to control and guide specific cell response (Folkman et al. 1988). The first evidence of the existence of an interplay between cells and their ECM was the identification, on the cell membrane, of specific heterodimeric transmembrane receptors, the integrins, which are actively involved in the specific binding with the ECM components (Van der Fuler and Sonnenberg 2001). Anchorage-dependent cells recognize specific amino acid sequences of the ECM molecules through their surface receptors (Hynes 1992; Schwartz et al. 1995; Ruoslahti 1999). After ligand binding, the integrin receptors are recruited into distinct, dot-like micro-domains on cell membrane and cluster to form specific structures, called focal adhesions (Zamir and Geiger 2001; Buzzoni and Hemler 1998). In these regions, the integrins are in contact and communicate with many specific structural (paxillin and vinculin) and signalling (protein kinase C, the GTPases Rac and Rho, and MAP kinase) molecules (Burridge and Chrzanowska-Wodnicka 1996; Rottner et al. 1999; Laukaitis et al. 2001; DeMali et al. 2002). This communication influences intracellular processes important for controlling cell behaviour, including transport and secretion of various molecules, endocytosis, decision between cell proliferation, differentiation or death. In this context, integrins act as bridges between extracellular and intracellular domains by regulating cell-matrix interaction and cell behaviour (Hynes 1992). The interactions between cells and ECM are, therefore, dynamic and bidirectional.

Furthermore, the presence and the specific spatial distribution of insoluble signals, such as adhesion signals, can function also as a guide for cellular recruitment in tissue

development and repair. A controlled spatial distribution of fibronectin, for instance, is involved in the correct embryogenesis process or in wound repair by guiding cell migration according a process called haptotaxis (Rhoads and Guan 2007).

Moreover, besides acting as repository for positional signals (Folkman 1982; Jiang et al. 1994; Stupack and Cheresch 2002), solid state components of the ECM (Sage and Vernon 1994) have been proven to function also as depot for diffusable signalling molecules, such as GFs (Rapraeger 2000; Wijelath et al. 2002). Indeed, the ECM macromolecules are able to bind, store and release the soluble signalling factors in the right temporal window. Hence, once synthesised, growth factors can follow two different fates: they can immediately act by binding the specific cellular receptor and activating the signal cascade leading to specific gene expression or they can be entrapped in ECM through electrostatic interactions with the ECM molecules and be released, successively by ECM degradation upon cellular demand (by cell-secreted or cell-activated proteases, such as metalloproteinases (MMP) and serine-proteases). The binding of soluble factors to ECM molecules allows: stabilization of the factor (e.g. preserving them from enzymatic degradation) and hence the long-term delivery of functional protein; optimization of the receptor/ligand interaction and, hence, localized morphogenetic activity; finally, optimization of local concentration level for signalling.

Most of the research work has focused on specific cell functions, largely ignoring the biological context in which the cells are naturally embedded and the way in which the biological signals are displayed (Massia and Hubbell 1990; Massia et al. 1993; Mrksich et al. 1996, 1997; Mrksich 2000). Recently, it has been reported that cells, grown in tridimensional matrices, form focal adhesions, called “3D-matrix adhesions”, different, in their content of integrins, paxillin, other cytoskeletal components, and tyrosine phosphorylation of focal adhesion kinase (FAK), from the focal adhesions formed in cell culture dishes (Cukierman et al. 2001; Yamada et al. 2003). Cells embedded in the ECM network are exposed to matrix biological signals which are either solubilized or bound to the matrix. Therefore, even though a tuning and quantitative balance between both insoluble and soluble factors has been proposed (Ferrara and Davis-Smyth 1997), it is fundamental to also consider the right combination of signalling molecules needed to be detected by the responsive cells at the right time frame and how that combination is translated into a precise architectural organization, including three-dimensional distribution and size of the tissue (Borselli et al. 2007a).

Cellular morphogenetic processes are the result of a complex interplay of several signalling pathways involving more than one factor and acting, each of them in specific temporal frames. Therefore, recent efforts have focused on developing novel schemes for mimicking physiological anisotropic architecture of the native ECM environments with a sequential delivery of spatially-controlled multiple factors in the bulk of the polymeric gels. At this regard, it is worth to be mentioned the relevant work of Richardson et al. (2001) in which a mature new vascular network was obtained by designing a controlled release polymeric device able to sequential deliver the two main factors involved in angiogenesis, VEGF and PDGF-BB, controlling respectively the proliferative and the maturation steps of this process.

In this context, the work of our laboratory has been focused on studying cell response on 2D functionalised surfaces and within 3D polymeric matrices, both with a random and a gradient spatial configuration of biological signals. In particular, we have evaluated the possibility of providing a directional guidance for in vitro morphogenetic processes by shaping the distribution of solid state molecules within two- and three-dimensional scaffolds with particular regard on cell adhesion, migration, growth, differentiation and angiogenesis, since these processes are all critical in the control of tissue regeneration processes. In the following we briefly overview the main results obtained by the study of the role of matricellular cues in controlling cell functions.

11.2.1 Effect of Matrix on Cell Migration

Cell migration is an essential process in many physiological conditions (embryonic development, inflammation, wound healing and angiogenesis) as well as in pathological events (tumour metastasis) (Gobin and West 2002; Friedl and Brocker 2000; Raeber et al. 2005; Friedl and Wolf 2003). It is determinant in controlling the rate of tissue formation and, hence, it is important in tissue engineering applications. Indeed, the possibility of predicting cell migration along 2D and through 3D scaffolds plays a crucial role in designing appropriate systems allowing cell invasion in a timely and appropriate fashion. Migration is a dynamic and cyclic multi-step process involving the propedeutic polarization of cell in the direction of the movement and further pruning of protrusions, followed by the formation of adhesions, cell contraction and detachment at the rear extremity (Li et al. 2005; Raucher and Sheetz 2000; Lauffenburger and Horwitz 1996). In cell migration process, at least three classes of structural macromolecules are involved: the ECM macromolecules, the cell membrane receptors (the integrins) and the intracellular cytoskeleton with associated proteins (Li et al. 2005; Maheshwari and Lauffenburger 1998). Migration can occur in response to gradients of soluble factors (chemotaxis), of insoluble factors (haptotaxis) or of mechanical properties (durotaxis) (Lauffenburger and Horwitz 1996, Lauffenburger and Linderman 1993). In isotropic matrices and in absence of signal gradients, cell migration can be described as a Brownian-like movement, when the direction of the movement frequently changes, or as a persistent random walk, when the cellular path is relatively straight, respectively for long or short time intervals (Tranquillo 1991).

The persistent random walk has been widely reviewed by Tranquillo (1991) and by Di Milla et al. (1991). According to this theoretical model, cell movement is defined by two parameters, persistence time (P), which is the measure of the time between “significant” direction changes, and cell speed (S), that measures the movement/displacement of cell centroid per unit time.

The speed of cell movement is regulated by different parameters including the type of receptor/ligand interaction, the ligand affinity for cell adhesion receptors, the ligand concentration and its spatial distribution, as shown by the following summary of the main results obtained in the recent years.

11.2.1.1 Effect of Concentration of Matricellular Cues on Cell Migration

As previously mentioned, there are different mechanisms of cell migration, namely chemotaxis, aptotaxis and durotaxis. Hence, cell migration can be controlled by a large number of signals, including insoluble ECM proteins, growth factors and cytokines. Among these factors, fibronectin (FN), the entire protein or only its binding-fragment (RGD peptide), is one of the several critical chemo- and aptotactic ECM proteins.

By culturing different type of cells, RPE, Hela, NIH3T3, U2OS, onto inert substrates opportunely pre-coated with FN at different concentrations ranging from 0.2 to 80 $\mu\text{g/mL}$, we found that both cell adhesion and migration on the substratum are cell-type specific. The measurement of cell migration parameters (S, P) was carried out by using a time-lapse videomicroscopy. The images were collected every 5 or 15 min for 8–16 h. The coordinates of cell displacement were calculated in order to evaluate the parameters of cell migration following the Stokes–Lauffenburger theoretical model (Di Milla et al. 1991). The resulted plot shows the cell displacement, $\langle D^2 \rangle$, calculated by the trajectory of cell centroids as a function of time. The parameters Speed (S) and Persistence length (P) were then calculated by fitting the $\langle D^2 \rangle$ versus time curve using the Stokes–Lauffenburger model. By analysing a series of images acquired by the Metamorph software, it is possible to track and visualize the pathway followed by a single cell clearly, as shown in Fig. 11.1.

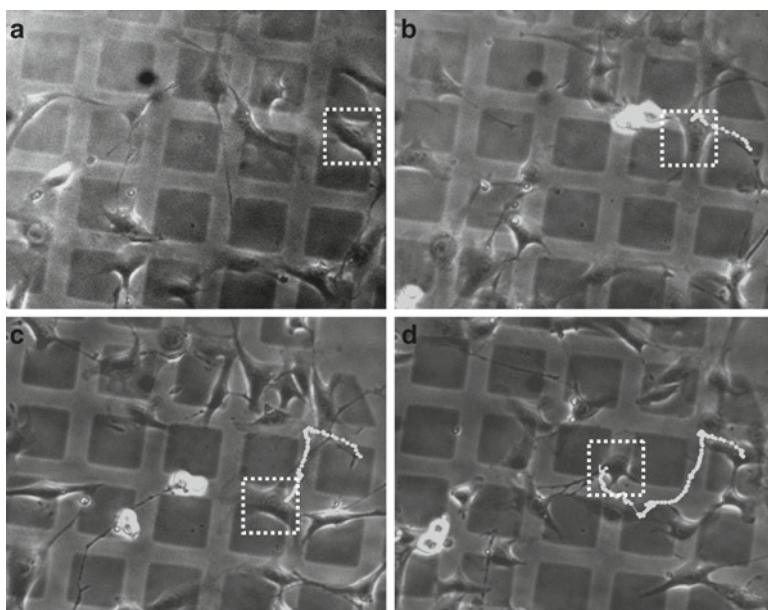


Fig. 11.1 Microscopic images acquired during a time-lapse video microscopy at 0 (a), 4 (b), 8 (c) and 12 (d) h. The cell is indicated with a *square* while the *line* shows the path followed by the cell (cell tracking)

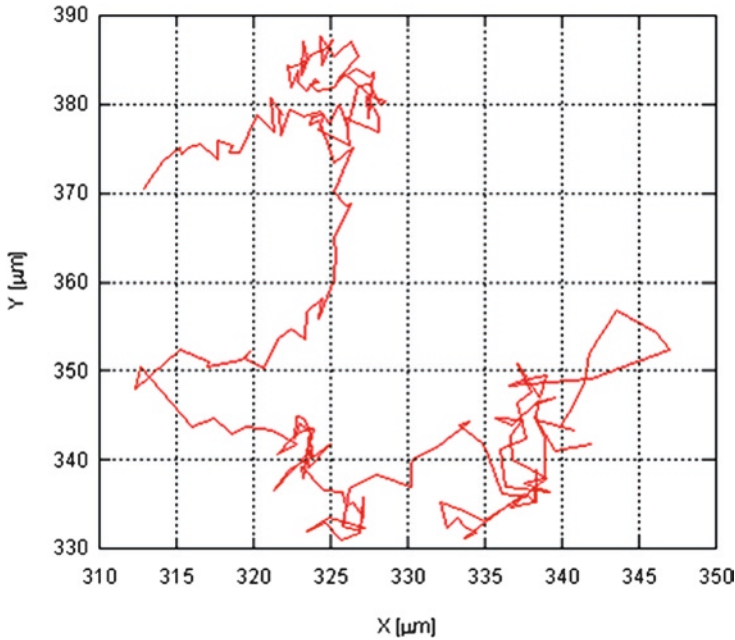


Fig. 11.2 Typical trajectory of a cell undergoing random motility in an isotropic environment. Cellular centroid position (x, y) of the same cell obtained after 15 min intervals

The graph in Fig. 11.2 shows the position of the centroid (x, y) of a single cell during the interval time analysed. As expected from the Stokes–Lauffenburger theoretical model, without a controlled spatial distribution of a chemotactic signal, the migration is random. Figure 11.3 shows a fit of the migration of NIH 3T3 fibroblasts onto a FN coating. FN deposition was obtained by incubating a 10 $\mu\text{g}/\text{mL}$ FN solution for 2 h on a Petri dish surface. This graph shows how well the experimental data, $\langle D^2 \rangle$ as a function of time, fit the Stokes–Lauffenburger theoretical model. The numerical values of S and P for four cell lines, RPE, HeLa, NIH3T3, U2OS, were determined for different fibronectin concentrations. In accordance with the previous reports (Massia and Hubbell 1991; Lutolf and Hubbell 2003), results show that for all the analysed cell types, there exists an intermediate adhesion strength for optimal cell migration (Fig. 11.4). In fact, the speed of migration initially increased up to a maximum value in correspondence of an optimal value of FN concentration. For further increase of FN concentration, the speed decreases. This behaviour is in agreement with previous studies (Irvine et al. 2002) showing that the optimal rate of cell migration is observed at certain value of density of ligands that are cell type-specific, while at either too low or too high concentrations of ligands cell migration was inhibited. The particular behaviour of different cells depends on the type and the number of cellular adhesion receptors present on the cell surface and on the quality of cell adhesion. Indeed, at low concentrations of ligands cells weakly adhere

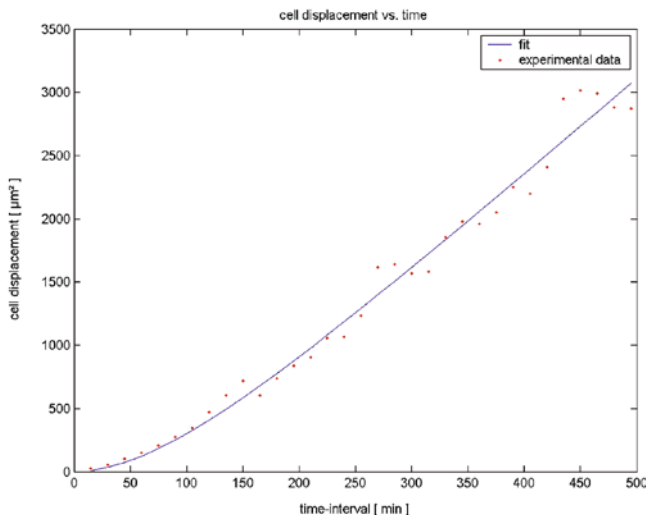


Fig. 11.3 Plots of mean square displacement versus time for NIH3T3 fibroblast cells cultured onto a coat of fibronectin. Data interpolation curve of cell displacement versus time according to Stokes–Lauffenburger model. The speed S and the persistence time P were computed by fitting the persistent random walk model equation (*solid lines*) to experimental data (*dots*). $\pm SD < 0.1$ (not shown). The experiments were repeated in triplicate and about 30 cells for each experiment were analysed

to the substrate and can not migrate, on the other hand at high concentration of ligands, the adhesion to the substrate is very strong and prevents cell movement.

This study, together with other relevant studies (Gobin and West 2002; Irvine et al. 2002; Koo et al. 2002; Lutolf and Hubbell 2003; Massia and Hubbell 1991; Palecek et al. 1997), provides an example that well-controlled adhesiveness substratum can yield into basic cell biological principles essential for deciphering the cell-ECM signalling complexity for tissue-engineering biomaterial design. However, many other aspects need to be considered in controlling cell migration process. In fact, although it has been demonstrated that density of adhesion signals can influence cell movement, also the exposure and spatial distribution of these signals can affect this biological mechanism.

11.2.1.2 Effect of Topography on Cell Migration

Recent advances in cell-material interaction have demonstrated that both chemical and topographical properties of the material surface can regulate and control cell shape and functions (Rogers et al. 2000). Since basal membranes, in vivo, have a complex tridimensional topography deriving from the presence of pores, fibers, channels and other superficial nanometric elements, it is likely that surface structure could contribute to determine specific cellular behaviors (Flemming et al. 1999).

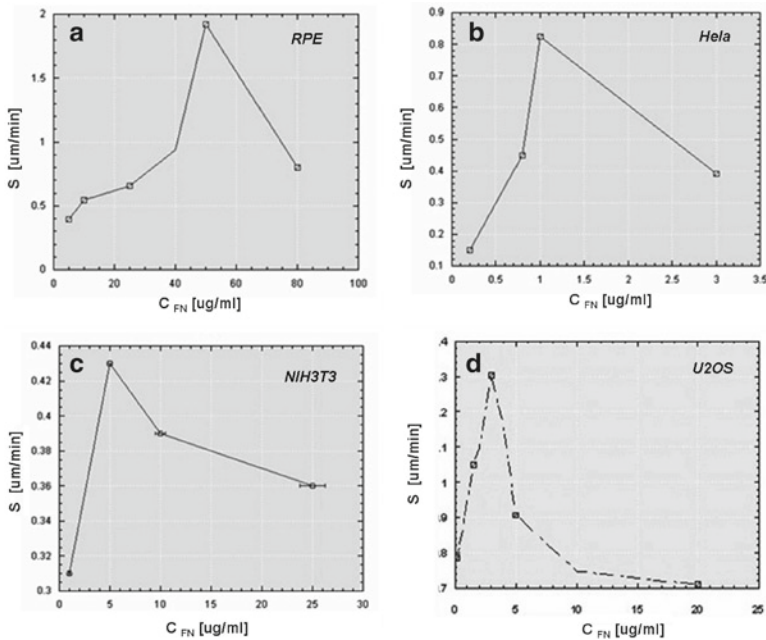


Fig. 11.4 Graphics of cellular speed versus FN concentration of RPE (a), HeLa (b), NIH3T3 (c) and U2OS (d). FN coatings were obtained by depositing different FN solutions (ranging from 0 to 80 $\mu\text{g}/\text{mL}$ of FN) for 2 h on Petri dish surfaces. For RPE and U2OS cells, the calculated S_{MAX} (about 1.92 $\mu\text{m}/\text{min}$) is obtained at a concentration of FN of 50 and 3 $\mu\text{g}/\text{mL}$, respectively; for HeLa cells, the S_{MAX} (about 0.83 $\mu\text{m}/\text{min}$) is obtained at a FN concentration of 1 $\mu\text{g}/\text{mL}$; finally, for NIH3T3 cells, the S_{MAX} (about 0.43 $\mu\text{m}/\text{min}$) is observed at 5 $\mu\text{g}/\text{mL}$ of FN

Several cell parameters, including cell orientation, motility, adhesion and shape, can be modulated by a specific surface micro- and nano-topography (Wilkinson et al. 2002; Dalby et al. 2002; Bourgoin et al. 1999). By using hydrogenated, amorphous carbon (a-C:H) grids with various interspace and height deposited on a glass substrate (Fig. 11.5), the influence of a micro-patterned surface topology on cell adhesion and migration parameters was studied (Pennacchi et al. 2004). It was shown that NIH 3T3 mouse embryo fibroblasts were able to recognize specific dimensions of the surface topography and to be guided on a material surface presenting well defined grid interspace. In particular, cells recognize topographic surfaces patterned with periodicities of 20–40 μm by showing a better adhesion and spreading (Fig. 11.6).

The effect of patterned surfaces is more evident when analyzing cell locomotion. Cell migration on patterned surfaces does not follow the 2D Stokes–Lauffenburger behaviour. Indeed, on surfaces with grid of 40 μm interspace, cells preferentially migrate along the carbon grooves paths, exhibiting a persistence length much longer compared to non-patterned surfaces (Fig. 11.1 and Table 11.1).

The correlation between cell movement and substrate topography can be better interpreted by the analysis of fractal dimension. According to Balakrishnan (1995),

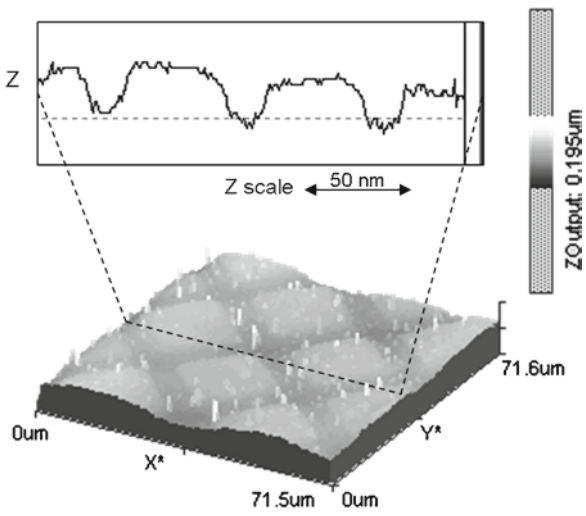


Fig. 11.5 AFM analysis indicating cross section line view and 3D topography of patterned surface of a-C:H

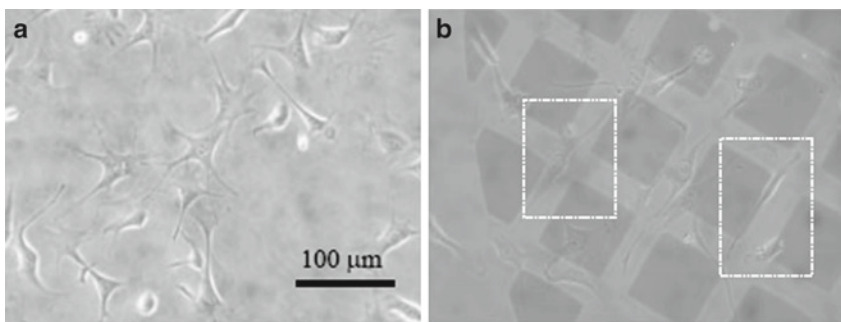


Fig. 11.6 Light microscope images (20× magnification) of NIH 3T3 cells on non-patterned surfaces (a) and on patterned surfaces with square length of 60 μm and spacing of 30 μm (b). On flat surfaces cells spread randomly. Conversely, on patterned surfaces some cells (evidenced by rectangles) are stretched and aligned along the edges. Scale bar, 100 μm

Table 11.1 Analysis of cell movement in function of grids dimensions (\pm SD < 0.1 [not shown])

Square length (μm)	Groove width (μm)	Depth (nm)	Persistence length (min)	Cell behaviour
40–80	20–40	30	154	Non random movement
100–200	30	30	68	Random movement
15–20	5–10	30	73	Random movement

a particle, moving randomly in an isotropic environment, follows a fractal trajectory. Conversely, on fractal structures, random movement becomes an anomalous diffusion (Aarão Reis 1996), depending on the fractal dimension of the structure. A fractal is a structure that can be subdivided in parts, each of which is a reduced-size copy of the whole, a property called “self-similarity”. In addition, fractals structures are characterized by a specific fractal dimension that is index of self-similarity level of the structure and can be measured according to Von Koch curve method (Balakrishnan 1995). Since carbon grids can also be considered fractal structures, the diffusion coefficient of cell movement has been correlated with fractal dimension of grids. The evaluation of a diffusion coefficient has been performed following a generalized diffusion model (Metzler and Klafter 2000). Preliminary results show that the diffusion coefficient evaluated by the analysis of the cell motion correlates well with the surface fractal dimension (data not shown), indicating that cell movement depends on the topography of the substrate.

In conclusion, the results show that the dimension of the square and the spacing affect fibroblast morphology and migration. By appropriate surface patterning it is possible to guide cell spreading and the direction of motion.

11.2.2 Matrix Effect on Embryonic Development

Cell-matrix interaction also plays an important role in cell differentiation process (Ingber 2006; Battista et al. 2005). A deep understanding of the role of the material in control and guidance of stem cell development and then commitment into complex and viable 3D tissues will be extremely useful to better design strategy for improving and enhancing their repairing potential. Among other ECM components, fibronectin (FN) and laminin (LM) have been proposed as main matricellular cues responsible for the control of development of embryonic bodies (EBs) and their specific tissue commitment (Battista et al. 2005). EBs, grown in 3D semi-interpenetrating polymer networks (SIPNs) of collagen-fibronectin (C-FN SIPNs) and collagen-laminin (C-LM SIPNs) at different ratios, displayed differentiation patterns dependent upon matrix composition.

The presence of FN in the SIPNs induces a dose-dependent enhancement of the EBs outgrowth compared to collagen alone. In particular, at FN concentration of 100 $\mu\text{g}/\text{mL}$, EBs outgrowth occurred at early time (after 24 h) (Fig. 11.7b), while at FN concentration of 5 $\mu\text{g}/\text{mL}$ outgrowth was delayed (Fig. 11.7a). After 12 days of culture, high FN concentrations induced the formation of organized capillary-like structures provided by open lumens (data not shown). At 24 days, specific endothelial cell marker (PECAM-1) staining was localized to the cord-like structures visualized by light microscopy in EBs grown in 100 $\mu\text{g}/\text{mL}$ FN (Fig. 11.7d). Conversely, tubular, PECAM-1-positive structures were almost absent in collagen gels without FN (data not shown) and in 5 $\mu\text{g}/\text{mL}$ FN SIPNs (Fig. 11.7c). These data indicate that the amount of FN within the 3D scaffold plays an important role in ES cells commitment toward blood vessels.

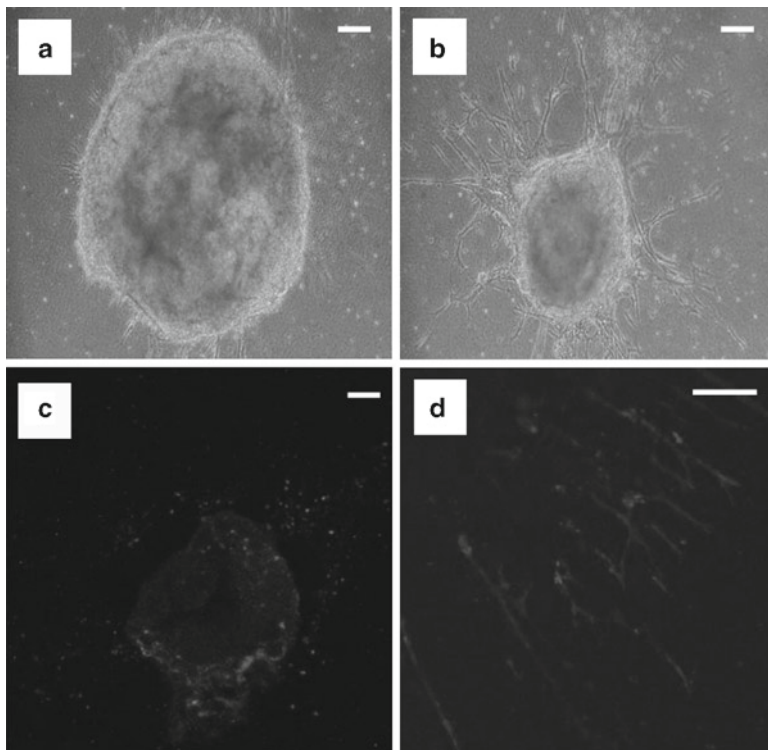


Fig. 11.7 Light microscopy evaluation of EBs outgrowth in 5 $\mu\text{g}/\text{mL}$ FN-based SIPNs (a) and in 100 $\mu\text{g}/\text{mL}$ FN-based SIPNs (b) after 24 h of culture. Immunofluorescence for PECAM1 antigen of EBs grown for 24 days in 5 $\mu\text{g}/\text{mL}$ FN-based SIPNs (c) and in 100 $\mu\text{g}/\text{mL}$ FN-based SIPNs (d). Scale bar, 50 μm

On the other hand, the presence of LM within collagen scaffold leads to an increase in EBs cardiac differentiation and this tendency increases with increasing LM concentration, as indicated by the percentage of EBs having beating areas (Fig. 11.8). In some LM-based SIPNs, it was observed that the tissue contraction generated a flux of hematopoietic cells inside the EB. These results indicate that the cellular adhesion cues provided by the presence of LM in the 3D scaffold guide EBs development toward cardiac tissue lineages.

In addition to their biological effect on EBs differentiation, FN and LM also exert a structural role in modifying collagen fiber structure and mechanical properties of collagen gel matrices. In particular, it has been observed that in cell-free collagen matrices, higher concentrations of both FN and LM (100 $\mu\text{g}/\text{mL}$) induce a decrease of elastic modulus (Table 11.2) and an increase of diffusion coefficient (Fig. 11.9). These results depend on the effect of FN and LM on collagen fibrillogenesis process (Makowski and Magdoff-Fairchild 1986; Weisel et al. 1987; Birk 2001). Indeed, in collagen gels, fibril cross-sections were irregular and appeared to be fusion products of laterally apposed smaller fibrils (Fig. 11.10a, b). Conversely, the

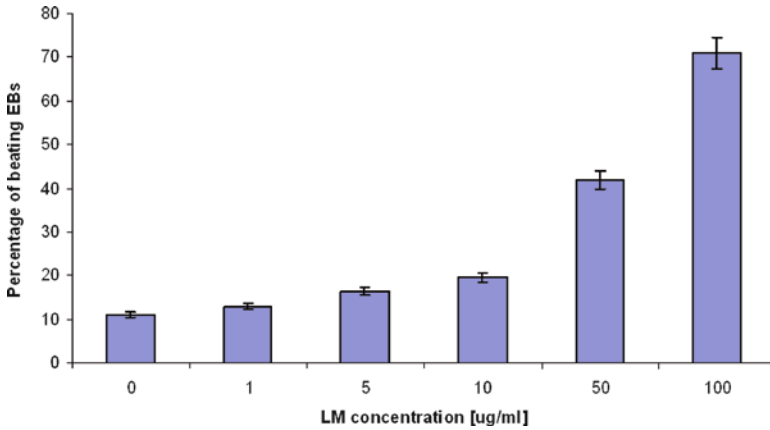


Fig. 11.8 Cardiac differentiation in LM-based SIPNs. Diagram showing the percentage of beating EBs as a function of LM concentration, in 3D LM-based SIPNs. The experiments were repeated in triplicate and about 30 EBs for each experiment were analysed

Table 11.2 Elastic moduli (G') at 1 Hz for 1.2 mg/mL collagen gel with varying concentration of fibronectin and laminin, evaluated by small amplitude oscillatory shear tests using a stress controlled rotational rheometer in a parallel plate geometry (15 mm of diameter)

Amount of FN or LM ($\mu\text{g/mL}$)	G' gel with FN (Pa)	G' gel with LM (Pa)
0	16	16
10	16	14.7
50	12.9	12.7
100	5.4	5

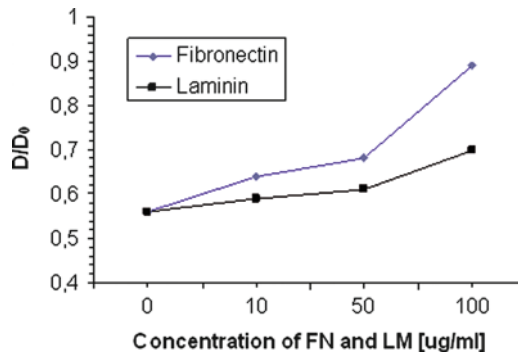


Fig. 11.9 Diffusion coefficient of dextran (500 kg/mol) in fibronectin (rhomb)- and laminin (square)-based semi-IPN, normalized respect its value in water, versus additive concentration, obtained by Fluorescence recovery after photobleaching (FRAP) analysis

addition of increasing amounts of fibronectin or laminin induced modification in fibril structure, by promoting the formation of linear collagen fibres, as shown by TEM images of a regular circular cross-section profile (Fig. 11.10c-f) and by reducing the tendency of fibrils to fuse together through the lateral apposition of intermediate

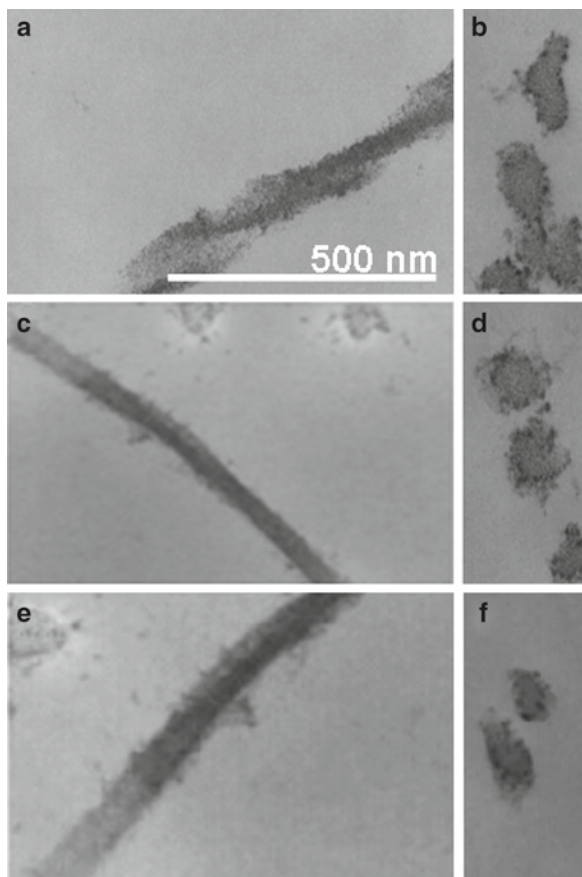


Fig. 11.10 TEM micrographs of collagen gels, FN-based semi-IPNs and LM-based semi-IPNs. (a) 1.2 mg/mL collagen gel; (b) 1.2 mg/mL collagen gel (*fibril cross sections*); (c) 1.2 mg/mL collagen gel + 100 $\mu\text{g/mL}$ of LM; (d) 1.2 mg/mL collagen gel + 100 $\mu\text{g/mL}$ of LM (*fibril cross sections*); (e) 1.2 mg/mL collagen gel + 100 $\mu\text{g/mL}$ of FN; (f) 1.2 mg/mL collagen gel + 100 $\mu\text{g/mL}$ of LM (*fibril cross sections*). Scale bar, 500 nm

fibrils. These results show that the addition of FN or LM to collagen gel matrices leads to the formation of a looser and weaker network of collagen fibres (Guarnieri et al. 2007).

Even if FN and LM have similar effects upon the structural organization and mechanical properties of collagen gel matrices, their effect on EBs development and differentiation is remarkable: FN induced a dose-dependent endothelial differentiation, whereas LM stimulated a cardiac pathway. Taking together, it can be concluded that, by modulating specific molecular signals within the scaffold, it is possible to induce EBs cavitation and guide EBs development. Whether this guidance is more likely provided by the cell adhesion motifs present on FN or LM than by the structure and mechanical properties of the material remains to be assessed. Immunofluorescence analyses on cell-free SIPNs showed a clustered distribution

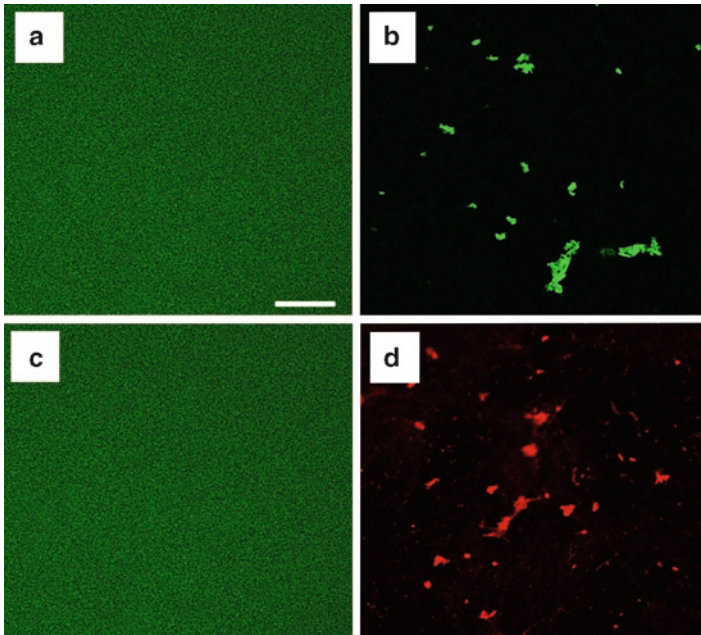


Fig. 11.11 Distribution of collagen (**a** and **c**), FN (**b**) and LM (**d**) in FN-based (**a** and **b**) and LM-based (**c** and **d**) collagen semi-IPNs by immunofluorescence analysis. Scale bar, 100 μm

of both FN and LM (Fig. 11.11b, d) (Guarnieri et al. 2007). Moreover, number and size of clusters increased at higher FN and LM concentrations. This spotted pattern and the biological responses generated in the EBs bring up the issue of the role of signal distribution and presentation in inducing cell response.

11.2.3 Matrix Effect on Angiogenic Processes

It has been widely demonstrated that matrix composition and signal presentation affect angiogenic process (Borselli et al. 2007b; Ruhrberg et al. 2002). In order to sustain tridimensional tissues, angiogenesis and vascularization are fundamental for determining the appropriate supply of oxygen and nutrients to cells. Since three-dimensional engineered tissues demand a correct and functional blood vessel network, the stimulation and the control of angiogenesis and vasculogenesis are critical for a successful material-guided tissue regeneration. Indeed, for long term endurance of any tissue repairing device, the formation and invasion of blood vessels into three-dimensional scaffolds are essential to determine the final functionality of the implanted device. There are many factors involved in controlling each step of the angiogenic process. Numerous studies have led to the identification of soluble factors (VEGFs, FGFs, TGFs, angiopoietins, ephrins, placental growth factors) and solid

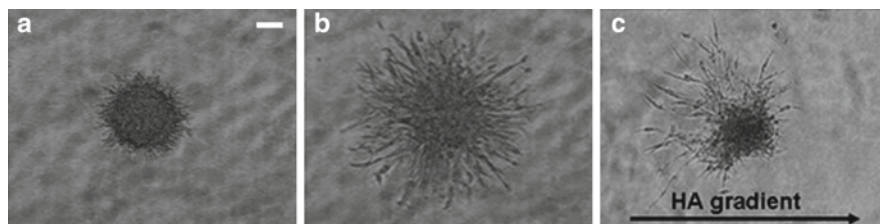


Fig. 11.12 Sprouting of ECs spheroids embedded in collagen-HA 5 mg/mL (a); in three-dimensional collagen gels (1.2 mg/mL) (b) and in gradients of matrices C-CHA5 at 24 h culture (c). Scale bar, 50 μ m

state components of the ECM (collagen, fibronectin, laminin, hyaluronic acid, etc.) that have been proven to be key effectors of endothelial cell behaviour (Kurz et al. 2003). Even though a tuning and quantitative balance between both insoluble and soluble pro-angiogenic stimulators and anti-angiogenic factors has been widely accepted, little is known about how these molecules control the spatial vascular architecture including distribution, branching, size and direction of outgrowth.

The vascular architecture *in vivo* is controlled, at least in part, by a specific and controlled spatial distribution of matricellular signals, and it has been demonstrated that the rate and the direction of vascular sprouts within a tridimensional scaffold may be guided by modulating the spatial distribution of the matricellular cues (Borselli et al. 2007b). Vascular sprouting of PAE spheroids embedded in isotropic semi-IPN collagen type I and hyaluronic acid (HA) indicates a clear effect of the composition of the material on angiogenic process. In particular, the presence of HA (MW: 1.55×10^5 Da) in collagen gel drastically inhibited ECs sprouting angiogenesis at early times when compared to the pure collagen gel (Fig. 11.12a–b). From the second day of culture, HA did not have a negative effect on the overall sprouting, but it significantly delayed endothelial proliferation and angiogenic sprouting.

The opposing effect of these two macromolecules were exploited to generate matrices with concentration gradients of collagen-HA in order to direct angiogenic sprouting growth within 3D gels. Different continuous linear gradients of C-HA matrices were realized by changing HA spatial distribution. In all the cases, it was observed that sprouting was directed toward the collagen rich matrices. In all the gradients, the spheroids displayed a polarized morphology (Fig. 11.12c). These findings demonstrate that gradients of matricellular cues can be used to direct and enhance angiogenic sprouting in 3D scaffolds.

11.3 Development of Novel Biofunctional Materials

The complex biochemical and biophysical structure of the native ECM serves as template for the design of tailor-made multifunctional synthetic biomaterials that require, to serve their specific biological functions, the incorporation of appropriate

bioactive domains deriving from the native proteins. Even though it is clear that the presence of biological signals is fundamental in designing biomaterials able to promote tissue growth and development both *in vitro* and *in vivo*, it is still not clear how these signals have to be presented to the cells. *In vivo*, cells constantly receive stimuli that are spatially and temporally regulated and controlled. Moreover, for recapitulating all the phases of tissue regeneration a well-orchestrated pattern of soluble and insoluble signals are needed. The spatial distribution of proteins, for example, can play an important role in the organization of tissues. Indeed, protein gradients can provide necessary biochemical cues that direct the organized formation of tissue (Swartz 2003). This role impacts embryogenesis, capillary sprouting, and wound healing. In angiogenic process, the formation of branching vessels is regulated by specific growth factors. VEGF, for example, is necessary for vessel formation. It has been demonstrated that a controlled distribution of VEGF can lead to the correct branching morphogenesis of blood vessels in mouse embryos. Indeed, changes in the extracellular localization of VEGF-A, in heparin-binding mutant embryos, resulted in an altered distribution of endothelial cells within the growing vasculature. Instead of being recruited into additional branches, nascent endothelial cells were preferentially integrated within existing vessels to increase lumen caliber. The disruption of the normal VEGF-A concentration gradient also impaired the directed extension of endothelial cell filopodia, suggesting that heparin-binding VEGF-A isoforms normally provide spatially restricted stimulatory cues that polarize and thereby guide sprouting endothelial cells to initiate vascular branch formation (Ruhrberg et al. 2002).

Also, in wound healing, chemotactic factors released by platelets and macrophages can recruit fibroblasts into the wound where the fibroblasts in part repopulate the wound and deposit connective tissue (Clark 1988). Likewise, protein gradients may be useful for optimizing engineered tissue formation by enhancing migration and the recruitment of cells into scaffolds for tissue engineering applications.

In this context, researchers are moving towards the identification of novel techniques to realize scaffolds presenting a controlled spatial and temporal distribution of biomacromolecular cues in order to understand the importance of signal presentation in regulating and guiding cell behaviour.

The first approaches to obtain substrates presenting biological signals in a controlled fashion regard methods for bi-dimensional applications (Fittkau et al. 2005). Photolithography techniques, for example, have made it possible to restrict cell adhesion to specific areas of a biomaterial surface. These techniques often involve the use of an elastomeric stamp to form patterns of protein-resistant and protein-adsorptive regions, which have been shown to lead to changes in both cell spreading and cell proliferation (Singhvi et al. 1994; Chen, and Ito 2001; Ito et al. 2001). These techniques can use self assembling molecules, such as alkanethiols, which can be easily modified by covalently attachment of biological molecules thus acting as spacers for exposing biochemical factors on the surface of the material (Mrksich et al. 1996, 1997; Mrksich 2000). It has been reported that the length of these spacers influences biological recognition, because it can prevent or promote the interaction between ligands and cellular receptors. The use of self

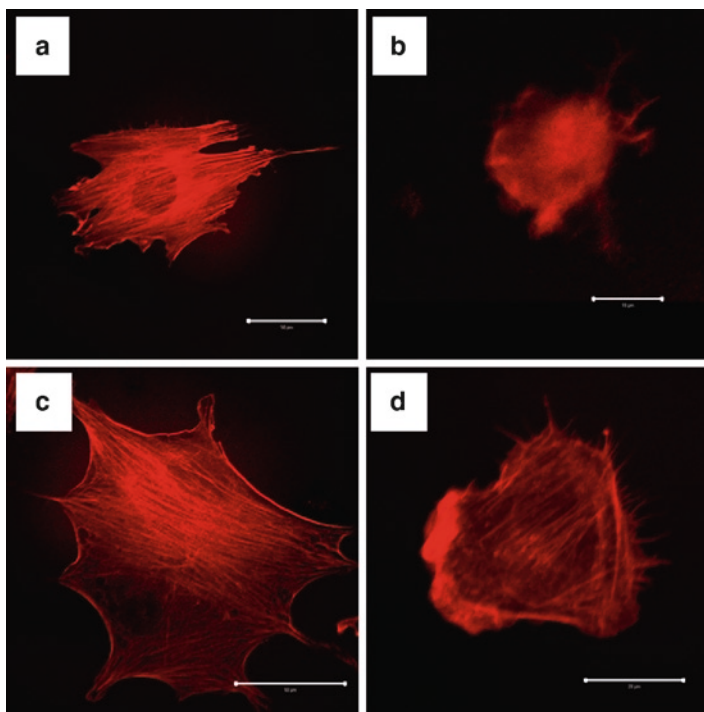


Fig. 11.13 Actin cytoskeleton staining of NIH3T3 cells seeded on control polystyrene cell culture dish (a); on PEG₃₄₀₀-SAMs (b); on RGD-PEG₃₄₀₀-SAMs (c); on RGD-PEG₆₈₀₀-SAM (d). Scale bar, 50 μ m (a–c) and 20 μ m (d)

assembled monolayers made of poly(ethylene glycol) chains (PEG-SAMs) represent an additional tool for studying the effect of biochemical signal exposure on promoting biological recognition and regulating cell activity (Zhu et al. 2001). Indeed, by covalently adding biochemical factors, such as RGD peptides, PEG can be easily functionalised, and, by varying its molecular weight, it is possible to change the spacer length. In the absence of RGD peptides, cell morphology, cytoskeleton organization and cell migration are drastically affected (Fig. 11.13b and Table 11.3). However, the addition of adhesion signals is not sufficient for a correct cell-material interaction. Cells do not adhere and migrate correctly on bioactivated PEG-SAMs substrates, made of PEG with high molecular weight (6,800 Da) (Fig. 11.13d and Table 11.3), because a long chain of PEG, being more flexible, tends to fold itself and mask the adhesion signal. Conversely, a shorter chain of RGD bioactivated PEG (3,400 Da) promoted cell adhesion and migration (Fig. 11.13c and Table 11.3), because it presents the adhesion signal in a more appropriate way.

Although these techniques are relatively simple to apply and flexible in providing a range of shapes and sizes that can be dictated, including protein gradients,

Table 11.3 Cell speed values of NIH3T3 cells migrating on PEG₃₄₀₀-SAMs; on RGD-PEG₃₄₀₀-SAMs; on RGD-PEG₆₈₀₀-SAMs

SAMs substrates	Cell speed ($\mu\text{m}/\text{min}$)
PEG ₃₄₀₀ -SH	1.18
RGD-PEG ₃₄₀₀ -SH	1.90
RGD-PEG ₆₈₀₀ -SH	1.26

it is difficult to apply this method to tri-dimensional systems (Chen and Ito 2001; Ito et al. 2001). Thus, other methods have been developed to enable cell guidance. Soluble protein gradients have been realised to study in vitro cellular response, in terms of cell migration (Boyden 1962; Nelson et al. 1975; Moghe et al. 1995; Knapp et al. 1999). These methods are based on the restricted diffusion of proteins from a region of higher concentration into another region at a lower concentration. For this kind of methods, polymeric gels, made of natural materials such as collagen or fibrin have been used in order to observe tri-dimensional chemotaxis within the scaffold (Moghe et al. 1995; Knapp et al. 1999). One of the main disadvantages of this kind of technique is the difficulty to maintain stable the concentration gradient for long time, because biochemical cues quickly diffuse away determining a uniform distribution of the cues in the scaffold and they are readily enzymatically digested or deactivated. Secondly, since these scaffolds are made of natural materials (fibrin or collagen) there are also biochemical cues intrinsic to the gels that can influence cell behaviour and migration making it difficult to control the presentation of bioactive factors (Mosesson et al. 2001; Van Hinsbergh et al. 2001). Thus, to overcome these limits, recent studies are using synthetic materials as scaffolds for the capability of modulating their mechanical and structural properties and of being feasibly bioactivated with biological signals. Hence, in construction of biocompatible synthetic biomaterial different approaches can be pursuit for modulating the cell-material interactions. The biologically functional building blocks, including cell adhesion ligands (such as RGD), proteins (such as growth factors) binding sites and degradation site for proteases, synthesized either chemically or by recombinant technology, can be cross-linked to form network in several ways. Two notable designs are the work of Nagai et al. (2006) who has designed supramolecular nanofibrillar hydrogel from ionic self-assembling bioactive peptide and of Lutolf and Hubbell (2003) who has proposed an engineered bioactive hydrogel through the chemical combination of synthetic peptides and PEG molecules. These molecules are assembled through their photopolymerization to obtain three-dimensional hybrid gel formed by end-functionalized chain of hydrophilic polymer. Examples include poly(ethylene glycol) based hydrogels functionalized with pendant RGD-containing peptides (Ruoslahti 1996), metalloproteinases-sensitive peptides and synthetic peptides exploiting the VEGF activity (Lutolf et al. 2003; Ruoslahti 1996; Zisch et al. 2003). These materials have been proven to stimulate and enhance vascular sprouting by reproducing the natural interplay that exists between matrix, cells and angiogenic factors.

Although several technologies exist that aid in controlling the pattern of bioactive factor presentation, most of these strategies fall short in enabling the sustained presentation of protein patterns in tridimensional biomaterials. In contrast, hydrogel scaffolds based on PEG provide the opportunity to control the presentation of biological signals, such as growth factors (DeLong et al. 2005a) or adhesive peptides (DeLong et al. 2005b), in terms of concentration and spatial distribution. Furthermore, the manipulation of laminar streams of fluids in microchannels makes possible the creation of gradients of high complexity, using small molecules, growth factors or other proteins either in solution or immobilized on the surface. Scaffold technology can thus take advantage of several techniques, such as microfluidics, to imprint within the scaffold a gradient of chemical signals to gain control of cell adhesion, migration, growth and proliferation.

One of the possible TE approaches to control molecular microenvironment is to use a chrono-programmed scaffold as a controlled release platform. Some relevant results have been achieved by the group of Mooney (Chen and Mooney 2003), who developed PLGA scaffolds for the sequential release of multiple GFs by mixing free VEGF with empty and PDGF-loaded polymer particles and subsequently assembling them into a porous scaffold (Richardson et al. 2001). More recently, they have also presented an anisotropic system based on a porous bi-layered PLGA scaffold able to expose only VEGF in one spatial region, and deliver VEGF and PDGF in an adjacent region (Chen et al. 2007). In a similar attempt, PLA microparticles plasticized with PEG were sintered into scaffolds formed by protein-free and protein-loaded layers, thus allowing a release of different bioactive molecules restricted to specific regions within the scaffold (Suciati et al. 2006). These scaffolds may find utility in applications where GF gradients or a region-dependent tissue growth are required. However these techniques present some disadvantages. The main limit is due to the partial modification of GF-loaded microspheres when formed into the scaffold. To overcome this limit, an alternative approach has been developed based on micromanipulation technique. It has been recently demonstrated that through the fine tuning of microsphere formulation and scaffold properties it is possible to realize platforms able to control the microenvironmental conditions in terms of time evolution of bioactive molecules delivery (Ungaro et al. 2006). Possible developments of these findings may benefit from advances in micro- and nanotechnologies so as to engineer templates embedding microspheres releasing GFs at known release rates in a predetermined and optimized spatial distribution within the scaffold. Actually, devices acting as single point source may be micropositioned by 3D printing and soft lithography to obtain highly regulated structures able to trigger the extent, and possibly the architecture/structure of tissue formation (Sun et al. 2004; Whitesides et al. 2001). The combination of micropositioning systems and mathematical modeling describing the complex and multiple mechanisms governing the release kinetics from single microspheres within the scaffold can be of help to realize scaffolds with highly controlled architecture by computer-aided scaffold design (CASD) (Sun et al. 2004; Hutmacher et al. 2004).

11.4 Conclusions

In designing scaffolds for tissue engineering, the principal objective is to recreate ECM function in a temporally coordinated and spatially organized structure. A key issue is the appropriate incorporation of the required biomolecular signals into the scaffold, so that the microenvironment may be tightly controlled and regulated. The increased understanding of the cellular and molecular mechanism of tissue development and regeneration has presented way towards more effective therapies for regenerative medicine and tissue engineering, however, many challenging questions regarding the spatial and temporal control of multiple signals presentation are still waiting for a satisfactory answer.

References

- Aarão Reis FDA (1996) Diffusion on regular random fractals. *J Phys A-Math Gen* 29:7803–7810
- Atala A (2007 March–April) Engineering tissues, organs and cells. *J Tissue Eng Regen Med* 1(2):83–96
- Balakrishnan V (1995) Random walk on fractals. *Mat Sci Eng B-Solid* 32:201–210
- Battista S, Guarnieri D, Borselli C, Zeppetelli S, Borzacchiello A, Mayol L, Gerbasio D, Keene DR, Ambrosio L, Netti PA (2005) The effect of matrix composition of 3D constructs on embryonic stem cell differentiation. *Biomaterials* 2631:6194
- Beningo KA, Dembo M, Wang YL (2004) Responses of fibroblasts to anchorage of dorsal extracellular matrix receptors. *Proc Natl Acad Sci USA* 101(52):18024–18029
- Biondi M, Ungaro F, Quaglia F, Netti PA (2008) Controlled drug delivery in tissue engineering. *Adv Drug Deliv Rev* 60:229–242
- Birk DE (2001) Type V collagen: heterotypic type I/V collagen interactions in the regulation of fibril assembly. *Micron* 32:223
- Borselli C, Battista S, Netti PA (2007a) Mind the matrix: role of scaffold in controlling cell function. In: *New research on biomaterials*. Nova Science Publishers, Hauppauge NY, USA, pp 181–195
- Borselli C, Oliviero O, Battista S, Ambrosio L, Netti PA (2007b) Induction of directional sprouting angiogenesis by matrix gradients. *J Biomed Mater Res A* 80(2):297–305
- Bourgoin D, Turgeon S, Ross GG (1999) Characterization of hydrogenated amorphous carbon films produced by plasma-enhanced chemical vapour deposition with various chemical hybridization. *Thin Solid Films* 357:2
- Boyden S (1962) The chemotactic effect of mixtures of antibody and antigen on polymorphonuclear leucocytes. *J Exp Med* 115:453–466
- Burridge K, Chrzanowska-Wodnicka M (1996) Focal adhesions, contractility, and signalling. *Annu Rev Cell Dev Biol* 12:463–518. Review
- Buzzoni G, Hemler ME (1998) Are changes in integrin affinity and conformation overemphasized? *Trends Biochem Sci* 23(1):30–34. Review
- Chen G, Ito Y (2001) Gradient micropattern immobilization of EGF to investigate the effect of artificial juxtacrine stimulation. *Biomaterials* 22:2453–2457
- Chen RR, Mooney DJ (2003) Polymeric growth factor delivery strategies for tissue engineering. *Pharm Res* 20:1103–1112
- Chen RR, Silva EA, Yuen WW, Mooney DJ (2007) Spatio-temporal VEGF and PDGF delivery patterns blood vessel formation and maturation. *Pharm Res* 24:258–264
- Clark RAF (1988) Wound repair: overview and general considerations. In: Clark RAF (ed) *The molecular and cellular biology of wound repair*. Plenum, New York, pp 3–35

- Cukierman E, Pankov R, Stevens DR, Yamada KM (2001) Taking cell-matrix adhesions to the third dimension. *Science* 294:1708–1712
- Curtis ASG, Casey B, Gallagher JO, Pasqui D, Wood MA, Wilkinson CDW (2001) Substratum nanotopography and the adhesion of biological cells. Are symmetry or regularity of nanotopography important? *Biophys Chem* 94:275–283
- Dalby MJ, Riehle MO, Johnstone HJ, Affrossman S, Curtis AS (2002 December) Polymer-demixed nanotopography: control of fibroblast spreading and proliferation. *Tissue Eng* 8(6):1099–1108
- DeLong SA, Gobin AS, West JL (2005a) Covalent immobilization of RGDS on hydrogel surfaces to direct cell alignment and migration. *J Control Release* 109:139–148b
- DeLong SA, Moon JJ, West JL (2005b) Covalently immobilized gradients of bFGF on hydrogel scaffolds for directed cell migration. *Biomaterials* 26(16):3227–3234a
- DeMali KA, Barlow CA, Burridge K (2002) Recruitment of the Arp2/3 complex to vinculin: coupling membrane protrusion to matrix adhesion. *J Cell Biol* 159:881–891
- DiMilla PA, Barbee K, Lauffenburger DA (1991 July) Mathematical model for the effects of adhesion and mechanics on cell migration speed. *Biophys J* 60(1):15–37
- Discher DE, Janmey P, Wang YL (2005) Tissue cells feel and respond to the stiffness of their substrate. *Science* 310(5751):1139–1143
- Ferrara N, Davis-Smyth T (1997) The biology of vascular endothelial growth factor. *Endocr Rev* 18(1):4–25
- Fittkau MH, Zilla P, Bezuidenhout D, Lutolf MP, Human P, Hubbell JA, Davies N (2005) The selective modulation of endothelial cell mobility on RGD peptide containing surfaces by YIGSR peptides. *Biomaterials* 26(2):167–174
- Flemming RG, Murphy CJ, Abrams GA, Goodman SL, Nealey PF (1999) Effects of synthetic micro- and nano-structured surfaces on cell behavior. *Biomaterials* 20:573–588
- Folkman J (1982) Angiogenesis: initiation and control. *Ann N Y Acad Sci* 401:212–227
- Folkman J, Klagsbrun M, Sasse J, Wadzinski M, Ingber D, Vlodavsky I (1988) A heparin-binding angiogenic protein–basic fibroblast growth factor is stored within basement membrane. *Am J Pathol* 130:393–400
- Friedl P, Brocker EB (2000) The biology of cell locomotion within three-dimensional extracellular matrix. *Cell Mol Life Sci* 57(1):41–64
- Friedl P, Wolf K (2003) Tumour-cell invasion and migration: diversity and escape mechanisms. *Nat Rev Cancer* 3(5):362–374
- Giancotti FG, Ruoslahti E (1999 August 13) Integrin signaling. *Science* 285(5430):1028–1032. Review
- Gobin AS, West JL (2002 May) Cell migration through defined, synthetic ECM analogs. *FASEB J* 16(7):751–753. Epub March 26
- Goldberg M, Langer R, Jia X (2007) Nanostructured materials for applications in drug delivery and tissue engineering. *J Biomater Sci Polym Ed* 18:241–268
- Guarnieri D, Battista S, Borzacchiello A, Mayol L, De Rosa E, Keene DR, Muscarello L, Barbarisi A, Netti PA (2007 February) Effects of fibronectin and laminin on structural, mechanical and transport properties of 3D collagenous network. *J Mater Sci Mater Med* 18(2):245–253
- Hay ED (ed) (1991) *Cell biology of extracellular matrix*. Plenum, New York
- Hsu S, Jamieson AM, Blackwell J (1994) Viscoelastic studies of extracellularmatrix interactions in a model native collagen gel system. *Biorheology* 31:21–36
- Humphries MJ, Newham P (1998) The structure of cell-adhesion molecules. *Trends Cell Biol* 8(2):78–83. Review
- Hutmacher DW (2001) Scaffold design and fabrication technologies for engineering tissues-state of the art and future perspectives. *J Biomater Sci Polym Ed* 12:107–124
- Hutmacher DW, Sitterling M, Risbud MV (2004) Scaffold-based tissue engineering: rationale for computer-aided design and solid free-form fabrication systems. *Trends Biotechnol* 22:354–362
- Hynes RO (1990) *Fibronectins*, 1st edn. Springer, New York, p 546
- Hynes RO (1992) Integrins: versatility, modulation, and signaling in cell adhesion. *Cell* 69:11–25

- Ingber DE (2006) Mechanical control of tissue morphogenesis during embryological development. *Int J Dev Biol* 50:255–266
- Irvine DJ, Hue KA, Mayes AM, Griffith LG (2002 January) Simulations of cell-surface integrin binding to nanoscale-clustered adhesion ligands. *Biophys J* 82(1 Pt 1):120–132
- Ito Y, Hayashi M, Imanish Y (2001) Gradient micropattern immobilization of heparin and its interaction with cells. *J Biomater Sci Polym Ed* 12:367–378
- Jiang B, Liou GI, Behzadian MA, Calwell RB (1994) Astrocytes modulate retinal vasculogenesis: effects on fibronectin expression. *J Cell Sci* 107:2499–2508
- Karp JM, Langer R (2007 October) Development and therapeutic applications of advanced biomaterials. *Curr Opin Biotechnol* 18(5):454–459. Epub 2007 Nov 5. Review
- Knapp DM, Helou EF, Tranquillo RT (1999) A fibrin or collagen gel assay for tissue cell chemotaxis: assessment of fibroblast chemotaxis to RGDSP. *Exp Cell Res* 247:543–553
- Koo LY, Irvine DJ, Mayes AM, Lauffenburger DA, Griffith LG (2002 April 1) Co-regulation of cell adhesion by nanoscale RGD organization and mechanical stimulus. *J Cell Sci* 115(Pt 7):1423–1433
- Kurz H, Burri PH, Djonov VG (2003) Angiogenesis and vascular remodeling by intussusception: from form to function. *News Physiol Sci* 18:65–70
- Lauffenburger DA, Horwitz AF (1996) Cell migration: a physically integrated molecular process. *Cell* 84(3):359–369
- Lauffenburger DA, Linderman JJ (1993) Receptors: models for binding. Trafficking and signaling. Oxford University Press, New York
- Laukaitis CM, Webb DJ, Donais K, Horwitz AF (2001) Differential dynamics of alpha 5 integrin, paxillin, and alpha-actinin during formation and disassembly of adhesions in migrating cells. *J Cell Biol* 153:1427–1440
- Lavik E, Langer R (2004) Tissue engineering: current state and perspectives. *Appl Microbiol Biotechnol* 65:1–8
- Li S, Guan JL, Chien S (2005) Biochemistry and biomechanics of cell motility. *Annu Rev Biomed Eng* 7:105–150
- Lo CM, Wang HB, Dembo M, Wang YL (2000) Cell movement is guided by the rigidity of the substrate. *Biophys J* 79(1):144–152
- Lu Y, Shansky J, Del TM, Ferland P, Wang X, Vandenberg H (2001) Recombinant vascular endothelial growth factor secreted from tissueengineered bioartificial muscles promotes localized angiogenesis. *Circulation* 104:594–599
- Lutolf MP, Hubbell JA (2003 May–June) Synthesis and physicochemical characterization of end-linked poly(ethylene glycol)-co-peptide hydrogels formed by Michael-type addition. *Biomacromolecules* 4(3):713–722
- Maheshwari G, Lauffenburger DA (1998) Deconstructing (and reconstructing) cell migration. *Microsc Res Tech* 43(5):358–368
- Maheshwari G, Brown G, Lauffenburger DA, Wells A, Griffith L (2000 May) Cell adhesion and motility depend on nanoscale RGD clustering. *J Cell Sci* 113(Pt 10):1677–1686
- Makowski L, Magdoff-Fairchild B (1986) Polymorphism of sickle cell hemoglobin aggregates: structural basis for limited radial growth. *Science* 234:1228
- Massia SP, Hubbell JA (1990 June) Covalent surface immobilization of Arg-Gly-Asp- and Tyr-Ile-Gly-Ser-Arg-containing peptides to obtain well-defined cell-adhesive substrates. *Anal Biochem* 187(2):292–301
- Massia SP, Hubbell JA (1991) An RGD spacing of 440 nm is sufficient for integrin alpha V beta 3 mediated fibroblast spreading and 140 nm for focal contact and stress fiber formation. *J Cell Biol* 114(5):1089–1100
- Massia SP, Rao SS, Hubbell JA (1993) Covalently immobilized laminin peptide Tyr-Ile-Gly-Ser-Arg (YIGSR) supports cell spreading and co-localization of the 67-kilodalton laminin receptor with alfa-actinin and vinculin. *J Biol Chem* 268(11):8053–8059
- Matsumoto T, Mooney DJ (2006) Cell instructive polymers. *Adv Biochem Eng Biotechnol* 102(113–37):113–137
- Metzler R, Klafter J (2000) The random walk's guide to anomalous diffusion: a fractional dynamics approach. *Phys Rep* 339:1–77

- Mikos AG, Herring SW, Ochareon P, Elisseeff J, Lu HH, Kandel R, Schoen FJ, Toner M, Mooney D, Atala A, Van Dyke ME, Kaplan D, Vunjak-Novakovic G (2006) Engineering complex tissues. *Tissue Eng* 12:3307–3339
- Moghe PV, Nelson RD, Tranquillo RT (1995) Cytokine-stimulated chemotaxis of human neutrophils in a 3-D conjoined fibrin gel assay. *J Immunol Methods* 180:193–211
- Mosesson MW, Siebenlist KR, Meh DA (2001) The structure and biological features of fibrinogen and fibrin. *Ann N Y Acad Sci* 936:11–30
- Mrksich M (2000) A surface chemistry approach to studying cell adhesion. *Chem Soc Rev* 29:267–273
- Mrksich M, Chen CS, Xia Y, Dike LE, Ingber DE, Whitesides GM (1996) Controlling cell attachment on contoured surfaces with self-assembled monolayers of alkanethiolates on gold. *Proc Natl Acad Sci USA* 93(20):10775–10778
- Mrksich M, Dike LE, Tien J, Ingber DE, Whitesides GM (1997) Using microcontact printing to pattern the attachment of mammalian cells to self-assembled monolayers of alkanethiolates on transparent films of gold and silver. *Exp Cell Res* 235(2):305–313
- Nagai Y, Unsworth LD, Koutsopoulos S, Zhang S (2006 September 28) Slow release of molecules in self-assembling peptide nanofiber scaffold. *J Control Release* 115(1):18–25. Epub 2006 July
- Nelson RD, Quie PG, Simmons RL (1975) Chemotaxis under agarose: a new and simple method for measuring chemotaxis and spontaneous migration of human polymorphonuclear leukocytes and monocytes. *J Immunol* 115:1650–1656
- Niklason LE, Langer R (2001) Prospects for organ and tissue replacement. *JAMA* 285:573–576
- Palecek SP, Loftus JC, Ginsberg MH, Lauffenburger DA, Horwitz AF (1997) Integrin-ligand binding properties govern cell migration speed through cell-substratum adhesiveness. *Nature* 385(6616):537–540
- Panyam J, Zhou W-Z, Prabha S, Sahoo SK, Labhasetwar V (2002) Rapid endo-lysosomal escape of poly(DL-lactide-co-glycolide) nanoparticles: implication for drug and gene delivery. *FASEB J* 16:1217–1226
- Pennacchi M, Armentano I, Zeppetelli S, Lanzaro L, Kenny JM, Netti PA (2004) Effects of material surface nanopatterning on cell morphology and orientation. In: *Advances in micro and nanoengineering*. Editura Academiei Romane, Bucarest, Romania, pp 9–22
- Raeber GP, Lutolf MP, Hubbell JA (2005) Molecularly engineered PEG hydrogels: a novel model system for proteolytically mediated cell migration. *Biophys J* 89(2):1374–1388
- Rapraeger AC (2000) Syndecan-regulated receptor signaling. *J Cell Biol* 149:995–998
- Raucher D, Sheetz MP (2000) Cell spreading and lamellipodial extension rate is regulated by membrane tension. *J Cell Biol* 148(1):127–136
- Rhoads DS, Guan JL (2007 November 1) Analysis of directional cell migration on defined FN gradients: role of intracellular signalling molecules. *Exp Cell Res* 313(18):3859–3867. Epub
- Richardson TP, Peters MC, Ennett AB, Mooney DJ (2001) Polymeric system for dual growth factor delivery. *Nat Biotechnol* 19(11):1029–1034
- Rogers JA, Chen CS, Xia Y, Dike LE, Ingber DE, Whitesides GM (2000) Printing, molding, and near-field photolithographic methods for patterning organic lasers, smart pixels and simple circuits. *Synthetic Met* 115:1–3
- Rottner K, Hall A, Small JV (1999) Interplay between Rac and Rho in the control of the substrate contact dynamics. *Curr Biol* 9:640–648
- Ruhrberg C, Gerhardt H, Golding M, Watson R, Ioannidou S, Fujisawa H, Betsholtz C, Shima DT (2002) Spatially restricted patterning cues provided by heparin-binding VEGF-A control blood vessel branching morphogenesis. *Genes Dev* 16:2684–2698
- Ruoslahti E (1996) RGD and other recognition sequences for integrins. *Annu Rev Cell Dev Biol* 12:697–715
- Sage EH, Vernon RB (1994) Regulation of angiogenesis by extracellular matrix: the growth and the glue. *J Hypertens Suppl* 12(10):S145–S152
- Savarino L, Baldini N, Greco M, Capitani O, Pinna S, Valentini S, Lombardo B, Esposito MT, Pastore L, Ambrosio L, Battista S, Causa F, Zeppetelli S, Guarino V, Netti PA (2007) The performance of poly-epsilon-caprolactone scaffolds in a rabbit femur model with and without autologous stromal cells and BMP4. *Biomaterials* 28:3101–3109

- Schoenwaelder SM, Burridge K (1999) Bidirectional signaling between the cytoskeleton and integrins. *Curr Opin Cell Biol* 11(2):274–286. Review
- Schwartz MA, Schaller MD, Gisser MH (1995) Integrins: emerging paradigms of signal transduction. *Annu Rev Cell Dev Biol* 11:549–599
- Shen H, Tan J, Saltzman WM (2004) Surface-mediated gene transfer from nanocomposites of controlled texture. *Nat Mater Des* 3:569–574
- Singhvi R, Kumar A, Lopez GP, Stephanopoulos GN, Wang DI, Whitesides GM, Ingber DE (1994) Engineering cell shape and function. *Science* 264:696–698
- Stupack DG, Cheresh DA (2002) ECM remodeling regulates angiogenesis: endothelial integrins look for new ligands. *Sci STKE* 119:PE7
- Suciati T, Howard D, Barry J, Everitt NM, Shakesheff KM, Rose FR (2006) Zonal release of proteins within tissue engineering scaffolds. *J Mater Sci Mater Med* 17:1049–1056
- Sun W, Darling A, Starly B, Nam J (2004) Computer-aided tissue engineering: overview, scope and challenges. *Biotechnol Appl Biochem* 39:29–47
- Swartz MA (2003) Signaling in morphogenesis: transport cues in morphogenesis. *Curr Opin Biotechnol* 14:547–550
- Tabata Y (2005) Significance of release technology in tissue engineering. *Drug Discov Today* 10:1639–1646
- Tranquillo RT (1991 July) Chemotactic movement of single cells. *ASGSB Bull* 4(2):75–85. Review
- Ungaro F, Biondi M, d'Angelo I, Indolfi L, Quaglia F, Netti PA, La Rotonda MI (2006) Microsphere-integrated collagen scaffolds for tissue engineering: effect of microsphere formulation and scaffold properties on protein release kinetics. *J Control Release* 113:128–136
- Van der Fuler A, Sonnenberg A (2001) Function and interactions of integrins. *Cell Tissue Res* 305:285–298
- Van Hinsbergh VW, Collen A, Koolwijk P (2001) Role of the fibrin matrix in angiogenesis. *Ann N Y Acad Sci* 936:426–437
- Weisel JW, Nagaswami C, Makowski L (1987) Twisting of fibrin fibers limits their radial growth. *Proc Natl Acad Sci USA* 84:8991
- Whitesides GM, Ostuni E, Takayama S, Jiang X, Ingber DE (2001) Soft lithography in biology and biochemistry. *Annu Rev Biomed Eng* 3:335–373
- Wijelath ES, Murray J, Rahman S, Patel Y, Ishida A, Strand K, Aziz S, Cardona C, Hammond WP, Savidge GF, Rafii S, Sobel M (2002) Novel vascular endothelial growth factor binding domains of fibronectin enhance vascular endothelial growth factor biological activity. *Circ Res* 91(1):25–31
- Wilkinson CDW, Riehle M, Wood M, Gallagher J, Curtis ASG (2002) The use of materials patterned on a nano- and micro-metric scale in cellular engineering. *Mat Sci Eng C* 19:1–2
- Yamada KM, Pankov R, Cukierman E (2003) Dimensions and dynamics in integrin function. *Braz J Med Biol Res* 36:959–966
- Zaari N, Rajagopalan P, Kim SK, Engler AJ, Wong JY (2004) Photopolymerization in microfluidic gradient generators: microscale control of substrate compliance to manipulate cell response. *Adv Mater* 16(23–24):2133–2137
- Zamir E, Geiger B (2001) Components of cell-matrix adhesions. *J Cell Sci* 114:3577–3579
- Zhu B, Eurell T, Gunawan R, Leckband D (2001 September 5) Chain-length dependence of the protein and cell resistance of oligo(ethylene glycol)-terminated self-assembled monolayers on gold. *J Biomed Mater Res* 56(3):406–416
- Zisch AH, Lutolf MP, Ehrbar M, Raeber GP, Rizzi SC, Davies N, Schmokel H, Bezuidenhout D, Djonov V, Zilla P, Hubbell JA (2003) Cell demanded release of VEGF from synthetic, biointeractive cell-ingrowth matrices for vascularized tissue growth. *FASEB J* 17(15):2260–2262

Chapter 12

Materials Surface Effects on Biological Interactions

Josep A. Planell, Melba Navarro, George Altankov, Conrado Aparicio, Elisabeth Engel, Javier Gil, Maria Pau Ginebra, and Damien Lacroix

Abstract At present it is well accepted that different surface properties play a strong role in the interaction between synthetic materials and biological entities. Surface properties such as surface energy, topography, surface chemistry and crystallinity affect the protein adsorption mechanisms as well as cell behaviour in terms of attachment, proliferation and differentiation. The aim of this chapter is to show the most relevant processes and interactions that take place during the first stages of contact between the material and the physiological environment. Some examples show that the modification of different biomaterials surfaces affects both protein adsorption and cell behaviour.

Keywords Surface properties • Topography • Surface chemistry • Cell–material interactions

12.1 Introduction

A multiplicity of parameters such as implant location, size, shape, micromotion, surface chemistry and topography, and porosity among others play a very relevant role in the behaviour in service of biomaterials. The host characteristics, namely, age and health condition, are also factors that need to be taken into account. Immediately after a prosthetic device is implanted into the body, a cascade of events is triggered. As soon as a biomaterial becomes implanted in vivo, it gets in direct contact with the physiological environment consisting in a highly corrosive aqueous medium containing different types of ions, different molecules such as proteins,

J.A. Planell (✉), C. Aparicio, E. Engel, J. Gil, M.P. Ginebra,
Technical University of Catalonia (UPC), Av. Diagonal 647,
Barcelona 08028, Spain
email: Joesp.A.Planell@upc.edu

polysaccharides and enzymes, as well as different types of cells non-adherent an even adherent. The initial events taking place on the biomaterial surface upon implantation will affect very strongly the future life in service of the implant.

The ability of the material to be wetted by the physiological fluids is the first factor to be taken into account immediately after implantation. The initial events occurring at the biomaterial surface are highly ruled by its surface properties and the complex interplay that exists between them. Indeed, the hydrophilicity or the hydrophobicity of the material surface is a consequence of its surface energy which turns out to be related with the electrical charges distribution. At the same time, the distribution of electrical charges is a consequence of the surface chemistry and crystallinity and all these properties are affected by the surface topography.

Cell adhesion requires the presence of an appropriate proteinaceous substrate where cell adhesion receptors such as integrins can be attached and form the cells anchoring points. The formation of the right adhesive layer of proteins or the opsonization of the surface at very early stages depends on the surface properties of the material. Opsonization is the process of coating microorganisms or material surface with plasma proteins such as C3b (activated constituent of the group of proteins circulating in the serum of blood known as the complement system) and IgG (Immunoglobulin G) to label them as a foreign body and target it for attack by phagocytic cells (Tang et al. 1998). This is what happens in the case of most biomaterials used in medical devices.

The foreign body response is basically an inflammatory response that persists as long as there is a foreign body present to respond to. An inflammatory reaction involves the migration of neutrophils and monocytes/macrophages to the injury site by chemotaxis of different cytokines in order to phagocytose all the material labelled as foreign and cellular debris. Neutrophils disappear after finishing their task leaving place to macrophages. A sustained macrophage response is typical of a chronic inflammatory reaction and is common in most implants.

According to some authors, foreign body reaction starts during this persistent response of macrophages (Hunt 2004). The sustained and numerous presences of macrophages lead the formation of multinucleated giant cells or foreign body giant cells (FBGC) as a response to the effort to overcome the frustrated phagocytosis process experienced by single cells (Anderson et al. 1996; Dee et al. 2002). At this stage, macrophages and also fibroblasts release chemotactic factors for the recruitment of more fibroblasts. Macrophages inactivate their attack mechanisms and fibroblasts become the main cell line. At this time, fibroblasts start secreting a collagen I and III-based extracellular matrix that will encapsulate the material. The thickness of this extracellular matrix will vary depending on the movement of the implanted device and will isolate the material from the host tissue.

The foreign body reaction is a serious limitation especially in those cases where materials have to be in direct contact and integrate with the surrounding tissues; it can also lead to chronic pain and eventual device rejection and failure. The result of all the previous considerations is that the implant or medical device surface plays the leading role in its interaction with the biological environment. Consequently, the study and

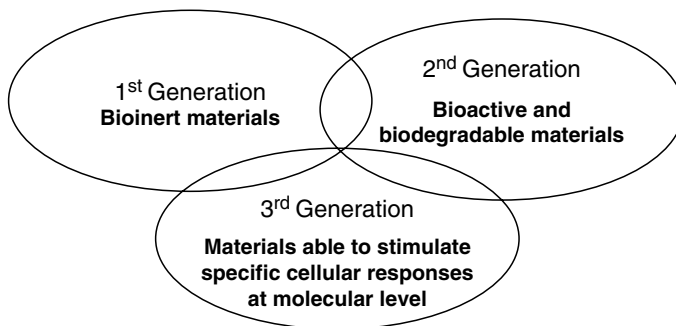


Fig. 12.1 Biomaterials generations

characterization, modification and functionalization of the biomaterials surfaces are probably the main strategies for success of implants and the tissue regeneration.

The development of materials with appropriate bulk and surface properties aiming at different goals such as support, fixation or substitution roles represents a very challenging scientific and technological issue. Most of the materials used for biomedical applications along most of the twentieth century were the same as those successfully used for other industrial sectors such as in the chemistry, energy, automotive, machine tool and aerospace industries.

The history of biomaterials' progress during the last 50 years can be understood in terms of three different generations (Fig. 12.1): a first generation (bioinert materials), a second generation (bioactive and biodegradable materials), and a third generation (materials designed to stimulate specific cellular responses at the molecular level) (Hench and Polak 2002). It is worth noting that this classification of the materials used for biomedical purposes does not imply that the appearance of a new generation of materials would exclude the use of preceding ones. In fact, materials used within the first generation of biomaterials are still successfully used in a wide spectrum of applications. Third generation materials are expected to overcome many limitations that still require adequate solutions, but by no means it is expected that third generation biomaterials should totally replace the materials from preceding ones.

12.1.1 First Generation

The progress of biomaterials has been taking place by continuously adding new demands to the list of required properties. New biomaterials have been developed as a response to these demands meant to cover new needs in the field. Concepts such as foreign body reaction, stress shielding, biocompatibility, biodegradability, bioactivity or osteoinduction are some of the demands that have steered the research for new biomaterials.

At the beginning, the main concern was to develop or select materials that combined the necessary physical properties for the devices in which they are used to match the functionality of the substituted tissue with a minimal toxic response of the host (Hench 1980). Thus, the first generation biomaterials were “inert materials” focused on achieving the minimum immune response and foreign body reaction. These first generation biomaterials consist in materials used and developed for different industrial applications, such as chemistry, food, transport and energy among others, that combine physical and chemical properties meant to endure the body aggressive environment. Among metallic materials only a few families of alloys can be selected, being the most widely used stainless steels, Co-Cr alloys and Ti and Ti alloys. Among ceramic materials, oxidic ceramics that cannot oxidize are the main candidates. Finally, among polymers and polymeric matrices in composites, fully polymerized thermoplastics and thermosetables are the most widely used.

12.1.2 Second Generation

Inertness reduces the toxic response of the host. However, it does not eliminate the foreign body reactions and the formation of a fibrous layer that envelops the implant or device avoiding the direct contact between the material surface and the surrounding tissue.

Second generation biomaterials are considered to appear between 1980 and 2000. This second generation was characterized by the development of materials aimed to overcome the formation of a fibrous layer that hindered the surface/tissue interaction. This goal was achieved along two different paths: (a) by promoting a specific biological response, and (b) by using biodegradable materials able to degrade progressively as the new tissue is regenerated. This was the generation of “bioactive materials” and “biodegradable materials”. For some authors the term “bioactivity” refers to the capacity of a material to elicit a specific biological response at its interface which results in the formation of a bond between the tissues and the material (Hench and Andersson 1993). Other authors proposed a definition that not only includes the ability of a material to bind to tissues but also their capacity to modulate other biological events (Black 2006).

In the case of materials used for bone applications, the most common expression of bioactivity is related to the formation of a mineral CaP layer that promotes direct binding between the implant and the tissue. Bioactivity was initially easy to associate to calcium phosphate ceramics. These materials do promote the *in vivo* deposition and formation of a biological hydroxyapatite layer at the material surface, improving in this way the interaction between the material surface and the bone tissue.

These materials have been used in a wide range of dental and orthopaedic applications aiming for bone tissue repair or regeneration. Bioactive materials accomplished clinical use by the mid-1980s in the form of bioactive glasses, ceramics, glass-ceramics, and composite materials.

In the case of metallic materials two strategies have been developed to obtain calcium phosphate bioactive surfaces for bone applications. One consists in coating the metallic implant surface with a calcium phosphate by different means, including plasma spray or other chemical methods, and the other consists in modifying the surface chemistry in order to induce in vivo or in vitro the nucleation of a CaP. A more general approach will consist in the material functionalization that will be described in the case of a polymer substrate.

Polymers bioactivity depends on the functional groups and binding sites available at the material surface. Thus, in the case of polymers, bioactivity can be improved by coupling certain biomolecules to their surface. This same strategy can be also used in the case of metals and ceramic materials.

Biodegradable materials are mainly represented by both natural and synthetic polymers that showed a controlled chemical breakdown and resorption of the polymer chains. The concept of bioabsorbable material was introduced in the late 1960s (Kulkarni et al. 1966; Kulkarni et al. 1971). In the last decades, these materials have been used in several orthopaedic applications such as bone substitution, repair of fractures (including ligament fixation), as sutures, rods, screws, pins and plates (Ciccone et al. 2001), and also in multiple non-orthopaedic applications such as cardiovascular, and nervous regeneration applications (Huang and Huang 2006; Teixeira et al. 2007).

12.1.3 Third Generation

Biomaterials developed during this generation are designed to be able to trigger specific cellular responses at the molecular level (Hench and Polak 2002). During this generation the biodegradability and bioactivity concepts are combined to generate biomaterials that are both degradable and bioactive. In addition to these two properties, it is also sought that materials have the ability to stimulate specific cellular events and behaviour depending on their final application.

The beginnings of this third generation of biomaterials coincide with the development of new 3D scaffolds for tissue engineering. Tissue engineering emerged as an alternative to overcome limitations such as donor site scarcity, rejection, diseases transfer, harvesting costs, and postoperative morbidity due to tissue transplantation (Banwart et al. 1995; Fernyhough et al. 1992; Goulet et al. 1997). The ultimate aim of tissue engineering is to regenerate and return the functionality to damaged tissues or organs. Thus, temporary 3D porous scaffolds are developed to be used as support and to stimulate cellular ingrowth, attachment, proliferation, and differentiation.

There are some tasks that cannot be achieved by the material itself. Therefore, growth factors and peptide sequences among others are used in combination with 3D scaffolds to repair and regenerate tissues and organs mimicking the natural signalling pathway (Hardouin et al. 2000).

Thus, 3D porous scaffolds and functionalized surfaces with biomolecules such as peptide motifs and proteins that simulate the extracellular matrix components as

to trigger specific cell responses are one of the most important achievements during the third generation (Agrawal and Ray 2001; Hutmacher et al. 2000; Temenoff and Mikos 2000).

12.1.4 Biomaterials for Substitution, Repair and Regeneration

Biomaterials development through these three generations has made possible the availability of materials exhibiting physical, chemical and biological properties as to satisfy numerous applications. These applications range from those that require materials for repair or substitution of tissues or organs to those requiring more sophisticated materials for more complex applications such as regeneration tasks. Thus, there are two main approaches that can be distinguished within the final applications of biomaterials. The first one is related to repair and substitution purposes, and the second one is related to regeneration of tissues and organs.

The first approach deals with those materials used for the elaboration of implants and prosthesis that are required to return the functionality of the tissue or organ in a short period of time, and where regeneration will not be possible. These materials are intended to fix, support or substitute the damaged tissue or organ, such as in traumatological treatments and pathologies that require urgent treatment as in the case of accidents. Most of these materials are included in the first and second generation categories of biomaterials.

The repair and substitution approach requires both non-degradable and degradable materials able to integrate and form a direct bond with the tissue as in the case of the osseointegration phenomenon. In this case, the aim is to develop materials whose surfaces stimulate and allow a direct union between the material and the osseous tissue to be formed while hindering the formation of a fibrous protein layer that envelops the implant and avoids proper material/tissue integration. Thus, there is a clear need to create surfaces able to overcome this problem. The strategies used to enhance material-protein and material-cell interactions will be discussed later in this chapter.

The second approach is related to the use of materials for tissue and organ regeneration purposes. Devices used for these applications must provide temporary support until the new tissue is regenerated and the damaged tissue/organ recovers its functionality. Thus, in this case, materials must be biodegradable and its degradation rate should match the healing process of the new tissue. This approach includes mainly materials from the second and third generation.

Another important issue within the regeneration approach is the use of cells, in particular stem cells which have raised great interest in the last years. Given the numerous limitations related to the use of autologous tissue and other alternative tissue sources such as allografts and xenografts, the use of new techniques involving the use of growth factors and stem cells has been boosted. The term “stem cell” implies that: (1) cells are capable of self-renewal, (2) cells have the ability to give rise to different cell lineages, and (3) cells are capable of in vivo functional regeneration of the tissues to which they give rise (Verfaillie 2002). Stem cells possess

the capacity to differentiate into a variety of cell phenotypes. This phenomenon is also known as “potency”, and varies depending on the cells source; cells able to differentiate in only one cell phenotype are unipotent cells, while cells able to differentiate into a wide variety of cells are pluripotent cells. Totipotent cells are those able to differentiate in any cell phenotype. The potency ability of stem cells is considered as a promising tool for tissue engineering applications and transplantation.

12.1.5 Stem Cells Sources

Stem cells can be obtained from both embryonic and adult tissues. Embryonic stem cells are collected at very early stages of embryogenesis. In spite of their totipotency, their collection and usage deals with important ethical issues. The potency of adult progenitor cells is more reduced than in the case of the embryonic ones, however, their collection does not involve ethical issues. These cells can be retrieved from bone marrow, brain, and adipose tissue (Stoltz et al. 2006) (Fig. 12.2).

Mesenchymal stem cells (MSCs) are together with muscle-derived stem cells, the most used for tissue engineering applications. The term MSCs is usually used to refer to connective tissue cells in adults tissues namely (myo)fibroblasts, bone, cartilage, fat, tendon, muscles, and nerve tissue. MSCs are a subgroup of stem cells that also have the ability to give rise to different cell lineages (Pittenger et al. 1999). These cells can be isolated from a variety of sources including bone marrow, fat, umbilical cord blood, and also peripheral blood (Chim and Schantz 2006, Fuchs et al. 2005; Kern et al. 2006), and may differentiate into osteoblasts, chondroblasts, myoblasts, and adipocytes.

Among the different MSC sources, bone marrow is the most currently used. Bone marrow is a natural reservoir of skeletal MSCs. These MSCs are found in the stromal compartment of bone marrow and represent a minimal fraction (0.001–0.01%) of the total population of nucleated cells in marrow (Chim and Schantz 2006).

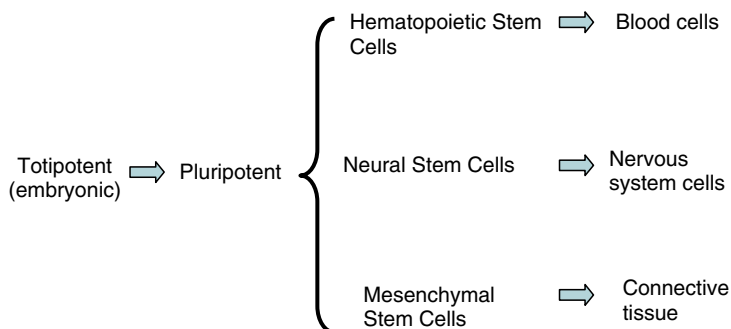


Fig. 12.2 Stem cells hierarchy

Therapies involving the use of progenitor cells require the presence of specific factors or cues that trigger the activation of particular cell behaviour and induce cell differentiation towards a determined cell lineage. Therefore, tissue regeneration supposes that not only materials' bulk properties are important but also their surface properties play a main role. Both topographical and chemical surface characteristics are of paramount importance in the interactions between materials and cells. Thus, it is expected that biomaterials aimed to regeneration purposes combine biodegradability and bioactivity together with surface properties that provide them the ability to stimulate specific cellular responses.

12.2 Surface Modification to Improve Cell–Material Interactions

In general, the success of a biomaterial strongly depends on its interaction with the biological environment. There are applications where a direct and tight contact between the tissue and the materials is required while there are other applications where a rather antifouling behaviour is needed. Within this context, material surface properties are of paramount importance.

Once a material is in contact with physiological fluids, the first interactions that take place are between the material surface and water molecules. The formation of a water coating layer involving the material occurs within a period of nanoseconds. This first stage is highly dependent on the surface properties of the material and will condition and determine which biomolecules and proteins will interact with the surface. After hydration, a second stage occurring from some seconds up to hours after implantation takes place. This stage consists in the interaction of the material surface with sugars, lipids and other macromolecules found in the physiological medium such as proteins. During this stage the “Vroman effect” is held and the material surface is covered by an adsorbed layer of proteins (McFarland et al. 1999). Finally, a third stage takes place after time periods ranging from minutes up to days after implantation. During this third stage, cells make contact with the surface and interact with it. This third stage is characterized by multiple complex interactions between the extracellular matrix proteins, cell membrane proteins and cytoskeleton proteins, surface chemistry and topography, the micro and macrostructure of the material (porosity, pore size and geometry, interconnectivity) and the released degradation by-products of the material if any. The complete process is illustrated in Fig. 12.4.

Thus, in general, biocompatibility and material biological responses are dependent on the protein adsorption process which is highly influenced by the materials' surface properties. Indeed, surface features such as its chemical composition, and surface energy determine the nature of the proteins adsorbed to the surface and their orientation and conformation.

Proteins' orientation and conformation are very important aspects affecting subsequent cell attachment and adhesion. Depending on these two parameters, the

protein peptide sequence availability will vary. Only those peptide sequences exposed to the cell–material interface are accessible to cell membrane receptors while those located in the interior of the protein are not.

Initial protein–material interactions are crucial given that they mediate cell attachment and adhesion processes. The proteins adsorbed on the material surface interact with specific cell adhesion proteins known as integrins. These are cell transmembrane proteins that possess two glycoproteic units (α and β) and three domains (cytoplasmic, transmembrane, and the extracellular one) as shown in (Fig. 12.3). The extracellular domains of the α and β units possess receptors for the specific recognition of cell adhesive peptide motifs that are contained in some adhesive proteins present in the extracellular matrix (ECM) (Siebers et al. 2005). The cytoplasmic domain interacts with the cytoskeleton fibres and other intracellular signalling molecules. Thus, integrins are able to mediate cell attachment and adhesion to the different surfaces. The cell adhesion process triggers some mechanical and chemical signals that affect further cell events such as proliferation and differentiation that indeed determine cell functionality (Anselme et al. 2000).

Cells interaction with the external medium and specifically, with the material surface is carried out through their cytoplasm, in particular, through cell structures known as lamellipodia or pseudopodia depending on the cell type, which are cell extensions formed by actin filaments (Anselme 2000). These lamellipodia possess smaller extensions which are also formed by actin filaments. These are very thin and long structures that sense the extracellular matrix and material surface. Fillopodia are the actuators of the adhesion, spreading and motility processes. Integrins located within these long and thin cytoplasm extensions interact with the substrate surface creating focal contacts that are points where several integrin receptors meet to form stronger adhesion points. Depending on the surface conditions, the fillopodia will receive more or less signals allowing the cell to attach or separate from the surface, to move in one direction or other, to get a very spread or rounded morphology, etc. (Benigno et al. 2001; Magel et al. 1993).

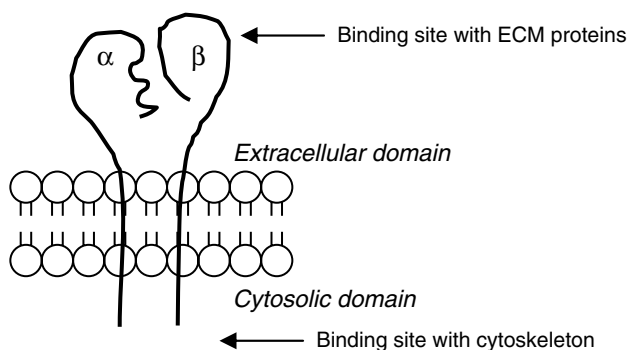


Fig. 12.3 Scheme of the structure of integrins

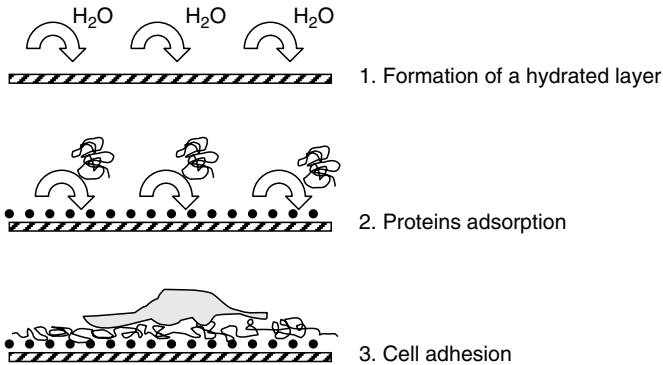


Fig. 12.4 Illustration of the sequence of events taking place at the material surface during the first stages of contact with the physiological medium

In addition to the adhesion process, cell–material interactions may be also controlled by adding some specific cues that induce their proliferation, differentiation or other cellular functions. These cues can be coupled to the materials surface by using different functionalization techniques.

In the cases where proteins adsorption, cell adhesion and formation of direct binding between the tissue and the material surfaces are not desired, materials surfaces must be modified in order to act as antifouling surfaces where proteins do not adsorb and cells do not attach and grow.

Thus, it is clear that materials surfaces are a key issue in order to enhance and control the biological response of biomaterials. Both surface chemistry and surface topography are the most important features affecting the biological response of a biomaterial.

12.2.1 Surface Topography

As shown in numerous works, surface roughness and topography are two important aspects that play a main role in cell response (Healy et al. 1996; Chesnel et al. 1995). It has been accepted that cell attachment, adhesion and proliferation on a surface can be guided by microtopography. In fact, numerous studies have been carried out and corroborate that topography influence cell adhesion (Anselme et al. 2000; Huang et al. 2004), morphology (Chen et al. 1997), migration (Tan and Saltzman 2002), orientation, focal adhesion (Diener et al. 2005), and differentiation (Zinger et al. 2005).

In some applications where cell orientation is critical to achieve a functional tissue, namely tendons, nerves, corneal stroma, and intervertebral disc regeneration, contact guidance of cells by micro–and nano-topographical features is a promising strategy. In the case of nervous tissue, it has been reported that aligned channels in

the micrometer scale are considered as the surface topographical patterns with the best results under in vitro conditions. In the case of bone tissue both micro and nanotopography have shown to induce bone cells response. Nanotopography, specifically random nanostructures have shown to elicit the best cell response to induce osteoblast differentiation for tissue regeneration (Dalby et al. 2007). In the case of implants to substitute and repair bone there seem to be an optimal roughness in the microscale that induces faster and appropriate bone growing in vitro and in vivo on rough titanium surfaces (Aparicio et al. 2003).

The use of micro or nanotopographic features depends mainly on the size of the cell structures to be influenced by the topographic changes and must be in accordance to the biological to be activated. As already mentioned, proteins are the first entities to become adsorbed to the implanted substrates. Microscale topographic structures are too large and can not be felt by proteins, in this case, nanotopographic features are closer to the dimension scale of proteins and adjust better to their size. Thus, it is possible to influence to some extent proteins adsorption behaviour by controlling the nano-topography of the substrates. However, there are many questions that remain unclear still today such as the possibility to control protein configuration upon adsorption, packing density, and arrangement among others.

Protein conformation is a very important issue since it determines the amount and type of functional peptide sequences exposed to the surface/cell interface. It has been shown that topographical changes of nanometric order of magnitude can modify the conformation and activity of the adsorbed proteins (Roach et al. 2007). A wide variety of studies conducted and reported by different research groups, where different substrates, conditions, and types of proteins and cells have been used, have been carried out. These studies have been done in order to substantiate the effects of topography, and more specifically, the relationship between the proteins adsorption mechanism and surface topographic differences. However, they have not been able to provide a clear and unambiguous understanding of the role of topography in the protein adsorption processes.

Cells are entities larger than proteins and therefore, they can be stimulated by using larger features. In general, it is well known that features ranging between 10 and 100 μm do influence cells (Mrksich and Whitesides 1995). Nevertheless, it must be highlighted that not all cell phenotypes react in the same manner to topographical changes; it seems that topographical stimulation is highly cell dependent (Meyer et al. 2005).

12.2.2 Surface Chemistry

Modification of surface chemistry is the most direct way to influence protein adsorption and cell behaviour. By tailoring the functional groups available at the material surface, it is possible to modify the surface properties, and consequently wettability, surface electrical charges, and free energy will change and as a result,

the affinity of some proteins for a particular substrate will be altered. Even though it is well accepted that certain functional groups enhance protein/surface interactions, at present there is no methodology that allows a full control of the protein conformation and orientation after adsorption (Roach et al. 2007).

Surface modification methods to improve the interactions between the material surface and cells have evolved during the last decades. One of the main goals of the second generation of biomaterials was the development of “bioactive materials”. Surface bioactivation can be achieved functionalizing surfaces with different biomolecules by means of a variety of methods where both chemical bonding and physical adsorption take place. Metallic and polymeric surfaces were studied and modified using methods such as dip-coating techniques, the formation of self-assembled monolayers (SAMs) and binding polymer chains to the surface to enhance the adhesion of cells, to influence proliferation and differentiation rates, and to achieve faster and more stable integration between the material and the tissue as in the case of dental implants and some orthopaedic prostheses (Blawas and Reichert 1998; Scotchford et al. 1998). Covalent chemical coupling of polymers and biomolecules to the substrates has been achieved through silanized titania surfaces, using amino- and carboxyl-directed immobilization mainly through glutaraldehyde chemistry, and photochemistry by “grafting to” biomolecules with a photoactive group (Xiao et al. 1998, 2001; Colloiod et al. 1993).

During the third generation more sophisticated “bottom-up” and “top-down” techniques have been developed to engineer surfaces with high specificity levels as well as the synthesis and tailoring of new biomolecules for specific applications. The development of more complex biopolymers and biomolecules such as elastin-like biopolymers including peptide sequences that induce mineralization and cell adhesion, or self-assembled amphiphilic peptides that include cell signalling cues are new approaches to mimic the natural process by which collagen induces the assembling of calcium phosphate, and hydroxyapatite crystallites within bone to generate its mineral rigid phase (Rodríguez-Cabello et al. 2007; Sergeant et al. 2008)

To provide evidences about the way in which surface properties affect the biological behaviour, some specific cases showing the importance and effect of surface chemistry and topography in biological response are described below.

12.3 Oxidation Treatment of NiTi Shape Memory Alloys to Obtain Ni-Free Surfaces and to Enhance Biocompatibility

NiTi shape memory alloys have raised great interest for different biomedical applications such as orthodontic wires, vascular, urological and gastroenterological stents, staples for orthopaedics, etc. This is due to their unique properties such as superelasticity, shape memory and their excellent damping characteristics. However, in spite of their attractive properties, these are quite controversial materials since they might cause negative effects such as allergies and potential carcinogenesis,

Table 12.1 Surface properties of the NiTi alloy before and after the oxidation treatment. Mean values \pm SD

NiTi alloy	Sa (nm)	Sz (nm)	Ssk	Sku	CA ($^{\circ}$)	γ^d (mJ/m 2)	γ_t (mJ/m 2)
Untreated	21.8 \pm 4.8	373.4 \pm 58.1	-0.5 \pm 0.3	10 \pm 4.2	63.2 \pm 2.6	11.3 \pm 2.3	49.4 \pm 2.3
Oxidized	103.5 \pm 9.7	863.2 \pm 93.3	0.1 \pm 0.1	3.1 \pm 0.2	59.0 \pm 2.2	13.3 \pm 1.8	52.1 \pm 1.9

Sa = spacing between local peaks; Sz =; Ssk = skewness surface plane; Sku = kurtosis of the surface; CA = Contact angle; γ^d = polar component of the total surface free energy; γ_t = total surface free energy

which are attributed to the Ni release to the surrounding medium (Wataha et al. 2001; Peltonen 1979; Dunlap et al. 1989).

To overcome this limitation and reduce the amount of Ni exposed at the material surface, an oxidation treatment was developed. It is based on a thermal treatment at a pressure of 3×10^{-2} mbar and 400 $^{\circ}$ C during 2 h 30 min that leads to the formation of a stoichiometric TiO $_2$ almost Ni-free protective layer (Michiardi et al. 2004).

The formation of this TiO $_2$ layer introduces some important modifications at the material surface. It increases its roughness from a mean Sa = 22 nm to Sa = 103 nm, and enhances the hydrophilic character of the surface, mainly by increasing the polar component of its surface free energy (Michiardi et al. 2006, 2007) (Table 12.1).

It has been shown in previous studies that the surface changes caused by the formation of the TiO $_2$ layer on the NiTi material surface induce significant differences in protein adsorption and cell behaviour.

In a protein adsorption study performed with fibronectin, which is one of the most important adhesive proteins and with albumin, the results obtained showed that the adsorption of both proteins on the material surface was highly affected by the presence of the TiO $_2$ layer (Howlet et al. 1994; Altankov and Groth 1994; Grinnel and Feld 1982). In fact, a significantly higher amount of both proteins was adsorbed in the materials with the oxidation treatment than in the material without any treatment. In the case of albumin, a direct correlation between surface energy and the amount of protein adsorbed was observed, showing the highest values of protein when the polar component reached its highest value. However, fibronectin did not show any correlation between the amount of protein adsorbed and the variations of surface energy. These results suggest that in the case of fibronectin there must be other factors besides the polar component that also influence its behaviour (Michiardi et al. 2007).

In vitro biocompatibility studies carried out with MG63 osteoblastic-like cells seeded on treated and untreated NiTi surfaces have also corroborated the influence of surface characteristics in cell behaviour. According to this study, the expression of osteoblastic differentiation markers such as alkaline phosphatase and osteocalcin was higher in the cells seeded in the material with the oxidation treatment than in the NiTi surface without treatment (Michiardi et al. 2008). These differences could be attributed to the physicochemical differences between the treated and non-treated

surfaces such as chemical composition, polarity, and even crystalline oxide structure that affect the adsorbed proteins in the surface and, in turn, affects the cell response, and also to their topographical differences. The Sa value of treated NiTi surfaces was five times greater than the one of the untreated surfaces. Even if both of them are in the nanometer length scale there seems to be an effect of nanotopography on cells behaviour which is in agreement with other studies where a faster differentiation process is enhanced by nanotopographic roughness (Larsson et al. 1996).

Thus, in this case the modification of the material surface leads to a lower release of Ni ions to the medium, to a higher nanoroughness and to changes in the polar component of the free surface energy, and the combination of all these factors enhanced the biocompatibility of the material.

12.4 Surface Characterisation of Fully Biodegradable Composite Scaffolds for Bone Regeneration

Biodegradable poly (α -hydroxyacids), in particular, polylactic acid (PLA) are currently used in diverse biomedical application namely, sutures, pins, screws, and drug delivery systems (Middleton and Tipton 2000; Rokkanen 2000). In addition, PLA is a very interesting candidate for the development of tissue engineering scaffolds due to its degradability that can be tuned according to the percentages of PLA stereoisomers present in the copolymer, and also because its degradation by-products can be metabolized and eliminated from the body following natural pathways in the form of H₂O and CO₂ (Grizzi et al. 1995). However, the use of PLA has been limited to some extent because it can not fully meet the mechanical requirements of some applications such the orthopaedic ones.

To overcome this limitation, PLA matrices have been reinforced with fibres and particles of polymeric and ceramic materials (Adriano et al. 1993; Kasuga et al. 2003). This is the case of the PLA/G5 glass biodegradable composite material, which has been reinforced with particles of a soluble CaP glass coded G5 (Navarro et al. 2003). It has been observed in previous works that the incorporation of bioabsorbable glass particles into the polymer matrix not only improve the mechanical properties of the material but also its bioactivity and biological behaviour (Navarro et al. 2005).

The addition of G5 glass particles (<40 μ m, 50% w/w) into the polymer leads to significant changes at the material surface. On one hand, relevant topographical changes took place as shown in Table 12.2. There is a clear increase of Sa values when G5 particles are present. Besides, other roughness values such as the Ssk (surface skewness), Sku (surface kurtosis) concerning the height and the distance between peaks and valleys revealed important differences between both surfaces.

Moreover, remarkable changes in the material's wettability and surface energy were also observed. Water contact angles varied from 73.6 for PLA to 67.6 for PLA/G5, whereas their surface energy varied from 31.1 to 41.7 mN/m.

Table 12.2 Topographical parameters for the PLA and PLA/glass composite material

Material	Sa (nm)	Sku	Ssk	SAI
PLA	74.41 ± 32.64	189.16 ± 365.74	-3.36 ± 8.24	1.01 ± 0.01
PLA/glass	3806.7 ± 587.28	5.01 ± 1.10	-0.407 ± 0.45	1.53 ± 0.16

Sa = spacing between local peaks; Sku = kurtosis of the surface; Ssk = skewness surface plane; SAI = surface area index

As in the case of the NiTi surfaces, variations in topography, and surface chemistry led to interesting differences in protein adsorption, and as a consequence, in cell behaviour. Indeed, it was reported that the amount of proteins adsorbed into the materials surfaces was higher in the case of the composite material than in the case of PLA. Moreover, the total amount of adsorbed protein increased with glass wt% significantly (Charles-Harris et al. 2005). Thus, in this particular case, protein adsorption seems to be sensitive to the chemical effect of the exposed glass particles.

In vitro cell cultures with MG63 osteoblast-like cells on PLA and PLA/G5 surfaces have shown interesting differences between the results obtained in both substrates. According to the reported results, there is a higher adhesion of cells in the case of the polymer reinforced with the glass particles than in plain PLA substrates. Moreover, there is a very clear difference in the morphology of the cells adhered to PLA or to the PLA/G5 composite material. In the case of PLA, cells showed a very well spread and flat morphology, whereas in the case of the composite material, cells adopted a more rounded and more voluminous configuration (Navarro et al. 2008). Topography has an important effect on cell behaviour as already mentioned (Boyan et al. 2001). In fact, surface roughness affect the interactions between the extracellular matrix and cells which in turn affects the formation and total amount of focal contacts as well as their type of adhesion and leads to changes in the cell cytoskeleton and in gene expression (Gronowicz et al. 1996). Thus, according to this statement, surface topography highly affects cell proliferation and differentiation processes.

The presence of glass particles and the interfaces and nonunions between the polymer matrix and the CaP glass particles promoted morphological changes in cells, so they could adapt better to the material topography.

12.5 Micro and Nanopatterned Surfaces for Biomedical Applications

As already discussed and described in the previous sections, there is a clear influence of surface topography and chemistry in cell response (Curtis and Wilkinson 1997). However, there is not a comprehensive understanding of the mechanisms of this effect.

Numerous studies have been done to elucidate the process by which cells are affected by both topography and chemistry. In the case of chemistry, there is a more

direct effect caused by the presence of well known specific functional groups, peptide motifs or proteins that are known to react with certain cell structures and activate some signalling cascades that trigger specific cell behaviours.

In the case of topography, the effect is not so obvious. Nevertheless, it has been observed that in general, the studies reported at the moment suggest that using a determined micro and nanotopography may cause cells to spread and elongate, to align following the direction of the surface pattern (Wilkinson et al. 2002; Charest et al. 2007) to rearrange the extracellular matrix in contact with the surface (Dalby et al. 2004; Johansson et al. 2006), and to internally re-organize cellular components (Gadegaard 2006), leading to variations in cellular responses. Nevertheless, there are well defined differences between surfaces presenting features in the micro or nano length scale.

Cell studies on PMMA non-structured surfaces and on PMMA surfaces structured with posts and holes using the hot embossing technique (Mills et al. 2007) have shown that in general, cells prefer to grow on non-structured surfaces than on the structured ones. In the case of the structured surfaces, there seems to be a slight difference in the cell response whenever posts or holes are used. It seems that cells use the posts as anchorage points to hold themselves to the surface. This work also showed that cells are also affected by the features size and separation between them; this in turn affects cell alignment. As the dimensions of the structures become smaller and the dimension differences between cells and features increase, the cell morphology seems to be less affected by the surface structures. Smaller features with subcellular dimensions affect through smaller cell receptors such as integrins.

Micro and nanopatterning of surfaces has also been combined with chemical patterns in order to study cell behaviour under different conditions. Micro and nanofabrication techniques such as nanoembossing together with surface functionalization techniques like microcontact printing, nanoplotting and dip-pen nanolithography have been used to covalently attach selectively adhesion proteins such as fibronectin to 2D substrates (Martínez et al. 2007).

References

- Adriano KP, Daniels AU, Smutz WP, Wyatt RWB, Heller J (1993) Preliminary biocompatibility screening of several biodegradable phosphate fiber reinforced polymers. *J Appl Biomater* 4:1–12
- Agrawal CM, Ray RB (2001) Biodegradable polymeric scaffolds for musculoskeletal tissue engineering. *J Biomed Mater Res* 55:141–150
- Altankov G, Groth T (1994) Reorganization of substratum-bound fibronectin on hydrophilic and hydrophobic materials is related to biocompatibility. *J Mater Sci Mater Med* 5:732–737
- Anderson JM, Gristina AG, Hanson SR, Harker LA, Johnson RJ, Merrit K, Naylor PT, Schoen FJ (1996) Host reactions to biomaterials and their evaluation. In: Ratner BD, Horffman AS, Schoen FJ, Lemons JE (eds) *Biomaterials science: an introduction to materials in medicine*. Academic, San Diego, CA, pp 127–146
- Anselme K (2000) Osteoblast adhesion on biomaterials. *Biomaterials* 21(7):667–681
- Anselme K, Bigerelle M, Noel B, Dufresne E, Judas D, Iost A, Hardouin P (2000) Qualitative and quantitative study of human osteoblast adhesion on materials with various surface roughnesses. *J Biomed Mater Res* 49:155–166

- Aparicio C, Gil F, Fonseca C, Barbosa M, Planell JA (2003) Corrosion behaviour of commercially pure titanium shot blasted with different materials and sizes of shot particles for dental implant applications. *Biomaterials* 24:263–273
- Banwart JC, Asher MA, Hassanein RS (1995) Iliac crest bone graft harvest donor site morbidity. A statistical evaluation. *Spine* 20:1055–1060
- Beningo KA, Dembo M, Kaverina I, Small JA, Wang YL (2001) Nascent focal adhesions are responsible for the generation of strong propulsive forces in migrating fibroblasts. *J Cell Biol* 153(4):881–887
- Black J (2006) Biocompatibility: definitions and issues. In: Black J (ed) *Biological performance of materials*, 4th edn. Taylor & Francis, Boca Raton, FL, p 6
- Blawas AS, Reichert WM (1998) Protein patterning. *Biomaterials* 19(7–9):595–609
- Boyan BD, Dean DD, Lohmann CH, Cochran DL, Sylvia VL, Schwartz Z (2001) The titanium-bone cell interface in vitro: the role of the surface in promoting osteointegration. In: Brunette D, Tengvall P, Textor M, Thomsen P (eds) *Titanium in medicine*. Springer, Berlin, pp 562–585
- Charest JL, Garcia AJ, King WP (2007) Myoblast alignment and differentiation on cell culture substrates with microscale topography and model chemistries. *Biomaterials* 28(13):2202–2210
- Charles-Harris M, Navarro M, Engel E, Aparicio C, Ginebra MP, Planell JA (2005) Surface characterisation of completely degradable composite scaffolds. *J Mater Sci Mater Med* 16:1125–1130
- Chen CS, Mrksich M, Huang S, Whitesides GM, Ingber DE (1997) Geometric control of cell life and death. *Science* 276(5317):1425–1428
- Chesnel KD, Clark CC, Brighton CT, Black J (1995) Cellular responses to chemical and morphologic aspect of biomaterial surfaces 2: the biosynthetic and migratory response of bone cell-populations. *J Biomed Mater Res* 29:110–1110
- Chim H, Schantz JT (2006) Human circulating peripheral blood mononuclear cells for calvarial bone tissue engineering. *Plast Reconstr Surg* 117(2):468–478
- Ciccone W, Motz C, Bentley C, Tasto J (2001) Bioabsorbable implants in orthopaedics: new developments and clinical applications. *J Am Acad Orthop Surg* 9:280–288
- Colloiodi A, Clemence JF, Sanger M, Sigrist H (1993) Oriented and covalent immobilization of target molecules to solid supports: synthesis and application of a light-activatable and thiol-reactive crosslinking reagent. *Bioconjugate Chem* 4:528–536
- Curtis A, Wilkinson C (1997) Topographical control of cells. *Biomaterials* 18:1573–1583
- Dalby MJ, Giannaras D, Riehle MO, Gadegaard N, Affrossman S, Curtis ASG (2004) Rapid fibroblast adhesion to 27 nm high polymer demixed nano-topography. *Biomaterials* 25:77–83
- Dalby MJ, Gadegaard N, Tare R, Andar A, Riehle M, Herzyk P, Wilkinson C, Oreffo R (2007) The control of human mesenchymal cell differentiation using nanoscale symmetry and disorder. *Nat Mater* 6:997–1003
- Dee KC, Puleo DA, Bizios R (2002) Wound healing. In: Dee KC, Puleo DA, Bizios R (eds) *An introduction to tissue-biomaterial interactions*. Wiley, Hoboken, NJ, pp 165–214
- Diener A, Nebe B, Lüthen F, Becker P, Beck U, Neumann H, Rychly J (2005) Control of focal adhesion dynamics by material surface characteristics. *Biomaterials* 26(4):383–392
- Dunlap CL, Vincent SK, Barker BF (1989) Allergic reaction to orthodontic wire: report of case. *JADA* 118:449–450
- Fernyhough JC, Schimandle JJ, Weigel MC, Edwards CC, Levine AM (1992) Chronic donor site pain complicating bone graft harvest from the posterior iliac crest for spinal fusion. *Spine* 17:1474–1480
- Fuchs JR, Hannouche D, Terada S, Zand S, Vacanti JP, Fauza DO (2005) Cartilage engineering from ovine umbilical cord blood mesenchymal progenitor cells. *Stem Cells* 23(7):958–964
- Gadegaard N (2006) Atomic force microscopy in biology: technology and techniques. *Biotech Histochem* 81(2–3):87–97
- Goulet JA, Senunas LE, DeSilva GL, Greengield MLVH (1997) Autogeneous iliac crest bone graft. Complications and functional assessment. *Clin Orthop* 339:76–81
- Grinnel F, Feld MK (1982) Adsorption characteristics of plasma fibronectin in relationship to biological-activity. *J Biomed Mater Res* 15:363–381
- Grizzi I, Garreau H, Li S, Vert M (1995) Hydrolytic degradation of devices based on poly(DL-lactic acid) size-dependence. *Biomaterials* 16(4):305–311

- Gronowicz G, McCarthy MB, Ahmad M (1996) Direct integrin-mediated attachment of human osteoblasts to implants. *J Bone Miner Res* 11:S323
- Hardouin P, Anselme K, Flautre B, Bianchi F, Bascouleguet G, Bouxin B (2000) Tissue engineering and skeletal diseases. *Joint Bone Spine* 67:419–424
- Healy KE, Thomas CH, Rezania A, Kim JE, McKeown PJ, Lom B, Hockberger PE (1996) Kinetics of bone cell organization and mineralization on materials with patterned surface chemistry. *Biomaterials* 17:195–208
- Hench LL (1980) *Biomaterials*. Science 208:826–831
- Hench LL, Anderson Ö (1993) Bioactive glasses. In: Hench LL, Wilson J (eds) *An introduction to bioceramics*. World Scientific, Hackensack, NJ, p 41
- Hench LL, Polak J (2002) Third generation biomedical materials. *Science* 295:1014–1017
- Howlet CR, Evans MDM, Walsh WR, Johnson G, Steele JG (1994) Mechanism of initial attachment of cells derived from human bone to commonly used prosthetic materials during cell-culture. *Biomaterials* 15:213–222
- Huang YC, Huang YY (2006) Biomaterials and strategies for nerve regeneration. *Artif Organs* 30(7):514–522
- Huang HH, Ho CT, Lee TH, Lee TL, Liao KK, Chen FL (2004) Effect of surface roughness of ground titanium on initial cell adhesion. *Biomol Eng* 21(3–5):93–97
- Hunt J (2004) Foreign body response. In: Wnek GE, Bowlin GL (eds) *Encyclopedia of biomaterials and biomedical engineering*. Marcel Dekker, New York, pp 641–646
- Hutmacher D, Hürzeler MB, Schliephake H (2000) A review of material properties of biodegradable and bioresorbable polymer for GTR and GBR. *J Oral Maxillofac Implants* 11:667–678
- Johansson F, Carlberg P, Danielsen N, Montelius L, Kanje M (2006) Axonal outgrowth on nano-imprinted patterns. *Biomaterials* 27(8):1251–1258
- Kasuga T, Maeda H, Kato K, Nogami M, Hata KI, Ueda M (2003) Preparation of poly(lactic acid) composites containing calcium carbonate (vaterite). *Biomaterials* 24:3247–3253
- Kern S, Eichler H, Stoeve J, Kluter H, Bieback K (2006) Comparative analysis of mesenchymal stem cells from bone marrow, umbilical cord blood, or adipose tissue. *Stem Cells* 24(5):1294–1301
- Kulkarni R, Pani KC, Neuman C, Leonard F (1966) Polylactic acid for surgical implants. *Archives Surg* 93:839
- Kulkarni R, Moore RG, Hegyeli AF, Leonard F (1971) Biodegradable poly(lactic acid) polymers. *J Biomed Mater Res* 5:169–181
- Larsson C, Thomsen P, Aronsson BO, Rodahl M, Lausmaa J, Kasemo B, Ericson LE (1996) Bone response to surface-modified titanium implants: studies on the early tissue response machined and electropolished implants with different oxides thicknesses. *Biomaterials* 17:605–616
- Magel S, Vogler EA, Firment L, Watt T, Haynie S, Sogah DY (1993) Peptide, protein and cellular interactions with self-assembled monolayer model surfaces. *J Biomed Mater Res* 27(12):1463–1476
- Martínez E, Ríos-Mondragón I, Pla-Roca M, Rodríguez-Segui S, Engel E, Mills CA, Sisquella X, Planell JA, Samitier J (2007) Cell-surface interactions studies to trigger stem cell differentiation. *Nanomedicine* 3(4):346–346
- McFarland CD, Mayer S, Scotchford C, Dalton BA, Steele JG, Downes S (1999) Attachment of cultured human bone cells to novel polymers. *J Biomed Mater Res* 44(1):1–11
- Meyer O, Buchter A, Wiesmann HP, Joos U, Jones DB (2005) Basic reactions of osteoblasts on structured material surfaces. *ECMjournal* 9:39–49
- Michiardi A, Aparicio C, Planell JA, Gil FJ (2004) Nuevo tratamiento de oxidación en aleaciones de NiTi para la disminución de la liberación de iones y la mejora de la biocompatibilidad. Spanish Patent no P2004024004
- Michiardi A, Aparicio C, Planell JA, Gil FJ (2006) New oxidation treatment of NiTi shape memory alloys to obtain Ni-free surfaces and to improve biocompatibility. *J Biomed Mater Res* 77B:249–456
- Michiardi A, Aparicio C, Ratner BD, Planell JA, Gil J (2007) The influence of surface energy on competitive protein adsorption on oxidized NiTi surfaces. *Biomaterials* 28:586–594

- Michiardi A, Engel E, Aparicio C, Planell JA, Gil FJ (2008) Oxidized NiTi surfaces enhance differentiation of osteoblast-like cells. *J Biomed Mater Res* 85A:108–114
- Middleton JC, Tipton AJ (2000) Synthetic biodegradable polymers as orthopaedic devices. *Biomaterials* 21(23):2335–2346
- Mills CA, Martínez R, Errachid A, Engel E, Funes M, Moormann C, Wahlbrink T, Gomila G, Planell JA, Samitier J (2007) Nanoembossed polymer substrates for biomedical surface interaction studies. *J Nanosci Nanotechnol* 7:4588–4594
- Mrksich M, Whitesides GM (1995) Patterning self-assembled monolayers using microcontact printing: a new technology for biosensors? *TIBTECH* 13:228–235
- Navarro M, Ginebra MP, Clement J, Martínez S, Avila G, Planell JA (2003) Physicochemical degradation of titania-stabilized soluble phosphate glasses for medical applications. *J Am Ceram Soc* 86(8):1345–1352
- Navarro M, Ginebra MP, Planell JA, Barrias C, Barbosa M (2005) In vitro degradation behavior of a novel bioresorbable composite material based on PLA and a soluble CaP glass. *Acta Biomater* 1:411–419
- Navarro M, Engel E, Planell JA, Amaral I, Barbosa M, Ginebra MP (2008) Surface characterisation and cell response of a PLA/CaP glass biodegradable composite material. *J Biomed Mater Res* 85 A:477–486
- Peltonen L (1979) Nickel sensitivity in general population. *Contact Dermatitis* 5:27–32
- Pittenger MF, Mackay AM, Beck SC, Jaiswal RK, Douglas R, Mosca JD et al (1999) Multilineage potential of adult human mesenchymal stem cells. *Science* 284(5411):143–147
- Roach P, Eglin D, Rohde K, Perry CC (2007) Modern biomaterials: a review-bulk properties and implications of surface modifications. *J Mater Sci Mater Med* 18:1263–1277
- Rodríguez-Cabello JC, Prieto S, Reguera J, Arias FJ, Riberiro A (2007) Biofunctional design of elastin-like polymers for advanced applications in nanobiotechnology. *J Biomater Sci Polym Ed* 18(3):269–286
- Rokkanen P (2000) Bioabsorbable fixation in orthopaedic surgery and traumatology. *Biomaterials* 21:2607–2613
- Scotchford CA, Cooper E, Leggett GJ, Downes S (1998) Growth of human osteoblast-like cells on alkanethiol on gold self-assembled monolayers: the effects of surface chemistry. *J Biomed Mater Res* 41:431–442
- Sergeant TD, Rao MS, Koh CY, Stupp SI (2008) Covalent functionalization on NiTi surfaces with bioactive peptide amphiphile nanofibers. *Biomaterials* 29(8):1085–1098
- Siebers MC, Brugge PJ, Wlaboomers XF, Jansen JA (2005) Integrins as linker proteins between osteoblasts and bone replacing materials. A critical review. *Biomaterials* 26(2):137–146
- Stoltz JF, Bensoussan D, Decot V, Netter P, Ciree A, Gillet P (2006) Cell and tissue engineering and clinical applications: an overview. *Biomed Mater Eng* 16(4):S3–S18
- Tan J, Saltzman WM (2002) Topographical control of human neutrophil motility on micropatterned materials with various surface chemistry. *Biomaterials* 23(15):3215–3225
- Tang L, Liu L, Elwing HB (1998) Complement activation and inflammation triggered by model biomaterial surfaces. *J Biomed Mater Res* 41(2):333–340
- Teixeira A, Duckworth JK, Hermanson O (2007) Getting the right stuff: controlling neural stem cell state and fate in vivo and in vitro with biomaterials. *Cell Res* 17(1):56–61
- Temenoff JS, Mikos AG (2000) Tissue engineering for regeneration of articular cartilage. *Biomaterials* 21:431–440
- Verfaillie CM (2002) Adult stem cells: assessing the case for pluripotency. *Trends Biotechnol* 12(11):502–508
- Wataha JC, O'Dell NL, Singh BB, Ghazi M, Whitford GM, Lockwood pE (2001) Relating nickel-induced tissue inflammation to nickel release in vivo. *J Biomed Mater Res B Appl Biomater* 58:537–544
- Wilkinson CDW, Riehle M, Wood M, Gallagher J, Curtis ASG (2002) The use of materials patterned on a nano-and micro-metric scale in cellular engineering. *Mater Sci Eng C* 14:263–269

- Xiao SJ, Textor M, Spencer ND, Wieland M, Keller B, Sigrist H (1998) Covalent attachment of cell-adhesive peptides containing (arg-gly-asp) sequences to titanium surfaces. *Langmuir* 14:5507–5516
- Xiao SJ, Kenausis G, Textor M (2001) *Biochemical modification of titanium surfaces*. Springer, Berlin
- Zinger O, Zhao G, Schwartz Z, Simpson J, Weiland M, Landolt D, Boyan B (2005) Differential regulation of osteoblast by substrate microstructural features. *Biomaterials* 26(14):1837–1847

Chapter 13

Chemical and Physical Modifications of Biomaterial Surfaces to Control Adhesion of Cells

Thomas Groth, Zhen-Mei Liu, Marcus Niepel, Dieter Peschel, Kristin Kirchhof, George Altankov, and Nathalie Faucheux

Abstract Cell adhesion is a prerequisite for healing of implant materials and colonization of tissue engineering scaffolds. Hence, it is a crucial task to control adhesion of cells on biomaterials, which can be achieved by surface modification. Different techniques can be used to modify the surface of materials, which have the desired physical and chemical properties, but lack sufficient biocompatibility. Among the techniques of surface modification, a number of self assembly methods have the advantage to work in solutions, so that different shaped materials can be modified easily. Self assembly methods selected in this study were chemisorption and covalent binding of alkylsiloxanes on glass (i), photochemical binding of polyethylene glycol on hydrophobic polymers (ii) and alternating adsorption of polyanions and polycations to assemble nanostructured multilayers on charged surfaces (iii). These methods enable to obtain control on adhesion of cells on different classes of biomaterials, which eventually may promote subsequent processes like cell growth and differentiation.

Keywords Biomaterials • Surface modification • Self assembled monolayer • Poly (ethylene glycol) • Layer-by-layer technique • Cell adhesion

T. Groth (✉), Z.-M. Liu, M. Niepel, D. Peschel, and K. Kirchhof
Biomedical Materials Group, Institute of Pharmacy, Martin Luther University Halle-Wittenberg ,
06120, Halle (Saale), Germany
e-mail: thomas.groth@pharmazie.uni-halle.de

G. Altankov
ICREA & Institute of Bioengineering Catalunya, Barcelona, Spain

N. Faucheux
Chemical Engineering Department, University of Sherbrooke, Canada

13.1 General Introduction

13.1.1 Basics of Cell Adhesion on Material Surfaces

Adhesion of cells is a crucial event in many physiological and patho physiological processes such as development of organism, wound healing, inflammation but also cancer and metastasis. Cell adhesion represents a prerequisite for a multitude of cellular functions such as movement, growth, differentiation, survival and others as depicted in Fig. 13.1 (Grinnell 1978). It has been found that the strength of adhesion controls the degree of cell spreading and hence the shape of cells on a substratum (Huang and Ingber 1999). The shape of cells however, seems to be a regulator of cellular functions (Huang and Ingber 2000; Altankov et al. 1996).

Adhesion of cells to substrata is related to physical long and short range interaction forces. Long range interaction forces are represented by Coulomb or electrostatic force, which is dependent on the presence of charges on the cell surface and the substratum (Bongrand 1982). Cell surfaces are predominantly negatively charged, while substrata can possess negative or positive surface charges. Accordingly, there can be repulsive or attractive forces between cells and surfaces (Bongrand 1982; Vitte et al. 2005). Furthermore, the presence of salt ions has an impact on the range of electrostatic forces. At low ionic strength the forces act at longer distances, while higher salt concentrations may shield the charges on cells and surfaces to certain degree (Trommler et al. 1985). There is a multitude of short range interaction forces. Attractive interactions are so called van-der-Waals force, hydrogen bonding, acid-base interactions and hydrophobic interactions. Repulsive short-range forces are exerted by hydration forces due to the presence of bound water molecules on polar moieties or steric hindrance due to the presence of hydrophilic, mobile macromolecules on the material or cell surface. A comprehensive overview on physics of cell adhesion can be found elsewhere (Bongrand 1982;

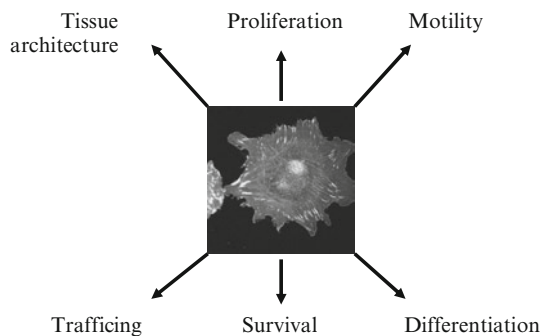


Fig. 13.1 Impact of cell adhesion on different cellular processes

Vitte et al. 2005). Basic studies have shown that cell adhesion is dependent on the surface charge of materials. Positively charged surfaces promote cell adhesion, while negatively charged surface reduce it (Bongrand 1982; Vitte et al. 2005). Also the effect of ionic strength has been studied extensively. Cell adhesion on negatively charged surfaces becomes low or negligible at low ionic strength, when the range of electrostatic force is long. Cell adhesion is strong at high ionic strength when electrostatic repulsion becomes negligible and van-der-Waals attraction dominates (Trommler et al. 1985). Also the effect of binding of water by polar surfaces has been exploited to prevent adhesion of cells. Water binds tightly to head groups of certain phospholipids, such as phosphatidylcholine (PC) (Israelachvili and Wennerstrom 1996; Bird et al. 1994). Accordingly, functionalization of surfaces with PC may be used to generate adhesion-preventing materials (Bird et al. 1994; Ishihara et al. 1993; Iwasaki et al. 1999). This may be also achieved by the immobilization of hydrophilic macromolecules like poly (ethylene glycol) and others, which lead to steric repulsion and inhibiting this way the attachment of cells (Lee et al. 1989; Morra 2000; Tziampazis et al. 2000). Beside these physicochemical surface properties also the topography of surface has an impact on cell adhesion. In general, cells may attach better on rough than on smooth surfaces (Deligianni et al. 2002; Diener et al. 2005). In this respect it has been found also that specific topographical features in micro and nanometer scale may control adhesion and subsequent reactions of cells. Pioneering work has been carried out by Curtis and coworkers (Curtis and Clark 1990; Wilkinson et al. 2002; Dalby et al. 2002). Last but not least, cells may also sense the viscoelastic properties of substrata. Soft, flexible substrata may inhibit attachment and spreading while stiff, solid surfaces may promote it (Pelham and Wang 1997).

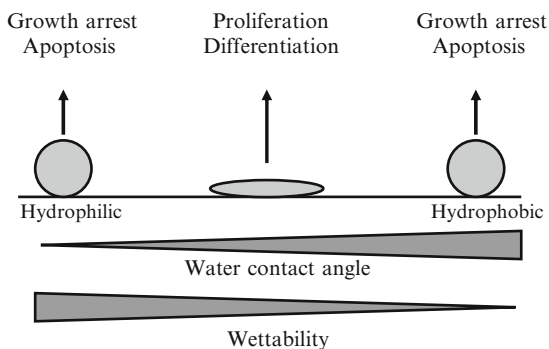
On the other hand, under physiological conditions cells contact material surfaces never directly, because of the presence of proteins in the surrounding body fluids. This holds also for the majority of *in vitro* culture conditions, when serum is used as component of culture medium. Moreover, most cell types are able to secrete a multitude of proteins. Hence, before cells contact biomaterial surfaces, proteins are transported to the substratum by diffusion or convection (Jauregui 1987). For adsorption of proteins hold principally the same conditions as described for cell adhesion. Indeed, the physicochemical properties of substrata control adsorption of proteins. Since proteins represent copolymers of different amino acids, most proteins carry acidic and basic groups, and hydrophilic and hydrophobic moieties. Therefore they are both amphoteric and amphiphilic. Depending on the isoelectrical point of proteins they may possess a positive or negative net charge at physiological conditions (Andrade and Hlady 1986). Moreover, even the net charge of a protein is negative it may carry positively charged residues and vice versa. Proteins possess also a number of amino acids with hydrophobic residues, which may be part of the protein core, but also form hydrophobic patches at the outer part of three-dimensional protein structure. Protein-containing body fluids contain many different types of proteins which differ in their amino acid composition, secondary and tertiary structure, and size (Norde and Lyklema 1991).

Consequently, proteins adsorb to almost all types of material surfaces except on those, which are highly hydrophilic with tight water binding (e.g. phosphatidylcholine) (Bird et al. 1994; Ishihara et al. 1993; Iwasaki et al. 1999) or having a close coverage with hydrophilic, mobile macromolecules such as poly (ethylene glycol), which create a repulsive barrier (Lee et al. 1989; Morra 2000; Tziampazis et al. 2000). On the other hand, surfaces, which are apolar or highly charged, may promote structural rearrangements by hydrophobic or electrostatic interactions, which cause conformational changes of proteins. The mechanisms and driving forces for these processes have been described in more detail by Norde and Lyklema and others (Andrade and Hlady 1986; Norde and Lyklema 1991; Tsai et al. 2002). Ultimately, conformational changes of proteins upon adsorption on biomaterials may induce unwanted physiological effects, such as activation of blood clotting, inflammation or delay of implant healing (Groth et al. 1992, 1994; Anderson et al. 1990; Tang and Eaton 1993). On the other hand, highly hydrophilic substrata may allow only traces of proteins to adsorb, which is desirable for blood-contacting applications, but detrimental to colonization of implants or scaffolds with tissue cells (Andrade and Hlady 1986).

The majority of biomaterial applications in tissue engineering and regenerative medicine require that tissue cells adhere on material surfaces (Hubbell 1995). It has been shown that cell adhesion is linked to the presence and conformation of specific attachment proteins on material surfaces (Altankov et al. 1996). Adhesive proteins such as fibrinogen, fibronectin, vitronectin and von Willebrand factor are normal components of blood plasma and may adsorb on biomaterial surfaces (Jauregui 1987). The extracellular matrix (ECM), which surrounds cells in tissues is composed of structural proteins like collages, adhesive proteins and glycosaminoglycans (Lodish et al. 2004). These proteins provide attachment to cellular receptors mainly integrins and deliver signals important for survival, growth and differentiation (Hynes 2002; Frisch and Ruoslahti 1997). The important role of integrins and presence of their specific ligands on biomaterial surfaces has been highlighted in other chapters of this book (Altankov this volume; Pankov this volume) and will be also briefly discussed later in this paper.

It has been found that the physicochemical properties of the material surface such as surface energy (wettability), and electrical surface potential (zeta potential), which are dependent on the chemical composition have an impact on the adsorption of proteins from surrounding liquids, such as blood or tissue fluids (Groth et al. 1997; Mullaney et al. 1999). Accordingly cell growth and function was found to be strongly related to the wettability of materials (van Kooten et al. 2004; Altankov and Groth 1996; Groth and Altankov 1996), which has been outlined in Fig. 13.2. The presence of charged functional groups, such as amino or carboxylic groups has been identified as promoting, while apolar groups like methyl may inhibit cellular attachment, growth and function (Keselowsky et al. 2003; Altankov et al. 2003). Overall, the molecular composition of material surfaces dictates the response of the biological systems in terms of protein adsorption, cell adhesion and subsequent events. Therefore, the modification of material surfaces can be used as a tool to optimize the biocompatibility of materials.

Fig. 13.2 Simplified view on dependence of cell adhesion on interfacial forces characterized by water contact angle measurements



13.1.2 Short Overview on Techniques to Modify Surfaces of Biomaterials

Many contemporary materials possess excellent physical and chemical properties, which make them attractive candidates for a variety of biomedical applications. However, the clinical use can be hampered by undesired side effects, which are caused by uncontrolled adsorption of proteins and subsequent conformational changes. Since, only material surfaces are in intimate contact with the biological environment it may be sufficient to modify the outermost part of the materials in a size-scale of a few nano up to micrometers. Techniques used for surface modification can be divided principally into two categories: physical or chemical techniques. Physical surface modification techniques include surface coating or entrapment (Bacakova et al. 2001; Vonarbourg et al. 2006), vapour deposition (Klee et al. 2003) and surface self assembly (Croll et al. 2006; Tang et al. 2006) methods. Physical interactions related to these techniques are electrostatic interaction, van der Waals force, hydrogen bonding, hydrophobic interaction, etc. Physical techniques are often simple methods, which sometimes do not require large and expensive equipments. However, some of the techniques have also the drawback of limited stability if the interaction force between substrate and immobilized molecules is relatively weak. Numerous methods have been developed for chemical modification of surfaces to generate functional groups or to bind other molecules on surfaces (Goddard and Hotchkiss 2007; Albrecht et al. 2003; Seifert et al. 2002). Some of these methods represent principally physical methods such as plasma treatment with glow or corona-discharge (Liu et al. 2006) or ion beam irradiation (Xu et al. 2006) but result in a chemical modification of material surfaces as it is achieved by surface etching (Guo et al. 2008) and surface grafting (Kondyurin et al. 2006; Hu et al. 2002; Hamerli et al. 2003a; Guo et al. 2008) methods. In principle, plasma treatment in different gas environments is able to generate various types and quantities of functional groups on substrata by controlling gas composition, distance between

samples and electrodes as well as power and time of plasma treatment (Liu et al. 2005; Hamerli et al. 2003b). Surface grafting is an important method for chemical surface modification since various functional compounds can be utilized to modify surface properties of biomaterials (Singh et al. 2007). The grafting methods can be divided into two classifications known as ‘grafting to’ and ‘grafting from’ (Zhao and Brittain 2000). Polymers with functional side or end groups can be easily grafted onto substrata via covalent binding. However, the complication inherent in the ‘grafting to’ process is the intrinsic limitation of the number of functional groups per surface area due to thermodynamic reasons (Zajac and Chakrabarti 1995). ‘Grafting from’ method utilizes active species existing on substrate surfaces with a high grafting density to initiate the polymerization of monomers from the surface. For surfaces without active groups, plasma, UV, ozone treatment or high energy irradiation can be used to generate immobilized initiators (i.e. radicals) followed by polymerization of monomers from the surrounding (Liu et al. 2004; Goda et al. 2006). However, the uncertainty of initiator types and quantity may lead to low grafting density and hence-tethered polymer since the reactions are not quantitative. A further disadvantage is that side reactions from the initiator-generation steps may introduce undesired structures on the surfaces (Fukuda et al. 2000). Surface-initiated atom transfer radical polymerization (ATRP) emerged as a new ‘grafting from’ technique due to its feasibility to control grafting density, grafting chain length and mono dispersity and its versatility in monomer types (Choi et al. 2007).

13.1.3 Methods to Generate Nanostructured Surface

It has been revealed that surface features in the nanometer scale may provoke distinct cellular reactions regarding adhesion, morphology, cytoskeletal arrangement, migration, proliferation, surface antigen display and gene expression (Curtis 2004; Gates et al. 2005). Based on these facts techniques for the fabrication of materials with nanoscale-controlled surface properties have been developed during the past few decades by making surface patterns with adjustable chemical, topographical and micromechanical properties. Methods used to generate nanoscale structures are commonly subdivided into two groups according to the manufacturing approach: ‘top down’ and ‘bottom-up’ (Chen and Pépin 2001). The top-down methods use various techniques of lithography to pattern nanoscale structures, including electron beam lithography, focused ion beam lithography, optical projection lithography, X-ray lithography, electron and ion projection lithography, and extreme UV lithography (Brétagnol et al. 2007). These techniques generally require expensive equipment. A further disadvantage is a certain lack of flexibility. The bottom-up methods, on the other hand, benefit basically from interactions between molecules or colloidal particles to assemble discrete nanoscale structures in two or three dimensions (Ahn et al. 2004). Techniques for the bottom-up approach include nanoimprinting, micro-contact printing, soft-lithography, near-field optical lithography and proximity probe lithography but also self-assembly procedures such as Langmuir–Blodgett

films or the layer-by-layer method. Most of these techniques are less costly and more easily to handle. New techniques, like scanning probe lithography and self-assembly, bridge top-down and bottom-up strategies for nanofabrication. Not only can they conserve the lithographic printing strategy but also allow pattern processing at molecular levels by self-assembly or self-organization in which molecular building blocks will automatically link together to form desired nanostructures (Brétagne et al. 2007; Ahn et al. 2004).

A few examples of self-assembly methods that can be employed to generate nano-structured surface coatings will be presented in this article. Techniques like self-assembled monolayers (SAM) or adsorption of amphiphilic molecules have been developed to build thin films onto various substrata. They can be used as bottom-up methods to generate distinct patterns on different types of material surface involving covalent bonds between molecules and surfaces. The layer-by-layer technique can be considered as further bottom-up method to obtain nano-structured multilayers on charged substrata. The binding between molecules and surfaces is based on physical interaction forces and does not involve covalent bonds. All methods can be used to modify the wettability, chemical composition and viscoelastic properties of biomaterial surfaces since they can be composed of a variety of molecules and deposited onto almost any kind of substrate. Overall, the methods presented provide means to control cell adhesion and hence subsequent cellular reactions.

13.2 Self Assembled Monolayers Based on Organosiloxanes

13.2.1 Background

Conventional biomaterials like polymers can have a large degree of surface heterogeneity regarding the type and distribution of functional groups, the presence of hydrophilic and hydrophobic domains, surface roughness, etc. Since all these parameters contribute to the cellular behaviour it is difficult to understand how surfaces should be composed to obtain the desired interactions with cells. Therefore, the variation of selected surface parameters, such as the chemical composition, without variation of other characteristics, such as morphology or domain structure, is required to obtain detailed outlines for advanced biomaterials for specific applications.

Self-assembled monolayers (SAMs) of organosiloxanes represent a class of organic surfaces that are perfectly suited to investigate interactions of surfaces with cells (Mrksich and Whitesides 1996). Figure 13.3 shows the three important elements of SAMs with coupling unit establishing a covalent link to different substrata (i), the alkyl chain as assembling structure (ii) and the head group (iii). The ability to control the composition and properties of SAMs precisely through synthesis, combined with the simple methods to arrange their functional groups in monolayers, makes this class of surfaces the best to tailor material surfaces to obtain control over the molecular composition and the resulting integral properties with well ordered organic surfaces (Mrksich and Whitesides 1996; Webb et al. 2000).

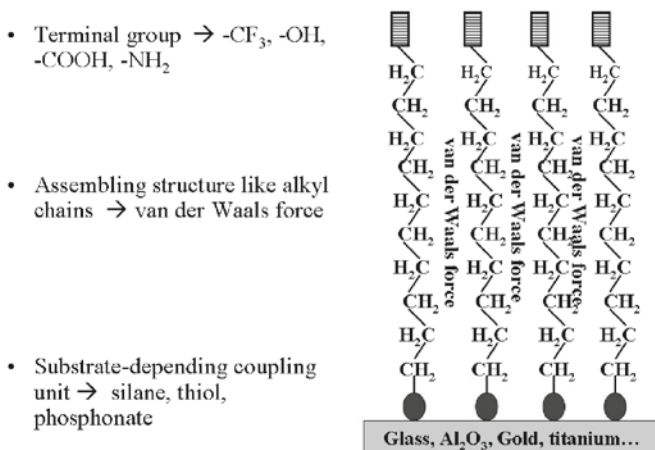


Fig. 13.3 Structure of self assembled monolayers composed of coupling unit, assembling structure and terminal group

Recent studies used SAMs to evaluate the effect of surface charge, wettability and topography on protein adsorption and cell behaviour using in vitro assay systems (Mrksich and Whitesides 1996; Webb et al. 2000; Healy et al. 1994). The strength of cell adhesion and spreading on SAMs has been especially studied (Webb et al. 2000; Healy et al. 1994; Sukenik et al. 1990). For example it was shown that hydrophobic methyl-terminated alkanethiol SAMs on gold induce minimal cell attachment and cannot support spreading and formation of focal contacts by mouse fibroblasts (McClary et al. 2000). However, most of these studies were performed using pre-adsorbed single protein solutions.

13.2.2 *Effect of SAM on Fibroblast Adhesion, Spreading and Growth*

Hence, this study was carried out in the presence of serum to investigate the relationships between surface properties of SAMs and cell attachment, spreading, cytoskeleton organization and subsequent cell proliferation. For this purpose a set of SAMs was prepared differing in their wettability from hydrophobic to hydrophilic surfaces by the adsorption of alkylsiloxanes onto glass cover slides, which were cleaned with Piranha solution. The SAMs varied primarily in the type of the functional end groups, such as amine (NH_2), carboxyl (COOH), hydroxyl (OH), methyl (CH_3) and polyethylene glycol (PEG). The surface properties of each SAM were analysed by measuring wettability (water contact angle), layer thickness (ellipsometry) and roughness (atomic force microscopy). Details of these experiments have been published elsewhere (Faucheux et al. 2004). Here only the effect of terminal head groups on wettability of surfaces is shown (see Fig. 13.4). It is visible that apolar head groups like methyl generate hydrophobic material

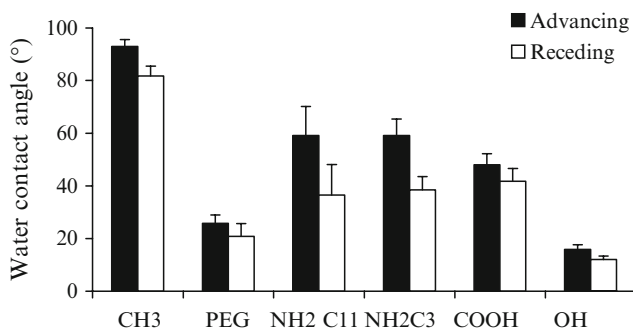


Fig. 13.4 Dynamic water contact angles of SAMs on glass with different terminal head groups, such as methyl (CH₃), poly (ethylene glycol) (PEG), amino groups linked to C3 or C11 alkyl chain length (NH₂ C11 or NH₂ C3), carboxyl (COOH) and hydroxyl (OH)

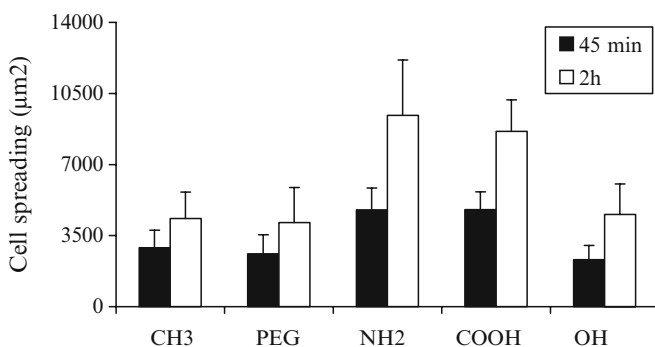


Fig. 13.5 Analysis of spreading of fibroblast cultured on serum-coated SAMs for 45 min or 2 h. Analysis was performed from phase contrast micrographs with image analysis software KS 300, Carl Zeiss Germany

surfaces, which is indicated by the high advancing and receding water contact angles. Polar head groups like hydroxyl and ethylene glycol are hydrophilic and cause low water contact angles, while the application of amino and carboxylic groups resulted in moderate wettable surfaces with contact angles around 50°.

Figure 13.5 shows significantly higher spreading of human fibroblasts attached to NH₂ and COOH in comparison to CH₃ ($p < 0.05$), PEG ($p < 0.05$) and OH ($p < 0.01$). The results for CH₃, PEG and OH terminated SAMs were similar ($p > 0.05$). This is in accordance with previous investigations showing that attachment and spreading of cells is enhanced on moderate wettable surface while hydrophobic or hydrophilic material surfaces inhibit interaction with cells because of conformational changes or absence of adhesive proteins (Goldstein and DiMilla 2002; Filippini et al. 2001; Steele et al. 1992).

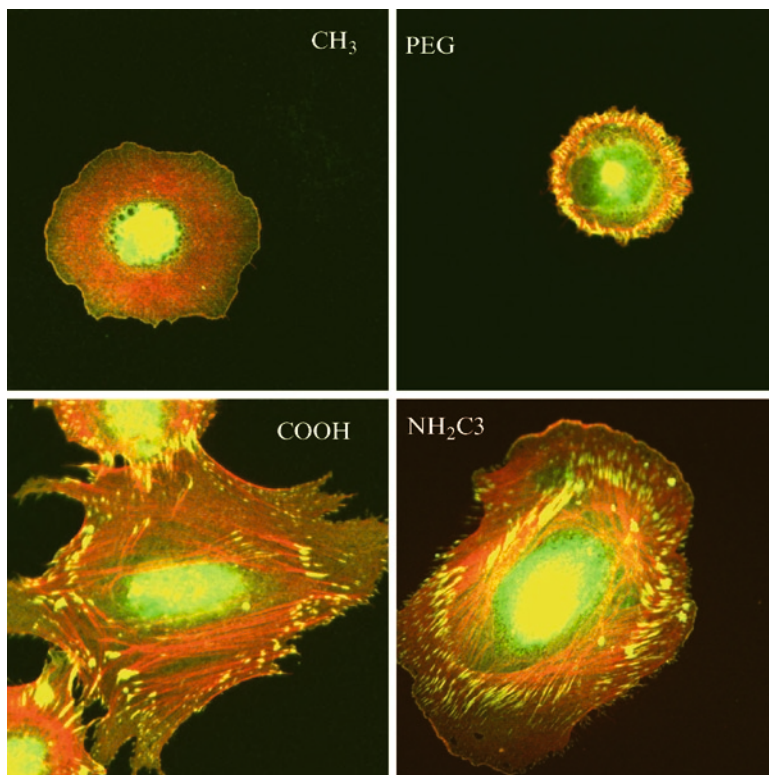


Fig. 13.6 Visualization of focal adhesion plaques by staining of vinculin (*green*) and actin stress fibres (*red*) after 45 min adhesion on serum-coated SAMs. Please note the *orange/yellow* colour of focal adhesions plaques, which originates from the overlap with inserting actin stress fibres

The differences in cell spreading were related to the formation of focal adhesion complexes and polymerization of actin as shown in Fig. 13.6. Since images obtained from OH and PEG terminated SAMs were similar only micrographs of cells plated on PEG are compared to CH₃, COOH and NH₂. Human fibroblasts attached to NH₂ and COOH contained extended linear focal adhesion plaques at the cell periphery and longitudinal actin stress fibres. Actin was mostly co-localised with vinculin in focal adhesion plaques indicated by the orange/yellow colour. In contrast on CH₃ no focal adhesions were observed nor any formation of actin stress fibres. Cells plated on PEG or OH started to develop very small punctuate focal adhesions but stress fibre formation was absent, too.

The initial interaction of fibroblasts with the various SAMs was also compared with growth and survival of cells. The growth index shown in Fig. 13.7 represents the ratio between the cell number at the beginning and after 48 h incubation. Significantly more fibroblasts were found on NH₂ and COOH terminated SAMs after 48 h than at time zero ($p < 0.05$). In contrast, fibroblasts did not grow on CH₃, PEG and OH

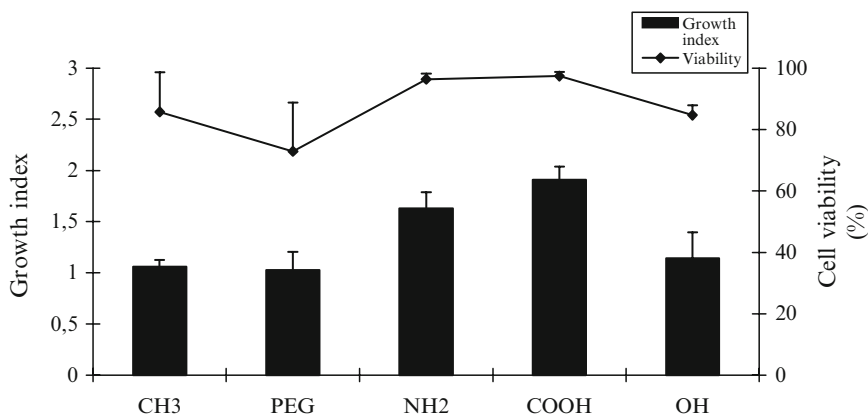


Fig. 13.7 Growth index and viability of fibroblasts plated for 48 h on the various SAMs. Cells were cultured in DMEM supplemented with 10% fetal bovine serum

terminated SAMs. The number of cells on these SAMs after 48 h was nearly the same compared to that at the beginning ($p > 0.05$). The lack of cell growth was accompanied by a slight decrease in cell viability ($<90\%$) which indicates beginning cell death particularly on PEG. Similar results were obtained from Filippini et al. (2001), who showed that Saos-2 human osteosarcoma cell growth was inhibited on either CH₃ or OH terminated SAMs. This illustrates that the starting conditions are very important for the subsequent reactions of cells. The underlying reasons for this phenomenon are the absence of attachment proteins on hydrophilic substrata or the conformational changes on hydrophobic materials (Juliano et al. 1993; Grinnell and Feld 1982; Jonsson et al. 1982), which lead to impaired interaction with integrin receptors followed by inadequate signalling responses in cells (Groth and Altankov 1996; Altankov et al. 1997). As a consequence cell growth and matrix synthesis are reduced, and cells may undergo apoptosis (Ruoslahti 1999). Garcia et al. used the same types of SAM except PEG and investigated adsorption and biological activity fibronectin, indicated by the binding of a monoclonal antibody against the cell binding domain. It was found that hydroxyl-terminated SAMs bound very low quantities of fibronectin with high biological activity, while methyl-terminated SAMs bound large quantities with considerable decreased biological activity (Garcia et al. 1999). In contrast on moderate wetttable carboxyl or amine-terminated SAMs biological activity of fibronectin was conserved (Garcia et al. 1999). Further findings of the current study were the absence of vitronectin adsorption from serum on OH and PEG-terminated SAMs, while no fibronectin adsorption was detectable on any of the SAMs (Faucheux et al. 2004). Consequently, human fibroblasts attached, spread and grew poorly on OH and PEG, but also on CH₃ terminated SAMs. Favourable outside-in signalling seemed to occur on both NH₂ and COOH supported by the observation of well-expressed focal adhesions with the formation of pronounced actin stress fibres. Groth and Altankov have

shown the connection of morphological features with tyrosine phosphorylation involved in outside-in signalling on biomaterials that was significantly lowered in human fibroblasts attached to CH_3 surfaces in comparison to NH_2 (Groth and Altankov 1996).

Overall, it can be concluded that the well-characterised chemistry of SAMs used in this study can provide a tool for the deeper understanding of early biochemical events such as signal transduction (Bergeron et al. 2007) provoked by cell-substratum interactions and their impact on the subsequent cellular behaviour (Faucheux et al. 2006). Moreover, different types of SAMs can be generated on a variety of substrate chemistries, such as glass, metal oxides, ceramics, gold, silver, titanium and hence used to tailor the biocompatibility of materials.

13.3 Photochemical Immobilization of Polyethyleneglycol on Hydrophobic Biomaterials

13.3.1 Background

Poly (ethylene glycol) (PEG) is a water soluble molecule and flexible in aqueous solutions. PEG has gained attraction because of properties like protein resistance and biocompatibility due to its high exclusion volume affected by great conformational entropy. Hence, surface attached PEG layers dramatically reduce non-specific binding of proteins (Lee et al. 1989; Morra 2000). It has been shown recently that the molecular weight or chain length of PEG and density on surface can controls the adsorption of proteins (Sofia et al. 1998).

According to the various interactions between proteins and surfaces, a favorable approach to prevent protein adsorption is to immobilize well-solvated polymers like PEG in the form of brushes on the surface (Szeleifer 1997; Halperin 1999). However, it has been observed that still the adsorption of proteins can occur, which has been proposed to happen by three mechanism (Halperin 1999; Halperin et al. 1992). First, the invasive mechanism explains adsorption due to diffusion of proteins through the interfacial region to the underlying substratum and subsequent adsorption there. Second, adsorption at the outer surface of the brush can happen due to protein-brush interactions. Third, compressive mechanism allows the adsorption of proteins upon compression of the polymer layer. Thus, the density of the grafted PEG layer or PEG chain length must be large enough to block protein-substrate interactions. Apart from PEG chain length, the ionic strength controls electrostatic forces between surface charges and proteins acting through the PEG layer (Pasche et al. 2005). Charge neutralization is effective in eliminating electrostatic interactions between a protein and the surface, which is usually the case at high salt concentrations decreasing the Debye-Hueckel length. However, only neutralization of charges on the surface is not sufficient to prevent protein adsorption, only sufficiently thick and dense PEG layer can resist protein adsorption. Consequently, the

brush chain density or surface coverage must be sufficiently high to screen diffusion through this steric layer (Sofia et al. 1998; Szeleifer 1997). In this sense, PEG has been applied to passivate surfaces to block adsorption of proteins and thus to prevent adhesion of cells. However, it must be noted that these effects can be observed only at high coating densities, when a brush regime of PEG on the surface has been achieved. In this context a large number of studies were carried out to produce inert, biocompatible surface coatings that prevent fouling of polymer membranes, activation of blood clotting on biomedical materials, to prevent activation of the immune system i.e. inflammation and other (Kim and Kim 2002; Vert and Domurado 2000; Zhang et al. 2007). In contrast to these studies the following investigation was aimed at the immobilization of PEG at lower coating densities to obtain control over adsorption of proteins and possibly subsequent adhesion of cells.

13.4 Effect of Photochemical Immobilization of Poly (Ethylene Glycol) on Adhesion of Cells

PEG of different molecular weights was covalently modified to obtain α -4-azidobenzoyl ω -methoxy (polyethylene glycol) as described by Thom et al. (2000). After adsorption of ABMPEG from aqueous solutions to polysulfone (PSf) films and exposure to UV light, a covalent link between the photolinker and PSf is established. The preparation of ABMPEG and the photochemical reactions have been described in more detail in recent papers (Thom et al. 2000; Altankov et al. 2000). The surface modification of PSf was monitored by a number of methods (Thom et al. 2000). Dynamic contact angle measurements showed that an increase of the ABMPEG concentration in the coating solution leads to a concomitant decrease in advancing and receding water contact angles (see Fig. 13.8). At the same time, it was observed that the hysteresis i.e. the difference between advancing and receding water contact angles increased. The observed water contact angles indicate a significant but incomplete PEG coating of the underlying PSf even for the highest solution concentration of ABMPEG. Surfaces saturated (brush regime) with PEG moieties would effectively shield the underlying PSf completely and typically show advancing receding contact angles lower than of 30° (Lazos et al. 2005). The increased hysteresis indicates certain heterogeneity of the substratum, which means that hydrophobic PSf is covered partly with hydrophilic PEG.

Figure 13.9 shows immunofluorescence images of human dermal fibroblasts seeded on different ABMPEG modified PSf after pre-coating with $20 \mu\text{g/mL}$ fibronectin. Focal adhesions were visualized by labeling vinculin with monoclonal antibodies. It was evident that spreading and formation of focal adhesions was slightly inhibited on PSf. This observation indicates that the hydrophobic PSf causes conformational changes of fibronectin as it was observed by others (Steele et al. 1992; Juliano et al. 1993; Grinnell and Feld 1982; Jonsson et al. 1982). However, low coating concentrations of ABMPEG lead to a significant increase in cell spreading and formation of focal adhesion plaques as visible up to 0.1 g/L .

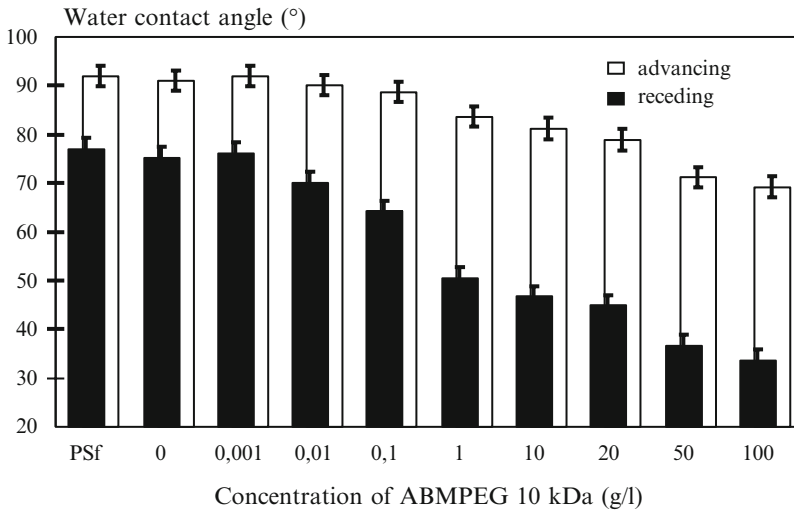


Fig. 13.8 Dynamic water contact angle measurements of plain polysulfone (PSf), PSf incubated in water (0) and after pre-incubation with different concentrations of ABMPEG dissolved in water and exposed to UV. Note the increasing hysteresis with rising ABMPEG concentrations. Data modified from Thom et al. (2000)

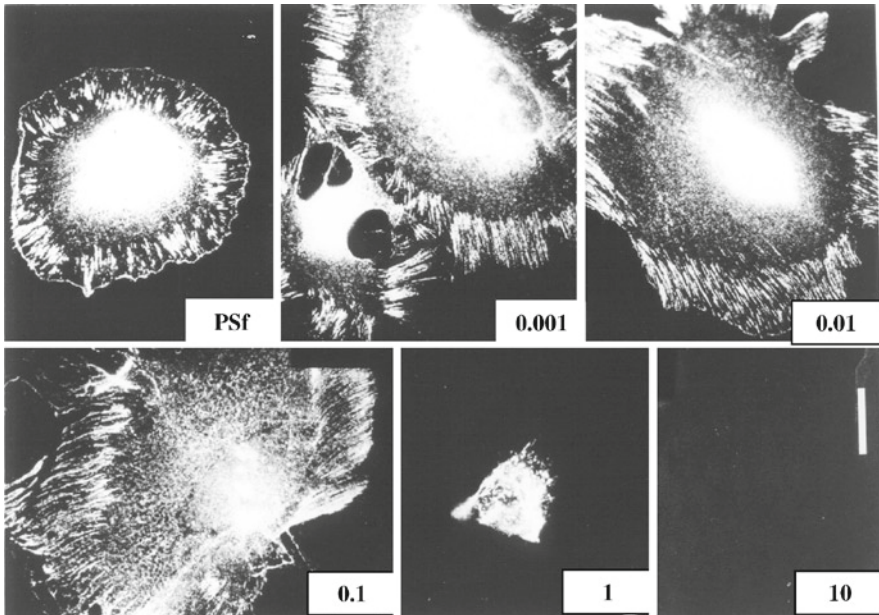


Fig. 13.9 Formation of focal adhesion plaques in human dermal fibroblast plated on ABMPEG modified polysulfone (PSf) after pre-coating with 20 µg/mL fibronectin. Cells were cultured for 2 h, fixed, permeabilized and stained for vinculin. Bar 10 µm

Indeed, higher coating concentrations such as 1 or 10 g ABMPEG/L reduced adhesion and spreading, which is related to the repelling effect of PEG on protein adsorption described previously (Lee et al. 1989; Morra 2000; Sofia et al. 1998; Szleifer 1997; Halperin 1999). In this context also the adsorption of fibronectin on ABMPEG modified PSf was measured with ellipsometry showing a pronounced decrease with increasing ABMPEG concentration (Thom et al. 2000; Altankov et al. 2000). However, fibronectin adsorption was still observable even at the highest coating density of 10 g/L ABMPEG.

The growth of fibroblasts in the presence of 10% fetal bovine serum on the different surfaces was strongly related to cell adhesion and spreading shown above. Figure 13.10 shows phase contrast micrographs of fibroblasts cultured over 7 days on the various plain or ABMPEG-modified PSf. Cells on plain PSf represented a slightly reduced cell growth. It was also observed that the number of cells was lower after 7 days of culture. Intermediate coating concentrations of ABMPEG corresponded to a maximum growth of cells. A slight shift was also observed in the maximal cell numbers at lower ABMPEG concentrations such as 0.001 g/L and

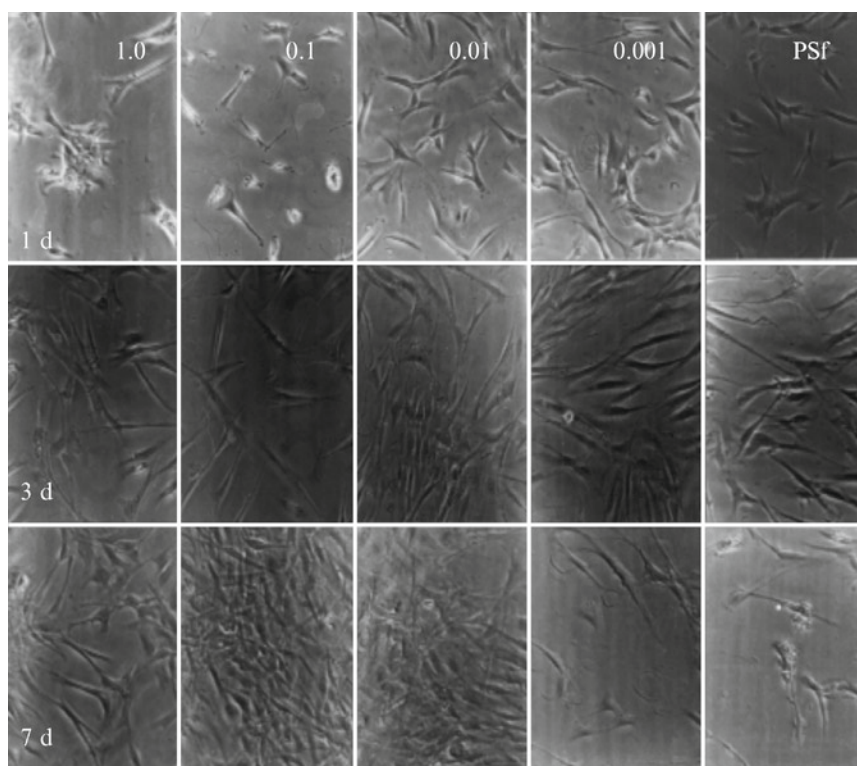


Fig. 13.10 Growth of fibroblasts on plain or PSf modified with various concentrations of ABMPEG. Cells were cultured for 7 days in the presence of 10% fetal bovine serum. Photographs were taken with phase contrast microscopy

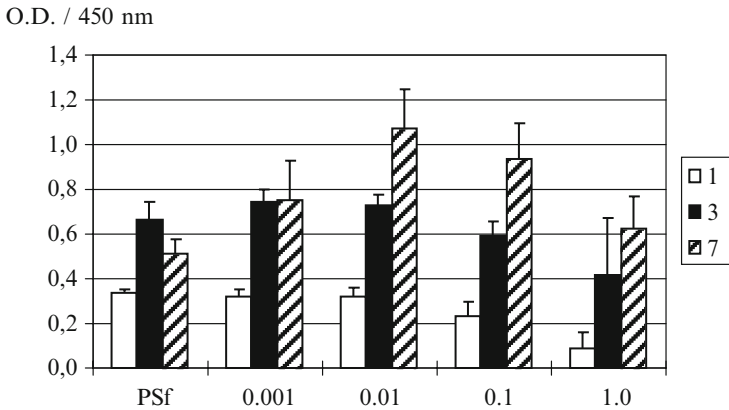


Fig. 13.11 Metabolic activity of fibroblasts on plain PSf or PSf modified with various concentrations of ABMPEG measured by XTT assay. Cells were cultured for 1, 3 and 7 days in the presence of 10% fetal bovine serum. Results are given as optical densities (O.D.) measured at 450 nm

0.01 g/L at day 1 and 3 to higher cell growth after 7 days at 0.1 g/L ABMPEG. An inhibition of cell growth was evident at higher coating concentrations like 1 g/L.

The qualitative results were confirmed by colorimetric XTT assay based on the quantification of the activity of cytosolic esterases, which is related to the number of viable cells. Figure 13.11 shows that the quantity of viable cells was reduced on plain PSf and at higher coating concentrations of ABMPEG. The maximum number of cells after 7 days culture was obtained at 0.01 and 0.1 g/L ABMPEG. Taken together these results, a remarkable finding can be noted, that intermediate concentrations of surface-bound PEG promote adhesion and growth of fibroblasts on PSf. It was also shown that functional activity of fibroblasts in terms of fibronectin synthesis and matrix formation was significantly enhanced at intermediate coating concentrations of ABMPEG as well (Altankov et al. 2000).

Recent work from Lazos et al. (2005) confirmed these previous findings and showed that an incomplete coverage of PEG on polystyrene was able to regulate the binding of proteins through size selective adsorption. It was stated that the protein binding to PEG-modified polystyrene surfaces is driven by hydrophobic interactions with uncovered polystyrene sites. Surface-bound PEGs control the size and density of sites thus allowing selective sizes of protein to be bound. The PEG coating density has an influence on PEG architecture on the surface such as brush at high density, overlapping mushroom at moderately high density, non-overlapping mushroom at a moderate density and pancake at a low density (Vermette and Meagher 2003). Jeon and Andrade studied the effect of surface density related to protein size (Jeon and Andrade 1991). A primary adsorption which is defined as proteins diffusing through the layer and adsorbing onto the underlying surface can be prevented by a dense PEG coating (brush regime). PEG chains in a brush conformation provide undesirable entropy, if proteins compress the PEG layer (Pasche et al. 2005). A larger PEG molecules like those used in the study presented here, with a greater excluded volume cannot pack as densely on the surface to get the

same grafting density as a smaller PEG molecule (Sofia et al. 1998). Thus, adhesive proteins like vitronectin or fibronectin may adsorb from serum on such substratum. However, in contrast to their adsorption on plain hydrophobic polysulfone, where conformational changes alter the biological activity of proteins, here the neighbouring PEG molecules compress adsorbed protein molecules and presumably limit their unfolding on ABMPEG-modified PSf. Hence, although less proteins bind to ABMPEG modified PSf (Thom et al. 2000), a high biological activity is maintained.

It is interesting to note that not only fibroblast express this specific behaviour. Other types of cells such as endothelial cells, keratinocytes and hepatocytes also show a strong dependence of adhesion and growth from ABMPEG coating concentration on PSf and again with a maximum activity at intermediate densities. Figure 13.12 shows as an example the growth behaviour of C3A hepatoblastoma cells in dependence on the ABMPEG concentration. It is obvious that a maximum of cell number can be observed at a coating concentration of 0.1 g/L ABMPEG. Overall it can be concluded that the photochemical immobilisation of PEG at low or intermediate coating densities can be used as a tool to control adsorption and biological activity of proteins from the surrounding media and hence adhesion of cells.

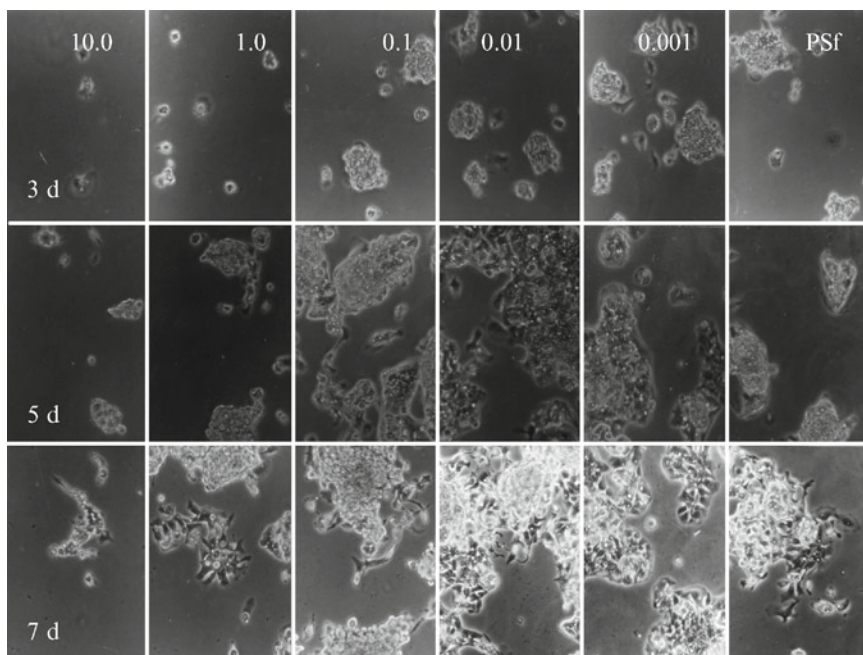


Fig. 13.12 Growth of C3A hepatoblastoma cells on ABMPEG modified polysulfone (PSf) in dependence on the ABMPEG concentration (gABMPEG/L) over 7 days of culture. Note that maximum number of cells can be observed at low and intermediate ABMPEG concentrations. Micrographs were obtained by phase contrast microscopy

13.5 Application of Layer-by-Layer Technique on Charged Surfaces

13.5.1 Background of Layer-by-Layer Technique

Based on the work of Iler in 1966 (Iler 1966), Decher and co-workers (Decher et al. 1992) established the layer-by-layer technique (LbL) as novel bottom-up method in the 1990s. In principle, the layer-by-layer method represents the alternating adsorption of oppositely charged polyelectrolytes (PEL) from aqueous solutions onto charged surfaces. The adsorption of negatively and positively charged molecules including washing steps for the removal of loosely bound material can be repeated in cycles, which leads to polyelectrolyte multilayers (PEM) of adjustable composition and thickness (see Fig. 13.13).

The thickness of the single layers is dependent on the conformation and nature of the applied macromolecules and lies in the nanometer range. The polycations and polyanions are being deposited primarily by electrostatic forces, but also other kinds of interactions such as van-der-Waals, hydrophobic and hydrogen bonding may play an important role (Tang et al. 2006). In this respect also other primary types of forces have been employed such as hydrophobic interaction using amphiphilic molecules for the generation of multilayers. Moreover, depending on the conformation of PEL the entanglement of molecules may occur, which increases the stability of the multilayers. Therefore the layers are not sharply separated but intermingle and are therefore considered as “fuzzy layers” (Decher 1997).

PEL are macromolecules that bear ionogenic groups. Their charge depends on ambient conditions, which particularly holds for weak polyelectrolytes. The adjustment

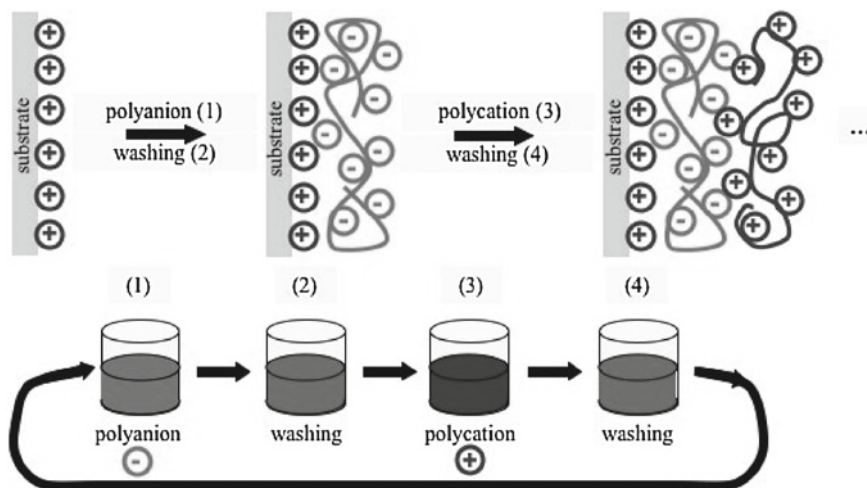


Fig. 13.13 Experimental set-up for generation of polyelectrolyte multilayers

and control of process parameters like the pH value, ionic strength of the solutions as well as the temperature can have a strong impact on the PEL conformation and hence on the morphology and features of the PEM (Tang et al. 2006; Decher 1997; Hammond 2004; Behrens and Grier 2001). Moreover, the properties of the PEL such as molar mass, charge density and structure, the substrates physicochemistry (type of functional groups, charges, etc.) and roughness can lead to a tremendous variety of characteristics of the resulting multilayers (Tang et al. 2006). The researcher is therefore given a great freedom of choice and application of molecules for LbL.

It is important to note that many biomacromolecules found in mammals such as DNA, proteins and polysaccharides represent PEL and can be used for the formation of PEMs (Tang et al. 2006). Hence, components of the extracellular matrix like collagen, fibronectin and other proteins or glycosaminoglycans like heparin may be incorporated into multilayers on charged biomaterial surfaces. For that reason, the LbL method might be a useful tool to mimic the natural environment of cells i.e. the extracellular matrix incorporating specific adhesion and growth factors. Consequently, PEM may be used to regulate adhesion of cells on biomaterials by changing general physicochemical surface properties (e.g. wettability) or incorporation of biological cues.

13.5.2 Application of LbL Technique to Inorganic Surfaces

This study was carried out to investigate the effect of PEMs composed of poly (ethylene imine) (PEI) and heparin (HEP) on cell adhesion and subsequent cell proliferation. Glass was used as a model material for other inorganic materials with a negative surface charge at physiological pH (Behrens and Grier 2001). The formation of PEMs was performed using PEI with a molecular weight of about 750 kDa as (weak) polycation and HEP with an activity of 186 IU/mg as (strong) polyanions, both dissolved in distilled water at a concentration of 2 mg/mL. During the layer formation process the pH value from the first to the seventh layer was not adjusted. For the assembly of the eighth and tenth layer the pH value of the heparin solution was adjusted to acidic, neutral and alkaline values.

Figure 13.14 shows water contact angles during the alternating adsorption of PEI and HEP with a successive multilayer formation up to ten layers. Static water contact angle measurements showed a regular oscillation of contact angles with lower values for HEP and higher for PEI up to the seventh layer. It has been shown previously that layers of PEI are moderately and layers of HEP are highly wettable due to the presence of polar amino groups and charged sulphate and carboxylic groups (Atkin et al. 2003; Yoo et al. 1998). However, a novel finding was here that the variation of pH values of the HEP solutions caused a distinct change in wettability. Especially layers prepared from HEP solutions at pH 9 were less hydrophilic than layers at pH 5 or 7.

The properties of PEM are depending on the solution pH and temperature during the layer formation process, particularly if weak PEL are used (Yoo et al. 1998).

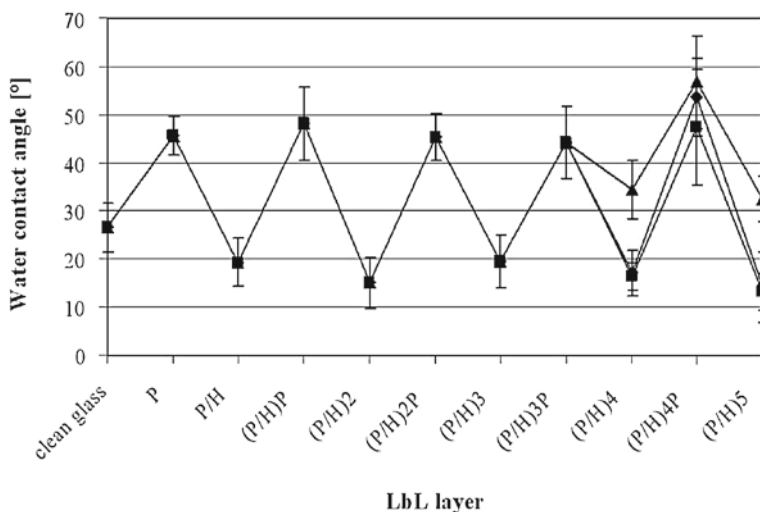


Fig. 13.14 Static water contact angle after each step of PEL adsorption onto glass substrates in dependence on the solution pH value (pH 5 [◆], pH 7 [■], pH 9 [▲])

The polymer chains of weak polycations tend to adsorb as thin layers with flat chain conformations at lower pH when they are highly charged and as thicker, loopy type structures when they are less charged at high pH (Yoo et al. 1998; Richert et al. 2004). Vice versa, the same is known for weak polyanions. The observed changes in wettability at pH 9.0 can be explained basically by the properties of the (weak) polycation in the outer regions of the multilayers (Richert et al. 2004). The deprotonation of adsorbed PEI (e.g. seventh layer PEI) at pH 9 during the addition of the HEP solution causes probably a reduced electrostatic attraction for HEP molecules in solution. Accordingly, less HEP shall be adsorbed, which causes a rise of water contact angle. Due to the negative charge of the eighth HEP layer PEI is still adsorbed at the ninth layer (Gopinadhan et al. 2007), which goes along a rise in water contact angles. Overall, the anticipated domination of the weak, less wettable polycation PEI in the subsequent layers after the increase to pH 9 should be the reason for the slightly diminished wettability of PEM.

The impact of multilayer composition and formation conditions (HEP or PEI, pH value) on cells was studied with human fibroblasts. Cell adhesion was visualized after plating cells 4 h on serum (FBS, 10%) or fibronectin (FN, 2 $\mu\text{g}/\text{mL}$) coated PEM (both with HEP or PEI as terminal layer) using immunofluorescence microscopy staining vinculin to show focal adhesions. Fibronectin matrix deposition was studied after 24 h culture of cells on the plain PEM in medium containing 10% serum.

Figure 13.15 shows micrographs of fibroblasts stained for vinculin cultured on the eighth layer, which represents HEP. The left column shows cells on FBS-coated, the middle on FN-coated HEP. The right column represents FN matrix

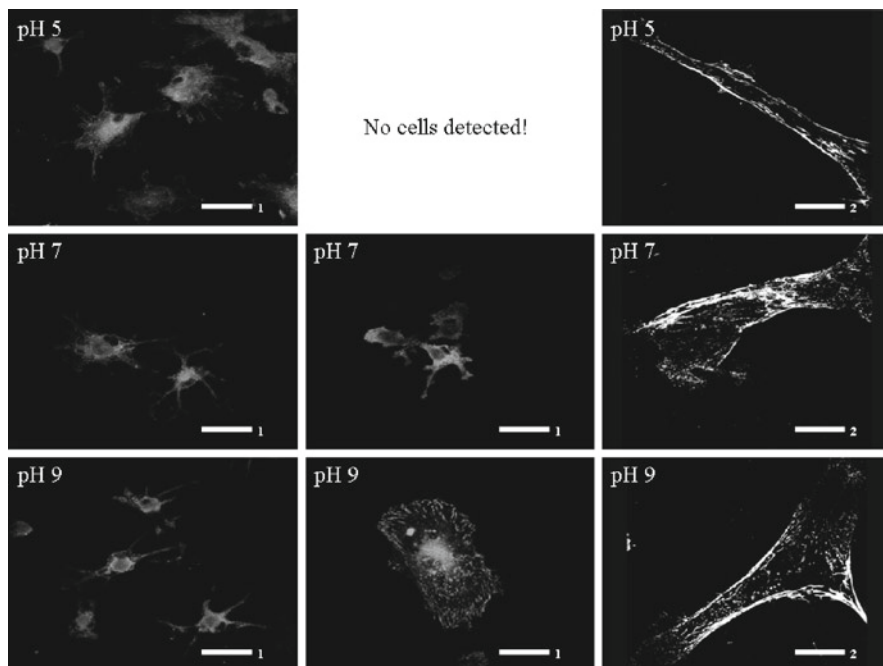


Fig. 13.15 Fibroblasts plated on $(\text{PEI}/\text{HEP})_4$ after 4 h. Staining of vinculin after pre-treating with 10% FBS (*left column*) and 2 $\mu\text{g}/\text{ml}$ FN (*middle column*) (bar1 = 50 μm); Fibronectin matrix formation was studied after 24 h cultivation of cells in serum-containing medium (10% FBS, *right column*) (bar2 = 25 μm)

formation on plain HEP in the presence of serum. The pictures reveal that adhesion and spreading on serum-coated HEP was not very much dependent on pH. Here cell spreading was low and shape of cells irregular with some pseudopodia formation. No expression of focal adhesion complexes was observed. It seems that those serum components are preferentially adsorbed, which do not support adhesion of cells. On the other hand, if FN was used as coating no cells adhered at pH 5. This implies that HEP layers formed at pH 5 do not allow adsorption of proteins. Cell spreading was still low at pH 7 with complete absence of focal adhesions. In contrast, cell spreading was greatly increased on HEP layers formed at pH 9. Here, focal adhesions positive for vinculin were well expressed. A similar finding was made for FN matrix formation. Pictures show that cell spreading was again maximal at pH 9 with more pronounced formation of FN matrix compared to cells plated on PEM formed at pH 5. A possible explanation of these findings is that large quantities of HEP are bound at pH 5, when the previously bound PEI is positively charged. Under this circumstance a high negative surface potential can be expected, which represents a repulsive barrier for protein adsorption (Müller et al. 1999). Hence, cell adhesion is diminished or absent. In contrast, at pH 9 less HEP is bound to the previous PEI

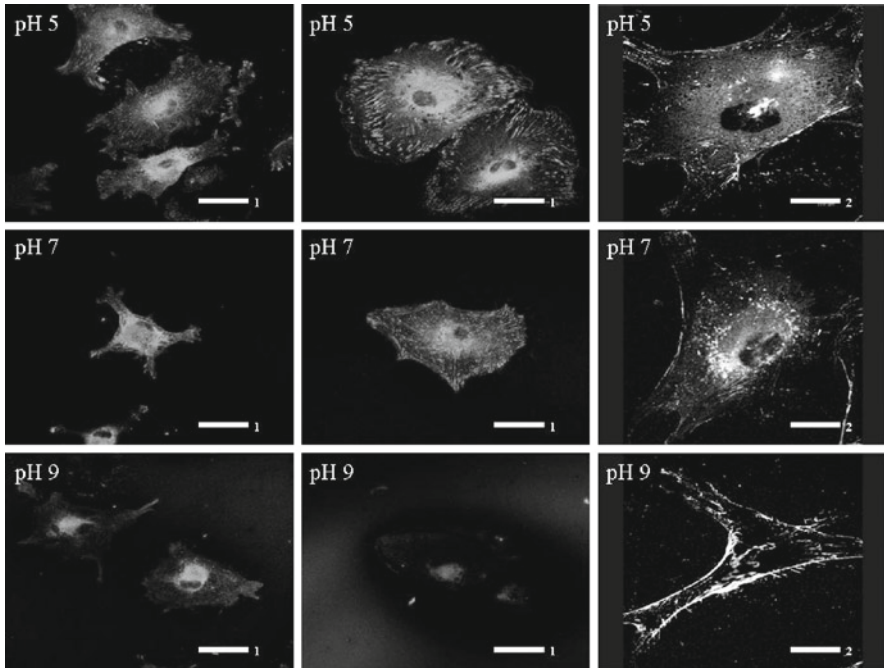


Fig. 13.16 Fibroblasts plated on $(\text{PEI}/\text{HEP})_4$ PEI after 4 h. Staining of vinculin after pre-treating with 10% FBS (*left column*) and 2 $\mu\text{g}/\text{mL}$ FN (*middle column*) (bar1 = 50 μm); Fibronectin matrix formation after 24 h cultivation of cells in serum-containing medium (10% FBS, *right column*) (bar2 = 25 μm)

layer so that enhanced FN binding is possible (Müller et al. 1999; 2001), which should promote cell adhesion and focal adhesion formation. Since, fibroblast secrete normally large quantities of FN, the results of matrix formation support this assumption. Here, more pronounced FN matrix deposition could be observed at pH 9, which went along with an improved spreading of cells.

On the terminal PEI layer the cells showed a nearly opposite behaviour compared to HEP layer (see Fig. 13.16). Under these circumstances spreading of cells was higher on terminal PEI layers adsorbed on HEP prepared at pH 5. The pre-treatment of the samples with FBS allowed to formation of vinculin-positive adhesion plaques on PEI at pH 5 (left column). No focal adhesions were observed in fibroblasts plated on PEI layers related to pH 9. After pre-adsorption of FN the adhesion plaques were much better developed on PEI layers at pH 5 while vinculin was weakly organized in focal adhesions in cells on layers at pH 9. Also the formation of FN matrix shown in the right column of Fig. 13.16 followed this trend. Again, the domination of the weak polycation PEI may be a reason for observed effects. At low pH 5, more HEP was bound to the previous layer, which allows sufficient adsorption of PEI and shall compensate for the prior negative charged of the HEP layer. As a result, probably a positively charged terminal PEI layer is established,

which will bind proteins like FN quite well (Müller et al. 1999, 2001) promoting adhesion and function of cells. In contrast, at pH 9, less PEI binds to the reduced quantities of HEP present in the terminal layer. PEI adsorption may cause a charge neutralisation, which may reduce adsorption of FN. Hence, cell adhesion, spreading and focal adhesion formation are diminished. Of course, these explanations have to be considered as preliminary. Further studies measuring zeta potentials of terminal layers and protein adsorption will allow more profound clarifications of the observed effects. In general, the current findings are in accordance with our previous work showing that adhesion of cells is diminished on surfaces with negative surface potential and enhanced on those having positive potential (Seifert et al. 2002; Altankov et al. 2003; Tzoneva et al. 2008).

In conclusion, tailoring the layer thickness and wettability of multilayers and hence the adhesion strength of surfaces for cells due to the variation of the pH may lead to various biomedical applications. For example, the established use of poly (ethylene imine) for complex formation with DNA may pave the way for in situ transfection of cells in the field of tissue engineering with the system presented here (Rémy-Kristensen et al. 2001).

13.5.3 Application of LbL Technique to Poly (L-Lactide) (PLLA) for Tissue Engineering Applications

PLLA is one of the few synthetic degradable polymers, which are approved by the Food and Drug Administration (FDA) for certain clinical applications. However, the application of PLLA and other polyesters in the emerging field of tissue engineering is hampered by their relatively low tissue compatibility, which is partly due to the hydrophobic nature of the polymers (Lendlein 1999). To overcome this limitation various surface modifications were conducted by different researchers to improve its biocompatibility (Ma et al. 2003). A novel approach to modify the surface of PLLA could be based on LBL technique (Iler 1966; Decher et al. 1992; Tang et al. 2006). However, due to the polymer composition PLLA lacks sufficient surface charges. Therefore it represents per se not a useful material for LbL technique. Hence, PEI was immobilized as primary layer in LbL on PLLA either by simple physical adsorption or covalent binding. The covalent immobilization of PEI onto PLLA surface was based on the chemical activation of the carboxylic end group of PLLA backbone and subsequent reaction with primary amino groups of PEI. Particularly the latter approach resulted in an efficient and durable modification of PLLA with PEI. The modified surfaces were characterized by acid orange assay to determine amino group density, AFM to investigate surface morphology/roughness changes, and water contact angle to evaluate surface hydrophilicity. Details of this investigation have been published elsewhere (Liu and Groth submitted). Main results are summarized in Table 13.1 showing that particularly the covalent modification of PLLA with a high molecular weight PEI (HMW) resulted in highest amino group density, lowest water contact angles and a certain increase in surface

Table 13.1 Surface properties of blank and modified PLLA films

Samples	Surface element composition (%)			Amino groups density (*10 ¹⁶ /cm ²)	Water contact angle	Surface roughness (Rms, nm)
	C	N	O			
Blank PLLA	61.6	–	38.4	–	72.4 ± 0.3	3.24 ± 0.62 *
Phys. LMW	64.2	0.5	35.3	2.51 ± 0.19	60.5 ± 0.9	6.70 ± 1.71
Chem. LMW	63.7	0.5	35.8	9.36 ± 0.62	59.4 ± 0.6	1.95 ± 0.71
Phys. HMW	65.1	1.0	33.9	12.14 ± 0.40	56.8 ± 2.7	7.91 ± 2.62
Chem. HMW	63.3	3.7	33.0	12.79 ± 0.36	56.2 ± 1.9	39.00 ± 9.60

PLLA – poly L lactic acid, Phys – adsorbed PEI, Chem. – covalent bound PEI, LMW – low molecular weight PEI (70.000), HMW – high molecular weight PEI (750.000)

roughness. In comparison the application of a low molecular weight PEI (LMW) did not result in comparable changes of the surface chemistry. If the biocompatibility of the PEI-modified PLLA was studied all PEI modified surfaces were superior to blank PLLA in terms of MG-63 osteoblasts adhesion, growth and functional activity, which has been published recently (Liu et al. submitted).

After PEI modification, positive charges were generated as demonstrated by zeta potential measurements (Liu et al. submitted), which paved the way for LBL assembly of biomacromolecules on PLLA to obtain control on cell adhesion. Polyanions selected for this study were components of connective tissue matrices like hyaluronic acid (HA) or a chemical modified highly sulfated HA (sHA). Due to the presence of carboxylic acid groups HA represents a weak polyelectrolyte, which makes its conformation dependent on ambient conditions like the pH value (Toole 2004). Many cells, such as osteoblasts, chondrocytes and other possess a specific receptor for HA, the CD 44 cell adhesion receptor. In this respect, it has been observed that HA can promote cell adhesion, proliferation, and differentiation (Brown and Jones 2005). Sulphation of HA can not only preserve the properties of HA but is also supposed to improve its antithrombogenic properties (Satoh et al. 2004). As polycation, chitosan was selected. CHI, a random copolymer of d-glucosamine and N-acetyl-d-glucosamine, is a polysaccharide having structural characteristics similar to the GAGs in the ECM. It is derived from the alkaline deacetylation of chitin obtained from the exoskeleton of crustaceans (Yi et al. 2005). Although CHI is not naturally present within the human body, a number of studies have demonstrated that it evokes a minimal immune response when implanted in animals. Since CHI is a biodegradable, biocompatible, and anti-infective material, it has been used for formation of scaffold material in tissue engineering (Yi et al. 2005). LBL assembly was carried using 2 mg/mL CHI (pH 5.0, in 0.05 M acetic acid containing 0.14 M NaCl) and sHA (pH 7.0 in water containing 0.14 M NaCl) solutions.

Water contact angle measurements shown in Fig. 13.17 revealed a change of wettability with increasing layer number. Obviously, the change in wettability was quite different compared to that observed for multilayer formation using PEI and HEP on glass as shown in Fig. 13.14. The water contact angle dropped in an oscillating

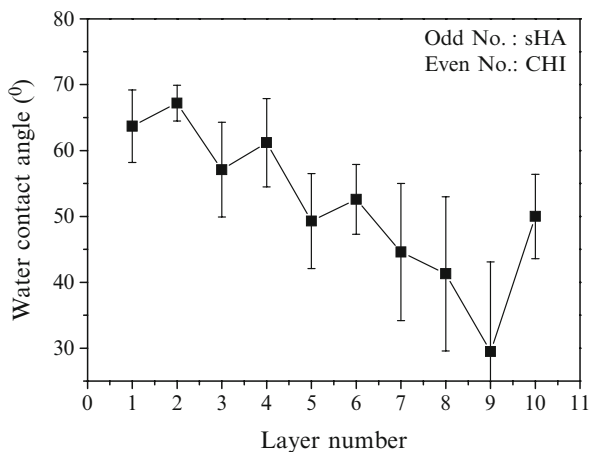


Fig. 13.17 Water contact angles on PEI-PLLA surface after adsorption of sHA (*odd numbers*) and CHI (*even numbers*)

manner from rather high values for PEI-PLLA to lower values after subsequent adsorptions of polycation CHI

and polyanion sHA. Figure 13.17 shows also that the decrease of WCA was greater after adsorption of sHA, which must be due to the strong acidic nature of the sulfate group compared to the basic CHI possessing amino and hydroxyl groups. It was also observed that the regular behavior of WCA changes ends with the seventh layer. The reason for this could be beginning intermixing of both polyions and/or formation of clusters, which could be responsible for the unexpected changes of water contact angles. The observed effects will be unraveled in future experiments.

LBL assembly of CHI and sHA on PLLA was also monitored by quartz crystal microbalance (QCM) spectroscopy, which can relate frequency changes of sensor oscillations to mass changes due to adsorption or desorption of molecules. PLLA was first spin-coated on the sensor to obtain a thin polymer film. Subsequently the PLLA film was chemically modified with HMW PEI as described previously. Figure 13.18 shows the frequency changes of the sensor. It can be seen that the subsequent alternating adsorption of sHA and CHI on the sensor, caused a decrease of resonance frequency, indicating an augmented mass of the adsorbed material according to Sauerbrey's law (Sauerbrey 1959). Hence, it can be stated that the experimental setting results in a continuous mass increase due to the alternating adsorption of either sHA or CHI.

After assembly of multilayers from sHA and CHI, the adhesion of MG-63 osteoblasts was studied plating the cells in the presence of serum for 4 h on the various surfaces. Both number of adherent cells and their size was quantified with image analyzing software. The results are shown in Fig. 13.19. Compared to blank PLLA surface, the number but also size of cells was quite different on either PEI modified

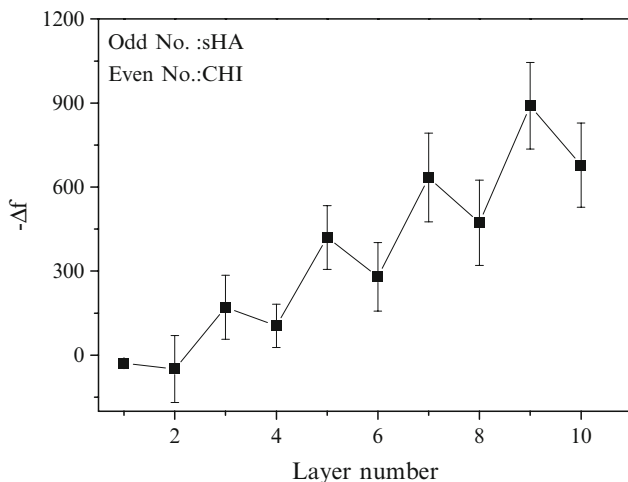


Fig. 13.18 Results of QCM measurements showing a mass increase as indicated by the decrease in resonance frequency after subsequent alternating adsorption of sulfated hyaluronic acid (sHA) and chitosan (CHI)

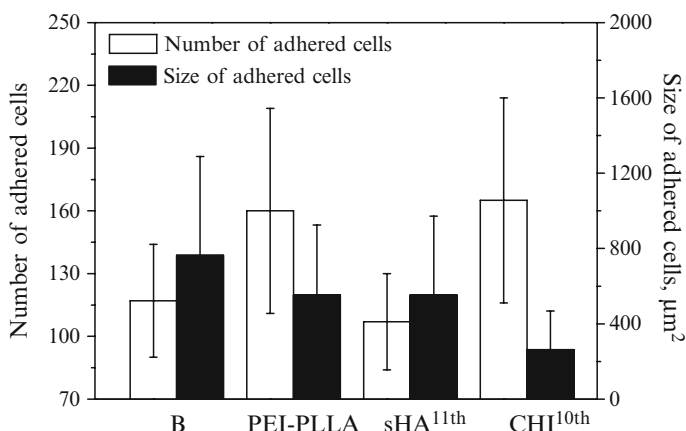


Fig. 13.19 Number and size of adhered MG-63 cells after 4 h on B: blank PLLA; PEI-PLLA: high molecular weight PEI-modified PLLA; sHA^{11th}: multilayers composed of sHA and CHI with sHA as terminal layer or CHI^{10th}: sHA-CHI multilayers with CHI^{10th} as terminal layer

or sHA/CHI multilayer surface. It was evident that cell adhesion was highest on PEI-modified PLLA or CHI terminated multilayers, which is related due to the presence of amino groups of PEI or CHI. As discussed before this could lead to improved adsorption of proteins like fibronectin or vitronectin promoting the adhesion of cells (Hamerli et al. 2003b; Webb et al. 2000; Faucheux et al. 2004; Altankov et al. 2003; Rémy-Kristensen et al. 2001). However, it must be also noted

that size of cells was quite small on CHI. In contrast, on sHA terminal layers both adhesion and size of cells was low. This can be related to the presence of negatively charged sulfate and carboxylate groups in sHA, which may result in hydrophilic surfaces with negative surface potential. This can be related to decreased adsorption of adhesive proteins and suppression of cell adhesion as it has been shown previously (Webb et al. 2000; Altankov et al. 2003; Tzoneva et al. 2008). Overall, the study presented here shows clearly that also degradable polyesters for tissue engineering applications can be chemically modified to allow subsequent physical adsorption of polyelectrolyte to generate multilayers. This can be used to control the adhesion of cells, which may open the way for a variety of applications in tissue engineering and regenerative medicine.

13.6 Summary and Conclusions

Generic methods have been selected in this study to modify the surface of different classes of materials such as inorganic materials, but also polymer surfaces. Basically all techniques presented here work in solutions, which are able to wet the surface of 3-D objects with different geometry. This should allow an even modification of implant materials or tissue engineering scaffolds. The techniques share also as a common feature that they represent bottom-up methods which allow basically the generation of micro and nanostructured on surfaces. It has been shown in this paper that all methods allow the adjustment of materials surface chemistry and thus wettability, which may be used to control adhesion of cells and hence subsequent cellular reactions such as proliferation and function. Moreover, the application of biogenic molecules or bio-related molecules as performed with the LbL method may itself represent the incorporation of biological cues or enable their subsequent binding to immobilized molecules like glycosaminoglycans. Overall, the methods presented here represent low cost solutions to tailor the surface of biomaterials in the nanometer scale for a variety of applications in tissue engineering and regenerative medicine.

Acknowledgments A part of the results presented here is based on contributions from previous projects and co-operations with Mathias Ulbricht, University Essen-Duisburg and Volkmar Thom, Sartorius AG. Financial support for these studies was provided by Deutsche Forschungsgemeinschaft (Gr 1290/4-1 and Gr 1290/4-2) and European Union funded Marie-Curie-Fellowships to George Altankov (HPMF-CT-2001-01275), Nathalie Faucheux (HPMF-CT-2000-00883) and Zhen-Mei Liu (MIF1-CT2005-021845).

References

- Ahn SJ, Kaholek M, Lee W-K, LaMattina B, Labean TH, Zauscher S (2004) Surface-initiated polymerization on nanopatterns fabricated by electron-beam lithography. *Adv Mater* 16(23–24):2141–2145

- Albrecht W, Seifert B, Weigel T, Holländer M, Groth T, Hilke R (2003) Amination of poly(ether imide) membranes using di- and multivalent amines. *Macromol Chem Phys* 204:510–521
- Altankov G, Groth T (1996) Fibronectin matrix formation and the biocompatibility of materials. *J Mater Sci Mater Med* 7:425–429
- Altankov G, Grinnell F, Groth T (1996) Studies on the biocompatibility of materials: fibroblast reorganization of substratum-bound fibronectin on surfaces varying in wettability. *J Biomed Mater Res* 30:385–391
- Altankov G, Groth T, Krasteva N, Albrecht W, Paul D (1997) Morphological evidence for a different fibronectin receptor organization and function during fibroblast adhesion on hydrophilic and hydrophobic glass substrata. *J Biomater Sci Polym Ed* 8:721–740
- Altankov G, Thom VH, Groth T, Jankova K, Jonsson G, Ulbricht M (2000) Modulating the biocompatibility of polymer surfaces with poly(ethylene glycol): effect of fibronectin. *J Biomed Mater Res A* 52(1):219–230
- Altankov G, Richau K, Groth T (2003) The role of surface zeta potential and substratum chemistry for regulation of dermal fibroblast interaction. *Materialwiss Eng* 34:1120–1128
- Anderson JM, Bonfield TL, Ziats NP (1990) Protein adsorption and cellular adhesion and activation on biomedical polymers. *Int J Artif Organs* 13:375–382
- Andrade JD, Hlady V (1986) Protein adsorption and materials biocompatibility: a tutorial review and suggested hypotheses. *Adv Polym Sci* 79:1–63
- Atkin R, Craig VSJ, Wanless EJ, Biggs S (2003) Mechanism of cationic surfactant adsorption at the solid–aqueous interface. *Adv Colloid Interface Sci* 103:219–304
- Bacakova L, Walachova K, Svorcik V, Hnatovicz V (2001) Adhesion and proliferation of rat vascular smooth muscle cells on polyethylene implanted with O⁺ and C⁺ ions. *J Biomater Sci Polym Ed* 12:817–834
- Behrens SH, Grier DG (2001) The charge of glass and silica surfaces. *J Chem Phys* 115(14): 6716–6721
- Bergeron E, Lord E, Marquis ME, Groth Th, Fauchoux N (2007) Modulation of cyclic AMP production in fibroblasts attached to substrata with different surface chemistries. In: Kendall JB (ed) *Biomaterials research advances*. Nova Science Publisher Inc., ISBN 978-1-60021-892-7, pp 21–36
- Bird RI, Hall B, Kojima M, Chapman D (1994) Phosphatidylcholine reduces polyester thrombogenicity shown by material thromboelastography (MTEG). *Clin Sci* 78:P78–P78
- Bongrand P (1982) Physics of cell adhesion. *Prog Surf Sci* 12:217–286
- Brétagnol F, Valsesia A, Sasaki T, Ceccone G, Colpo P, Rossi F (2007) Direct nanopatterning of 3D chemically active structures for biological applications. *Adv Mater* 19:1947–1950
- Brown MB, Jones SA (2005) Hyaluronic acid: a unique topical vehicle for the localized delivery of drugs to the skin. *JEADV* 19:308–318
- Chen Y, Pépin A (2001) Nanofabrication: conventional and nonconventional methods. *Electrophoresis* 22:187–207
- Choi C-H, Hagvall SH, Wu BM, Dunn JCY, Beygui RE, Kim C-J (2007) Cell interaction with three-dimensional sharp-tip nanotopography. *Biomaterials* 28:1672–1679
- Croll TI, O'Connor J, Stevens GW, Cooper-White JJ (2006) A blank state? Layer-by-layer deposition of hyaluronic acid and chitosan onto various surfaces. *Biomacromolecules* 7:1610–1622
- Curtis A (2004) Tutorial on the biology of nanotopography. *IEEE Trans Nanobioscience* 3:293–295
- Curtis ASG, Clark P (1990) The effects of topography and mechanical properties of materials on cell behaviour. *Crit Rev Biocompat* 5:343–362
- Dalby MJ, Childs S, Riehle MO, Johnstone H (2002) Fibroblast reaction to island topography: changes in cytoskeleton and morphology with time. *Biomaterials* 24:927–935
- Decher G (1997) Fuzzy nanoassemblies: toward layered polymeric multicomposites. *Science* 277:1232–1237
- Decher G, Hong JD, Schmitt J (1992) Buildup of ultrathin multilayer films by self-assembly process III. Consecutively alternating adsorption of anionic and cationic polyelectrolytes on charged surfaces. *Thin Solid Films* 210/211:831–835

- Deligianni DD, Katsala ND, Koutsoukos PG, Missirlis Y (2002) Effect of surface roughness of hydroxyapatite on human bone marrow cell adhesion, proliferation, differentiation and detachment strength. *Biomaterials* 22:87–96
- Diener A, Nebe B, Luethen F, Becker P, Beck U, Neumann HG, Rychly J (2005) Control of focal adhesion dynamics by material surface characteristics. *Biomaterials* 26:383–392
- Fauchoux N, Schweiss R, Lützwow K, Werner C, Groth T (2004) Self-assembled monolayers with different terminating groups as model substrates for cell adhesion studies. *Biomaterials* 25:2721–2730
- Fauchoux N, Tzoneva R, Nagel M-D, Groth T (2006) The dependence of fibrillar adhesions in human fibroblasts on substratum chemistry. *Biomaterials* 27:234–245
- Filippini P, Rainaldi G, Ferrante A, Mecheri B, Gabrielli G, Bombace M, Indovina PL, Santini MT (2001) Modulation of osteosarcoma cell growth and differentiation by silane-modified surfaces. *J Biomed Mater Res* 55:338–349
- Frisch SM, Ruoslahti E (1997) Integrins and anoikis. *Curr Opin Cell Biol* 9:701–706
- Fukuda T, Goto A, Ohno K (2000) Mechanisms and kinetics of living radical polymerizations. *Macromol Rapid Comm* 21:151–165
- Garcia AJ, Vega MD, Boettiger D (1999) Modulation of cell proliferation and differentiation through substrate-dependent changes in fibronectin conformation. *Mol Biol Cell* 10:785–798
- Gates BD, Xu Q, Stewart M, Ryan D, Willson CG, Whitesides GM (2005) New approaches to nanofabrication: molding, printing, and other techniques. *Chem Rev* 105(4):1171–1196
- Goda T, Konno T, Takai M, Moro T, Ishihara K (2006) Biomimetic phosphorylcholine polymer grafting from polydimethylsiloxane surface using photo-induced polymerization. *Biomaterials* 27:5151–5160
- Goddard JM, Hotchkiss JH (2007) Polymer surface modification for the attachment of bioactive compounds. *Prog Polym Sci* 32:698–725
- Goldstein AS, DiMilla PA (2002) Effect of adsorbed fibronectin concentration on cell adhesion and deformation under shear on hydrophobic surfaces. *J Biomed Mater Res* 59:665–675
- Gopinadhan M, Ivanova O, Ahrens H, Günther J-U, Steitz R, Helm CA (2007) The influence of secondary interactions during the formation of polyelectrolyte multilayers: layer thickness, bound water and layer interpenetration. *J Phys Chem B* 111:8426–8434
- Grinnell F (1978) Cellular adhesiveness and extracellular substrata. *Int Rev Cytol* 53:65–144
- Grinnell F, Feld M (1982) Fibronectin adsorption on hydrophilic and hydrophobic surfaces detected by antibody binding and analyzed during cell adhesion in serum-containing medium. *J Biol Chem* 257:4888–4893
- Groth T, Altankov G (1996) Studies on the cell-biomaterial interaction: role of tyrosine phosphorylation during fibroblasts spreading on surfaces varying in wettability. *Biomaterials* 17:1227–1234
- Groth T, Derdau K, Strietzel F, Foerster F, Wolf H (1992) The hemocompatibility of biomaterials in vitro - Investigations on the mechanism of the whole blood clot formation test. *ATLA* 20:390–395
- Groth T, Herrmann K, Campbell EJ, New RRC, Hall B, Hesse R, Goering H (1994) Protein adsorption, lymphocyte adhesion and platelet adhesion/activation on polyurethane ureas is related to hard segment content and composition. *J Biomater Sci Polym Ed* 6:497–510
- Groth T, Synowitz J, Malsch G, Richau K, Albrecht W, Lange K-P, Paul D (1997) Contact activation of plasmatc coagulation on polymeric membranes measured by the activity of kallikrein in heparinized plasma. *J Biomater Sci Polym Ed* 8:797–808
- Guo L, Kawazoe N, Fan Y, Ito Y, Tanaka J, Tateishi T, Zhang X, Chen G (2008) Chondrogenic differentiation of human mesenchymal stem cells on photoreactive polymer-modified surfaces. *Biomaterials* 29:23–32
- Halperin A (1999) Polymer brushes that resist adsorption of model proteins: design parameters. *Langmuir* 15:2525–2533
- Halperin A, Tirrel N, Lodge TP (1992) Tethered chains in polymer microstructures. *Adv Polym Sci* 100:31–71
- Hamerli P, Weigel T, Groth T, Paul D (2003a) Surface properties of and cell adhesion onto allylamine-plasma coated polyethylenterephthalat membranes. *Biomaterials* 24:3989–3999

- Hamerli P, Weigel T, Groth T, Paul D (2003b) Enhanced tissue-compatibility of polyethylene-terephthalat membranes by plasma aminofunctionalisation. *Surf Coat Tech* 174–175:574–578
- Hammond PT (2004) Form and function in multilayer assembly: new applications at the nano-scale. *Adv Mater* 16:1271–1293
- Healy KE, Lom B, Hockberger PE (1994) Spatial distribution of mammalian cells dictated by material surface chemistry. *Biotechnol Bioeng* 43:792–800
- Hu Y, Winn SR, Krajchich I, Hollinger JO (2002) Porous polymer scaffolds surface-modified with arginine-glycine-aspartic acid enhance bone cell attachment and differentiation *in vitro*. *J Biomed Mater Res* 64A:583–590
- Huang S, Ingber DE (1999) The structural and mechanical complexity of cell growth control. *Nat Cell Biol* 1:131–138
- Huang S, Ingber DE (2000) Shape-dependent control of cell growth, differentiation and apoptosis: switching between attractors in cell regulatory networks. *Exp Cell Res* 261:91–103
- Hubbell JA (1995) Biomaterials in tissue engineering. *Biotechnology* 13:565–576
- Hynes RO (2002) Integrins: bidirectional, allosteric signaling machines. *Cell* 110:673–687
- Iler RK (1966) Multilayers of colloidal particles. *J Colloid Interface Sci* 21:569–594
- Ishihara K, Oshida H, Endo Y, Watanabe A, Ueda T, Nakabayashi N (1993) Effect of phospholipid adsorption on nonthrombogenicity of polymer with phospholipid head groups. *J Biomed Mater Res* 27:1309–1314
- Israelachvili J, Wennerstrom H (1996) Role of hydration and water structure in biological and colloidal interactions. *Nature* 379:219–225
- Iwasaki Y, Nakabayashi N, Nakatani M, Mihara T, Kurita K, Ishihara K (1999) Competitive adsorption between phospholipid and plasma protein on a phospholipid polymer surface. *J Biomater Sci Polym Ed* 10:513–529
- Jauregui HO (1987) Cell adhesion to biomaterials. The role of several extracellular matrix components in the attachment of non-transformed fibroblasts and parenchymal cells. *ASAIO Trans* 33(2):66–74
- Jeon SI, Andrade JD (1991) Protein-surface interactions in the presence of polyethylene oxide II. Effect of protein size. *J Colloid Interface Sci* 142:159–165
- Jonsson U, Ivarson B, Lundstrom I, Berghem L (1982) Adsorption behavior of fibronectin on well characterized silica surfaces. *J Colloid Interface Sci* 90:148–163
- Juliano DJ, Saavedra SS, Truskey GA (1993) Effect of the conformation and orientation of adsorbed fibronectin on endothelial cell spreading and the strength of adhesion. *J Biomed Mater Res* 27:1103–1113
- Keselowsky BG, Collard DM, Garcia AJ (2003) Surface chemistry study on the enhancement of the osteointegration of a novel synthetic hydroxyapatite scaffold *in vivo*. *J Biomed Mater Res* 66A:247–259
- Kim JH, Kim SC (2002) PEO-grafting on PU/PS IPNs for enhanced blood compatibility – effect of pendant length and grafting density. *Biomaterials* 23:2015–2025
- Klee D, Ademovic Z, Bosserhoff A, Hoecker H, Maziolis G, Erli H-J (2003) Surface modification of poly (vinylidene fluoride) to improve the osteoblast adhesion. *Biomaterials* 24:3663–3670
- Kondyurin A, Gan BK, Bilek MMM, Mizuno K, McKenzie DR (2006) Etching and structural changes of polystyrene films during plasma immersion ion implantation from argon plasma. *Nucl Instrum Meth B* 251:413–418
- Lazos D, Franzka S, Ulbricht M (2005) Size-selective protein adsorption to polystyrene surfaces by self-assembled grafted poly (ethylene glycols) with varied chain lengths. *Langmuir* 21:8774–8784
- Lee JH, Kopecek J, Andrade JD (1989) Protein-resistant surfaces prepared by PEO-containing block copolymer surfactants. *J Biomed Mater Res* 23:351–368
- Lendlein A (1999) Polymers for implants with biomedical applications. *Chem Unserer Zeit* 33:279–295
- Liu Z-M, Groth T (2010) Modification of poly (L-lactide) with poly (ethylene imine) for tissue engineering applications. *Eur Polym J* (submitted)

- Liu Z-M, Lee S, Sarun S, Peschel D, Groth T Immobilization of poly (ethylene imine) on poly-lactide to control MG-63 cell adhesion, proliferation and function. *Biomaterials* (submitted)
- Liu Z-M, Xu Z-K, Wang J-Q, Wu J, Fu J-J (2004) Surface modification of polypropylene microfiltration membranes by graft polymerization of N-vinyl-2-pyrrolidone. *Eur Polym J* 40:2077–2087
- Liu Z-M, Xu Z-K, Wan L-S, Wu J, Ulbricht M (2005) Surface modification of polypropylene microfiltration membranes by the immobilization of poly(N-vinyl-2-pyrrolidone): a facile plasma approach. *J Membrane Sci* 249(1–2):21–31
- Liu Z-M, Tingry S, Innocent C, Durand J, Xu Z-K, Seta P (2006) Modification of microfiltration polypropylene membranes by allylamine plasma treatment: influence of the attachment routes on peroxidase immobilization and enzyme efficiency. *Enzyme Microb Technol* 39(4):868–876
- Lodish H, Berk A, Matsudaira P, Kaiser CA, Krieger M, Scott MP, Zipursky SL, Darnell J (2004) *Molecular cell biology*, 5th edn. Freeman, New York
- Ma Z, Gao C, Shen J (2003) Surface modification of poly-L-lactid acid (PLLA) membrane by grafting acrylamide: an effective way to improve cytocompatibility for chondrocytes. *J Biomater Sci Polym Ed* 14:13–25
- McClary KB, Ugarova T, Grainger DW (2000) Modulating fibroblast adhesion, spreading, and proliferation using self-assembled monolayer films of alkythioliates on gold. *J Biomed Mater Res* 50:428–439
- Morra M (2000) On the molecular basis of fouling resistance. *J Biomater Sci Polym Ed* 11:547–569
- Mrksich M, Whitesides GM (1996) Using self-assembled monolayers to understand the interactions of man-made surfaces with proteins and cells. *Annu Rev Biophys Biomol Struct* 25:55–78
- Mullaney M, Groth T, Darkow R, Hesse R, Albrecht W, Paul D, von Sengbusch G (1999) Investigation of plasma protein adsorption on functionalized nanoparticles for application in apheresis. *Artif Organs* 23:87–97
- Müller M, Rieser T, Lunkwitz K, Meier-Haack J (1999) Polyelectrolyte complex layers: a promising concept for antifouling coatings verified by in-situ ATR-FTIR spectroscopy. *Macromol Rapid Comm* 20:607–611
- Müller M, Rieser T, Dubin PL, Lunkwitz K (2001) Selective interaction between proteins and the outermost surface of polyelectrolyte multilayers: influence of the polyanion type, pH and salt. *Macromol Rapid Comm* 22:390–395
- Norde W, Lyklema J (1991) Why proteins prefer interfaces. *J Biomater Sci Polym Ed* 2(3):183–202
- Pasche V, Vörös J, Griesser HJ, Spencer ND, Textor M (2005) Effects of ionic strength and surface charge on protein adsorption at PEGylated surfaces. *J Phys Chem B* 109:17545–17552
- Pelham RJ, Wang Y-L (1997) Cell locomotion and focal adhesions are regulated by substrate flexibility. *Proc Natl Acad Sci USA* 94:13661–13665
- Rémy-Kristensen A, Clamme J-P, Vuilleumier C, Kuhry J-G, Mély Y (2001) Role of endocytosis in the transfection of L929 fibroblasts by polyethylenimine/DNA complexes. *Biochim Biophys Acta* 1514:21–32
- Richert L, Arntz Y, Schaaf P, Voegel J-C, Picart C (2004) pH dependent growth of poly(L-lysine)/poly(L-glutamic) acid multilayer films and their cell adhesion properties. *Surf Sci* 570:13–29
- Ruoslahti E (1999) Fibronectin and its integrin receptors in cancer. *Adv Cancer Res* 76:1–20
- Satoh T, Nishiyama K, Nagahata M, Teramoto A, Abe K (2004) The research on physiological property of functionalized hyaluronan: interaction between sulphated hyaluronan and plasma proteins. *Polym Adv Technol* 15:720–725
- Sauerbrey G (1959) Verwendung von Schwingquarzen zur Wägung dünner Schichten. *Z Physik* 155:206–222
- Seifert B, Mihanetzi G, Groth T, Albrecht W, Richau K, Missirlis Y, Paul D, von Sengbusch G (2002) Polyetherimide – a new membrane forming polymer for biomedical applications. *Artif Organs* 26:189–199
- Singh N, Cui X, Boland T, Husson SM (2007) The role of independently variable grafting density and layer thickness of polymer nanolayers on peptide adsorption and cell adhesion. *Biomaterials* 27:763–771

- Sofia SJ, Premnath V, Merrill EW (1998) Poly (ethylene oxide) grafted to silicon surfaces: grafting density and protein adsorption. *Macromolecules* 31:5059–5070
- Steele JG, Johnson G, Underwood PA (1992) Role of serum vitronectin and fibronectin in adhesion of fibroblasts following seeding onto tissue culture polystyrene. *J Biomed Mater Res* 26:861–884
- Sukenik CN, Balachander N, Culp LA, Lewandowska K, Merritt K (1990) Modulation of cell adhesion by modification of titanium surfaces with covalently attached self-assembled monolayers. *J Biomed Mater Res* 24:1307–1323
- Szleifer I (1997) Protein adsorption on tethered polymer layers: effect of polymer chain architecture and composition. *Physica A* 244:370–388
- Tang L, Eaton JW (1993) Fibrin(ogen) mediates acute inflammatory responses to biomaterials. *J Exp Med* 178(6):2147–2156
- Tang Z, Wang Y, Podsiadlo P, Kotov NA (2006) Biomedical applications of layer-by-layer assembly: from biomimetics to tissue engineering. *Adv Mater* 18:3203–3224
- Thom VH, Altankov G, Groth T, Jankova K, Jonsson G, Ulbricht M (2000) Optimizing cell-surface interactions by photografting of poly(ethylene glycol). *Langmuir* 16:2756–2765
- Toole BP (2004) Hyaluronan: from extracellular glue to pericellular cue. *Nat Rev Cancer* 4:528–539
- Trommler A, Wolf H, Gingell D (1985) Red blood cells experience electrostatic repulsion but make molecular adhesions with glass. *Biophys J* 48:835–841
- Tsai WB, Grunkemeier JM, McFarland CD, Horbett TA (2002) Platelet adhesion to polystyrene-based surfaces preadsorbed with plasmas selectively depleted in fibrinogen, fibronectin, vitronectin, or von Willebrand's factor. *J Biomed Mater Res* 60(3):348–359
- Tziampazis E, Kohn J, Moghe PV (2000) PEG variant biomaterials as selectively adhesive protein templates: model surfaces for controlled cell adhesion and migration. *Biomaterials* 21:511–520
- Tzoneva R, Seifert B, Albrecht W, Richau K, Lendlein A, Groth T (2008) Poly (ether imide) membranes – studies on the effect of surface modification and protein preadsorption on endothelial adhesion, growth and function. *J Biomater Sci Polym Ed* 19:837–852
- van Kooten TG, Spijker HT, Busscher HJ (2004) Plasma-treated polystyrene surfaces: model surfaces for studying cell–biomaterial interactions. *Biomaterials* 25:1735–1747
- Vermette P, Meagher L (2003) Interactions of phospholipid- and poly (ethylene glycol)-modified surfaces with biological systems: relation to physico-chemical properties and mechanisms. *Colloids Surf B Biointerfaces* 28:153–198
- Vert M, Domurado D (2000) Poly (ethylene glycol): protein repulsive or albumin compatible? *J Biomater Sci Polym Ed* 11:1307–1317
- Vitte J, Benoliel A-M, Pierres A, Bongrand P (2005) Regulation of cell adhesion. *Clin Hemorheol Microcirc* 33:167–188
- Vonarbourg A, Passirani C, Saulnier P, Benoit J-P (2006) Parameters influencing the stealthiness of colloidal drug delivery systems. *Biomaterials* 27:4356–4373
- Webb K, Hlady V, Tresco PA (2000) Relationships among cell attachment, spreading, cytoskeletal organization, and migration rate for anchorage-dependent cells on model surfaces. *J Biomed Mater Res* 49:362–368
- Wilkinson CDW, Riehle M, Wood M, Gallagher J, Curtis ASG (2002) The use of materials patterned on a nano and micrometer scale in cellular engineering. *Mat Sci Eng C* 19:263–269
- Xu X, Kwok RWM, Lau WM (2006) Surface modification of polystyrene by low energy hydrogen ion beam. *Thin Solid Films* 514:182–187
- Yi H, Wu L-Q, Bentley WE, Ghodssi R, Rubloff GW, Culver JN, Payne GF (2005) Biofabrication with chitosan. *Biomacromolecules* 6(6):2881–2894
- Yoo D, Shiratori SS, Rubner MF (1998) Controlling bilayer composition and surface wettability of sequentially adsorbed multilayers of weak polyelectrolytes. *Macromolecules* 31:4309–4318
- Zajac R, Chakrabarti A (1995) Irreversible polymer adsorption from semidilute and moderately dense solutions. *Phys Rev E* 52:6536–6549
- Zhang TXuN, Nichols HL, Shi D, Wen X (2007) Modification of nanostructured materials for biomedical applications. *Mat Sci Eng C* 27:579–594
- Zhao B, Brittain WJ (2000) Polymer brushes: surface-immobilized macromolecules. *Prog Polym Sci* 25:677–710

Chapter 14

Results of Biocompatibility Testing of Novel, Multifunctional Polymeric Implant Materials In-Vitro and In-Vivo

Dorothee Rickert, Rosemarie Fuhrmann, Bernhard Hiebl,
Andreas Lendlein, and Ralf-Peter Franke

Abstract Extensive in-vitro and in-vivo evaluation of the biocompatibility of biomaterials intended for clinical applications is necessary to provide information on the interactions that take place between the organism and these materials under specific implant conditions. Sterilization of polymer-based implant materials is a basic requirement but can lead to their damage or destruction. Low-temperature plasma (LTP) or ethylene oxide (EO) sterilization are objects of intensive research and were applied on the materials used in this program. After 4 weeks of polymer incubation in minimal essential medium (MEM), samples, sterilized by LTP, gave a markedly higher mean cell lysis rate ($3.7 \pm 2.5\%$) than EO sterilized samples ($0.9 \pm 0.3\%$). To achieve relevant in-vitro results on biomaterial-cell interactions, biocompatibility testing was carried out with cultures of locotypical cells, e.g. cells of the upper aerodigestive tract (ADT). Primary cell cultures of the oral cavity, the pharynx and the esophagus showed region-typical varying relationships between epithelial, fibroblastic and smooth muscle cells. Proper wound healing is thought to be required for the integration of biomaterials and angiogenesis is a prerequisite for this process. A focus of the present work was the influence of polymer-based implant materials and their degradation products on angiogenesis in-vivo. After 48 h, none of the polymer samples demonstrated development of an avascular region in the chorioallantoic membrane (CAM) test. A key process in proper wound

D. Rickert (✉)

Marienhospital Stuttgart, Böheimstr. 37, 70199 Stuttgart, Germany
e-mail: D.Rickert@gmx.de

R. Fuhrmann and R.-P. Franke

Central Institute for Biomedical Engineering, Department of Biomaterials, University of Ulm,
Albert-Einstein-Allee 47, 89081 Ulm, Germany

B. Hiebl and A. Lendlein

Institute of Polymer Research, GKSS Research Center Geesthacht GmbH,
Kantstraße 55, 14513 Teltow, Germany
e-mail: Lendlein@gkss.de

healing is the tightly controlled degradation and regeneration of the extracellular matrix (ECM). A biomaterial for the reconstruction of the upper ADT is subjected to varying pH values and enzymatic, bacterial and mechanical stress during the digestive and the swallowing process. These complex conditions can currently only be investigated in-vivo in an animal model. As a model the stomach of the rat was selected, in which a biomaterial can be investigated under extreme chemical, enzymatic, bacteriological and mechanical conditions. Other parameters investigated are the impermeability of the polymer-tissue closure and the tissue regeneration after defect reconstruction. The fluid tight integration of a long term resorbable AB-copolymer network in the surrounding tissue of the gastric wall of Sprague Dawley rats could be demonstrated.

Keywords Regenerative medicine • Multifunctional biomaterials • Sterilization • Biocompatibility testing • Extracellular matrix remodeling • Biofunctionality testing in-vivo

14.1 Introduction

14.1.1 *Regenerative Medicine*

Regenerative medicine is an innovative scientific field in which the problems and problem solving approaches of clinical medicine are integrated in the natural and engineering sciences (Ahsan and Nerem 2005; Atala 2005). Regenerative medicine, in the widest sense, is concerned with the restoration of impaired function of cells, tissues, and organs either by biological replacement, e.g. with tissues cultured in-vitro, or by providing the stimulus for the body's own reparative and regenerative mechanisms (Shastri and Lendlein 2009). The focus of this field moves beyond the replacement of organs and tissues (tissue engineering) and encompasses both innovative development and advancement in classical transplantation medicine and cell therapy including stem cell technologies (Breyman et al. 2006; Reed and Patarca 2006), as well as a pharmacological approach to targeted stimulation of tissue regeneration in-vivo (Ioannidou 2006). The goal of regenerative medicine is to translate research findings into the development and establishment of innovative therapeutic options in clinical medicine (Humes 2005; Kume 2005; Spector 2006).

Due to the morbidity shift in the last few decades and in view of the current demographic transition in Western industrialized nations, clinical medicine today is increasingly occupied with diseases that bring about a gradual decline in function of vital cell and organic systems resulting from different causes. Most often, classical therapies do not offer an effective cure for these diseases that require permanent treatment and on which a considerable amount of time and effort is spent.

The approaches of regenerative medicine are expected to present therapy solutions for a number of these diseases, among which are most of the widespread diseases with high morbidity rates, reduced quality of life and high health care costs. It is expected that the solutions offered by regenerative medicine to substitute destroyed or damaged tissues with fully functional replacements will prove to be the curative therapy that could make permanent symptomatic treatment unnecessary to the benefit of patients and health care funding bodies.

14.1.2 Functionalized Implant Materials

A current trend in polymer science is the preparation of degradable biomaterials that are designed to be multifunctional, i.e. containing specific functionalities such as e.g. hydrolytic degradability, tissue compatibility, and shape-memory effects that can be adjusted selectively according to the requirements of the specific sites of application (Gall et al. 2005; Langer and Tirrell 2004; Lendlein and Kelch 2005a). AB-copolymer networks are prepared by photo curing of oligo(ϵ -caprolactone) and poly(butyl acrylate) segments (Lendlein et al. 2001; Lendlein and Kelch 2005b; Kelch et al. 2007). The integration of the highly elastic poly(butyl acrylate) segments enables customizable elasticity of the materials which is an essential prerequisite for the biomechanical functionality of these polymer systems especially within the temperature range of room and body temperature (Lendlein et al. 2001). AB-copolymer networks based on polyester segments are hydrolytically degradable. Besides the hydrolysable ester bonds, the polymer networks contain oligomethacrylate and poly(butyl acrylate) chains that are not hydrolytically cleavable. With progressive hydrolytic degradation, oligomers of methacrylic acid and acrylic acid derivatives emerge increasingly from these segments. The copolymer networks can be defined as multifunctional, and due to their biomechanical functionality and/or tissue compatibility, be regarded as suitable for use as hydrolytically degradable implant materials.

14.1.3 Clinical Application of Polymer-Based Implant Materials

14.1.3.1 Biocompatibility Testing In-Vitro

An extensive in-vitro and in-vivo evaluation of the biocompatibility of biomaterials intended for clinical application is necessary to provide information on the interactions that take place between the organism and these materials under specific implant conditions (Raghunath et al. 2007; Stangegaard et al. 2006). It is therefore of current interest to study the biocompatibility of novel biomaterials with standardized and established methods.

14.1.3.2 Sterilization of Polymer-Based, Degradable Implant Materials

It is a basic requirement that biomaterials for biomedical applications are sterile. The thermal and chemical stability of polymer-based, hydrolytically degradable biomaterials is much lower than that of ceramics or metal-based materials. Therefore, they usually cannot be sterilized by conventional methods such as heat sterilization (with temperatures between 160–190°C), or steam sterilization (121–134°C), without destroying the material. Sterilization under ionizing radiation can result on the one hand in chain degradation and on the other in cross-linking processes that change the chemical structure of polymers. Ionizing radiation, furthermore, can influence the surface properties as well as the thermal and mechanical properties of a material (Goldman et al. 1998). Since special requirements are necessary when sterilizing polymer-based biomaterials, low-temperature sterilization methods such as plasma (LTP, low-temperature plasma sterilization) and ethylene oxide (EO) sterilization are presently objects of intensive research.

14.1.3.3 The Importance of Angiogenesis

When biomaterials are to be incorporated into the surrounding tissue *in-vivo*, proper wound healing is required. Wound healing is a complex, interactive and dynamic process involving numerous mediators, cells and components of the extracellular matrix (Clark 1995). Angiogenesis is an essential prerequisite for the normal wound healing process. Interactions between biomaterial and tissue *in-vivo* require adequate capillary and blood vessel formation to ensure transport between the tissue and the implanted biomaterial. To date, inadequate microvasculature formation presents a limitation to the biomedical application of several biomaterials (Sieminski and Gooch 2000). The current object of research is to influence the angiogenesis process both pro and antiangiogenically using degradable implant materials (Stayton et al. 2005). Therefore, a subject of investigation in the present work was the influence of polymer-based implant materials and their degradation products on angiogenesis *in-vivo*.

14.1.3.4 Primary Cell Cultures of the Upper Aerodigestive Tract

Cell culture is a standardized method in biomedical research. To achieve relevant *in-vitro* results on biomaterial-cell interactions, biocompatibility testing of materials should be conceived in accordance with the site of biomedical application and be carried out with cultures of locotypical cells (Falconnet et al. 2006). Thus the evaluation of the biocompatibility of novel polymers that have been selected as suitable materials for application in the upper aerodigestive tract (ADT) could involve cell culture experiments using primary cultures of cells of the oral cavity, pharynx or esophagus as a possibility to investigate biomaterial-cell interactions and ensure optimal adaptation of these materials to the specific requirements

of the upper ADT. In order to study these specific cell-polymer interactions, primary cell cultures of the upper ADT were established and characterized biochemically in the present work.

14.1.3.5 Wound Healing

The most important processes in wound healing are cell migration and proliferation, angiogenesis, matrix degradation and remodeling of granulation tissue (Clark 1995). The key process involved in proper wound healing is the tightly controlled degradation of the extracellular matrix. A disturbed balance between matrix degradation and synthesis during wound healing with a shift toward matrix degradation could lead to disturbed wound healing with the development of fistulae and ulcers or with a shift toward matrix synthesis to the formation of scars and keloids (Singer and Clark 1999).

Matrix metalloproteinases (MMPs) are zinc-dependent, endogenous peptidases capable of cleaving almost all components of the extracellular matrix and therefore have a critical function in the wound healing process (Ravanti and Kahari 2000). The proteolytic function of the MMPs is inhibited specifically by their endogenous inhibitors (Tissue Inhibitor of Matrix Metalloproteinases, TIMPs). Four TIMPs have been identified and cloned to date (TIMP 1–4) (Nagase et al. 2006). In the literature, differential expressions of TIMPs and MMPs could be shown for normal and impaired wound healing (Moses et al. 1996; Vaalamo et al. 1999). Well-balanced MMP and TIMP activity is an important parameter for the establishment of a stable extracellular matrix architecture.

14.1.3.6 Biocompatibility Testing In-Vivo

A degradable biomaterial designed for use in the upper ADT must meet high demands in terms of the chemical, enzymatic, bacteriological and mechanical stability of the material. Premature degradation of the biomaterial may lead to the development of a persistent salivary fistula associated with high mortality caused by fatal bleeding due to internal carotid artery arrosion. Given the chemical conditions predominating in the upper ADT such as varying pH values, and the enzymatic, bacterial and mechanical stress they are subjected to during the digestive and the swallowing process, degradable biomaterials intended for reconstruction of the upper ADT must consist of an implant material with adequate chemical, enzymatic, bacterial and mechanical stability. These complex conditions can currently only be investigated in-vivo in an animal model. In the present study, an animal model was established, in which a standardized full-thickness gastric wall defect in rats was closed with an elastic, long term resorbable, polymeric biomaterial. In this model the stomach of the rat was selected as the site of application so that the stability of the biomaterial could be investigated under extreme chemical, enzymatic, bacteriological and mechanical conditions. In addition to chemical and

mechanical stability testing of the material, other important parameters investigated in the present study were impermeability of the polymer-tissue closure, integration of the polymer into the surrounding tissue and also tissue regeneration after defect reconstruction.

14.2 Materials and Methods

14.2.1 *Polymer-Based, Biodegradable Implant Materials*

As a model system of a degradable and biomechanically adjustable polymer, a long term resorbable, elastic copolymer network based on poly(ϵ -caprolactone) dimethacrylate obtained through end group functionalization with methacryloyl chloride of poly(ϵ -caprolactone) diol (Sigma-Aldrich, St. Louis, USA), number average molecular weight (M_n) of 10,000 g·mol⁻¹ and polydispersity index of 1.4 was chosen. After photopolymerization, the material was extracted with chloroform and subsequently dried to constant weight under vacuum. The final copolymer network was prepared from 40 wt% of poly(ϵ -caprolactone) dimethacrylate and 60 wt% of butylacrylate via radical polymerization initiated by UV irradiation without addition of a photoinitiator (Lendlein et al. 2001, 2000).

14.2.2 *Sterilization Methods*

For the biocompatibility experiments in-vitro, the polymer samples were sterilized using LTP or EO sterilization according to clinical sterilization methods used for thermolabile equipment and materials.

14.2.3 *Investigation of In-Vitro Toxicity*

The agarose overlay assay was used, among others, to assess the cytotoxicity of the polymeric implant materials. Degradation of the polymer under in-vivo conditions was simulated by incubating the polymer samples for 24 h, 1 week, and 2 and 4 weeks in a simulated physiological solution (Minimal Essential Medium; MEM) at 37°C in a shaking incubator (EB, Edmund Bühler, TM 10).

14.2.3.1 *Agarose Overlay Assay*

The agarose diffusion test according to ASTM International standards (American Society for Testing and Materials) is a well-established method for biocompatibility testing in-vitro (ASTM International 1992). Furthermore, by using an image

analysis system, it was possible to evaluate the influence of soluble contents of the material on cells in more detail. A comprehensive description of the agarose diffusion assay and the image analysis system can be found in the literature (Rickert et al. 2002).

14.2.3.2 Direct Cell Seeding Tests

For the present work, primary cell cultures of cells of the oral cavity, pharynx and esophagus of the animal model were established and characterized biochemically. The methods used for cell characterization and the procedure for establishing the cell cultures have been described in detail in the literature (Rickert et al. 2007). These primary cells were then used in the direct cell seeding tests performed on the polymeric implant materials.

14.2.4 In-Vivo Assessment of Tissue Compatibility of Biomaterials

14.2.4.1 Chick Chorioallantoic Membrane (CAM) Assay

Fertilized chicken eggs were incubated at 37°C with a humidity of 65–70% for 3 days. Each egg shell was then opened under sterile conditions and the chicken embryo was transferred to a petri dish which was placed in a cell culture incubator at 37°C, with 2–4% CO₂ and a relative humidity of 65–70%. Then EO sterilized polymer samples (10 × 10 mm) were placed on the vascularized CAM and incubated for 48 h. Vascularization of the CAM, well visible through the polymer, was assessed microscopically and quantified.

14.2.5 Animal Model

14.2.5.1 Mucosal Reconstruction in an Animal Model

The application for permission of the animal experiments was approved by the federal governmental authority Regierungspräsidium Tübingen (application no. 729). Eighty-four male wild-type Sprague-Dawley rats (Charles River, Sulzfeld, Germany) were used. The animals were assigned by a 2:1 randomization to the implant group, to the control group and to the baseline group. In the animals of the implant group a standardized full-thickness gastric wall defect was performed and then closed with the polymer network samples that were 10 mm in diameter and 200 µm in thickness. In the control group the defect was closed by a primary wound closure without biomaterial implantation. The untreated animals of the baseline

group were kept under the same conditions as the animals of the other groups. The implantation or investigation periods were 1 week, 4 weeks and 6 months. After removing the stomach by dissecting the superior part of the duodenum and the distal part of the esophagus, the connection between the polymer and the surrounding tissue in the implant group and the scar of the primary wound closure in the control group were tested for leak tightness by an impermeability testing procedure. Using the same procedure, the maximum inflation of the stomachs of the animals of the baseline group was documented.

14.2.6 Statistical Evaluation

Statistical evaluation of the in-vitro and in-vivo investigations was carried out using the SPSSPC+ statistical software, version 10.0.5. (SPSS, Chicago, USA). The paired sample *t* test was used for comparison between the different groups. The difference observed was regarded as statistically significant when the *p*-value was ≤ 0.05 .

14.3 Results

14.3.1 Detailed Evaluation of In-Vitro Biocompatibility Testing

Microscopic image analysis of the agarose assay revealed characteristic distributions of cell lysis in defined zones of the controls (sterilized, non-toxic glass samples) as well as of experimental polymer samples (Fig. 14.1, Rickert et al. 2002). The highest percentage of lysed cells was found in the transitional zones in the areas adjacent to the outer rim of the polymer or glass samples. Besides the zone specificity of mean cell lysis distribution, it was seen that polymer samples incubated for 4 weeks in a physiological solution (MEM) showed a statistically significant higher cell lysis (mean cell lysis of $4.73 \pm 0.09\%$) than samples that had not been incubated (mean cell lysis of $2.04 \pm 0.105\%$).

14.3.1.1 Influence of Different Sterilization Methods on Biocompatibility

Image analysis revealed statistically significant differences ($p \leq 0.01$) in mean cell lysis rates between EO and LTP sterilized polymer samples not subjected to degradation (without MEM incubation) as well as after 2 and 4 weeks of MEM incubation (Fig. 14.2, Rickert et al. 2003). Especially after 4 weeks of MEM incubation, a markedly higher mean cell lysis rate was observed for the LTP sterilized samples (mean cell lysis of $3.67 \pm 2.54\%$) compared to EO sterilized samples (mean cell lysis of $0.93 \pm 0.3\%$).

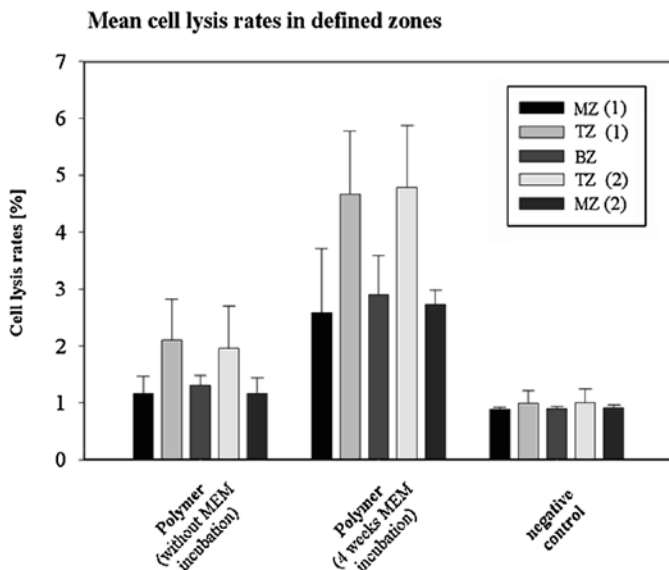


Fig. 14.1 Mean cell lysis rates in defined zones of polymer samples without MEM incubation, after incubation in MEM for 4 weeks, and of negative controls. MZ: marginal zone; TZ: transitional zone; BZ: biomaterial zone. Taken from Rickert et al. 2002, Copyright 2006 by Walter de Gruyter Berlin, New York

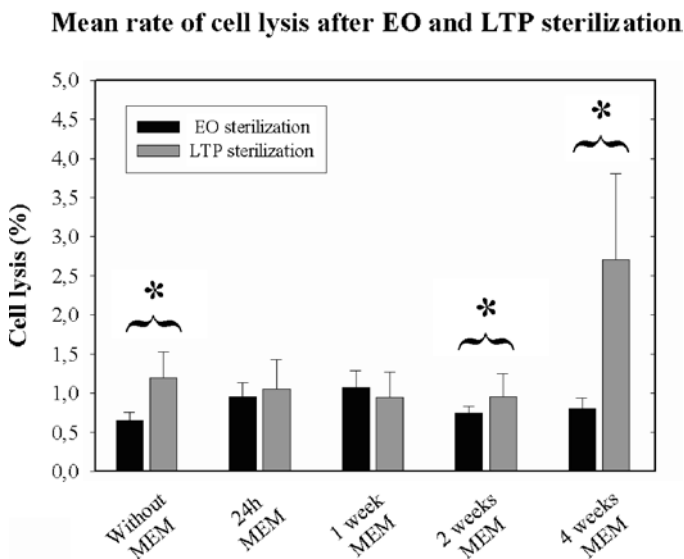


Fig. 14.2 Comparison of mean cell lysis rates after sterilization of polymer samples with different methods. Statistically significant differences in cell lysis rates ($p \leq 0.01$) between EO and LTP sterilized samples are marked with *asterisks*. MEM: minimal essential medium; EO: ethylene oxide sterilization; LTP: low temperature plasma sterilization. Taken from Rickert et al 2003, Copyright 2003, John Wiley & Sons, Inc

14.3.2 *In-Vivo Assessment of Tissue Compatibility of Biomaterials*

14.3.2.1 Chick Chorioallantoic Membrane (CAM) Assay

Quantification of vascularization of the chorioallantoic membrane (CAM) in the CAM assays with polymer samples and controls (CAM assays without polymer) (Fig. 14.3, Rickert et al. 2006a) did not reveal any differences.

14.3.2.2 Mucosal Reconstruction in an Animal Model

Gastric wall reconstruction with a copolymer network material in a rat model is shown in Fig. 14.4, Rickert et al. 2006b; Rickert et al. 2007b. The fluid-tight integration of a long term resorbable AB-copolymer network in the surrounding tissue of the gastric wall of Sprague-Dawley rats could be demonstrated in an animal model (Fig. 14.5, Rickert et al. 2006b). None of the animals of the implant group ($n = 42$), or control group ($n = 21$) with primary wound closure without biomaterial implantation, developed gastrointestinal complications such as fistulae, perforation or peritonitis in the periods of investigation (1 week, 4 weeks and 6 months).

The results of intragastric pressure measurements at maximum inflation of the explanted stomachs exhibited no statistically significant differences between the implant, control and baseline groups at the investigated time points (Fig. 14.6, Rickert et al. 2006b). The tightness of the suture closure between the polymer and the surrounding tissue was verified for all animals of the implant group.

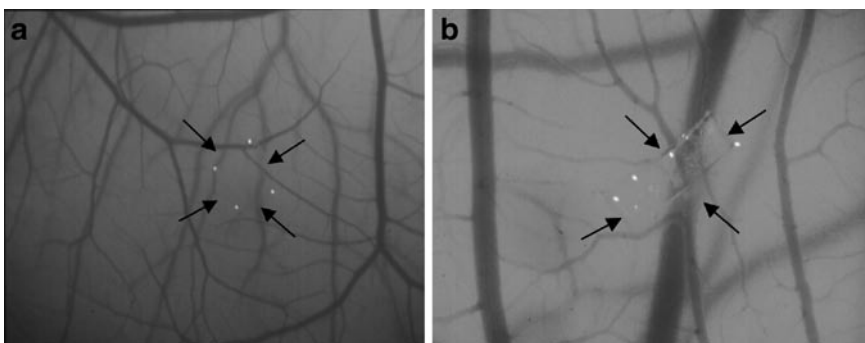


Fig. 14.3 The chorioallantoic membrane (CAM) after a 48-h incubation period with polymer samples. After 48 h, none of assays with polymer samples demonstrated development of an avascular region (a and b). Moreover, there was no evidence of thrombi and/or hemorrhages in any of the assays with polymer samples (magnification seven- to tenfold). Taken from Rickert et al. 2006a, with kind permission from Springer Science+Business Media

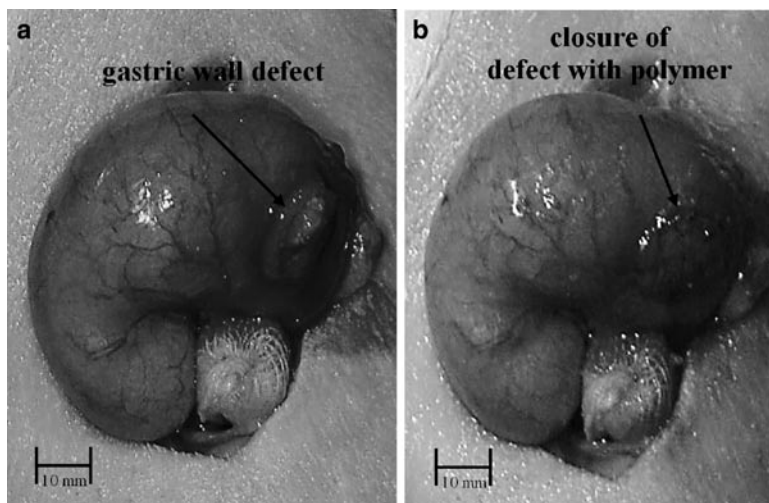


Fig. 14.4 (a) shows the luxated stomach with the full-thickness gastric wall defect (indicated by *arrows*). In (b) the gastric wall defect has been closed with the polymer. Taken from Rickert et al. 2006b, Copyright 2006 by Walter de Gruyter Berlin, New York and Rickert et al. 2007b, Copyright 2007, with permission from IOS Press

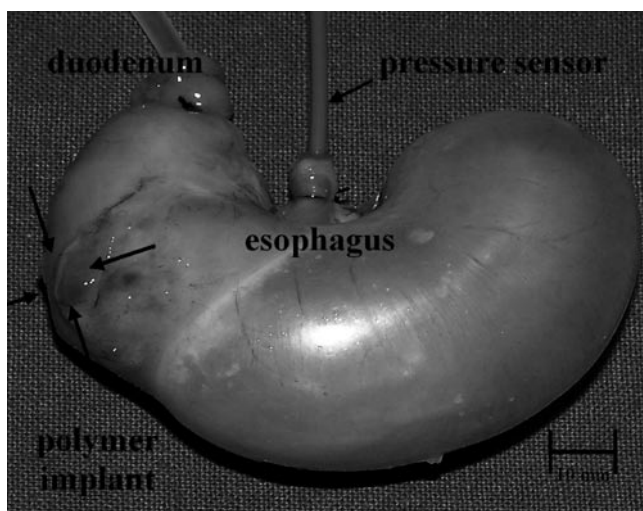


Fig. 14.5 Depiction of the explanted stomach after the 1-week implantation period. The implantation site of the polymer is marked by *arrows*. Air was pumped into the stomach through a tube fixed into the duodenum. Pressure was measured by a pressure sensor fixed in the esophageal stump. The pressure sensor is marked by an *arrow*. Taken from Rickert et al. 2006b, Copyright 2006 by Walter de Gruyter Berlin, New York

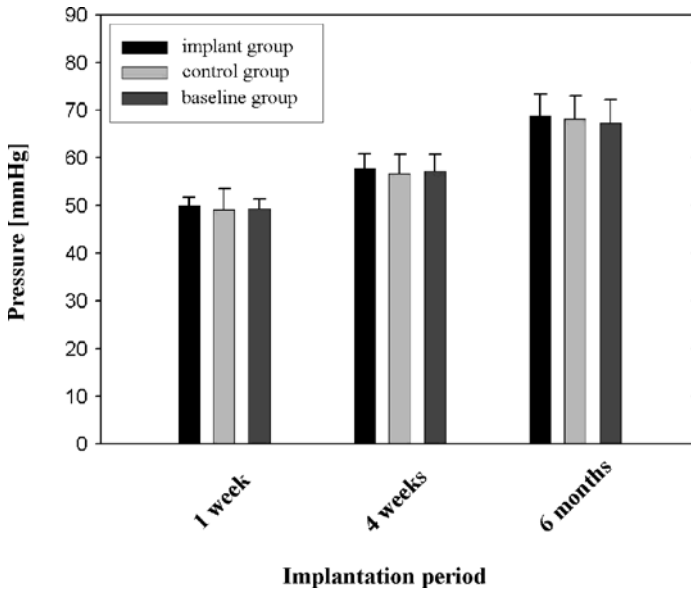


Fig. 14.6 Intra-gastric pressure (mmHg) measured after maximum inflation of the explanted stomachs of the implant, control and baseline group at the end of the 1-week, 4-week and 6-month investigation period. Taken from Rickert et al. 2006b, Copyright 2006 by Walter de Gruyter Berlin, New York

14.4 Discussion

The higher cell lysis rates in the transitional zones around the polymer as well as the control samples are attributed to mechanical cell damage, among other reasons. According to the literature, it has been known for many years that fibroblasts react sensitively to mechanical stress (Grierson and Meldolesi 1995; Lemmon et al. 2005; Messer et al. 2006). The significant differences in the mean cell lysis rates of the polymer samples without and with 4-weeks MEM incubation suggest that degradation and leaching of substances takes place during the incubation of the polymer samples in the physiological solution (Shen et al. 2007). The method mentioned for detailed evaluation of the agarose assay seems to demonstrate a sufficiently high sensitivity so that L-929 cells may be used to assess the influence of polymer samples incubated for different time periods in aqueous solutions (MEM), though these cells are not specific to the application site. Further in-vitro biocompatibility tests should be carried out with specific cells corresponding to the biomedical application site of the materials. Nonspecific cells limit the validity of the agarose assay as they indicate only a general toxicity of diffusible substances.

It is not yet known completely what influence LTP sterilization has on the degradation behavior of the investigated polymer samples. In the literature, oxidation of the surface of various polymers after LTP sterilization has been reported (El Mansouri et al. 1999; Lerouge et al. 2000). Surface oxidation causes, among other

things, the hydrophilicity of polymeric materials to increase. Besides surface oxidation, an influence on the hydrolytic stability of the material with a higher release of oligomers could be shown in the literature. For example, it is known that particularly in the near-surface layer of the polymer there is an accumulation of oligomers (Burslem and Stevenson 2005; Simmons et al. 2006). The factors mentioned may cause a change in biocompatibility in-vitro. To what extent these modifications affect biocompatibility of the material in-vivo, however, is not known to date and can only be investigated by implantation of the materials in-vivo.

Influential factors to be considered, which may affect the cytotoxicity of polymer samples in-vitro in addition to differing sterilization methods and incubation times in physiological solution are other physicochemical properties such as weight, porosity and permeability and also the movements of the samples on the agarose layer and the interactions between the polymer surface and the agarose layer as well as the metabolic products produced by the cells. Surface modifications of the polymer samples through various sterilization methods and incubation times in MEM could result in a change of the gaseous exchange between cells and nutrient availability. This mechanism, however, cannot be primarily ascribed to the weight of the samples since the heavier weight negative glass controls (weight: $0.038 \pm 1.26 \times 10^{-4}$ g), were not associated with higher cell lysis rates compared to the polymer samples (weight: $0.021 \pm 0.83 \times 10^{-4}$ g). To assess the influence of different sterilization methods on polymer biocompatibility and to evaluate the mechanical properties and degradation behavior of polymer biomaterials, it will be necessary to conduct comprehensive material characterization testing in-vitro and in-vivo.

The availability or lack of components of the extracellular matrix during the cell adhesion process of the different primary cell cultures of the upper ADT seems to have a decisive influence on subsequent cell proliferation, cell differentiation and biochemical activity of the cells. These results are consistent with data in the literature which could show that gene expression, and the synthesis of enzymes that are directly involved with the remodeling process of the extracellular matrix, were affected by the surface topography of the substrate material (Chou et al. 1998; Mudera et al. 2000; Nakashima et al. 1998). The differences observed between the kinetics and activity levels of the oral and pharyngeal cells on one hand, and the esophageal cells on the other, seem to be a result of the divergent functional requirements and differentiation of cells in the different regions of the upper ADT. To date, there is little knowledge of the mechanisms of wound healing and MMP expression of cells of the upper ADT in-vitro and in-vivo (Bennett et al. 2000; Stephens et al. 2001). The comprehensive characterization of the cells of the upper ADT is a prerequisite for the establishment of novel therapeutic options in the field of otolaryngology and head and neck surgery for the treatment of chronic disorders in wound healing after surgical interventions or the development of novel biomaterials for the reconstruction of the upper ADT after surgical resections of tumors.

Regular angiogenesis after polymer incubation in the CAM assays demonstrated the adequate biocompatibility and biofunctionality of the polymers. A current object of research is to influence angiogenesis in order to optimize the wound healing process through the release of relevant growth factors.

In an animal model for gastric wall reconstruction, the stability of the polymeric implant material as well as its biomechanical functionality could be shown under the extreme chemical, hydrolytical and enzymatic conditions prevalent in the stomach. The results of the intragastric impermeability measurements and the fact that no postoperative gastrointestinal complications were observed show that the degradable, elastic AB-copolymer network did not induce wound healing disorders at the time of investigation but, on the contrary, supported tissue regeneration. In further experiments, it will be necessary to investigate the underlying mechanisms of biomaterial integration into the surrounding tissue as well as analyze polymer degradation and the tissue remodeling process.

References

- Ahsan T, Nerem RM (2005) Bioengineered tissues: the science, the technology, and the industry. *Orthod Craniofac Res* 8(3):134–140
- Atala A (2005) Tissue engineering, stem cells and cloning: current concepts and changing trends. *Expert Opin Biol Ther* 5(7):879–892
- Bennett JH, Morgan MJ, Whawell SA, Atkin P, Roblin P, Furness J, Speight PM (2000) Metalloproteinase expression in normal and malignant oral keratinocytes: stimulation of MMP-2 and-9 by scatter factor. *Eur J Oral Sci* 108(4):281–291
- Breyman C, Schmidt D, Hoerstrup S (2006) Umbilical cord cells as a source of cardiovascular tissue engineering. *Stem Cell Rev* 2(2):87–92
- Burslem R, Stevenson P (2005) Plasma processing of surfaces. *Med Device Technol* 16(7):40–41
- Chou LS, Firth JD, Uitto VJ, Brunette DM (1998) Effects of titanium substratum and grooved surface topography on metalloproteinase-2 expression in human fibroblasts. *J Biomed Mater Res* 39(3):437–445
- Clark RAF (1995) *The molecular and cellular biology of wound repair*. Plenum, New York
- El Mansouri H, Yagoubi N, Scholler D, Feigenbaum A, Ferrier D (1999) Propylene oligomers: extraction methods and characterization by FTIR, HPLC, and SEC. *J Appl Polym Sci* 71(3):371–375
- Falconnet D, Csucs G, Grandin HM, Textor M (2006) Surface engineering approaches to micro-pattern surfaces for cell-based assays. *Biomaterials* 27(16):3044–3063
- Gall K, Yakacki CM, Liu YP, Shandas R, Willett N, Anseth KS (2005) Thermomechanics of the shape memory effect in polymers for biomedical applications. *J Biomed Mater Res A* 73A(3):339–348
- Goldman M, Gronsky R, Pruitt L (1998) The influence of sterilization technique and ageing on the structure and morphology of medical-grade ultrahigh molecular weight polyethylene. *J Mater Sci Mater Med* 9(4):207–212
- Grierson JP, Meldolesi J (1995) Shear stress-induced $[Ca^{2+}]_i$ transients and oscillations in mouse fibroblasts are mediated by endogenously released Atp. *J Biol Chem* 270(9):4451–4456
- Humes DH (2005) Stem cells: the next therapeutic frontier. *Trans Am Clin Climatol Assoc* 116:167–184
- ASTM International (1992) ASTM designation: F 813-83: standard practice for direct contact cell culture evaluation of materials for medical devices. ASTM International, pp 239–241
- Ioannidou E (2006) Therapeutic modulation of growth factors and cytokines in regenerative medicine. *Curr Pharm Des* 12(19):2397–2408

- Kelch S, Steuer S, Schmidt AM, Lendlein A (2007) Shape-memory polymer networks from oligo [(epsilon-hydroxycaproate)-co-glycolate] dimethacrylates and butyl acrylate with adjustable hydrolytic degradation rate. *Biomacromolecules* 8(3):1018–1027
- Kume S (2005) Stem-cell-based approaches for regenerative medicine. *Dev Growth Differ* 47(6):393–402
- Langer R, Tirrell DA (2004) Designing materials for biology and medicine. *Nature* 428(6982):487–492
- Lemmon CA, Sniadecki NJ, Ruiz SA, Tan JL, Romer LH, Chen CS (2005) Shear force at the cell-matrix interface: enhanced analysis for microfabricated post array detectors. *Mech Chem Biosyst* 2(1):1–16
- Lendlein A, Kelch S (2005a) Degradable, multifunctional polymeric biomaterials with shape-memory. *Mater Sci Forum* 492–493:219–223
- Lendlein A, Kelch S (2005b) Shape-memory polymers as stimuli-sensitive implant materials. *Clin Hemorheol Microcirc* 32(2):105–116
- Lendlein A, Neunschwander P, Suter UW (2000) Hydroxy-telechelic copolyesters with well-defined sequence structure through ring-opening polymerization. *Macromol Chem Phys* 201(11):1067–1076
- Lendlein A, Schmidt AM, Langer R (2001) AB-polymer networks based on oligo(epsilon-caprolactone) segments showing shape-memory properties. *Proc Natl Acad Sci USA* 98(3):842–847
- Lerouge S, Guignot C, Tabrizian M, Ferrier D, Yagoubi N, Yahia L (2000) Plasma-based sterilization: effect on surface and bulk properties and hydrolytic stability of reprocessed polyurethane electrophysiology catheters. *J Biomed Mater Res* 52(4):774–782
- Messer RLW, Davis CM, Lewis JB, Adams Y, Wataha JC (2006) Attachment of human epithelial cells and periodontal ligament fibroblasts to tooth dentin. *J Biomed Mater Res A* 79A(1):16–22
- Moses MA, Marikovsky M, Harper JW, Vogt P, Eriksson E, Klagsbrun M, Langer R (1996) Temporal study of the activity of matrix metalloproteinases and their endogenous inhibitors during wound healing. *J Cell Biochem* 60(3):379–386
- Mudera VC, Pleass R, Eastwood M, Tarnuzzer R, Schultz G, Khaw P, McGrouther DA, Brown RA (2000) Molecular responses of human dermal fibroblasts to dual cues: Contact guidance and mechanical load. *Cell Motil Cytoskeleton* 45(1):1–9
- Nagase H, Visse R, Murphy G (2006) Structure and function of matrix metalloproteinases and TIMPs. *Cardiovasc Res* 69(3):562–573
- Nakashima Y, Sun DH, Maloney WJ, Goodman SB, Schurman DJ, Smith RL (1998) Induction of matrix metalloproteinase expression in human macrophages by orthopaedic particulate debris in vitro. *J Bone Joint Surg Br* 80B(4):694–700
- Raghunath J, Rollo J, Sales KM, Butler PE, Seifalian AM (2007) Biomaterials and scaffold design: key to tissue-engineering cartilage. *Biotechnol Appl Biochem* 46:73–84
- Ravanti L, Kahari VM (2000) Matrix metalloproteinases in wound repair (Review). *Int J Mol Med* 6(4):391–407
- Reed JA, Patarca R (2006) Regenerative dental medicine: stem cells and tissue engineering in dentistry. *J Environ Pathol Toxicol Oncol* 25(3):537–569
- Rickert D, Lendlein A, Kelch S, Fuhrmann R, Franke RP (2002) Detailed evaluation of the agarose diffusion test as a standard biocompatibility procedure using an image analysis system. Influence of plasma sterilization on the biocompatibility of a recently developed photoset-polymer. *Biomed Technik* 47(11):285–289
- Rickert D, Lendlein A, Peters I, Moses MA, Franke RP (2006a) Biocompatibility Testing of Novel Multifunctional Polymeric Biomaterials for Tissue Engineering Applications in Head and Neck Surgery: An Overview. *Eur Arch Oto-Rhino-Laryn* 263(3):215–222
- Rickert D, Franke RP, Fernandez CA, Kilroy S, Yan L, Moses MA (2007a) Establishment and biochemical characterization of primary cells of the upper aerodigestive tract. *Clin Hemorheol Microcirc* 36(1):47–64
- Rickert D, Scheithauer MO, Coskun S, Kelch S, Lendlein A, Franke RP (2007b) The influence of a novel, polymeric biomaterial on the concentration of acute phase proteins in an animal model. *Clin Hemorheol Microcirc* 36(4):301–311

- Rickert D, Scheithauer MO, Coskun S, Lendlein A, Kelch S, Franke RP (2006b) First results of the investigation of the stability and tissue integration of a degradable, elastomeric copolymer in an animal model. *Biomed Tech* 51(3):116–124
- Rickert D, Lendlein A, Schmidt AM, Kelch S, Roehlke W, Fuhrmann R, Franke RP (2003) In vitro cytotoxicity testing of AB-polymer networks based on oligo(epsilon-caprolactone) segments after different sterilization techniques. *J Biomed Mater Res B* 67B(2):722–731
- Shastri VP, Lendlein A (2009) Materials in regenerative medicine. *Adv Mater* 21(32–33):3231–3234
- Shen JY, Pan XY, Lim CH, Chan-Park MB, Zhu X, Beuerman RW (2007) Synthesis, characterization, and in vitro degradation of a biodegradable photo-cross-linked film from liquid poly(epsilon-caprolactone-co-lactide-co-glycolide) diacrylate. *Biomacromolecules* 8(2):376–385
- Sieminski AL, Gooch KJ (2000) Biomaterial-microvasculature interactions. *Biomaterials* 21(22):2233–2241
- Simmons A, Hyvarinen J, Poole-Warren L (2006) The effect of sterilisation on a poly(dimethylsiloxane)/poly(hexamethylene oxide) mixed macrodiol-based polyurethane elastomer. *Biomaterials* 27(25):4484–4497
- Singer AJ, Clark RAF (1999) Mechanisms of disease – cutaneous wound healing. *N Engl J Med* 341(10):738–746
- Spector M (2006) Biomaterials-based tissue engineering and regenerative medicine solutions to musculoskeletal problems. *Swiss Med Wkly* 136(19–20):293–301
- Stangegaard M, Wang Z, Kutter JP, Dufva M, Wolff A (2006) Whole genome expression profiling using DNA microarray for determining biocompatibility of polymeric surfaces. *Mol Biosyst* 2(9):421–428
- Stayton PS, El-Sayed MEH, Murthy N, Bulmus V, Lackey C, Cheung C, Hoffman AS (2005) ‘Smart’ delivery systems for biomolecular therapeutics. *Orthod Craniofac Res* 8(3):219–225
- Stephens P, Davies KJ, Ocleston N, Pleass RD, Kon C, Daniels J, Khaw PT, Thomas DW (2001) Skin and oral fibroblasts exhibit phenotypic differences in extracellular matrix reorganization and matrix metalloproteinase activity. *Br J Dermatol* 144(2):229–237
- Vaalamo M, Leivo T, Saarialho-Kere U (1999) Differential expression of tissue inhibitors of metalloproteinases (TIMP-1,-2,-3, and-4) in normal and aberrant wound healing. *Hum Pathol* 30(7):795–802

Chapter 15

UFOs, Worms, and Surfboards: What Shapes Teach Us About Cell–Material Interactions

Julie A. Champion and Samir Mitragotri

Abstract The success of regenerative materials is dependent on the ability to elicit cell interactions. Cell–material interactions, both desired and undesired, are dictated by the physical properties of the material. Previous research has focused on surface chemistry and feature size of biomaterials. The role of shape, in particular the ability of cells to recognize and respond to shape, has not been determined. This is primarily due to the limited availability of techniques to produce materials with features of controlled and varied morphologies. To this end, we have created a diverse collection of novel polymer micro- and nano-particle shapes and studied their phagocytosis by macrophages. The macrophage immune response to biomaterials is a formidable obstacle in delivery and integration of materials for successful tissue regeneration, engineering, and drug delivery. The results show that particle shape, from the point of view of the macrophage, profoundly impacts phagocytosis, more than particle size and independent of surface chemistry. We can use this understanding to design material features that will direct desired macrophage response and, in the future, study the effects of shape on other cell functions. This work demonstrates the importance of shape in the design of biomaterials and its influence on cell–material interactions.

Keywords Shape • Microspheres • Drug delivery • Phagocytosis

J.A. Champion
School of Chemical and Biomolecular Engineering, Georgia Institute of Technology,
Atlanta, GA 30332, USA

S. Mitragotri (✉)
Department of Chemical Engineering, University of California Santa Barbara,
Santa Barbara, CA 93106, USA
e-mail: samir@engineering.ucsb.edu

15.1 Introduction

The goal of regenerative materials is to provide an interactive environment conducive to healing, growth or differentiation of individual cells and larger scale tissues. Interaction is the key to regeneration and materials that encourage desired interactions while discouraging undesired interactions will be most successful in promoting regeneration. Cell–material interactions are dictated by the physical properties of the material such as chemistry, size and shape. Biomaterials presenting many different surface chemistries and a range of feature sizes have been evaluated for cell interactions with a variety of cell types. Shape investigations of cell–material interactions, however, have been limited to micro-fabricated features on 2-D surfaces and fibrous 3-D matrices (Yim and Leong 2005; Ball et al. 2007). An extensive understanding of the effects of material shape on cell interactions does not exist as it does for chemistry and size. This is primarily due to the limited availability of techniques to produce materials with features of controlled and varied morphologies. To address this void, we have created a diverse collection of novel polymer micro- and nano-particle shapes with which to study the dependence of cell–material interactions on shape.

In addition to serving as tools for revealing the role of shape in cell–material interactions, polymer particles can be used to encapsulate therapeutic drugs with several benefits over traditional formulations (Langer 1990). Drug delivery is a critical component of regenerative medicine. In many cases delivery of soluble growth factors and other proteins are essential to induce cellular behavior required for successful tissue regeneration. A great deal of research has been performed on this type of drug delivery system, investigating the effects of particle properties such as polymer chemistry, surface chemistry and particle diameter. In spite of this work, significant challenges still exist for successful drug delivery with polymeric particles.

In this work, we use polymer particles of various geometries to reveal the effect of shape on phagocytosis by macrophages, one example of cell–material interactions. As components of the immune system and producers of inflammatory factors, the macrophage response to biomaterials is critical to successful *in vivo* incorporation and tissue regeneration. In addition, macrophages serve as a significant barrier to drug delivery particles by internalizing them and thus preventing delivery of therapeutic molecules. The following chapter describes the preparation of geometrically distinct polymer particles and the effect of shape on the ability of macrophages to internalize these particles.

15.2 Particulate Drug Delivery Systems

Traditionally, delivery of therapeutic drugs has been accomplished by injection or oral ingestion. Though oral administration is painless and convenient, injections are painful and require sterile needles and training. Both methods, however, suffer

significant therapeutic limitations. Usually frequent dosing, daily or more often, is required due to the high rate of metabolism and/or degradation of the drug in the body. This leads to greater time spent above or below the therapeutic concentration, which increases side effects and decreases the effectiveness of the drug. Additionally, injection and oral administration are not suited towards new types of complex biological therapeutics such as proteins, peptides and DNA, which are often required for integration of regenerative materials. These molecules cannot survive the harsh environment of the gastrointestinal tract or enzymes and degradation processes in the blood and tissue. These methods of drug administration also cannot target drug molecules to specific tissues and therefore require higher systemic concentrations to achieve the required concentration in the desired tissue. Often this results in exposure of healthy tissues to high drug concentrations, sometimes at levels toxic to healthy cells. The limitations described here are not only a result of the administration route, but also the drug formulation. Typically, the active drug molecule is administered with fillers or other non-active ingredients with little, if any function of their own. In order to address these issues and realize the full potential of therapeutic molecules, the field of drug delivery has emerged with the appreciation that a drug is only as good as its delivery system. The goals of drug delivery systems are not only to deliver drug into the body, but at the ideal systemic or local concentration with the minimum number of doses (Langer 1990). A variety of different approaches have been taken to cover a range of therapeutic molecules, diseases and administration routes. Some examples include transdermal delivery systems, macromolecular conjugates and encapsulating polymer particles, to name a few (Langer 1990; Prausnitz et al. 2004; Patri et al. 2002). Polymer particles are uniquely suited as controlled release systems to meet drug delivery requirements for a wide range of applications. Particulate delivery systems have already had some success both in the laboratory and in the clinic. However, there are still significant challenges to overcome in order to achieve all the goals of a successful drug delivery system.

Encapsulation of therapeutic agents into polymeric carriers provides important benefits over traditional formulations (Langer 1990). Prior to release, the polymer protects the drug from degradation or premature metabolism. Controlled release of the therapeutic agent is sustained over days to months, thereby maintaining drug concentrations at constant therapeutic levels for longer periods of time. This reduces the frequency of administration and increases patient compliance. Targeting ligands can also be attached to the particle surface to direct accumulation of particles at a particular site, thereby increasing the drug concentration locally while minimizing systemic side effects. Polymeric particles are versatile and can be used to deliver drugs via subcutaneous, pulmonary, intravascular and oral routes, each with different design requirements. In addition to these advantages, the main disadvantage suffered by drug delivery particles is their recognition and uptake by immune cells called macrophages in a process known as phagocytosis (Illum et al. 1982; Moghimi et al. 2001).

Particles can have a variety of different functions or interactions with cells and tissues in the body. Some are dependent on the route of administration while others are not. The primary function of all drug delivery particles is controlled release of

therapeutic molecules. There are several different release mechanisms depending on the particle design. Release can be water driven or depend on local environmental factors such as pH or the presence of enzymes, which may vary according to administration route. The ability of particles to accumulate at a target site is another important function of drug delivery particles. The goal of targeting is attachment to, and often uptake by, the desired cell type. While targeting or circulating, particles should avoid uptake by undesired cells, particularly cells of the immune system such as macrophages. This is perhaps the most important function of particles since they are unable to deliver their therapeutic load, systemically or locally, if they have been sequestered by the immune system. Phagocytosis is one of the most difficult barriers of particulate drug delivery systems.

15.2.1 Role of Physical Properties in Particle Function

Physical properties of drug delivery particles dictate every aspect of their function. Some property–function relationships are well characterized while others have not yet been investigated. The physical properties that are primarily responsible for particle function are surface chemistry, size and shape. The first two properties have been studied extensively and many of their roles in particle function are understood. Their roles in cell–material interactions are summarized below. Shape is, by far, the least studied of these properties and this work aims to fill that gap.

15.2.1.1 Surface Chemistry

Surface chemistry primarily influences the interactions of particles with cells and proteins in the body. Towards that end, significant attention has been paid to chemical modification of the particle surface so as to minimize protein adsorption and recognition by the components of the immune system, making them “stealth” particles (Stolnik et al. 1995). The most commonly used strategy involves modification of the surface with a hydrophilic polymer brush to reduce opsonization, the adsorption of antibodies and complement on the particle surface, which promotes recognition by the immune system. Localization of hydrophilic polymers on the particle surface has been achieved by physical or chemical adsorption or by incorporation of the stealth polymer into the carrier at the polymer synthesis stage (Storm et al. 1995). For example, di-block co-polymers of PLGA with PEG have been used to fabricate particles enriched with hydrophilic PEG at the surface and hydrophobic PLGA at the core (Gref et al. 1994). Surface chemistry can not only be exploited to avoid biological interaction but also to encourage specific, desired biological interaction. Surface modification has been actively used to target particles to specific tissues or cell types for localized drug delivery. A plethora of targeting ligands for cell-surface receptors, including small molecules, antibodies, carbohydrates and peptides have been used to target cells in various tissues including brain, liver and tumors (Poste and Kirsh 1983; Reddy et al. 2006; Liang et al. 2006).

15.2.1.2 Size

The impact of particle size on carrier function has also been actively investigated. Size influences almost every aspect of particle function including degradation, flow properties, clearance and uptake mechanisms (Illum et al. 1982; Moghimi et al. 2001; Stolnik et al. 1995; Panyam et al. 2003; Dunne et al. 2000; Goldsmith and Turitto 1986; Patil et al. 2001; Lamprecht et al. 2001; Tabata and Ikada 1990). In terms of cell–material interactions, size primarily influences attachment and internalization of particles by cells. Depending on the surface chemistry, particles can bind to receptors on many different kinds of cells. Spherical particle attachment is dependent on size because the probability of attachment is based on the surface area of attachment between the particle and cell membranes of varying curvature. Particles larger than $\sim 0.5 \mu\text{m}$ can be phagocytosed by macrophages and smaller particles can be endocytosed by phagocytic or non-phagocytic cells (Rejman et al. 2004; May and Machesky 2001). The velocity of phagocytic internalization is not size dependent (see Section 15.5). However, the size of the particle dictates the type of internalization process that will occur: phagocytosis, endocytosis or pinocytosis.

15.2.1.3 Shape

In contrast to significant research focused on investigating the effect of particle size and surface chemistry on *in vivo* performance, there is a striking lack of research on the effect of particle shape. The precise role of particle shape in drug delivery has not been fully elucidated, most likely due to the lack of easy-to-use methods available to control particle shape. Certainly shape, along with size and chemistry, is a critical feature of drug delivery particles. Particle geometry is likely to affect all aspects of drug delivery including degradation and release, *in vivo* transport, clearance, targeting and individual cell–particle interactions (Champion et al. 2007a). Shape effects on cell behavior have been demonstrated in non-particulate systems. For example, differences cell adhesion, motility and differentiation have been documented on various 2-D surfaces with micro-fabricated channels and posts as well as fibrous 3-D matrices (Yim and Leong 2005; Ball et al. 2007).

Shape of particles will likely influence their targeting ability to specific cell types. Not only is the overall surface area available for targeting ligands important, but the local curvature also affects ligand and opsonin adsorption and the degree to which particles fit the contours and attach to target cell membranes. Internalization of targeted particles, whether intended or undesired, should also be dictated by particle shape. Due to the specified upper limits on size of (spherical) particle uptake by non-phagocytic cells in the literature, particle shape and orientation could prove to be very important. Particle shape could not only affect the cells' ability to internalize successfully, but also the transport and sorting of particles inside the cell.

Unlike targeted uptake, macrophage phagocytosis is usually undesirable. Phagocytosis is a critical interaction between particles and phagocytic immune cells.

Natural phagocytic targets such as bacteria and environmental particles have diverse shapes and sizes. This suggests that phagocytosis will also be affected by particle shape. Internalization of particles by macrophages prevents delivery of drugs to required tissues. Given the importance of drug delivery in regenerative medicine and the negative effect of macrophage-particle interactions on delivery, phagocytosis is the first system we chose to investigate shape driven cell–material interactions.

15.3 Phagocytosis

The first line of defense against infection is provided by the innate immune system. Phagocytosis, which means “cell-eating”, is a process of innate immunity involving ingestion of particulate matter primarily by cells of the mononuclear phagocytic system and neutrophils. It is typically defined as actin-dependent internalization of large, $>0.5 \mu\text{m}$, particulate targets (Aderem and Underhill 1999). Phagocytosis is different from endocytosis and pinocytosis on the basis of particle size and the role of actin (Koval et al. 1998). Internalized matter includes infectious organisms, dead host cells, and cellular and foreign debris. Polymeric particles are identified as foreign and rapidly eliminated from the body by phagocytosis, an unconquered hurdle in the development of novel particulate drug delivery systems. There are four steps of phagocytosis: chemotaxis, attachment, engulfment and digestion (Goldsby et al. 2003). Of these, attachment and engulfment are expected to be impacted the most by particle geometry.

15.3.1 Attachment

Macrophages encounter phagocytic targets either by chemotactic migration or random collisions. Random interactions of particles and cells may be described purely based on probabilistic events, taking into account the most important long-range particle-cell forces, van der Waals, electrostatic and steric-polymer forces (Israelchvili 1992) and the fact that contact does not ensure attachment. Macrophages are faced with the challenging task of distinguishing foreign particles from indigenous ones, a task usually performed by phagocytic surface receptors. Attachment is the result of binding between particles and receptors on the cell surface. It is required for engulfment and can be rather complicated because some phagocytic targets can be recognized by more than one receptor (Aderem and Underhill 1999). There are two groups of phagocytic receptors, pattern-recognition receptors (PRRs) and opsonic receptors. PRRs are components of innate immunity that recognize and bind a variety of conserved surface motifs on pathogens (Aderem and Underhill 1999; Ross and Auger 2002). Also included in this group are scavenger receptors (SRs) that exhibit broad ligand-binding specificities (Pearson 1996). Class A scavenger receptors (SR-A) bind most non-opsonized poly(styrene) (PS) and other non-biological or environmental

particles (Arredouani et al. 2005). Opsonic receptors identify and bind to opsonins, proteins produced by the body that coat the surface of particles and increase the efficiency of phagocytosis (Aderem and Underhill 1999; Ross and Auger 2002). Complement receptors that bind to complement fragments non-specifically opsonized to pathogens or particles. Alternatively, antibodies specifically opsonize during the adaptive immune response and bind to the activation class of Fc receptors on macrophages. However, IgG has also been observed to bind non-specifically to silica and PS particles indicating that an adaptive immune response is not necessary for FcR mediated phagocytosis (Hetland et al. 2000; O'Brien and Melville 2003).

15.3.2 *Internalization*

Internalization is the most defining and remarkable step in phagocytosis. Regardless of the cell type or receptor involved, phagocytosis is a product of coordinated rearrangement of the actin cytoskeleton (May and Machesky 2001). The mechanism to internalize particles is dependent on which receptor begins the signaling pathway required for actin polymerization. The first event triggered by the binding of particles is the clustering and cross-linking of receptors at the binding site (Aderem and Underhill 1999; Swanson and Hoppe 2004). Signaling from subsequent activation steps recruits cytoskeletal proteins that initiate and regulate the polymerization of actin filaments beneath the particle and leads to the formation of the phagocytic cup. The major actin nucleator is the Arp2/3 complex which can be activated to induce actin polymerization by a variety of proteins included members of the WASP family. As the growing actin network pushes the leading edge of the membrane forward, the actin network in the rear is being remodeled and depolymerized, leading to the transformation of the actin cup to an actin ring structure (Lee et al. 1997, 2001; Aizawa et al. 1997). After the plasma membrane surrounds the particle completely, it fuses with itself and breaks off from the rest of the membrane. The particle is released into the cytoplasm still tightly surrounded by membrane. FcR-mediated engulfment is thought to occur by a “zipper” model. The advance of the membrane occurs as an ordered progression of FcR-IgG interactions leading to the events described above. Internalization via CRs is a more passive version of FcR-mediated internalization. The particle sinks into the cell as the membrane invaginates with small or no pseudopodia. It is believed that different mechanisms are employed when PRRs initiate binding but they are similar to FcR internalization (Aderem and Underhill 1999).

15.4 **Fabrication of Non-spherical Polymer Particles**

Though metal particles have been synthesized into a variety of non-spherical geometries, polymer particles cannot take advantage of the same techniques. Only a few methods of fabricating non-spherical polymer particles existed prior to the

development of this technique. By extensive adaptation of the sphere stretching method of Ho et al. (1993), we created a technique that produces particles displaying regions of varying concavity, curvature, aspect ratio and surface texture (Champion et al. 2007b). With this method, it is possible to make particles where important properties such as volume, shape, surface area, curvature and texture can be systematically and independently varied. This ability is essential in determining the role of shape in any application, including cell–material interactions.

15.4.1 General Method

Uncrosslinked spherical PS particles with diameters of 60 nm to 10 μm are used as a starting material for preparing particles with complex shapes. In order to manipulate the PS spheres, they are embedded in a poly(vinyl alcohol) (PVA) film. PVA is used for its ability to form films and because it is water soluble, unlike PS. Most importantly, PVA has the ability to form hydrogen bonds to surface groups on particles through hydroxyl groups which results in strong attraction between particles and film. To form the film, PVA is dissolved in water, particles are added, and the particle/PVA solution is then cast and dried. A combination of liquefying and stretching induces morphological changes in the spheres. Newly shaped particles are collected by solidifying the particles and dissolving the film.

Since PS particles, and many other polymer particles of interest, are solid at room temperature, liquefaction is necessary to manipulate the particle. This can be accomplished two ways, through heat or solvent. Particles must be heated above 90°C, their glass transition temperature (T_g), to liquefy them. At the T_g a polymer possesses sufficient free volume for chain rearrangement (Painter and Coleman 1997). Above its T_g , a polymer softens to a liquid with high viscosity. As it is heated further the polymer viscosity decreases and it becomes a liquid that flows easily. Another way to fluidize particles is with solvent. PS has many good solvents including toluene, an aromatic hydrocarbon (Roff and Scott 1971). Soaking film-embedded particles in toluene completely liquefies them but they do not disperse because they are trapped in the film. Toluene does not adversely affect the PVA film. The viscosity of the particles after soaking in toluene is much lower than particles heated to 125–155°C, the temperature range used in this method.

The PVA film must also be modified to make stretching possible, either by heating or the addition of a plasticizer. Since the T_g of PS (90°C) is higher than the T_g of PVA (85°C), the film stretches well if the particles are simultaneously being heat-liquefied. Stretching of toluene-liquefied or solid particles is performed at room temperature. Since PVA film will not stretch at room temperature, the T_g of the film was decreased to below room temperature by the addition of a plasticizer, glycerol (Painter and Coleman 1997). Stretching of films, under any conditions, was performed on machined stretching devices in either one dimension or simultaneously in two dimensions.

The method for engineering shape can be classified into two general approaches (Champion et al. 2007b). In the first approach, termed scheme A, PS particles are liquefied and then stretched. In the second approach, scheme B, PVA films are stretched first to create voids around the particles. These voids are then filled by liquefying the particles. In both schemes re-solidifying the particles after manipulation sets their new shape. Heated films are cooled to room temperature while still on the stretching device. Toluene-immersed films are air-dried on the stretching device to evaporate the toluene, removed from the device and immersed in isopropanol to remove any residual toluene. Finally, the particles are collected by dissolving the film in warm water. The particle-film solution is washed by centrifugation in 30% isopropanol to remove PVA.

These two manipulation approaches, though apparently simple, can give rise to an incredibly diverse range of particle shapes. Final particle shape is dictated by the material properties of the film (T_g and thickness), the material properties of the particles (T_g and viscosity), interactions between particles and film (adhesion strength) and the stretching parameters (extent and dimensionality). Particle volume remains constant during stretching, governed entirely by the volume of the initial sphere. Thus, size and shape of particles can be independently controlled. The shapes made from this method, pictured in Fig. 15.1, were made primarily from 1 to 5 μm particles. However, the method has been easily extended to nanoparticles as small as 60 nm for several shapes.

15.4.2 Specific Shapes

Particles made using scheme A are shown in Fig. 15.1b–h. These particles share the same general mechanism of formation, the liquefied particle is stretched due to its strong association with the film arising from H-bonding. However, the final shape depends strongly on the details of key parameters. For example, stretching particles in a thin film (35 μm) produces flatter particles (Fig. 15.1b) whereas stretching in a thicker film (70 μm) produces rods with a nearly circular cross-section (Fig. 15.1c). In each case, the aspect ratio can be controlled independently of the shape, from 1 to ~ 11 , and is typically smaller than the extension ratio of the film itself. The ends of rectangular disks (Fig. 15.1b) and cylindrical rods (Fig. 15.1c) are relatively flat owing to the high viscosity of liquefied droplet, which in turn can be attributed to the use of low temperatures used for liquefaction (120°C). Increasing the liquefaction temperature created sharp-ended worm-like particles (Fig. 15.1d). The exact shape and tortuosity of worms varied from particle to particle. Two dimensional (2-D) stretching of heat-liquefied particles led to oblate ellipsoids with aspect ratios dictated by the extent of stretching (Fig. 15.1e).

Replacing heat with toluene as a mode of liquefying particles led to entirely different shapes due to decreased PS viscosity. Specifically, 1-D stretching of films after toluene-liquefaction formed thin elliptical disks with curved ends (Fig. 15.1f) under conditions where heat-liquefied particles formed rectangular disks with blunt

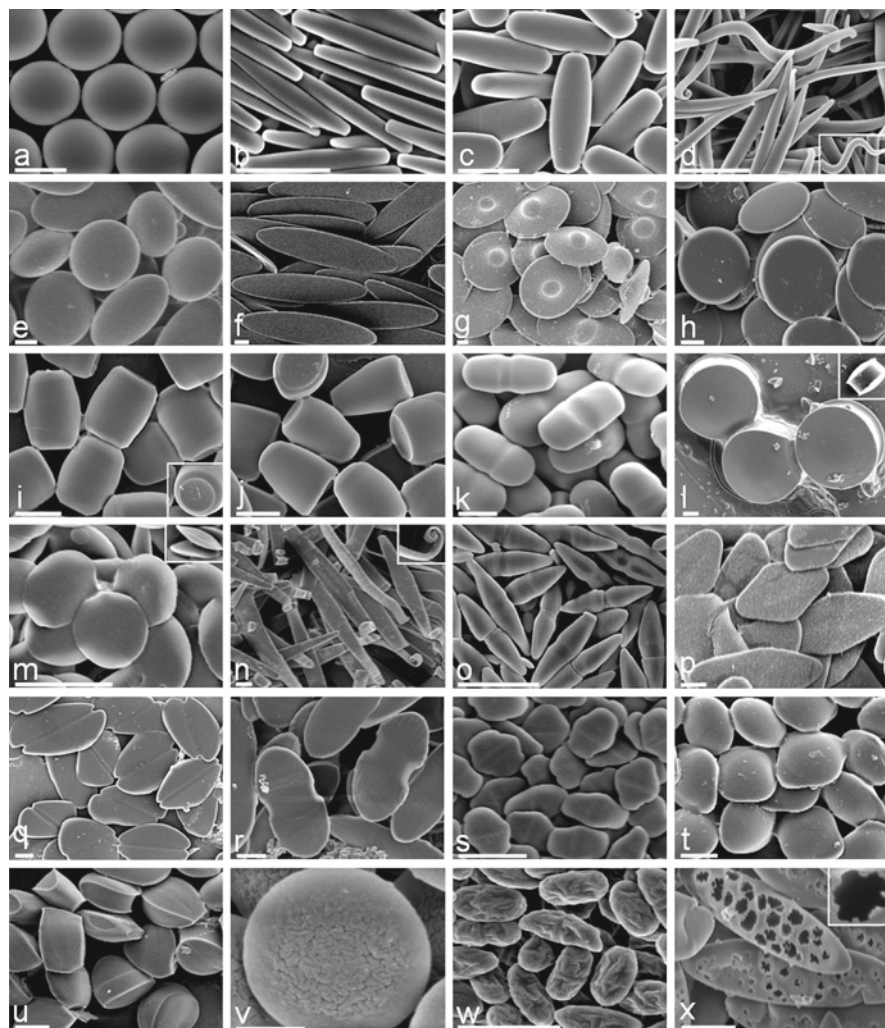


Fig. 15.1 Scanning electron micrographs of polystyrene (a) spheres stretched into (b) rectangular disks, (c) rods, (d) worms, (e) oblate ellipsoids, (f) elliptical disks, (g) UFOs, (h) circular disks, (i) barrels, (j) bullets, (k) pills, (l) pulleys, (m) bi-convex lenses, (n) ribbons with curled ends, (o) bicones, (p) diamond disks, (q) emarginate disks, (r) flat pills, (s) elongated hexagonal disks, (t) ravioli, (u) tacos, (v) wrinkled prolate ellipsoids, (w) wrinkled oblate ellipsoids and (x) porous elliptical disks. Scale bars = 2 μm except for (w) (400 nm)

ends. Peculiar results were obtained when toluene-liquefied particles were stretched in 2-D. Moderate stretching of toluene-liquefied particles led to UFO-like particles (Fig. 15.1g) due to preferential stretching of the particle around the equator. Extensive stretching under the same conditions or comparable stretching of smaller particles eliminated the dome and produced flat circular disks (Fig. 15.1h).

More complex shapes were made using scheme B, shown in Fig. 15.1i–m. One-dimensional stretching of the film without particle-liquefaction creates an ellipsoidal void around the particle. Upon heat-induced liquefaction, PS fills the void by wetting the film. However, at relatively low liquefaction temperatures (130°C) the high viscosity of PS inhibits complete filling of the void and leads to barrel-like particles upon solidification (Fig. 15.1i, inset shows concave regions at both ends). Interestingly, liquefaction at higher temperatures (140°C), keeping all other parameters the same, decreases PS viscosity and induces distribution of PS to one end of the void, increasing the contact area between PS and PVA, and forming bullet-like structures (Fig. 15.1j). Once again, replacing heat with toluene, as a means of liquefaction, after dry-stretching of film produced different shapes due to further reduction of viscosity. One-dimensional stretching in air followed by toluene-induced liquefaction formed pill-like particles (Fig. 15.1k). Moderate 2-D stretching of the film in air followed by toluene-induced liquefaction led to pulley-shaped particles (Fig. 15.1l, a circular disk with a groove in the middle, inset shows side view). Repeating the same procedure with extensive stretching produced bi-convex lenses (Fig. 15.1m, inset shows side view).

Combination and/or repetition of schemes A and B led to even more unusual shapes pictured in Fig. 15.1n–u. These combination shapes include ribbon-like particles with curled ends (Fig. 15.1n, inset shows a curl), bicones (Fig. 15.1o), diamond disks (Fig. 15.1p), emarginate disks (Fig. 15.1q), flat pills (Fig. 15.1r), elongated hexagonal disks (Fig. 15.1s), ravioli (Fig. 15.1t) and tacos (Fig. 15.1u).

This method can be further modified to control additional design features, such as surface texture, while keeping size and shape constant. Particles with unique surface textures are shown in Fig. 15.1v–x. For example, scheme B was modified to make wrinkled prolate ellipsoids (Fig. 15.1v). In this modification, the film was stretched while keeping the particles solid and it was removed from the stretcher prior to particle liquefaction. This allowed the film to relax and produced wrinkles at the film-void interface. Subsequent toluene-induced liquefaction produced particles with wrinkled surfaces. A similar procedure performed by 2D stretching produced wrinkled oblate ellipsoids (Fig. 15.1w). In another example, porous elliptical disks (Fig. 15.1x) were formed when toluene-liquefied particles stretched according to scheme A were immediately immersed in isopropanol to remove toluene, omitting the air drying step. This led to rapid removal of toluene from the particle and created holes on one side of the particle surface.

This shape fabrication method generates particles of incredibly diverse shapes. The resultant shapes can be explained by the physical properties of the particle and film and the interaction between them. Scheme A generally leads to simpler shapes since fewer properties, primarily particle viscosity and film thickness, are relevant to the final shape. Particle viscosity, for example, dictates whether a shape will have pointy ends (worms, elliptical disks) or flatter ends (rectangular disks, rods). Higher viscosity of particles (arising from stretching at low temperature) prevents the film from stretching to a sharp point due to preservation of width of the particle during stretching. Regardless of viscosity, thinner films led to creation of flatter particles and thicker films led to the creation of particles with circular cross sections.

Scheme B leads to generally more complex shapes because of the introduction of an additional design parameter, particle-film wetting properties. In particular, the interplay between particle-film wetting properties and particle viscosity introduced further diversities in shape.

15.5 Effect of Particle Shape on Phagocytosis

Normally occurring phagocytic targets include pathogens such as rod-shaped *Escherichia coli* and spiral-shaped *Campylobacter jejuni*, disk-shaped senescent cells such as aged erythrocytes, and airborne irregularly shaped particles such as dust and pollen. These targets vary widely in both shape and size. Since macrophages in the human body encounter targets with such diversity, it is expected that target geometry impacts phagocytosis in some way. Several studies have been conducted specifically to address this question, however a generalized answer is still lacking. The main reason behind this shortcoming is that all phagocytosis studies have been performed using spherical targets (Tabata and Ikada 1990; Koval et al. 1998; Simon and Schmidtschonbein 1988; Kawaguchi et al. 1986; Rudt and Muller 1993; Cannon and Swanson 1992). Exclusive use of spherical particles originated partly due to a presumption that size is the principal parameter of interest and partly due to difficulties in fabricating non-spherical particles of controlled dimensions. Use of spherical particles not only concealed the role of particle shape in phagocytosis but also creates an inaccurate picture of the actual role of particle size since all parameters that describe size (volume, surface area etc.) scale with particle radius. Our ability to create particles with controlled non-spherical morphologies allowed us to explore the role of particle shape in phagocytosis.

15.5.1 Shape Internalization

Particles representing six distinct geometric shapes were fabricated for internalization experiments (Fig. 15.1a, c, e–g): spheres, rectangular disks, oblate ellipsoids, elliptical disks, and UFOs. IgG-opsonized and non-opsonized particles were incubated with alveolar macrophages and observed with time-lapse video microscopy. Internalization of both opsonized and non-opsonized particles exhibited a strong dependence on local particle shape from the perspective of the phagocyte. Local shape varies not only for different particles but also for different points of initial contact on the same particle, except for spheres. For example, macrophages that attached to elliptical disks along the major axis internalized them within minutes (Fig. 15.2a). The macrophage membrane can be seen moving along the length of the particle in a coordinated, unified fashion. On the other hand, cells that attached to the same elliptical disks along the minor axis or flat side did not internalize them, even after 15 h (Fig. 15.2b). They did, however, spread on the particle surface but

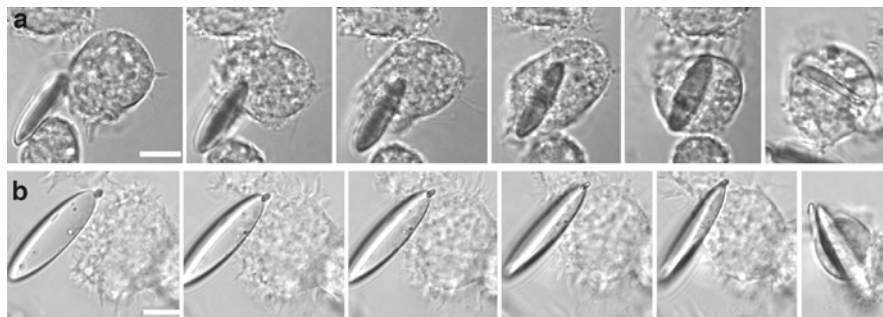


Fig. 15.2 Time-lapse video microscopy images at 0, 1, 1.5, 2, 3 and 39 min after attachment of identical non-opsonized elliptical disks to alveolar macrophages. **(a)** Cell attaches along the major axis of elliptical disk and internalizes it completely in 3 min. **(b)** Cell attaches to the flat side of an identical elliptical disk and spreads but does not internalize the particle. Continued observation indicated this particle was not internalized for over 110 min. Scale bars = 10 μm

with non-synchronized, separate fronts moving in different directions at different times. Macrophages attached to the flat side of IgG-opsonized elliptical disks exhibited more spreading than those attached to non-opsonized particles but the final result was the same, no phagocytosis. Since the particles used for these studies possessed identical properties (dimensions, surface area, volume, and chemistry), observations in Fig. 15.2 clearly show that the local particle shape at the point of initial contact, not the overall size, determined their phagocytic fate. Similar results were seen for all shapes. Rectangular disks were internalized from the corners but not from the blunt ends, sides or faces. Oblate ellipsoids were internalized from the edge, but not from either face. UFO-shaped particles were internalized from either dome or the edge but not from the concave region in between. Spheres could be internalized from any point, due to their symmetry.

Scanning electron microscopy (SEM) provided more evidence for this orientation bias (Fig. 15.3). As seen in the micrographs, the cell membrane showed marked progression on elliptical disks when approached along the major axis. In contrast, cells that attached to the flat side of elliptical disks exhibited spreading but no engulfment of particles, even after 2 h. As a reference point, consistent engulfment was observed on spheres.

Further insight for orientation-dependent particle phagocytosis was gained by staining macrophages for polymerized actin at various times during phagocytosis. As discussed in Section 15.3.2, actin polymerization is the principal mechanism by which macrophages push the leading edge membrane and engulf particles (May and Machesky 2001). Spheres and elliptical disks that attached to macrophages along the major axis exhibited an actin cup at short times that later transformed to a ring around the particle as phagocytosis progressed. Macrophage attachment to the flat side of elliptical disks, in spite of actin polymerization at points of contact and spreading, did not exhibit an actin cup or ring. Formation of an actin cup is a clear indicator of initialization of internalization and was observed only at the same local shapes that induced internalization in time-lapse video microscopy.

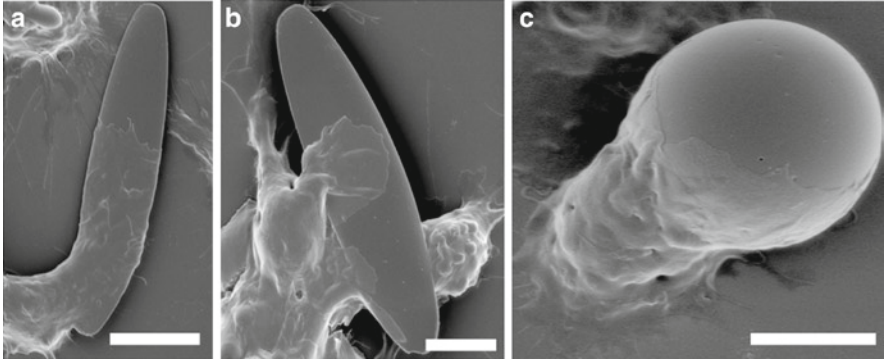


Fig. 15.3 Micrographs of cells and particles. (a) The cell body can be seen at the end of an opsonized elliptical disk and the membrane has progressed down the length of the particle. Scale bar = 10 μm . (b) A cell has attached to the flat side of an opsonized elliptical disk and has spread on the particle. Scale bar = 5 μm . (c) An opsonized spherical particle has attached to the top of a cell and the membrane has progressed over approximately half the particle. Scale bar = 5 μm

15.5.2 Quantification of Shape

To arrive at a generalized and quantitative statement about the role of shape in phagocytosis, local shape had to be quantified. Although curvature qualitatively seemed to describe the experimental observations, previous experiments with spheres of different diameters demonstrated that internalization velocity was not purely a function of curvature. Since the macrophage membrane moves tangentially along the surface of the particle, we chose to define local shape in terms of tangent angles. We defined the angle Ω between the membrane normal at the point of initial contact, $\bar{\mathbf{N}}$, and a vector $\bar{\mathbf{T}}$ whose angle represents the mean direction of tangents drawn to the target contour from the point of initial contact to the center line of the target (Fig. 15.4).

$$\Omega = \cos^{-1}(\bar{\mathbf{N}} \cdot \bar{\mathbf{T}}) = \left\langle \int_0^{\theta} \frac{ds}{d\theta} \kappa(\theta) d\theta \right\rangle_{0, \pi/2}$$

$\kappa(\theta)$ is curvature and $ds/d\theta$ is the angular gradient of the arc length (Weisstein 1999). $\theta = 0$ is defined as the point of contact. Ω , evaluated numerically for each case, is a dimensionless parameter and depends only on the particle's shape and its point of attachment to the macrophage. Essentially, Ω is a measure of curvature that is normalized for size. It indicates the mean angle made by the membrane with $\bar{\mathbf{N}}$ as it travels around the particle during phagocytosis. For each attachment site on a particle, there exist two values of Ω defined for two orthogonal views of the particle, the larger of which is used in further analysis. For all sized spheres, the dome or

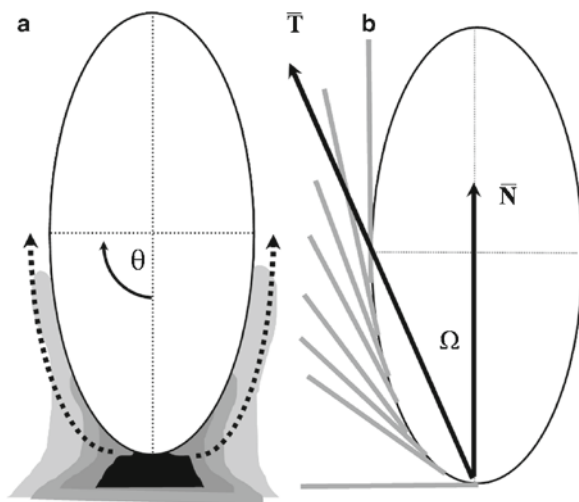


Fig. 15.4 A schematic diagram illustrating how membrane (gray) progresses tangentially around an ED (a). \bar{T} represents the average of tangential angles from $\theta = 0$ to $\theta = \pi/2$. Ω is the angle between \bar{T} and membrane normal at the site of attachment, \bar{N} (b). Ω is essentially curvature normalized for size

ring of UFOs, and the edge of oblate ellipsoids, $\Omega = 45^\circ$. For an elliptical disk with a major axis a , minor axis b and relatively small thickness, $\Omega \sim \arctan(b/a)$ for a particle attaching along the major axis (Fig. 15.4, top), $\Omega \sim \arctan(a/b)$ for attachment along the minor axis, and $\Omega \approx 90^\circ$ for a cell attaching on the flat side (Fig. 15.4, bottom). For the concave region of a UFO, $\Omega > 90^\circ$. Since Ω depends only on particle shape, dependence of phagocytosis on size and shape can be clearly separated and understood.

15.5.3 Correlation Between Internalization, Shape and Size

Dependence of the rate of internalization on Ω can be seen in Fig. 15.5 where internalization velocity (total distance traveled by macrophage membrane to complete phagocytosis, evaluated in the two-dimensional projected view of the particle (Fig. 15.4), divided by the time required to complete phagocytosis) is plotted against Ω . Phagocytosis velocity decreased with increasing Ω . Furthermore, there was an abrupt transition in internalization velocity to zero at $\Omega \sim 45^\circ$. Zero velocity is assigned when phagocytosis is not completed within the normal period of observation (2 h). Any lack of internalization in Fig. 15.5 is not due to particle size since all particles in this figure were successfully internalized from at least one attachment orientation. IgG-coated particles exhibited the same Ω -dependence as non-opsonized particles, confirming the binding receptor generality of the dependence of phagocytosis on particle shape.

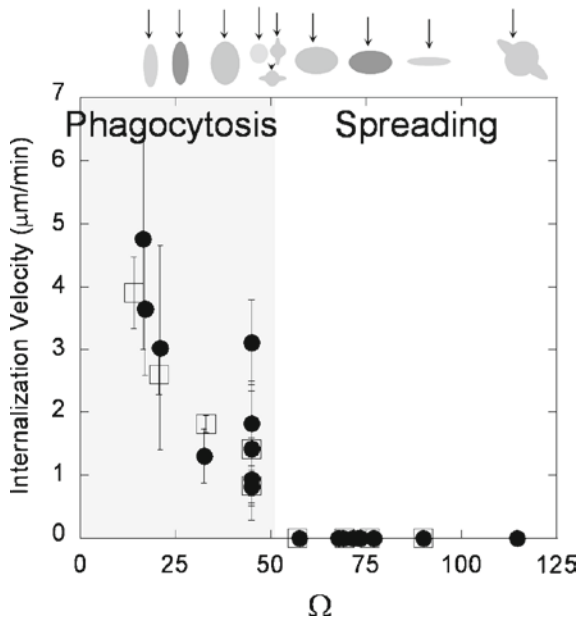


Fig. 15.5 Membrane velocity (distance traveled by the membrane divided by time to internalize) decreases with increasing Ω for a variety of shapes and sizes of particles, IgG-opsonized (\square) and non-opsonized (\bullet). Each data point represents a different shape, size or aspect ratio particle. Internalization velocity is positive for $\Omega \leq 45^\circ$ ($p < 0.001$). Above a critical value of Ω , $\sim 45^\circ$, internalization velocity is zero ($p < 0.001$) and there is only membrane spreading following particle attachment, not internalization. The *arrows* above the plot indicate the point of attachment for each shape that corresponds to the value of Ω on the x-axis. Error in Ω error is due to the difference in the actual point of contact in time-lapse microscopy from that used to calculate Ω . Only points of contact within 10° of that used to calculate Ω were selected. All *data points* at the critical point, $\Omega = 45^\circ$, do not have error associated with Ω , except UFOs, due to their asymmetry ($n \geq 3$, error bars show one standard deviation)

The sudden transition from phagocytosis to spreading at $\Omega \sim 45^\circ$ is rather striking. Particles with $\Omega > 45^\circ$ were capable of inducing significant spreading of cells but not internalization. Spreading has been likened to “frustrated” phagocytosis and phagocytosis has even been proposed as a simple model for spreading since many of the same proteins are involved in both processes (Cougoule et al. 2004; Welch and Mullins 2002; Castellano et al. 2001). In fact, the leading membrane edge during phagocytosis in Fig. 15.3 visually appears very much like that of a cell spreading on a flat surface. Apparent similarities between the two have led researchers to believe that cells cannot distinguish target shape, comparing the membrane appearance on an attached microsphere to a flat glass coverslip (Koval et al. 1998). However, the observations described here show a clear difference in features of actin remodeling during phagocytosis and simple spreading. Although actin is present at the membrane-particle interface in both cases, formation of an actin cup and

ring, clearly visible during phagocytosis, is absent during spreading. More importantly, the fine line between phagocytosis and spreading is defined by the shape of the particle from the cell's perspective.

The overall process of phagocytosis is a result of the complex interplay between shape and size. However, sphere diameter did not affect internalization velocity of non-spherical particles. The phase diagram in Fig. 15.6 shows whether or not internalization was initialized and completed for particles with different combinations of Ω and V^* , the ratio of particle volume to macrophage volume. Initiation of internalization was judged by formation of an actin cup or ring (Fig. 15.4) and completion was judged by closure of the membrane. The diagram shows three regions: the successful phagocytosis region ($\Omega \leq 45^\circ$, $V^* \leq 1$) where phagocytosis is initiated and completed quickly, the attempted phagocytosis region ($\Omega \leq 45^\circ$, $V^* > 1$) where phagocytosis is initiated but not completed within the period of observation, and the spreading region ($\Omega > 45^\circ$) where particle attachment takes place and macrophages spread on the particle but phagocytosis is not initiated. This diagram clearly shows that initiation of phagocytosis is governed by Ω while V^*

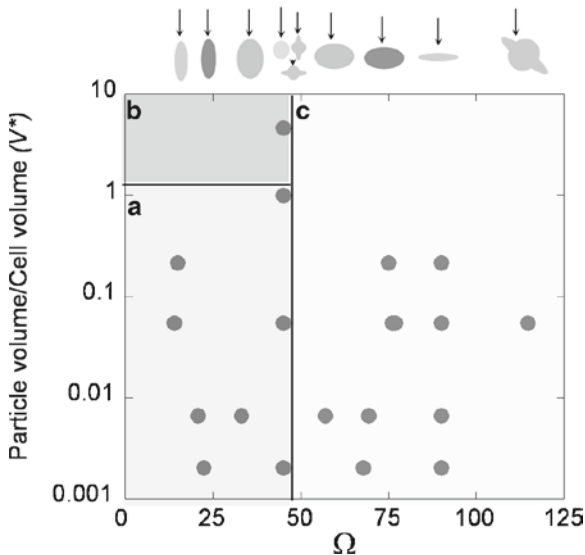


Fig. 15.6 Phagocytosis phase diagram with Ω and dimensionless particle volume V^* (particle volume divided by cell volume) as governing parameters. Initialization of internalization is judged by the presence of an actin cup or ring. There are three regions: Cells attaching to particles at areas of high Ω , $>45^\circ$, spread but do not initiate internalization (Region c). Cells attaching to particles at areas of low Ω , $<45^\circ$, do initiate internalization (Regions a and b). If $V^* \leq 1$, internalization is completed (Region a). If $V^* > 1$, internalization is not complete due to the size of the particle (Region b). The arrows above the plot indicate the point of attachment for each shape that corresponds to the value of Ω on the x-axis. Data points indicate more than 95% of observed cells belonged in the category. Each data point represents a different shape, size, or aspect ratio particle ($n = 5$ for each point)

primarily influences completion. Macrophages phagocytosed particles as large as themselves when approached from the preferred orientation ($\Omega \leq 45^\circ$). Even in the case of particles larger than the cells, macrophages started the internalization process as judged by actin cups. Completion of internalization was not possible however due to the large volume of the particle. On the contrary, particles with volumes as small as 0.2% of the cell volume were not internalized when approached from an undesired orientation ($\Omega > 45^\circ$).

The mechanism for shape-dependence of phagocytosis requires further examination. Since the formation of a coordinated actin cup is crucial to initializing phagocytosis, it is likely that the dynamics of actin remodeling plays a central role in the shape-dependence of phagocytosis. As the membrane surrounds a particle during phagocytosis, the circumference of the actin ring follows the local geometry of the particle. During early stages of phagocytosis the ring expands to surround the particle on all sides and the magnitude of expansion necessary to surround a certain length of the particle increases with increasing Ω . Since actin remodeling is an energy dependent process (May and Machesky 2001), it is likely that particles that require only gradual expansion of actin ring (that is, particles with low Ω) are phagocytosed more effectively. In fact, closer inspection of the macrophage in Fig. 15.2a reveals that even within the same particle, the time required for the cell to internalize the middle third of an elliptical disk (region of relatively constant circumference) is half that required to internalize first third of the elliptical disk (region of expanding circumference). Beyond a certain value of Ω , the large magnitude of expansion necessary to form an actin cup may inhibit phagocytosis completely.

15.6 Design of Non-spherical Particles for Drug Delivery

Through the fabrication of non-spherical PS particles and observation of macrophage behavior with five of these shapes, we have established the role of shape in macrophage-particle interactions. However, to extend this technology to the fields of drug delivery and regenerative medicine requires optimization of shape for phagocytosis and other drug delivery functions, use of biodegradable polymers, and encapsulation and targeting abilities.

15.6.1 *Optimal Shapes for Avoiding Phagocytosis*

Through the experiments described in Section 15.5, we discovered the effect that local particle shape has on phagocytosis using five non-spherical shapes. Macrophage attachment to particle regions with low Ω values induced phagocytosis while attachment to regions with Ω values greater than 45° inhibited phagocytosis. It is geometrically impossible to fabricate shapes with no regions of $\Omega < 45^\circ$. However, one can design shapes that minimize the area of regions with low Ω values.

15.6.2 Fabrication of Non-spherical Biodegradable Drug Carriers

Most of the work creating non-spherical polymer particles and studying the effect of shape on phagocytosis has been performed with PS particles. While an excellent model polymer for the previously described experiments, PS is not a biodegradable polymer and cannot be used to encapsulate and deliver therapeutic molecules. In order for any shape fabrication method to be used for producing drug carriers, a variety of requirements must be met. First, the method must be able to accommodate drug delivery polymers such as PLGA or PEG. Like PS, PLGA is a hydrophobic polymer and PVA can hydrogen-bond with PLGA. We have adapted the film stretching method to make PLGA shapes without major changes from the protocol used to make PS particles. PLGA spheres were prepared by single emulsion solvent evaporation method and stretched into elliptical disks and oblate ellipsoids.

Another requirement for drug delivery particle fabrication methods is that the method must allow for incorporation of therapeutic drug molecules and not require any conditions which could inactivate the drug molecules. In the film stretching method, therapeutic agents are encapsulated in the particles prior to stretching. Therapeutic molecules are incorporated in either organic or aqueous phases, depending upon their solubility and stability, during the sphere fabrication process using current technology. As an example, 66 kDa FITC-labeled bovine serum albumin (BSA) was encapsulated in PLGA by the double emulsion solvent evaporation method and stretched into elliptical disks. No leaching of BSA occurred during the stretching process due to its insolubility in the solvents. However, if the encapsulated material is soluble and is small enough to diffuse through the PVA film, leaching may occur. Stretched films may be exposed to a highly concentrated solution of the encapsulated material in solvent, this has been successfully performed with fluorescein and PS particles. Though stretching particles in solvents can be damaging to encapsulated proteins and other biological therapeutics, current encapsulation technologies utilize the same techniques. In order to stabilize encapsulated proteins, co-encapsulation of amphiphilic molecules, which are preferentially adsorbed on the aqueous organic interface while shielding vulnerable therapeutic protein molecules, may be employed (Manning et al. 1989). Another route to protect sensitive protein therapeutics is to utilize hydrophilic biodegradable polymers instead of the more traditional hydrophobic ones. Theoretically, hydrophilic polymer particles can be stretched in a hydrophobic film made from poly(dimethylsiloxane) co-polymers (Mohraz and Solomon 2005), ethyl cellulose or others. Since some shapes are formed using solvent and others using heat, shape selection should take into account the method of liquefaction.

The shape fabrication method should also not inhibit post-production processing, such as tethering of targeting ligands or stealth moieties to the particle surface. This has been verified with the BSA-encapsulated PLGA ellipses. After shape fabrication, fluorescent IgG was physically adsorbed on the surface of the particles and confirmed with fluorescence microscopy.

15.7 Conclusions and Future Directions

We have established a simple shape manipulation method and fabricated polymer particles with varied and controlled morphologies. Using these particles we revealed, for the first time, that the local particle shape at the point of macrophage attachment is critical to the success of phagocytosis. Size, on the other hand, only dictates attachment to the membrane and in the case of very large particles affects completion of phagocytosis. Prompted by our initial motivation of successful particulate drug delivery systems, we identified optimal shapes for avoiding phagocytosis and demonstrated the generality of our shape manipulation method to biodegradable, drug encapsulating particles. Together, these results bring a fresh view to drug delivery particle design that will enable delivery of therapeutic molecules for many applications including tissue regeneration.

15.7.1 Drug Delivery

The single most important outcome of this work is a new tool in the drug delivery particle design toolbox – shape. From now on, for any application, shape should be considered along with polymer chemistry, surface chemistry and size. In some cases spheres may be the best shape for a certain application, but that should be a conscious decision and not due to a lack of ability to alter particle morphology. The fabrication methods described here create a group of particles where important properties such as shape, dimensions, volume, surface area, curvature and surface chemistry can be systematically and independently varied. This is critical in determining exactly what aspect of shape influences particle behavior and also the interplay between shape, size and surface chemistry.

The phagocytosis results presented here leave no doubt that shape is a critical parameter for drug delivery particles. With the shapes that are now available, future effort should be focused on uncovering the effect of shape in degradation, transport, targeting and non-phagocytic internalization. Though each of these areas can be studied separately, ultimately optimization must be performed to identify the shape or shapes that perform best in all categories for a given application. Current drug delivery literature has recently begun to reflect the growing realization of the importance of shape even though its many roles have not yet been uncovered (Rolland et al. 2005; Geng et al. 2007).

15.7.2 Cell–Material Interactions

The effect of shape on biological interactions is not obvious, as evidenced by the intriguing dependence of phagocytosis on shape. These observations demonstrate the complexity of cell-particle interactions and reveal the ability of cells to sense,

identify and respond to particle shape. Currently available non-spherical particles can not only be used as tools in determining the role of shape, but also as guides in the design of even more new shapes that exhibit the best performance for a given application.

Understanding the complex interplay between shape and size is essential to fully elucidate phagocytosis of natural targets. One of the most intriguing questions is whether the orientation-bias of phagocytosis disappears for smaller targets. Cells are not able to detect macroscopic properties such as volume until phagocytosis is complete. However, it is not known if there is any size inference upon detection of shape. Size limits for internalization processes have been established for spherical particles. Large particles, $>0.5 \mu\text{m}$, are internalized by actin-dependent phagocytosis described in this work. Smaller particles, $0.2 \mu\text{m} < \text{diameter} < 0.5 \mu\text{m}$, exhibit decreased actin dependence and increased dependence on receptor-mediated endocytosis mechanisms as size decreases (Koval et al. 1998). This is obviously complicated by the fact that these definitions only apply to spheres and a cell may detect multiple smaller or larger dimensions on a non-spherical particle. It is possible that the role of shape changes as internalization becomes less actin dependent. We observed that shape dictates the *initiation* of internalization for large particles. This shape dependence on initiation may still hold true for smaller particles, even in the case of endocytosis, because the signaling pathways responding to particle-receptor binding are directing subsequent internalization events. The spatial orientation of bound receptors corresponds directly to the local particle shape at the point of contact. It seems logical, however, that a lower size limit must exist at which shape is indistinguishable to a cell. Certainly the role of shape in smaller particles both in phagocytic and non-phagocytic internalization processes is a worthwhile topic to explore. In addition to internalization processes, the ability of geometrically distinct particles to alter other cellular behaviors should be investigated. Cell adhesion, spreading, motility and differentiation are all important processes in tissue regeneration and may be affected by cell interaction with free or embedded non-spherical particles.

References

- Aderem A, Underhill DM (1999) Mechanisms of phagocytosis in macrophages. *Annu Rev Immunol* 17(1):593–623
- Aizawa H, Fukui Y, Yahara I (1997) Live dynamics of Dictyostelium cofilin suggests a role in remodeling actin latticework into bundles. *J Cell Sci* 110(19):2333–2344
- Arredouani MS, Palecanda A, Koziel H, Huang YC, Imrich A, Sulahian TH, Ning YY, Yang ZP, Pikkarainen T, Sankala M, Vargas SO, Takeya M, Tryggvason K, Kobzik L (2005) MARCO is the major binding receptor for unopsonized particles and bacteria on human alveolar macrophages. *J Immunol* 175(9):6058–6064
- Ball MD, Prendergast U, O’Connell C, Sherlock R (2007) Comparison of cell interactions with laser machined micron- and nanoscale features in polymer. *Exp Mol Pathol* 82(2):130–134
- Cannon GJ, Swanson JA (1992) The macrophage capacity for phagocytosis. *J Cell Sci* 101(4):907–913

- Castellano F, Chavrier P, Caron E (2001) Actin dynamics during phagocytosis. *Semin Immunol* 13(6):347–355
- Champion JA, Katare YK, Mitragotri S (2007a) Particle shape: a new design parameter for micro- and nanoscale drug delivery carriers. *J Control Release* 121(1–2):3–9
- Champion JA, Katare YK, Mitragotri S (2007b) Making polymeric micro- and nanoparticles of complex shapes. *Proc Natl Acad Sci USA* 104(29):11901–11904
- Cougoule C, Wiedemann A, Lim J, Caron E (2004) Phagocytosis, an alternative model system for the study of cell adhesion. *Semin Cell Dev Biol* 15(6):679–689
- Dunne M, Corrigan OI, Ramtoola Z (2000) Influence of particle size and dissolution conditions on the degradation properties of polylactide-co-glycolide particles. *Biomaterials* 21(16):1659–1668
- Geng Y, Dalhaimer P, Cai S, Tsai R, Tewari M, Minko T, Discher DE (2007) Shape effects of filaments versus spherical particles in flow and drug delivery. *Nat Nanotechnol* 2(4):249–255
- Goldsbey RA, Kindt TJ, Osborne BA, Kuby J (2003) *Immunology*. Freeman, New York
- Goldsmith HL, Turitto VT (1986) Rheological aspects of thrombosis and hemostasis - basic principles and applications. *Thromb Haemost* 55(3):415–435
- Gref R, Minamitake Y, Peracchia MT, Trubetskoy V, Torchilin V, Langer R (1994) Biodegradable long-circulating polymeric nanospheres. *Science* 263(5153):1600–1603
- Hetland G, Namork E, Schwarze PE, Aase A (2000) Mechanism for uptake of silica particles by monocytic U937 cells. *Hum Exp Toxicol* 19(7):412–419
- Ho CC, Keller A, Odell JA, Ottewill RH (1993) Preparation of monodisperse ellipsoidal polystyrene particles. *Colloid Polym Sci* 271(5):469–479
- Illum L, Davis SS, Wilson CG, Thomas NW, Frier M, Hardy JG (1982) Blood clearance and organ deposition of intravenously administered colloidal particles – the effects of particle size, nature and shape. *Int J Pharm* 12(2–3):135–146
- Israelchvili J (1992) *Intermolecular and surface forces*. Academic, San Diego, CA
- Kawaguchi H, Koiwai N, Ohtsuka Y, Miyamoto M, Sasakawa S (1986) Phagocytosis of latex-particles by leukocytes. 1. Dependence of phagocytosis on the size and surface-potential of particles. *Biomaterials* 7(1):61–66
- Koval M, Preiter K, Adles C, Stahl PD, Steinberg TH (1998) Size of IgG-opsonized particles determines macrophage response during internalization. *Exp Cell Res* 242(1):265–273
- Lamprecht A, Schafer U, Lehr CM (2001) Size-dependent bioadhesion of micro- and nanoparticulate carriers to the inflamed colonic mucosa. *Pharm Res* 18(6):788–793
- Langer R (1990) New methods of drug delivery. *Science* 249(4976):1527–1533
- Lee E, Shelden EA, Knecht DA (1997) Changes in actin filament organization during pseudopod formation. *Exp Cell Res* 235(1):295–299
- Lee EY, Pang KM, Knecht D (2001) The regulation of actin polymerization and cross-linking in Dictyostelium. *Biochim Biophys Acta* 1525(3):217–227
- Liang HF, Chen CT, Chen SC, Kulkarni AR, Chiu YL, Chen MC, Sung HW (2006) Paclitaxel-loaded poly(gamma-glutamic acid)-poly(lactide) nanoparticles as a targeted drug delivery system for the treatment of liver cancer. *Biomaterials* 27(9):2051–2059
- Manning MC, Patel K, Borchardt RT (1989) Stability of protein pharmaceuticals. *Pharm Res* 6(11):903–918
- May RC, Machesky LM (2001) Phagocytosis and the actin cytoskeleton. *J Cell Sci* 114(6):1061–1077
- Moghimi SM, Hunter AC, Murray JC (2001) Long-circulating and target-specific nanoparticles: theory to practice. *Pharm Rev* 53(2):283–318
- Mohraz A, Solomon MJ (2005) Direct visualization of colloidal rod assembly by confocal microscopy. *Langmuir* 21(12):5298–5306
- O'Brien DK, Melville SB (2003) Multiple effects on *Clostridium perfringens* binding, uptake and trafficking to lysosomes by inhibitors of macrophage phagocytosis receptors. *Microbiol SGM* 149:1377–1386
- Painter PC, Coleman MM (1997) *Fundamentals of polymer science*. CRC, Boca Raton, FL

- Panyam J, Dali MA, Sahoo SK, Ma WX, Chakravarthi SS, Amidon GL, Levy RJ, Labhasetwar V (2003) Polymer degradation and in vitro release of a model protein from poly(D, L-lactide-co-glycolide) nano- and microparticles. *J Control Release* 92(1–2):173–187
- Patil VRS, Campbell CJ, Yun YH, Slack SM, Goetz DJ (2001) Particle diameter influences adhesion under flow. *Biophys J* 80(4):1733–1743
- Patri AK, Majoros IJ, Baker JR (2002) Dendritic polymer macromolecular carriers for drug delivery. *Curr Opin Chem Biol* 6(4):466–471
- Pearson AM (1996) Scavenger receptors in innate immunity. *Curr Opin Immunol* 8(1):20–28
- Poste G, Kirsh R (1983) Site-specific (targeted) drug delivery in cancer-therapy. *Biotechnology* 1(10):869–878
- Prausnitz MR, Mitragotri S, Langer R (2004) Current status and future potential of transdermal drug delivery. *Nat Rev Drug Discov* 3(2):115–124
- Reddy GR, Bhojani MS, McConville P, Moody J, Moffat BA, Hall DE, Kim G, Koo YEL, Woolliscroft MJ, Sugai JV, Johnson TD, Philbert MA, Kopelman R, Rehemtulla A, Ross BD (2006) Vascular targeted nanoparticles for imaging and treatment of brain tumors. *Clin Cancer Res* 12(22):6677–6686
- Rejman J, Oberle V, Zuhorn IS, Hoekstra D (2004) Size-dependent internalization of particles via the pathways of clathrin- and caveolae-mediated endocytosis. *Biochem J* 377:159–169
- Roff WJ, Scott JR (1971) *Fibres, films, plastics and rubbers*. Butterworths, London
- Rolland JP, Maynor BW, Euliss LE, Exner AE, Denison GM, DeSimone JM (2005) Direct fabrication and harvesting of monodisperse, shape-specific nanobiomaterials. *J Am Chem Soc* 127(28):10096–10100
- Ross JA, Auger MJ (2002) The biology of the macrophage. In: Burke B, Lewis CE (eds) *The macrophage*. Oxford University Press, Oxford
- Rudt S, Muller RH (1993) In vitro phagocytosis assay of nano- and microparticles by chemiluminescence. 3. Uptake of differently sized surface-modified particles, and its correlation to particle properties and in vivo distribution. *Eur J Pharm Sci* 1(1):31–39
- Simon SI, Schmidtschonbein GW (1988) Biophysical aspects of microsphere engulfment by human-neutrophils. *Biophys J* 53(2):163–173
- Stolnik S, Illum L, Davis SS (1995) Long circulating microparticulate drug carriers. *Adv Drug Deliv Rev* 16(2–3):195–214
- Storm G, Belliot SO, Daemen T, Lasic DD (1995) Surface modification of nanoparticles to oppose uptake by the mononuclear phagocyte system. *Adv Drug Deliv Rev* 17(1):31–48
- Swanson JA, Hoppe AD (2004) The coordination of signaling during Fc receptor-mediated phagocytosis. *J Leukoc Biol* 76(6):1093–1103
- Tabata Y, Ikada Y (1990) Phagocytosis of polymer microspheres by macrophages. *Adv Polym Sci* 94:107–141
- Weisstein EW (1999) <http://mathworld.wolfram.com/Ellipse.html>
- Welch MD, Mullins RD (2002) Cellular control of actin nucleation. *Annu Rev Cell Dev Biol* 18:247–288
- Yim EK, Leong KW (2005) Significance of synthetic nanostructures in dictating cellular response. *Nanomedicine* 1(1):10–21

Chapter 16

Nano-engineered Thin Films for Cell and Tissue-Contacting Applications

Richard F. Haglund Jr.

Abstract Thin films of bioactive, biocompatible and biotherapeutic materials are crucial to many applications in bioengineering and medicine, but the susceptibility of these materials to thermal damage forbids the application of many conventional thin-film deposition technologies. Here we describe a novel approach to depositing thin nanostructured thin films using resonant mid-infrared laser ablation. This vapor-phase technique – which can be employed either in vacuum or in air or another ambient gas environment – circumvents many difficulties attendant to conventional liquid-phase deposition technologies, such as spin- and dip-coating. It makes possible, for example, multilayer deposition with sharp interfaces, and patterning by means of shadow-masking. Examples of the technique on biocompatible and -degradable polymers, nucleic acids, fluoropolymers and functionalized nanoparticles are described. In conclusion, current developments in laser technology are discussed that can enable this thin-film deposition technique, now based on tunable, picosecond mid-infrared free-electron lasers, to be realized using mid-infrared solid-state, table-top laser sources with similar characteristics.

Keywords Pulsed laser deposition of nanostructured thin films • Tunable picosecond, mid-infrared lasers • Thin films of poly(ethylene glycol), poly(DL-lactide-co-glycolide), poly(tetrafluoroethylene), silica nanoparticles

16.1 Introduction

Thin-film coatings of biologically compatible or even bioactive materials are increasingly being employed to add functionality to prosthetics, implants and biomedical devices. Drug-eluting stents are only the most obvious and widely used

R.F. Haglund (✉)

Department of Physics and Astronomy and W. M. Keck Foundation Free-Electron Laser Center,
Vanderbilt University, Nashville, TN 37235-1807, USA
email: richard.haglund@vanderbilt.edu

example of biologically active coatings that improve the medical performance of a device – in this case, by releasing drugs that help to prevent restenosis of blood vessels after blockages have been cleared by angioplasty. The conventional techniques for thin-film deposition of polymers, biopolymers and proteins rely on liquid-phase techniques, such as spin- or dip-coating and aerosol spraying, because these can be carried out at room temperature, thus avoiding damage to delicate or thermally labile biomaterials. However, some of the most desirable biocompatible polymers – such as the fluoropolymers used to make non-reactive surfaces – are insoluble, and thus not amenable to such techniques. In other cases, interfacial diffusion makes it difficult to maintain sharp interfaces that are desirable in time-release applications. Finally, these solution-phase coatings do not work very well when patterned surfaces or thin nanoparticle films are desired. Hence the need and opportunity for a vapor-phase coating technique that circumvents these problems as needed for specific biomedical applications.

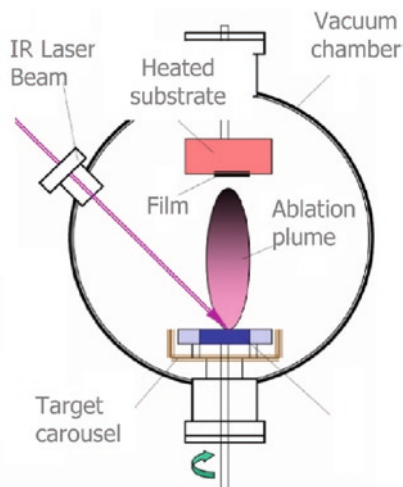
In this paper, we first describe deposition of nanostructured thin films by means of resonant infrared pulsed laser deposition (RIR-PLD). We then present specific examples of biologically interesting polymers, biopolymers, fluoropolymers and nanoparticles that have been deposited by RIR-PLD. We discuss the mechanism of this unusually gentle method for the vaporization of thermally labile polymers and nanoparticles without inducing photofragmentation or destructive photo-thermal effects. Finally, we consider the evidence for the low-temperature nature of this deposition technique and the status of near-term developments in laser technology that could conceivably support widespread adoption of RIR-PLD for fabricating nanostructured, multi-functional surfaces and interfaces to cells and tissue.

16.2 Resonant Infrared Pulsed Laser Deposition of Thin Films

Pulsed laser deposition (PLD) is already used for prototyping inorganic thin films and even complex functional devices (Thin Solid Films et al. 1994). Its most widely known instantiation uses ultraviolet lasers with nanosecond pulse duration and pulse repetition rates up to hundreds of Hz, and is particularly effective in depositing thin films of complex oxides, such as high-temperature superconductors and magneto-resistive quaternary oxides.

Reduced to its essentials, PLD begins with an ablation target – holding the desired thin-film material either in a neat preparation or embedded in a matrix – in a suitable container. When irradiated by a high-power laser pulse, the target is volatilized and transferred to a substrate on which the film may then grow by any of several different mechanisms, depending on the substrate temperature, the diffusion coefficient of the deposited atoms, molecules or clusters, and the bonding mechanisms operating to create the thin film. The general experimental configuration for an infrared PLD experiment is illustrated schematically in Fig. 16.1.

Fig. 16.1 Schematic of a PLD apparatus using an IR laser. The target is usually mounted so that it can be rotated, while the focusing optics often include a beam-scanning device to insure uniform ablation of the target



Even though there have been a few successful deposition experiments on polymers by matrix-assisted pulsed-laser evaporation (MAPLE) with UV lasers, UV photochemistry leads to photofragmentation and undesirable material modifications when applied to polymers. Resonant infrared (RIR) PLD avoids the destructive photochemistry that is characteristic of UV-PLD and UV-MAPLE by virtue of the low photon energies employed (0.1–0.5 eV versus 5.0–6.4 eV). In RIR-PLD, weakly resonant excitation of monomer IR vibrations leads to photomechanical or photo-thermal bond-breaking of the weak interchain bonds (Bubb et al. 2006a). Fragmentation of the polymers can also be avoided in many cases by exciting end-group or side-chain moieties. These bonds are *localized, anharmonic* modes of the monomer groups, which communicate the absorbed laser energy only slowly to the *delocalized, harmonic* vibrational manifold that constitutes the heat bath of the polymer.

Figure 16.2 shows the most common vibrational modes that are targeted when using RIR-PLD to ablate neat polymer or matrix materials with embedded polymers. The fluoropolymer modes are not shown, but are typically CF_2 vibrations found in the 8.0–8.5 μm region.

During the past 5 years, we have successfully employed resonant infrared laser ablation to deposit thin films of many different polymers (Bubb and Haglund 2006). “Successful” is defined as the deposition of a film in which the polymers retain the local and long-range structure, mass distribution and polydispersity that were typical of the polymer before ablation and deposition. Quantitative characterization techniques have demonstrated how laser pulse duration, pulse-repetition frequency, wavelength, intensity and fluence affect film quality. Details about the generic effects of these parameters on RIR-PLD are deferred to Section 16.5 of this paper.

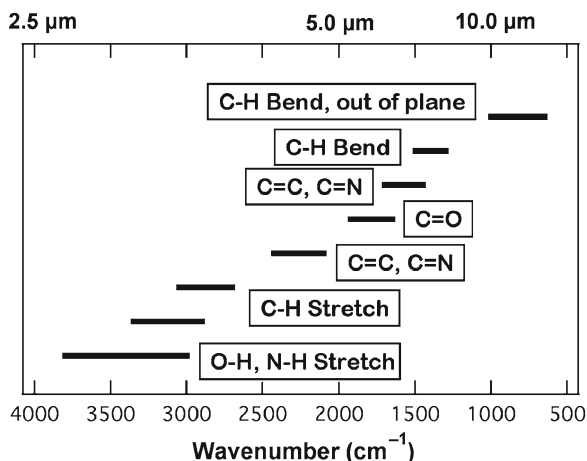


Fig. 16.2 Wavelength bands showing where the most important polymer vibrational modes can be excited to produce resonantly enhanced thin-film deposition

16.3 Resonant Infrared Laser Ablation of Thermally Labile Polymers

The following paragraphs present specific examples to illustrate the potential of RIR-PLD for thin-film deposition of bioactive materials. We show the importance of resonant excitation, laser tunability, fluence and intensity in achieving volatilization of intact polymers. Except where otherwise noted, all the experiments were carried out using the Vanderbilt free-electron laser (FEL) to carry out the resonant IR ablation. This FEL is based on an S-band radio-frequency linear accelerator, and produces mid-IR light continuously tunable from 2 to 10 μm (Edwards et al. 1996). The temporal pulse structure of the FEL is unusual, in that it delivers 1-ps duration micropulses in a burst or *macropulse* lasting 4–5 μs , at a macropulse repetition frequency of 30 Hz. With a fundamental micropulse repetition frequency of 2.865 GHz, the spacing between micropulses is about 350 ps, and there are some 2×10^4 micropulses in each macropulse. Macropulse energies are typically a few millijoules. While none of the experiments reported here exhibited phenomena that could be explicitly attributed to the micropulse structure, there are reasons to believe that the micro/macropulse structure is important (see Section 16.5.2).

16.3.1 Poly(Ethylene Glycol) – PEG

Our initial studies compared RIR-PLD with UV-PLD of poly(ethylene glycol) (PEG) to demonstrate the importance of resonant vibrational excitation. The deposited films were characterized by: Fourier-transform infrared spectroscopy (FTIR) to

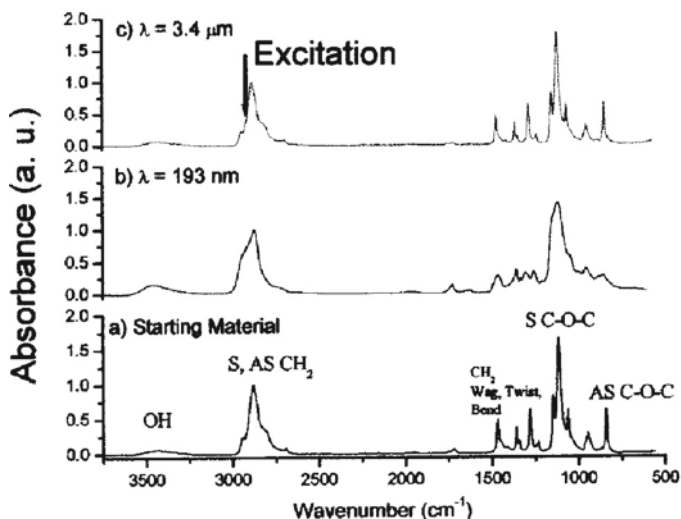


Fig. 16.3 Fourier-transform infrared (FTIR) spectra of poly(ethylene glycol) (a) from the laser ablation target before deposition; (b) when ablated by an ArF laser; and (c) when ablated by a free-electron laser tuned to the $3.4\ \mu\text{m}$ C–H stretching vibration

monitor local binding and electronic structure; size-exclusion chromatography (SEC) to monitor polydispersity; and matrix-assisted laser desorption-ionization mass spectrometry (MALDI-MS) and electrospray ionization mass spectrometry (ESI-MS) to monitor the polymer chain-length distribution before and after deposition. The major vibrational modes targeted for resonant laser excitation were $-\text{CO}$, $-\text{CH}$ and $-\text{OH}$ (Fig. 16.3).

Comparison of the FTIR spectra of UV-PLD ($\lambda = 193\ \text{nm}$) and RIR-PLD of PEG ($2.90\ \mu\text{m}$, the O–H stretch) shows that resonant IR ablation produced thin films whose local electronic structure and polydispersity accurately match the IR spectra of the starting material. In contrast, PEG thin films deposited using an ArF UV laser exhibited FTIR spectra so drastically modified that the films could only be described as ‘PEG-like.’

Molecular weight distributions of the deposited films, measured by ESI and displayed in Fig. 16.4, suggest a similar conclusion. The concentrations of the solutions injected into the ESI time-of-flight mass spectrometer were the same in all cases. The agreement between the mass spectrum of the RIR-PLD film and the starting material is evident. Although apparently random and noisy, there are real peaks in the UV-PLD deposited film’s spectrum. Due to the alteration of the UV-PLD film’s chemical structure, we once again refer to it as “PEG-like,” as there is no correlation between the peaks in its spectrum and the native material. Similar results were obtained using a fixed frequency Er:YAG ($2.94\ \mu\text{m}$) laser operating either in free-running mode with a pulse width of about $300\ \mu\text{s}$ or Q-switched with

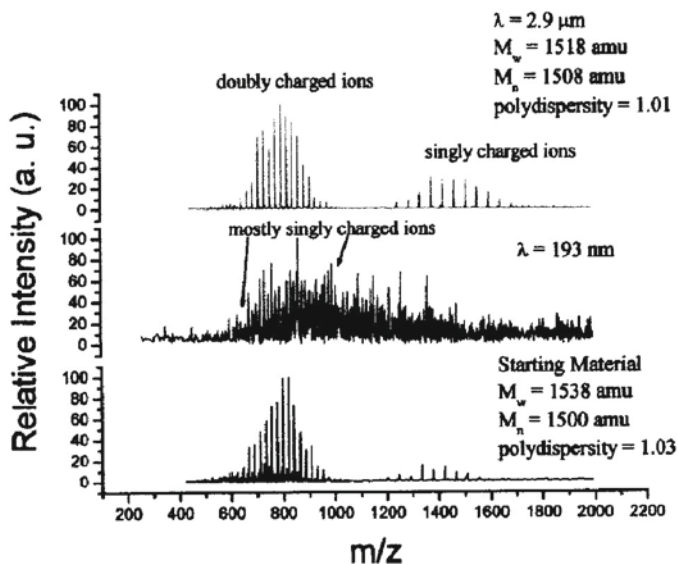


Fig. 16.4 Mass distributions of poly(ethylene glycol) measured by electrospray ionization mass spectrometry. *Bottom*: ablation target material; *middle*: from film deposited by UV PLD at 193 nm; and *top*: from film deposited by RIR-PLD, with the laser tuned to the O–H stretching vibration at 2.90 μm

a pulse duration of 50 ns (Bubb et al. 2006b). This suggests that RIR-PLD may also be possible using table-top lasers in some cases.

Additional RIR-PLD studies of PEG deposition, not further discussed here, have shown that PEG films deposited with off-resonance IR irradiation are also chemically altered compared to both the native polymer and its resonant counterpart, although the changes were not as striking as those observed in UV-PLD. What may be most interesting about RIR-PLD, from a scientific standpoint, is the apparent mode-specific behavior with respect to the deposition rate and molecular weight distributions of the deposited films. For example, comparison of PEG films deposited by excitation of –OH (2.90 μm) versus –CH (3.45 μm) stretching modes showed that the films deposited by excitation of the terminal –OH group showed no alteration even up to extremely high fluences while the –CH deposited films were fragmented.

The deposition rate – an important quantity for thin-film technology – also depends strongly on the vibrational mode being excited. In the case of PEG, the bond (–OH) with the smallest oscillator strength gave the highest deposition rate while the one with the largest oscillator strength (–CO) showed the smallest deposition rate. One is led to conclude that exciting the bond most responsible for the inter-chain interactions leads to the most efficient desorption while doing the least damage to the polymer, a result that is also borne out in experiments on RIR-PLD of polystyrene.

16.3.2 Poly(DL-Lactide-Co-Glycolide) – PLGA

Thin films used in drug-delivery or drug-release applications must satisfy stringent criteria for the integrity of their electronic properties. A good example is furnished by PLGA, a co-polymer of poly(lactic acid) and poly(D-,L-glycolide) that breaks down into PLA and PGA by hydrolysis. PLGA has been used as a drug-delivery coating; indeed, optimum drug delivery in the lungs can be facilitated by a thin porous time-release coating of PLGA on 1–5 μm drug particles (Hardy and Chadwick 2000). PLGA releases controlled therapeutic drug doses by creating a thin permeable barrier on drug particles that degrades over time. PLA is hydrolyzed to lactic acid, which is metabolized through the Krebs cycle and then excreted as carbon dioxide and water. PGA, on the other hand, is converted to glycolic acid monomers by hydrolysis and esterases. These monomers are either excreted in urine or may form glycine, which is converted into serine and subsequently to pyruvic acid, which also enters the Krebs cycle (Athanasidou et al. 1998). Evidently then, for PLGA to form an effective time-release coating, it must not be chemically altered since other products cannot be guaranteed to have a metabolic pathway in the Krebs cycle.

In general, polymers contain strongly UV absorbing moieties (such as C=O linkages in PLGA) and will certainly undergo photolysis. When PLGA is deposited by UV-PLD, the intense UV laser light can generate photochemical reactions, such as $\sigma-\sigma^*$ transitions, that directly dissociate and rupture bonds. This can lead, in principle, to the loss of entire pendant groups. UV irradiation also induces $\pi-\pi^*$ transitions; the subsequent delocalization of electrons can lead to reversals of bond order and other photochemical rearrangements. The question then becomes, is the deposited material photochemically altered or are oligomeric fragments deposited with a substantial part of the polymer destroyed, cross-linked or volatilized?

Since the excitation process involves both electronic and thermal degrees of freedom, the relaxation channels can be expected to be similarly complex. The form of the deposited film will depend intimately on the reaction pathways that are made available through energy randomization. For these reasons, biodegradable coatings require a method of processing that does not raise concerns about potential toxicity that may arise if the chemical structure of PLGA is altered, since the byproducts may not break down into biodegradable components.

As a test case for the utility of RIR-PLD in making biocompatible or biodegradable thin films, PLGA (50:50) was deposited by exciting the –CH, and –OH stretch vibrations at macropulse fluences of 7.8 and 6.7 J/cm^2 , respectively (Bubb et al. 2002). The deposition rate was 100–200 nm/min , which is extremely high. Given that the process conditions were not optimized, this suggests that industrial-scale processing may be achievable for RIR-PLD.

While the infrared absorbance spectrum of the PLGA films is nearly identical to that of the native polymer, the average molecular weight of the films is only about 40% of that of the starting material. The results for GPC measurements on native material and RIR-PLD thin films are displayed in Fig. 16.5. Although there is some

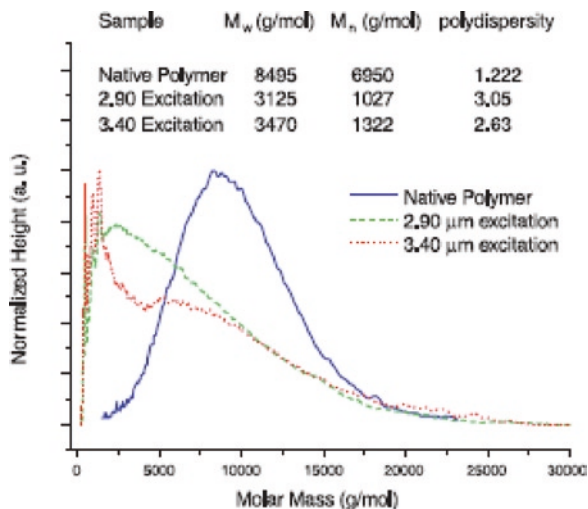


Fig. 16.5 Mass distributions from size-exclusion chromatography of (a) the PLGA material prior to ablation (blue curve); (b) the PLGA film as deposited following laser ablation at 2.90 μm (O–H stretch); and (c) the PLGA film as deposited following laser ablation at 3.40 μm (C–H stretch)

segmentation of the chains, these results show that coatings of PLGA could be reasonably expected to be broken down and metabolized in the Krebs cycle, and as such are suitable for time release applications.

16.3.3 Proteins and Nucleic Acids

Direct desorption or ablation of biological molecules has been attempted with ultraviolet excimer lasers in the past, but with mixed results (Ringeisen et al. 2001, 2002). The most successful experiments have used a UV-MAPLE protocol, in which the molecules are diluted to a low concentration (of order 10^{-4}) in a matrix that strongly absorbs UV light. The matrix shields the biomolecules from collisions and entrains them in a cooling supersonic expansion jet during the desorption or ablation process. However, the mass transfer efficiency is directly proportional to concentration; moreover, when the concentration is increased in order to enhance mass-transfer rates, collisional damage to the vast majority of molecules destroys their biological activity. Here we provide two examples of successful deposition of a protein and a nucleic acid (Haglund Jr et al. 2003).

In an IR-MAPLE experiment, a solution of a biotinylated protein standard mixture (BioRad, Catalog Number 161-0319) in water was prepared for IR-MAPLE. The mixture include bovine serum albumin (BSA, molecular weight – 166 kDa). The concentration was of order 1%, much greater than would be typical of a UV-MAPLE experiment.

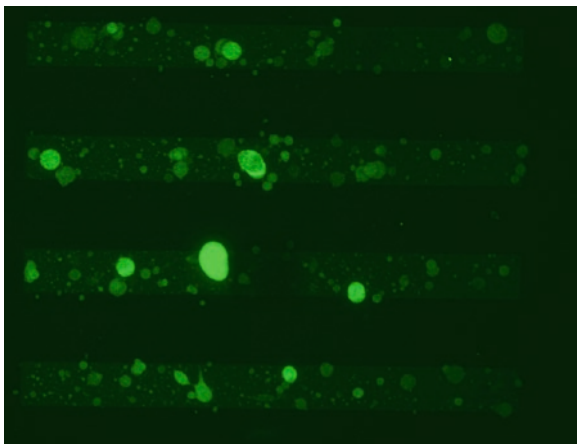


Fig. 16.6 Photomicrograph of luminescing biotinylated bovin serum albumin following deposition by RIR-PLD through a shadow mask with 1 mm stripes. The *bright spots* are the fluorescence spots from the streptavidin-labeled BSA that has been deposited through the shadow mask

The sample was frozen in liquid nitrogen prior to insertion into the vacuum chamber. A thin film of the labeled BSA protein was transferred by resonant IR laser ablation to a nitrocellulose-coated glass slide through a gold shadow mask using IR-MAPLE; the laser was tuned to $3.0\ \mu\text{m}$, near the absorption maximum in water ice. After deposition, the deposited material was bioassayed by washing the slide with a uptake-blocking protein, and then tagging with a site-specific fluorescent streptavidin label. An image of the fluorescence from the structured film is shown in Fig. 16.6. This indicates successful transfer and preservation of the site-selective biological activity in the deposited proteins, as well as the patterning potential indicated by the shadow-mask technique.

In another experiment, we showed the possibility of thickness-controlled, conformal transfer of nucleic acids without fragmentation, provided that the fluence was low enough. Frozen solutions of salmon-sperm and pBluescript II DNA were used as the targets, which were again irradiated by $2.94\ \mu\text{m}$ light from the FEL, corresponding to the O-H stretching vibration of liquid water. Electrophoresis of the transferred material indicated that the DNA underwent virtually no fragmentation in the regime of moderate macropulse fluences. Interestingly, it proved impossible to transfer DNA successfully using a 100-ns pulse-length Er:YAG laser at similar fluence levels, possibly indicating a role for ultrashort pulses.

The importance of the intensity dependence indicated by this experiment cannot be overemphasized. It suggests that the denaturation of the DNA is a direct result of thermal loading experienced during the laser-induced transfer process at high macropulse energy; this is consistent with the failure to transfer DNA using an Er:YAG laser at $2.94\ \mu\text{m}$. In that sense, the energy budget is a sensitive thermometer for the transport mechanism.

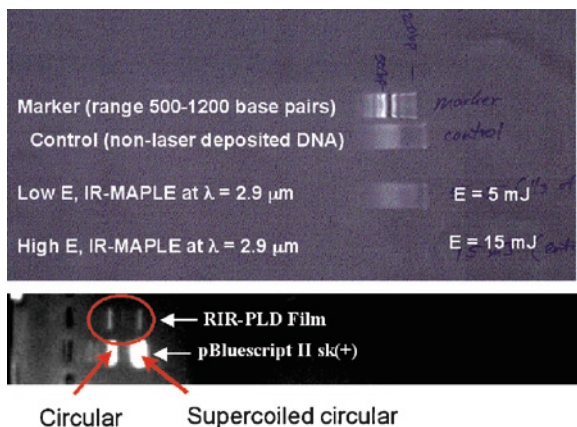


Fig. 16.7 *Top panel:* Electrophoresis traces for salmon-sperm DNA, showing a marker for the mass range of the DNA, a control trace for non-laser deposited DNA, and a laser-deposited DNA marker at a laser pulse energy of 5 mJ. Note the absence of a DNA marker for an IR-MAPLE experiment at higher pulse energy, probably indicating fragmentation of the DNA. *Bottom panel:* Comparison of the electrophoresis traces for a standard sample of pBluescript II DNA, one deposited by RIR-PLD (IR-MAPLE) and the other a non-laser deposited film

The transport of the salmon-sperm DNA is not a particularly severe test of the IR-MAPLE technique, because the salmon-sperm DNA has a rather broad mass distribution and is globular like a protein – thus somewhat insensitive to photofragmentation. The second electrophoresis trace is thus the more interesting one, showing the successful IR-MAPLE transfer of pBluescript DNA, a standard used by molecular biologists as a calibration marker, which has two distinct forms: one a circular DNA fragment, the other supercoiled. In the lower panel of Fig. 16.7, the two bands of the sample as received and the sample from the transferred film are shown without any alteration in their masses. The fact that the mass distributions are identical indicates that the DNA has been transferred intact from the ice matrix to the film plate.

16.3.4 Poly(Tetrafluoroethylene)

From an applications perspective, poly(tetrafluoroethylene) (PTFE) and other similar fluoropolymers have an impressive panoply of desirable mechanical, optical, thermal, chemical, rheological and tribological properties that have led to its widespread use in a variety of thin film technologies and has long been of interest to practitioners of PLD (Schwodiauer et al. 1998). However, PTFE is insoluble, so that solution-phase deposition techniques are out of the questions. Moreover, previous experiments in UV-PLD of PTFE resulted in flash pyrolysis, “unzipping”

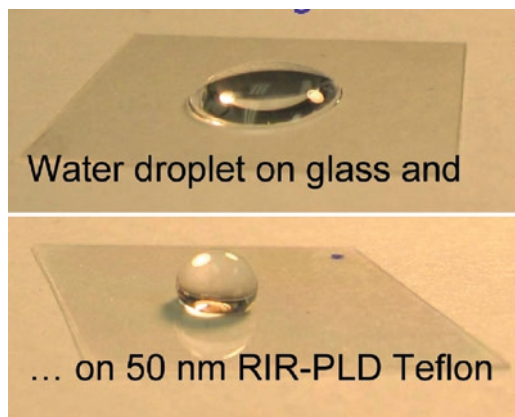


Fig. 16.8 Water droplet on a glass slide (*top*) and on a 50 nm film of PTFE deposited by RIR-PLD at 8.26 μm . The contact angle of the water droplet on the PTFE film is greater than 105° , indicating the extreme degree of hydrophobicity consistent with the known properties of PTFE thin films

the polymer during the ablation process; the monomers and small oligomers that were deposited on the substrate could be repolymerized only by high-temperature polymerization in the presence of radicals. Needless to say, such a high-temperature synthesis is not likely to be compatible with many polymers that would be desirable in a cell- or tissue-contacting context.

In RIR-PLD experiments on neat PTFE targets, both a commercial PTFE rod (Teflon) and pressed pellets from PTFE powder (Goodfellow) were used; the pressed pellets were sintered at 275°C for several days before use. The FEL was tuned to either the C-F₂ vibrational mode at 8.26 μm or a weak combination band at 4.2 μm (Papantonakis and Haglund 2004).

Figure 16.8 shows a clean glass microscope slide and a slide that has been coated with a 50 nm film of PTFE deposited by RIR-PLD at 8.26 μm . The contact angle of the droplet on the PTFE film is greater than 105° , indicating that the film is extremely hydrophobic, consistent with the properties of bulk PTFE films.

The deposition rate for both modes was 20–25 $\text{\AA}/\text{s}$ for a fluence of $2 \text{ J}/\text{cm}^2$ at 8.26 μm . This corresponds to deposition of a 0.5 μm thick film in less than 5 min which is very similar to that obtained with PLGA. However, the films deposited at 8.26 μm were substantially smoother than those deposited at 4.2 μm .

PTFE films deposited in this way were found to have good crystalline quality as evidenced by X-ray photoelectron spectroscopy, even when deposited at room temperature. The film is relatively free of particulates and the feature size is about 100 nm (Fig. 16.9). These properties compare favorably with other reports in the literature, even though they were obtained at far lower processing temperatures.

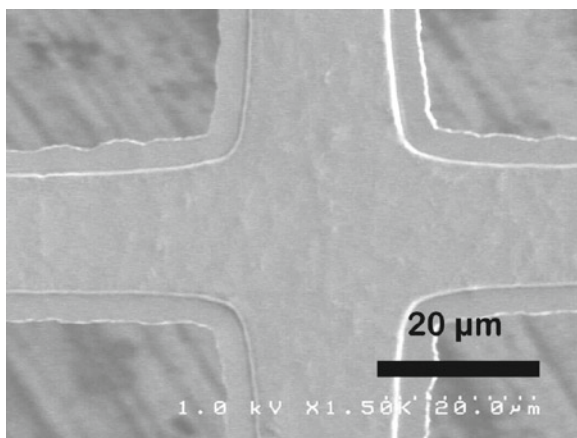


Fig. 16.9 PTFE film covering Ni mesh from an electron microscope grid. Note the *smooth edges* of the PTFE film, and also the way it has retracted from the edge of the mesh

16.4 Deposition of Functional Nanoparticles

Functionalized nanoparticles offer some of the most tantalizing prospects for nano-engineering surfaces to provide specific functionality when in contact with cells or tissues. For example, enhanced cell growth on silica nanoparticles has recently been demonstrated (Lipski et al. 2007), and it is likely that all kinds of biochemical processes can be catalyzed effectively on the high surface-area substrates that nanoparticles make possible. The list of widely cited nanomaterials for diagnostic and therapeutic purposes, not surprisingly, also includes gold nanocrystals (Pan et al. 2007) and carbon nanotubes (Abarrategi et al. 2008). Thus there are many reasons to look for an effective deposition technique for nanoscale materials. However, making thin films of nanoparticles has proven to be quite difficult. Spin-coating and ink-jet printing suffer from the spatially inhomogeneous distribution of nanoparticles known as the “coffee-ring” morphology. As we now demonstrate, however, RIR-PLD seems to have a unique capability to realize this potential.

Nanoparticles of varying compositions, sizes (diameters from 50 nm to 3 μm) and with various surface-bound ligands were successfully transferred from frozen solutions using resonant IR laser ablation. The average coverage for 0.46 μm polystyrene spheres – between one to two nanoparticle layers – was in some cases less uniform than desired, but further studies showed that this was frequently due to agglomeration of nanoparticles prior to freezing the target. Sonicating the suspension prior to the freezing resulted in a more even layer-by-layer coverage. Despite being less than ideal, however, the particle coverage is more uniform than what is achieved by many solvent- and spray-based particle coating techniques.

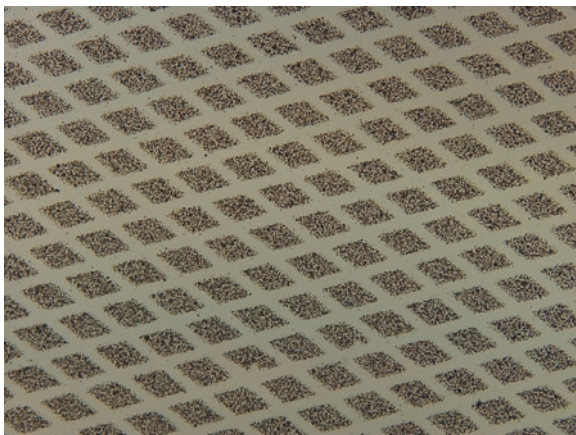


Fig. 16.10 Pattern deposition of TiO_2 nanoparticles (50–100 nm diameter) through a shadow mask onto a silicon substrate. The width of the lanes between patches of nanoparticles is 23 μm , defined by a shadow mask in contact with the substrate

When used in conjunction with a shadow mask, RIR-LANT can be used to pattern specific areas on a device platform. Figure 16.10 shows an optical image of patterned TiO_2 nanoparticles (50–100 nm diameter) obtained by placing a TEM grid in contact with the silicon substrate. The lighter areas represent the area blocked by the 23 μm wide wires. Attempts to measure a sticking coefficient of the nanoparticles were inconclusive, but the spheres seem to have a significant mobility when deposited on a silicon surface.

For applications in surface-engineered coatings, it is vital to demonstrate that the functionalities of the nanoparticles are not altered by the ablation and transport processes intrinsic to RIR-PLD. We did this by comparing emission spectra of functionalized silica nanoparticles before and after laser transfer. These particular NPs were synthesized with a core rich in the dye tetramethylrhodamine isothiocyanate (TRITC) with a second dye fluorescein isothiocyanate (FITC) on the outer surface of the sphere (Burns et al. 2006a, b). The reactivity and fragility of the dyes made them a good test case of the non-destructive nature of the laser transfer process. As-prepared silica nanoparticles were drop cast onto silicon substrates at similar densities to the laser transferred samples, and their emission spectra compared to the laser-transferred samples. The spectra were normalized to the maximum intensity of the TRITC emission peak near 580 nm. Photoluminescence measurements performed on these particles show no significant alteration of their emission properties, suggesting that no damage occurred to the encapsulated or surface-bound dye either during the ablation event (Fig. 16.11). Small shifts in the peak emission wavelength or intensity ratio of the two dyes seen in the figure are due in part to unequal photo-bleaching during the data acquisition and possibly due to intrinsic differences in the dye ratios which occurred during nanoparticle synthesis, as well as slight modifications associated with the resonant ablation process even at IR wavelengths.

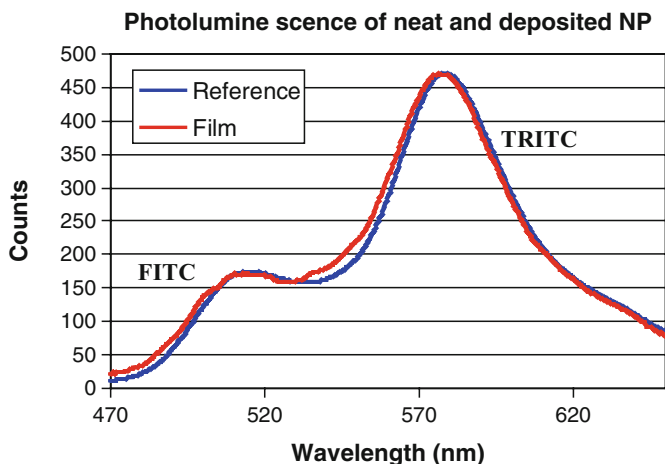


Fig. 16.11 Photoluminescence spectra of nanoparticles deposited by RIR laser assisted nanoparticle transfer, showing the preservation of the fluorescence during the ablation and deposition procedure

Other work not presented here has demonstrated the ability to combine resonant IR-laser transfer with pulsed laser deposition to create composite or layered materials, such as PTFE films interspersed with layers of polystyrene nanoparticles. Successive depositions of different types of functionalized particles, in conjunction with appropriate masks, could allow one to impart different functionalities to specific areas of a device platform. In a similar manner, a stratified architecture could be produced, comprising layers of different nanoparticles alternating with each other or with another material such as a polymer. Alternating layers of nanoparticles would be much more difficult to fabricate by solvent-based techniques, since the deposition of a fresh layer of nanoparticle-bearing solvent might disturb the previously deposited layer by hydrodynamic motion or, in the case of organic films, by dissolution of the layer beneath.

16.5 Discussion and Conclusions

The experiments described in [Section 16.4](#) build a plausible case that RIR-PLD could be a useful way to deposit complex multilayer, multifunctional and patterned films of bioactive materials for tissue engineering, prosthetic devices and other applications where a surface in contact with cells or tissues needs to be nanoengineered to produce a desired biological or therapeutic effect. However, if RIR-PLD is to be a viable tool for bioengineering, it needs to be demonstrated to be a low-temperature process the mechanism of which is reasonably well understood and that can be reduced to practice using conventional lasers. In the final section of the paper, we address each of these three questions in turn.

16.5.1 Evidence for Low-Temperature Character of RIR-PLD

The polymers whose deposition by RIR-PLD is described in Section 16.4 are thermoplastic, meaning that they undergo melting or denaturation above a well-defined temperature. There is, however, another large family of polymers, the so-called thermosets, in which the polymer is initially part of a precursor that polymerizes and cross-links only upon the application of heating above the glass transition temperature. Polyimides such as KaptonTM, introduced by Dupont in the early 1960s, are a classic example. And although their potential uses in bioengineering applications are probably very limited, their recent successful deposition by RIR-PLD gives the best evidence so far that RIR-PLD is inherently a low-temperature process unlikely to denature thermally labile biomaterials.

This evidence rests on a recent demonstration that it is possible to transfer the precursor polymer for polyimide without initiating cross-linking, that is, without curing. Polyimides are synthesized by a two-step process. First, pyromellitic dianhydride (PMDA) and 4, 4'-oxydianiline (ODA) are dissolved in the polar solvent N-methyl pyrrolidinone (NMP), to form the prepolymer solution poly(amic acid), PAA. The solvent determines the degree of cross linking and the chain length in the polymer; NMP promotes longer chains prior to the cross-linking step by increasing melt flow. The second step requires a thermal cure, temperatures above 150°C, to induce cyclodehydration. Generally the PAA is cured around 250°C to ensure complete conversion of PAA to polyimide. The water-removal step requires that the film be thin and uniform to prevent water vapour from becoming trapped.

In our experiments, liquid PAA targets with a polymer concentration of 15% were frozen in a liquid nitrogen bath and ablated at a wavelength of 3.45 μm, resonant with a strong absorption band in the NMP; the NMP thus acts as a matrix to assist in the ejection of intact PAA molecules. The precursor PAA material was deposited at fluences above 0.5 J/cm² in both air and vacuum. When the deposited material was wiped with the solvent NMP immediately after deposition, the material was easily removed, demonstrating that neither curing nor cross-linking occurred in PAA during the laser transfer. After heating to 150°C on a laboratory hotplate for 30 min, on the other hand, the deposited film could not be removed with an NMP wipe. At this curing temperature the PAA was probably not fully imidized, but still resisted the solvent action of the NMP, an important benchmark for the imidization process. Additionally the as-transferred PAA did not exhibit the color change to the amber hue that accompanies the imidization process.

The relevance of this experiment to deposition of thermally labile material by RIR-PLD is straightforward: Even though relatively large amounts of PAA were transferred to a substrate by resonant IR ablation, the temperature of the PAA did not exceed 150°C. In fact, similar experiments on poly(amide imide) that cures at temperatures near 125°C show the same result. This is probably attributable to the fact that the plume expands during ablation at nearly sonic velocities, thus providing a significant cooling effect. This picture is consistent, incidentally, with similar experiments on resonant IR laser ablation of inorganic materials.

16.5.2 The RIR-PLD Mechanism and Its Consequences

RIR-PLD is perhaps the best example to date of a laser-processing regime that uses ultrashort pulses at high pulse-repetition frequency (PRF) rather than nanosecond pulses at low PRF. This approach, grounded in basic theory (Gamaly et al. 1999) and demonstrated in thin-film deposition of amorphous carbon (Rode et al. 1999) by a group from the Australian National University, is based on the idea that thin-film deposition initiated by laser ablation is best accomplished using small pulse energies, high intensities and high pulse repetition frequency (PRF). The first of these criteria insures that collateral damage, particulate emission, and undue thermal loading are minimized. The second follows from the fact that reaction *rates* are proportional to laser intensity, rather than to fluence. Third, high PRF serves to maximize throughput and to produce a nearly continuous vapor stream during deposition.

The defining dynamical or mechanistic feature of RIR-PLD is that it takes place under conditions of high spatio-temporal densities of *vibrational* excitation. In resonant IR excitation of vibrational modes, the IR photons transfer their energy to specific molecular degrees of freedom. These anharmonic vibrations couple relatively slowly to the harmonic vibrations that constitute the phonon bath. Typical relaxation times for such anharmonic excitations are in the 1–10 ps range, so that nuclear motion and bond-breaking can begin, if the density of excitation is sufficiently high, before the energy leaks out of the excited mode (Dlott and Fayer 1989).

At the intensities characteristic of the FEL micropulses, the ablation yield or deposition rate scales with energy per unit volume (E/V), but it includes an intensity-dependent absorption term:

$$\text{Yield} \propto (E/V) \cong F_L \alpha(\omega, I) \cong I_0 \tau_L [\alpha_0(\omega) + \beta I] \quad (16.1)$$

where F_L and τ_L are the laser fluence and pulse duration, respectively; α is the linear and β the nonlinear (third-order) absorption coefficient; and ω and I are the laser-light frequency and intensity, respectively. Because the FEL micropulse duration is short compared to the relaxation time of the initial anharmonic vibrational excitation, we are justified in considering the 1-ps FEL micropulses as “ultrafast” in the same sense as this terminology is usually applied to femtosecond laser processing by electronic excitation.

The apparently efficient surface vaporization process observed in RIR-PLD is not typical of thermal evaporation, for several reasons. First, velocity distributions and shock-wave measurements are consistent with a relatively low-velocity, sub-sonic plume expansion. Second, the experiments with poly(amic acid) show that the temperature of the material does not exceed 150°C during ablation, since otherwise the PAA would cross-link and imidize. Third, temperature-rise calculations show that at the fluences characteristics of RIR-PLD, the temperature only rises by tens of degrees.

In some cases, such as PTFE, it is plausible that ablation is initiated by multiple- or multi-quantum absorption by near-surface PTFE molecules, leading to the rupture of the weak intermolecular van der Waals bonds in the target. Indeed, for conditions

typical of those experiments, the two-, three- and four-photon excitation probabilities range from 1% to 20%. These probabilities are probably enhanced by the bandwidth ($\sim 16 \text{ cm}^{-1}$) of the FEL micropulses, which is large enough to overcome the inherent anharmonicity that would otherwise inhibit vibrational ladder-climbing. This suggests that the generation of a highly excited vibrational state before the onset of non-radiative relaxation processes is quite likely. Evidence for nonlinear absorption is found in dramatically reduced optical penetration depths in IR ablation of NaNO_3 , CaCO_3 and amorphous SiO_2 (Ermer et al. 2000). In other cases, such as the ablation of polystyrene, it appears that efficient ablation is initiated by the excitation of side-chain C-H modes that can likewise break the weak hydrogen bonds between neighboring polystyrene chains (Bubb et al. 2006a).

Therefore, in conceptualizing the process mechanistically we have to account for how the polymers might be ejected intact into the gas phase. There are at least two distinct processes at work. In thermal equilibrium, due to the long macropulse, the temperature is raised by some tens of degrees. Since the viscosity satisfies the Volger-Fulcher law:

$$\frac{\eta}{\eta_0} = \exp\left(\frac{B}{T - T_0}\right) \quad (16.2)$$

with $B \sim 710$ and $T_0 \sim 50^\circ\text{C}$, the rise of about 100°C during the macropulse means that the viscosity decreases by a factor of more than 100. At the same time, the polymer is expanding due to the rise in temperature in the focal volume, and PS molecules near the surface of the melt zone can reduce their free energy by uncoiling and evaporating due to competition between the entropic configuration energy and the gain in energy from the loss of free volume in the coiled polymer (Jones 2002). If in addition there is a stress wave, with propagation times of order nanoseconds in the drop-cast target, this could power the ejection of surface molecules, as indeed shadowgraphs of the ablation plume seem to indicate (Dyger et al. 2007).

16.5.3 Prospects for Table-Top RIR-PLD Laser Technology

Tunable, picosecond free-electron lasers have furnished an ideal testing ground for RIR-PLD in the high PRF, ultrashort pulse regime. With micropulse durations in the 0.5–2 ps range, FELs deliver energy in a time scale comparable to or shorter than vibrational relaxation times. Producing up to tens of μJ in picosecond micropulses, they achieve intensities in the $10^{10-11} \text{ W/cm}^2$ range, sufficient to initiate multiphoton processes if desired and to sustain high reaction rates. And with micropulse repetition frequencies in the 50 MHz–3 GHz range, and macropulse repetition rates ranging from 30 Hz to continuous, they can deliver extremely high average powers (Neil et al. 2000). Finally, because FELs can be tuned to select the desired mode of material absorption, the spatio-temporal density of vibrational excitation can be calculated and controlled.

However, the FEL is probably viable only as a research tool even for high-value biomedical or bioengineering applications (Edwards et al. 2005). The capital cost of the Vanderbilt FEL, for example, was of order \$3 million, and has annual maintenance and operating costs of order one million dollars (Edwards et al. 1996). This is a level of complexity and expenditure that is simply not consistent with the requirements of a commercial thin-film deposition tool. Replacing the FEL will in all probability require the generation of an appropriate macropulse-micropulse temporal pulse sequence in a solid-state laser, and to provide at least sufficient tunability in the mid-infrared by frequency down-conversion to deposit energy in the wavelength ranges relevant to polymers.

Recent publications (Innerhofer et al. 2003; Keller 2003; Brunner et al. 2004) suggest that the combination of a high repetition-rate pump laser such as Nd:YAG or Yb:YAG coupled to a synchronously pumped optical parametric oscillator (OPO) (Innerhofer et al. 2004) may well be capable of producing a high-repetition rate pulse structure with significant average power in the mid-infrared range. A solid-state laser system with 1 W average power in the 3–3.5 μm range, delivering a mode-locked train of 13 ps pulses at a PRF of 1 MHz has operated at the Australian National University for a couple years with high reliability. The tunability is based on multi-stage difference-frequency mixing combining pulses from the Nd:VO₄ solid-state amplifier with the output of a telecommunications-type Er:YAG fiber amplifier in periodically poled LiNbO₃ crystals (Kolev et al. 2006).

So far, no solid-state laser has been developed with the macropulse-micropulse structure that appears to be so effective with the FEL. However, this would not seem to be a significant practical difficulty, as broad-band infrared electro-optic switches, with variable opening times ranging from 0.1 to 10 μs , have been demonstrated (Becker et al. 1994). Moreover, the development of mid-infrared materials to cover the wavelength bands of interest at these intensities and average powers, and to find suitable sources of radiation to provide the idler beam for the OPO, poses a significant challenge.

The most important early applications are likely to be the O-H, C-H and N-H stretching vibrations in the 2.5–4.0 μm region (Fig. 16.12). Moreover, some fluoropolymers of great technological significance – such as the insoluble polytetrafluoroethylene (trade name, Teflon[®]) – can be deposited by exciting the C-F₂ stretching modes around 8 μm (Papantonakis and Haglund 2004). The challenge is how to reach these various wavelength bands using presently available nonlinear infrared materials. The demonstrated paths to achieve wavelengths beyond 4 μm is at present to cascade successive OPO stages, with the attendant cost in efficiency at each stage. It may well be that the development of mode-locked Cr-doped ZnSe lasers in the 2 μm wavelength band, as well as the development of advanced IR frequency-conversion materials – e.g., glass-bonded GaAs laminates providing quasi-phase matched difference frequency generation (Fiore et al. 1998; Haidar et al. 2002) – will move the field toward ablation of polymers with interesting bands all across the mid-infrared region of the spectrum.

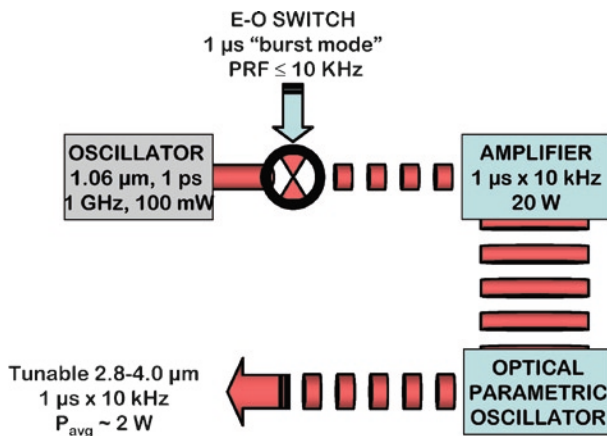


Fig. 16.12 Schematic of a table-top laser for RIR-PLD based on frequency down-conversion to the mid-infrared. The oscillator-amplifier chain is all fixed-frequency (1.06 μm wavelength), while the optical parametric oscillator is tunable over a modest range of wavelengths

16.6 Conclusions

This paper has described a novel method for depositing thermally labile, biocompatible or bioactive polymers and nanoparticles: resonant infrared pulsed laser deposition (RIR-PLD). So far, a variety of biocompatible, biodegradable, and bioactive polymers have been deposited, as well as functionalized nanoparticles. Thus RIR-PLD clearly has the inherent capability of depositing multilayer, multifunctional coatings on surfaces that can then be used to deposit cells or other biological structural elements. While RIR-PLD has not so far been used to deposit cells, there is no doubt that this is possible; cells and bacteria have been deposited by matrix-assisted pulsed laser evaporation (MAPLE) with ultraviolet lasers, albeit in frozen alcohol matrices. With its inherent capability of targeting matrix materials with strong vibrational resonances, such as water ice, RIR-PLD would no doubt be even more effective in depositing cells, bacteria and viruses if desired. Thus this new thin-film deposition technology opens new opportunities for creating nanoengineered thin films in contact with tissues and cells.

Acknowledgements It is a pleasure to acknowledge the expertise and insight of those who have contributed to much to the development of the RIR-PLD technique and to the understanding of the underlying mechanisms: Daniel D. M. Bubb (Rutgers University-Camden); James S. Horwitz, Michael R. Papantonakis and Duane L. Simonsen (Naval Research Laboratory); Erik Herz and Ulrich B. Wiesner (Cornell University); and Nicole L. Dygert, Stephen L. Johnson and Kenneth E. Schriver (Vanderbilt University). Financial support for the research at Vanderbilt has been provided by the Naval Research Laboratory, AppliFlex LLC and the Air Force Office of Scientific Research through the Medical Free-Electron Laser Program of the Department of Defense (F49620-01-1-0429), and is hereby gratefully acknowledged.

References

- Abarrategi A, Gutierrez MC, Moreno-Vicente C, Hortiguela MJ, Ramos V, Lopez-Lacomba JL, Ferrer ML, del Monte F (2008) Multiwall carbon nanotube scaffolds for tissue engineering purposes. *Biomaterials* 29(1):94–102
- Athanasios KA, Agrawal CM, Barber FA, Burkhart SS (1998) Orthopaedic applications for PLA-PGA biodegradable polymers. *Arthroscopy* 14(7):726–737
- Becker K, Johnson JB, Edwards GS (1994) Broadband Pockels cell and driver for a Mark III-type free electron laser. *Rev Sci Instrum* 65(5):6
- Brunner F, Innerhofer E, Marchese SV, Sudmeyer T, Paschotta R, Usami T, Ito H, Kurimura S, Kitamura K, Arisholm G, Keller U (2004) Powerful red-green-blue laser source pumped with a mode-locked thin, disk laser. *Opt Lett* 29(16):1921–1923
- Bubb DM, Haglund RF Jr (2006) Resonant infrared pulsed laser ablation and deposition of thin polymer films. In: Eason R (ed) *Pulsed laser deposition of thin films: applications-led growth of functional materials*. Wiley, New York, pp 35–61
- Bubb DM, Toftmann B, Haglund RF, Horwitz JS, Papantonakis MR, McGill RA, Wu PW, Chrisey DB (2002) Resonant infrared pulsed laser deposition of thin biodegradable polymer films. *Appl Phys A-Mater* 74(1):123–125
- Bubb DM, Johnson SL, Belmont R, Schriver KE, Haglund RF, Antonacci C, Yeung LS (2006a) Mode-specific effects in resonant infrared ablation and deposition of polystyrene. *Appl Phys A* 83(1):147–151
- Bubb DM, Sezer AO, Harris D, Rezae F, Kely SP (2006b) Steady-state mechanism for polymer ablation by a free-running Er:YAG laser. *Appl Surf Sci* 253(5):2386–2392
- Burns A, Ow H, Wiesner U (2006a) Fluorescent core-shell silica nanoparticles: towards “Lab on a Particle” architectures for nanobiotechnology. *Chem Soc Rev* 35(11):1028–1042
- Burns A, Sengupta P, Zedayko T, Baird B, Wiesner U (2006b) Core/shell fluorescent silica nanoparticles for chemical sensing: towards single-particle laboratories. *Small* 2(6):723–726
- Chrisey DB, Hubler GK (eds) (1994) *Pulsed laser deposition of thin solid films*. Wiley, New York
- Dlott DD, Fayer MD (1989) Application of a 2-color free-electron laser to condensed-matter. *J Opt Soc Am B* 6(5):977–994
- Dygert NL, Schriver KE, Haglund RF Jr (2007) Resonant infrared pulsed laser deposition of a polyimide precursor. *IOP Conference Series* 59(651–656)
- Edwards GS, Evertson D, Gabella W, Grant R, King TL, Kozub J, Mendenhall M, Shen J, Shores R, Storms S, Traeger RH (1996) Free-electron lasers: reliability, performance, and beam delivery. *IEEE J Sel Top Quant* 2(4):810–817
- Edwards GS, Allen SJ, Haglund RF, Nemanich RJ, Redlich B, Simon JD, Yang WC (2005) Applications of free-electron lasers in the biological and material sciences. *Photochem Photobiol* 81(4):711–735
- Ermer DR, Papantonakis MR, Baltz-Knorr M, Nakazawa D, Haglund RF (2000) Ablation of dielectric materials during laser irradiation involving strong vibrational coupling. *Appl Phys A* 70(6):633–635
- Fiore A, Berger V, Rosencher E, Bravetti P, Nagle J (1998) Phase matching using an isotropic nonlinear optical material. *Nature* 391(6666):463–466
- Gamaly EG, Rode AV, Luther-Davies B (1999) Ultrafast ablation with high-pulse-rate lasers. Part I: theoretical considerations. *J Appl Phys* 85(8):4213–4221
- Haglund RF Jr, Bubb DM, Ermer DR, Horwitz JS, Houser EJ, Hubler GK, Ivanov B, Papantonakis MR, Ringeisen BR, Schriver KE (2003) Resonant infrared laser materials processing at high vibrational excitation density: applications and mechanisms. In: Ostendorf A, Helvajian H, Sugioka K (eds) *Laser precision manufacturing*, Proc. SPIE, vol 5063
- Haidar R, Mustelier A, Kupecek P, Rosencher E, Triboulet R, Lemasson P, Mennerat G (2002) Largely tunable midinfrared (8–12 μm) difference frequency generation in isotropic semiconductors. *J Appl Phys* 91(4):2550–2552

- Hardy JG, Chadwick TS (2000) Sustained release drug delivery to the lungs – an option for the future. *Clin Pharmacokinet* 39(1):1–4
- Innerhofer E, Sudmeyer T, Brunner F, Haring R, Aschwanden A, Paschotta R, Honninger C, Kumkar M, Keller U (2003) 60-W average power in 810-fs pulses from a thin-disk Yb:YAG laser. *Opt Lett* 28(5):367–369
- Innerhofer E, Sudmeyer T, Brunner F, Paschotta R, Keller U (2004) Mode-locked high-power lasers and nonlinear optics a powerful combination. *Laser Phys Lett* 1(2):82–85
- Jones RAL (2002) *Soft condensed matter*. Oxford University Press, New York
- Keller U (2003) Recent developments in compact ultrafast lasers. *Nature* 424(6950):831–838
- Kolev VZ, Duering MW, Luther-Davies B, Rode AV (2006) Compact high-power optical source for resonant infrared pulsed laser ablation and deposition of polymer materials. *Opt Express* 14(25):12302–12309
- Lipski AM, Jaquiere C, Choi H, Eberli D, Stevens M, Martin I, Chen IW, Shastri VP (2007) Nanoscale engineering of biomaterial surfaces. *Adv Mater* 19(4):553–557
- Neil GR, Bohn CL, Benson SV, Biallas G, Douglas D, Dylla HF, Evans R, Fugitt J, Grippo A, Gubeli J, Hill R, Jordan K, Krafft GA, Li R, Meringa L, Piot P, Preble J, Shinn M, Siggins T, Walker R, Yunn B (2000) Sustained kilowatt lasing in a free-electron laser with same-cell. *Phys Rev Lett* 84(22):5238
- Pan Y, Neuss S, Leifert A, Fischler M, Wen F, Simon U, Schmid G, Brandau W, Jahnen-Dechent W (2007) Size-dependent cytotoxicity of gold nanoparticles. *Small* 3(11):1941–1949
- Papantonakis MR, Haglund RF (2004) Picosecond pulsed laser deposition at high vibrational excitation density: the case of poly(tetrafluoroethylene). *Appl Phys A* 79(7):1687–1694
- Ringeisen BR, Callahan J, Wu PK, Pique A, Spargo B, McGill RA, Bucaro M, Kim H, Bubb DM, Chrisey DB (2001) Novel laser-based deposition of active protein thin films. *Langmuir* 17(11):3472–3479
- Ringeisen BR, Chrisey DB, Pique A, Young HD, Modi R, Bucaro M, Jones-Meehan J, Spargo BJ (2002) Generation of mesoscopic patterns of viable *Escherichia coli* by ambient laser transfer. *Biomaterials* 23(1):161–166
- Rode AV, Luther-Davies B, Gamaly EG (1999) Ultrafast ablation with high-pulse-rate lasers. Part II: experiments on laser deposition of amorphous carbon films. *J Appl Phys* 85(8):4222–4230
- Schwodiauer R, Bauer-Gogonea S, Bauer S, Heitz J, Arenholz E, Bauerle D (1998) Charge stability of pulsed-laser deposited polytetrafluoroethylene film electrets. *Appl Phys Lett* 73(20):2941–2943

Chapter 17

Injectable Hydrogels: From Basics to Nanotechnological Features and Potential Advances

Biancamaria Baroli

Abstract The purpose of this contribution is twofold: firstly, to describe methods of preparation, physical chemical properties, and potential issues of injectable hydrogel-based formulations from a tissue engineering perspective, and, secondly, to highlight their nanotechnological features and future potentials.

Keywords Hydrogels • Injectable formulations • Reticulation processes • Swelling • Meshes • Nanochannels • Permissivity • Lower critical solution temperature (LCST) • Degradation • Nanotechnology • Tissue engineering • Drug delivery • Cell encapsulation

17.1 Introduction

Tissue engineering is an interdisciplinary field of investigation whose main objective is that of providing essential elements to body tissues and organs in order to induce them to self-regenerate from injuries (related with either war, or car-, labor- and home-accidents), deformities, pathological states, and medical ablation. Tissue engineering's most challenging goal would be that of *de novo* organ formation to provide alternatives to organ transplantation wait-lists and associated mortalities (Langer and Vacanti 1993, 1995, 1999; Vacanti and Langer 1999).

Over the last 2 decades, elements that have been identified as potential candidates to induce and/or support regeneration can be grouped in three main categories: cells, inducing substances, and scaffolds (Langer and Vacanti 1993, 1995, 1999; Vacanti and Langer 1999; Williams 1999). This classification is actually a simplified

B. Baroli (✉)

Dip. Farmaco Chimico Tecnologico, Facoltà di Farmacia, Università di Cagliari,
Via Ospedale 72, 09124, Cagliari, Italy
e-mail: bbaroli@unica.it; bbaroli@aruba.it

description of all signals and elements participating in a regenerative process (Satellite Consensus Conference 2005; Nerem 2007; Kirkpatrick et al. 2007). Therefore, this introduction starts by providing an evolutionary development in the concept, properties and function of scaffolds in order to prepare the readers for the main focus of this chapter.

17.1.1 The Concept of Scaffold

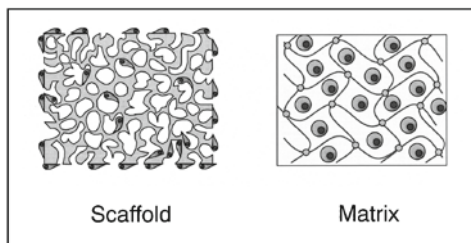
The origins of the word scaffold can be traced to the fourteenth century with the meaning of “*a temporary or movable platform for workers (as bricklayers, painters, or miners) to stand or sit on when working at a height above the floor or ground*” or of “*supporting framework*” (The Merriam-Webster online dictionary (November 15, 2007)). Both “*a temporary or movable platform*” and “*supporting framework*” suit well for an initial description of what a scaffold is in regenerative medicine.

The observation that organs are made from the association of different tissues, and tissues from the association of cells and extracellular matrix (ECM), which acts as a cell supporting structure, brought scientists to experiment whether cells could be grown on artificial supporting structures. It was also observed that ECM “*temporariness*” may be related with normal processes of ECM remodeling, which allow the maintenance of competent tissues (e.g., molecule renewal process, but also healing processes), body responses to insults, and body growth.

Starting from this first idea, there have been many articles describing the use of biodegradable polymers for the production of tissue engineering scaffolds (Hutmacher et al. 2001; Pişkin 2002; Xue and Greisler 2003; Gunatillake and Adhikari 2003; Webb et al. 2004; Nair and Laurencin 2006; Holland and Mikos 2006; Martina and Hutmacher 2007; Furth et al. 2007). However, it became clear pretty soon that cells would not survive and would not invade a thick polymer scaffold if they were respectively entrapped into, or seeded onto, a material that did not allow sufficient mass transport (Ko et al. 2007). Therefore, one of the most important scaffold requirements was uncovered. Porosity, interconnectivity of pores, dimension of pores, as well as thickness and surface properties of pore walls are all parameters that differently affects in vitro and in vivo experiments (Karande et al. 2004; Karageorgiou and Kaplan 2005; Hollister 2005). In fact, along with inward-outward movement of molecules, thick scaffolds also need to allow microvasculature invasion when implanted in vivo.

For gelling materials and for all other materials used to encapsulate or entrap cells, differences in mass transport are related to dimension and permissiveness of polymeric meshes (Lin and Metters 2006; Baroli 2007). In this case, water, nutrients, oxygen and waste products need to diffuse through the “*pores*” bounded by entangled or crosslinked polymer chains. Hence, permissiveness is not only related to meshes’ dimensions, but also to the interactions that may be established between

Fig. 17.1 Schematic cross-sectional representation of artificial supporting structures loaded with cells



nutrients/waste products and polymer chains (Lin and Metters 2006; Baroli 2007; Gehrke et al. 1997). In fact, at the nanoscale, where molecules diffuse through what we can image, in three dimensions, as tortuous nanochannels within the polymer network, hydrophobic interactions, Van der Waals forces, dipoles, hydrogen and ionic bonds predominate (Lin and Metters 2006; Baroli 2007; Gehrke et al. 1997). Microvasculature invasion is still related to permissiveness and also with cellular ability to make materials permissive by degradation and/or remodeling processes.

Beside temporariness, these initial comments distinguish two main categories of scaffolds (Fig. 17.1). Those that are literally termed *scaffolds* are rigid and porous supporting structures where cells, after colonizing their surfaces, eventually migrate into their interior. Even though cells may be considered macroscopically entrapped into the scaffolds, they will always lay onto polymer external or internal surfaces of the interconnected pores. The other type of scaffolds (in its broad terminology) is that grouping all those that are preferably named *matrices*. These are generally made of softer or gelled materials in which cells are microscopically entrapped. Cells are closely surrounded by polymers forming the matrix, which is porous only at the nanoscale.

Scaffolds and matrices differ in many other characteristics such as mechanical properties, production and fabrication methods, handling, water content, hydrophobicity, injectability, sterilizability, and ability to support cell adhesion, cell migration, and cell differentiation, to name some. All these features contribute to the success of the scaffold/matrix once implanted in an individual. As one can note, some of these characteristics are related to technological aspects, while some other are associated with the functionality of the scaffold/matrix. Therefore, supportive structures that sustain, induce, or transmit cellular signaling cannot longer be considered inert structures but engineered therapeutics.

To induce, sustain, and/or transmit cellular signaling from a polymer structure to cells it is important that cells and single polymer chains (or cells and what it is linked to the polymer chains) interact directly. It is becoming clearer and clearer that these interactions at the nanoscale and the micro-modifications of the environment around the cells are responsible for triggering and/or sustaining cellular signals (Clark 2007). Therefore, scientists are starting realizing that the development of next-generation scaffolds/matrices needs to be based on understanding, and on the ability to engineer and control, what may happen onto and inside of the

scaffold/matrix (Clark 2007; Causa et al. 2007; Kidoaki and Matsuda 2008; Ilkhanizadeh et al. 2007; Cheng et al. 2007; Dodla and Bellamkonda 2006, 2008; Liu et al. 2007; Zelzer et al. 2008). Although a great effort has been focused on cell attachment, spreading and chemotaxis, to understand (and possibly control) all possible signals involved in cell stimulation, investigations should also include not only the specific interactions between cells and polymers, but also all the gradients in nutrients/waste products, oxygen/carbon dioxide tension, degradation products, ionic strength and pH, pressure and osmotic pressure, strains and flows, cytokines and related molecules that may be generated inside of the scaffolds/matrices after implantation or during in vitro experimentations.

Under this perspective, hydrogel-based matrices are the structures that could potentially produce this type of signals more easily because of their close resemblance to natural ECMs, as justified by the increasing interest on these materials (Chen et al. 1997; Hoffman 2002; Nguyen and West 2002; Jeong et al. 2002; Baroli 2006; Prestwich et al. 2006; Boland et al. 2006; Fedorovich et al. 2007; De Laporte and Shea 2007; Gazit 2007; Brandl et al. 2007; Tessmar and Göpferich 2007; Kopeček 2007; Khademhosseini and Langer 2007). And this is also the perspective through which hydrogels will be presented, highlighting their tissue engineering and nanotechnological features, and suggesting potential nanotechnological advances.

17.2 Hydrogels

A hydrogel (HG) is defined as a polymer network that is insoluble in water, but in there swells up to an equilibrium volume retaining its shape. To satisfy this statement, polymer chains should contain a sufficient number of hydrophilic residues (e.g., hydroxylic, carboxylic, amidic, aminic, sulfonic, and others), and should be reticulated with each other by covalent bonds or other associative and cooperative forces (Lin and Metters 2006; Baroli 2007). Among these last ones there are hydrophobic associations/Van der Waals forces, micellar packing, hydrogen bonds, ionic bonds, crystallizing segments, and combinations of the above (Lin and Metters 2006; Baroli 2007). Consequently, the degree of swelling results from balancing hydrophilicity, that drives water inside of the polymer network, and type and degree of reticulation, that generate forces against a further distension of the polymer network (Lin and Metters 2006; Baroli 2007).

The nature of reticulation allows distinguishing HGs as *permanent or chemical hydrogels* and *reversible or physical hydrogels*, where polymer chains are covalently or physically crosslinked, respectively (Lin and Metters 2006; Baroli 2007).

Macroscopically, chemical and physical HGs may slightly differ in their mechanical properties, the first one being generally stiffer. However, HGs are known to have poor mechanical properties and to be very difficult to be handled. Therefore, these minimal differences are not sufficient to induce one to prefer chemical or physical HGs for tissue engineering applications. There are instead

some general and specific advances, but also some limitations, that should be carefully evaluated during the design and development of HG-based tissue engineering matrices (Lin and Metters 2006; Baroli 2007).

17.2.1 *Methods of Preparation*

HGs may be fabricated as matrices of different shapes, hollow tubes, fibers, films, macro- and microbeads, microspheres and microcapsules. Hence, preparation of HGs occurs by a few main principal processes that are carried out under different conditions to assure concomitant shaping. General methods of preparation have been extensively reviewed in literature (Baroli 2006, 2007; Gehrke et al. 1997; Chen et al. 1997; Hoffman 2002; Nguyen and West 2002; Jeong et al. 2002; Kúdela 1989; Peppas et al. 2000a, b; Guenet 1992; Qiu and Park 2001; Murakami et al. 2007; Hennink and van Nostrum 2002; Hern and Hubbell 1998; Elisseeff et al. 1999; Anseth and Burdick 2002). Therefore, in the following two paragraphs only references of specific cases will be given.

17.2.1.1 **Chemical Reticulation Processes**

There are essentially two chemical processes used to produce permanent HGs: polymerization (Odian 1991), and reaction of complementary residues located on different polymer chains to form inter-chain bridges (Hennink and van Nostrum 2002).

The first process is generally associated with the production of chemical HGs, while the second one is erroneously only associated with the secondary chemical reticulation of physical HGs. Nevertheless, considering all possible variants, chemical HGs may be produced by (1) polymerization of monomers that are successively crosslinked, (2) crosslinkage of polymers, (3) polymerization of multifunctional monomers, (4) copolymerization of monomers with crosslinkers, (5) copolymerization of monomers with multifunctional monomers, and (6) polymerization of monomers within HGs to produce IPNs (Fig. 17.2).

In general, polymerization follows a free radical mechanism, which is usually activated by radiation (e.g., UV or visible light, electron beams, gamma- and X-rays) or heat (Odian 1991). To undergo polymerization, formulations should be composed of monomers possessing polymerizable residues such as vinylic or methacrylic groups, and, in some cases, of an appropriate initiator system. In fact, during the very first phases of polymerization, the energy of radiation or heat is respectively transferred to initiator system (more common) or monomers, which will provide initiating radical species. From a chemical point of view, many factors contribute to the successfulness of polymerization, i.e. the maximum degree of monomer conversion. Several studies have pointed out the importance of fast initiation and propagation rates, and high initiation and propagation efficiencies, which in

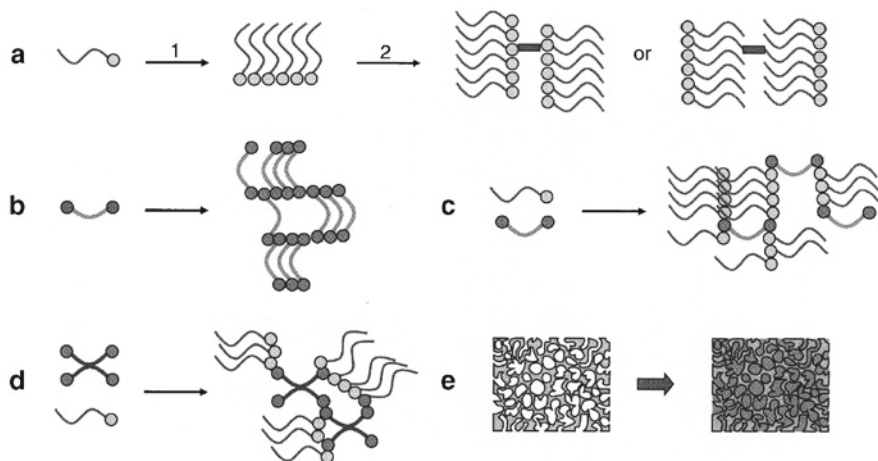


Fig. 17.2 Schematic representation of chemical reticulation processes. (a1) polymerization of monomers; (a2) crosslinkage of polymers; (b) polymerization of multifunctional monomers; (c) copolymerization of monomers with crosslinkers; (d) copolymerization of multifunctional monomers with monomers; (e) production of IPNs

turn are related with properties and efficiencies of both initiator system and triggering radiation (Baroli 2006; Nelson et al. 1995; Lovell et al. 1999; Andrzejewska 2001; Goodner and Bowman 2002; Burdick et al. 2003; Neumann et al. 2006; Tarle et al. 2006; Johnson et al. 2007).

Depending on formulation components, polymerization does not always assure to obtain reticulated polymer network (i.e., polymerization and reticulation are not concurrent). In these cases, hence, further chemical reactions are needed. As it was mentioned earlier, the rationale is that of forming inter-chain bridges (Hennink and van Nostrum 2002). This may be achieved by reacting complementary residues (e.g.; amine-carboxylic acid, $-\text{NH}/-\text{COOH}$; isocyanate-hydroxyl, $-\text{NCO}/-\text{OH}$; isocyanate-amine, $-\text{NCO}/-\text{NH}-$) under appropriate conditions. In addition, it has been shown that peptidyl chains may be crosslinked using dialdehyde (HCO-R-COH) (Hennink and van Nostrum 2002), and cysteine-residues ($\text{COR-CH(NHR')-CH}_2\text{-SH}$) through their sulfhydryl groups (R-SH) (Wathier et al. 2006; Ghosh et al. 2006; Rizzi and Hubbell 2005; Ehrick et al. 2005; Plunkett et al. 2005). Utilization of high-energy irradiation and enzymes has also been explored (Hennink and van Nostrum 2002).

Polymerization may be distinguished in bulk polymerization and interfacial polymerization. In the first case, HG components are blended, and resulting mixture is polymerized. Interfacial polymerization is instead used to produce particles or capsules, or films or sheets, that may be useful for encapsulating cells or to act as tissue sealants or barriers (Hubbell 1996; Cruise et al. 1998, 2000; Uludag et al. 2000; Desmangles et al. 2001; Couvreur et al. 2002; Mayer 2005). Thinness layers are produced by adsorbing initiators on tissues or cells, which are then exposed to the polymerizable mixture and irradiated. In general, specific shapes may be obtained by polymerizing the formulation within molds, by spraying

it and polymerizing the resultant aerosol to obtain small particles, by vortexing it within a non-solvent fluid and polymerizing the resultant emulsion to obtain particles, or finally by spatially and temporally controlling the polymerization process, as in 3D printing, to obtain complex structures.

However, general HG fragility and difficulties in handling have inspired scientists to design formulations that could be injected in the body location of interest and successively gelled in situ. This strategy allows production and implantation to become simultaneous and overcomes all the issues related to handling. In addition, since ungelled formulations may be delivered through small catheters/cannulas, implantation may be performed with minimally invasive surgery, potentially leading to easier and faster surgical procedures and higher patient compliance.

However, in vivo production poses some safety concerns. First, formulators should prove that monomers and initiators are non-toxic, or are used at non-toxic concentrations. In fact, once polymerizable formulations are implanted and converted into HGs, all unreacted monomers or toxic substances (if any) will be leached out into the body (Bryant et al. 1999, 2000; Trudel and Massia 2002; Pagoria et al. 2005; Williams et al. 2005; Hong et al. 2006). In addition, among potentially toxic substances there are the radicals generated during polymerization (Lovell et al. 1999; Andrzejewska 2001; Goodner and Bowman 2002; Burdick et al. 2003; Neumann et al. 2006; Tarle et al. 2006; Johnson et al. 2007). Obviously, their production cannot be overcome. However, formulators should be competent enough to propose blends able to efficiently polymerize in short times, and, eventually, to offer protection means for molecules/cells to be entrapped (Quick and Anseth 2003; Baroli et al. 2003). In such circumstances, cells and/or molecules to be entrapped and host tissues/fluids will be exposed to radicals for short times, and damages, if any, should be minimal or easily recoverable (Quick and Anseth 2003; Baroli et al. 2003; Shen et al. 2005). In contrast, during slow and inefficient polymerization, or in formulations undergoing post-polymerization processes (Truffier-Boutry et al. 2006), entrapped entities will endure a prolonged exposure to radicals, while host tissues/fluids will receive a continuous release of reactive species. A second important issue is the great amount of heat generated during polymerization due to its exothermicity (Lovell et al. 1999; Andrzejewska 2001; Goodner and Bowman 2002; Burdick et al. 2001, 2003; Neumann et al. 2006; Tarle et al. 2006; Johnson et al. 2007; Daronch et al. 2007; Michalakis et al. 2006; Dunne and Orr 2002). For instance, a common polymethyl-methacrylate (PMMA)-based bone cement has been shown to reach around 60°C at the host cell-cement interface, but up to 110°C in its interior during polymerization (Yamamuro et al. 1998). Therefore, uncontrolled thermic rises may be extremely dangerous for tissues located close to the implant because they could become necrotic and induce a strong inflammatory response (Jefferis et al. 1975). Besides these extreme cases, even milder thermal rises could compromise the vitality of cells and/or the activity of molecules. A temperature of 42–47°C is sufficient to induce cellular damage (Lundskog 1972). Proteins coagulate at around 50°C (De Wijn and van Mullem 1990) but may lose their activity at lower temperatures. Consequently, cytokines or growth factors to be entrapped in a chemical HG need to be thermoresistant or preventively prepared as a thermoresistant formulation.

It is clear that these safety issues may strongly influence the biocompatibility of final product, possibly extending the formulation phase or diminishing the attractive properties of the material.

17.2.1.2 Physical Reticulation Processes

Production of physical HGs is based on few mechanisms of reticulations such as ionic interactions, crystallization, hydrophobic interactions, hydrogen bond interactions, and protein interactions (Fig. 17.3).

Ionic interactions allow the simplest and most known process of physical reticulation, where anionic or cationic polymers may be crosslinked using counter ions (*ionotropic hydrogels*), or other polymers that are oppositely charged (*complex coacervate* or *polyion complex hydrogels*), as shown in Fig. 17.3 (scheme 1 and 2). There are several natural polymers that gel accordingly to this type of interactions. Alginate, chitosan, and hyaluronan are representative examples of such materials that have been, and still are, used for biomedical applications. For instance, alginate has been utilized for scaffold and matrix production, cell encapsulation, and cytokine, growth factor, gene, and DNA encapsulation and delivery (Hill et al. 2006;

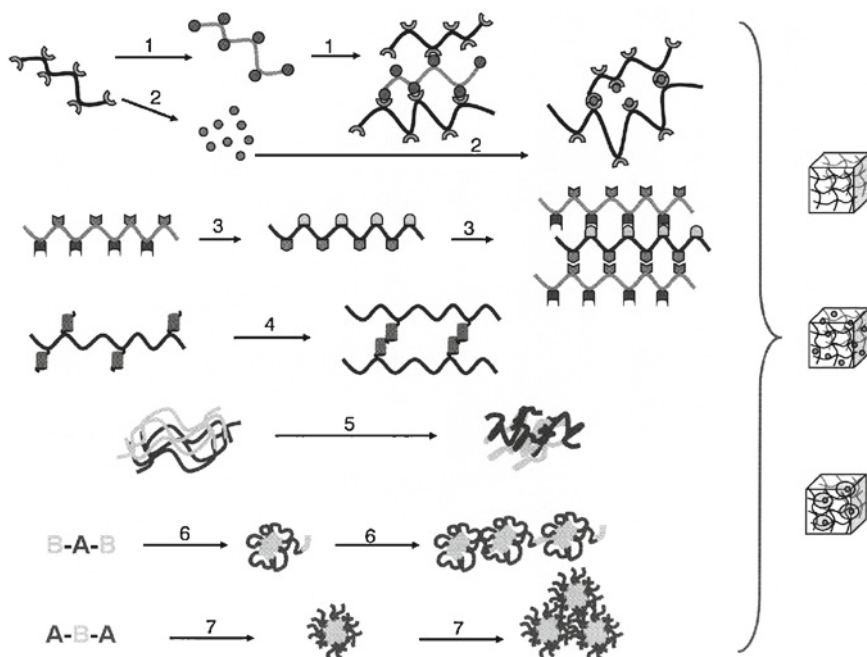


Fig. 17.3 Schematic representation of physical reticulation processes. (1 and 2) Respectively, complex coacervation and ionotropic gelation; (3) reticulation by hydrogen bonds; (4) reticulation by proteic interactions. Example of coiled coil-graft polymer; (5) crystallization process; (6 and 7) reticulation by hydrophobic interaction and self-assembly in supramolecular structures

Zachos et al. 2006; Paek et al. 2005; Simmons et al. 2004; Raymond et al. 2003; Sylven 2002; Dobie et al. 2002; Mierisch et al. 2002; Rokstad et al. 2002; Milella et al. 2001; Lee et al. 2000a; Peters et al. 1998; Tilakaratne et al. 2007; Lim et al. 2006; Vogelín et al. 2006; Li et al. 2006; Liao et al. 2005; Noushi et al. 2005; Gu et al. 2004; Peirce et al. 2004; Chinen et al. 2003). Chitosan-based formulations have been used for regeneration of neural tissue, liver, bone, cartilage, and skin, to produce vascular grafts, and to promote angiogenesis. Delivery of growth factors, plasmids, and adenoviral vectors has been also reported (Atala and Lanza 2002; Chenite et al. 2000; Delgado et al. 2006; Zhang et al. 2006a, b; Hsieh et al. 2006; Guo et al. 2006; Park et al. 2004a, 2006; Akbuga et al. 2004; Cho et al. 2004a; Lee et al. 2000b, 2002, 2004; Mizuno et al. 2003; Ozbas-Turan et al. 2002; Brown et al. 2001; Chellat et al. 2000; Hahn et al. 2006; Miralles et al. 2001). Hyaluronan gels are instead less common because of their extremely poor mechanical properties. However some formulations have been proposed for the restoration of vocal fold lamina propria, cartilage tissue engineering, and induction of neovascularization (Atala and Lanza 2002; Hahn et al. 2006; Miralles et al. 2001; Arimura et al. 2005; Giavaresi et al. 2005). Gelling by ionic interactions occurs very rapidly. Therefore, to develop an injectable formulation that will uniformly gel once deposited in a body cavity acting as a mold, it is important to slow down this reaction for at least the time required to mix components and deliver the formulation (possibly <5 min). For instance, aqueous solutions of chitosan and glycerophosphate disodium salt gel by ionic interaction but at 37°C (Chenite et al. 2000). In addition, the reaction of alginate with calcium ions may be delayed by using less soluble calcium salts, or by slowly increasing acidity of dispersing aqueous solutions (Novamatrix™ 2007; Liu et al. 2008).

HGs can be produced by crystallization when small portions of the polymeric chains crystallize (Fig. 17.3, scheme 5). This phenomenon produces solid regions acting as crosslinking spots. It has been reported that polyvinyl alcohol (PVA) gels according to this mechanism after a few cycles of freeze-thawing (Hassan and Peppas 2000; Gu et al. 1998; Cascone et al. 1999), while gelatin-silk fibroin blends after exposure to methanol or a methanol-water solution (Gil et al. 2005). No injectable formulations for biomedical purposes have been developed so far, because conditions cannot easily be reproduced in vivo.

A special attention should be given, instead, to those polymers that gel by hydrophobic interactions and assemble in supramolecular structures (Fig. 17.3, scheme 6 and 7). Fundamental characteristic of such polymers is that of possessing hydrophilic (A) and hydrophobic (B) polymeric segments in, or attached to, the main backbone chain (respectively amphiphilic block and graft co-polymers). ABA and BAB polymers, once dispersed in an aqueous solution, will initially form micelles due to segregation of hydrophobic segments. Successively, by increasing polymer concentration or temperature, micelles will aggregate in supramolecular structures (Fig. 17.3, scheme 6 and 7) (Baroli 2007; Hennink and van Nostrum 2002). Among these polymers there are the Pluronics® (PEO-b-PPO-b-PEO and PPO-b-PEO-b-PPO) and derivatives, and PEG-PLGA-PEG and PLGA-PEG-PLGA block copolymer families. Properties of each single polymer of a specific family change by

varying the molecular weight of each block, and type and length of residues attached to it. Therefore, it has been possible to synthesize polymers with desired properties, such as a lower critical solution temperature (LCST) close to body temperature (i.e., 25–37°C). Pluronics® (Gajewiak et al. 2006; Weinand et al. 2006; Ruszymah et al. 2005; Gu and Alexandridis 2005; Yoo et al. 2004), and in particular the F-127 (Cortiella et al. 2006; Chua et al. 2005; Arevalo-Silva et al. 2000; Saim et al. 2000; Cao et al. 1998), has been investigated as HG scaffolds for tissue engineering of cartilage, bone, lung and breast, and for drug delivery both in its cubic and micellar (nanocarrier) phases. PEG-PLGA-PEG (Lee et al. 2003; Li et al. 2003; Jeong et al. 2000a, b) and PLGA-PEG-PLGA (Moffatt and Cristiano 2006; Duvvuri et al. 2005; Qiao et al. 2005; Chen et al. 2005; Kwon and Kim 2004; Jeong et al. 2004; Choi and Kim 2003) have been studied for drug delivery systems, whose release kinetics are governed by diffusion and degradation.

Another well-known family of polymers that gel by hydrophobic interactions but without forming supramolecular structures are those related with poly(*N*-isopropylacrylamide) (PNIPAAm). It is well-known that these residues have an extended conformation below the LCST temperature. However, in proximity to LCST temperature, they rapidly start to aggregate into hydrophobic folded masses. IPAAm residues have been successfully used to produce synthetic and semi-synthetic injectable polymeric formulations that have been used for cartilage tissue engineering and delivery of proteins (Chen and Cheng 2006; Kwon and Matsuda 2006; Kim et al. 2005; Pişkin 2004; Cho et al. 2004b; Stile and Healy 2002; Ohya et al. 2001; An et al. 2001; Choi et al. 2002; Wu et al. 2005; Kim and Healy 2003; Makino et al. 2001).

It is also reminded that LCST properties have been used to profitably print polymeric dispersions of cells (and/or molecules) in an *in vitro* set-up. This technique allows to build up, drop-by-drop or fiber-by-fiber, complex structures, where cells and/or molecules may be distributed as desired and also in a gradient fashion (Boland et al. 2006; Fedorovich et al. 2007). Unfortunately, devices for *in vivo* 3D printing have not yet been realized, and by now *in vivo* applications of LCST polymers suffer this limitation.

Observing how well nature uses hydrogen bonds to assemble DNA chains and to fold proteins, scientists have driven some of their efforts to produce polymers that gel using this type of interaction (Fig. 17.3, scheme 3). It is reminded that hydrogen bonds can occur between proton donor (e.g., carboxylic, hydroxylic, aminic and amidic residues) and proton acceptor (e.g., oxygen, nitrogen, and halogen atoms, which have a lone pair electrons, and/or unsaturated residues) groups (Silverstein et al. 1991). Examples of such polymers are: PVA, PVA/PEO blends (Bromberg and Ron 1998), PVA/gelatin blends (Wang et al. 2008), PVA/chitosan blends (Mathews et al. 2008), PVA/phenyl boronic acid bearing-phospholipid polymer blends (Konno and Ishihara 2007), PVA/poly-gamma-glutamic acid blends (Lin et al. 2006), PVA/PEO-PPO-PEO blends (Oh et al. 2004), PVA/poly(vinyl pyrrolidone) (PVP) blends (Thomas et al. 2003), polyacrylamide/polyacrylic acid blends, and others (Kimura et al. 2004, 2005, 2007; Boucard et al. 2005; Petrini et al. 1999). Finally, DNA structure has inspired an interesting semi-synthetic polymer.

By grafting oligodeoxyribonucleotides (ODN) on poly(*N,N*-dimethylacrylamide-co-*N*-acryloyloxysuccinimide) this interesting polymer gel upon addition of free or grafted complementary ODN (Murakami and Maeda 2005; Lin et al. 2004; Nagahara and Matsuda 1996; Mirkin et al. 1996; Milam et al. 2003; Starr and Sciortino 2006; Um et al. 2006; Ding et al. 2007).

Even the advances in protein engineering are providing new tools for producing appealing semi-synthetic polymers. In fact, it is now possible to (a) produce proteins or oligopeptides with desired repeating units, (b) graft desired peptide chains of desired lengths onto synthetic polymers, (c) graft coiled coils (i.e., left-handed superhelices of two or more right-handed alpha-helices; Fig. 17.3, scheme 4) on synthetic polymers. This new type of polymer allows producing HGs that respond to temperature and pH changes, due to the interactions between proteic residues (Wang et al. 1999; Lao et al. 2007; Xu and Kopeček 2008; Hosseinkhani et al. 2006; Yang et al. 2006; Xu et al. 2005; Kretsinger et al. 2005; Tanaka et al. 2004; Schneider et al. 2002). In addition, the reactions between biotin and avidin (Segura et al. 2005; Vermette et al. 2003), and antigens and antibodies (Miyata et al. 1999) have been used to produce self-assembled matrices for drug and cell encapsulation as well.

The processes of physical reticulation proposed above are very mild and compatible with a body environment. What was discussed so far has shown that nanotechnological properties of injectable HG-based materials are not a consequence of a nanotechnological fabrication process, since the formulations are simply injected in the body to gel. Some variants of this general approach may contemplate the injection of preventively reticulated HG-based particles or micro-matrices suspended in an aqueous dispersant solution, as acellular drug loaded polymeric implantable materials. It could also be possible to suspend preventively reticulated HG-based particles or micro-matrices in a cell loaded, polymeric solution (Park et al. 2005; Holland et al. 2004), as schematized in Fig. 17.4.

Impressive nanotechnological advances in fabrication could be instead achieved by developing devices for in vivo 3D printing. In addition, other advances of this kind may be envisaged in tailored polymer syntheses. The polymeric sequence has

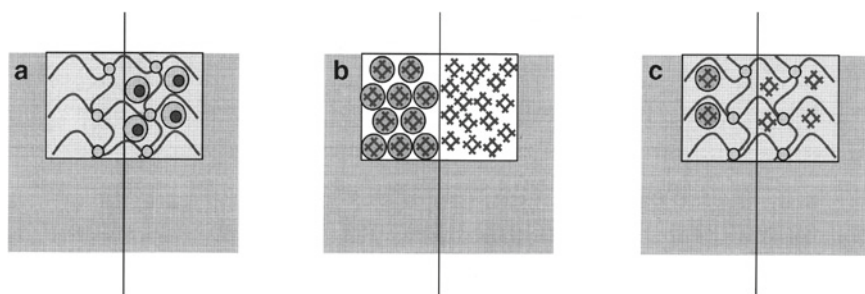


Fig. 17.4 Potential formulative combinations of injectable and HG-based systems. (a) Cell -free and -loaded gelable polymer dispersion; (b) formulation composed of HG-based particles and micro-matrices dispersed in an aqueous fluid; (c) formulation composed of HG-based particles and micro-matrices dispersed in a gelable polymer dispersion

the potential to establish, at the nanoscale, interactions between specific groups of the polymer and cells/molecules that may be converted in cellular signaling. In addition, the interactions between polymer chains and/or their residues in a reticulated network may be responsible of creating new HG properties. Finally, formulation of gelable polymers with nanomaterials should not be underestimated.

17.3 Properties Exploitable in Tissue Engineering

Historically, HGs have been developed for drug delivery systems and for in vitro cell encapsulation. Therefore, many properties celebrated for such systems could be less important for tissue engineering applications. This section discusses whether general properties of HGs may be useful for an implanted HG-based matrix that is used as host and/or implanted cell support, and which may be their nanotechnological aspects/potentialities.

The first property of HGs to be mentioned is the ability of swelling up to an equilibrium state (Baroli 2007; Kúdela 1989; Peppas et al. 2000a; Flory and Rehner 1943a, b; Flory 1950, 1953; Flory et al. 1949; Peppas and Merrill 1976, 1977; Peppas 1986; Peppas and Colombo 1997; Canal and Peppas 1989; Brannon-Peppas and Peppas 1990a, b; Khare and Peppas 1995; Anseth et al. 1996; Blanco et al. 1996; Díez-Peña et al. 2002; Lustig and Peppas 1988). This controlled enlargement of HG volume is the resultant of two forces acting in opposite directions. An osmotic pressure, generated by HG polymer concentration, will be responsible of driving water inside of the network, and thus will act toward volume expansion. Whereas, the sum of cohesive forces and the extent of extendability of polymer chains will produce a force acting against volume expansion. When these two forces reach the equilibrium, swelling process stops. Brainstorming on the applicability of this property leads to the following conclusions. A volume expansion of an implanted material may be advisable in a district where a permanent obstruction is needed, even despite a potential enlargement of such location. Swelling could also be intentionally used to capture, within the polymer network, host molecules found or circulating at the implantation site. Another application may be that of producing a slight compressive pressure on surrounding tissues. However, all these applications seems to be difficult to be realized and of questionable utility. In fact, surgeons should inject a formulation that is not possessing all the water needed to be at equilibrium; it would be necessary to preventively know the degree of swelling and dimensions of polymer meshes after HG expansion stabilization in that particular location (in this case implant site will negatively contribute to volume expansion); it would be most likely appropriated to inject a volume of ungelled formulation smaller than the receiving body cavity, which means that surgeons should be trained for that particular formulation and application. However, these potential applications may be complex and expensive.

Attention should be given to polymer mesh dimensions (Baroli 2007; Kúdela 1989; Peppas et al. 2000a; Flory and Rehner 1943a, b; Flory 1950, 1953; Flory et al. 1949;

Peppas and Merrill 1976, 1977; Peppas 1986; Peppas and Colombo 1997; Canal and Peppas 1989; Brannon-Peppas and Peppas 1990a, b; Khare and Peppas 1995; Anseth et al. 1996; Blanco et al. 1996; Díez-Peña et al. 2002; Lustig and Peppas 1988). Without entering into details of mathematical modeling, it can be intuitively recognized that this parameter describes a physical barrier whose cut-off will determine the size of molecules that might move inward and/or outward the gel. This parameter and its modification regulate HG-encapsulated cell survival both assuring an adequate mass transport and protection from host immune system (if necessary). In addition, polymer mesh dimensions control the release (total amount and diffusion pattern) of entrapped molecules. Polymer meshes become a physico-chemical barrier when one considers potential interactions between residues on polymer chains and diffusing molecules. It is especially the ionic character of these residues that may influence protein adhesion within HG nanochannels for example. Negative charge increases blood compatibility (no thrombogenicity) (Duncan et al. 1997; Gemmell et al. 1996; Llanos and Sefton 1992, 1993; Hari et al. 1993; Strzinar and Sefton 1992; Ishihara et al. 1990; Desai and Hubbell 1989; Ratner et al. 1978; Chen et al. 2007; Mequanint et al. 2006; Arica et al. 2005) while positive charges promote cell adhesion (De Rosa et al. 2004; Tanahashi and Mikos 2003; Sosnik and Sefton 2006). It can be clearly seen that the modification of charge has various implications that are almost all related with compatibility of materials toward tissue and fluids at the implantation site and/or toward encapsulated cells. Since these characteristics are developed with a specific synthesis, they do not depend on fabrication methods but on polymer sequence. Reticulation of polymer chains and the consequent proximity of ionic residues will transfer properties (or will generate new properties to be transferred) to the HG. The possibility of changing this parameter, which could be collectively termed permissivity of HG meshes and nanochannels, has nanotechnological potentialities going beyond simple but controlled molecule/cell interactions. It may be possible to synthesize self-assembling polymers that gel to form spatially-controlled meshes of different dimensions and thus nanochannels of different (or changing) internal diameter. This would allow the production of injectable materials that gel in vivo conditions to function as nanofluidic devices without the use of MEMs or 3D printing technologies. In addition, it would be possible to produce a gel possessing channels exploitable for microvasculature invasion.

Degradation is another property of materials to be used for regenerative purposes that is highly desirable. This meets the objective of inducing the host to replace an artificial, temporary supporting material with regenerated tissue with matched rates of loss and replacement. Physical HGs degrade via their polymer backbone and/or lateral chains. In contrast, chemical HGs may degrade through the polymer chains or the crosslinking bonds. From a toxicological perspective, processes that degrade HG polymer networks into small units would be preferable, since they could easily be eliminated by glomerular filtration without further metabolic processes. From a tissue engineering perspective, instead, the critical issue is related to the type of degradation, namely on whether it would be advisable to have materials degrading by a bulk or surface process. It is well known that a material undergoing bulk degradation will maintain its volume while decreasing its mechanical

properties, whereas it will suffer an opposite situation if it is eroded by surface degradation (Fig. 17.5).

Consequently, the following scenarios may occur after implantation. (a) An unloaded non-permissive gel would cause host cells to invade its external surfaces. With surface-degrading materials, the front of cells and their associated ECM will move forward as polymer disappears. Bulk-degrading materials, instead, will eventually become permissive, and cells may colonize HG interior where they can deposit ECM and slowly convert bulk polymeric materials into bulk ECM-cell constructs. Finally, hybrid situations should be expected for cell-free permissive and surface degrading gels. (b) A cell-loaded non-permissive gel would not allow entrapped cells to directly communicate with host cells until it became permissive or degraded (Fig. 17.6).

Initial debate on required mechanical properties was based on the potential mechanical failure of scaffolds/matrices once implanted in the body of an individual that had to withstand his/her own weight. Logically, this led to the conclusion that mechanical properties of scaffolds/matrices should suit those of the host tissue.

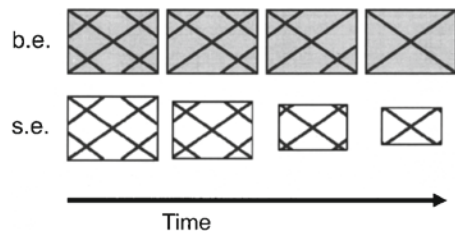


Fig. 17.5 Schematic representation of bulk-degrading (b.e.) and surface-degrading (s.e.) materials over time

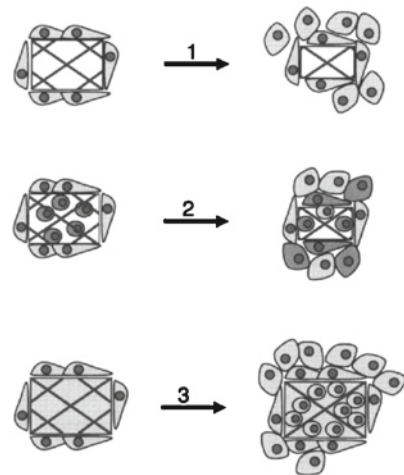


Fig. 17.6 Potential scenarios after implantation of degradable HGs. (1) Cell-unloaded non-permissive surface-degrading HG; (2) cell-loaded non-permissive surface-degrading HG; (3) cell-unloaded non-permissive bulk-degrading HG

Therefore, surface-degrading materials were recommended for hard tissues, and preferably bulk-degrading ones for soft tissues. Nevertheless, some scientists hypothesized that mechanical properties of scaffolds/matrices could be of minor importance if a normal process of regeneration would have occurred. In this case, it would have been the regenerating tissue to provide required properties.

The later observation that tissues arise from a condensation of mesenchyme, occurring close or far away from blood vessels, but around non-fully differentiated cells (Kierszenbaum 2002) (which can be seen as a sort of cell encapsulation) led scientists to suppose that simple mechanical signals could induce progenitors cells to differentiate toward a lineage or another. This observation seems to support the importance of scaffold/matrix mechanical properties. The *in vitro* proliferation of cardiomyocytes under cyclic mechanical stress can produce more competent tissue (Birla et al. 2007; Lal et al. 2007; Gwak et al. 2008; Gupta and Grande-Allen 2006), which supports the importance of matrix/scaffold mechanical properties. Perhaps a discriminating selection of materials based only on macroscopic mechanical properties of host tissue is not appropriate, since it seems the suitable mechanical signals vary with cell phenotype. In addition, it seems that signals that involve or surround whole cells are more efficacious. Following this reasoning, then, one would be prompted to conclude that cell permissive, or eventually permissive, bulk-degrading materials would suit this scenario. In fact, focusing on hard tissues as an example, surface-degrading materials would be too tough and compact to allow cell encapsulation,¹ therefore the only signals they may transfer to cells are those arising from the cell-material boundary. One day, it may be possible to develop an extremely porous and tough material that could be interpenetrated with a permissive ECM-like gel solving issues of hard tissues. Some advances in mechanical properties of HGs have been already achieved (Kopeček 2007). Nanotechnological advances may be envisaged in future and further development of HG-based materials resembling the ECM of specific hosting tissues that may be degraded by the endogenous matrix metallo-proteases (MMPs) (Kim et al. 2005; Kim and Healy 2003; Hong et al. 2007; Ahmed et al. 2007; Lévesque and Shoichet 2007; He and Jabbari 2007; Moss et al. 2006; Raeber et al. 2005; Park et al. 2004b; Seliktar et al. 2004; Lutolf et al. 2003a, b), or other enzymes found at implant site or produced by entrapped and/or host cells. It would also be interesting to develop HG-based matrices that upon degradation may release ECM self-assembling building blocks. According to this hypothesis, HGs would work as supportive/filling material and ECM-block drug delivery systems.

It has been mentioned that, depending on their composition, HGs may suffer volume phase and sol-gel phase transitions when exposed to particular signals. In the first case, HGs will swell or shrink; in the latter case, HGs will pass from a gel state to a sol state, or the reverse. Signals able to trigger these events may be

¹In this case the use of a non-porous scaffold would be the best solution since porosity decreases mechanical properties.

changes in temperature, pH, ionic strength, concentration of particular molecules, electric field, light, and many others, alone or as a combination, or temporal combination, of the above (Baroli 2007; Jeong et al. 2002; Guenet 1992; Qiu and Park 2001). Focusing on tissue engineering potential applications of these properties, it is clear that it would not be advisable to have a cell support that might dissolve (sol-gel transition) or modify its volume below or above the dimension of body cavity where it has been implanted. Only the ability to dissolve when tissues are completely formed could be contemplated for non-degradable permissive three-dimensional physical gels, or non-degradable non-permissive two-dimensional physical gel-based layers, as a way to remove the temporal support. In most common cases, utility of such properties should be restricted to transitions of limited extent or that are confined to some narrow regions within the three-dimensional HG. These small and/or localized deformations may be strategically used to produce pulsatile release of entrapped molecules, without modifying the entire HG structure. Another application could be that of allowing cell invasion and/or growth under controlled, pulsatile deformations that would transfer pulsatile mechanical signals to cells. It may also be possible to obtain a gel that will pulse (small and controlled swell-shrink transitions) by wireless electrical/magnetic signals, and that could be dissolved (to eliminate it) when cells become fully differentiated. Design and control of localized transitions may be indeed considered nanotechnological advances. At this time just few explorative studies can be found in literature (Hu et al. 2007; Frimpong et al. 2007; Nayak and Lyon 2005; Satarkar and Hilt 2008). Their potential is clear.

HGs have been and still are extensively investigated and developed as drug delivery systems. It has been already mentioned that HGs used for tissue engineering applications may also entrap molecules. These, in particular, may comprehend growth factors, cytokines, angiogenic molecules, cell chemoattractants, and DNA fragments, plasmids, or vectors, among others. In case of injectable formulations, molecules to be successively delivered may be found in their free form or preventively entrapped/encapsulated/precipitated into/onto colloidal carriers (e.g., polymeric micro- and nanoparticles, gold and/or other metallic and/or magnetic nanoparticles), as shown in Fig. 17.7.

The use of pre-formulated molecules will protect them from gelling environment that, in case of chemical HGs, might be aggressive. However, the principal reason for using pre-formulated molecules is that of controlling their release from the HG. In fact, hydrophilic polymer networks share in general fast releases due to their high water content. With this in mind, several combinations may be proposed. One could use free and encapsulated molecules to obtain release both at short and longer times. One could also combine, in the same HG, different molecules that have been pre-formulated with different microencapsulation systems when multiple releases and different release profiles are needed. In addition, nothing excludes that colloidal carriers may be part of the HG; in fact, appropriately functionalized particles that entrap desired molecule(s) may be physically or chemically cross-linked with polymer chains. This solution may be advantageous to avoid concerns related with the release of the entire colloidal system from the HG.

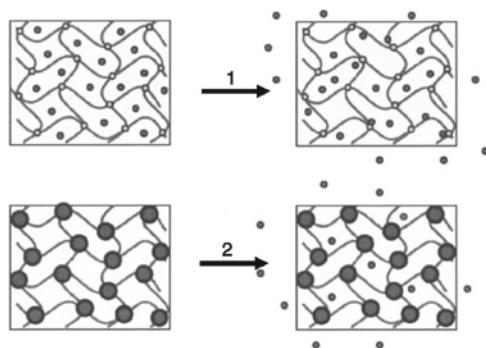


Fig. 17.7 Schematic representation of drug-loaded HGs. (1) When a drug is directly entrapped in a HG, it is free to move outward the gel. In contrast, (2) if it is entrapped in a pre-encapsulated formulations, and colloidal particles linked to HG, drug would need first to diffuse from the particle into the gel, and then from the gel to the surroundings

In this paragraph a short digression is made to present a special case of drug delivery system and to distinguish tissue engineering devices from cell-based devices. In fact, another way to deliver desired molecules is that of encapsulating those cells that are able to produce them. In this case, a biotechnological drug delivery device whose function is not regenerative but substitutive will be obtained. These devices are generally produced *in vitro* and then implanted *in vivo*, and have been used as artificial pancreas, artificial liver, or to deliver molecules useful for the treatment of CNS diseases and tumors (Yasuhara and Date 2007; Nakama et al. 2006; Orive et al. 2006; Bloch et al. 2006; Haque et al. 2005; Bjerkvig et al. 2003; Emerich and Salzberg 2001; Davalli et al. 2000). Maybe in the future, it would be possible to engineer those cell phenotypes needed for regenerative scopes to have a controllable switch that allow them to produce specific cytokines/growth factors on command, thus overcoming all delivery issues.

Nanotechnological aspects may be found on previously mentioned HG properties that could be used to control the localized delivery of entrapped drugs, and on the choice and properties of supplemental colloidal carriers that could be added to the HG. Metallic (Murthy et al. 2008; Bikram et al. 2007; Thomas et al. 2007; Wang et al. 2005) and/or magnetic particles (Hu et al. 2007; Frimpong et al. 2007; Nayak and Lyon 2005; Satarkar and Hilt 2008), carbon nanotubes (Kawaguchi et al. 2006; Joshi et al. 2005; Kovtyukhova et al. 2003), and quantum dots (Liedl et al. 2007; Sirpal et al. 2007) alone² or entrapped in polymeric microspheres (or related colloidal particles) are lately receiving a great attention, and are believed to fulfill expected nanotechnological advances. For instance, it has been shown that carbon nanotubes may act as gelators and corresponding gels as redox-based biosensors. Using magnetic nanoparticles, instead, it has been possible to modify gel nano-porosity depending on magnetic field, and who knows what other discoveries are awaiting for our future studies!

²References proposed in this sentence refer to nanomaterials that have been directly incorporated into HGs.

17.4 Major Issues of Injectable Materials in Tissue Engineering

General issues of HG-based materials are weak mechanical properties, difficulty in handling, and cell adhesion. While mechanical properties have been attempted to be modified by acting on the degree of HG reticulation or by using mixtures of polymers and strengtheners (Prestwich et al. 2006), difficulties in handling can be solved with the development of injectable formulations that gel *in vivo*. Moreover, cell adhesion, when needed, may be increased by introducing positive charges or peptidyl adhesive sequences (e.g., RGD, YIGSR) in the polymer chains (Hern and Hubbell 1998; Ghosh et al. 2004, 2006; Rizzi and Hubbell 2005; Ehrick et al. 2005; Loh et al. 2001; Burdick and Anseth 2002; Ito et al. 2007; Comisar et al. 2007; Ferreira et al. 2007; Cui et al. 2006; Yeo et al. 2007; Weber et al. 2007; Newman et al. 2006; Santiago et al. 2006; Patel et al. 2005; Li et al. 2005; Yu et al. 1999). Toxicological issues related with the *in vivo* reticulation of chemical HGs have been addressed elsewhere within this chapter.

Other issues, not specifically associated with HG materials, are related with viscosity, sterilizability and product packaging, and will determine how easy would be to prepare a sterile, homogeneous, fully-active formulation in a surgical room during surgical preparation of implant site.

Injectable formulations may be developed as extemporaneous or ready-to-use blends depending on their composition. However, due to their high water content, extemporaneous blends should be preferred for long shelf-life products and for cell-entrapping formulations. At this regard, the easiest way to package injectable formulations would be that of a sterile glass vial containing the lyophilized formulation (to speed dissolution process) that will be reconstituted with sterile water before implantation. If it could not be possible to lyophilize the entire formulation, single components may be lyophilized in different vials, and each single reconstituted fluid added to the syringe that will be used to inject final blend in the body. Once components are dissolved and/or dispersed, cells could be added, and formulations injected. It would be advisable that the entire process of formulation mixing is short, to be easily carried out in the surgical room during patient preparation. It should also be highlighted that ungelled formulations should be neither too viscous nor too little viscous to respectively be manually injectable through small cannulas, thus allowing minimal invasive surgeries, and to avoid or minimize sedimentation of formulation components. Overly viscous blends may require special devices to be injected.

Finally, the other major issue, which, in general, is superficially taken in consideration by university research laboratories, but that makes the difference when one would like to market his/her own product, is the respect of obligatory requisites for injectable/implantable formulations. These are sterility, apyrogenicity, purity, and biocompatibility with human tissues and fluids. It is reminded that some natural and synthetic polymers and proteins cannot be autoclaved if maintenance of native structure is desired, and that polymers may shorten their molecular weight or degrade faster after gamma-rays sterilization. Therefore, sterilization by filtration

of single components or final formulation seems to be a good compromise. In fact, in this case, damage to formulation components may be overcome. In addition, costs of the sterilization process may be decreased since the clean room could be used only for lyophilizing/evaporating filtered solutions of HG components, and for the production of cell dispersions. The concern of pyrogenicity may be considered to be related with a lack in product purity, since pyrogenic materials are contaminated with bacterial endotoxins. This is a problematic issue because pyrogen removal requires materials to be exposed for long times to high temperatures (180°C for 3 h, or 250°C for 30 min). It is therefore necessary to assay and control the level of material bio-burden, or move production to clean rooms thus increasing costs. Finally, for what concern biocompatibility, and beside everything else commented in previous paragraphs, it should not be underestimated that animal-derived natural polymers used to produce HGs may trigger immunogenic responses when implanted in vivo (e.g., collagen versus atelocollagen).

17.5 Conclusions

This chapter has reviewed classical methods of preparation and properties of injectable gelable polymeric materials for tissue engineering applications. Discussion has put in evidence that HGs may be adequately formulated to induce, sustain and/or transmit cellular signaling both to hosting tissues, and potentially encapsulated cells. Soft reticulation methods and environmentally-stimulated gelation are supplemental features allowing in situ production through minimal invasive procedures. Great advances are expected from tailored synthetic projects and from development of hybrid formulations containing nanomaterials, as potential strategies to furnish gelled polymer networks of new properties.

Acknowledgements This work has been supported by MIUR (PRIN 2005, project number: 2005035525) and Fondazione Banco di Sardegna (project number: 2003.0476).

References

- Ahmed TA, Griffith M, Hincke M (2007) Characterization and inhibition of fibrin hydrogel-degrading enzymes during development of tissue engineering scaffolds. *Tissue Eng* 13(7):1469–1477
- Akbuga J, Ozbas-Turan S, Erdogan N (2004) Plasmid-DNA loaded chitosan microspheres for in vitro IL-2 expression. *Eur J Pharm Biopharm* 58(3):501–507
- An YH, Webb D, Gutowska A, Mironov VA, Friedman RJ (2001) Regaining chondrocyte phenotype in thermosensitive gel culture. *Anat Rec* 263(4):336–341
- Andrzejewska E (2001) Photopolymerization kinetics of multifunctional monomers. *Prog Polym Sci* 26(4):605–665
- Anseth KS, Burdick JA (2002) New directions in photopolymerizable biomaterials. *MRS Bull* 27(2):130–136

- Anseth KS, Bowman CN, Brannon-Peppas L (1996) Mechanical properties of hydrogels and their experimental determination. *Biomaterials* 17(17):1647–1657
- Arevalo-Silva CA, Eavey RD, Cao Y, Vacanti M, Weng Y, Vacanti CA (2000) Internal support of tissue-engineered cartilage. *Arch Otolaryngol Head Neck Surg* 126(12):1448–1452
- Arica MY, Bayramoglu G, Arica B, Yalçin E, Ito K, Yagci Y (2005) Novel hydrogel membrane based on copoly(hydroxyethyl methacrylate/p-vinylbenzyl-poly(ethylene oxide)) for biomedical applications: properties and drug release characteristics. *Macromol Biosci* 5(10):983–992
- Arimura H, Ouchi T, Kishida A, Ohya Y (2005) Preparation of a hyaluronic acid hydrogel through polyion complex formation using cationic polylactide-based microspheres as a biodegradable crosslinking agent. *J Biomater Sci Polym Ed* 16(11):1347–1358
- Atala A, Lanza RP (eds) (2002) *Methods in tissue engineering*. Academic, San Diego, CA
- Baroli B (2006) Photopolymerization in drug delivery, tissue engineering and cell encapsulation: issues and potentialities. *J Chem Technol Biotechnol* 81(4):491–499
- Baroli B (2007) Hydrogels for tissue engineering and delivery of tissue-inducing substances. *J Pharm Sci* 96(9):2197–2223
- Baroli B, Shastri VP, Langer R (2003) A method to protect sensitive molecules from a light-induced polymerizing environment. *J Pharm Sci* 92(6):1186–1195
- Bikram M, Gobin AM, Whitmire RE, West JL (2007) Temperature-sensitive hydrogels with SiO₂-Au nanoshells for controlled drug delivery. *J Control Release* 123(3):219–227
- Birla RK, Huang YC, Dennis RG (2007) Development of a novel bioreactor for the mechanical loading of tissue-engineered heart muscle. *Tissue Eng* 13(9):2239–2248
- Bjerkvig R, Read TA, Vajkoczy P, Aebischer P, Pralong W, Platt S, Melvik JE, Hagen A, Dornish M (2003) Cell therapy using encapsulated cells producing endostatin. *Acta Neurochir Suppl* 88:137–141
- Blanco MD, Garcia O, Rosa RM, Teijon JM, Katime I (1996) 5-Fluorouracil release from copolymeric hydrogels of itaconic acid monoester. I. Acrylamide-co-monomethyl itaconate. *Biomaterials* 17(11):1061–1067
- Bloch K, Vorobeychik M, Yavrians K, Azarov D, Bloch O, Vardi P (2006) Improved activity of streptozotocin-selected insulinoma cells following microencapsulation and transplantation into diabetic mice. *Cell Biol Int* 30(2):138–143
- Boland T, Xu T, Damon B, Cui X (2006) Application of inkjet printing to tissue engineering. *Biotechnol J* 1(9):910–917
- Boucard N, Viton C, Domard A (2005) New aspects of the formation of physical hydrogels of chitosan in a hydroalcoholic medium. *Biomacromolecules* 6(6):3227–3237
- Brandl F, Sommer F, Goepferich A (2007) Rational design of hydrogels for tissue engineering: impact of physical factors on cell behavior. *Biomaterials* 28(2):134–146
- Brannon-Peppas L, Peppas NA (1990a) Dynamic and equilibrium swelling behavior of pH-sensitive hydrogels containing 2-hydroxyethyl methacrylate. *Biomaterials* 11(9):635–644
- Brannon-Peppas L, Peppas NA (1990) The equilibrium swelling behavior of porous and non-porous hydrogels. In: Brannon-Peppas L, Harland RS (eds) *Absorbent polymer technology*. Elsevier, Amsterdam, pp 67–102
- Bromberg LE, Ron ES (1998) Temperature-responsive gels and thermogelling polymer matrices for protein and peptide delivery. *Adv Drug Deliv Rev* 31(3):197–221
- Brown CD, Kreilgaard L, Nakakura M, Caram-Lelham N, Pettit DK, Gombotz WR, Hoffman AS (2001) Release of PEGylated granulocyte-macrophage colony-stimulating factor from chitosan/glycerol films. *J Control Release* 72(1–3):35–46
- Bryant SJ, Nuttelman CR, Anseth KS (1999) The effects of crosslinking density on cartilage formation in photocrosslinkable hydrogels. *Biomed Sci Instrum* 35:309–314
- Bryant SJ, Nuttelman CR, Anseth KS (2000) Cytocompatibility of UV and visible light photoinitiating systems on cultured NIH/3T3 fibroblasts in vitro. *J Biomater Sci Polym Ed* 11(5):439–457
- Burdick JA, Anseth KS (2002) Photoencapsulation of osteoblasts in injectable RGD-modified PEG hydrogels for bone tissue engineering. *Biomaterials* 23(22):4315–4323

- Burdick JA, Peterson AJ, Anseth KS (2001) Conversion and temperature profiles during the photoinitiated polymerization of thick orthopaedic biomaterials. *Biomaterials* 22(13):1779–1786
- Burdick JA, Lovestead TM, Anseth KS (2003) Kinetic chain lengths in highly cross-linked networks formed by the photoinitiated polymerization of divinyl monomers: a gel permeation chromatography investigation. *Biomacromolecules* 4(1):149–156
- Canal T, Peppas NA (1989) Correlation between mesh size and equilibrium degree of swelling of polymeric network. *J Biomed Mater Res* 23(10):1183–1193
- Cao YL, Lach E, Kim TH, Rodriguez A, Arevalo CA, Vacanti CA (1998) Tissue-engineered nipple reconstruction. *Plast Reconstr Surg* 102(7):2293–2298
- Cascone MG, Maltinti S, Barbani N, Laus M (1999) Effect of chitosan and dextran on the properties of poly(vinyl alcohol) hydrogels. *J Mater Sci Mater Med* 10(7):431–435
- Causa F, Netti PA, Ambrosio L (2007) A multi-functional scaffold for tissue regeneration: The need to engineer a tissue analogue. *Biomaterials* 28(34):5093–5099
- Chellat F, Tabrizian M, Dumitriu S, Chornet E, Magny P, Rivard CH, Yahia L (2000) In vitro and in vivo biocompatibility of chitosan-xanthan polyionic complex. *J Biomed Mater Res* 51(1):107–116
- Chen JP, Cheng TH (2006) Thermo-responsive chitosan-graft-poly(N-isopropylacrylamide) injectable hydrogel for cultivation of chondrocytes and meniscus cells. *Macromol Biosci* 6(12):1026–1039
- Chen J, Jo S, Park K (1997) Degradable hydrogels. In: Domb AJ, Kost J, Wiseman DM (eds) *Handbook of biodegradable polymers*. Overseas Publishers Association, Amsterdam, pp 203–230
- Chen S, Pieper R, Webster DC, Singh J (2005) Triblock copolymers: synthesis, characterization, and delivery of a model protein. *Int J Pharm* 288(2):207–218
- Chen YM, Tanaka M, Gong JP, Yasuda K, Yamamoto S, Shimomura M, Osada Y (2007) Platelet adhesion to human umbilical vein endothelial cells cultured on anionic hydrogel scaffolds. *Biomaterials* 28(10):1752–1760
- Cheng SY, Heilman S, Wasserman M, Archer S, Shuler ML, Wu M (2007) A hydrogel-based microfluidic device for the studies of directed cell migration. *Lab Chip* 7(6):763–739
- Chenite A, Chaput C, Wang D, Combes C, Buschmann MD, Hoemann CD, Leroux JC, Atkinson BL, Binette F, Selmani A (2000) Novel injectable neutral solutions of chitosan form biodegradable gels in situ. *Biomaterials* 21(21):2155–2161
- Chinen N, Tanihara M, Nakagawa M, Shinozaki K, Yamamoto E, Mizushima Y, Suzuki Y (2003) Action of microparticles of heparin and alginate crosslinked gel when used as injectable artificial matrices to stabilize basic fibroblast growth factor and induce angiogenesis by controlling its release. *J Biomed Mater Res A* 67(1):61–68
- Cho BC, Kim JY, Lee JH, Chung HY, Park JW, Roh KH, Kim GU, Kwon IC, Jang KH, Lee DS, Park NW, Kim IS (2004) The bone regenerative effect of chitosan microsphere-encapsulated growth hormone on bony consolidation in mandibular distraction osteogenesis in a dog model. *J Craniofac Surg* 15(2):299–311; discussion 312–333
- Cho JH, Kim SH, Park KD, Jung MC, Yang WI, Han SW, Noh JY, Lee JW (2004b) Chondrogenic differentiation of human mesenchymal stem cells using a thermosensitive poly(N-isopropylacrylamide) and water-soluble chitosan copolymer. *Biomaterials* 25(26):5743–5751
- Choi S, Kim SW (2003) Controlled release of insulin from injectable biodegradable triblock copolymer depot in ZDF rats. *Pharm Res* 20(12):2008–2010
- Choi SH, Yoon JJ, Park TG (2002) Galactosylated poly(N-isopropylacrylamide) hydrogel submicrometer particles for specific cellular uptake within hepatocytes. *J Colloid Interface Sci* 251(1):57–63
- Chua KH, Aminuddin BS, Fuzina NH, Ruzymah BH (2005) Insulin-transferrin-selenium prevent human chondrocyte dedifferentiation and promote the formation of high quality tissue engineered human hyaline cartilage. *Eur Cell Mater* 9:58–67; discussion 67
- Clark RAF (2007) Special Issue, Natural and artificial cellular microenvironments for soft tissue repair. *Adv Drug Deliv Rev* 59(13):1291–1292

- Comisar WA, Kazmers NH, Mooney DJ, Linderman JJ (2007) Engineering RGD nanopatterned hydrogels to control preosteoblast behavior: a combined computational and experimental approach. *Biomaterials* 28(30):4409–4417
- Cortiella J, Nichols JE, Kojima K, Bonassar LJ, Dargon P, Roy AK, Vacant MP, Niles JA, Vacanti CA (2006) Tissue-engineered lung: an in vivo and in vitro comparison of polyglycolic acid and pluronic F-127 hydrogel/somatic lung progenitor cell constructs to support tissue growth. *Tissue Eng* 12(5):1213–1225
- Couvreur P, Barratt G, Fattal E, Legrand P, Vauthier C (2002) Nanocapsule technology: a review. *Crit Rev Ther Drug Carrier Syst* 19(2):99–134
- Cruise GM, Hegre OD, Scharp DS, Hubbell JA (1998) A sensitivity study of the key parameters in the interfacial photopolymerization of the poly(ethylene glycol) diacrylate upon porcine islets. *Biotechnol Bioeng* 57(6):655–665
- Cruise GM, Hegre OD, Lamberti FV, Hager SR, Hill R, Scharp DS, Hubbell JA (2000) *In vitro* and *in vivo* performance of porcine islets encapsulated in interfacially photopolymerized poly(ethylene glycol) diacrylate membranes. *Cell Transplant* 8(3):293–306
- Cui FZ, Tian WM, Hou SP, Xu QY, Lee IS (2006) Hyaluronic acid hydrogel immobilized with RGD peptides for brain tissue engineering. *J Mater Sci Mater Med* 17(12):1393–1401
- Daronch M, Rueggeberg FA, Hall G, De Goes MF (2007) Effect of composite temperature on in vitro intrapulpal temperature rise. *Dent Mater* 23(10):1283–1288
- Davalli AM, Galbiati F, Bertuzzi F, Polastri L, Pontiroli AE, Perego L, Freschi M, Pozza G, Folli F, Meoni C (2000) Insulin-secreting pituitary GH3 cells: a potential beta-cell surrogate for diabetes cell therapy. *Cell Transplant* 9(6):841–851
- De Laporte L, Shea LD (2007) Matrices and scaffolds for DNA delivery in tissue engineering. *Adv Drug Deliv Rev* 59(4–5):292–307
- De Rosa M, Carteni M, Petillo O, Calarco A, Margarucci S, Rosso F, De Rosa A, Farina E, Grippo P, Peluso G (2004) Cationic polyelectrolyte hydrogel fosters fibroblast spreading, proliferation, and extracellular matrix production: Implications for tissue engineering. *J Cell Physiol* 198(1):133–143
- De Wijn JR, van Mullem PJ (1990) In: Williams D (ed) *Concise encyclopedia of medical and dental materials*. MIT, Cambridge, pp 14–21
- Delgado JJ, Evora C, Sanchez E, Baro M, Delgado A (2006) Validation of a method for non-invasive in vivo measurement of growth factor release from a local delivery system in bone. *J Control Release* 114(2):223–229
- Desai NP, Hubbell JA (1989) The short-term blood biocompatibility of poly(hydroxyethyl methacrylate-co-methyl methacrylate) in an in vitro flow system measured by digital videomicroscopy. *J Biomater Sci Polym Ed* 1(2):123–146
- Desmangles AI, Jordan O, Marquis-Weible F (2001) Interfacial photopolymerization of beta-cell clusters: approaches to reduce coating thickness using ionic and lipophilic dyes. *Biotechnol Bioeng* 72(6):634–641
- Díez-Peña E, Quijada-Garrido I, Barales-Rienda JM (2002) Hydrogen-bonding effects on the dynamic swelling of P(N-iPAAm-co-MAA) copolymers. A case of autocatalytic swelling kinetics. *Macromolecules* 35(23):8882–8888
- Ding K, Alemdaroglu FE, Börsch M, Berger R, Herrmann A (2007) Engineering the structural properties of DNA block copolymer micelles by molecular recognition. *Angew Chem Int Ed* 46(7):1172–1175
- Dobie K, Smith G, Sloan AJ, Smith AJ (2002) Effects of alginate hydrogels and TGF-beta 1 on human dental pulp repair in vitro. *Connect Tissue Res* 43(2–3):387–390
- Dodla MC, Bellamkonda RV (2006) Anisotropic scaffolds facilitate enhanced neurite extension in vitro. *J Biomed Mater Res A* 78(2):213–221
- Dodla MC, Bellamkonda RV (2008) Differences between the effect of anisotropic and isotropic laminin and nerve growth factor presenting scaffolds on nerve regeneration across long peripheral nerve gaps. *Biomaterials* 29(1):33–46
- Duncan AC, Sefton MV, Brash JL (1997) Effect of C4-, C8- and C18-alkylation of poly(vinyl alcohol) hydrogels on the adsorption of albumin and fibrinogen from buffer and plasma: limited correlation with platelet interactions. *Biomaterials* 18(24):1585–1592

- Dunne NJ, Orr JF (2002) Curing characteristics of acrylic bone cement. *J Mater Sci Mater Med* 13(1):17–22
- Duvvuri S, Janoria KG, Mitra AK (2005) Development of a novel formulation containing poly(d, l-lactide-co-glycolide) microspheres dispersed in PLGA-PEG-PLGA gel for sustained delivery of ganciclovir. *J Control Release* 108(2–3):282–293
- Ehrick JD, Deo SK, Browning TW, Bachas LG, Madou MJ, Daunert S (2005) Genetically engineered protein in hydrogels tailors stimuli-responsive characteristics. *Nat Mater* 4(4):298–302
- Elisseeff J, Anseth K, Sims D, McIntosh W, Randolph M, Langer R (1999) Transdermal photopolymerization for minimally invasive implantation. *Proc Natl Acad Sci USA* 96(6):3104–3107
- Emerich DF, Salzberg HC (2001) Update on immunoisolation cell therapy for CNS diseases. *Cell Transplant* 10(1):3–24
- Fedorovich NE, Alblas J, de Wijn JR, Hennink WE, Verbout AJ, Dhert WJ (2007) Hydrogels as extracellular matrices for skeletal tissue engineering: state-of-the-art and novel application in organ printing. *Tissue Eng* 13(8):1905–1925
- Ferreira LS, Gerecht S, Fuller J, Shieh HF, Vunjak-Novakovic G, Langer R (2007) Bioactive hydrogel scaffolds for controllable vascular differentiation of human embryonic stem cells. *Biomaterials* 28(17):2706–2717
- Flory PJ (1950) Statistical mechanics of swelling of network structure. *J Chem Phys* 18(1):108–111
- Flory PJ (1953) Principles of polymer chemistry. Cornell University Press, Ithaca, NY
- Flory PJ, Rehner J (1943a) Statistical mechanics of cross-linked polymer networks. I. Rubberlike elasticity. *J Chem Phys* 11(11):512–520
- Flory PJ, Rehner J (1943b) Statistical mechanics of cross-linked polymer networks. II. Swelling. *J Chem Phys* 11(11):521–526
- Flory PJ, Rabjohn N, Schaffer MC (1949) Dependence of elastic properties of vulcanized rubber on the degree of cross linking. *J Polym Sci* 4(3):225–245
- Frimpong RA, Fraser S, Hilt JZ (2007) Synthesis and temperature response analysis of magnetic-hydrogel nanocomposites. *J Biomed Mater Res A* 80(1):1–6
- Furth ME, Atala A, Van Dyke ME (2007) Smart biomaterials design for tissue engineering and regenerative medicine. *Biomaterials* 28(34):5068–5073
- Gajewiak J, Cai S, Shu XZ, Prestwich GD (2006) Aminoxy pluronics: synthesis and preparation of glycosaminoglycan adducts. *Biomacromolecules* 7(6):1781–1789
- Gazit E (2007) Self-assembled peptide nanostructures: the design of molecular building blocks and their technological utilization. *Chem Soc Rev* 36(8):1263–1269
- Gehrke SH, Fisher JP, Palasis M, Lund ME (1997) Factors determining hydrogel permeability. *Ann N Y Acad Sci* 831:179–207
- Gemmell CH, Black JP, Yeo EL, Sefton MV (1996) Material-induced up-regulation of leukocyte CD11b during whole blood contact: material differences and a role for complement. *J Biomed Mater Res* 32(1):29–35
- Ghosh K, Liu Y, Palumbo FS, Luo Y, Clark RA, Prestwich GD (2004) Attachment and spreading of fibroblasts on an RGD peptide-modified injectable hyaluronan hydrogel. *J Biomed Mater Res A* 68(2):365–375
- Ghosh K, Ren XD, Shu XZ, Prestwich GD, Clark RA (2006) Fibronectin functional domains coupled to hyaluronan stimulate adult human dermal fibroblast responses critical for wound healing. *Tissue Eng* 12(3):601–613
- Giavaresi G, Torricelli P, Fornasari PM, Giardino R, Barbucci R, Leone G (2005) Blood vessel formation after soft-tissue implantation of hyaluronan-based hydrogel supplemented with copper ions. *Biomaterials* 26(16):3001–3008
- Gil ES, Frankowski DJ, Spontak RJ, Hudson SM (2005) Swelling behavior and morphological evolution of mixed gelatin/silk fibroin hydrogels. *Biomacromolecules* 6(6):3079–3087
- Goodner MD, Bowman CN (2002) Development of a comprehensive free radical photopolymerization model incorporating heat and mass transfer effects in thick films. *Chem Eng Sci* 57(5):887–900

- Gu Z, Alexandridis P (2005) Drying of films formed by ordered poly(ethylene oxide)-poly(propylene oxide) block copolymer gels. *Langmuir* 21(5):1806–1817
- Gu ZQ, Xiao JM, Zhang XH (1998) The development of artificial articular cartilage-PVA-hydrogel. *Biomed Mater Eng* 8(2):75–81
- Gu F, Amsden B, Neufeld R (2004) Sustained delivery of vascular endothelial growth factor with alginate beads. *J Control Release* 96(3):463–472
- Guenet JM (1992) Thermoreversible gelation of polymers and biopolymers. Academic, London
- Gunatillake PA, Adhikari R (2003) Biodegradable synthetic polymers for tissue engineering. *Eur Cell Mater* 5:1–16
- Guo T, Zhao J, Chang J, Ding Z, Hong H, Chen J, Zhang J (2006) Porous chitosan-gelatin scaffold containing plasmid DNA encoding transforming growth factor-beta1 for chondrocytes proliferation. *Biomaterials* 27(7):1095–1103
- Gupta V, Grande-Allen KJ (2006) Effects of static and cyclic loading in regulating extracellular matrix synthesis by cardiovascular cells. *Cardiovasc Res* 72(3):375–383
- Gwak SJ, Bhang SH, Kim IK, Kim SS, Cho SW, Jeon O, Yoo KJ, Putnam AJ, Kim BS (2008) The effect of cyclic strain on embryonic stem cell-derived cardiomyocytes. *Biomaterials* 29(7):844–856
- Hahn MS, Teply BA, Stevens MM, Zeitel SM, Langer R (2006) Collagen composite hydrogels for vocal fold lamina propria restoration. *Biomaterials* 27(7):1104–1109
- Haque T, Chen H, Ouyang W, Martoni C, Lawuyi B, Urbanska AM, Prakash S (2005) In vitro study of alginate-chitosan microcapsules: an alternative to liver cell transplants for the treatment of liver failure. *Biotechnol Lett* 27(5):317–322
- Hari PR, Ajithkumar B, Sharma CP (1993) Hydrogen grafted polymer surfaces: interaction and morphology of platelets. *J Biomater Appl* 8(2):174–182
- Hassan CM, Peppas NA (2000) Structure and morphology of freeze/thawed PVA hydrogels. *Macromolecules* 33(7):2472–2479
- He X, Jabbari E (2007) Material properties and cytocompatibility of injectable MMP degradable poly(lactide ethylene oxide fumarate) hydrogel as a carrier for marrow stromal cells. *Biomacromolecules* 8(3):780–792
- Hennink WE, van Nostrum CF (2002) Novel crosslinking methods to design hydrogels. *Adv Drug Deliv Rev* 54(1):13–16
- Hern DL, Hubbell JA (1998) Incorporation of adhesion peptides into nonadhesive hydrogels useful for tissue resurfacing. *J Biomed Mater Res* 39(2):266–276
- Hill E, Boonthekul T, Mooney DJ (2006) Designing scaffolds to enhance transplanted myoblast survival and migration. *Tissue Eng* 12(5):1295–1304
- Hoffman AS (2002) Hydrogels for biomedical applications. *Adv Drug Deliv Rev* 54(1):3–12
- Holland TA, Mikos AG (2006) Biodegradable polymeric scaffolds. Improvements in bone tissue engineering through controlled drug delivery. *Adv Biochem Eng Biotechnol* 102:161–185
- Holland TA, Tessmar JK, Tabata Y, Mikos AG (2004) Transforming growth factor-beta 1 release from oligo(poly(ethylene glycol) fumarate) hydrogels in conditions that model the cartilage wound healing environment. *J Control Release* 94(1):101–114
- Hollister SJ (2005) Porous scaffold design for tissue engineering. *Nat Mater* 4(7):518–524. Erratum in: *Nat Mater* 5(7):590 (2006)
- Hong Y, Mao Z, Wang H, Gao C, Shen J (2006) Covalently crosslinked chitosan hydrogel formed at neutral pH and body temperature. *J Biomed Mater Res* 79(4):913–922
- Hong H, McCullough CM, Stegemann JP (2007) The role of ERK signaling in protein hydrogel remodeling by vascular smooth muscle cells. *Biomaterials* 28(26):3824–3833
- Hosseinkhani H, Hosseinkhani M, Tian F, Kobayashi H, Tabata Y (2006) Ectopic bone formation in collagen sponge self-assembled peptide-amphiphile nanofibers hybrid scaffold in a perfusion culture bioreactor. *Biomaterials* 27(29):5089–5098
- Hsieh CY, Hsieh HJ, Liu HC, Wang DM, Hou LT (2006) Fabrication and release behavior of a novel freeze-gelled chitosan/gamma-PGA scaffold as a carrier for rhBMP-2. *Dent Mater* 22(7):622–629
- Hu SH, Liu TY, Liu DM, Chen SY (2007) Nano-ferrosponges for controlled drug release. *J Control Release* 121(3):181–189

- Hubbell JA (1996) Hydrogel systems for barriers and local drug delivery in the control of wound healing. *J Control Release* 39(2):305–313
- Hutmacher DW, Goh JC, Teoh SH (2001) An introduction to biodegradable materials for tissue engineering applications. *Ann Acad Med Singapore* 30(2):183–191
- Ilkhanizadeh S, Teixeira AI, Hermanson O (2007) Inkjet printing of macromolecules on hydrogels to steer neural stem cell differentiation. *Biomaterials* 28(27):3936–3943
- Ishihara K, Aragaki R, Ueda T, Watanabe A, Nakabayashi N (1990) Reduced thrombogenicity of polymers having phospholipid polar groups. *J Biomed Mater Res* 24(8):1069–1077
- Ito A, Akiyama H, Kawabe Y, Kamihira M (2007) Magnetic force-based cell patterning using Arg-Gly-Asp (RGD) peptide-conjugated magnetite cationic liposomes. *J Biosci Bioeng* 104(4):288–293
- Jefferis CD, Lee AJC, Ling RSM (1975) Thermal aspects of self-curing poly(methyl methacrylate). *J Bone Joint Surg* 57B:511–518
- Jeong B, Bae YH, Kim SW (2000a) In situ gelation of PEG-PLGA-PEG triblock copolymer aqueous solutions and degradation thereof. *J Biomed Mater Res* 50(2):171–177
- Jeong B, Bae YH, Kim SW (2000b) Drug release from biodegradable injectable thermosensitive hydrogel of PEG-PLGA-PEG triblock copolymers. *J Control Release* 63(1–2):155–163
- Jeong B, Kim SW, Bae YH (2002) Thermosensitive sol-gel reversible hydrogels. *Adv Drug Deliv Rev* 54(1):37–51
- Jeong JH, Kim S, Park TG (2004) Biodegradable triblock copolymer of PLGA-PEG-PLGA enhances gene transfection efficiency. *Pharm Res* 21(1):50–54
- Johnson PM, Stansbury JW, Bowman CN (2007) Photopolymer kinetics using light intensity gradients in high-throughput conversion analysis. *Polymer* 48(21):6319–6324
- Joshi PP, Merchant SA, Wang Y, Schmidtke DW (2005) Amperometric biosensors based on redox polymer-carbon nanotube-enzyme composites. *Anal Chem* 77(10):3183–3188
- Karageorgiou V, Kaplan D (2005) Porosity of 3D biomaterial scaffolds and osteogenesis. *Biomaterials* 26(27):5474–5491
- Karande TS, Ong JL, Agrawal CM (2004) Diffusion in musculoskeletal tissue engineering scaffolds: design issues related to porosity, permeability, architecture, and nutrient mixing. *Ann Biomed Eng* 32(12):1728–1743
- Kawaguchi M, Fukushima T, Hayakawa T, Nakashima N, Inoue Y, Takeda S, Okamura K, Taniguchi K (2006) Preparation of carbon nanotube-alginate nanocomposite gel for tissue engineering. *Dent Mater J* 25(4):719–725
- Khademhosseini A, Langer R (2007) Microengineered hydrogels for tissue engineering. *Biomaterials* 28(34):5087–5092
- Khare AR, Peppas NA (1995) Swelling/deswelling of anionic copolymer gels. *Biomaterials* 16(7):559–567
- Kidoaki S, Matsuda T (2008) Microelastic gradient gelatinous gels to induce cellular mechanotaxis. *J Biotechnol* 133(2):225–230
- Kierszenbaum AL (2002) Histology and cell biology. An introduction to pathology. Mosby, St. Louis, MO
- Kim S, Healy KE (2003) Synthesis and characterization of injectable poly(N-isopropylacrylamide-co-acrylic acid) hydrogels with proteolytically degradable cross-links. *Biomacromolecules* 4(5):1214–1223
- Kim S, Chung EH, Gilbert M, Healy KE (2005) Synthetic MMP-13 degradable ECMs based on poly(N-isopropylacrylamide-co-acrylic acid) semi-interpenetrating polymer networks. I. Degradation and cell migration. *J Biomed Mater Res A* 75(1):73–88
- Kimura M, Fukumoto K, Watanabe J, Ishihara K (2004) Hydrogen-bonding-driven spontaneous gelation of water-soluble phospholipid polymers in aqueous medium. *J Biomater Sci Polym Ed* 15(5):631–644
- Kimura M, Fukumoto K, Watanabe J, Takai M, Ishihara K (2005) Spontaneously forming hydrogel from water-soluble random- and block-type phospholipid polymers. *Biomaterials* 26(34):6853–6862
- Kimura M, Takai M, Ishihara K (2007) Biocompatibility and drug release behavior of spontaneously formed phospholipid polymer hydrogels. *J Biomed Mater Res A* 80(1):45–54

- Kirkpatrick CJ, Fuchs S, Hermanns MI, Peters K, Unger RE (2007) Cell culture models of higher complexity in tissue engineering and regenerative medicine. *Biomaterials* 28(34):5193–5198
- Ko HC, Milthorpe BK, McFarland CD (2007) Engineering thick tissues – the vascularisation problem. *Eur Cell Mater* 14:1–18; discussion 18–19
- Konno T, Ishihara K (2007) Temporal and spatially controllable cell encapsulation using a water-soluble phospholipid polymer with phenylboronic acid moiety. *Biomaterials* 28(10):1770–1777
- Kopeček J (2007) Hydrogel biomaterials: A smart future? *Biomaterials* 28(34):5185–5192
- Kovtyukhova NI, Mallouk TE, Pan L, Dickey EC (2003) Individual single-walled nanotubes and hydrogels made by oxidative exfoliation of carbon nanotube ropes. *J Am Chem Soc* 125(32):9761–9769
- Kretsinger JK, Haines LA, Ozbas B, Pochan DJ, Schneider JP (2005) Cytocompatibility of self-assembled beta-hairpin peptide hydrogel surfaces. *Biomaterials* 26(25):5177–5186
- Kúdela V (1989) In: Kroschwitz JI (ed) *Polymers: biomaterials and medical applications*. Wiley, New York, pp 228–252
- Kwon YM, Kim SW (2004) Biodegradable triblock copolymer microspheres based on thermosensitive sol-gel transition. *Pharm Res* 21(2):339–343
- Kwon IK, Matsuda T (2006) Photo-iniferter-based thermoresponsive block copolymers composed of poly(ethylene glycol) and poly(N-isopropylacrylamide) and chondrocyte immobilization. *Biomaterials* 27(7):986–995
- Lal H, Verma SK, Smith M, Guleria RS, Lu G, Foster DM, Dostal DE (2007) Stretch-induced MAP kinase activation in cardiac myocytes: differential regulation through beta1-integrin and focal adhesion kinase. *J Mol Cell Cardiol* 43(2):137–147
- Langer R, Vacanti JP (1993) Tissue engineering. *Science* 260(5110):920–926
- Langer R, Vacanti JP (1995) Artificial organs. *Sci Am* 273(3):130–133
- Langer RS, Vacanti JP (1999) Tissue engineering: the challenges ahead. *Sci Am* 280(4):86–89
- Lao UL, Sun M, Matsumoto M, Mulchandani A, Chen W (2007) Genetic engineering of self-assembled protein hydrogel based on elastin-like sequences with metal binding functionality. *Biomacromolecules* 8(12):3736–3739
- Lee KY, Peters MC, Anderson KW, Mooney DJ (2000a) Controlled growth factor release from synthetic extracellular matrices. *Nature* 408(6815):998–1000
- Lee YM, Park YJ, Lee SJ, Ku Y, Han SB, Klokkevold PR, Chung CP (2000b) The bone regenerative effect of platelet-derived growth factor-BB delivered with a chitosan/tricalcium phosphate sponge carrier. *J Periodontol* 71(3):418–424
- Lee JY, Nam SH, Im SY, Park YJ, Lee YM, Seol YJ, Chung CP, Lee SJ (2002) Enhanced bone formation by controlled growth factor delivery from chitosan-based biomaterials. *J Control Release* 78(1–3):187–197
- Lee PY, Li Z, Huang L (2003) Thermosensitive hydrogel as a Tgf-beta1 gene delivery vehicle enhances diabetic wound healing. *Pharm Res* 20(12):1995–2000
- Lee JE, Kim KE, Kwon IC, Ahn HJ, Lee SH, Cho H, Kim HJ, Seong SC, Lee MC (2004) Effects of the controlled-released TGF-beta 1 from chitosan microspheres on chondrocytes cultured in a collagen/chitosan/glycosaminoglycan scaffold. *Biomaterials* 25(18):4163–4173
- Lévesque SG, Shoichet MS (2007) Synthesis of enzyme-degradable, peptide-cross-linked dextran hydrogels. *Bioconjug Chem* 18(3):874–885
- Li Z, Ning W, Wang J, Choi A, Lee PY, Tyagi P, Huang L (2003) Controlled gene delivery system based on thermosensitive biodegradable hydrogel. *Pharm Res* 20(6):884–888
- Li F, Griffith M, Li Z, Tanodekaew S, Sheardown H, Hakim M, Carlsson DJ (2005) Recruitment of multiple cell lines by collagen-synthetic copolymer matrices in corneal regeneration. *Biomaterials* 26(16):3093–3104
- Li AA, Shen F, Zhang T, Cironi P, Potter M, Chang PL (2006) Enhancement of myoblast microencapsulation for gene therapy. *J Biomed Mater Res B Appl Biomater* 77(2):296–306
- Liao IC, Wan AC, Yim EK, Leong KW (2005) Controlled release from fibers of polyelectrolyte complexes. *J Control Release* 104(2):347–358
- Liedl T, Dietz H, Yurke B, Simmel F (2007) Controlled trapping and release of quantum dots in a DNA-switchable hydrogel. *Small* 3(10):1688–1693

- Lim SH, Liao IC, Leong KW (2006) Nonviral gene delivery from nonwoven fibrous scaffolds fabricated by interfacial complexation of polyelectrolytes. *Mol Ther* 13(6):1163–1172
- Lin CC, Metters AT (2006) Hydrogels in controlled release formulations: network design and mathematical modeling. *Adv Drug Deliv Rev* 58(12–13):1379–1408
- Lin DC, Yurke B, Langrana NA (2004) Mechanical properties of a reversible, DNA-crosslinked polyacrylamide hydrogel. *J Biomech Eng* 126(1):104–110
- Lin WC, Yu DG, Yang MC (2006) Blood compatibility of novel poly(γ -glutamic acid)/polyvinyl alcohol hydrogels. *Colloids Surf B Biointerfaces* 47(1):43–49
- Liu L, Ratner BD, Sage EH, Jiang S (2007) Endothelial cell migration on surface-density gradients of fibronectin, VEGF, or both proteins. *Langmuir* 23(22):11168–11173
- Liu H, Wang C, Gao Q, Liu X, Tong Z (2008) Fabrication of novel core-shell hybrid alginate hydrogel beads. *Int J Pharm* 351(1–2):104–112
- Llanos GR, Sefton MV (1992) Heparin-poly(ethylene glycol)-poly(vinyl alcohol) hydrogel: preparation and assessment of thrombogenicity. *Biomaterials* 13(7):421–424
- Llanos GR, Sefton MV (1993) Immobilization of poly(ethylene glycol) onto a poly(vinyl alcohol) hydrogel: 2. Evaluation of thrombogenicity. *J Biomed Mater Res* 27(11):1383–1391
- Loh NK, Woerly S, Bunt SM, Wilton SD, Harvey AR (2001) The regrowth of axons within tissue defects in the CNS is promoted by implanted hydrogel matrices that contain BDNF and CNTF producing fibroblasts. *Exp Neurol* 170(1):72–84
- Lovell LG, Newman SM, Bowman CN (1999) The effects of light intensity, temperature, and comonomer composition on the polymerization behavior of dimethacrylate dental resins. *Dent Res* 78(8):1469–1476
- Lundskog J (1972) Heat and bone tissue. *Scand J Plast Reconstr Surg Suppl* 9:1–80
- Lustig SR, Peppas NA (1988) Solute diffusion in swollen membranes. 9. Scaling laws for solute diffusion in gels. *J Appl Polym Sci* 36:735–747
- Lutolf MP, Weber FE, Schmoekel HG, Schense JC, Kohler T, Müller R, Hubbell JA (2003a) Repair of bone defects using synthetic mimetics of collagenous extracellular matrices. *Nat Biotechnol* 21(5):513–518
- Lutolf MP, Lauer-Fields JL, Schmoekel HG, Metters AT, Weber FE, Fields GB, Hubbell JA (2003b) Synthetic matrix metalloproteinase-sensitive hydrogels for the conduction of tissue regeneration: engineering cell-invasion characteristics. *Proc Natl Acad Sci USA* 100(9):5413–5418
- Makino K, Hiyoshi J, Ohshima H (2001) Effects of thermosensitivity of poly(N-isopropylacrylamide) hydrogel upon the duration of a lag phase at the beginning of drug release from the hydrogel. *Colloids Surf B Biointerfaces* 20(4):341–346
- Martina M, Hutmacher DW (2007) Biodegradable polymers applied to tissue engineering research: a review. *Polym Int* 56(2):145–157
- Mathews DT, Birney YA, Cahill PA, McGuinness GB (2008) Vascular cell viability on polyvinyl alcohol hydrogels modified with water-soluble and -insoluble chitosan. *J Biomed Mater Res B Appl Biomater* 84(2):531–540
- Mayer C (2005) Nanocapsules as drug delivery systems. *Int J Artif Organs* 28(11):1163–1171
- Mequanint K, Patel A, Bezuidenhout D (2006) Synthesis, swelling behavior, and biocompatibility of novel physically cross-linked polyurethane-block-poly(glycerol methacrylate) hydrogels. *Biomacromolecules* 7(3):883–891
- Michalakakis K, Pissiotis A, Hirayama H, Kang K, Kafantaris N (2006) Comparison of temperature increase in the pulp chamber during the polymerization of materials used for the direct fabrication of provisional restorations. *J Prosthet Dent* 96(6):418–423
- Mierisch CM, Cohen SB, Jordan LC, Robertson PG, Balian G, Diduch DR (2002) Transforming growth factor-beta in calcium alginate beads for the treatment of articular cartilage defects in the rabbit. *Arthroscopy* 18(8):892–900
- Milam VT, Hiddessen AL, Crocker JC, Graves DJ, Hammer DA (2003) DNA-driven assembly of biodisperse, micron-sized colloids. *Langmuir* 19(24):10317–10323
- Milella E, Barra G, Ramires PA, Leo G, Aversa P, Romito A (2001) Poly(L-lactide)acid/alginate composite membranes for guided tissue regeneration. *J Biomed Mater Res* 57(2):248–257

- Miralles G, Baudoin R, Dumas D, Baptiste D, Hubert P, Stoltz JF, Dellacherie E, Mainard D, Netter P, Payan E (2001) Sodium alginate sponges with or without sodium hyaluronate: in vitro engineering of cartilage. *J Biomed Mater Res* 57(2):268–278
- Mirkin CA, Letsinger RL, Mucic RC, Storhoff JJ (1996) A DNA-based method for rationally assembling nanoparticles into macroscopic materials. *Nature* 382(6592):607–609
- Miyata T, Asami N, Uragami T (1999) A reversibly antigen-responsive hydrogel. *Nature* 399(6738):766–769
- Mizuno K, Yamamura K, Yano K, Osada T, Saeki S, Takimoto N, Sakurai T, Nimura Y (2003) Effect of chitosan film containing basic fibroblast growth factor on wound healing in genetically diabetic mice. *J Biomed Mater Res A* 64(1):177–181
- Moffatt S, Cristiano RJ (2006) PEGylated J591 mAb loaded in PLGA-PEG-PLGA tri-block copolymer for targeted delivery: in vitro evaluation in human prostate cancer cells. *Int J Pharm* 317(1):10–13
- Moss JA, Stokols S, Hixon MS, Ashley FT, Chang JY, Janda KD (2006) Solid-phase synthesis and kinetic characterization of fluorogenic enzyme-degradable hydrogel cross-linkers. *Biomacromolecules* 7(4):1011–1016
- Murakami Y, Maeda M (2005) DNA-responsive hydrogels that can shrink or swell. *Biomacromolecules* 6(6):2927–2929
- Murakami Y, Yokoyama M, Okano T, Nishida H, Tomizawa Y, Endo M, Kurosawa H (2007) A novel synthetic tissue-adhesive hydrogel using a crosslinkable polymeric micelle. *J Biomed Mater Res A* 80(2):421–427
- Murthy PS, Murali Mohan Y, Varaprasad K, Sreedhar B, Mohana Raju K (2008) First successful design of semi-IPN hydrogel-silver nanocomposites: a facile approach for antibacterial application. *J Colloid Interface Sci* 318(2):217–224
- Nagahara S, Matsuda T (1996) Hydrogel formation via hybridization of oligonucleotides derivatized in water-soluble vinyl polymers. *Polym Gels Netw* 4(2):111–127
- Nair LS, Laurencin CT (2006) Polymers as biomaterials for tissue engineering and controlled drug delivery. *Adv Biochem Eng Biotechnol* 102:47–90
- Nakama H, Ohsugi K, Otsuki T, Date I, Kosuga M, Okuyama T, Sakuragawa N (2006) Encapsulation cell therapy for mucopolysaccharidosis type VII using genetically engineered immortalized human amniotic epithelial cells. *Tohoku J Exp Med* 209(1):23–32
- Nayak S, Lyon LA (2005) Soft nanotechnology with soft nanoparticles. *Angew Chem Int Ed Engl* 44(47):7686–7708
- Nelson EW, Jacobs JL, Scranton AB, Anseth KS, Bowman CN (1995) Photo-differential scanning calorimetry studies of cationic polymerization of divinyl ethers. *Polymer* 36(24):4651–4656
- Nerem RM (2007) Cell-based therapies: from basic biology to replacement, repair, and regeneration. *Biomaterials* 28(34):5074–5077
- Neumann MG, Schmitt CC, Ferreira GC, Corrêa IC (2006) The initiating radical yields and the efficiency of polymerization for various dental photoinitiators excited by different light curing units. *Dent Mater* 22(6):576–584
- Newman KD, McLaughlin CR, Carlsson D, Li F, Liu Y, Griffith M (2006) Bioactive hydrogel-filament scaffolds for nerve repair and regeneration. *Int J Artif Organs* 29(11):1082–1091
- Nguyen KT, West JL (2002) Photopolymerizable hydrogels for tissue engineering applications. *Biomaterials* 23(22):4307–4314
- Noushi F, Richardson RT, Hardman J, Clark G, O’Leary S (2005) Delivery of neurotrophin-3 to the cochlea using alginate beads. *Otol Neurotol* 26(3):528–533
- Novamatrix™, Norway (November 16, 2007) <https://www.novamatrix.biz/default.asp?KategoriID=4&SubKategoriID=19&ArtikelID=57>
- Odian G (1991) Principles of polymerization. Wiley, New York
- Oh KS, Han SK, Choi YW, Lee JH, Lee JY, Yuk SH (2004) Hydrogen-bonded polymer gel and its application as a temperature-sensitive drug delivery system. *Biomaterials* 25(12):2393–2398
- Ohya S, Nakayama Y, Matsuda T (2001) Thermoresponsive artificial extracellular matrix for tissue engineering: hyaluronic acid bioconjugated with poly(N-isopropylacrylamide) grafts. *Biomacromolecules* 2(3):856–863

- Orive G, Tam SK, Pedraz JL, Hallé JP (2006) Biocompatibility of alginate-poly-L-lysine microcapsules for cell therapy. *Biomaterials* 27(20):3691–3700
- Ozbas-Turan S, Akbuga J, Aral C (2002) Controlled release of interleukin-2 from chitosan microspheres. *J Pharm Sci* 91(5):1245–1251
- Paek HJ, Campaner AB, Kim JL, Aaron RK, Ciombor DM, Morgan JR, Lysaght MJ (2005) In vitro characterization of TGF-beta1 release from genetically modified fibroblasts in Ca(2+)-alginate microcapsules. *ASAIO J* 51(4):379–384
- Pagoria D, Lee A, Geurtsen W (2005) The effect of camphorquinone (CQ) and CQ-related photosensitizers on the generation of reactive oxygen species and the production of oxidative DNA damage. *Biomaterials* 26(19):4091–4099
- Park JH, Kwon S, Nam JO, Park RW, Chung H, Seo SB, Kim IS, Kwon IC, Jeong SY (2004a) Self-assembled nanoparticles based on glycol chitosan bearing 5beta-cholanic acid for RGD peptide delivery. *J Control Release* 95(3):579–588
- Park Y, Lutolf MP, Hubbell JA, Hunziker EB, Wong M (2004b) Bovine primary chondrocyte culture in synthetic matrix metalloproteinase-sensitive poly(ethylene glycol)-based hydrogels as a scaffold for cartilage repair. *Tissue Eng* 10(3–4):515–522
- Park H, Temenoff JS, Holland TA, Tabata Y, Mikos AG (2005) Delivery of TGF-beta1 and chondrocytes via injectable, biodegradable hydrogels for cartilage tissue engineering applications. *Biomaterials* 26(34):7095–7103
- Park YJ, Kim KH, Lee JY, Ku Y, Lee SJ, Min BM, Chung CP (2006) Immobilization of bone morphogenetic protein-2 on a nanofibrous chitosan membrane for enhanced guided bone regeneration. *Biotechnol Appl Biochem* 43(Pt 1):17–24
- Patel PN, Gobin AS, West JL, Jr Patrick CW (2005) Poly(ethylene glycol) hydrogel system supports preadipocyte viability, adhesion, and proliferation. *Tissue Eng* 11(9–10):1498–1505
- Peirce SM, Price RJ, Skalak TC (2004) Spatial and temporal control of angiogenesis and arterIALIZATION using focal applications of VEGF164 and Ang-1. *Am J Physiol Heart Circ Physiol* 286(3):H918–H925
- Peppas NA (1986) *Hydrogel in medicine and pharmacy*. CRC, Boca Raton, FL
- Peppas NA, Colombo P (1997) Analysis of drug release behavior from swellable polymer carriers using the dimensionality index. *J Control Release* 45(1):35–40
- Peppas NA, Merrill EW (1976) Poly(vinyl alcohol) hydrogels – reinforcement of radiation-crosslinked networks by crystallization. *J Polym Sci [A1]* 14:441–457
- Peppas NA, Merrill EW (1977) Crosslinked poly(vinyl alcohol) hydrogels as swollen elastic networks. *J Appl Polym Sci* 21:1763–1770
- Peppas NA, Bures P, Leobandung W, Ichikawa H (2000a) Hydrogels in pharmaceutical formulations. *Eur J Pharm Biopharm* 50(1):27–46
- Peppas NA, Huang Y, Torres-Lugo M, Ward JH, Zhang J (2000b) Physicochemical foundations and structural design of hydrogels in medicine and biology. *Annu Rev Biomed Eng* 2:9–29
- Peters MC, Isenberg BC, Rowley JA, Mooney DJ (1998) Release from alginate enhances the biological activity of vascular endothelial growth factor. *J Biomater Sci Polym Ed* 9(12):1267–1278
- Petrini P, Tanzi MC, Moran CR, Graham NB (1999) Linear poly(ethylene oxide)-based polyurethane hydrogels: polyurethane-ureas and polyurethane-amides. *J Mater Sci Mater Med* 10(10/11):635–639
- Pişkin E (2002) Biodegradable polymeric matrices for bioartificial implants. *Int J Artif Organs* 25(5):434–440
- Pişkin E (2004) Molecularly designed water soluble, intelligent, nanosize polymeric carriers. *Int J Pharm* 277(1–2):105–118
- Plunkett KN, Berkowski KL, Moore JS (2005) Chymotrypsin responsive hydrogel: application of a disulfide exchange protocol for the preparation of methacrylamide containing peptides. *Biomacromolecules* 6(2):632–637
- Prestwich GD, Shu XZ, Liu Y, Cai S, Walsh JF, Hughes CW, Ahmad S, Kirker KR, Yu B, Orlandi RR, Park AH, Thibeault SL, Duflo S, Smith ME (2006) Injectable synthetic extracellular matrices for tissue engineering and repair. *Adv Exp Med Biol* 585:125–133

- Qiao M, Chen D, Ma X, Liu Y (2005) Injectable biodegradable temperature-responsive PLGA-PEG-PLGA copolymers: synthesis and effect of copolymer composition on the drug release from the copolymer-based hydrogels. *Int J Pharm* 294(1–2):103–112
- Qiu Y, Park K (2001) Environment-sensitive hydrogels for drug delivery. *Adv Drug Deliv Rev* 53(3):321–339
- Quick DJ, Anseth KS (2003) Gene delivery in tissue engineering: a photopolymer platform to coencapsulate cells and plasmid DNA. *Pharm Res* 20(11):1730–1737
- Raeber GP, Lutolf MP, Hubbell JA (2005) Molecularly engineered PEG hydrogels: a novel model system for proteolytically mediated cell migration. *Biophys J* 89(2):1374–1388
- Ratner BD, Hoffman AS, Whiffen JD (1978) The thrombogenicity of radiation grafted polymers as measured by the vena cava ring test. *J Bioeng* 2(3–4):313–323
- Raymond J, Metcalfe A, Desfaits AC, Ribourtout E, Salazkin I, Gilmartin K, Embry G, Boock RJ (2003) Alginate for endovascular treatment of aneurysms and local growth factor delivery. *AJNR Am J Neuroradiol* 24(6):1214–1221
- Rizzi SC, Hubbell JA (2005) Recombinant protein-co-PEG networks as cell-adhesive and proteolytically degradable hydrogel matrixes. Part I: Development and physicochemical characteristics. *Biomacromolecules* 6(3):1226–1238
- Rokstad AM, Holtan S, Strand B, Steinkjer B, Ryan L, Kulseng B, Skjak-Braek G, Espevik T (2002) Microencapsulation of cells producing therapeutic proteins: optimizing cell growth and secretion. *Cell Transplant* 11(4):313–324
- Ruszymah BH, Chua K, Latif MA, Hussein FN, Saim AB (2005) Formation of in vivo tissue engineered human hyaline cartilage in the shape of a trachea with internal support. *Int J Pediatr Otorhinolaryngol* 69(11):1489–1495
- Saim AB, Cao Y, Weng Y, Chang CN, Vacanti MA, Vacanti CA, Eavey RD (2000) Engineering autogenous cartilage in the shape of a helix using an injectable hydrogel scaffold. *Laryngoscope* 110(10 Pt 1):1694–1697
- Santiago LY, Nowak RW, Peter Rubin J, Marra KG (2006) Peptide-surface modification of poly(caprolactone) with laminin-derived sequences for adipose-derived stem cell applications. *Biomaterials* 27(15):2962–2969
- Satarkar NS, Hilt JZ (2008) Hydrogel nanocomposites as remote-controlled biomaterials. *Acta Biomater* 4(1):11–16
- ESB Satellite Consensus Conference (2005) Proceedings of “19th European Conference on Biomaterials”
- Schneider JP, Pochan DJ, Ozbas B, Rajagopal K, Pakstis L, Kretsinger J (2002) Responsive hydrogels from the intramolecular folding and self-assembly of a designed peptide. *J Am Chem Soc* 124(50):15030–15037
- Segura T, Anderson BC, Chung PH, Webber RE, Shull KR, Shea LD (2005) Crosslinked hyaluronic acid hydrogels: a strategy to functionalize and pattern. *Biomaterials* 26(4):359–371
- Seliktar D, Zisch AH, Lutolf MP, Wrana JL, Hubbell JA (2004) MMP-2 sensitive, VEGF-bearing bioactive hydrogels for promotion of vascular healing. *J Biomed Mater Res A* 68(4):704–716
- Shen F, Li AA, Cornelius RM, Cirone P, Childs RF, Brash JL, Chang PL (2005) Biological properties of photocrosslinked alginate microcapsules. *J Biomed Mater Res B Appl Biomater* 75(2):425–434
- Silverstein RM, Bassler GC, Morrill TC (1991) Spectrometric identification of organic compounds, 5th edn. Wiley, New York
- Simmons CA, Alsberg E, Hsiung S, Kim WJ, Mooney DJ (2004) Dual growth factor delivery and controlled scaffold degradation enhance in vivo bone formation by transplanted bone marrow stromal cells. *Bone* 35(2):562–569
- Sirpal S, Gattás-Asfura KM, Leblanc RM (2007) A photodimerization approach to crosslink and functionalize microgels. *Colloids Surf B Biointerfaces* 58(2):116–120

- Sosnik A, Sefton MV (2006) Methylation of poloxamine for enhanced cell adhesion. *Biomacromolecules* 7(1):331–338
- Starr FW, Sciortino F (2006) Model for assembly and gelation of four-armed DNA dendrimers. *J Phys-Condens Mat* 18(26):L347–L353
- Stile RA, Healy KE (2002) Poly(N-isopropylacrylamide)-based semi-interpenetrating polymer networks for tissue engineering applications. 1. Effects of linear poly(acrylic acid) chains on phase behavior. *Biomacromolecules* 3(3):591–600
- Strzinar I, Sefton MV (1992) Preparation and thrombogenicity of alkylated polyvinyl alcohol coated tubing. *J Biomed Mater Res* 26(5):577–592
- Sylvén C (2002) Angiogenic gene therapy. *Drugs Today* 38(12):819–827
- Tanahashi K, Mikos AG (2003) Protein adsorption and smooth muscle cell adhesion on biodegradable agmatine-modified poly(propylene fumarate-co-ethylene glycol) hydrogels. *J Biomed Mater Res A* 67(2):448–457
- Tanaka S, Ogura A, Kaneko T, Murata Y, Akashi M (2004) Adhesion behavior of peritoneal cells on the surface of self-assembled triblock copolymer hydrogels. *Biomacromolecules* 5(6):2447–2455
- Tarle Z, Knezevic A, Demoli N, Meniga A, Sutalo J, Unterbrink G, Ristic M, Pichler G (2006) Comparison of composite curing parameters: effects of light source and curing mode on conversion, temperature rise and polymerization shrinkage. *Oper Dent* 31(2):219–226
- Tessmar JK, Göpferich AM (2007) Matrices and scaffolds for protein delivery in tissue engineering. *Adv Drug Deliv Rev* 59(4–5):274–291
- The Merriam-Webster online dictionary (November 15, 2007); <http://www.m-w.com>
- Thomas J, Lowman A, Marcolongo M (2003) Novel associated hydrogels for nucleus pulposus replacement. *J Biomed Mater Res A* 67(4):1329–1337
- Thomas V, Yallapu MM, Sreedhar B, Bajpai SK (2007) A versatile strategy to fabricate hydrogel-silver nanocomposites and investigation of their antimicrobial activity. *J Colloid Interface Sci* 315(1):389–395
- Tilakaratne HK, Hunter SK, Andracki ME, Benda JA, Rodgers VG (2007) Characterizing short-term release and neovascularization potential of multi-protein growth supplement delivered via alginate hollow fiber devices. *Biomaterials* 28(1):89–98
- Trudel J, Massia SP (2002) Assessment of the cytotoxicity of photocrosslinked dextran and hyaluronan-based hydrogels to vascular smooth muscle cells. *Biomaterials* 23(16):3299–3307
- Truffier-Boutry D, Demoustier-Champagne S, Devaux J, Biebuyck JJ, Mestdagh M, Larbanois P, Leloup G (2006) A physico-chemical explanation of the post-polymerization shrinkage in dental resins. *Dent Mater* 22(5):405–412
- Uludag H, De Vos P, Tresco PA (2000) Technology of mammalian cell encapsulation. *Adv Drug Deliv Rev* 42(1–2):29–64
- Um SH, Lee JB, Kwon SY, Umbach CC, Luo D (2006) Enzyme-catalyzed assembly of DNA hydrogel. *Nat Mater* 5(10):797–801
- Vacanti JP, Langer R (1999) Tissue engineering: the design and fabrication of living replacement devices for surgical reconstruction and transplantation, *Lancet* 354(Suppl 1):SI32–34
- Vermette P, Gengenbach T, Divisekera U, Kambouris PA, Griesser HJ, Meagher L (2003) Immobilization and surface characterization of NeutrAvidin biotin-binding protein on different hydrogel interlayers. *J Colloid Interface Sci* 259(1):13–26
- Vogelin E, Baker JM, Gates J, Dixit V, Constantinescu MA, Jones NF (2006) Effects of local continuous release of brain derived neurotrophic factor (BDNF) on peripheral nerve regeneration in a rat model. *Exp Neurol* 199(2):348–353
- Wang C, Stewart RJ, Kopecek J (1999) Hybrid hydrogels assembled from synthetic polymers and coiled-coil protein domains. *Nature* 397(6718):417–420
- Wang X, Haasch RT, Bohn PW (2005) Anisotropic hydrogel thickness gradient films derivatized to yield three-dimensional composite materials. *Langmuir* 21(18):8452–8459

- Wang M, Li Y, Wu J, Xu F, Zuo Y, Jansen JA (2008) In vitro and in vivo study to the biocompatibility and biodegradation of hydroxyapatite/poly(vinyl alcohol)/gelatin composite. *J Biomed Mater Res A* 85(2):418–426
- Wathier M, Johnson CS, Kim T, Grinstaff MW (2006) Hydrogels formed by multiple peptide ligation reactions to fasten corneal transplants. *Bioconjug Chem* 17(4):873–876
- Webb AR, Yang J, Ameer GA (2004) Biodegradable polyester elastomers in tissue engineering. *Expert Opin Biol Ther* 4(6):801–812
- Weber LM, Hayda KN, Haskins K, Anseth KS (2007) The effects of cell-matrix interactions on encapsulated beta-cell function within hydrogels functionalized with matrix-derived adhesive peptides. *Biomaterials* 28(19):3004–3011
- Weinand C, Pomerantseva I, Neville CM, Gupta R, Weinberg E, Madisch I, Shapiro F, Abukawa H, Troulis MJ, Vacanti JP (2006) Hydrogel-beta-TCP scaffolds and stem cells for tissue engineering bone. *Bone* 38(4):555–563
- Williams DF (1999) *The Williams dictionary of biomaterials*. Liverpool University Press, Liverpool
- Williams CG, Malik AN, Kim TK, Manson PN, Elisseeff JH (2005) Variable cytocompatibility of six cell lines with photoinitiators used for polymerizing hydrogels and cell encapsulation. *Biomaterials* 26(11):1211–1218
- Wu JY, Liu SQ, Heng PW, Yang YY (2005) Evaluating proteins release from, and their interactions with, thermosensitive poly (N-isopropylacrylamide) hydrogels. *J Control Release* 102(2):361–372
- Xu C, Kopeček J (2008) Genetically engineered block copolymers: Influence of the length and structure of the coiled-coil blocks on hydrogel self-assembly. *Pharm Res* 25(3):674–682
- Xu C, Breedveld V, Kopecek J (2005) Reversible hydrogels from self-assembling genetically engineered protein block copolymers. *Biomacromolecules* 6(3):1739–1749
- Xue L, Greisler HP (2003) Biomaterials in the development and future of vascular grafts. *J Vasc Surg* 37(2):472–480
- Yamamoto T, Nakamura T, Iida H, Kawanabe K, Matsuda Y, Ido K, Tamura J, Senaha Y (1998) Development of bioactive bone cement and its clinical applications. *Biomaterials* 19(16):1479–1482
- Yang J, Xu C, Wang C, Kopecek J (2006) Refolding hydrogels self-assembled from N-(2-hydroxypropyl)methacrylamide graft copolymers by antiparallel coiled-coil formation. *Biomacromolecules* 7(4):1187–1195
- Yasuhara T, Date I (2007) Intracerebral transplantation of genetically engineered cells for Parkinson's disease: toward clinical application. *Cell Transplant* 16(2):125–132
- Yeo Y, Geng W, Ito T, Kohane DS, Burdick JA, Radisic M (2007) Photocrosslinkable hydrogel for myocyte cell culture and injection. *J Biomed Mater Res B Appl Biomater* 81(2):312–322
- Yoo MK, Kweon HY, Lee KG, Lee HC, Cho CS (2004) Preparation of semi-interpenetrating polymer networks composed of silk fibroin and poloxamer macromer. *Int J Biol Macromol* 34(4):263–270
- Yu X, Dillon GP, Bellamkonda RB (1999) A laminin and nerve growth factor-laden three-dimensional scaffold for enhanced neurite extension. *Tissue Eng* 5(4):291–304
- Zachos TA, Shields KM, Bertone AL (2006) Gene-mediated osteogenic differentiation of stem cells by bone morphogenetic proteins-2 or -6. *J Orthop Res* 24(6):1279–1291
- Zelzer M, Majani R, Bradley JW, Rose FR, Davies MC, Alexander MR (2008) Investigation of cell-surface interactions using chemical gradients formed from plasma polymers. *Biomaterials* 29(2):172–184
- Zhang Y, Cheng X, Wang J, Wang Y, Shi B, Huang C, Yang X, Liu T (2006a) Novel chitosan/collagen scaffold containing transforming growth factor-beta1 DNA for periodontal tissue engineering. *Biochem Biophys Res Commun* 344(1):362–369
- Zhang X, Yu C, Xushi S, Zhang C, Tang T, Dai K (2006b) Direct chitosan-mediated gene delivery to the rabbit knee joints in vitro and in vivo. *Biochem Biophys Res Commun* 341(1):202–208

Chapter 18

Polyelectrolyte Complexes as Smart Nanoengineered Systems for Biotechnology and Gene Delivery

Vladimir A. Izumrudov

Abstract Preparation and properties of water-soluble non-stoichiometric polyelectrolyte complexes are described. It is demonstrated that the data accumulated on studying kinetics and equilibrium of competitive reactions in solutions of the complexes form a basis for the development of stimuli responsive polyelectrolyte systems that are used for (bio)separation, gene delivery, immunoassay, design of (oligomeric) enzymes with controlled thermoaggregation and thermostability, preparation of ultrathin multilayered polyelectrolyte films and hollow capsules, creation of artificial chaperones.

Keywords (Bio)Polyelectrolyte complexes • Competitive interpolyelectrolyte reactions • Self-assembly and self-adjusted phenomena • Selectivity and molecular recognition • Controlled phase separations • Stimuli responsive systems

18.1 Introduction

Scaffolds serve a central role in many tissue engineering and regenerative medicine strategies by providing the means to control the local environment (De Laporte and Shea 2007). Scaffolds have been fabricated from a range of natural and synthetic materials, with biodegradable materials being desirable to avoid a second surgical procedure. Scaffolds have also been employed as controlled release vehicles that can maintain therapeutic concentrations of diffusible tissue inductive factors (Langer 1998, 2001; Salvay and Shea 2006). Gene therapy approaches can be employed to increase the expression of above factors or block the expression of

V.A. Izumrudov (✉)

Polymer Chemistry Department, Moscow State University, Leninskiye Gory,
Moscow 119991, Russia

factors that would inhibit tissue formation (Pannier and Shea 2004). Direct gene delivery from a scaffold enables localized transgene expression primarily to the implant site. The scaffold-based delivery has the potential to maintain effective levels of the vector for prolonged times providing the sustained release formulations that can compensate for vectors lost due to clearance or degradation. Additionally, scaffold can protect the vector from attack by immune responses or limiting degradation by serum nucleases or proteases (Roy et al. 2003).

Nucleic acids (e.g., DNA, RNA, siRNA) can be delivered alone, or packaged using viral or nonviral vectors. For delivery, vectors must evade the immune system and be transported to the cell microenvironment for internalization, typically into an endosome, from which the vector must escape prior to being degraded as the endosome transitions into a lysosome. Viral vectors are composed of either DNA or RNA surrounded by a capsid, which provides greater efficiency than nonviral vectors yet provokes an immune response that can lead to clearance of the vector or infected cells (Medzhitov and Janeway 2002; Yang et al. 1994). Although nonviral vectors are less efficient than viral vectors, they are easier to prepare and display high gene complexation capabilities. Most often, nonviral vectors are positively charged peptides or polymers that are commonly named polycations. Nucleic acids are condensed with cationic polymers to decrease particle size, protect the nucleic acid from degradation, create a less negative particle relative to naked plasmid to promote interaction with negatively charged cell membranes, and facilitate endosomal release via the proton sponge effect (De Laporte et al. 2006).

Viral and nonviral vectors interact with polymeric biomaterials through non-specific mechanisms, including hydrophobic, electrostatic, and van der Waals interactions that have been well-characterized for adsorption and release of proteins from polymeric systems (Norde and Lyklema 1991). Thus, the non-specific interactions between plasmid and a collagen matrix were promoted by modifying the collagen with cationic polypeptide poly-L-lysine (Cohen-Sacks et al. 2002). DNA has been encapsulated with either natural or synthetic polycations to form micro- and nanospheres, porous scaffolds and hydrogels for sustained DNA release (Storrie and Mooney 2006). Among numerous polycations, cationic soluble polysaccharides are considered as attractive supports for tissue formation and nonviral gene vectors since they are nontoxic, biodegradable, and can be modified for improved physicochemical properties. In particular, cationic polysaccharide DEAE-pullulan was successfully used as a gene vector and as a 3D-cationic matrix for transfection (San Juan et al. 2007a). This approach may be useful to design implantable biochemical devices for gene therapy *in vivo*.

More recently, vectors have been immobilized in polyelectrolyte multilayers (PEMs) on surfaces using a technique termed polyelectrolyte layer-by-layer deposition. Nanoscale multilayer films are created with alternating layers of negatively charged plasmid and positively charged polymers that are deposited on materials such as stainless steel stents (Hammond 2004; Jewell et al. 2005, 2006; Zhang et al. 2004). Tissue development can often be characterized as occurring in sequential phases, with differential gene expression between the different phases. The strategy of multilayer films formation could have one vector close to the material that would

be released after different vectors located at the exterior (Wood et al. 2006; Zhang et al. 2007). This type of coating offers the possibility for either simultaneous or sequential interfacial delivery of different DNA molecules aimed at cell transfection (Jessel et al. 2006). Mixed architectures made of PEMs and hydrolysable polymeric layers could act as coating which allows body to induce a time scheduled cascade of biological activities (Garza et al. 2005).

In comparison to conventional coating methods, the multilayer films are easy to prepare from different pairs of oppositely charged components that could be both commonly-used polyelectrolytes and charged biopolymers (e.g., proteins, enzymes, nucleic acids). No special apparatus is required, and nanofilms can be prepared under mild, physiological conditions. The procedure can be performed on the solid of any shape (Zhu et al. 2004), and PEMs retain their biological activity after storage as dry material. These very flexible systems are feasible for use in medicine, e.g., for the development of implants, drug delivery and tissue engineering. The embedding of bioactive molecules in the multilayer architectures not only anchors them irreversibly on the biomaterial, but also presents the possibility to control of their activity (Chluba et al. 2001). PEMs coated with poly(styrenesulfonate) (PSS) layer constitute a good microenvironment at the material-cell interface for HCS-2/8 cells (Vautier et al. 2002). The same approach was used for the development of biocompatible coatings for bone implants (Tryoen-Toth et al. 2002). Highly ionically reticulated multilayer films attracted cells, whereas weakly ionically cross-linked multilayers, which swell substantially under physiological conditions, resisted fibroblast attachment (Mendelsohn et al. 2003). On the surfaces of most hydrophobic multilayer films, the A7r5 cells adhered, spread, and exhibited little indication of motility, whereas on the most hydrophilic surfaces, the cells adhered poorly (Salloum et al. 2005). The use of the multilayer films as the cell adhesive substrates was neither accompanied by induced cytotoxic effects nor altered the phenotype of the endothelial cells, whereas the initial cell attachment was enhanced as compared to the polyelectrolyte monolayer (Boura et al. 2003). The revealed ability of PEMs to encourage neuron-like cells attachment greatly simplifies neuronal culture methodology and enables neuronal investigations in new environments (Forry et al. 2006). The study of protein structure has inspired the design of polypeptide multilayer films and pointed out new opportunities for technology development, e.g. coatings for medical implant devices, scaffolds for tissue engineering, coating for targeted drug delivery, artificial cells for oxygen therapeutics, and artificial viruses for immunization (Haynie et al. 2006).

The stability and cell adhesion properties of PEMs can be modulated by the degree of chemical reticulation (Richert et al. 2004a, 2006). The greater spreading of smooth muscle cells occurred on the stiffer films (Richert et al. 2004b). For cross-linked PEMs, the Young's modulus can be varied over two orders of magnitude that drastically change the adhesion and spreading of human chondrosarcoma cells (Schneider et al. 2006). Cross-linked PEMs are still biodegradable, which make them interesting candidates for biomedical applications. The results reported by Schneider et al. (2007) prove that it is possible to design multifunctional films that combine mechanical resistance, biodegradability, and bioactive properties into

a single multilayer architecture. Elasticity of the multilayer films with weak polyelectrolyte as one of the component can be also varied over several order of magnitude. The attachment and proliferation of human microvascular endothelia cells can be regulated by these multilayer substrata (Thompson et al. 2005).

Layer-by-layer self-assembly technique was successively employed to surface engineer titanium and enhanced its cell biocompatibility that could be important for fabrication of titanium-based implant surfaces (Cai et al. 2005). The expanded poly(tetrafluoroethylene) surface modified with PEMs facilitated attachment of the cells and their function showing promise of the treatment for synthetic small-diameter vascular grafts (Moby et al. 2007). To improve adhesion and spreading of the cells, PEMs were built on the surface of poly(dimethylsiloxane) that is widely used in biomedical applications, membrane technology, and microlithography (Kidambi et al. 2007). The ultrathin multilayer films have the potential to assemble extracellular matrix components and may be further functionalized by inclusion of active drugs and proteins to produce tunable biomaterial interfaces (Zhang et al. 2005).

To summarize, the forementioned consideration of the recently reported data on PEMs and gene delivery clearly shows the important role of polyelectrolytes and polyelectrolyte complexes in the current development of tissue engineering and regenerative medicine. It is apparent that for practical implementation, e.g., the desirable surfaces modification by PEMs building or preparing of the appropriate polyelectrolyte nonviral vectors for gene delivery, a detailed knowledge of the factors that could efficiently control the polyelectrolyte systems is required. Accordingly, the accumulated information on polyelectrolyte complexes (PECs) and protein-polyelectrolyte complexes (PPCs) merits consideration (for reviews see Xia and Dubin 1994; Shief and Glatz 1994; Kokufuta 1994; Kabanov 1994; Kabanov and Kabanov 1995, 1998; Izumrudov et al. 1999a). The unique properties of PECs revealed on studies the complex formation, phase behavior, and competitive interpolyelectrolyte reactions in their solutions allow one to regard the complexes as polymer compounds produced as a result of equilibrium reactions with inherent permanent exchange of polyions in water-salt solutions. The capacity of PECs to take part in the competitive reactions that could be rather selective provides self-assembly of the complexes in solutions and ensures behavior of PECs as self-adjusted systems. The important feature of some polyelectrolyte complexes is their ability to dissolve in aqueous solutions and form stimuli responsive polyelectrolyte systems with controlled phase separations. This view on PECs and their properties is fundamental and can be extended to different complexes, specifically DNA-containing PECs and PPCs based on globular proteins, enzymes, antibodies, and conjugates.

This paper summarizes the main properties of PECs and PPCs with special emphasis on the features that are the most important to formulate general principles of interpolyelectrolyte reactions and their potential application in biotechnology, materials science and gene delivery, in particular for development of novel processes and materials in tissue engineering and regenerative medicine. As covered below, these principles could be developed into highly efficient means of isolation and purification of protein and nucleic acids, enhanced immunoassay procedures,

suppression of thermoaggregation of (oligomeric) enzymes, creation of reversibly soluble biocatalysts, multilayer ultrathin films and hollow capsules, artificial chaperones and gene delivery systems.

18.2 Complex Formation and Competitive Reactions in Solutions of Oppositely Charged Polyelectrolytes

18.2.1 *Polyelectrolyte Complexes and Their Properties*

PECs are formed as a result of a cooperative coupling reaction between two oppositely-charged polyions which are characterized by high charge density (for review see Philipp et al. 1989). The degree of conversion in the reaction, Θ , is determined as the ratio of equilibrium number of interpolymer ionic pairs to the ultimate one. In the discussion that follows the systems with Θ close to 1 will be dealt with. If one of the interacting polyelectrolytes is a weak polyion, Θ is controlled by pH. The comparison of experimental dependencies of Θ on pH and pH dependencies of ionization degree of the weak polyelectrolyte indicated that a highly charged component of the PEC could induce charges on a weakly charged partner (for review see Kabanov 1994). It suggests a pronounced widening of pH region corresponding to the existence of PEC as a product of complete interpolyelectrolyte reaction, $\Theta \approx 1$ and increase of a number of polyelectrolyte pairs suitable for preparing of such PECs.

Practical ramification of this finding might be extended to different spheres, e.g. the development of highly efficient bioseparation processes (for review see Izumrudov et al. 1999a), significant improvement of cell transfection by DNA-containing PECs (San Juan et al. 2007b), and construction of stimuli responsive ultrathin multilayer films or nanocapsules (Kharlampieva and Sukhishvili 2003a, b).

PECs possess two main properties that might appear at first sight to be mutually exclusive, i.e. being both rather highly stable and a labile. The lability is manifested by the participation of PECs in interpolyelectrolyte reactions accompanied by a transfer of polyions from one complex to another one. The combination of above properties with selectivity of the cooperative binding provides self-assembly of PECs in solutions and forms the basis for the development of stimuli responsive polyelectrolyte systems.

18.2.1.1 Stability of Polyelectrolyte Complexes

A cooperative character of the multisite binding makes PECs extremely stable with respect to dissociation. The dissociation constant of a polycomplex sharply decreases with increasing oligomer length (Papisov and Litmanovich 1989) and reaches practically zero even for relatively short charged oligomers (Tsuchida and Abe 1982).

The “critical” chain length required to form a stable PEC in aqueous solution slightly varies for different pairs of polyions being four to six repeat units (Tsuchida and Abe 1982; Kabanov 1994). Therefore, after this small “critical” length of polyions is exceeded, their binding becomes apparently irreversible. It implies that the samples of polyions with broad molecular mass distribution also could be put to practical use if PECs are formed by mixing of salt-free water solutions of the components.

Addition of simple salts destroys ion pairs in PECs increasing the “critical” chain length. Thus, concentration of sodium chloride required for complete destruction of PEC formed by relatively long poly(methacrylate) (PMA) anion and poly(N-ethyl-4-vinylpyridinium) (PEVP) polycations of different degree of polymerization (DP) increased drastically with PEVP lengthening up to $DP \approx 100$ and then changed only slightly (Pergushov et al. 1995). The same regularity is inherent in various pairs of polyions, with the only difference in the value of the critical salt concentration. So, in the water–salt media, a practical implementation should be accomplished by PECs consisted of relatively long charged chains, in particular PEVP with $DP > 100$. For the interaction at physiological ionic strength, above requirement is not so rigid, and for the great majority of the polyelectrolyte pairs 20 repeat units proved to be enough for the stable PEC formation.

Stability of PECs is dependent on the nature of the salt added and determined by the affinity of the counter ions to the polyion. With respect to their ability to induce PEC(PMA-PEVP) dissociation, the ions exhibit the orders: $Br^- > Cl^- > F^-$ and $Li^+ > Na^+ > K^+$ (Pergushov et al. 1993). Noteworthy, that substitution of one halide anion with another resulted in much more pronounced change of complex stability and hence, could be a powerful tool for fine tuning and functionalization of the polyion systems, specifically DNA-containing PECs (Izumrudov and Zhiryakova 1999).

18.2.1.2 Soluble Polyelectrolyte Complexes and Competitive Reactions

The discovery of soluble non-stoichiometric PECs (NPECs) (Tsuchida et al. 1972) marked a serious breakthrough in studies of interpolyelectrolyte reactions bringing them to a qualitatively new level. The possibility of soluble NPECs formation, on the other hand, could be undesirable when the complete precipitation of PEC is required, e.g. in the bioseparation processes or on layer-by-layer deposition of oppositely charged polyions that is used for preparing of ultrathin multilayer films and nanocapsules. So, the identification of the conditions of NPECs formation is worth consideration.

Soluble NPECs can be prepared from any pairs of oppositely charged polyions having a wide variety of chemical structures. These data and conditions of NPECs formation are summarized in reviews of Kabanov and Zezin (1982), and Kabanov (1994). A simple and universal method of NPECs preparation is a direct mixing of aqueous solutions of oppositely charged polyelectrolytes taken in non-equivalent proportions in the pH range where they are both fully charged and in the presence of small amounts of a low-molecular-weight electrolyte. The study of water–salt

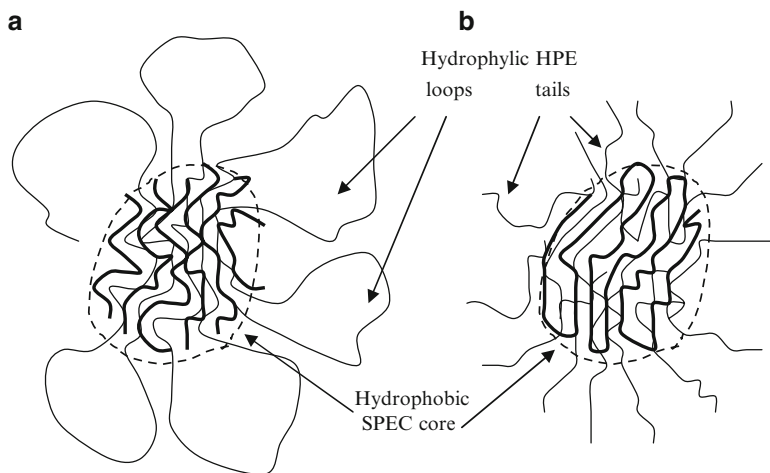
solutions of NPECs by light scattering (Kharenko et al. 1979) evidenced that their molecular mass and size are independent on the way of the complex preparation and comparable with these molecular characteristics of the polymer components. So, the NPECs might be considered as macromolecular compounds that are consisted of a limited number of the electrostatically bound chains (specifically, one relatively long polyanion chain and a number of short chains of the polycation) that corresponds to the composition of the mixture.

Poor electrostatic complementary of the interacting ionene polycations and PSS polyanion has made possible the interpolyelectrolyte exchange followed by the self-assembly of soluble NPEC even in the salt-free media (Tsuchida et al. 1972). Analogously, if the mixing of salt-free aqueous solutions of strongly binding PMA polyanion and PEVP polycation did not result in the soluble NPEC formation due to kinetic restrictions, than in the mixture of PMA with non-complementary half-alkylated PEVP polycation (which contained only a half of positively charged pyridinium units randomly distributed along the chain) the soluble NPEC formed in a matter of minutes regardless the length of the polycations (Izumrudov et al. 1986a). These findings suggest that the decisive factor of kinetics of the exchange is the difference in the arrangement of the charges (or charge density) of the chains rather than a number of ion pairs between polyions.

Local disruptions of the system of the ion pairs could be also achieved by the added low-molecular-weight electrolyte. Studies of kinetics and mechanism of interpolyelectrolyte reactions (Bakeev et al. 1992) evidenced that in salt-free solutions the reactions, as a rule, are kinetically restricted, whereas an addition of even small amount of the salt proved to be enough for systems to reach quickly an equilibrium state characterized by permanent exchange of polyions between NPECs (Izumrudov et al. 1984a).

According to the accepted terminology (Kabanov 1994), soluble NPEC consists of host polyelectrolyte (HPE) and oppositely charged guest polyelectrolyte (GPE). Molar ratio, φ , of GPE and HPE charged units should not exceed a definite critical value, $\varphi = [\text{GPE}]/[\text{HPE}] < \varphi_{cr}$ which is mainly not too different from 0.5. The fragments of HPE and GPE chains, stabilized by ion pairs, form hydrophobic double-stranded sequences that tend to segregate in aqueous solutions in a hydrophobic core. The hydrophilic periphery of NPEC is formed by charged HPE segments sticking out in solution as loops and/or tails.

Negatively charged NPECs of “A” type with relatively long chains of solubilizing host polyanion (Scheme 18.1) are the most extensively studied complexes (for review see Kabanov 1994). Formation of NPEC of “B” type (Izumrudov et al. 1987, 1988) with relatively short host polyanions (Scheme 18.1) is accompanied by unfavorable change of entropy of the system. The shorter HPE chain relative to GPE chain, the more HPE chains should be immobilized to reach the critical molar ratio φ_{cr} providing NPEC solubility and hence, the more is the loss of entropy due to a decrease in a total number of the particles in solution. This has the effect of diminishing the stability of such NPECs in water–salt solutions, reflected by the lowering of critical salt concentration, $[\text{NaCl}]^*$, corresponding to the onset of phase separation with the shortening of HPE chains (Fig. 18.1).



Scheme 18.1 A schematic sketch of structure of water-soluble NPECs with different relationship of a degree of polymerization (DP) of the guest and host components: $DP(\text{HPE}) > DP(\text{GPE})$ (a), and $DP(\text{HPE}) < DP(\text{GPE})$ (b)

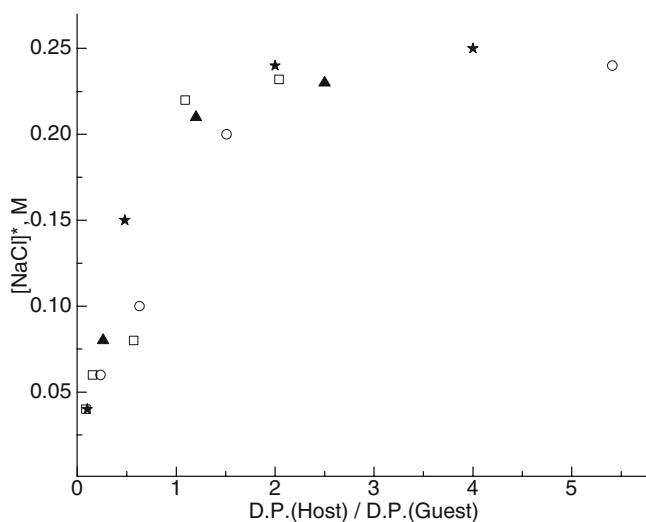


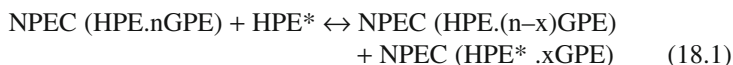
Fig. 18.1 Dependence of critical salt concentration, corresponding to onset of phase separation on the ratio of DP of the components in solution of NPEC formed by host PMA polyanion (*open symbols*) and host hydrolyzed copolymer of divinyl ether and maleic anhydride (DIVEMA) (*filled symbols*) with PEVP polycation of different DP: 900 (*squares*), 560 (*stars*), and 340 (*triangles and circles*). The data are reconstructed from the results reported by Izumrudov et al. (2005a) for DIVEMA-PEVP and Izumrudov et al. (2006) for PMA-PEVP pairs

So, the region of ionic strength wherein the salt concentration is enough to allow exchange of the polymer components but not so high to transform soluble NPEC to the insoluble stoichiometric PEC is narrowed with the shortening of HPE chains. This caused problems in preparation of such NPECs and even led to the mistaken conclusion (Kasaikin et al. 1979; Zezin et al. 1984) about the impossibility to obtain soluble NPECs with $DP(HPE) < DP(GPE)$.

Positively charged NPECs with host polycation were prepared from PMA and PEVP after substitution of bromide counter ions that strongly bound with PEVP polycation for weakly bound fluoride ones (Nefedov et al. 1985). Quite recently, positively charged NPECs of both “A” and “B” type were obtained from host PEVP bromide and guest PMA (Izumrudov et al. 2006). Similarly to negatively charged NPECs, the positively charged NPECs were relatively stable in water–salt solutions at $DP(HPE) > DP(GPE)$, whereas at $DP(HPE) < DP(GPE)$ the shortening of HPE chains was accompanied by the progressive decrease in their solubilizing capacity.

To ensure the complete precipitation of PEC as it is required in some practical applications, the above features of the NPECs should be taken into account. To avoid the PEC solubilization, relatively short polycations or, better still, the polycations with strongly bound Br^- counter ions should be used since an overdose of the host polycations would not lead to formation of soluble NPEC in water–salt media. Analogously, by using the relatively short host polyanions one can rather safely overdose the polyanion.

The solubility of NPECs facilitated the study of competitive reactions that proceed in homogeneous aqueous solutions and imply the competition between different HPE molecules for binding with GPE chains (18.1).



The transfer of GPE chains from the initial NPEC to HPE^* of the same chemical nature as HPE in the NPEC is referred to as the exchange reaction. Otherwise, if HPE and HPE^* have different chemical structures, then the transfer (18.1) is denoted as interpolyelectrolyte substitution reaction.

The position of the equilibrium (18.1) might be quite different, from the uniform distribution of GPE chains between HPE and HPE^* chains of the same length ($x = n/2$) to a highly selective binding of GPE with HPE^* chains ($x \approx n$). The latter case is of primary concern for the design of target drug delivery and self-adjusted systems.

18.2.1.3 Molecular Selectivity

The phenomenon of molecular “recognition” in NPECs solutions and factors leading to the selective binding of polyions are described in reviews of Izumrudov et al. (1991, 1999a). Polycation recognizes and binds polyanion which forms more stable NPEC even if the difference between the free energy changes counted per pair of oppositely charged units is very small.

Thus in solutions containing relatively long and relatively short PMA polyanions, PEVP polycation prefers to bind with the long chains (Izumrudov et al. 1987). Similarly, relatively long polyphosphate anion (PPh) completely displaced PMA chains from NPEC(PMA-PEVP), whereas short PPh chains proved to be impotent to compete with PMA chains for binding with PEVP (Izumrudov et al. 1988).

A minute amount (one group per 400 repeat units) of hydrophobic pyrenyl groups covalently attached to PMA polyanions proved to be enough for PEVP polycation to choose unmistakably the modified polyanions among the unmodified ones and to bind them (Bakeev et al. 1987). This result appears to be rather promising for the development of drug and gene delivery, bioseparation and assay procedures using conjugates of polyions with a small number of antibodies, antigens or antigen determinants.

Introduction of sulfonate (or sulfate) groups in the macromolecule endows the polyanions with the ability to be particularly attractive for polycations. Thus, PEVP polycation recognizes negatively charged polysaccharides with sulfate groups in the chain and blocks such sites (Izumrudov et al. 1999b). This feature might be a key point in the study of structure-function relation of the heparin-like polyanions (Chaubet et al. 2003). The extremely high affinity of polycations to polyanions with a high density of sulfonate (or sulfate) groups in the chains (e.g. potassium poly(vinylsulfate), sodium poly(anetholesulfonate), PSS, heparin) made the polyanions of this family the favorite objects for preparing of multilayer films and capsules, to judge from a great majority of the reported data. On the other hand, this imposes kinetic restrictions on the interpolyelectrolyte exchange and hence, hinders preparation of soluble NPECs from the strongly binding polyanions (Karibyants et al. 1997; Zintchenko et al. 2003). Nevertheless, by proper choice of concentration of the external salt (which could be an order of magnitude higher than in the case of carboxylic or phosphate polyanions) one can minimize the kinetics restrictions and prepare the soluble complexes (Izumrudov et al. 1985). The properties of NPECs of this family (Izumrudov et al. 2006) have much in common with properties of NPECs discussed above. The strongly binding polyanions irreversibly substitute carboxylate or polyphosphate polyanions in their NPECs (Izumrudov et al. 1985; Kabanov et al. 1985) that could be rather attractive for the development of final stage of bioseparation procedure when the quantitative removal (regeneration) of anionic species from the precipitated PECs or PPCs is required. The high affinity of heparin to polyamines was used as a basis for the application of soluble NPEC as a depot for polyamines playing the role of antiheparin agent (Kabanov 1994).

If the difference in affinities of both competitive polyanions to the polycation is not so pronounced, the direction of the substitution reaction can be significantly dependent on the outside conditions.



Thus the equilibrium (18.2) is completely shifted to the right in 0.3 M LiCl, whereas at the same ionic strength but in 0.3 M KCl it is completely shifted to the left being intermediate in 0.3 M NaCl solution (Izumrudov et al. 1988).

At fixed salt concentration, PEVP polycation preferentially bound with PPh anion at lower temperatures and with PMA polyanion at higher temperatures (Izumrudov et al. 1996a). However, the competition of the polyanions for binding with poly(N-methyl-4-vinylpyridinium) polycation (PMVP) is in favor of PPh polyanion, the equilibrium (18.3) is completely shifted to the right in the studied range 5–60°C (Izumrudov et al. 1998).



High selectivity of cooperative interpolyelectrolyte reactions, sensitivity to the change of environmental conditions and a rather high reaction rate define a self-adjustment of the systems. Both formation of the complexes and their transformation following a change of the media are accomplished by the method of trial and errors via interpolyelectrolyte reactions until the equilibrium state is achieved.

This view of polyelectrolyte complexes and their properties is fundamental and quite widespread. The principles of the competitive binding and chain transfer discovered in solutions of NPECs can be extended to the interpolyelectrolyte reactions with the participation of biopolymers and their conjugates.

18.3 DNA-Containing PECs and Their Properties

During the past decade, PECs of polycations with DNA, so-called “polyplexes”, have attracted increasing attention as nonviral vehicles for gene delivery to the cell (for reviews see Kabanov and Kabanov 1995, 1998; Kabanov 1999; Pouton and Seymour 2001; Cho et al. 2003). The prospects for improving the cell transfection have motivated extensive study of polyplexes in order to give a precise control over their stability.

18.3.1 Stability of DNA-Containing Complexes

The capacity of the added cations and anions to dissociate PEC(DNA-PEVP) decreased in the orders $\text{Ca}^{++} > \text{Mg}^{++} \gg \text{Li}^+ > \text{Na}^+ > \text{K}^+$ (Izumrudov et al. 1995a, b, 1996b) and $\text{I}^- > \text{Br}^- > \text{Cl}^- \gg \text{F}^-$ (Izumrudov and Zhiryakova 1999). The similar row $\text{Ca}^{++} \geq \text{Sr}^{++} \gg \text{Li}^+ > \text{Na}^+ \geq \text{K}^+ > \text{Cs}^+$ was reported by Schindler and Nordmeier (1997) for PECs formed by DNA with different quaternized polyamines.

The dependence of the stability of PEC(DNA-PEVP) on PEVP chain length (Izumrudov and Zhiryakova 1999) is a perfect analog to that of PEC(PMA-PEVP) (Pergushov et al. 1995). The critical salt concentration in solutions of both PECs increased sharply with the lengthening of short PEVP polycation up to $\text{DP} \approx 100$ and then goes up only slightly.

The variation in structure of amino groups of the polycations might be a powerful tool in design of PECs with desirable stability. The dissociation of polyplexes

formed by quaternized polyamines is pH-independent and particularly sensitive to the destruction action of the added salt, whereas the primary polyamines form the most stable PECs in a wide pH-region (Izumrudov et al. 2000). The same regularities were revealed on studying DNA complexes with cationic micelles formed by C_{12} surfactants with amino groups of different structure in the “heads” (Izumrudov et al. 2002). The best stability of polyplexes with primary polyamines can be assigned to the most closed contact between the oppositely charged groups in the complex. This assumption was supported by the stabilization of polyplexes formed by different poly(N-alkyl-4-vinylpyridinium) polycations upon the shortening of N-alkyl substituent of the polycation (San Juan et al. 2007b).

The revealed ability of polycations with primary amino groups to form the most stable PECs provides an explanation for the widespread use of primary polyamines, specifically polyallylamine for preparing multilayer films and nanocapsules. Since the invention in the past decade of the layer-by-layer deposition procedure and up to the present day, polyallylamine and PSS has been remaining the most favorable polymer pair for PEMs construction due to the extremely high interpolyelectrolyte interaction that strongly prohibits the polyelectrolyte exchange, and hence, suppresses undesirable formation of the soluble NPEC during the deposition.

The high density of charged phosphate groups that are fixed on a rigid DNA double helix provides the advantages of native DNA over other negatively charged components of the cell in complex formation with polyamines. Rather flexible, complicated and less defined conformation of RNA molecules weakens the electrostatic interaction, and the dissociation of PECs formed by RNA with polyamines is completed at the ionic strength insufficient even for the onset of dissociation of the corresponding insoluble DNA-containing PEC (Wahlund et al. 2003). The specific quantitative precipitation of DNA from DNA/RNA mixtures suggests a simple, cheap, efficient and easy-scaleable method for the large scale purification of DNA, for instance, isolation of plasmids (Wahlund et al. 2004a, b).

18.3.2 *Selectivity of Competitive Reactions in DNA Solutions*

As might be expected from the presence of phosphate groups in both PPh and DNA, competitive reactions in solutions of these polyanions have much in common. Just as the reaction (18.2) with PPh polyanion, the reaction (18.4) proved to be sensitive to the concentration and the nature of the added salt.



The equilibrium (18.4) is significantly shifted to the right in 0.25 M NaCl and completely shifted to the left in 0.25 M LiCl being intermediate in 0.25 M KCl solution (Izumrudov et al. 1996b). This regularity differs from the row $\text{Li}^+ > \text{Na}^+ > \text{K}^+$ revealed for reaction (18.2) with PPh polyanion. The antipodal position of Li^+ in the above series is probably caused by abnormally high affinity of this cation to native DNA.

Denatured DNA interacts with Li^+ without any abnormalities and in solutions of denatured DNA equilibrium (18.4) obeys the expected order $\text{Li}^+ \approx \text{Na}^+ > \text{K}^+$.

Direction of substitution (18.4) is also determined by the degree of polymerization of the components, specifically by the ratio $\psi = \text{DP (PMA)}/\text{DP (PEVP)}$ (Izumrudov et al. 1995b). If NPEC(PMA-PEVP) of “A” type (Scheme 18.1) is used, the equilibrium (18.4) is shifted to the left, whereas in the case of the NPEC of “B” type, the decrease of ψ leads to entropy favorable shift of the equilibrium to the right.

The ability of guest aliphatic n,n -ionene bromides to recognize and bind host DNA or PMA was shown to be determined by either DP of the ionene polycation or a number n of methylene groups between charges in the ionene molecule (Trukhanova et al. 2005). The lengthening of the ionene chains resulted in a steady growth of the selectivity with preferential binding to PMA or DNA of the ionene chains of the higher or the lower charge densities, respectively. Eventually, for the ionenes with relatively high DP = 100, the equilibrium (18.5) was completely shifted to the left in the case of 3,3-ionene, whereas 10,10-ionene bound only DNA.



These findings can serve as groundwork for creation of smart gene delivery vehicles that liberate the cargo DNA upon a change of external conditions at desired surrounding environment.

18.3.3 *Complexing of DNA with Polycations for Cell Transfection*

To bind strongly with negatively charged cell membranes, the vehicle should be oppositely charged. A great majority of cell transfection is carried out by low-density, soluble subpopulations of positively charged DNA-polycation complexes, which is normally only a small part of the total complexed DNA (Eichman et al. 2001). Recently (Zelikin et al. 2002), a close correlation was found between the efficacy of cell transfection by DNA delivered as positively charged PEC and the tolerance of the PEC to the addition of salt. Therefore, the elaborating of strategies for preparing of soluble DNA-containing positively charged NPECs stable at physiological pH and ionic strength is one of the “hottest” areas in the current research.

A huge molecular mass of DNA present a considerable challenge to the experimenters since commonly used polyamines are much shorter than DNA plasmid and hence, form with DNA the positively charged complexes of “B” type (Scheme 18.1) that are particularly sensitive to the added salt. Accordingly, the positively charged NPECs with $\psi \ll 1$ which are formed by relatively short host PEVP with guest DNA (or PMA) undergo phase separation at rather low ionic strength and practically regardless the charge/charge composition $\chi = [\text{GPE}]/[\text{HPE}] \equiv [-]/[+]$ of the

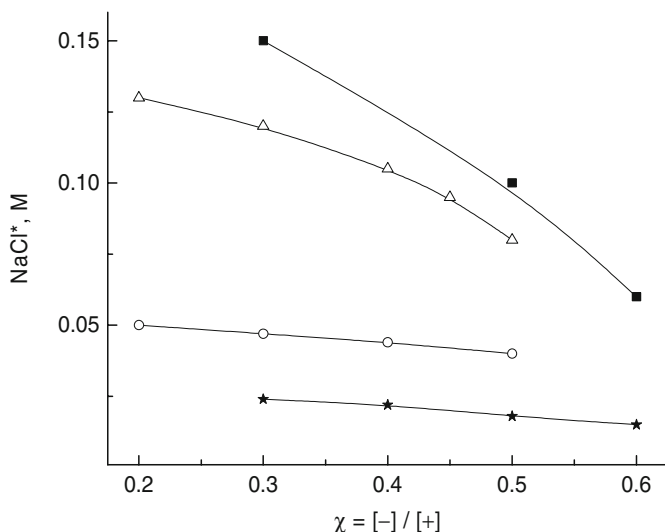


Fig. 18.2 Dependence of critical salt concentration, corresponding to onset of phase separation on the ratio of concentration of the charged groups in solution of positively charged NPEC formed by host PEVP polycation (DP 1640) with guest PMA polyanion (*open symbols*) or guest DNA (*filled symbols*) at different $\psi = \text{DP (HPE)}/\text{DP (GPE)}$: $\psi = 0.1$ (*stars*), 0.4 (*circles*), 2 (*squares*) and 7 (*triangles*). The data are reconstructed from the results reported by Izumrudov et al. (2006)

mixture (Fig. 18.2, curves 1, 2) (Izumrudov et al. 2003, 2006). On the contrary, the corresponding positively charged NPECs of “A” type with $\psi \geq 1$ are significantly more stable, specifically at lower values of χ (Fig. 18.2, curves 3, 4). It is particularly remarkable that curve 4 of NPEC formed by guest DNA with 300–500 base pairs is partly arranged in the region of salt concentrations close to physiological ionic strength. This gives promise that the target positively charged NPEC can be prepared even from relatively long nucleic acid if the chains of host polycation are long enough, i.e. at $\psi > 1$. In line with this reasoning, the use of guest oligonucleotides should considerably extend the DP range of polyamines that are able to play the role of host polycation in the target soluble NPEC.

Another line of attack on the problem of the cell transfection improvement appears to be the using of above mentioned effect of compulsive charging of a weak polyelectrolyte in the presence of a highly charged polyion (Kabanov 1994) to promote the escape of the DNA into cytosol. Boussif et al. (1995) proposed a proton sponge hypothesis that asserts the acting of polymers with high cationic charge potential as a proton sponge upon acidification within endosomes or lysosomes. The hypothesis has been built essentially around the transfecting activities of some cationic polymers, specifically poly(ethylenimine) with apparent pK_a of values closed to pH 5.5, in relation to the acidic environment of endosomes and lysosomes. Partly alkylated PEVP polycation is protonated in more acidic

media in accordance with relatively low apparent pK_a of 3.25 determined for poly-4-vinylpyridine (Kirsh et al. 1973). Yet in the presence of highly charged DNA, the charging of the non-alkylated pyridine moieties occurs at pH 5–6 that results in a pronounced growth in the efficacy of cell transfection by this polyamine (San Juan et al. 2007b). Thus the DNA binding effect extends the range of polycations capable of improving the transfection and demonstrates the advantages of the partly alkylated tertiary polyamines for the preparation of efficient nonviral gene delivery vectors.

18.4 Complexes of Proteins with Oppositely Charged Polyions

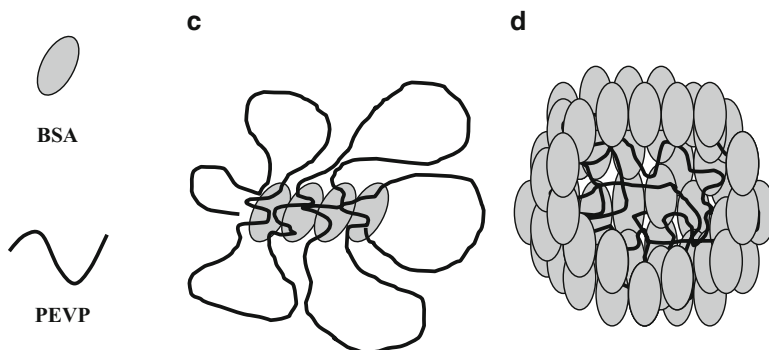
The revealed kinetic and thermodynamic factors controlling the formation, reconstruction and rearrangement of PPCs are summarized in the reviews of Izumrudov (1996) and Izumrudov et al. (1999a). The complex of bovine serum albumin (BSA) with PEVP polycation has received the most study as suitable model system to elucidate the main features of PPCs.

18.4.1 Soluble Complexes and Competitive Reactions in Their Solutions

Interaction of PEVP polycation with negatively charged BSA globules might lead to the formation of either water-soluble or insoluble PPCs. Positively charged soluble PPCs are formed at more than threefold excess of PEVP charge units relative to the negatively charged groups of BSA located on a surface of the protein globules (Kabanov et al. 1980a). Segments of PEVP chain carrying excess charge act as solubilizing fragments of PPC (Scheme 18.2, C) that consists of one PEVP chain and the corresponding number of BSA globules (Izumrudov et al. 1981).

Negatively charged soluble PPCs with the protein as solubilizing component are formed at more than 2.5-fold excess of the negatively charged BSA groups (Zaitsev et al. 1992a). The soluble PPCs consist of one polycation chain and the minimum amount of BSA globules to provide PPC solubility (Scheme 18.2, D). The system is heterogeneous at intermediate compositions of PEVP and BSA mixture.

Spontaneous formation of the water-soluble PPCs in the mixtures of solutions of the components suggests self-assembly of the complex particles due to the exchange of the protein globules between PPCs of different composition. The protein transfer that was evidenced experimentally for PPC(PEVP-BSA) of type “C” (Izumrudov et al. 1984b) occurred relatively quickly in solutions of PPC of type “D” even in salt-free media and was accelerated by the addition of sodium chloride (Izumrudov et al. 1986b).



Scheme 18.2 A schematic sketch of structure of positively charged (c) and negatively charged (d) particles of soluble PPC(BSA-PEVP)

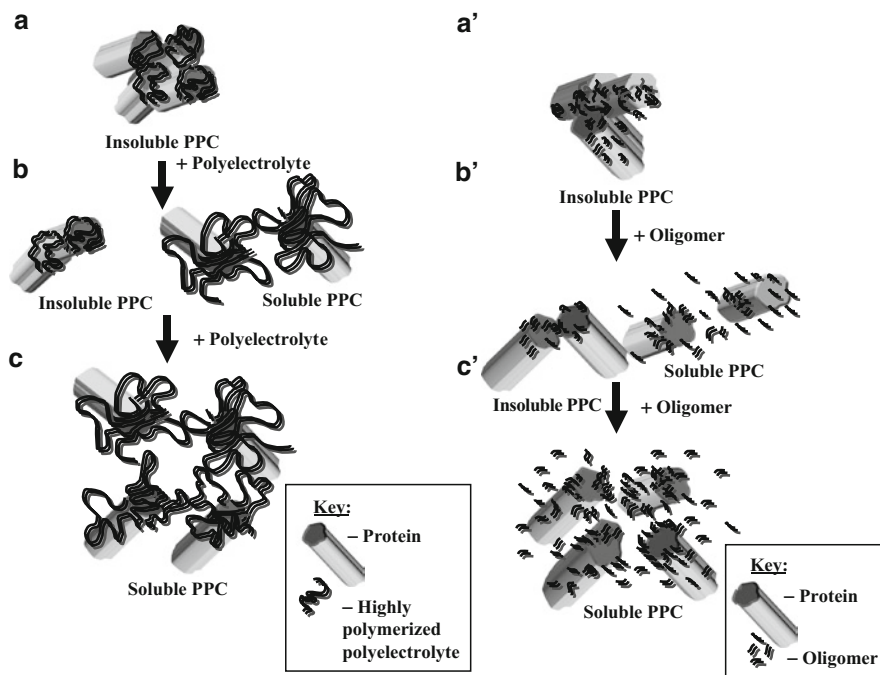
The phenomenon of molecular “recognition” in the mixture of PEVP polycation with different proteins of serum was reported by Kabanov et al. (1980b). The equilibrium state of the system corresponded to a coexistence of soluble PPCs of type “C” each consists of one PEVP chain and protein globules of only one sort.

The competition of PEVP polycation (DP = 650) and PEVP oligocation (DP = 30) for binding with BSA was in favor of the polymer.



The equilibrium (18.6) was completely shifted to the right (Zaitsev et al. 1992b) due to entropy favorable increase of a number of particles in solutions. Just as for PECs described above, the critical salt concentration corresponding to complete destruction of the PPC slightly decreased with the shortening of PEVP chains up to DP \approx 100 and then reduced abruptly (Zaitsev et al. 1992b). For the same reason, the solubilizing ability of the charged chains decreased on their shortening. Thus, very short oligomeric PMA anions proved to be impotent to prevent thermoaggregation of positively charged glyceraldehyde-3-phosphate dehydrogenase (GAPDH), whereas the lengthening of PMA chains and the rise in their relative content favored the reduction of thermoaggregation (Shalova et al. 2005) (Scheme 18.3). The same trends in suppression of thermoaggregation due to formation of soluble PPCs were revealed in the mixtures of negatively charged GAPDH with PEVP polycations of different DP (Shalova et al. 2007).

The potential uses of this thermodynamic limitation of the formation of soluble oligomer-protein complexes of type “C” are intriguing. Thus, oligomers could be employed as overdose proof precipitate agents for proteins separation with the recovery of the components that could be readily achieved by addition of a relatively small amount of the salt. On the other hand, the failure of the charged oligomer to solubilize PPC sets limits on the polyions capable to prevent protein thermodenaturation.



Scheme 18.3 A schematic sketch of transformation of insoluble PPC to the soluble one by addition of highly polymerized polyion (a–c) or charged oligomer (a'–c')

The reported data show that properties of soluble NPECs and PPCs as well as self-assembly and self-adjustment phenomena in their solutions are quite similar (for review see Izumrudov et al. 1999a). Formation of complexes of both types is governed by the hydrophilic-lipophilic balance of their particles. The complexes are composed of a few molecules of the components providing their solubility. The similarity is also observed in the course of the competitive reactions that are controlled by the same factors reflecting the similarity of driving forces of these processes.

The relatively low stability of PPCs in water–salt media (Zaitsev et al. 1992b) is conditioned by a less extended or poorly ordered systems of the ion pairs in PPC as compared to PEC. For the same reason, in the multicomponent systems highly charged synthetic polyions displaced globular proteins from their PPCs with oppositely charged polyelectrolytes (Margolin et al. 1985a), whereas the proteins specifically bound to PPC (e.g. by enzyme-inhibitor interactions) remained in the insoluble PEC formed (Margolin et al. 1985b). These findings are important for improving immunochemical methods, since the assay could be done in solution, followed by the isolation of the components in the precipitate, i.e. the advantages of both homogeneous and heterogeneous assays could be combined. The study of the antigens interactions with antibodies covalently attached to PMA polyanion reinforced the mechanism of the competitive binding (Dzantiev et al. 1988) and

formed the basis for the development of so-called “pseudohomogeneous immunoassay” (Dzantiev et al. 1988) that allowed one to decrease considerably the time of the determination without noticeable loss of the assay sensitivity.

Covalent attachment of proteins to polyelectrolytes endows the conjugates with attractive properties. Direct mixing of the corresponding amounts of water–salt solutions of the enzyme–polyion conjugate and oppositely charged polyion results in self-assembly of the NPEC. The presence of the enzyme was not attended with noticeable changes in the properties of NPEC (Margolin et al. 1981) whereas the immobilized enzyme acquired the unique abilities of NPEC, e.g. to undergo reversible and quantitative phase transitions under slight changes in pH, ionic strength or polymer/polymer composition of the mixture (Margolin et al. 1983). The features of these reversibly soluble immobilized enzymes are described in detail by Margolin et al. (1985b) and reviewed by Zezin et al. (1989). The application of reversibly soluble immobilized enzymes allows: (a) the combination of all advantages of the homogeneous catalysis with an easy separation of the enzyme molecules from the reaction mixture at the end of the process; (b) the significant increase of thermostability of the immobilized enzyme via its precipitation by pH change; (c) the protection of the enzyme from high-molecular-weight inhibitors either in precipitate or in solution; (d) the creation of stimuli responsive enzyme systems in which an attainment of the certain conversion degree results in the termination of the process; (e) the design of reversibly soluble multienzyme systems.

18.4.2 Artificial Chaperones

In the last decades, a lot of papers devoted to investigation of chaperones and chaperonines, in particular the elucidation of their role in protein folding, were published (for reviews see Ellis and Van der Vies 1991; Guise et al. 1996; Ellis 1998). A number of works reported the attempts to create artificial chaperones. The ultimate objective of this line of inquiry is to design relatively sophisticated systems capable of simulating various steps of chaperone action, i.e. (i) the recognition and binding of non-native protein forms, (ii) the deposition of the non-native forms in a complex with chaperones to suppress their aggregation, and (iii) the dosed liberation of the non-native forms into solution after folding to the native conformation.

A system based on conjugates of antigens and antibodies with synthetic polyelectrolytes is a promising model for mimicking the first step of the chaperone action (Dainiak et al. 1998). Monoclonal antibodies specific for misfolded non-active dimeric forms of GAPDH but not binding the native tetrameric form of the enzyme were covalently coupled to PMA polyanion. Partially activated enzyme was treated with the immobilized antibodies to bind inactivated dimers and the product was precipitated by the addition of an equimolar (per charges) amount of PEVP polycation. The immobilized antibodies recognize misfolded dimers like the chaperone recognize the misfolded polypeptides, bind them and remove from the reaction medium.

As to mimicking the second and further steps, the suppression of the enzymes aggregation due to soluble PPC formation was reported for mixtures of GAPDH with either PMA polyanion (Shalova et al. 2005) or PEVP polycation (Shalova et al. 2007). The highly polymerized polyion of proper concentrations could form with the oppositely charged GAPDH the soluble PPC of type “A” (Scheme 18.2) in which a mutual repulsion of the non-bound charged groups of the polyion keeps the protein globules from the contact and hence, weakens GAPDH aggregation on heating. The efficacy of thermoaggregation suppression proved to be significantly higher if the polyelectrolyte chains with hydrophobic moieties were used. The hydrophobic sites of the chain interacted with hydrophobic patches of the protein that was exposed of the surface of the bound globule on the heating and block them from the contact with hydrophobic patches of other protein molecules. The hydrophobic interactions not only suppressed thermoaggregation, but they also changed significantly the enzyme structure that was reflected by the decrease in the enzymatic activity (Shalova et al. 2007). In other words, the polyion mimics the important function of chaperone, i.e. the binding of the protein in the complex that prevents aggregation of the non-native forms and acts efficiently on the structure of the bound misfolded polypeptides. The destruction of the PPC by the added salt or by means of a competitive displacement of the enzyme from the PPC by the oppositely charged polyion restored markedly the activity. The latter can be considered as an important step in mimicking the final stage of chaperone action, i.e. the liberation of the non-native forms into solution after folding to the native conformation. The revealed important role of hydrophobicity of the charged chains in preventing thermoaggregation might be of particular interest for control the aggregation of proteins that are prone to form the amyloid structures responsible for the development of neurodegenerative diseases.

18.5 Polyelectrolyte Multilayer Films and Capsules

Alternating deposition of oppositely charged polyelectrolytes from their solutions at a surface has recently become a widely used technique for surface functionalization and construction of multilayer films and capsules (Decher 1997; Schlenoff and Dubas 2001; Kotov et al. 1998; Graul et al. 1999). The fundamentals and applications of these novel nanoscopically structured materials are summarized in recent reviews (Cooper et al. 2005; Sukhishvili 2005). The deposition procedure is temptingly simple and is often viewed as being applicable to virtually any pair of synthetic polyions or charged biopolymers. Limitations of layer-by-layer technique were recognized as comparatively uncommon cases when no interpolyelectrolyte binding occurred, such as for polymers whose charge density is lower than critical (Steitz et al. 2001; Glinel et al. 2002). Disruption of the binding also lies in the heart of salt- and pH-induced dissolution of multilayers (Mendelsohn et al. 2000; Dubas and Schlenoff 2001; Kharlampieva and Sukhishvili 2003a, b; Izumrudov and Sukhishvili 2003).

Modern theories of PEMs growth describe the buildup of these films as irreversible (Casrelново and Joanny 2000; Dobrynin and Rubinstein 2005). However, from the thermodynamic point of view, the fact that multilayer films can be successfully deposited at surfaces might seem to contradict the knowledge accumulated on soluble NPECs formation. Thus during each step of deposition, PEMs are exposed to a large excess, compared to film surface charge, of polyelectrolyte chains in solution. In other words, one could expect that, on the basis of thermodynamic arguments only, the growth of PEMs would be severely impeded if conditions favorable for the formation of NPECs are employed.

Desorption of polyelectrolytes from a multilayer resulting from competitive binding with polyelectrolyte chains in solution has also been reported by several authors (Hoogeveen et al. 1996; Sui et al. 2003; Schoeler et al. 2002). The main feature of PEMs destruction via above solubilization is that the chains remain strongly associated both in the PEMs and soluble NPEC, and the redistribution of chains occurs due to a competitive reaction, favoring NPECs and resulting in PEMs erosion.

The understanding of relationship between multilayer deposition and the phase diagrams of NPECs (Kovačević et al. 2002, 2003; Izumrudov et al. 2004) is important for efficient control the transition between stable film growth and the deposition regime opposed by polymer desorption in a wide range of conditions (pH, ionic strength, ratio of chain length, etc.). In the recent review of Sukhishvili et al. (2006), the reported data on the relationship between PEMs growth and behavior

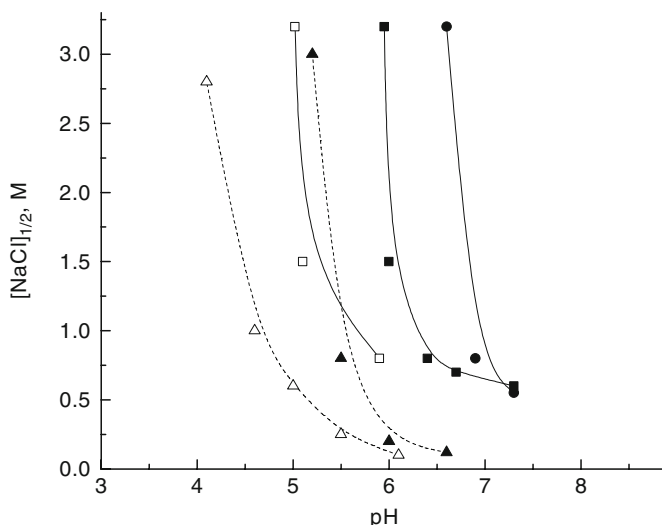


Fig. 18.3 Concentration of sodium chloride corresponding to release of a half of the positively charged partner from a ten-layer of PMA-containing PEMs (*filled symbols*) or the PAA-containing PEMs (*open symbols*) as a function of solution pH for PEVP- β polycation with alkylation degree $\beta = 84$ (*squares*), $\beta = 50$ (*circles*), or lysozyme (*triangles*, *dash lines*). The data are reconstructed from the results reported by Izumrudov and Sukhishvili (2003) for the polyamines and Izumrudov et al. (2005b) for lysozyme

of NPECs in water–salt solution has been summarized. It is shown that the accumulated knowledge on stability of NPECs, phase separations in their water–salt media, and kinetics of the interpolyelectrolyte exchange reactions can form the basis for generalization and prediction the likelihood of the chains removal from PEMs during the film growth. The revealed factors of control of these processes in NPECs solutions that were described in detail in earlier sections could eventually provide a materials scientist with a “map” of PEMs growth which will allow one to rationally avoid unstable regimes during the deposition.

Note that the reversible switching from the regime of stable PEMs growth to unstable one can be accomplished upon very small change of the external conditions. An illustrative example is pH-dependent stabilization of polyelectrolyte complexes formed by PMA polyanion or poly(acrylic) acid (PAA) with polyamines that occurs in neutral and slightly acidic media (Izumrudov and Sukhishvili 2003). The drastic increase in NaCl concentration corresponding to destruction of PEMs (Fig. 18.3, solid lines) is attributed to formation of a network of the hydrogen bonds between protonated carboxylic groups of the polyacid which reinforces multilayer film. The stabilization proceeds in enzyme-friendly and rather narrow pH regions and could be efficiently controlled by either acidity of the polyacids and/or a charge density of the polyamines chains. Moreover, PEMs of the polyacids with basic proteins, specifically lysozyme (Fig. 18.3, dash lines) were shown to obey the same regularities (Izumrudov et al. 2005b). These findings support the proposed mechanism of PEMs stabilization and can be used for the development of stimuli responsive PEMs suitable for application at physiological pH and ionic strength.

References

- Bakeev KN, Izumrudov VA, Zezin AB, Kabanov VA (1987) Phenomenon of molecular recognition in interpolyelectrolyte reactions. *Vysokomol Soedin (in Russian)* 29B:483–484
- Bakeev KN, Izumrudov VA, Kuchanov SI, Zezin AB, Kabanov VA (1992) Kinetics and mechanism of interpolyelectrolyte exchange and addition reactions. *Macromolecules* 25:4249–4254
- Boura C, Menu P, Payan E, Picart C, Voegel JC, Muller S, Stoltz JF (2003) Endothelial cells growth on thin polyelectrolyte multilayered films: an evolution of a new versatile surface modification. *Biomaterials* 24:3521–3530
- Boussif O, Lezoualc’h F, Zanta MA, Mergny MD, Scherman D, Demeneix B, Behr J-P (1995) A versatile vector for gene and oligonucleotide transfer into cells in culture and in vivo: polyethylenimine. *Proc Natl Acad Sci USA* 92:7297–7301
- Cai K, Rechtenbach A, Hao J, Bossert J, Jandt KD (2005) Polysaccharide-protein surface modification of titanium via a layer-by-layer technique: characterization and cell behavior aspects. *Biomaterials* 26:5960–5971
- Casrelnovo M, Joanny J-F (2000) Formation of polyelectrolyte multilayers. *Langmuir* 16:7524–7532
- Chaubet F, Izumrudov VA, Boisson-Vidal C, Jozefonvicz J (2003) Poly(N-ethyl-4-vinylpyridinium) bromide as a potential probe to select heparin-like anticoagulant polyanions. *Carbohydr Polym* 51:33–36
- Chluba J, Voegel JC, Decher G, Erbacher P, Schaaf P, Ogier J (2001) Peptide hormone covalently bound to polyelectrolytes and embedded into PEM architectures conserving full biological activity. *Biomacromolecules* 2:800–805

- Cho YW, Kim J-D, Park K (2003) Polycation gene delivery systems: escape from endosomes to cytosol. *J Pharm Pharmacol* 55:721–734
- Cohen-Sacks H, Elazar V, Gao J, Golomb A, Adwan H, Korchoy N, Levy RJ, Berger MR, Colomb G (2002) Delivery and expression of pDNA embedded in collagen matrices. *J Control Release* 95:309–320
- Cooper CL, Dubin PL, Kayitmazer AB, Turksen S (2005) Polyelectrolyte-protein complexes. *Curr Opin Colloid Interface Sci* 10:52–78
- Dainiak MB, Izumrudov VA, Muronetz VI, Galaev IYu, Mattiasson B (1998) Conjugates of monoclonal antibodies with polyelectrolyte complexes – an attempt to make an artificial chaperone. *BBA* 1381:279–285
- De Laporte L, Shea LD (2007) Matrices and scaffolds for DNA delivery in tissue engineering. *Adv Drug Deliv Rev* 59:292–307
- De Laporte L, Cruz RJ, Shea LD (2006) Design of modular non-viral gene therapy vectors. *Biomaterials* 27:947–954
- Decher G (1997) Fuzzy nanoassemblies: toward layered polymeric multicomposites. *Science* 277:1232–1237
- Dobrynin AV, Rubinstein M (2005) Theory of polyelectrolytes in solutions and at surfaces. *Prog Polym Sci* 30:1049–1118
- Dubas ST, Schlenoff JB (2001) Polyelectrolyte multilayers combining a weak polyacid: construction and deconstruction. *Macromolecules* 34:3736–3740
- Dzantiev BB, Blintsov AN, Tsivilyova LS, Berezin IV, Egorov AM, Izumrudov VA, Zezin AB, Kabanov VA (1988) Binding of antigens with the conjugates of antibodies and a synthetic water-soluble polyelectrolyte. *Dokl Biochem* 302:279–282
- Eichman JD, Bielinska AU, Kukovska-Latallo JF, Donovan BW, Baker JR (2001) Bioapplications of PAMAM dendrimers. In: Fréchet MJM, Tomalia DA (eds) *Dendrimers and other dendritic polymers*. Wiley, New York, pp 442–461
- Ellis RJ (1998) Steric chaperones. *Trends Biochem Sci* 23:43–45
- Ellis RJ, Van der Vies SM (1991) Molecular chaperones. *Annu Rev Biochem* 60:321–347
- Forry SP, Reyes DR, Gaitan M, Locascio LE (2006) Facilitating the culture of mammalian nerve cells with polyelectrolyte multilayers. *Langmuir* 22:5770–5775
- Garza JM, Jessel N, Ladam G, Dupray V, Muller S, Stoltz JF, Schaaf P, Voegel JC, Lavallo P (2005) Polyelectrolyte multilayers and degradable polymer layers as multicompartiment films. *Langmuir* 21:12372–12377
- Glinel K, Moussa A, Jonas AM, Laschewsky A (2002) Influence of polyelectrolyte charge density on the formation of multilayers of strong polyelectrolytes at low ionic strength. *Langmuir* 18:1408–1412
- Graul WG, Li M, Schlenoff JB (1999) Ion exchange in ultrathin films. *J Phys Chem B* 103:2718–2723
- Guise AD, West SM, Chaundhuri JB (1996) Protein folding in vivo and renaturation of recombinant proteins from inclusion bodies. *Mol Biotechnol* 6:53–64
- Hammond PT (2004) Form and function in multi-layer assembly: new applications at the nano-scale. *Adv Mater* 16:1271–1293
- Haynie DT, Zhang L, Zhao W, Rudra JS (2006) Protein-inspired multilayer nanofilms: science, technology and medicine. *Nanomedicine* 2:150–157
- Hoogeveen NG, Cohen Stuart MA, Fleer GJ, Böhmer MR (1996) Formation and stability of multilayers of polyelectrolytes. *Langmuir* 12:3675–3681
- Izumrudov VA (1996) Competitive reactions in solutions of protein-polyelectrolyte complexes. *Ber Bunsenges Phys Chem* 100:1017–1023
- Izumrudov VA, Sukhishvili SA (2003) Ionization-controlled stability of polyelectrolyte multilayers in salt solutions. *Langmuir* 19:5188–5191
- Izumrudov VA, Zhiryakova MV (1999) Stability of DNA-containing interpolyelectrolyte complexes in water–salt solutions. *Macromol Chem Phys* 200:2533–2540
- Izumrudov VA, Kasaikin VA, Ermakova LN, Mustafaev MI, Zezin AB, Kabanov VA (1981) Study of structure of water-soluble complexes of bovine serum albumin with poly(N-ethyl-4-vinylpyridinium) bromide by light-scattering. *Vysokomol Soedin (in Russian)* 23A:1365–1373

- Izumrudov VA, Savitskii AP, Bakeev KN, Zezin AB, Kabanov VA (1984a) A fluorescence quenching study of interpolyelectrolyte reactions. *Macromol Chem Rapid Commun* 5:709–714
- Izumrudov VA, Zezin AB, Kabanov VA (1984b) Macromolecular exchange in solutions of complexes of globular proteins with synthetic polyelectrolytes. *Dokl Phys Chem* 275:335–338
- Izumrudov VA, Bronich TK, Zezin AB, Kabanov VA (1985) Kinetics and mechanism of intermacromolecular reactions in polyelectrolyte solutions. *J Polym Sci [B]* 23:439–444
- Izumrudov VA, Bakeev KN, Zezin AB, Kabanov VA (1986a) Influence of polyion charge density on kinetics of interpolyelectrolyte reactions. *Dokl Akad Nauk (in Russian)* 286:1442–1445
- Izumrudov VA, Zezin AB, Kabanov VA (1986b) Kinetics of macromolecular exchange in solutions of protein-polyelectrolyte complexes. *Dokl Phys Chem* 291:1127–1130
- Izumrudov VA, Nyrkova TYu, Zezin AB, Kabanov VA (1987) Influence of chain length of lyophilizing polyion on direction and kinetics of interpolyelectrolyte exchange reaction. *Vysokomol Soedin (in Russian)* 29B:474–478
- Izumrudov VA, Bronich TK, Saburova OS, Zezin AB, Kabanov VA (1988) The influence of chain length of a competitive polyanion and nature of monovalent counterions on the direction of the substitution reaction of polyelectrolyte complexes. *Macromol Chem Rapid Commun* 9:7–12
- Izumrudov VA, Zezin AB, Kabanov VA (1991) Equilibrium of interpolyelectrolyte reactions and the phenomenon of molecular “recognition” in solutions of interpolyelectrolyte complexes. *Russ Chem Rev* 60:792–806. Translated from *Uspekhi Khimii*, 1991, 60:1570–1595
- Izumrudov VA, Zezin AB, Kargov SI, Zhiryakova MV, Kabanov VA (1995a) Competitive displacement of ethidium cations intercalated in DNA by polycations. *Dokl Phys Chem* 342:150–153. Translated from *Dokl Akad Nauk* 342:626–629
- Izumrudov VA, Kargov SI, Zhiryakova MV, Zezin AB, Kabanov VA (1995b) Competitive reactions in solutions of DNA and water-soluble interpolyelectrolyte complexes. *Biopolymers* 35:523–531
- Izumrudov VA, Ortega Ortiz H, Zezin AB, Kabanov VA (1996a) Temperature controlled reversible substitution of polyions in an interpolyelectrolyte complex. *Dokl Phys Chem* 349:190–192. Translated from *Dokl Akad Nauk* 349:630–633
- Izumrudov VA, Zhiryakova MV, Kargov SI, Zezin AB, Kabanov VA (1996b) Competitive reactions in solutions of DNA-containing polyelectrolyte complexes. *Macromol Chem Macromol Symp* 106:179–192
- Izumrudov VA, Ortega Ortiz H, Zezin AB, Kabanov VA (1998) Temperature-controllable interpolyelectrolyte substitution reactions. *Macromol Chem Phys* 199:1057–1062
- Izumrudov VA, Galaev IYu, Mattiasson B (1999a) Polycomplexes – potential for bioseparation. *Bioseparation* 7:207–220
- Izumrudov VA, Chaubet F, Clairbois A-S, Jozenfonvicz J (1999b) Interpolyelectrolyte reactions in solutions of functionalized dextrans with negatively charged groups along the chains. *Macromol Chem Phys* 200:1753–1760
- Izumrudov VA, Zhiryakova MV, Kudaibergenov SE (2000) Controllable stability of DNA-containing polyelectrolyte complexes in water–salt solutions. *Biopolymers (Nucleic Acid Sci)* 52:94–108
- Izumrudov VA, Zhiryakova MV, Goulko AV (2002) Ethidium bromide as a promising probe for studying DNA interaction with cationic amphiphiles and stability of the resulting complexes. *Langmuir* 18:10348–10356
- Izumrudov VA, Wahlund P-O, Gustavsson P-E, Larsson P-O, Galaev IYu (2003) Factors controlling phase separations in water–salt solutions of DNA and polycations. *Langmuir* 19:4733–4739
- Izumrudov VA, Kharlampieva E, Sukhishvili SA (2004) Salt-induced multilayer growth: correlation with phase separation in solution. *Macromolecules* 37:8400–8406
- Izumrudov VA, Gorshkova MYu, Volkova IF (2005a) Controlled phase separations in solutions of soluble polyelectrolyte complex of DIVEMA (copolymer of divinyl ether and maleic anhydride). *Eur Polym J* 41:1251–1259

- Izumrudov VA, Kharlampieva E, Sukhishvili SA (2005b) Multilayers of a globular protein and a weak polyacid: role of polyacid ionization in growth and decomposition in salt solutions. *Biomacromolecules* 6:1782–1788
- Izumrudov VA, Parashchuk VV, Sybachin AV (2006) Controlled phase separations in solutions of polyelectrolyte complexes. Potential for gene delivery. *J Drug Deliv Sci Technol* 16:267–274
- Jessel N, Oulad-Abdelghani M, Meyer F, Lavalle P, Haikel Y, Schaaf P, Voegel J-C (2006) Multiple and time-scheduled in situ DNA delivery mediated by β -cyclodextrin embedded in a polyelectrolyte multilayer. *Proc Natl Acad Sci USA* 103:8618–8621
- Jewell CM, Zhang J, Fredin NJ, Lynn DM (2005) Multilayered polyelectrolyte films promote the direct and localized delivery of DNA to cells. *J Control Release* 106:214–223
- Jewell CM, Zhang J, Fredin NJ, Wolff MR, Lynn DM (2006) Release of plasmid DNA from intravascular stents coated with ultrathin multilayered polyelectrolyte films. *Biomacromolecules* 7:2483–2491
- Kabanov VA (1994) Basic properties of soluble interpolyelectrolyte complexes applied to bioengineering and cell transformation. In: Dubin PL, Bock J, Davis RM, Schulz DN, Thies C (eds) *Macromolecular complexes in chemistry and biology*. Springer, Berlin, pp 151–174
- Kabanov AV (1999) Taking polycation gene delivery systems from in vitro to in vivo. *PSTT* 2:365–372
- Kabanov AV, Kabanov VA (1995) DNA complexes with polycations for the delivery of genetic material into cells. *Bioconjug Chem* 6:7–20
- Kabanov AV, Kabanov VA (1998) Interpolyelectrolyte and block ionomer complexes for gene delivery: physico-chemical aspects. *Adv Drug Deliv Rev* 30:49–60
- Kabanov VA, Zezin AB (1982) Water-soluble nonstoichiometric polyelectrolyte complexes: a new class of synthetic polyelectrolytes. *Sov Sci Rev* 4:207–282
- Kabanov VA, Zezin AB, Mustafaev MI, Kasaikin VA (1980a) Soluble interpolymer complexes of polyamines and polyammonium salts. In: Goethals EJ (ed) *Polymer amines and ammonium salts*. Pergamon, Oxford/New York, pp 173–192
- Kabanov VA, Mustafaev MI, Blokhina VD, Agafieva VS (1980b) About competitive relationships of the reactions of serum proteins with polycations. *Mol Biol (in Russian)* 14:64–75
- Kabanov VA, Zezin AB, Izumrudov VA, Bronich TK, Bakeev KN (1985) Cooperative interpolyelectrolyte reactions. *Macromol Chem Suppl* 13:137–155
- Karibyants N, Dautzenberg H, Cölfen H (1997) Characterization of PSS/PDADMAC-co-AA polyelectrolyte complexes and their stoichiometry using analytical ultracentrifugation. *Macromolecules* 30:7803–7809
- Kasaikin VA, Kharenko OA, Kharenko AV, Zezin AB, Kabanov VA (1979) The principles of formation of water-soluble polyelectrolyte complexes. *Vysokomol Soedin (in Russian)* 21B:84–85
- Kharenko OA, Kharenko AV, Kalyugnaya RI, Izumrudov VA, Kasaikin VA, Zezin AB, Kabanov VA (1979) Nonstoichiometric polyelectrolyte complexes as a new water-soluble macromolecular complexes. *Vysokomol Soedin (in Russian)* 21A:2719–2725
- Kharlampieva E, Sukhishvili SA (2003a) Ionization and pH stability of multilayers formed by self-assembly of weak polyelectrolytes. *Langmuir* 19:1235–1243
- Kharlampieva E, Sukhishvili SA (2003b) Polyelectrolyte multilayers of weak polyacid and cationic copolymer: competition of hydrogen-bonding and electrostatic interactions. *Macromolecules* 36:9950–9956
- Kidambi S, Udpa N, Schroeder SA, Findlan R, Lee I, Chan C (2007) Cell adhesion on polyelectrolyte multilayer coated polydimethylsiloxane surfaces with varying topographies. *Tissue Eng* 13:2105–2117
- Kirsh Yu, Komarova O, Lukovkin G (1973) Physico-chemical study of ionic equilibria for poly-2 and poly-4-vinylpyridines in alcohol-water solutions. *Eur Polym J* 9:1405–1408
- Kokufuta E (1994) Complexation of proteins with polyelectrolytes in a salt-free system. In: Dubin PL, Bock J, Davis RM, Schulz DN, Thies C (eds) *Macromolecular complexes in chemistry and biology*. Springer, Berlin, pp 301–325

- Kotov NA, Magonov S, Tropsha E (1998) Layer-by-layer self assembly of aluminosilicate-polyelectrolyte composites: mechanism of deposition, crack resistance, and perspectives for novel membrane materials. *Chem Mater* 10:886–895
- Kovačević D, van der Burgh S, de Keizer A, Cohen Stuart MA (2002) Kinetics of formation and dissolution of weak polyelectrolyte multilayers: role of salt and free polyion. *Langmuir* 18:5607–5612
- Kovačević D, van der Burgh S, de Keizer A, Cohen Stuart MA (2003) Specific ionic effects on weak polyelectrolyte multilayer formation. *J Phys Chem B* 107:7998–8002
- Langer R (1998) Drug delivery and targeting. *Nature* 392:5–10
- Langer R (2001) Drug delivery. *Drugs on target. Science* 293:58–59
- Margolin AL, Izumrudov VA, Svedas VK, Zezin AB, Kabanov VA, Berezin IV (1981) Preparation and properties of penicillin amidase immobilized in polyelectrolyte complexes. *BBA* 660:359–365
- Margolin AL, Izumrudov VA, Sherstyuk SF, Svedas VK, Zezin AB, Kabanov VA (1983) Enzymes immobilized in polyelectrolyte complexes. Influence of conformational changes in the matrix and phase transitions in solutions on the catalytic properties. *Mol Biol (in Russian)* 17:1001–1008
- Margolin AL, Sherstyuk SF, Izumrudov VA, Svedas VK, Zezin AB, Kabanov VA (1985a) Enzymes in polyelectrolyte complexes. The effect of phase transition on thermal stability. *Eur J Biochem* 146:625–632
- Margolin AL, Sherstyuk SF, Izumrudov VA, Svedas VK, Zezin AB, Kabanov VA (1985b) Protein-protein interactions in the systems containing synthetic polyelectrolytes. *Dokl Chem* 284:313–316
- Medzhitov R, Janeway CA Jr (2002) Decoding the patterns of self and nonself by the innate immune system. *Science* 296:298–300
- Mendelsohn JD, Barret CJ, Chan VV, Pal AJ, Mayes AM, Rubner MF (2000) Fabrication of microporous thin films from polyelectrolyte multilayers. *Langmuir* 16:5017–5023
- Mendelsohn JD, Yang SY, Hiller J, Hochbaum AI, Rubner MF (2003) Rational design of cytophilic and cytophobic polyelectrolyte multilayer thin film. *Biomacromolecules* 4:96–106
- Moby V, Boura C, Kerdjoudj H, Voegel LC, Marchal L, Dumas D, Schaaf P, Stoltz JF, Menu P (2007) Poly(styrenesulfonate)/poly(allylamine) multilayers: a route to favor endothelial cell growth on expanded poly(tetrafluoroethylene) vascular grafts. *Biomacromolecules* 8:2156–2160
- Nefedov NK, Ermakova TG, Kasaikin VA, Zezin AB, Lopiryov VA (1985) Influence of a nature of counterion on formation and properties of nonstoichiometric polyelectrolyte complexes. *Vysokomol Soedin (in Russian)* 27A:1496–1499
- Norde W, Lyklema J (1991) Why proteins prefer interfaces. *J Biomater Sci Polym Ed* 2:183–202
- Pannier AK, Shea LD (2004) Controlled release systems for DNA delivery. *Mol Ther* 10:19–26
- Papisov IM, Litmanovich AD (1989) Molecular recognition in interpolymer interactions and matrix polyreactions. *Adv Polym Sci* 90:139–179
- Pergushov DV, Izumrudov VA, Zezin AB, Kabanov VA (1993) Effect of low-molecular mass salts on the behavior of water-soluble nonstoichiometric polyelectrolyte complexes. *Polym Sci* 35A:940–944. Translated from *Vysokomol Soedin* (1993) 35:844–849
- Pergushov DV, Izumrudov VA, Zezin AB, Kabanov VA (1995) Stability of interpolyelectrolyte complexes in aqueous saline solutions. *Polym Sci* 37A:1081–1087. Translated from *Vysokomol Soedin* (1995) 37:1739–1746
- Philipp B, Daurzenberg H, Lonow KJ, Kötzt J, Dawydoff W (1989) Polyelectrolyte complexes – recent developments and open problems. *Prog Polym Sci* 14:91–172
- Pouton CW, Seymour LW (2001) Key issues in non-viral gene delivery. *Adv Drug Deliv Rev* 46:187–203
- Richert L, Boulmedais F, Lavalle P, Mutterer J, Ferreux E, Decher G, Schaaf P, Voegel JC (2004a) Improvement of stability and cell adhesion properties of polyelectrolyte multilayer films by chemical cross-linking. *Biomacromolecules* 5:284–294

- Richert L, Engler AJ, Discher DE, Picart C (2004b) Elasticity of native and cross-linked polyelectrolyte multilayer films. *Biomacromolecules* 5:1908–1916
- Richert L, Schneider A, Vautier D, Vodouhe C, Jessel N, Payan E, Schaaf P, Voegel JC, Picart C (2006) Imaging cell interactions with native and crosslinked polyelectrolyte multilayers. *Cell Biochem Biophys* 44:273–285
- Roy K, Wang D, Hedley ML, Barman SP (2003) Gene delivery with in-situ crosslinking polymer networks generates long-term systemic protein expression. *Mol Ther* 7:401–408
- Salloum DS, Olenych SG, Keller TC, Schlenoff JB (2005) Vascular smooth muscle cells on polyelectrolyte multilayers: hydrophobicity-directed adhesion and growth. *Biomacromolecules* 6:161–167
- Salvay DM, Shea LD (2006) Inductive tissue engineering with protein and DNA-releasing scaffolds. *Mol Biosyst* 2:36–48
- San Juan A, Hlawaty H, Chaubet F, Letourneur D, Feldman LJ (2007a) Cationized pullulan 3D matrices as new materials for gene transfer. *J Biomed Mater Res* 82A:354–362
- San Juan A, Letourneur D, Izumrudov VA (2007b) Quaternized poly-4-vinylpyridines as model gene delivery polycations: elucidation of structure–function relationship through modification of side chains hydrophobicity and degree of alkylation. *Bioconjug Chem* 18:922–928
- Schindler T, Nordmeier E (1997) The stability of polyelectrolyte complexes of calf-thymus DNA and synthetic polycations: theoretical and experimental investigations. *Macromol Chem Phys* 198:1943–1972
- Schlenoff JB, Dubas ST (2001) Mechanism of polyelectrolyte multilayer growth: charge overcompensation and distribution. *Macromolecules* 34:592–598
- Schneider A, Francius G, Obeid R, Schwinte P, Hemmerle J, Frisch B, Schaaf P, Voegel JC, Zenger B, Picart C (2006) Polyelectrolyte multilayers with a tunable Young's modulus: influence of film stiffness on cell adhesion. *Langmuir* 22:1193–2000
- Schneider A, Vodouhe C, Richert L, Francius G, Le Guen E, Schaaf P, Voegel JC, Frisch B, Picart C (2007) Multifunctional polyelectrolyte multilayer films: combining mechanical resistance, biodegradability, and bioactivity. *Biomacromolecules* 8:139–145
- Schoeler B, Kumaraswamy G, Caruso F (2002) Investigation of the influence of polyelectrolyte charge density on the growth of multilayer thin films prepared by the layer-by-layer technique. *Macromolecules* 35:889–897
- Shalova IN, Asryants RA, Sholukh MV, Saso L, Kurganov BI, Muronetz VI, Izumrudov VA (2005) Interaction of polyanions with basic proteins, 2. Influence of complexing polyanions on the thermoaggregation of oligomeric enzymes. *Macromol Biosci* 5:1184–1192
- Shalova IN, Naletova IN, Saso L, Muronetz VI, Izumrudov VA (2007) Interaction of polyelectrolytes with proteins, 2. Influence of complexing polycations on the thermoaggregation of oligomeric enzyme. *Macromol Biosci* 7:929–939
- Shief JY, Glatz CE (1994) Precipitation of proteins with polyelectrolytes: role of polymer molecular weight. In: Dubin PL, Bock J, Davis RM, Schulz DN, Thies C (eds) *Macromolecular complexes in chemistry and biology*. Springer, Berlin, pp 272–284
- Steitz R, Jaeger W, Klitzing R (2001) Influence of charge density and ionic strength on the multilayer formation of strong polyelectrolytes. *Langmuir* 17:4471–4474
- Storrie H, Mooney DJ (2006) Sustained delivery of plasmid DNA from polymeric scaffolds for tissue engineering. *Adv Drug Deliv Rev* 58:500–514
- Sui Z, Salloum D, Schlenoff JB (2003) Effect of molecular weight on the construction of polyelectrolyte multilayers: stripping versus sticking. *Langmuir* 19:2491–2495
- Sukhishvili SA (2005) Responsive polymer films and capsules via layer-by-layer assembly. *Curr Opin Colloid In* 10:37–44
- Sukhishvili SA, Kharlampieva E, Izumrudov VA (2006) Where polyelectrolyte multilayers and polyelectrolyte complexes meet. *Macromolecules* 39:8873–8881
- Thompson MT, Berg MC, Tobias IS, Rubner MF, Van Vliet KJ (2005) Tuning compliance of nanoscale polyelectrolyte multilayers to modulate cell adhesion. *Biomaterials* 26:6836–6845
- Trukhanova ES, Izumrudov VA, Litmanovich AA, Zelikin AN (2005) Recognition and selective binding of DNA by ionenes of different charge density. *Biomacromolecules* 6:3198–3201

- Tryoen-Toth P, Vautier D, Haikel Y, Voegel JC, Schaaf P, Chluba J, Ogier J (2002) Viability, adhesion, and bone phenotype of osteoblast-like cells on polyelectrolyte multilayer films. *J Biomed Mater Res* 60:657–667
- Tsuchida E, Abe K (1982) Interactions between macromolecules in solution and intermacromolecular complexes. *Adv Polym Sci* 45:1–130
- Tsuchida E, Osada Y, Sanada K (1972) Interaction of poly(styrene sulfonate) with polycations carrying charges in the chain backbone. *J Polym Sci* 10:3397–3403
- Vautier D, Karsten V, Egles C, Chluba J, Schaaf P, Voegel JC, Ogier J (2002) Polyelectrolyte multilayer films modulate cytoskeletal organization in chondrosarcoma cells. *J Biomater Sci Polym Ed* 13:713–732
- Wahlund P-O, Izumrudov VA, Gustavsson P-E, Larsson P-O, Galaev IYu (2003) Phase separations in water–salt solutions of polyelectrolyte complexes formed by RNA and polycations: comparison with DNA complexes. *Macromol Biosci* 3:404–414
- Wahlund P-O, Gustavsson P-E, Izumrudov VA, Larsson P-O, Galaev IYu (2004a) Precipitation by polycation as capture step in purification of plasmid DNA from a clarified lysate. *Biotech Bioeng* 87:675–684
- Wahlund P-O, Gustavsson P-E, Izumrudov VA, Larsson P-O, Galaev IYu (2004b) Polyelectrolyte complexes as a tool for purification of plasmid DNA. Background and development. *J Chromatogr* 807:121–127
- Wood KC, Chuang HF, Batten RD, Lynn DM, Hammond PT (2006) Controlling interlayer diffusion to achieve sustained, multiagent delivery from layer-by-layer thin films. *Proc Natl Acad Sci USA* 103:10207–10212
- Xia J, Dubin PL (1994) Protein-polyelectrolyte complexes. In: Dubin PL, Bock J, Davis RM, Schulz DN, Thies C (eds) *Macromolecular complexes in chemistry and biology*. Springer, Berlin, pp 247–271
- Yang Y, Ertl HC, Wilson JM (1994) MHC class I-restricted cytotoxic T lymphocytes to viral antigens destroy hepatocytes in mice infected with E1-deleted recombinant adenoviruses. *Immunity* 1:433–442
- Zaitsev VS, Izumrudov VA, Zezin AB, Kabanov VA (1992a) Water-soluble protein-polyelectrolyte complexes containing excess of the protein as a liophylizing component. *Dokl Phys Chem* 322:17–21
- Zaitsev VS, Izumrudov VA, Zezin AB, Kabanov VA (1992b) Influence of polymerization degree of poly-N-ethyl-4-vinylpyridinium cations on solubility and reversible transformations of their complexes with bovine serum albumin. *Dokl Phys Chem* 323:177–181
- Zelikin AN, Putnam D, Shastri P, Langer R, Izumrudov VA (2002) Aliphatic ionenes as gene delivery agents: elucidation of structure-function relationship through modification of charge density and polymer length. *Bioconjug Chem* 13:548–553
- Zezin AB, Kasaikin VA, Kabanov NM, Kharenko OA, Kabanov VA (1984) Influence of the ratio of degrees of polymerization of components on formation of nonstoichiometric polycomplexes. *Vysokomol Soedin (in Russian)* 26A:1519–1524
- Zezin AB, Izumrudov VA, Kabanov VA (1989) Interpolyelectrolyte complexes as a new family of enzyme carriers. *Makromol Chem Macromol Symp* 26:249–264
- Zhang J, Chua LS, Lynn DM (2004) Multilayered thin films that sustain the release of functional DNA under physiological conditions. *Langmuir* 20:8015–8021
- Zhang J, Senger B, Vautier D, Picart C, Schaaf P, Voegel JC, Lavalle P (2005) Natural polyelectrolyte films based on layer-by-layer deposition of collagen and hyaluronic acid. *Biomaterials* 26:3353–3361
- Zhang J, Montanez SI, Jewell CM, Lynn DM (2007) Multilayered films fabricated from plasmid DNA and a side-chain functionalized poly(β -amino ester): surface-type erosion and sequential release of multiple plasmid constructs from surfaces. *Langmuir* 23:11139–11146
- Zhu H, Ji J, Shen J (2004) Construction of multilayer coating onto poly-(DL-lactide) to promote cytocompatibility. *Biomaterials* 25:109–117
- Zintchenko A, Rother G, Dautzenberg H (2003) Transition highly aggregated complexes – soluble complexes via polyelectrolyte exchange reactions: kinetics, structural changes, and mechanism. *Langmuir* 19:2507–2513